

VOLUME 33

MAY 1955

NUMBER 5

Canadian Journal of Chemistry

This issue

is dedicated to

PROFESSOR OTTO MAASS

in recognition of his contribution to science

Published by **THE NATIONAL RESEARCH COUNCIL**

OTTAWA

CANADA

CANADIAN JOURNAL OF CHEMISTRY

(Formerly Section B, Canadian Journal of Research)

Under the authority of the Chairman of the Committee of the Privy Council on Scientific and Industrial Research, the National Research Council issues THE CANADIAN JOURNAL OF CHEMISTRY and six other journals devoted to the publication, in English or French, of the results of original scientific research. Matters of general policy concerning these journals are the responsibility of a joint Editorial Board consisting of: members representing the National Research Council of Canada; the Editors of the Journals; and members representing the Royal Society of Canada and four other scientific societies.

The Chemical Institute of Canada has chosen the Canadian Journal of Chemistry and the Canadian Journal of Technology as its medium of publication for scientific papers.

EDITORIAL BOARD

Representatives of the National Research Council

A. N. Campbell, *University of Manitoba*
G. E. Hall, *University of Western Ontario*
E. G. D. Murray, *McGill University*
D. L. Thomson, *McGill University*
W. H. Watson (Chairman), *University of Toronto*

Editors of the Journals

D. L. Bailey, *University of Toronto*
J. B. Collip, *University of Western Ontario*
E. H. Craigie, *University of Toronto*
G. A. Ledingham, *National Research Council*
Léo Marion, *National Research Council*
R. G. E. Murray, *University of Western Ontario*
G. M. Volkoff, *University of British Columbia*

Representatives of Societies

D. L. Bailey, *University of Toronto*
Royal Society of Canada
J. B. Collip, *University of Western Ontario*
Canadian Physiological Society
E. H. Craigie, *University of Toronto*
Royal Society of Canada
R. G. E. Murray, *University of Western Ontario*
Canadian Society of Microbiologists
H. G. Thode, *McMaster University*
Chemical Institute of Canada
T. Thorvaldson, *University of Saskatchewan*
Royal Society of Canada
G. M. Volkoff, *University of British Columbia*
Royal Society of Canada; Canadian Association of Physicists

Ex officio

Léo Marion (Editor-in-Chief), *National Research Council*

Manuscripts for publication should be submitted to Dr. Léo Marion, Editor-in-Chief, Canadian Journal of Chemistry, National Research Council, Ottawa 2, Canada.

Proof, correspondence concerning proof, and orders for reprints should be sent to the Manager, Editorial Office (Research Journals), Division of Administration, National Research Council, Ottawa 2, Canada.

Subscriptions, renewals, requests for single or back numbers, and all remittances should be sent to Division of Administration, National Research Council, Ottawa 2, Canada. Remittances should be made payable to the Receiver General of Canada, credit National Research Council.

The journals published, frequency of publication, and prices are:

Canadian Journal of Biochemistry and Physiology	Bimonthly	\$3.00 a year
Canadian Journal of Botany	Bimonthly	\$4.00 a year
Canadian Journal of Chemistry	Monthly	\$5.00 a year
Canadian Journal of Microbiology*	Bimonthly	\$3.00 a year
Canadian Journal of Physics	Monthly	\$4.00 a year
Canadian Journal of Technology	Bimonthly	\$3.00 a year
Canadian Journal of Zoology	Bimonthly	\$3.00 a year

The price of single numbers of all journals is 75 cents.

*Volume 1 will combine three numbers published in 1954 with six published in 1955 and will be available at the regular annual subscription rate of \$3.00.

Reprinted in entirety by photo-offset.

To

PROFESSOR OTTO MAASS
this issue is dedicated by his
friends and former students as
a tribute on the occasion of his
retirement as Macdonald Pro-
fessor of Physical Chemistry
and Head of the Department,
at McGill University



O. Maass

Professor Otto Maass

C.B.E., Ph.D., F.R.S., F.R.S.C., D.Sc. (Hon.), LL.D. (Hon.)

Otto Maass retires this June from his position of Macdonald Professor of Physical Chemistry and Head of the Department, at McGill University. This issue of the Canadian Journal of Chemistry, consisting of papers by a few of his friends and former students, is dedicated to him in recognition of his unique place in Canadian science. A mere recital of his achievements and of the honours awarded him, or an account of the many positions he has filled so brilliantly, would fail to explain his influence among the Canadian scientific fraternity. In what follows, an attempt is made to describe his career, and to indicate the importance of his work and his character to Canadian chemists.

Dr. Maass was born in New York City, of Dutch and German parents, in 1890. His family moved to Westmount, P.Q., and Dr. Maass received his early education in Montreal schools, then attended McGill University as a student in the honour course of mathematics and physics. He was persuaded to forsake this branch of learning for the field of physical chemistry by Douglas McIntosh, who later became Macdonald Professor of Physical Chemistry. McIntosh had the greatest admiration for Dr. Maass, and in later years, when the latter's achievements were so universally acclaimed, would boast that he had played the part of Humphrey Davy to Michael Faraday. Since Davy's greatest discovery was Faraday, so McIntosh insisted that his best contribution was to interest Otto Maass in chemistry. After taking an M.Sc. degree with McIntosh in 1912, Maass went to Harvard to work with T. W. Richards as holder of the Royal Exhibition of 1851 Scholarship, and there obtained his Ph.D. degree. After a short period in Europe, he returned to McGill, and became Macdonald Professor of Physical Chemistry in 1923 and Head of the Department in 1937. Under his supervision a large and active research group rapidly formed. Dr. Maass also soon became associated with the Pulp and Paper Research Institute of Canada and began to study the fundamental physical chemistry associated with the preparation of pulp and paper. At the same time he trained in the laboratory of that Institute men who have themselves contributed important advances to the Canadian processes of pulp and paper manufacture. Dr. Maass has retained his association with that organisation, and is presently its General Director of Research.

It would take too long to list the important publications which Maass and his students published from these two laboratories. Suffice it to say that in various calorimetric studies, in the investigations of the critical state, in the determinations of the surface energies of solids, in the preparation and the study of the properties of hydrogen peroxide, in the basic studies of cellulose and cellulose systems, and in the fundamentals of the chemical pulping of wood, the work done still remains some of the best work produced in these fields.

The breadth of these endeavours should be noted. In an age of increasing specialization, Dr. Maass's interest was aroused in many fields, and he made important advances in all of them. Recognition of his outstanding contributions has been made in many ways over the years. He received the Tory Medal of the Royal Society of Canada in 1944, and was elected a Fellow of the Royal Society of London in 1940. For outstanding achievement in the field of paper technology, the Society of Chemical Industry Medal was awarded him in 1943, and more recently, for contributions to both pure and applied chemistry, he was awarded the Chemical Institute of Canada Medal in 1952. In addition to these honours, Dr. Maass has been granted an honorary degree by three Canadian universities, namely, the University of Manitoba, the University of Laval and the University of Toronto. The University of Rochester has also made him an alumnus of that institution by the award of the D.Sc. degree in 1947.

A record of such scholarly achievement would seem sufficient for any man. To it, however, must be added the accomplishments of the great teacher. Particularly with graduate students, Dr. Maass's talent for stating the problem in simple terms and suggesting an experimental attack upon it was clearly in evidence. Many research directors no doubt possess these attributes, but only the very few possess the blend of colourfulness and sympathy which established the spirit and enthusiasm found in Dr. Maass's group at McGill, and which, by a happy kind of contagion, spread throughout the department. Whenever a group of Canadian chemists relaxes, the talk is frequently turned at some stage by a former student, to some exploit, or even prank, which is to be credited to O. M., as he is universally called. Less frequently, but with equal delight, is sometimes recounted a particularly apt, though charitable, chastisement, administered by him. These memories are cherished, and McGill graduates, at least, never tire of retelling or rehearsing these tales, which are handed down from one generation of students to the next. The close feeling among these former associates, which stems from the personality of the teacher, has had important consequences, as will become apparent. All told, Dr. Maass supervised the graduate work of one hundred and thirty-seven students. The vast majority of these took the Ph.D. degree.

Maass's students have frequently gained prominence in both the academic and industrial life of Canada and of the United States. Although the situation has changed to some extent, there was a time when almost every university across Canada had, as its departmental head in Chemistry, or as a prominent member of its chemistry staff, a former member of Dr. Maass's research group. Nor have the Federal Government's laboratories escaped these inroads, as a glance at the names of the scientists will show. Thus Dr. Maass's influence has pervaded the whole scene of Canadian chemistry.

No account of Maass's endeavours would be complete without reference to his association with Canada's effort during the last War, and his continued interest in Canada's preparedness for the future. Dr. Maass, himself, obviously considers the problems of defence of major importance, since he devotes

himself unstintingly to them as a member of the Defence Research Board's committees, and as Scientific Adviser (Special Weapons) to the Chief of Staff.

Prior to 1939, Dr. Maass was one of the few Canadians who foresaw that war was inevitable. Through the Associate Committees of the National Research Council, he did his best to see that organisations were established and manned, to provide the various branches of the Armed Services with required technical information. From the outset of the war, no research was carried on in his McGill laboratory which did not have a direct bearing on wartime activities. He further succeeded in creating an organisation by which all Canadian universities, with their staffs and graduate students, could make direct contributions to the scientific problems confronting the Services. He was one of those who helped establish the Chemical Warfare Laboratories in Ottawa, the Suffield Experimental Station in Alberta, and other establishments of similar type. At the same time he served as an Assistant to the President of the Research Council, Dr. C. J. Mackenzie, and finally also as Director, The Directorate of Chemical Warfare and Smoke, Department of National Defence. These many activities could not have been managed except by a man whose prestige and associations were of the unique type possessed by Dr. Maass. Even in time of war, it is unlikely that any other Canadian scientist could have called forth the effort and co-operation of his fellows which were required. For this work he was honoured by the King, who made him a Commander of the Order of the British Empire, and by the Civil Service, which awarded him the gold medal of the Professional Institute of the Public Service. Since his energy, tact, and knowledge were also drawn upon by the United States, that Government also recognised his services with the award of the United States Medal of Freedom with Bough.

In 1926 Dr. Maass married Carol Robertson, who was herself a Ph.D. in physical chemistry, gained at McGill with Dr. Maass, and therefore also a member of the "O.M. Club" as well. Mrs. Maass must certainly be given some of the credit for her husband's success, for the war years in particular would have taken greater toll of an almost indestructible health, without her understanding and help.

It is difficult indeed to believe that Dr. Maass will ever really retire. He will undoubtedly continue to make contributions to chemistry and education as long as his health permits. Whatever his ventures, he carries with him the best wishes of all who know him.

R. L. McINTOSH,
UNIVERSITY OF TORONTO,
TORONTO, CANADA.

Canadian Journal of Chemistry

Issued by THE NATIONAL RESEARCH COUNCIL OF CANADA

VOLUME 33

MAY 1955

NUMBER 5

STUDIES IN THE POLYOXYPHENOL SERIES

IX. THE SYNTHESIS OF PAPAVERINE AND PAPAVERALDINE BY THE POMERANZ-FRITSCH METHOD¹

BY DONALD A. GUTHRIE,² ARLEN W. FRANK,³ AND C. B. PURVES

ABSTRACT

Fritsch's cyclization of N-(α -veratrylveratrylidene)-aminoacetal in sulphuric acid was shown to give 1.1% of papaverine and 23% of an isomer, m.p. 164.5–165.5°C.; hydrochloride, m.p. 212°C. decomp., which was supposed to be 4,5-bis(3,4-dimethoxyphenyl)-2H-pyrrolenine, produced by an internal condensation of the acetal or the corresponding aldehyde with the reactive methylene group. A similar structure was proposed for another unidentified isomer prepared by Schlittler and Müller. Hydrogenation of Fritsch's acetal gave N-(α -veratrylveratryl)-aminoacetal, m.p. 69.5–70°C., which was cyclized to a base, m.p. 155.5–156°C.; N-acetyl derivative, m.p. 203.5–204°C., formulated as 2,3-bis(3,4-dimethoxyphenyl)-3-pyrroline. Substances presumed to be the intermediate aldehyde and aldol were isolated as colorless oils. Condensation of the diketone veratril with aminoacetal, followed by cyclization of the crude product, constituted a new two-step synthesis of papaveraldine in 8% yield, and the reduction of the latter to papaverine was known.

Other crystalline compounds prepared incidentally and thought to be new were veratril monoanil, m.p. 172–173°C.; α,α' -biveratrylideneaminoacetal, m.p. 101–102°C.; a compound formulated as 2,3-bis(3,4-dimethoxyphenyl)-4-ethylmercaptopyrrolidine hydrochloride, m.p. 184–185°C.; from this an unidentified mercury complex, m.p. 109°C. decomp.; 4,4'-dibenzyloxy-3,3'-dimethoxydesoxybenzoin, m.p. 141–142°C.; and its oxime, m.p. 137.5°C.

INTRODUCTION

The opium alkaloid papaverine is now produced in about 15% yield from vanillin by the Bischler-Napieralski isoquinoline synthesis (3, 4), but the possible application of the less familiar Pomeranz-Fritsch synthesis is still of interest because the product would in theory be obtained in fewer steps. Pomeranz (15) was the first to plan this application, but the attempts of Allen and Buck (1), Fritsch (8), and Schlittler and Müller (17) to put it into effect gave disappointing results. The present article reveals some of the factors that caused these attempts to fail, and describes modifications that lead to syntheses of papaverine and papaveraldine. Manske (14) reviewed the general methods available for the synthesis of isoquinolines.

¹Manuscript received December 31, 1954.

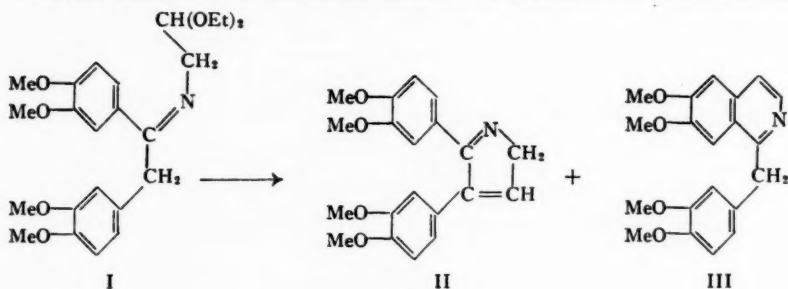
Contribution from the Division of Industrial and Cellulose Chemistry, McGill University, and from the Wood Chemistry Division, Pulp and Paper Research Institute of Canada, Montreal, Que. Abstracted from Ph.D. theses submitted to the University in May 1952 by D.A.G. and in August 1954 by A.W.F.

²Present address: Esso Laboratories, Standard Oil Development Co., P.O. Box 51, Linden, N.J., U.S.A.

³Present address: Division of Pure Chemistry, National Research Council, Ottawa, Canada.

Fritsch (8) reported in 1903 that N-(α -veratrylveratrylidene)-aminoacetal (I), prepared by condensing desoxyveratroin with aminoacetal, was cyclized with 75% sulphuric acid at room temperature to give a 13% yield (based on desoxyveratroin) of a yellow compound melting at 162°C., or 15°C. higher than papaverine (III). Found: C, 70.7; H, 6.4; N, 4.8%. Calc. for papaverine, $C_{20}H_{21}O_4N$: C, 70.7; H, 6.2; N, 4.1%. Like papaverine, the yellow compound was soluble in acetone and sparingly soluble in ethanol and ether. On the basis of these results, Fritsch claimed that the compound was isomeric with papaverine, but he did not attempt to establish its structure.

As a preliminary to repeating Fritsch's synthesis, it was noted that one mole of water was expelled and one mole of aminoacetal was retained when benzoin was boiled with an excess of the acetal, and formation of the Schiff base was presumably complete. A new compound, the desoxybenzoin from O-benzylvanillin, was incidentally prepared in crystalline form. Desoxyveratroin was then condensed with aminoacetal by distilling a mixture of the two substances at atmospheric pressure and up to 245°C. until the water and the excess of aminoacetal were removed. Several attempts to carry out the condensation under milder conditions failed. The product, the Schiff base (I),

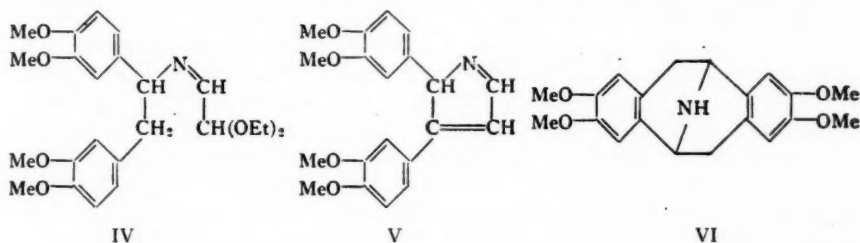


was an uncrystallized, viscous yellow oil, just as described by Fritsch (8). Cyclization of the Schiff base in 83% sulphuric acid gave an 18–23% yield of yellow needles melting at 164.5–165.5°C., whose composition confirmed the supposition that the compound was an isomer of papaverine. A small amount of papaverine (1.1%) was isolated from the mother liquor by chromatography on an alumina column.

One possible isomer, 5,6-dimethoxy-1-veratrylisoquinoline, which might have arisen by cyclization at position 2 rather than position 6 in the veratryl nucleus, could be dismissed immediately, since this isomer had been prepared unambiguously by the Bischler-Napieralski method as a white crystalline solid, m.p. 89–91°C. (13). Another possibility was the isomer 4,5-bis(3,4-dimethoxyphenyl)-2H-pyrroline (II), formed by an internal aldol condensation of the acetal, or of the aldehyde produced by hydrolysis, with the reactive methylene group in (I). A mass of evidence was assembled in support of this structure. The absence of active hydrogen (Zerewitinoff) and an inability to prepare an acetyl or benzoyl derivative indicated the absence of the N—H

group. The base formed no methiodide, but a solution in hydrochloric acid and acetone deposited an orange-colored crystalline hydrochloride which was somewhat unstable to hot solvents and was sparingly soluble in water. Further support for structure (II) was gained from the infrared absorption spectrum of the base. The presence of two very close bands at $805\text{--}810\text{ cm}^{-1}$, corresponding to two unsymmetrical triply-substituted benzene rings, excluded the isoquinoline ring structure (papaverine has only one band in this region). A $\text{C}=\text{N}$ band at 1566 cm^{-1} and the absence of the N-H band showed that, if a pyrrole ring were present, the hydrogen atoms would have to be distributed around the ring in an abnormal manner.

In accord with structure (II), we would like to propose a structure for another unidentified isomer of papaverine, obtained by Schlittler and Müller in 1948 (17). The Schiff base *N*-(α -veratrylveratryl)-iminoacetal (IV), prepared by condensing 1,2-bis(3,4-dimethoxyphenyl)-ethylamine with glyoxal semiacetal, was cyclized with 75% sulphuric acid in 10% yield to a white crystalline compound melting at $222\text{--}223^\circ\text{C}$. and with the carbon and hydrogen content required for $\text{C}_{20}\text{H}_{21}\text{O}_4\text{N}$. The product was probably 2,3-bis(3,4-

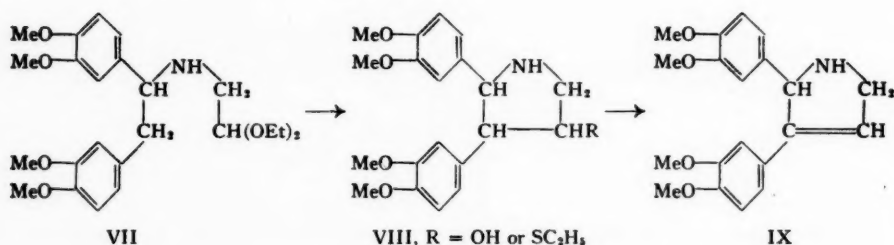


dimethoxyphenyl)-2*H*-pyrrolenine (V), differing from (II) only in the position of the $\text{C}=\text{N}$ bond.

An attempt was made by Allen and Buck (1) in 1930 to synthesize papaverine by the Fischer-Rügheimer modification of the Pomeranz-Fritsch synthesis. This modification, which was the subject of a recent paper (7), consisted of cyclizing *N*-benzylaminoacetals with sulphuric acid in the presence of an oxidizing agent such as arsenic pentoxide. Allen and Buck found that condensation of 1,2-bis(3,4-dimethoxyphenyl)-ethylamine with bromoacetal at 150°C . yielded a red oil, presumably *N*-(α -veratrylveratryl)-aminoacetal (VII), which could not be crystallized and which gave no crystalline derivatives. When the oil was treated with arsenic pentoxide in sulphuric acid solutions of various strengths, nothing but black amorphous material was obtained. In the present work, attempts were made to condense the amine with excess chloroacetal in boiling xylene, or with a slight excess of bromoacetal in cold benzene, but the first experiment yielded a black gum, and the second a white amorphous solid containing almost no nitrogen. In both cases much of the original amine could not be recovered. Allen and Buck (1) apparently employed the dimethyl acetal of bromoacetaldehyde instead of the more common

diethyl acetal used in the above experiments, and a direct comparison with their results was not possible.

It was then discovered that the desired secondary amine, *N*-(α -veratryl-veratryl)-aminoacetal (VII), could be prepared in good yield as a white crystalline solid by hydrogenation of the Schiff base (I) over Raney nickel. Cyclization of this crystalline amine (VII) under the conditions of the Rügheimer synthesis gave a white crystalline solid, m.p. 155.5–156°C., in yields of up to 56%. The product had the composition of dihydropapaverine, $C_{20}H_{22}O_4N$, but differed from the known substances 3,4-dihydropapaverine, m.p. 97–98°C., and pavine (VI), m.p. 201–202°C. (2, 18). Analogy with the cyclization of the Schiff base (I) suggested that the new substance was either the hitherto unknown 1,2-dihydropapaverine, or 2,3-bis(3,4-dimethoxyphenyl)-3-pyrroline (IX), formed by an internal aldol condensation of the acetal (or aldehyde) with the reactive methylene group. The former, however, was shown to be an unstable intermediate in the reduction of papaverine with tin and hydrochloric acid, cyclizing spontaneously in the acid solution to pavine (VI) (18). The absence of pavine in the acidic reaction mixture from the cyclization of (VII) was, therefore, an indication that no 1,2-dihydropapaverine was produced.



The over-all pattern of the infrared spectrum of the new base favored a structure similar to the pyrrolenine (II). A double band at 799–808 cm^{-1} indicated, as in the pyrrolenine, the presence of two unsymmetrical triply-substituted benzene rings. The presence of an N—H group was established by the presence of the N—H stretching frequency and by the preparation of a crystalline acetyl derivative. The base was, however, completely destroyed when attempts were made at dehydrogenation to the pyrrolenine with selenium at 250°C., with palladium-on-charcoal at 190°C., or with palladium black in boiling decalin.

Other experiments on the cyclization of the secondary amine (VII) at 20°C. showed that sulphuric acid of 20 to 65% strength was capable of hydrolyzing the acetal, but was unable to convert the product (aldehyde or aldol; see below) to the pyrroline (IX). At an acid strength of 75 or 83%, fair yields of the pyrroline were obtained, with or without arsenic pentoxide, but the duration of the reaction was critical (Fig. 1) because the product was unstable toward the condensing agent. When samples of the crystalline pyrroline were

dissolved in 83% sulphuric acid at room temperature and worked up in the usual manner after 2 and 18 hr., the recovery of the pyrroline was only 48% and 18%, respectively. The fact that the conditions of cyclization were so narrowly defined constituted another reason why Allen and Buck (1) failed to isolate the pyrroline.

The hydrolysis of *N*-(α -veratrylveratryl)-aminoacetal (VII) to the free aldehyde was studied in the hope that this procedure would reduce the time required for the subsequent cyclization. When the hydrolysis was carried out with 2 *N* hydrochloric acid for seven hours at 100°C. there was obtained, as anticipated, a product exhibiting a very strong positive dinitrophenylhydrazine test for the carbonyl function, and 92% of the theoretical amount of ethanol was recovered. The crude, gummy product was cyclized in 83% sulphuric acid over a four-hour period to the pyrroline (IX) in 32% yield (based on the acetal). When the acetal was hydrolyzed with concentrated hydrochloric acid at 20°C. for 0.5, 3, 6, 24, and 51 hr., the ethanol recovered amounted to 14, 71, 98, 100, and 99%, respectively, of the theoretical amount. Even after six hours, when the hydrolysis was complete, the colorless gum which formed the product gave a negative dinitrophenylhydrazine test for the carbonyl function. This product was probably the intermediate aldol, 2,3-bis(3,4-dimethoxyphenyl)-4-pyrrolidinol (VIII, R = OH). Concentrated hydrochloric acid, then, was presumably capable of cyclizing the acetal or aldehyde to the aldol, but not of dehydrating the aldol to the pyrroline.

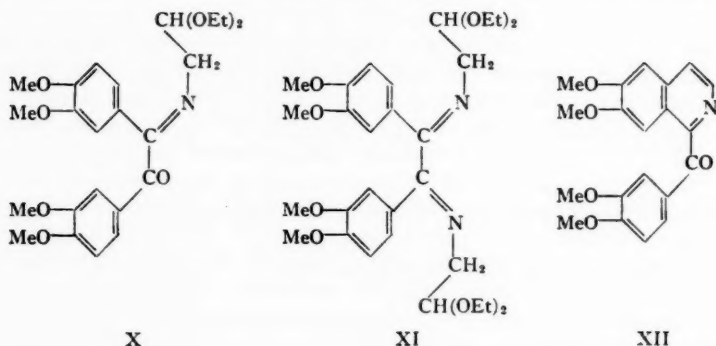
Support for this argument was unintentionally provided by the results of an attempt to prepare the free aldehyde, *N*-(α -veratrylveratryl)-aminoacetaldehyde, by conversion of the acetal (VII) to the thioacetal, followed by cleavage of the thioacetal with mercuric chloride and cadmium carbonate (22). Instead of the expected thioacetal, the crystalline product, isolated from the reaction of the acetal with ethyl mercaptan in concentrated hydrochloric acid, had the composition of the sulphide, 2,3-bis(3,4-dimethoxyphenyl)-4-ethylmercaptopyrrolidine hydrochloride (VIII, R = SC₂H₅). The concentrated hydrochloric acid had effected, at some stage in the reaction, an aldol condensation.

Treatment of the sulphide with mercuric chloride and cadmium carbonate, under the conditions normally employed for the hydrolysis of a thioacetal to the corresponding aldehyde (22), gave a brilliant yellow mercury complex, m.p. 109°C. decomp., which contained nitrogen atoms, methoxyl groups, and mercury atoms in the ratio 2:8:1. When the complex was decomposed with hydrogen sulphide a colorless oil resulted, which was probably the aldol (VIII, R = OH), since tests for halogen and carbonyl groups were negative, and the oil yielded up to 34% of the pyrroline (IX) when aliquots were treated with 83% sulphuric acid.

In retrospect, it appeared that a major obstacle to the completion of the synthesis of papaverine by the Pomeranz-Fritsch method was the reactivity of the methylene group in *N*-(α -veratrylveratrylidene)-aminoacetal (I), and that this obstacle might be removed by replacing the group with, for example, a hydroxyl or keto group. Veratroin was not a suitable starting material,

because it was difficult to purify (12), and would probably not withstand the drastic conditions required for condensation with aminoacetal. On the other hand, the diketone veratril was a stable, crystalline compound, readily prepared by mild oxidation of veratroin (10, 12), or by methylation of vanillil, a substance now isolated from oxidized waste sulphite liquor and of potential commercial importance. It was found advantageous to methylate the vanillil in the form of its bright yellow crystalline disodium salt.

Many attempts were made to prepare the desired mono-Schiff base, N-(α -veratroylveratrylidene)-aminoacetal (X), by condensing veratril with various proportions of boiling aminoacetal. The conditions finally employed were slightly milder than those for the similar condensation of desoxyveratroin, but efforts to employ a lower temperature resulted only in the quantitative recovery of the veratril. After isolation, the product soon deposited a substantial quantity of the disubstituted compound, α,α' -biveratrylidene-aminoacetal (XI), as white crystals. Since this compound yielded veratril on hydrolysis with dilute acid, no further internal condensation, such as formation of an imidazole (11), had occurred. The remainder of the product was a yellow oil which resisted attempts at purification by chromatography on Magnesol or cellulose columns. A paper chromatogram of the oil, developed with petroleum ether saturated with water, and sprayed with acid 2,4-dinitrophenyl-



hydrazine, showed a yellow spot at R_f 0.79 and a red spot at R_f 0.68. Reference chromatograms with veratril and the crystalline di-Schiff base showed yellow spots at the base line and at R_f 0.79, respectively. The oil therefore contained some of the di-Schiff base and also a carbonyl compound which was assumed to be the sought-for mono-Schiff base (X). The oil, however, could not be crystallized, and repeated attempts to isolate the mono-Schiff base ended in failure. Attempts to reach the same goal by partial hydrolysis of the di-Schiff base were also fruitless. These failures were unexpected, because a preliminary condensation of veratril with boiling aniline readily gave the pale yellow crystalline monoanil in good yield.

An attempt was also made to isolate the secondary amine corresponding to the mono-Schiff base (X). The Schiff base mixture, or the pure di-Schiff base

alone, consumed no hydrogen when shaken with Adams' platinum oxide catalyst and 30–40 p.s.i. of hydrogen for 25 hr. at room temperature. Hydrogenation of the Schiff base mixture over freshly prepared Raney nickel at 1500 p.s.i. for three hours at 80–90°C. gave an oil which slowly deposited 2% of the unchanged di-Schiff base, but none of the desired secondary amine. Only 7% of veratril was recovered after hydrolysis of the residual oil with dilute hydrochloric acid, and neutralization of the acidic mother liquor caused the separation of a red ether-soluble oil (83% of the original veratril) which was not examined in detail.

In default of the pure mono-Schiff base (X), the experiments on cyclization were carried out on the original crude mixture. No papaveraldine (XII) was isolated from attempted cyclizations in 83% sulphuric acid for 20 hr. at room temperature, or in concentrated sulphuric acid for three minutes at 150°C., but an 8% yield, based on veratril, resulted from a cyclization carried out with 72% acid at room temperature or less. This result amounted to a new synthesis of papaverine (III), for papaveraldine was known to be reduced to papaverine with zinc dust and acetic anhydride (5, 19), as well as in a less direct way (5).

EXPERIMENTAL

Melting points were not corrected. The infrared spectra were obtained from Nujol mulls.

Materials

Veratroin was prepared from veratraldehyde by the benzoin condensation, and was reduced to desoxyveratroin substantially as described by Kubiczek (12). After the observation of Fritsch (8) that desoxyveratroin could not be separated from traces of veratril by crystallization had been confirmed, the crude product, 11.3 gm., was boiled for two hours under reflux with 100 ml. of anhydrous ethanol, 10 ml. of glacial acetic acid, and 6.7 gm. of Girard's "T" reagent for carbonyl compounds (the hydrochloride of N-trimethyl-aminoacethydrazide) (9). When cool, the solution was poured into 300 gm. of ice and water containing 21.5 gm. of potassium carbonate and was extracted with benzene until the extracts were colorless. The adduct was decomposed by acidifying the aqueous residue to pH 1 with hydrochloric acid, and an hour later the precipitated desoxyveratroin, 4.6 gm., was collected. The best overall yield was 18%, and m.p. 103.5–104.5°C., the recorded values being 106°C. (12, 21) or 107°C. (1).

Desoxyveratroin oxime, melting correctly at 128.5–129°C. (1, 12), was obtained in 99% yield by stirring a slurry of desoxyveratroin, hydroxylamine hydrochloride, and sodium acetate in aqueous ethanol for three days at room temperature. A yield of only 67% was obtained when the hydrochloride was used in pyridine solution (1). This oxime was reduced to 1,2-bis(3,4-dimethoxyphenyl)-ethylamine in 78% yield by sodium amalgam (1, 10), and in 69% yield by hydrogenation for 50 min. at 80–100°C. and 1300 p.s.i. over a Raney nickel catalyst. This catalyst was apparently more suitable than palladium-on-charcoal, which recently failed to give the expected result (21).

To prepare veratril, a mixture of 30.2 gm. (0.1 mole) of vanillil, m.p. 233–233.5°C. (diacetate, m.p. 139–140°C.), 24 gm. of sodium hydroxide, and 200 ml. of water was shaken rapidly until solution was complete. In a few minutes the red solution began to deposit in practically quantitative yield the bright yellow needles of the disodium salt of vanillil, which was washed with ethanol and dried *in vacuo* over solid potassium hydroxide. This salt melted above 265°C., was insoluble in all common organic liquids, but dissolved readily in water to give a yellow solution. A mixture of the dry, powdered salt with 28 ml. of dimethyl sulphate and 500 ml. of toluene was heated for five hours under reflux, and was then cooled. The next day the solid product, 55 gm., was freed from sodium salts by being ground in a mortar with 10% sodium carbonate, and the residue of almost pure veratril weighed 26.6 gm. (80.5%). One recrystallization from glacial acetic acid raised the melting point to 224–225°C., the recorded value being 223°C. (12). Veratril was also obtained by methylating vanillil with dimethyl sulphate and aqueous sodium carbonate or methanolic sodium hydroxide, but the yields were only 31% and 66%, respectively. Oxidation of the crude veratroin described above with copper sulphate in pyridine (10), or by air and alkali (12), gave veratril in over-all yields of 10% or less from veratraldehyde.

Aminoacetaldehyde diethyl acetal was prepared in 35% yield from chloroacetal as described by Richmond and Wright (16); the colorless product had the right composition, boiled correctly at 160–165°C., and yielded a picrate melting correctly at 142–143°C. When the chloroacetal was replaced by bromoacetal the yield of aminoacetal decreased to 14% or less; none was obtained from chloroacetal and sodamide suspended in boiling liquid ammonia, ether, or toluene.

4,4'-Dibenzyloxy-3,3'-dimethoxydesoxybenzoin

In accord with Kubiczek's general procedure (12), a solution of 35 gm. of O-benzylvanillin, m.p. 61°C., and 5.2 gm. of potassium cyanide in 100 ml. of ethanol was boiled under reflux for four and one-half hours in an atmosphere of hydrogen. The gum which precipitated when the solution was poured into 400 ml. of cold water was dissolved in 400 ml. of ether, and the ethereal solution was washed with dilute sodium carbonate, dilute sodium bisulphite, and finally with water. After the solution had been dried, evaporation of the ether left the benzoin as a crude oil, which was then dissolved in a boiling mixture of methanol, 300 ml., acetic acid, 150 ml., and water, 75 ml., and reduced by the gradual addition of 39 gm. of zinc dust during one and one-half hours. The white solid that separated when the solution cooled was extracted with acetone from excess zinc dust, and the extract was poured into water. The long white needles that separated weighed 9.5 gm. (28%) and their melting point of 141–142°C. was not changed by recrystallization from ethanol. Found: OCH₃, 13.0, 13.2%. Calc. for C₂₀H₁₈O₅: OCH₃, 13.2%. The oxime could not be prepared by stirring the desoxybenzoin with hydroxylamine hydrochloride and sodium acetate in 80% ethanol, but an 85% yield resulted when the substance was boiled for five and one-half hours with a solution of

the hydrochloride in pyridine. After three recrystallizations from ethanol, the melting point of the oxime was 137–137.5°C., depressed to 124–133°C. by admixture with the original desoxybenzoin.

Cyclization of N-(α -Veratrylveratrylidene)-aminoacetal (I)

A 125 ml. distillation assembly containing 25 gm. (0.079 mole) of desoxyveratroin and 30 gm. (0.225 mole) of aminoacetal was swept out with nitrogen and the heating was adjusted from time to time to give slow, uniform distillation of the excess aminoacetal. The temperature of the liquid rose steadily over the course of one hour from 165°C. to 245°C., as the last traces of the excess aminoacetal were carried over. The light yellow still residue of crude Schiff base (I) weighed 29.8 gm. (calc. 34.1 gm.).

Part of this oil (15.0 gm.) was dissolved in 160 ml. of chilled 83% sulphuric acid, the crimson solution was stirred for 20 hr. at room temperature, and was then mixed with 500 gm. of chopped ice. The slurry was made alkaline with aqueous sodium hydroxide and extracted with benzene. Extraction of the benzene solution with 0.1 *N* hydrochloric acid and addition of excess aqueous sodium hydroxide to the aqueous extract gave a slightly brown solid, which was then taken up in hot ethanol, decolorized with charcoal, and filtered. On cooling, there separated 2.89 gm. (21.5% based on desoxyveratroin) of yellow needles melting at 164–165°C. The melting point was raised slightly to 164.5–165.5°C. by recrystallization from ethanol. Found: C, 70.5, 70.8; H, 6.3, 6.2; N, 4.01, 4.02; OCH₃, 35.9, 36.1%; mol. wt., determined cryoscopically in benzene, 354, 336. Calc. for C₂₀H₂₁O₄N: C, 70.7; H, 6.2; N, 4.13; OCH₃, 36.6%; mol. wt., 339. Determinations made in anisole by the Zerevitinoff method showed the presence of only 0.12, 0.07 gm. of active hydrogen per mole. The compound was very soluble in chloroform, pyridine, glacial and aqueous acetic acid, sparingly soluble in acetone, methanol, and ethanol, and insoluble in water and ether.

The hydrochloride, prepared by adding a little concentrated hydrochloric acid to an acetone solution of the base, melted with decomposition at 212°C. Found: Cl, 9.36, 9.33%. Calc. for C₂₀H₂₁O₄NCl: Cl, 9.46%. This orange-colored substance was only sparingly soluble in water, and was rather unstable to recrystallization from hot solvents.

The brown ethanol filtrate, from which the yellow base had been removed, was evaporated to dryness and the residue digested exhaustively with boiling petroleum ether. Filtration and evaporation of the extract left 0.39 gm. of a pale yellow solid melting over the range 134–138°C. This solid was dissolved in dry benzene and chromatographed on an alumina column; the yellow base, C₂₀H₂₁O₄N, washed through the column weighed 0.17 gm. (1.3%) and melted at 164–165°C. The column was then extruded and all but the upper 0.5 cm., which was deep brown in color, was extracted with 5% pyridine in methanol. This extract yielded, on filtration and evaporation, 0.15 gm. (1.1%) of papaverine, m.p. 146.5–147.5°C. The base was converted to its hydrochloride, m.p. 221–222°C. The melting points of the base and its hydrochloride were identical with those of authentic papaverine and its hydrochloride, respectively, and no depression in the melting points was observed on admixture.

N-(α -Veratrylveratryl)-aminoacetal (VII)

The crude Schiff base (I), obtained as a pale yellow oil from a condensation of 20.0 gm. of desoxyveratrin with 33.7 gm. of aminoacetal, was dissolved in 100 ml. of ethanol and hydrogenated with 2 gm. of Raney nickel in a 300 ml. steel bomb at 1300 p.s.i. and 80–100°C. for 80 min. The yellow oil remaining after filtration and evaporation of the bomb contents was dissolved in 150 ml. of *N* hydrochloric acid and the solution was extracted several times with ether. A small amount (1.8 gm.; 9%) of desoxyveratrin was recovered from the ether extract. Neutralization of the acidic aqueous solution with sodium hydroxide caused the deposition of a mass of white crystals, which after washing and drying weighed 16.5 gm. (61% based on desoxyveratrin) and melted at 66–68°C. Repeated crystallization from methanol gave fine white felted needles and raised the melting point to 69.5–70°C. Found: C, 66.5, 66.5; H, 8.3, 8.3; N, 3.25, 3.29; OCH₃, 42.6, 42.2%. Calc. for C₂₄H₃₈O₆N: C, 66.5; H, 8.2; N, 3.24; OCH₃ (OC₂H₅ calc. as OCH₃), 43.0%. The product was very soluble in dilute mineral acids, ether, ethyl acetate, chloroform, and benzene, was only slightly less soluble in ethanol and methanol, and was insoluble in water.

In subsequent preparations under apparently identical conditions the yield of *N*-(α -veratrylveratryl)-aminoacetal (VII) was only 20–25% of the desoxyveratrin used.

2,3-Bis(3,4-dimethoxyphenyl)-3-pyrroline (IX) (Fig. 1)

The following experiment was typical of the series. A solution of 1.0 gm. of the acetal (VII) in 11 ml. of chilled 83% sulphuric acid was allowed to stand for seven hours at room temperature, and was then poured into ice water. After extraction with benzene, the acid solution was made alkaline and

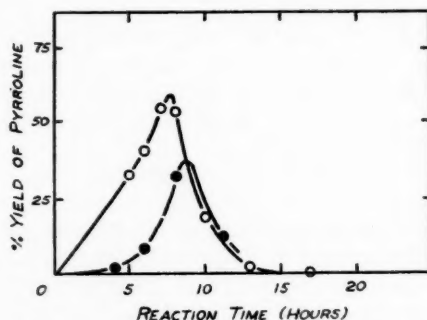


FIG. 1. Per cent yield of 2,3-bis(3,4-dimethoxyphenyl)-3-pyrroline (IX) from cyclization of *N*-(α -veratrylveratryl)-aminoacetal (VII) in sulphuric acid at 20°C. for various times; ○ in 83% acid, ● in 75% acid.

filtered. The acid-soluble white precipitate weighed 0.44 gm. (56%) and melted at 150–154°C. The melting point was raised to 155.5–156°C. by successive precipitation from hydrochloric acid solution with alkali. Found:

C, 70.3, 70.2; H, 6.9, 6.8; N, 4.05, 4.11, 4.02; OCH_3 , 35.7, 35.5%. Calc. for $\text{C}_{20}\text{H}_{23}\text{O}_4\text{N}$: C, 70.3; H, 6.8; N, 4.10; OCH_3 , 36.4%.

Treatment of the base with acetic anhydride in pyridine for three days at room temperature gave a 94% yield of the N-acetyl derivative melting at 203.5–204°C. Found: N, 3.56, 3.60; OCH_3 , 32.1, 32.2%. Calc. for $\text{C}_{22}\text{H}_{25}\text{O}_5\text{N}$: N, 3.66; OCH_3 , 32.4%.

2,3-Bis(3,4-dimethoxyphenyl)-4-ethylmercaptopyrrolidine Hydrochloride (VIII, R = SC_2H_5)

The acetal (VII), 3.65 gm. (0.0084 mole), was added to a stirred suspension of 15 ml. (0.20 mole) of ethyl mercaptan in 100 ml. of concentrated hydrochloric acid. After 24 hr., the mixture was poured into 100 ml. of water and the solution was washed with benzene. The solution was made alkaline with aqueous sodium hydroxide and again extracted with benzene. The benzene extract, on drying over anhydrous sodium sulphate and evaporating, yielded 1.98 gm. of a colorless oil. This oil was dissolved in acetone and converted to the hydrochloride by treatment with a few drops of the concentrated acid; the gum left on evaporation of the solution slowly crystallized when heated at 60°C. *in vacuo* for two hours. The product, washed with dry acetone and dry ether and then dissolved in a little methanol, was precipitated into dry ether. Weight, 1.38 gm. (37.5%), and m.p. 184–185°C. Found: C, 60.0; H, 5.9; N, 3.08, 2.99; S, 6.90, 7.08; OCH_3 , 28.0, 27.9%. Calc. for $\text{C}_{22}\text{H}_{30}\text{O}_4\text{NSCl}$: C, 60.0; H, 6.9; N, 3.18; S, 7.28; OCH_3 , 28.2%. The base, prepared from the hydrochloride by treatment with alkali, was an oil which appeared to decompose.

A solution of 1.29 gm. (0.003 mole) of the crystalline hydrochloride in water was made alkaline and extracted with benzene. The colorless oil left after evaporation of the dried extract was dissolved in 70 ml. of acetone to which had been added 3.75 gm. of mercuric chloride, 4.8 gm. of cadmium carbonate, and 1.0 ml. of water. The mixture was stirred for 24 hr. at room temperature, and was then filtered. The residue left after evaporation of the filtrate was dissolved in a large volume of chloroform and was washed with dilute aqueous potassium iodide followed by water. Evaporation of the dried chloroform solution left 1.17 gm. of a brilliant yellow solid melting with decomposition at 85°C. The melting point was raised to 109°C. by repeated solution in acetone and precipitation with ether. Found: N, 1.88, 1.90; OCH_3 , 16.9, 17.2; Hg, 13.8%. These figures were in the ratio 1.96 N: 8.0 OCH_3 : 1.0 Hg.

A solution of 0.800 gm. of this mercury complex in aqueous acetone containing a few drops of acetic acid was treated with hydrogen sulphide until no further precipitation of black mercuric sulphide occurred. This precipitate was dried and weighed to yield the analytical figure for mercury quoted above. The acetone solution was diluted with water, made alkaline, and extracted with benzene. Evaporation of the dried extract left 0.468 gm. of a colorless oil which was negative to tests for halogen and carbonyl groups; yield as the aldol (VIII, R = OH) based on the sulphide (VIII, R = SC_2H_5), 65%.

This oil was treated with 5 ml. of 83% sulphuric acid at room temperature. Aliquots were removed at various intervals and the pyrroline (IX) was

isolated as outlined previously. After 1.5, 3, 5, 7, and 15 hr. the yields of IX (based on the oil) were 22, 30, 34, 19, and 2% respectively. The authenticity of these products was established by mixed melting point with samples of the pyrroline (IX).

Condensation of Veratril with Aminoacetal

A mixture of 16.5 gm. (0.05 mole) of veratril and 25.0 gm. (0.17 mole) of aminoacetal was boiled gently under reflux in a nitrogen atmosphere until all of the veratril was dissolved. After cooling, the viscous red product was dissolved in ether and the solution was filtered to remove the unchanged veratril, which in this run weighed only 0.1 gm. The ethereal solution was extracted several times with water to remove the excess aminoacetal, then was dried over anhydrous potassium carbonate and evaporated. On rubbing with a little ethanol, the residue partly crystallized in well-formed white hexagonal plates, which weighed 3.3 gm. (12%) and melted at 98.5–100°C. after one recrystallization from ethanol–water. Two more recrystallizations from ethanol–water raised the melting point to 101–102°C., unchanged by recrystallization from ligroin. Found: C, 64.3, 63.8; H, 7.8, 7.7; N, 4.82, 4.84, 4.89, 4.84; OCH_3 , 43.3, 43.4%. Calc. for α, α' -biveratrylideneaminoacetal (XI), $\text{C}_{10}\text{H}_{14}\text{O}_3\text{N}_2$: C, 64.3; H, 7.9; N, 5.00; OCH_3 (OC_2H_5 calc. as OCH_3), 44.3%. Another 1.2 gm. of this di-Schiff base was recovered from the eluates of the experiments on column chromatography, bringing the total yield up to 16%. The product was very soluble in methanol, ethanol, ether, chloroform, and benzene, less soluble in hot ligroin, and insoluble in water.

A solution of 47.6 mgm. of the di-Schiff base, 2 ml. of ethanol, and 10 ml. of *N* hydrochloric acid was kept for 10 hr. at room temperature and then filtered. The veratril weighed 6.5 mgm. (23%) and melted at 223.5–224°C. (mixed m.p. undepressed). The recovery of veratril was increased to 42% when the reaction was carried out on the steam bath for six hours under reflux.

Papaveraldine (XII)

Condensation of 3.30 gm. of veratril with 5.0 gm. of aminoacetal as described above gave 6.6 gm. of a partly crystalline red oil, and 0.33 gm. of veratril was recovered. Part of this mixture of Schiff bases, 4.7 gm., was dissolved cautiously in 50 ml. of 72% sulphuric acid and kept for two days at 5°C. and for another three days at room temperature. The dark red solution was poured onto 50 gm. of chopped ice, filtered, and extracted twice with ether. When the aqueous portion was neutralized with 10% sodium carbonate an amorphous buff-colored solid separated, together with much black gummy material. A solution of the solid in benzene was combined with a benzene extract of the filtrate, and applied to a 6 in. alumina column. The black material remained at the top of the column. The benzene eluates were separately evaporated, the residues taken up in dilute hydrochloric acid, and the solutions distilled to dryness under reduced pressure. Some of the fractions yielded a crystalline hydrochloride, m.p. 189–192°C. These fractions were combined, taken up in hot water, and neutralized with concentrated ammonia. The

base which separated, when collected on a filter and washed thoroughly with water, weighed 0.177 gm. (8%) and melted at 205–207°C. One recrystallization from methyl ethyl ketone gave 0.135 gm. of papaveraldine melting at 208–209°C., not depressed on admixture with an authentic sample, m.p. 208–209°C., prepared by oxidation of papaverine with selenium dioxide as described by Taylor (20).

The hydrochloride, prepared by covering the base with 10% hydrochloric acid, heating the mixture on a steam bath, and adding water dropwise until solution was complete, crystallized on cooling in fine yellow needles, m.p. 198–199°C., undepressed on admixture with a sample similarly prepared from authentic papaveraldine. Papaveraldine was reported to melt at 210°C. corr., and its hydrochloride at 200°C. corr. (6, 20).

Veratril Monoanil

A mixture of 3.30 gm. (0.01 mole) of veratril and 4.65 gm. (0.05 mole) of freshly distilled aniline was heated under nitrogen for three hours with steady reflux (bath temp. 230°C.). The mixture partly crystallized on cooling. After being triturated with ether in a mortar, the mixture left a residue of 1.75 gm. which was identified as veratril (52% recovery).

The ethereal mother liquor was evaporated to dryness and the residual oil was mixed with 5 ml. of ethanol. A crop of yellow crystals, 0.757 gm., slowly separated. Further dilution with ethanol yielded two more crops of 0.826 gm. and 0.476 gm. Recrystallization of the middle crop from ethanol gave a product, m.p. 172–173°C. with strong sintering at 159°C., which appeared to be a mixture of two crystalline substances, one pale yellow and the other golden yellow. Recrystallization from ethyl acetate removed the golden yellow impurity, and the veratril monoanil then melted at 172–173°C. Found: C, 70.8, 70.7; H, 5.7, 5.8; N, 3.33, 3.36; OCH_3 , 30.5, 30.5%. Calc. for $\text{C}_{24}\text{H}_{21}\text{O}_6\text{N}$: C, 71.1; H, 5.7; N, 3.45; OCH_3 , 30.6%. The anil was very soluble in chloroform, soluble in benzene, ether, and hot ethyl acetate, slightly soluble in ethanol, and insoluble in water and hexane.

A solution of 30.2 mgm. of veratril monoanil, 2 ml. of ethanol, and 5 ml. of *N* hydrochloric acid was heated on the steam bath for six hours under reflux. After cooling, the mixture was poured into water, allowed to stand undisturbed for several hours, and filtered. The veratril weighed 22.8 mgm. (93%) and melted at 223.5–224°C. (mixed m.p. undepressed).

ACKNOWLEDGMENTS

We wish to thank Mr. A. W. Pross of Canadian Industries (1954) Limited, McMasterville, Que. for determining and interpreting the infrared spectra, and Dr. C. A. Sankey of the Ontario Paper Company, Thorold, Ont. for a generous gift of vanillin. Two of us are grateful for assistance in the form of scholarships from Canadian Industries Limited (D.A.G.), from the Spruce Falls Power and Paper Company (A.W.F.), from the Pulp and Paper Research Institute of Canada (A.W.F.), and from the National Research Council of Canada (D.A.G. and A.W.F.).

REFERENCES

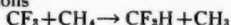
1. ALLEN, I. and BUCK, J. S. *J. Am. Chem. Soc.* 52: 310. 1930.
2. BATTERSBY, A. R. and BINKS, R. *Chemistry & Industry*, 1455. 1954.
3. BISCHLER, A. and NAPIERALSKI, B. *Ber.* 26: 1903. 1893.
4. British Intelligence Objectives Subcommittee, Final Rept. 766: 119. 1945; 1774: 1. 1947.
5. BUCK, J. S., PERKIN, W. H., JR., and STEVENS, T. S. *J. Chem. Soc.* 127: 1462. 1925.
6. DOBSON, B. and PERKIN, W. H., JR. *J. Chem. Soc.* 99: 135. 1911.
7. FRANK, A. W. and PURVES, C. B. *Can. J. Chem.* 33: 365. 1955.
8. FRITSCH, P. *Ann.* 329: 37. 1903.
9. GIRARD, A. and SANDULESCO, G. *Helv. Chim. Acta*, 19: 1095. 1936.
10. HARTWELL, J. L. and KORNBERG, S. R. L. *J. Am. Chem. Soc.* 67: 1606. 1945.
11. JAPP, F. R. and DAVIDSON, W. B. *J. Chem. Soc.* 67: 32. 1895.
12. KUBICZEK, G. *Monatsh.* 76: 55. 1945.
13. LINDENMANN, A. *Helv. Chim. Acta*, 32: 69. 1949.
14. MANSKE, R. H. F. *Chem. Revs.* 30: 145. 1942.
15. POMERANZ, C. *Monatsh.* 14: 116. 1893.
16. RICHMOND, H. H. and WRIGHT, G. F. *Can. J. Research, B*, 23: 158. 1945.
17. SCHLITTLER, E. and MÜLLER, J. *Helv. Chim. Acta*, 31: 914. 1948.
18. SCHÖPF, C. *Experientia*, 5: 201. 1949.
19. STUCHLIK, L. *Monatsh.* 21: 813. 1900.
20. TAYLOR, E. P. *J. Pharm. and Pharmacol.* 2: 324. 1950.
21. WALKER, G. N. *J. Am. Chem. Soc.* 76: 3999. 1954.
22. WOLFROM, M. L. *J. Am. Chem. Soc.* 51: 2188. 1929.

THE VAPOR PHASE PHOTOLYSIS OF HEXAFLUOROACETONE IN THE PRESENCE OF METHANE AND ETHANE¹

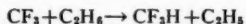
BY P. B. AYS COUGH,² J. C. POLANYI,³ AND E. W. R. STEACIE

ABSTRACT

The photolytic decomposition of hexafluoroacetone by light of wavelength 3130 Å has been used to produce trifluoromethyl radicals for a study of their reactions with methane and ethane. It has been shown that these radicals abstract hydrogen with greater facility than do methyl radicals. The activation energies for the two reactions



and



are found to be 10.3 ± 0.5 kcal./mole and 7.5 ± 0.5 kcal./mole respectively, if one can assume zero activation energy for the recombination of trifluoromethyl radicals.

INTRODUCTION

Relatively few kinetic studies have been made on the reactions of fluoroalkyl radicals and most of those so far reported have not yielded very precise data about the elementary reactions of these radicals. In part this is the result of analytical difficulties in handling the mixtures of fluorinated compounds in the reaction products. Further difficulties have arisen because of low quantum yields (as in the photolysis of trifluoromethyl iodide (2, 4, 6)), side reactions caused by the necessity of using high temperatures for pyrolyses (as in the pyrolysis of tris(trifluoromethyl)arsine (1)), or the production of more than one type of radical in the primary breakdown (as in the photolysis of trifluoroacetone (12)). Some exploratory work on the photolysis of hexafluorodimethyl mercury (11) showed that trifluoromethyl radicals were produced by straightforward fission of the mercury-carbon bonds but the total yield was small on account of the low volatility of the substrate.

During a preliminary study of the photolysis of hexafluoroacetone it was found that this compound fulfills most of the requirements of a source of trifluoromethyl radicals and that a simple analytical procedure can be devised for estimating the products. It was therefore decided to begin a study of the elementary reactions of these radicals with an investigation of their reactions with the simpler hydrocarbons, using the photolysis of hexafluoroacetone as the source of the radicals.

Between 80° and 300°C. hexafluoroacetone yields on photolysis only hexafluoroethane and carbon monoxide, in the stoichiometric proportions. The quantum yield is independent of light intensity and is only slightly affected by pressure in the range used (20–100 mm.). In the presence of hydrocarbons fluoroform is found in the products and under certain conditions replaces the hexafluoroethane almost completely. For instance when 25 mm. hexafluoroacetone is photolyzed at 120°C. in the presence of an equal amount of isobutane

¹Manuscript received November 30, 1954.

Contribution from the Division of Pure Chemistry, National Research Council, Ottawa, Canada. Issued as N.R.C. No. 3554.

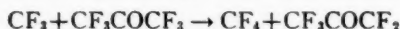
²National Research Council of Canada Postdoctorate Fellow, 1953–55.

³National Research Council of Canada Postdoctorate Fellow, 1952–54.

over 99% of the fluorine appears in the products as fluoroform. It therefore seems that above 80°C. the primary decomposition is a simple split into radicals



and that these radicals can abstract hydrogen or dimerize according to the composition of the reaction mixture. Above 300°C. some attack on the walls of the vessel takes place with the formation of silicon tetrafluoride and carbon dioxide, though the rate of this reaction can be considerably reduced by placing on the inside of the vessel a thin coating of calcium fluoride. No carbon tetrafluoride was found even at the highest temperatures used (about 350°C.) so it appears that the activation energy for reactions such as



is quite high.

A more detailed report on the photolysis of hexafluoroacetone will be presented elsewhere. The present paper describes experiments in which this compound was photolyzed in the presence of methane and ethane.

EXPERIMENTAL

Apparatus

The apparatus was essentially the same as that used in experiments on the photolysis of acetone described in earlier papers from this laboratory. The light source was a B.T.H. high pressure mercury lamp (type ME/D, 250 watts) operated on 220 v. d-c. This lamp gives a concentrated beam of light which was easily collimated by a single quartz lens and a stop. The quartz reaction vessel (10 cm. long, 5 cm. diam.) had a volume of about 190 ml. It was found desirable to use a beam of light of smaller diameter than the vessel in order to reduce attack on the walls by fluorinated radicals at high temperatures, so the illuminated volume was only 62 ml. A layer of calcium fluoride a few wavelengths in thickness was sputtered on to the inside of the vessel to further prevent access of the radicals to the quartz. (It should be stated that there is no proof that these precautions are necessary at the lower temperatures used in studying hydrogen-abstraction reactions such as those reported here. The vessel and optical system were designed for experiments at high temperatures at which this form of attack is troublesome.) The reaction cell was heated in an aluminum block furnace, the temperature of which could be controlled to within 1°C.

All the runs described in this paper were carried out using a combination of 5 cm. nickel sulphate (200 gm./l.), 1 cm. potassium chromate (0.2 gm./l.), 1 cm. potassium hydrogen phthalate (5 gm./l.), and a 3 mm. C.S. 7-54 (9863) filter to isolate the 3130 Å line.

Materials

Two samples of hexafluoroacetone were presented by the Minnesota Mining and Manufacturing Co., to whom we are greatly indebted. Further samples were prepared in collaboration with Dr. L. C. Leitch and Mr. A. T. Morse by the permanganate oxidation of perfluoroisobutene (3, 10). The final sample

after drying over P_2O_5 was distilled in a Podbielniak column and a small middle cut taken for use. This material had a b.p. of -27.8°C . at 754 mm. pressure, and when analyzed on the mass spectrometer showed a spectrum which could be completely identified with that expected from CF_3COCF_3 . It was stored in a blackened bulb at liquid air temperature because some decomposition was observed at room temperature. The methane and ethane were Phillips Research Grade and were found by mass spectrometric analysis to contain less than one per cent impurity (mainly higher hydrocarbons).

Procedure

Hexafluoroacetone was admitted to the heated reaction vessel and its pressure measured on a mercury manometer. When methane was to be added the hexafluoroacetone was condensed in a cold finger close to the cell at -180°C . while the methane was admitted. After allowing the hexafluoroacetone to warm up to cell temperature the total pressure was measured. From this the pressure of methane could be obtained. After the reactants were mixed for at least five minutes by means of a Toepler type pump the reaction vessel was isolated by closing a cutoff valve and the light switched on. When ethane was used the two reactants were condensed separately into the cold finger and then mixed as before. The photolyses were allowed to proceed until the amount of decomposition was about five per cent. No correction for pyrolysis was necessary in the experiments described.

Analytical Methods

The products were analyzed by means of two LeRoy stills in conjunction with a mercury diffusion pump and a combined Toepler and gas burette. The bulk of the hexafluoroacetone was condensed in the first still at -145°C . while the second still was maintained at -210°C . to retain all the products except CO (and CH_4 in reactions with this gas). Mixtures of CO and CH_4 were estimated mass spectrometrically. The second still was then raised to -155°C . to collect the C_2F_6 , CF_3H , C_2H_6 , and SiF_4 and CO_2 if present. Two methods were used to analyze this fraction; the mass spectrometer was used when an approximate estimate of all the components was needed, but in most of the experiments described here C_2F_6 and CF_3H accounted for at least 95% of this fraction and it was found more convenient and probably more accurate to use the infrared absorption of these compounds for the estimation. Both have very strong and sharp bands in the region 1300 cm^{-1} to 1100 cm^{-1} and there is very little overlapping. In the presence of a large excess of ethane correction must be made for the pressure broadening of the CF_3H band. When mass spectrometric and infrared analyses were made on the same mixtures the agreement was excellent. The hexafluoroacetone remaining was examined mass spectrometrically for the presence of other products such as CF_3CH_3 and $\text{CF}_3\text{CH}_2\text{CH}_3$, but quantitative analysis for such substances is very uncertain.

RESULTS

In Table I are presented the results of experiments in which hexafluoroacetone was photolyzed in the presence of methane or ethane, together with a

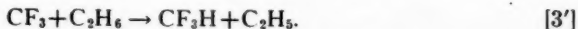
TABLE I

Temp., °K.	Press. CF ₃ COCF ₃ , mm.	Press. RH, mm.	Time, sec.	Products, moles/sec. × 10 ¹⁰			$\frac{R_{CF_3H}}{R_{C_2F_6}[RH]} \times 10^{11}$
				C ₂ F ₆	CF ₃ H	CO	$\frac{1}{R_{C_2F_6}[RH]}$ (molecules/cc.) ⁻¹ sec. ⁻¹
<i>Hexafluoroacetone alone</i>							
394	51.0	—	3600	24.7	—	25.4	—
406	49.0	—	1800	25.3	—	27.1	—
433	25.0	—	2700	18.4	—	19.5	—
494	24.7	—	2400	16.3	—	17.4	—
<i>RH = methane</i>							
395	25.1	92.5	5100	10.72	2.11		0.282
400	24.6	89.7	6600	11.8	2.62		0.348
407	24.7	84.0	3600	10.72	2.74		0.415
409.5	25.0	93.6	3300	12.52	3.12	17.8	0.394
416	23.4	46.6	4200	10.7	1.77	12.4	0.494
433	24.6	85.2	4200	10.9	5.08	15.2	0.801
441.5	25.0	72.8	4500	10.2	5.61		1.09
451	25.8	56.3	3600	10.85	5.00		1.25
451	24.8	94.5	6000	10.75	8.79		1.31
457.5	23.0	55.0	3000	9.74	5.08	13.8	1.385
469	24.9	43.0	3600	7.97	5.48	10.3	2.17
477.5	24.5	54.9	3000	8.42	9.11		2.79
485	25.4	55.9	3600	9.39	10.95	15.5	3.07
491.5	24.3	58.0	3600	7.20	12.4		4.01
503	25.2	48.5	4200	8.86	13.5	18.9	4.80
510	25.0	50.6	3300	8.39	16.0		5.67
524	24.7	42.5	2430	8.10	17.4		7.71
<i>RH = ethane</i>							
353.5	25.4	27.2	6000	0.88	2.16	2.78	2.61
362.5	25.7	26.5	6000	1.53	3.42	4.66	3.74
366	24.0	25.4	6000	2.02	4.06	5.01	3.68
385	25.5	24.7	5400	2.96	7.18	7.68	6.17
391	24.5	23.9	3600	1.88	6.67	5.98	8.18
403	25.2	56.6	3600	0.59	11.95	8.00	11.3
421.5	25.8	25.4	3900	2.66	14.35	9.78	14.9
428.5	24.1	25.8	3600	1.86	13.95		17.4
439	25.6	26.0	3000	1.32	15.8	9.20	23.7
443.5	24.5	24.1	2400	1.42	18.65	10.0	29.5
454	38.0	25.2	2400	1.99	22.4	13.0	29.3
471.5	39.5	24.0	2400	2.03	27.5	16.9	38.9
489	25.1	25.4	2400	0.59	24.7	12.2	63.3

few runs without hydrocarbon. The runs were carried out in several series with different light intensities to show that the value of the ratio $R_{CF_3H}/R_{C_2F_6}^{1/2}$ (CH_4) is not affected by changes in intensity. This method of grouping the results also had the effect of showing that there was none of the progressive change in rate constants due to surface effects that had been a feature of previous investigations (1).

Hexafluoroethane and fluoroform are major products at all temperatures and these clearly result from dimerization and hydrogen-abstraction reactions of trifluoromethyl radicals. The following reaction scheme will account for these products.





Since CF_3CH_3 and C_2H_6 were found in appreciable amounts in the products from experiments with methane as substrate it is reasonable to assume that the methyl radicals produced in reaction [3] disappear by reactions such as



and



The disappearance of the ethyl radicals produced in reaction [3'] can be accounted for by the analogous reactions



and



The amount of CF_3CH_3 and C_2H_6 increases markedly with temperature as would be expected from this mechanism. Further support for this reaction scheme can be provided by evaluating the functions

$$R_1 = [2(\text{C}_2\text{F}_6) + (\text{CF}_3\text{H}) + (\text{CF}_3\text{CH}_3)]/\text{CO} \text{ and } R_2 = [2(\text{C}_2\text{H}_6) + (\text{CF}_3\text{CH}_3)]/\text{CO}$$

which should both be equal to unity if all the radicals can be accounted for in this way. For three runs in which complete analyses were made the values were, for R_1 , 0.97, 0.95, 0.97 and for R_2 , 0.85, 0.90, 1.05. This is considered satisfactory in view of the difficulty of estimating small quantities of CF_3CH_3 in the presence of excess hexafluoroacetone.

If the reaction mechanism suggested is substantially correct, the rate of formation of C_2F_6 can be expressed by

$$R_{\text{C}_2\text{F}_6} = k_2[\text{CF}_3]^2$$

and the rate of formation of CF_3H by

$$R_{\text{CF}_3\text{H}} = k_3[\text{CF}_3][\text{CH}_4] \\ k_3'[\text{CF}_3][\text{C}_2\text{H}_6].$$

or

From these equations it follows that

$$k_3/k_2^{1/2} = R_{\text{CF}_3\text{H}}/R_{\text{C}_2\text{F}_6}^{1/2}[\text{CH}_4] = A_3/A_2^{1/2} \cdot e^{-(E_3 - \frac{1}{2}E_2)/RT}$$

$$\text{and } k_3'/k_2^{1/2} = R_{\text{CF}_3\text{H}}/R_{\text{C}_2\text{F}_6}^{1/2}[\text{C}_2\text{H}_6] = A_3'/A_2^{1/2} \cdot e^{-(E_3' - \frac{1}{2}E_2)/RT}.$$

Reference to Fig. 1 will show that the Arrhenius plots for both reactions are straight lines within the experimental error, in the temperature range used. The values obtained by the method of least squares for the differences in activation energy are

$$E_3 - \frac{1}{2}E_2 = 10.3 \text{ kcal./mole}$$

$$E_3' - \frac{1}{2}E_2 = 7.5 \text{ kcal./mole.}$$

Assuming an effective cell volume of 62 ml., the ratios of rate constants at 182°C. (455°K.) are

$$k_3/k_2^{1/2} = 1.52 \times 10^{-12} \text{ (molecule/cc.)}^{-1/2} \text{sec.}^{-1}$$

$$k_3'/k_2^{1/2} = 3.18 \times 10^{-11} \text{ (molecule/cc.)}^{-1/2} \text{sec.}^{-1}$$

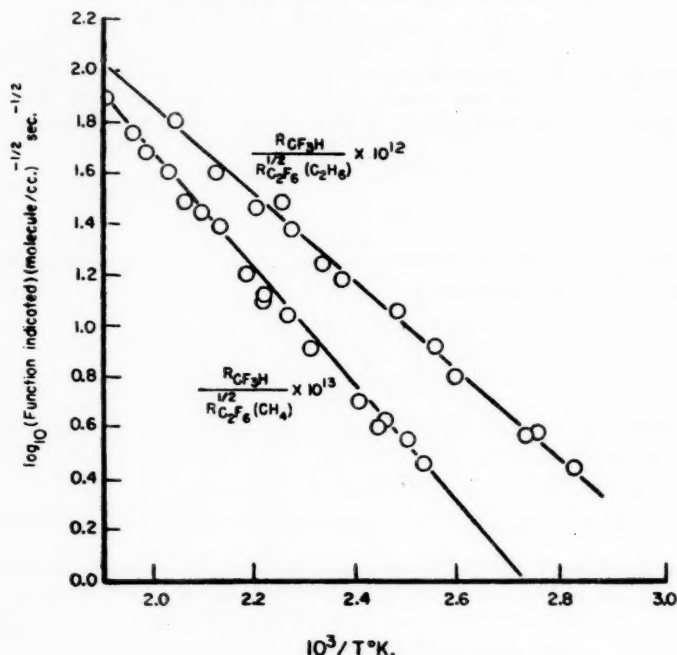


FIG. 1. Arrhenius plots for the photolysis of hexafluoroacetone.

and the ratio of steric factors

$$\begin{aligned} P_3/P_2^{\frac{1}{2}} &= 5 \times 10^{-3} \\ P_3'/P_2^{\frac{1}{2}} &= 3 \times 10^{-3} \end{aligned}$$

For these calculations the collision diameters assumed were as follows: CH_3 , 3.5 Å; CH_4 , 3.5 Å; C_2H_6 , 4.5 Å; CF_3 , 4.0 Å. The mean square deviation of the values of the activation energies is 0.22 kcal./mole in each case, but the systematic errors in the analyses are probably greater and the error is more likely to be about 0.5 kcal./mole.

DISCUSSION

It has been shown that hexafluoroacetone is a convenient source of trifluoromethyl radicals and that the technique used for studies of the reactions of methyl radicals may be applied in a very similar manner to these radicals. At the moment lack of sufficient quantitative data makes a close comparison between methyl and trifluoromethyl radicals rather speculative. In order to use the available data it is necessary to make certain assumptions about the steric factors and activation energies for the dimerization reactions of methyl and trifluoromethyl radicals. It is now reasonably certain that the steric factor for the recombination of methyl radicals is about unity and the activa-

tion energy zero or very nearly so (5, 7, 8), and there seems to be no reason to suppose that the steric factor is markedly different for the dimerization of trifluoromethyl radicals. This suggestion is supported by the fact that the steric factors obtained in this study are "normal" (compare the value 6×10^{-4} obtained by Trotman-Dickenson, Birchard, and Steacie (13) for the reaction $\text{CH}_3 + \text{C}_2\text{H}_6 \rightarrow \text{CH}_4 + \text{C}_2\text{H}_5$). However, it does not appear to be entirely justifiable to assume zero activation energy for the dimerization of trifluoromethyl radicals. Sieger and Calvert (12) have mentioned this possibility, basing their suggestion on configurational differences between methyl and trifluoromethyl radicals. It seems to us that even if there is no important difference in configuration the marked polarity of the carbon-fluorine bonds will result in dipole-dipole interaction at some stage of the reaction which may cause an energy barrier of significant proportions. However, it is extremely unlikely that it would be as high as 5-6 kcal. which would be necessary to bring the values of E_a and E_a' into line with the currently accepted values for the analogous reactions $\text{CH}_3 + \text{CH}_4 \rightarrow \text{CH}_4 + \text{CH}_3$ (13-14 kcal.) (14, 9), and $\text{CH}_3 + \text{C}_2\text{H}_6 \rightarrow \text{CH}_4 + \text{C}_2\text{H}_5$ (about 10.4 kcal.) (13). Thus there is little doubt that trifluoromethyl radicals do abstract hydrogen with greater facility than do methyl radicals, though it would not be wise to suggest that the observed differences in activation energies for abstraction by methyl and trifluoromethyl radicals have any great quantitative significance. On the basis of present information the difference appears to be about 3 kcal./mole, assuming for the moment zero activation energy for the reaction $2 \text{CF}_3 \rightarrow \text{C}_2\text{F}_6$. Sieger and Calvert give a value of 2.3 kcal./mole for this difference in the case of abstraction of hydrogen from trifluoroacetone (12). It is, however, clearly desirable to determine the rate constants of the dimerization reaction with sufficient accuracy to evaluate the activation energy and pre-exponential factors before discussing this question further.

ACKNOWLEDGMENT

We are indebted to Mr. R. Lauzon for assistance in the infrared analyses and to Miss F. Gauthier and Miss J. Fuller for the mass spectrometric analyses.

REFERENCES

1. AYSCOUGH, P. B. and EMELEUS, H. J. *J. Chem. Soc.* 3381. 1954.
2. BANUS, J., EMELEUS, H. J., and HASZELDINE, R. N. *J. Chem. Soc.* 3041. 1950.
3. BRICE, T. J., LAZERTE, J. D., HALS, L. J., and PEARLSON, W. H. *J. Am. Chem. Soc.* 75: 2698. 1953.
4. DACEY, J. R. *Discussions Faraday Soc.* 14: 84. 1953.
5. GOMER, R. and KISTIAKOWSKY, G. B. *J. Chem. Phys.* 19: 85. 1951.
6. HASZELDINE, R. N. *Discussions Faraday Soc.* 14: 134. 1953.
7. INGOLD, K. U. and LOSSING, F. P. *J. Chem. Phys.* 21: 368. 1953.
8. INGOLD, K. U. and LOSSING, F. P. *J. Chem. Phys.* 21: 1135. 1953.
9. MCNESBY, J. R. and GORDON, A. S. *J. Am. Chem. Soc.* 76: 4196. 1954.
10. MORSE, A. T., AYSCOUGH, P. B., and LEITCH, L. C. *Can. J. Chem.* 33: 453. 1955.
11. POLANYI, J. Unpublished work.
12. SIEGER, R. A. and CALVERT, J. G. *J. Am. Chem. Soc.* 76: 5197. 1954.
13. TROTMAN-DICKENSON, A. F., BIRCHARD, J. R., and STEACIE, E. W. R. *J. Chem. Phys.* 19: 163. 1951.
14. TROTMAN-DICKENSON, A. F. and STEACIE, E. W. R. *J. Chem. Phys.* 19: 329. 1951.

FREE RADICAL RECOMBINATION IN THE PHOTOLYSIS OF ACETONE¹

By S. N. NALDRETT²

ABSTRACT

(CH₃CO)₂-1-C¹⁴ (I) was prepared by irradiating (CH₃)₂CO in the presence of CH₃I-C¹⁴. Acetone was then irradiated at room temperature with light of 2537 Å in the presence of (I). Radioactivity was found in all products which contained methyl groups but not in any carbon monoxide product. The amount of carbon-14 ultimately found in acetone confirms that the quantum efficiency of the primary photolytic process is nearly unity and that extensive recombination of methyl and acetyl radicals to form acetone is responsible for the low over-all quantum efficiency of decomposition.

INTRODUCTION

The photolysis of acetone has been exhaustively investigated. (For reviews see Dorfman and Noyes (2) and Steacie (7).) One important feature of the mechanism is the explanation of the low quantum yield at low temperatures by the recombination reaction:



It seemed of value to make a direct check of this reaction by the use of radioactive carbon.

EXPERIMENTAL

The Photolysis System

Irradiations were carried out in a cylindrical quartz vessel 45 mm. in diameter and 108 mm. long with polished plane parallel windows. Illumination was supplied by a neon-mercury resonance lamp in a quartz envelope with a filter of chlorine gas so that the light was mostly 2537 Å. Three different lamps were used in the course of the experiments. All irradiations were carried out at room temperature.

Measurement of Radioactivity

All samples were counted in Geiger-Mueller tubes as gases, so that no counts were lost because of self-absorption or window absorption and only a geometry correction was necessary. The counting efficiency of each gas mixture was checked by the response given to an external radioactive standard. Usually no external quench was required, but if necessary a Neher-Harper type of electronic quenching circuit was used. Sufficient counts were observed so that the uncertainty in the count rate recorded was less than other errors such as measurement of sample size, loss by adsorption, or in stopcock grease, etc.

Preparation of Biacetyl-1-C¹⁴

Active (CH₃CO)₂ was prepared by irradiating a mixture of CH₃COCH₃ and CH₃I-C¹⁴ in the vapor phase. In the first attempt a mixture of 2.7×10^{-3}

¹Manuscript received October 22, 1964.

Contribution from Division of Chemistry, National Research Council, Ottawa, Canada, and Royal Military College, Kingston, Canada.

²Present address: Royal Military College, Kingston, Canada.

moles acetone and 8.6×10^{-8} moles of active methyl iodide with an activity of 1.9×10^7 disintegrations per minute was irradiated for 110 hr. with a current of 30 ma. through the lamp in the irradiation system described. Less than 0.5% of the activity was recovered as $(\text{CH}_3\text{CO})_2\text{-C}^{14}$ and since the amount was not sufficient, the preparation was repeated. For the second preparation a mixture of 5.6×10^{-8} moles of acetone and 2.3×10^{-8} moles of $\text{CH}_3\text{I-C}^{14}$ with an activity of 8.5×10^7 d.p.m. was irradiated for 690 hr. with a lamp current of 100 ma. The light absorbed in the cell was of the order of 10^{19} quanta/hour. A tubulation which had been added to the irradiation cell was kept at 0°C . and served to reduce the amount of biacetyl vapor in the light beam, so that reaction to carbon monoxide and ethane was reduced. The 3.8×10^{-4} moles of biacetyl recovered had an activity of 7.4×10^6 d.p.m. This amounts to 9.1% of the total methyl groups and 8.7% of the total activity in the reaction cell. Although neither of these figures is very reliable, the similarity between them seems to indicate that there has been a very high degree of exchange of methyl radicals amongst the molecules CH_3I , CH_3COCH_3 , and $(\text{CH}_3\text{CO})_2$.

Purification of Biacetyl-1-C¹⁴

Radioactive tracers and also mass spectrometer analysis showed that biacetyl and acetone were not separated by low pressure fractionation in a Ward type still to the extent expected from their relative vapor pressures. However, for the purpose of this project the presence of acetone in the biacetyl was not a disadvantage, provided that the acetone was not radioactive. To ensure this, bulk amounts of inactive biacetyl (about 0.75 gm.) and of inactive acetone (about 0.3 gm.) were added to the micro amount of active biacetyl product, and the acetone fraction was then separated in the Ward type still. Further additions of inactive acetone and fractionations were made until the process had been repeated seven times. No further changes in the specific radioactivities of either the biacetyl or acetone fractions were observed in the last three fractionations, indicating that the removal of radioactive acetone was complete. Mass spectrometer analysis showed that there was about 14% inactive acetone in the active biacetyl sample.

Analysis of the Products

After the irradiation the products were separated into fractions by means of a Ward-Savelli still (5). The temperatures of the four condensers were set at -183° ; -140° ; -78° ; -60° respectively, and the fractions as separated consisted largely of (1) CH_4 and CO ; (2) C_2H_6 ; (3) $(\text{CH}_3)_2\text{CO}$, and (4) $(\text{CH}_3\text{CO})_2$. The carbon monoxide was removed from the methane fraction by oxidation over hot copper oxide and absorption in Ascarite. No measurable amount of hydrogen was found in preliminary runs and attempts to estimate it separately from the carbon monoxide were discontinued. The volumes of the fractions were measured and the quantities are shown in Table I as moles $\times 10^6$. The analysis of the products of Photolyses Nos. 6 and 7 was made by means of a mass spectrometer.

TABLE I
 PHOTOLYSIS OF ACETONE AND BIACETYL-1-C¹⁴

Photo- lysis number	Irradiation conditions		Substance	Reactants		Products		Degree of ex- change in acetone	Quanta ab- sorbed
	Lamp	Quanta ×10 ⁻²⁰ esti- mated from CO		Moles ×10 ⁵	CH ₃ -C ¹⁴ ×10 ⁷	Moles ×10 ⁵	CH ₃ -C ¹⁴ ×10 ⁷		Mole- cules re- actant
1	B	2.8	(CH ₃ CO) ₂ (CH ₃) ₂ CO C ₂ H ₆ CO CH ₄ Total or av.	15.2 15.2	36.0 36.0	7.35 2.25 3.73 9.25 0.55 34.1	35.4 33.2 32.6 34.0 		
2	B	1.9	(CH ₃ CO) ₂ (CH ₃) ₂ CO C ₂ H ₆ CO CH ₄ Total or av.	 167.2 167.2	 	14.5 130.2 17.5 6.35 0.69 	 		
3	A	0.95	(CH ₃ CO) ₂ (CH ₃) ₂ CO C ₂ H ₆ CO CH ₄ Total or av.	10.3 22.0 32.3	2.95 0.94	9.06 15.90 5.00 3.08 1.12 1.03	1.53 0.61 1.37 1.90 	0.59	0.5
4	C	3.4	(CH ₃ CO) ₂ (CH ₃) ₂ CO C ₂ H ₆ CO CH ₄ Total or av.	26.8 119.9 146.7	35.9 6.57	19.6 116.0 13.8 11.1 4.15 2.19	7.80 1.30 1.49 2.84 	0.59	0.37
5	C	4.7	(CH ₃ CO) ₂ (CH ₃) ₂ CO C ₂ H ₆ CO CH ₄ Total or av.	25.3 206.6 231.9	36.0 3.92	30.4 156.2 27.4 15.6 1.28 3.11	12.0 1.39 3.83 2.9 	0.45	0.34
6	C	3.8	(CH ₃ CO) ₂ (CH ₃) ₂ CO C ₂ H ₆ CO CH ₄ Total or av.	15.2 158.7 173.9	36.0 3.15	26.6 104.4 20.6 12.6 1.36 1.75	4.38 0.86 2.59 3.3 	0.49	0.37
7	C	3.0	(CH ₃ CO) ₂ (CH ₃) ₂ CO C ₂ H ₆ CO CH ₄ Total or av.	16.7 313.2 329.9	36.0 1.82	28.3 281.9 26.8 19.7 2.74 1.09	7.71 0.44 1.01 2.61 	0.40	0.30
8	A	0.8	(CH ₃ CO) ₂ (CH ₃) ₂ CO C ₂ H ₆ CO CH ₄ Total or av.	9.25 263.3 272.6	36.2 1.23	16.4 241.6 7.85 2.58 1.61 0.84	10.9 0.17 0.54 1.24 	0.20	0.049

The radioactivity of each of the fractions was measured directly in Experiments 1, 3, and 5. In the other experiments each fraction was further treated after the volume was measured, by addition of carriers and hold-back carriers and refractionated until radiochemical purity was attained. For example, after the volume of the acetone product had been measured, there was added to it convenient amounts of ethane, acetone, and biacetyl, and the acetone fraction was again recovered by fractionation in the Ward-Savelli still. The process was repeated, usually three times, until it was assured that the radioactivity was definitely associated with the substance being determined and not with a contaminant. Some of the product was sacrificed to the more volatile and to the less volatile carriers at each fractionation, and in the end the total radioactivity recovered in all of the products was only about one half the total activity of the reactants.

OBSERVATIONS AND DISCUSSIONS

The results of some typical experiments are listed in Table I. Experiment No. 2 shows results which are typical of the behavior of pure acetone when irradiated in this system; the results are quite similar to what has been reported by others. Experiment No. 1 shows typical behavior of pure biacetyl; these observations also are similar to what has been reported by others (1). The remainder of the table indicates what was observed when mixtures of radioactive biacetyl and inactive acetone were irradiated. The products obtained in these experiments are not far different from the composite which would result from the separate irradiation of the biacetyl and the acetone. The addition of biacetyl therefore does not seem to have any particular effect on the decomposition of acetone and the conclusions can probably be applied to the photolysis of pure acetone.

The most significant feature of the observations is that after irradiation, radioactivity is present in every substance which contains methyl radicals, but no radioactivity was found in the carbon monoxide fraction in any experiment. This confirms the fact that free radicals play a major role in the photolysis reactions and that recombination of free radicals to acetone occurs.

The next to the last column in the table shows an estimate of the degree of exchange of radicals amongst acetone and the other substances. This figure is simply the ratio of the specific activity of the methyl groups in acetone to the average specific activity of all methyl groups recovered. However, for some experiments only about half of the original radioactivity was recovered, and in using this figure as a measure of the extent of exchange, it is assumed that the fraction of active acetone lost between the first measurement of volume and the counting after purification is the same as the average loss of the other active compounds. Of course this assumption may be in error; the only justification for it is that it gives results which are consistent with those obtained in experiments in which nearly all of the radioactivity was recovered, and in which this assumption does not enter. It would appear that exchange was from one fifth to three fifths completed by the irradiation given in these experiments.

The results indicate that the exchange increased with irradiation, although a precise measurement of the number of quanta absorbed was not made. The dimensions and the intensity of the light beam in these experiments were not carefully controlled since the irradiations extended over several days and had to be left unattended. However, an estimate of limited value can be made from the yield of carbon monoxide. The quantum efficiency for the production of carbon monoxide in the photolysis of acetone at room temperature by light of 2537 Å was determined by Herr and Noyes (3) to be 0.22 for somewhat similar light intensities and pressures of acetone. The validity of this figure for the conditions of the experiments described here was established by determining the amount of hydrolysis of a solution of monochloroacetic acid (6) under the same experimental conditions before and after Photolysis No. 6. The light absorbed by the cell from Lamp C during Photolysis No. 6 was thereby determined to be 2.8×10^{18} quanta per hour, and the quantum efficiency of carbon monoxide production from these data is 0.20. This figure was used to calculate the total quanta absorbed, and the quanta per molecule for each photolysis as shown in the table. The differences in the absorption coefficients of biacetyl and acetone for the radiation involved is certainly less than 10% (4) and therefore equal absorption has been assumed in making the calculations.

On the simplest assumption that one quantum per molecule will produce free radicals and permit exchange, it would be expected that the figure for degree of exchange would be similar to the figure for quanta absorbed per molecule. These figures are reasonably similar except for Photolysis No. 8, and for this experiment the estimate of quanta absorbed from carbon monoxide production seems too low by comparison with Photolysis No. 3 in which the same lamp was used for a shorter irradiation. These observations are confirmatory evidence that the quantum efficiency is close to unity for the primary process: $\text{CH}_3\text{COCH}_3 + h\nu = \text{CH}_3 + \text{CH}_3\text{CO}$ and that the recombination of radicals to reform acetone accounts for the low over-all quantum efficiency of decomposition of acetone.

The behavior of C^{12}H_3 and $\text{C}^{12}\text{H}_3\text{CO}$ will, of course, not be quite the same as that of the C^{14} compounds. The isotope effect will, however, be negligible as far as our present purpose is concerned.

ACKNOWLEDGMENT

The author is grateful to Dr. F. P. Lossing for the mass-spectrometer analyses, and to Dr. E. W. R. Steacie for generous assistance with the photochemical technique, and many helpful discussions.

REFERENCES

1. ANDERSON, H. W. and ROLLEFSON, G. K. *J. Am. Chem. Soc.* 63: 816. 1941.
2. DORFMAN, L. M. and NOYES, W. A., JR. *J. Chem. Phys.* 16: 557. 1948.
3. HERR, D. S. and NOYES, W. A., JR. *J. Am. Chem. Soc.* 62: 2052. 1940.
4. LARDY, G. C. *Compt. rend.* 176: 1548. 1923.
5. SAVELLI, J. J., SEYFRIED, W. D., and FILBERT, B. M. *Ind. Eng. Chem. Anal. Ed.* 13: 868. 1941.
6. SMITH, R. N., LEIGHTON, P. A., and LEIGHTON, W. G. *J. Am. Chem. Soc.* 61: 2299. 1939.
7. STEACIE, E. W. R. *Atomic and free radical reactions.* 2nd ed. Reinhold Publishing Corporation, New York. 1954.

THE DETERMINATION OF MOLECULAR WEIGHT¹

BY A. F. SIRIANNI AND I. E. PUDDINGTON

ABSTRACT

The molecular weights of organic compounds of known constitution have been determined with satisfactory accuracy, using milligram quantities of materials, by a static measurement of the vapor pressure difference between pure solvents and solutions of the compounds. The method may be used over a considerable temperature range. The suitability of solvents is governed by their chemical stability and vapor pressure. Results obtained using compounds in the molecular weight range of 600-1000 are reported.

INTRODUCTION

A previous publication (4) indicated some success in using static measurements of the difference in vapor pressure between pure solvents and solutions to estimate the molecular weights of non-ionizing solutes. The procedure utilized a mercury micromanometer that was relatively insensitive to the vibration normally encountered in laboratories. In the previous work compounds having molecular weights below about 350 were used and the measurements were all made at 20°C., using solvents to which a hydrocarbon base stopcock lubricant was substantially inert.

Since the method appeared to be applicable to the measurement of the molecular weights of polymers with relatively low degrees of polymerization, it seemed desirable to extend the temperature range of the instrument and to increase the number of usable solvents, by eliminating the possible contamination from stopcock grease. As this has involved considerable modification in the construction and operation of the apparatus, the present communication is intended to record some of the more essential refinements that have been suggested as the result of several years of use and to indicate results that have been obtained. Compounds of molecular weight up to about 1000 that had known constitutions, with a variety of solvents, concentrations, and temperatures, have now been used successfully.

APPARATUS AND EXPERIMENTAL

The apparatus that was eventually adopted is shown in Fig. 1. Part A was built in such a way that it could be enclosed by a thermostat constructed of "aluminum foil backed masonite" and "ten test", equipped with heaters, fans, and thermoregulators to give temperatures that varied not more than $\pm 1^\circ\text{C}.$ in various locations within the box and $\pm 0.1^\circ\text{C}.$ in any one location, over the range 30° to 100°.

Continuous resistance heaters controlled by variacs were located on the side walls of the thermostat and a low power intermittent heater controlled by the thermoregulator was located in the slip stream of a 10 in. fan. The manometer and burette were enclosed in a secondary ten-test box, open at

¹Manuscript received January 6, 1955.

Contribution from the Division of Applied Chemistry, National Research Council, Ottawa, Canada. N.R.C. No. 3555.

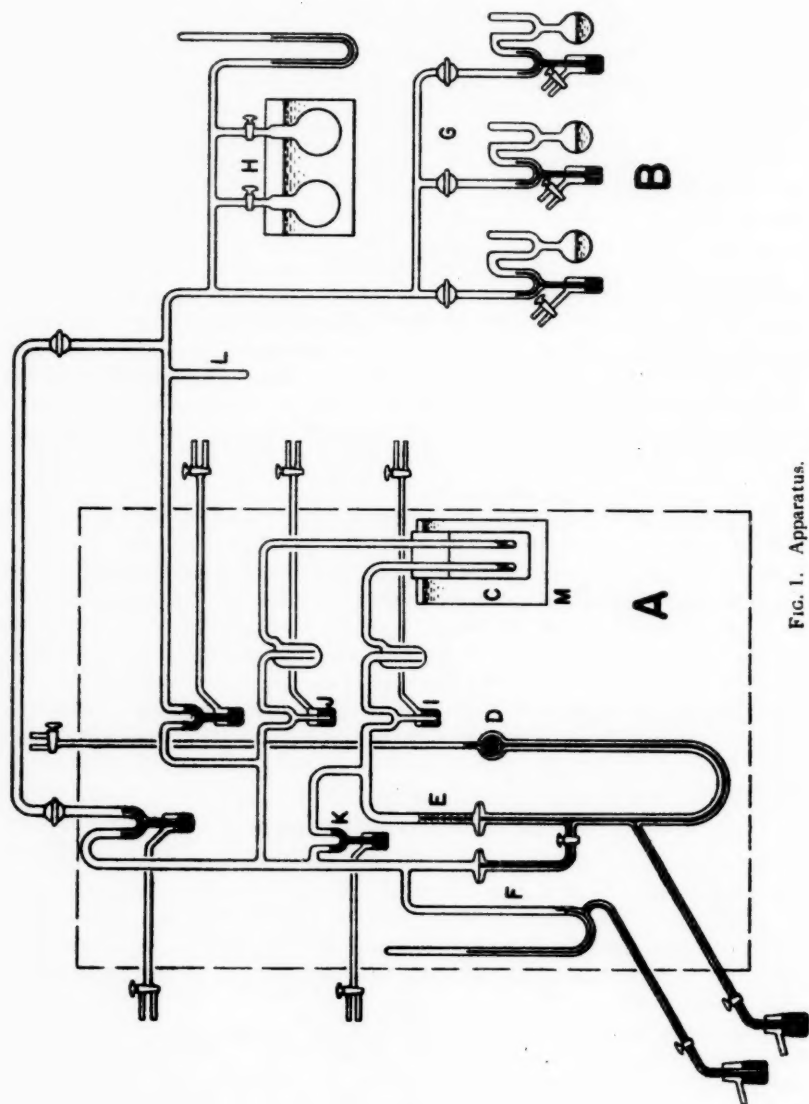


FIG. 1. Apparatus.

the top and containing an 8 in. fan blowing outward, located in one side near the bottom, to give a continuous downward flow of air through the box. The temperature within this box did not vary by more than 0.2°C . Thermostat "C" contained the solution and solvent holders enclosed in a copper block, the details of which are shown in Fig. 2. This thermostat consisted of a

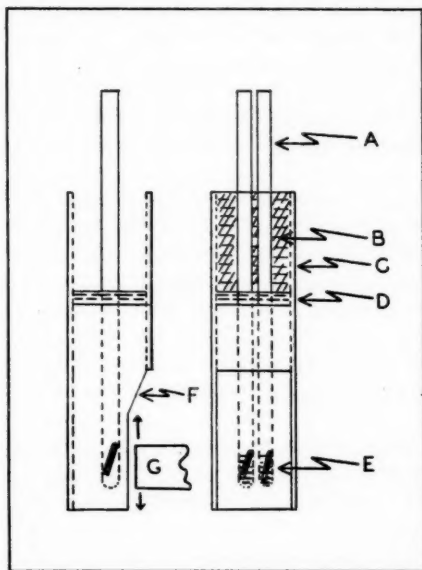


FIG. 2. Enlarged view of copper block. A, sample holders; B, glass wool insulation; C, cellulose acetate sleeve; D, mercury film; E, stirrers; F, recessed portion of copper block; G, magnet.

2 liter, wide mouth, dewar flask. It was maintained at $10\text{--}30^{\circ}$ below the air thermostat to prevent solvent condensation in the connecting tubing. The temperature of the oil contained in the thermostat was controlled to $\pm 0.0005^{\circ}\text{C}$. Good thermal contact was maintained between the sample holders and the copper block with a film of mercury and the copper block itself was partially insulated from the bath with a piece of cellulose acetate tubing and a heavy coat of shellac. Both solution and solvent were stirred with glass sheathed bars of iron, actuated by an alnico magnet that oscillated in a vertical direction with a frequency of about 20–25 cycles per minute.

As suggested in the earlier paper, etching of the inside of the two bulbs forming the arms of the U tube was found desirable to give reproducible contact angles at the mercury–glass–vapor interface. This is important since the operation of the manometer assumes that the volume of mercury transferred between the arms of the U tube is proportional to the pressure change. Experiments have indicated that the contact angle is quite sensitive to temperature changes, changes in the type of vapor contained in the bulb, and probably to large differences in the pressure of any one vapor. No pair of

bulbs yet used seems to behave in an identical fashion and while the zero point of the instrument has remained constant to ± 0.001 mm. for periods up to 10 days, if conditions are kept reasonably constant, it may change substantially if, for example, alcohol vapor is substituted for benzene or the vapor pressure of the solvent is raised by several centimeters with mercury cutoff *K* open. These effects obviously become more important as the magnification factor of the instrument is increased. The behavior of the manometer was invariably good if the contact angle was sufficiently diffuse that no sharp line of contact was visible at the mercury-glass interface. It could frequently be improved by contaminating the mercury surface with about 10^{-7} to 10^{-9} gm. of lithium stearate added in distilled methanol. Contact angles rarely gave any trouble, however, at temperatures above about 30°C.

The most convenient method found for etching the bulbs to the desired degree consists in placing a few grams of 200-325 mesh carborundum in the bulbs along with a few cubic centimeters of water and sections of flattened lead shot. The bulbs are then rotated for 16-24 hr. at a speed just below that required to carry the pieces of lead around with the rotating bulb. This must be followed by a thorough cleaning and steaming before the bulbs are fixed into the rest of the apparatus. Final traces of grinding residues were sometimes removed by reducing the pressure suddenly when the glass surface was wet with methanol.

All of the stopcocks within the thermostat in contact with the solvent vapor were replaced with short arm mercury cutoffs equipped with glass check valves. The cutoffs could be controlled by two way stopcocks located outside the thermostat. The stopcock separating the two arms of the U tube was lubricated with a film of dried aquadag* plus a very thin film of heavy lithium stearate grease. This tap was operated by a felt lined stirrup attached to an iron rod extending through the top of the thermostat. It did not have to be relubricated more frequently than once in two years. It was exposed to temperatures up to 90°C. A mercury sealed 4 mm. pyrex stopcock similar to Corning 7500 was found quite satisfactory for this valve. The large bulbs and the stopcock were set in plaster of Paris to ensure rigidity.

In order to increase the range of the manometer, a series of small bulbs about equal to the measuring capillary in volume were located in the short piece of capillary (*E*) above the right hand arm of the U tube. These bulbs were marked volumetrically with etches. If, during a measurement, the tail end of the mercury thread was off scale when the advancing end reached the first etch, it was merely pushed on to the etch that allowed a reading to be made on the measuring capillary. In the present case three bulbs were used to give a total range of about two millimeters pressure difference, with a magnification of approximately 2000. The diameters of the bulbs that formed the arms of the U tubes were about 5 cm.

A change in manometer design was examined wherein the essential difference was the reversal of the positions of the measuring capillary and bulb *D*.

*A dispersion of graphite in water prepared by the Acheson Colloids Corp., Port Huron, Michigan, U.S.A.

The expansions in capillary *E* were then placed below the bulb forming the right hand arm of the U tube. In this model the volume of mercury in the right hand arm was measured by withdrawing it into the empty bulb *D* and again noting the location of the mercury thread in the measuring capillary when the tail end of the mercury was at a convenient etch. While this design offered the advantages at high magnifications of using much less mercury and of a considerable saving of time, during readings, owing to the fact that only a small thread of mercury rather than a large volume had to pass through the measuring capillary, the older model was quite satisfactory for most work.

In making a molecular weight determination, the solute in amounts varying from 0.1 to about 2 mgm. was weighed into a 3 to 4 mm. i.d. pyrex tube. After placing the stirrer within the tube, it was sealed to the apparatus and the pressure reduced to about 10^{-6} mm. Pure solvents, previously deaired by refluxing *in vacuo* until a sample of the vapor could be condensed into a 1 mm. capillary to give a thread of liquid containing no bubbles, were stored in the bulbs *B* outside of the air thermostat.

A cold finger containing dry ice made a satisfactory reflux condenser for the deairing procedure. Although slightly different methods were used with the various solvents, the Reagent Grade compounds were usually passed through a chromatographic column packed with silica gel and alumina, and dried with calcium hydride (1, 2) wherever practicable, prior to degassing. The amount of solvent to be used was measured in the vapor state in the calibrated volumes *H* contained in a thermostat. After the solvent vapor in the connecting tubing was condensed into the reservoir, the vapor in one of the bulbs "*H*" was quantitatively condensed on the solute sample. The requirement on the solvent side could then be supplied from the other bulb, and the solvent and solution connected to their respective sides of the manometer. If the determination was the first after the interior of the apparatus had been exposed to the air, it was flushed with solvent vapor, to displace residual air or water vapor adsorbed on the glass walls, and re-evacuated.

In the early operation of the apparatus it was learned that the manometer provided a sensitive means of testing the purity of the solvent. If pure solvent was condensed in about the same volume in both the solvent and solution holders, no vapor pressure difference should be detectable after successive portions were removed from one of the containers. Solvents of this purity are not infrequently difficult to obtain, however, and in order to reduce any fractionation of solvent that might occur to a minimum during a determination, two closely similar volumes were used at *H*. The dead space on either side of the U tube was made the same, the final adjustment being made by selection of the position in *F* to which the mercury was adjusted to read the vapor pressure of the pure solvent. Small compensating adjustments in volume required by the use of different size sample holders could be made by changing slightly the position of the mercury level in the necks of cutoffs *I* and *J* before a vapor pressure difference was measured. Since the apparatus was contained in a thermostat, thermal expansion of the mercury was not a problem. The zero point of the manometer needed to be checked only in-

frequently, usually after a series of readings for one concentration. The null point not infrequently varied from run to run but this appeared to be due to the distillation of mercury within the system when no solvent vapor was present. There was no indication of a zero point change during a run.

As observed by Frazer and his associates (3) the attainment of vapor pressure equilibrium required only about 30 min. provided the solvent was air free; a trace of air increased this time considerably, however. When high vapor pressures were used, it was necessary to know the dead space on the solution side of the manometer accurately since the concentration of the solution was determined by making the appropriate dead space correction on the amount of solvent measured in H .

By condensing the solvent in side arm L after a determination was completed, the solvent could be used over again to prepare a slightly more concentrated solution for a second determination. It was thus possible to measure the vapor pressure difference on a rather wide range of solution concentration on a single solute sample and with a minimum expenditure of pure solvent. A usual solution contained between 15 and 90 mgm. of solvent.

Consecutive readings of vapor pressure lowering on the same sample normally did not vary by more than one per cent.

RESULTS

The results of the determination of molecular weight of sucrose octaacetate (mol. wt. = 678), raffinose hendecaacetate* (mol. wt. = 967), and three samples of bitumen† in various solvents and at a number of temperatures are shown in the accompanying graphs. Variations from the mean are normally

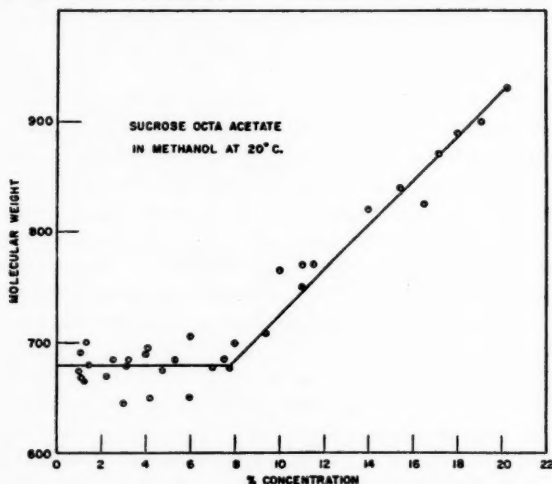


FIG. 3. Variation in molecular weight of sucrose octaacetate with concentration in methanol at 20°C.

*Kindly supplied by Dr. R. P. A. Sims.

†Kindly supplied by Dr. D. S. Montgomery.

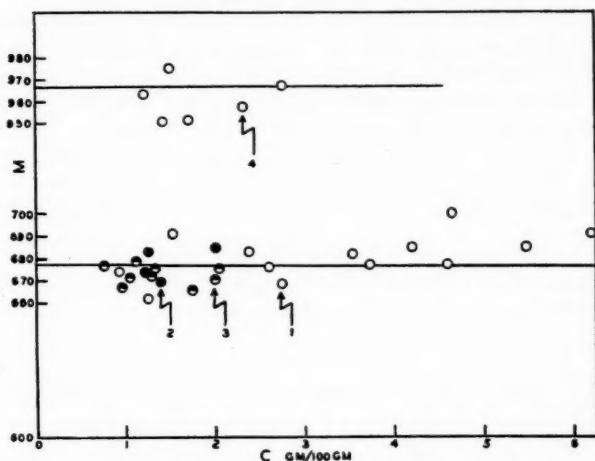


FIG. 4. Molecular weight of sucrose octaacetate and raffinose hendecaacetate in benzene at various temperatures: (1) sucrose octaacetate at 30°C., (2) sucrose octaacetate at 55°C., (3) sucrose octaacetate at 55°C., (4) raffinose hendecaacetate at 55°C. Solid lines in each case represent theoretical molecular weight.

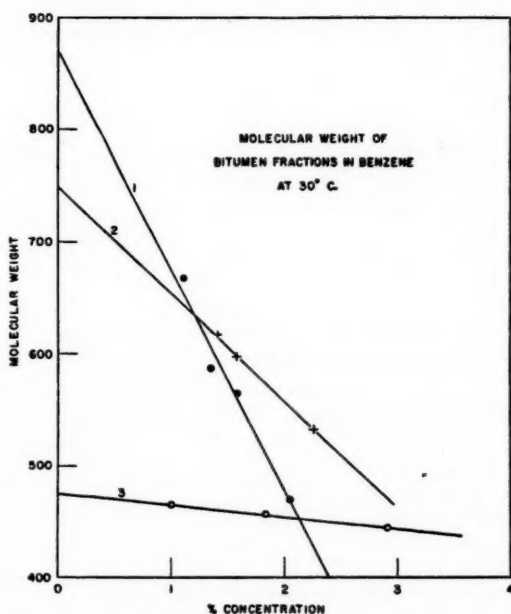


FIG. 5. Molecular weight vs. concentration for three samples of bitumen in benzene at 30°C.

not more than two per cent. With the crystalline materials dependence of molecular weight on concentration over the range examined was noted only with sucrose octaacetate in methanol at 20°C. and in concentrations in excess of 8% by weight. This is probably due to association of the solute. The bitumen samples on the other hand behaved like polymers. The weight of solute used in all cases was between 0.3 and 1.1 mgm. The method has been used successfully to determine the molecular weights of polymers up to about 20,000. The results of this work will be presented in a future publication.

ACKNOWLEDGMENT

It is a pleasure to acknowledge the substantial contributions made by G. Stainsby and R. A. Campbell to this work.

REFERENCES

1. BROWN, A. S., LEVIN, P. M., and ABRAHAMSON, E. W. *J. Chem. Phys.* 19: 1226. 1951.
2. DAVIS, R. T. and SCHIESSLER, R. *J. Phys. Chem.* 57: 966. 1953.
3. FRAZER, J. W. C. and LOVELACE, B. F. *J. Am. Chem. Soc.* 36: 2439. 1914.
4. PUDDINGTON, I. E. *Can. J. Research, B*, 27: 151. 1949.

PARTICLE MOTIONS IN SHEARED SUSPENSIONS

III. FURTHER OBSERVATIONS ON COLLISIONS OF SPHERES¹

By R. ST. J. MANLEY² AND S. G. MASON

ABSTRACT

Two-body interactions between glass spheres of diameters a_1 and a_2 caused by velocity gradients vary with a_1/a_2 . When $1 < a_1/a_2 < 2$, well-defined collisions similar to those previously reported for spheres of equal size can be observed. Fair agreement is found between the experimentally observed and calculated collision frequencies over a range of particle concentrations and velocity gradients. When $a_1/a_2 > 2$ the particles are separated at all times and the phenomena of interaction are more complex. Single air bubbles rotate at the same angular velocity as rigid spheres. When two air bubbles of equal size are brought into collision a doublet is formed; instead of the mirror-image separation observed with neutral rigid spheres, the doublet continues to rotate for as many as 60 rotations before coalescence occurs. Less frequently a doublet with distinct particle separation is observed. Periods of rotation of both types of doublet and certain details of the rotational orbit of a doublet of touching air bubbles have been measured and compared with values predicted from Jeffery's theoretical equations for rigid ellipsoids. Apart from their intrinsic interest, the phenomena described are of importance in theories of viscosity and coagulation of suspensions and colloidal dispersions.

INTRODUCTION

In an earlier paper (5), the two-body collisions of rigid neutral spheres of equal size suspended in a liquid subjected to a velocity gradient were described in some detail. It was shown experimentally that in a simple field of fluid shear described by

$$\begin{aligned} [1] \quad u &= Gy, \\ v, w &= 0 \end{aligned}$$

where u , v , and w are the respective velocities along the X -, Y -, and Z -axes and G is the rate of shear, two spheres can approach one another along an undisturbed rectilinear path parallel to the X -axis until they come into apparent collision at the rate

$$\begin{aligned} [2] \quad f &= 4a^2nG/3 \\ [3] \quad &= 8cG/\pi. \end{aligned}$$

Here, f denotes the number of collisions per particle per unit time, a the particle diameter, n the number of particles per unit volume of suspension, and c the volume of particles in the suspension.

The doublet formed by two colliding spheres rotates about the Z -axis at a constant angular velocity

$$[4] \quad \omega = G/2$$

until it reaches the mirror image through the Y - Z plane of the initial position of contact; the two particles then separate.

¹Manuscript received January 17, 1955.

Contribution from Pulp and Paper Research Institute of Canada and the Department of Chemistry, McGill University, Montreal, Que.

²Holder of a Fellowship from the National Research Council of Canada.

The measured values of the mean and maximum doublet lives and the distribution function of doublet lives were shown to be in good agreement with values calculated from the experimentally established mechanism of doublet behavior. Most of the experimental evidence suggested that the contact between the spheres of the doublet is real, resulting from a force which is generated by distortion of the local field of fluid motion and which operates to push the particles together. In one set of experiments, however, in which the motion was interrupted by a period of quiescence, the behavior of the doublets suggested that the particles do not come into true contact (5).

Equations [2] and [3] are readily derived (5, 8) by calculating the number of particle centers which are carried in unit time along rectilinear paths parallel to the X -axis, at the translational velocities given by equation [1], into a "collision sphere" of radius a drawn about the center of a reference sphere. For simplicity the reference sphere is placed at the origin of the coordinate system. If two spheres of different diameters a_1 and a_2 approach one another in a similar manner until they collide, the binary collision frequency is obtained by substituting $(a_1 + a_2)/2$ for a in equation [2], i.e.

$$[5] \quad f_{12} = (a_1 + a_2)^3 n_2 G / 6$$

where f_{12} is the number of collisions per unit time suffered by a type-1 sphere with type-2 spheres, and n_2 is the number concentration of the latter. If c_2 is the volume fraction of type-2 spheres in the suspension, $\pi a_2^3 n_2 / 6 = c_2$, whence by substitution in equation [5]

$$[6] \quad f_{12} = \frac{(a_1 + a_2)^3}{\pi a_2^3} c_2 G.$$

The present paper deals with an experimental study of interactions in binary suspensions of rigid spheres of different diameter ratios and in suspensions of air bubbles of approximately equal size. These experiments were carried out to extend the earlier observations (5), to test equation [6], and to attempt to resolve the question of whether or not the two spheres of a doublet come into true physical contact. Although the question of contact remains incompletely answered, a number of interesting and, it is believed, significant observations were made which have application to theories of viscosity and coagulation of suspensions and colloidal dispersions.

EXPERIMENTAL PART

The experiments were conducted in the concentric cylinder apparatus previously described (9). Single particles and doublets were observed at the origin of a field of motion as defined by equation [1], through a microscope directed along the Y -axis of the coordinate system so that the particles were viewed as their projections on the X - Z plane (Fig. 1). The velocity gradient G could be calculated with a precision of 0.1% from the measured speeds of rotation and could be varied continuously from 0 to 2.5 sec⁻¹.

Binary suspensions of rigid spheres were prepared by suspending glass spheres ranging from 5 μ to 180 μ in diameter in corn sirup having a viscosity of about 50 poises and a density of 1.3 gm./cc. The experimental methods for

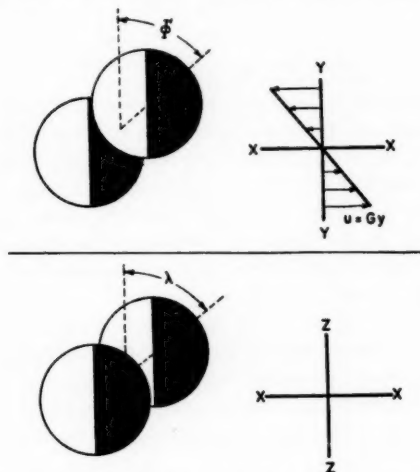


FIG. 1. Coordinate system for describing velocity gradients and motions of spherical doublets. Experimental observations are made along Y -axis so that particles are viewed as projections on the X - Z plane. ϕ' is the azimuthal angle referred to Z as the polar axis, and λ the azimuthal angle referred to Y as polar axis. The angular velocity $\omega = -d\phi'/dt$.

uniform dispersion and deaeration previously employed with monodisperse systems were used (5). For measurements of the collision frequency f_{12} , a supply of two sizes of glass spheres having a narrow size distribution was prepared by screen fractionation of bulk samples. The size spectra are given in Table I. Suspensions of volume concentration c_2 from 0.4 to 1.6% were prepared; each of these suspensions contained about 0.02 volume per cent of type-1 spheres which were used as reference particles.

TABLE I
SIZE DISTRIBUTION OF SPHERES

Diameter a_1 , μ	% of diameter < a_1	Diameter a_2 , μ	% of diameter < a_2
160	0.91	107	2.5
165	17.3	112	28.6
175	49.0	117	74.0
185	91.0	122	95.0
190	100.0	127	100.0
Number average diameter = 179 μ Standard deviation = 9.0 μ		Number average diameter = 117 μ Standard deviation = 4.4 μ	

Attempts to produce suitable uniform dispersions of fluid drops were only partly successful. However, dilute "foams" of air bubbles of unknown and variable concentration were prepared by vigorous mechanical stirring of viscous liquids such as corn sirup and glycerine. After agitation, the systems were allowed to stand so that larger bubbles rose to the surface leaving behind bubbles of fairly uniform diameter of about 150 μ .

RESULTS

1. Glass Spheres

General

The type of interaction between two spheres of diameters a_1 and a_2 (where $a_1 > a_2$) was found to depend upon the ratio a_1/a_2 . In systems in which $a_1/a_2 < 2$ approx., collisions were easily recognizable and, indeed, were similar to those of equal-sized spheres (5). The doublet formed by the two colliding particles appeared to rotate as a rigid dumbbell until a position was reached which was a mirror image about the Y - Z plane of the point of initial contact; separation then occurred and each sphere was restored to the same y -coordinate existing before the onset of collision.

When $a_1/a_2 > 2$, the interactions were much more complex and the particles could be seen to be separated at all times. One striking type which was repeatedly observed was as follows: upon approaching a large sphere, a small sphere began to describe the type of planetary motion around the large one as illustrated in Fig. 2, moving in a gradually widening spiral path past the

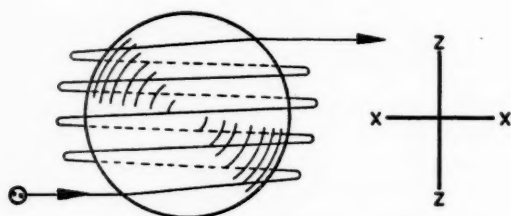


FIG. 2. Planetary motion of a sphere moving in an upward spiral path around a larger reference sphere (schematic).

equatorial plane until it attained a latitude roughly equivalent to that at which it started. It then separated from the large sphere at a velocity which appeared to be equal to that with which it approached. Upon reversal of the field of fluid motion (by reversing the directions of rotation of the two concentric cylinders), it was found that the smaller sphere continued to move upwards. In a number of instances, a "zig-zag" motion of the small sphere upwards in a roughly constant X - Z plane was also observed.

Collision Frequency

These measurements were made using spheres having the dimensions given in Table I. The collision frequency f_{12} was determined over a range of values of c_2 and G in the same manner as for monodisperse spheres (5). The results together with the values calculated from equation [6] are summarized in Table II. For a total of 857 observed collisions the ratio $f_{\text{obs}}/f_{\text{calc}} = 1.08$; since the standard deviation of this ratio is estimated to be 16% from the spreads in particle diameters given in Table I and 3% from the random sampling error of 900 collisions, the agreement may be considered satisfactory.

TABLE II
 COMPARISON OF OBSERVED AND CALCULATED COLLISION FREQUENCIES

Volume fraction, $c_2 \times 10^3$	G , sec. ⁻¹	N^*	f_{12} , Obs./Calc.
4.1	0.580	53	1.28
8.1	0.580	64	1.21
12.1	0.580	60	0.97
16.2	0.580	57	0.81
8.1	0.826	35	0.88
12.1	0.826	57	1.07
16.2	0.826	71	1.20
4.1	0.826	46	1.05
16.2	0.826	81	0.99
8.1	1.260	65	1.05
12.1	1.260	63	0.95
16.2	1.260	64	1.20
8.1	0.973	75	1.30
8.1	1.349	66	1.22
		Total 857	Mean 1.08

*Number of collisions counted.

2. Air Bubbles

General

Single air bubbles were not visibly deformed up to the highest velocity gradients attempted (2.5 sec.⁻¹) and were found to spin about the Z -axis in the same manner as rigid spheres (9). Two bubbles, upon approaching one another, formed a doublet which rotated about the Z -axis; however, instead of rotating through the angle 2ϕ , where $\phi (< \pi/2)$ is the azimuthal angle corresponding to the point of initial contact (Fig. 1), and then separating at the mirror image of the initial position of contact ($-\phi$) as was observed with equal-sized glass spheres (5), the doublet continued to rotate for as many as 60 complete rotations over a period as long as one-half hour, *until the pair suddenly coalesced into a single bubble*. During the interval between initial contact and coalescence, the doublet rotated about the Z -axis in a manner qualitatively similar to that of a rigid cylindrical particle, i.e. somewhat like

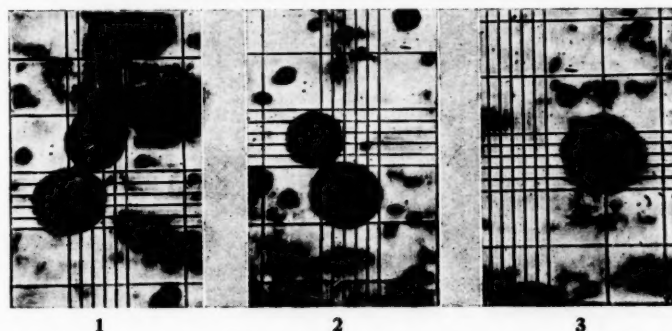


FIG. 3. Photomicrographs of a doublet of air bubbles (of different diameters) at $\lambda > 0$ (No. 1), $\lambda < 0$ (No. 2), and after coalescence to a single sphere (No. 3).

a precessing gyroscope (9). A doublet in two positions before and one position after coalescence to a single sphere is shown in the photomicrographs in Fig. 3.

Practically all of the interactions observed were as described above, i.e. the bubbles came into apparent contact and after a time coalesced. In many instances, a doublet of bubbles in contact collided with a singlet to form a triplet of which a pair eventually coalesced, thus forming a doublet which eventually coalesced into a singlet. In a number of cases doublets were formed in which the bubbles were clearly separated, but which executed a number of complete rotations as a pair and then separated.

Rotation of Single Bubbles

It has been shown theoretically (4, 11) and confirmed experimentally (9) that a single rigid sphere spins about the Z-axis at the angular velocity given by equation [4], i.e. with a period

$$[7] \quad T_1 = 4\pi/G.$$

It was considered to be of interest to see how closely equation [7] was followed by air bubbles.

Although the bubbles were opaque in the directly illuminated microscope field, their rotational motion could be followed by observing particles of carbon 2μ to 5μ in diameter which were dispersed in the liquid medium and became lodged at the air/liquid interface during the agitation process. One of these particles suitably chosen could be used as a convenient reference point. The time required by the particle to make two successive crossings of the X-Z plane (Fig. 1) was taken to be the half-period of rotation. The precision of these measurements was not as high as with glass spheres (5, 9); the latter were transparent in the microscope field and reference marks on the surface or inside of the particle could be seen throughout the rotation.

Table III contains the observed periods of rotation of an air bubble over a range of velocity gradients. For purposes of comparison the periods calculated from equation [7] are also given. The agreement is seen to be reasonably good considering the difficulty in making accurate measurements.

TABLE III
PERIODS OF ROTATION OF SINGLE AIR BUBBLES

$G, \text{sec.}^{-1}$	$T_1, \text{sec.}$						Observed Calculated
	Observed				Mean observed	Calculated	
0.625	22.4	23.6	19.2	22.8	22.0	20.1	1.09
0.737	18.6	17.4	18.0	18.0	18.0	17.1	1.05
0.985	12.0	11.8	12.4	12.4	12.1	12.8	0.94
1.34	8.4	8.2	9.0	8.8	8.6	9.4	0.91
2.33	4.8	6.2	7.0	7.2	6.0	5.4	1.11
							Mean 1.02

These results show that over the range of velocity gradients studied here, the air bubbles rotate like rigid spheres. This observation accords with Garner's

observation that at low Reynolds numbers sedimenting fluid spheres behave as though they were solid, i.e. they fall at the Stokes velocity without the expected circulation of fluid inside the drop (3).

Periods of Rotation of Air Doublets

A series of measurements of the periods of rotation T_2 about the Z-axis of the doublet formed by two colliding spheres which ultimately coalesced was made over a range of shear rates. The experimental method was similar to that previously described for cylindrical particles (9). In these experiments care was taken to select doublets having bubbles of equal size. Table IV shows

TABLE IV
PERIODS OF ROTATION OF DOUBLETS FORMED BY THE COLLISION
OF FLUID SPHERES

$G, \text{sec.}^{-1}$	Mean $T_2, \text{sec.}$	$T_2 G / 2\pi$
<i>Doublet No. 1</i>		
0.581	40.4	3.74
0.846	27.6	3.72
1.12	20.8	3.72
1.44	16.0	3.68
1.87	11.9	3.55
<i>Doublet No. 2</i>		
0.566	41.0	3.70
0.733	32.2	3.76
1.07	21.6	3.68
1.41	16.4	3.69
2.17	10.4	3.60
		Mean 3.68

typical results for two doublets over a range of shear rates. It will be noted from values shown in the last column that T_2 varies inversely with the velocity gradient.

Periods of rotation of two doublets of separated and hence non-coalescing bubbles were also measured; these are given in Table V.

TABLE V
PERIODS OF ROTATION OF AIR DOUBLETS WITHOUT
BUBBLE CONTACT

$G, \text{sec.}^{-1}$	Mean $T_2, \text{sec.}$	$T_2 G / 2\pi$
1.776	16.4	4.64
2.020	22.4	7.20

According to Jeffery (4), the period of rotation about the Z-axis of a rigid prolate spheroid of axis ratio r is given by

$$[8] \quad T_2 = 2\pi[r + (1/r)]/G$$

which for $r = 2$ yields a value $T_2 G / 2\pi = 5/2$. It is seen from Table IV that

the period of rotation of a doublet of contacting spheres is greater than that of a spheroid of corresponding axis ratio. The "equivalent ellipsoidal axis ratio" r_e may be calculated from equation [8] by inserting the *measured* value of $T_2 G / 2\pi$. This yields a value of $r_e/r = 1.69$ for contacting bubbles; this is considerably higher than the corresponding values of 0.5 for a doublet of neutral rigid spheres (equation [4]), and 0.6 to 0.7 for rigid cylindrical particles having r 's ranging from 130 to 20 (9).

Details of Orbit

It has been previously shown (9) that the spherical elliptical orbit of a prolate spheroid predicted by Jeffery (4) may be transformed to the form

$$[9] \quad \tan \lambda = \tan \lambda_{\max} \sin 2\pi t / T$$

where t is time, λ is the angle between the Z-axis and the X-Z projection of the major axis of the particle (Fig. 1), and λ_{\max} is the maximum value of λ achieved in a particular orbit. Equation [9], which describes the rocking to and fro between the angles $\pm \lambda_{\max}$ of the X-Z projection of the particle, has been confirmed experimentally for rigid cylindrical particles (9).

The variation of λ with time of a doublet of touching air bubbles was measured using a goniometric ocular on the microscope in the same manner as with cylindrical particles (9). The results, which are shown plotted over a half-rotation in Fig. 4, show excellent agreement with equation [9].

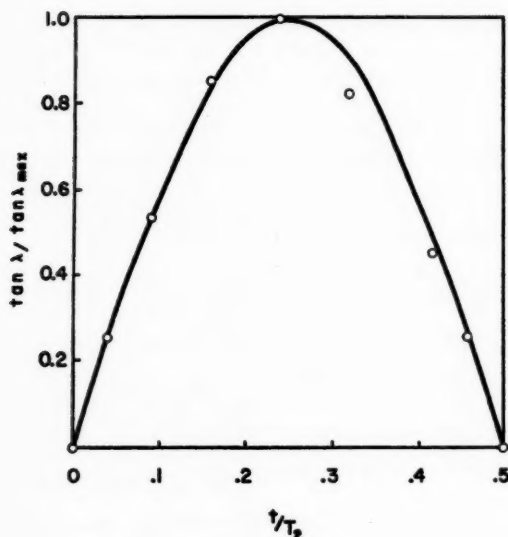


FIG. 4. Variation of the azimuthal angle λ (Fig. 1) with time for a semirootation of a doublet formed by the collision of two air bubbles of equal size. The points are calculated from measured values of λ and T_2 and the curve from Jeffery's equation for a rigid ellipsoid in the form of equation [9].

DISCUSSION

General

Except when $a_1/a_2 > 2$, when the particles can be seen to be separated at all times, the evidence of true contact between glass spheres from these experiments and from the more detailed experiments reported and discussed previously (5) is inconclusive.

The planetary motion observed when $a_1/a_2 > 2$, and which became more marked as the ratio was increased, is complex in nature but may be a manifestation of streamlines around the larger of the two spheres; circular streamlines in the X - Y plane around an isolated rigid sphere may be expected, but the details have not yet been worked out from theory. No explanation can be offered for the "zig-zag" motion. The upward motion of the smaller sphere relative to the larger, which has been shown to occur independent of the direction of rotation of the spheres, is most probably due to differential sedimentation, since a downward sedimentation of the glass spheres in the less dense liquid medium is to be expected.

The coalescence of the air bubbles, while not positive proof of contact, suggests an initial approach of the two spheres close enough so that they adhere with sufficient force to prevent separation in the mirror-image position observed with glass spheres. Owing to the uncertain nature of the long range London-van der Waal's attraction forces, and of the electrostatic repulsion and electroviscous effects existing in thin liquid films which are revealed in the experiments of Derjaguin (1), Elton (2), and others, caution must be exercised in interpreting the significance of the observations on coalescence until additional experiments are carried out.

The formation of air bubble doublets with complete separation cannot be explained although it is possible that it may be related to the planetary motion observed in the binary systems of glass spheres.

Steady State Concentration of Doublets

The persistence of a doublet of neutral rigid spheres for a finite period between collision and separation causes a steady state concentration of doublets to be built up when the suspension is stirred, caused to flow, or otherwise subjected to a velocity gradient. At statistical equilibrium, the number formed per unit time equals the number which die by separation. Thus if F is the total number of doublets formed in unit volume per unit time, and $\bar{\tau}$ is the mean doublet life, then the steady state number of doublets n' per unit volume is given by

$$[10] \quad n' = \bar{\tau}F.$$

For equal-sized spheres, $F = fn/2$ and $\bar{\tau} = \pi/G$ (5). It readily follows that the volume fraction of doublets (c') in the steady state becomes

$$[11] \quad c' = 8c^2$$

where c is the total volume concentration of singlets. Equation [11] can be valid only at low concentrations since the depletion of the system of singlets and the formation of triplets, etc., have been ignored. Several values from

equation [11] are shown in Table VI where it is seen that even at low concentrations an appreciable fraction of neutral spheres can exist in doublet form.

TABLE VI
STEADY STATE CONCENTRATION OF DOUBLETS IN A
SUSPENSION OF NEUTRAL SPHERES

c , volume %	c' , volume %	100 c'/c
2	0.3	15
4	1.3	32
8	5.1	64

We wish next to consider the doublet concentration in a binary system where $a_1/a_2 < 2$. Equation [6] gives the collision frequency per particle; the collision frequency per unit volume F_{12} is given by $f_{12}n_1$. Thus for collisions between k different species uniformly dispersed, the total number of two-body collisions of all types in unit time and unit volume is given by

$$[12] \quad F = \frac{1}{2} \sum_{j=1}^k \sum_{i=1}^k f_{ij}n_i,$$

the factor $\frac{1}{2}$ appearing since each collision has been counted twice under the summation sign. This reduces to

$$[13] \quad F = \frac{G}{12} \sum \sum (a_i + a_j)^3 n_i n_j.$$

For a binary system, i.e. $k = 2$, this yields

$$[14] \quad F = \frac{24G}{\pi^2} \left[\frac{c_1^2}{a_1^3} + \frac{c_2^2}{a_2^3} + \frac{(a_1 + a_2)^3}{4a_1^3 a_2^3} \right] c_1 c_2,$$

the first two terms corresponding to 1-1 and 2-2 collisions respectively, and the third to 1-2 collisions. Assuming that the doublet life for unequal spheres is the same as that for equal spheres, it follows that the steady state concentration of doublets is given by

$$[15] \quad c' = 8c_1^2 + 8c_2^2 + (1 + a_1/a_2)^3 (1 + a_2^3/a_1^3) c_1 c_2.$$

It is readily shown that c' is a minimum when $a_1 = a_2$; it follows therefore that polydispersity may increase the steady concentration of doublets.

Recently we have shown (6) how doublet formation as described above in monodisperse and polydisperse suspensions may be used to modify a theoretical equation due to Vand (11); this modification gives good agreement with measured values of the relative viscosity of rigid spheres at concentrations up to 18% by volume.

The interaction phenomena are of interest in connection with the well-known increase in rate of coagulation of hydrosols and aerosols caused by stirring, turbulent flow, etc. The theory of this effect, which is based upon the increase in collision frequency due to velocity gradients (orthokinetic collisions)

over the normal Brownian (perikinetiC) collisions, was first developed by Smoluchowski (8) and has since been extended by Tuorilla (10), Muller (7), and others.

ACKNOWLEDGMENT

We are indebted to A. P. Arlov for the preparation of the photomicrographs shown in Fig. 3.

REFERENCES

1. DERJAGUIN, B. V. Discussions Faraday Soc. In press.
2. ELTON, G. A. H. Proc. Roy. Soc. (London), A, 194: 275. 1948.
3. GARNER, F. H. Trans. Inst. Chem. Engrs. (London), 28: 88. 1950.
4. JEFFERY, G. B. Proc. Roy. Soc. (London), A, 102: 161. 1922.
5. MANLEY, R. ST. J. and MASON, S. G. J. Colloid Sci. 7: 354. 1952.
6. MANLEY, R. ST. J. and MASON, S. G. Can. J. Chem. 32: 763. 1954.
7. MULLER, H. Kolloidchem. Beih. 27: 223. 1928.
8. SMOLUCHOWSKI, M. VON. Z. Physik. Chem. 92: 129. 1917.
9. TREVELYAN, B. J. and MASON, S. G. J. Colloid Sci. 6: 354. 1951.
10. TUORILLA, P. Kolloidchem. Beih. 24: 1. 1927.
11. VAND, V. J. Phys. & Colloid Chem. 52: 277, 300. 1948.

THE RECIPROCAL SALT-PAIR SYSTEM: SODIUM CHLORIDE - AMMONIUM SULPHITE - SODIUM SULPHITE - AMMONIUM CHLORIDE - WATER AT 20°C. AND 60°C.

PART I. TERNARY SYSTEMS¹

BY J. A. LABASH² AND G. R. LUSBY

ABSTRACT

Solubility data have been obtained at 20°C. and 60°C. for the following ternary systems:

- | | |
|--|---|
| (1) $\text{NaCl-NH}_4\text{Cl-H}_2\text{O}$ | (2) $\text{NH}_4\text{Cl-(NH}_4)_2\text{SO}_3\text{-H}_2\text{O}$ |
| (3) $\text{Na}_2\text{SO}_3\text{-(NH}_4)_2\text{SO}_3\text{-H}_2\text{O}$ | (4) $\text{NaCl-Na}_2\text{SO}_3\text{-H}_2\text{O}$ |

No evidence of the formation of double salts or of solid solutions in the first three systems was obtained. Ammonium sulphite monohydrate does not appear to dehydrate at 60°C. in solutions saturated with sodium sulphite or ammonium chloride. In the study of the $\text{NaCl-NH}_4\text{Cl-H}_2\text{O}$ system, the data agree with average values obtained from the literature and some discrepancies in the published data have been noted. In the $\text{NaCl-Na}_2\text{SO}_3\text{-H}_2\text{O}$ system some anomalous results can be explained on the basis of the existence of solid solutions of the hydrated and anhydrous forms of sodium sulphite and sodium sulphate.

INTRODUCTION

The work described in the present paper and in a following paper was carried out for the purpose of obtaining data necessary for the development of a process for making sodium sulphite and ammonium chloride directly from sodium chloride, sulphur dioxide, and ammonia. The carrying out of such a process industrially requires careful control of liquor compositions in order that products of high purity may be obtained. Because the solubility data in the literature were insufficient for such control of the proposed process, a phase rule study was made of the reciprocal salt-pair system: $\text{NaCl-(NH}_4)_2\text{SO}_3\text{-Na}_2\text{SO}_3\text{-NH}_4\text{Cl-H}_2\text{O}$, at 20°C. and 60°C., and of the four associated ternary systems.

EXPERIMENTAL

(1) Chemicals

Analytical reagent (A.R.) ammonium sulphite was found to contain a relatively high percentage of sulphate and its use was abandoned after a series of preliminary experiments. Ammonia and sulphur dioxide gases were added in place of solid ammonium sulphite wherever possible. When the solid $[(\text{NH}_4)_2\text{SO}_3\cdot\text{H}_2\text{O}]$ was needed, it was freshly prepared from the constituent gases; the solid, thus prepared, was found to contain much less sulphate than the reagent chemical. Ammonium sulphite was used in some cases in the form of a thick slurry, in order to avoid the oxidation which occurs during filtering and drying operations.

Sodium sulphite heptahydrate for the 20°C. work was freshly prepared by cooling a saturated solution of anhydrous sodium sulphite. It, also, was used in the form of a slurry when it was possible to do so.

¹Manuscript received January 17, 1955.

Contribution from Central Research Laboratory, Canadian Industries (1964) Limited, McMasterville, Quebec.

²Present address: Canadian Industries (1964) Limited, Hamilton, Ontario.

The ammonium chloride, sodium chloride, and anhydrous sodium sulphite were of A.R. grade. The latter contained about 1% of sodium sulphate.

(2) Procedure

A constant temperature bath was used, of which the temperature was controlled to $\pm 0.1^\circ\text{C}$. For most of the work, solutions were stirred in three-necked flasks using glass propeller-type stirrers. In earlier work it was found that the sulphate content of the solution increased considerably over a period of a few days, particularly at 60°C . In most of the present work therefore the air was displaced with nitrogen in order to keep oxidation at a minimum. It was also found that ammonia has quite an appreciable vapor pressure over these solutions. Loss of ammonia therefore occurred and this resulted in the formation of bisulphite ion. Solutions were analyzed frequently for bisulphite, which was then neutralized by the addition of ammonia gas.

A solution was sampled by allowing salts to settle and then quickly drawing a sample up into a pipette. A short length of glass tubing containing a wad of absorbent cotton was attached by a rubber tube to the lower end of the pipette to prevent any salts being drawn up into the pipette. In the case of solutions above room temperature the pipette and filter tube were heated. The sample was run into a weighing bottle which was then stoppered and weighed. The sample was diluted in a volumetric flask and suitable aliquots were taken for analysis.

The procedure used in studying the ternary systems consisted in preparing a saturated solution of a single salt, to which portions of the second salt were then added, and the solution was stirred in the presence of an excess of the first salt. After time was allowed for equilibrium to be reached, the solution was analyzed. Additions of the second salt were continued until the composition of the solution became constant. When it was desired to determine the composition of the solid phase, the "rest" method of Schreinemakers was followed. Use was also made of the microscope for identification of solids.

Duplicate analyses were not usually carried out on solutions representing points on lines of ternary (or quaternary) systems. The data for solutions at points of intersections of lines (univariant points), however, are averages of two or more analyses.

(3) Analytical Methods

(a) Bisulphite

Owing to the buffering action of the sulphites, these solutions could not be analyzed accurately for bisulphite or free ammonia by a direct titration with standard alkali or acid respectively. The sulphite was therefore oxidized to sulphate and bisulphite to bisulphate by the addition of neutral hydrogen peroxide (A.R.). This oxidation was carried out at room temperature because the hydrogen peroxide contained a stabilizer which developed acidity in a hot solution. The oxidized solution was then titrated with standard alkali in the presence of methyl red to determine bisulphite, now in the form of bisulphate. Excess ammonia, when present, was titrated with standard acid in the presence of phenolphthalein, after oxidation of the sulphite.

(b) *Sulphite*

In order to minimize oxidation an aliquot was taken immediately after dilution of the sample and was added to *N*/10 iodine solution, the excess of which was then titrated with *N*/10 thiosulphate solution using starch indicator. The sulphite concentration was calculated in the usual way and a correction was made when bisulphite was present.

(c) *Sulphate*

An aliquot was oxidized with bromine water and the total sulphate was determined gravimetrically as barium sulphate. The actual sulphate content of the solution was then determined by subtracting from the total sulphate, the sulphate equivalent to the sulphite and bisulphite in the liquor.

(d) *Chloride*

A fourth aliquot was analyzed for chloride by the standard volumetric method using *N*/10 silver nitrate in excess and back-titrating with *N*/10 ammonium thiocyanate, using ferric alum indicator.

(e) *Ammonium*

Ammonium was determined by the method of Ronchèse (11), which is based on the fact that formaldehyde reacts with the ammonia contained in ammonium salts to form hexamethylene tetramine. The liberated acid can then be titrated to give a measure of the combined ammonia. Because formaldehyde reacts with sulphites, however, the solution used for the ammonium determination was that in which the sulphite had already been oxidized with iodine as described above (b). Methyl red was added to this solution at the end of the thiosulphate back-titration and the acid was exactly neutralized with sodium hydroxide solution. An excess of neutral 20% formaldehyde solution was added and the solution was heated to about 50°C. for a few minutes. The acid liberated by the reaction between ammonia in the ammonium salts and the formaldehyde was then titrated with standard sodium hydroxide solution using phenolphthalein indicator. The sodium hydroxide was standardized by the same procedure using dried A.R. ammonium chloride.

The neutralization of 20% formaldehyde solution was done by taking a measured quantity, diluting it with water to about the same extent as in a regular analysis, and then titrating it with sodium hydroxide, using phenolphthalein indicator. From the volume of sodium hydroxide used in this titration was calculated the amount to be added to the bottle containing the 20% formaldehyde. Alternatively, an electrometric titration was also found to be useful in exactly neutralizing the acidity of the 20% formaldehyde solution, which otherwise is difficult because of buffering action.

(f) *Sodium*

Sodium was determined by the standard method of converting all sodium salts to the sulphate, evaporating the solution to dryness, and heating the residue to constant weight.

The accuracy of the analytical methods was such that duplicate analyses checked within 2 parts per 1000 in the case of the sulphite, ammonium, and

chloride determinations, and within 4 parts per 1000 for sodium and total sulphate determinations.

EXPERIMENTAL RESULTS AND DISCUSSION

(1) NH_4Cl - NaCl - H_2O System

The data obtained in the present work at 20°C. and 60°C. are presented in Tables I and II.

TABLE I
SOLUBILITY DATA IN THE SYSTEM:
 NH_4Cl - NaCl - H_2O at 20°C. and 60°C.

(a) Temp. 20°C.			(b) Temp. 60°C.		
Composition of solution, weight %		Solid phases	Composition of solution, weight %		Solid phases
NaCl	NH_4Cl		NaCl	NH_4Cl	
26.36	0	NaCl	0	35.37	NH_4Cl
23.10	5.32	NaCl			
20.94	8.92	NaCl			
18.30	13.78	NaCl			
17.66	14.79	NaCl			
17.63	14.87	$\text{NaCl} + \text{NH}_4\text{Cl}$	13.60	24.70	$\text{NH}_4\text{Cl} + \text{NaCl}$
13.57	17.38	NH_4Cl			
8.41	20.96	NH_4Cl			
4.27	24.02	NH_4Cl	27.03	0	NaCl
0	27.26	NH_4Cl			

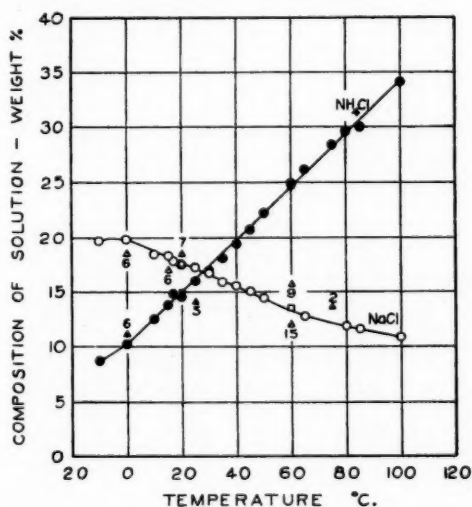


FIG. 1. Mutual solubilities of sodium chloride and ammonium chloride.

- ● Published data, averaged where possible.
- △ ▲ Published data, differing considerably from average values. Numeral indicates literature reference.
- ■ Data obtained in present work.

TABLE II
SUMMARY OF PUBLISHED SOLUBILITY DATA FOR AQUEOUS SOLUTIONS SATURATED WITH BOTH
NaCl AND NH_4Cl

Temp., °C.	Composition of solution, weight %		Authors
	NaCl	NH_4Cl	
-10	19.70	8.75	Yarlikov (14)
0	19.99	10.20	Fedotiev (1)
	19.78	10.26	Gerassimov (2)
	19.94	10.20	Lauffenburger and Brodsky (5)
	18.39*	11.06*	Mondain-Monval (6)
	19.9	10.2	Rivett (9)
	19.58	10.22	Sborgi and Franco (10)
	19.58	10.08	Yarlikov
10	18.27	12.49	Sborgi and Franco
	18.55	12.65	Yarlikov
15	18.20	13.56	Fedotiev
	17.04*	14.00	Mondain-Monval
	18.44	13.76	Toporescu (12)
17	17.78	14.88	Karsten (4)
20	18.52*	14.32	Rengade (7)
	17.52	14.78	Gerassimov
	17.54	14.50	Yarlikov
	17.63*	14.87*	Present work (Table I)
25	17.60	14.07*	Lauffenburger and Brodsky
	17.28	15.86	Restaino (8)
	17.10	15.9	Rivett
	16.83	16.16	Sborgi and Franco
30	16.55	16.97	Fedotiev
35	16.04	17.99	Toporescu
	15.82	18.29	Yarlikov
40	15.5	19.4	Rivett
45	15.03	20.70	Fedotiev
50	14.30	22.42	Gerassimov
	14.43	22.33	Restaino
	14.44	22.09	Toporescu
	14.48	21.98	Yarlikov
60	15.7*	24.4	Rivett
	11.96*	25.30	Zil'berman and Ivanov (15)
	13.60*	24.70*	Present work (Table I)
65	12.65	26.18	Yarlikov
75	13.57*	28.39	Gerassimov
80	12.0	29.5	Rivett
	11.55	29.76	Yarlikov
85	11.57	29.94	Zil'berman and Ivanov
100	10.82	34.13	Restaino
	10.77	33.98	Wurmser (13)

*Not used in averaging the data, and plotted separately in Fig. 1.

It was noted that there were quite large differences between the present data and those in the literature, for solutions saturated with both sodium and ammonium chlorides at 60°C. Consideration of these differences led to a survey of all the available literature data on the mutual solubilities of these two salts. The original papers, the International Critical Tables and the handbooks of Seidell and Landolt-Bornstein, were consulted. The data thus found are summarized in Table II and plotted in Fig. 1. In those cases where two or more sets of data were available at a given temperature, the average values were plotted. However, data differing considerably from the average were not included in the average but were plotted separately. In addition to these larger discrepancies which are shown in Fig. 1, several smaller ones are apparent from a study of the data in Table II.

An explanation of some of these discrepancies may be that sufficient time of agitation was not allowed for equilibrium to be reached. In some cases, the explanation may be the occurrence of typographical errors. For example, Yarlikov (14) gives the same value for NaCl at 35°C. and 50°C. The 50°C. value is evidently a typographical error as it can be calculated from other data which he gives in Table II of his paper that the value at 50°C. should be 22.8 instead of 23.9 gm. NaCl/100 gm. of H₂O. The 50°C. value of Yarlikov (14.48%), given in Table II of the present paper was calculated using the value of 22.8 gm./100 gm. of H₂O.

Data obtained in the present work at 20°C. and 60°C. for solutions saturated with both salts appear to be in quite good agreement with curves representing average values of the published data, as indicated in Fig. 1.

(2) $\text{NH}_4\text{Cl}-(\text{NH}_4)_2\text{SO}_4\text{-H}_2\text{O}$ System

(a) 20°C. Data

The data are given in Table III and Fig. 2.

Ishikawa and Murooka (3) showed that ammonium sulphate does not form solid solutions with ammonium sulphite and there is no evidence in the

TABLE III
SOLUBILITY DATA IN THE SYSTEM:
 $\text{NH}_4\text{Cl}-(\text{NH}_4)_2\text{SO}_4\text{-H}_2\text{O}$ AT 20°C.

Point in Fig. 2	Composition of solution, weight %			Composition of rest, weight %			Solid phases
	NH_4Cl	$(\text{NH}_4)_2\text{SO}_4$	$(\text{NH}_4)_2\text{SO}_4$	NH_4Cl	$(\text{NH}_4)_2\text{SO}_4$	$(\text{NH}_4)_2\text{SO}_4$	
S	27.26	0	0	—	—	—	NH_4Cl
	24.70	5.25	0.45	75.97	1.13	0.82	NH_4Cl
	22.45	10.00	1.06	70.70	2.90	1.54	NH_4Cl
	20.08	15.52	—	—	—	—	NH_4Cl
	18.39	19.13	—	—	—	—	NH_4Cl
F	16.61	23.57	1.20	52.28	24.20	0.28	$\text{NH}_4\text{Cl}+(\text{NH}_4)_2\text{SO}_4\cdot\text{H}_2\text{O}$
F	16.57	23.64	1.15	16.79	62.26	2.12	$\text{NH}_4\text{Cl}+(\text{NH}_4)_2\text{SO}_4\cdot\text{H}_2\text{O}$
	15.36	24.55	0.90	3.39	72.24	1.30	$(\text{NH}_4)_2\text{SO}_4\cdot\text{H}_2\text{O}$
	9.66	28.85	—	2.29	71.56	1.78	$(\text{NH}_4)_2\text{SO}_4\cdot\text{H}_2\text{O}$
	5.13	32.63	—	0.78	74.82	1.84	$(\text{NH}_4)_2\text{SO}_4\cdot\text{H}_2\text{O}$
R	0	37.34	0.49	—	—	—	$(\text{NH}_4)_2\text{SO}_4\cdot\text{H}_2\text{O}$

literature for the existence of solid solutions of ammonium chloride and ammonium sulphate. The sulphate content of a given rest could therefore only be due to ammonium sulphate in the adhering mother liquor and to oxidation of the sulphite by air during filtration. Because the sulphate content of the rest was usually much higher than that which could be accounted for by the adhering mother liquor, a correction was made by converting the ammonium sulphate in the rest to ammonium sulphite and adding this value to the $(\text{NH}_4)_2\text{SO}_3$ value before the rest composition was plotted in Fig. 2.

The data in Table III and Fig. 2 show no evidence of double salt or solid solution formation between ammonium chloride and ammonium sulphite at 20°C .

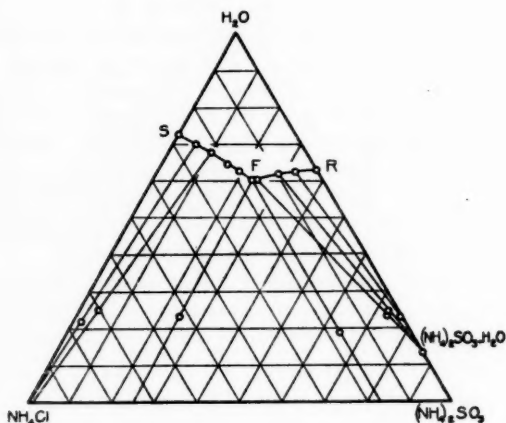


FIG. 2. Ammonium chloride - ammonium sulphite - water system at 20°C .

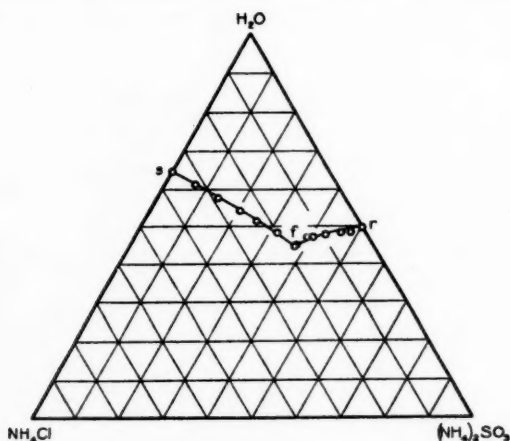


FIG. 3. Ammonium chloride - ammonium sulphite - water system at 60°C .

(b) 60°C. Data

The data in Table IV and in Fig. 3 show no evidence of the formation of a double salt or of solid solutions of ammonium chloride and ammonium sulphite at 60°C. The results also indicate that ammonium sulphite monohydrate does not dehydrate at 60°C. in solutions containing ammonium chloride, although no rest analyses were made to confirm this point.

The composition of the solution saturated with both salts is considerably different from that found by Zil'berman and Ivanov (15).

TABLE IV
SOLUBILITY DATA IN THE SYSTEM:
 $\text{NH}_4\text{Cl}-(\text{NH}_4)_2\text{SO}_3-\text{H}_2\text{O}$ AT 60°C.

Point in Fig. 3	Composition of solution, weight %					Solid phases
	NH_4Cl	$(\text{NH}_4)_2\text{SO}_3$	$(\text{NH}_4)_2\text{SO}_4$	NH_4HSO_3	NH_3	
s	35.37	0	0	0	0	NH_4Cl
	32.04	6.95	—	—	—	NH_4Cl
	28.56	13.97	—	0.23	0	NH_4Cl
	25.35	20.75	—	0.09	0	NH_4Cl
	22.98	25.75	—	0.22	0	NH_4Cl
	19.82	32.06	—	0.43	0	NH_4Cl
f	17.84	37.72	0.91	—	—	$\text{NH}_4\text{Cl} + (\text{NH}_4)_2\text{SO}_3 \cdot \text{H}_2\text{O}$
	(16.74)	(35.82)*	—	—	—	$\text{NH}_4\text{Cl} + (\text{NH}_4)_2\text{SO}_3 \cdot \text{H}_2\text{O}$
f	17.82	37.86	0.99	—	—	$\text{NH}_4\text{Cl} + (\text{NH}_4)_2\text{SO}_3 \cdot \text{H}_2\text{O}$
	17.71	37.7	—	0.17	—	$(\text{NH}_4)_2\text{SO}_3 \cdot \text{H}_2\text{O}$
	16.90	37.6	—	0	0.22	$(\text{NH}_4)_2\text{SO}_3 \cdot \text{H}_2\text{O}$
	13.82	39.6	—	0	0.02	$(\text{NH}_4)_2\text{SO}_3 \cdot \text{H}_2\text{O}$
	15.64	38.5	—	—	—	$(\text{NH}_4)_2\text{SO}_3 \cdot \text{H}_2\text{O}$
	12.29	40.7	0.89	—	—	$(\text{NH}_4)_2\text{SO}_3 \cdot \text{H}_2\text{O}$
	9.05	43.1	—	0	0.02	$(\text{NH}_4)_2\text{SO}_3 \cdot \text{H}_2\text{O}$
	5.35	46.2	—	0	0.05	$(\text{NH}_4)_2\text{SO}_3 \cdot \text{H}_2\text{O}$
	3.14	48.6	—	0.51	—	$(\text{NH}_4)_2\text{SO}_3 \cdot \text{H}_2\text{O}$
	0	50.48	—	0.13	0	$(\text{NH}_4)_2\text{SO}_3 \cdot \text{H}_2\text{O}$
r	0	50.48	—	0.13	0	$(\text{NH}_4)_2\text{SO}_3 \cdot \text{H}_2\text{O}$

*Zil'berman and Ivanov (15).

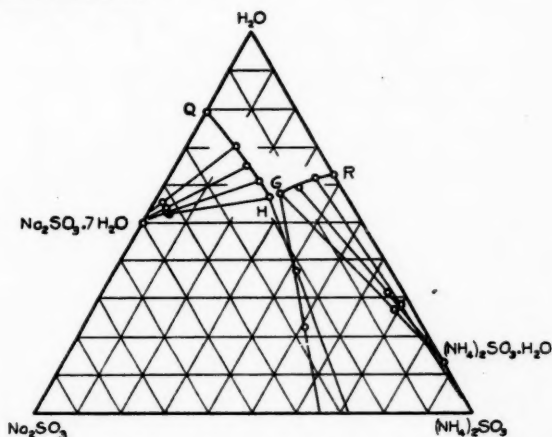


FIG. 4. Sodium sulphite-ammonium sulphite-water system at 20°C.

(3) $\text{Na}_2\text{SO}_3-(\text{NH}_4)_2\text{SO}_3-\text{H}_2\text{O}$ System

(a) 20°C. Data

When portions of each salt were added to a saturated solution of the other salt, it was found that the two final compositions at 20°C. were not the same (Table V and Fig. 4). This result indicates the formation of a new solid phase between *G* and *H*, but sufficient work was not done to establish its nature.

TABLE V
SOLUBILITY DATA IN THE SYSTEM:
 $\text{Na}_2\text{SO}_3-(\text{NH}_4)_2\text{SO}_3-\text{H}_2\text{O}$ AT 20°C.

Point in Fig. 4	Composition of solution, weight %			Composition of rest, weight %			Solid phases
	Na_2SO_3	$(\text{NH}_4)_2\text{SO}_3$	$(\text{NH}_4)_2\text{SO}_4$	Na_2SO_3	$(\text{NH}_4)_2\text{SO}_3$	$(\text{NH}_4)_2\text{SO}_4$	
<i>R</i>	0	37.34	0.49	—	—	—	$(\text{NH}_4)_2\text{SO}_3 \cdot \text{H}_2\text{O}$
	4.74	33.52	1.10	2.14	69.65	1.72	$(\text{NH}_4)_2\text{SO}_3 \cdot \text{H}_2\text{O}$
	9.91	30.91	0.62	3.78	64.60	0.41	$(\text{NH}_4)_2\text{SO}_3 \cdot \text{H}_2\text{O}$
	14.79	27.55	1.00	4.60	67.82	0.92	$(\text{NH}_4)_2\text{SO}_3 \cdot \text{H}_2\text{O}$
<i>G</i>	14.98	27.43	0.96	26.95	50.51	0.95	$(\text{NH}_4)_2\text{SO}_3 \cdot \text{H}_2\text{O}$ + unknown solid
<i>H</i>	17.26	25.75	1.30	21.56	41.24	1.95	Undetermined
	17.21	25.70	0.80	42.79	4.82	0.85	$\text{Na}_2\text{SO}_3 \cdot 7\text{H}_2\text{O}$
	17.97	20.87	0.88	43.03	3.77	0.87	$\text{Na}_2\text{SO}_3 \cdot 7\text{H}_2\text{O}$
	18.65	15.95	0.84	42.73	3.25	0.79	$\text{Na}_2\text{SO}_3 \cdot 7\text{H}_2\text{O}$
	19.34	10.44	0.87	42.79	1.57	1.44	$\text{Na}_2\text{SO}_3 \cdot 7\text{H}_2\text{O}$
<i>Q</i>			(Na_2SO_4)				
	20.58	—	0.77	—	—	—	$\text{Na}_2\text{SO}_3 \cdot 7\text{H}_2\text{O}$

60°C. Data

Little work was done on this system at 60°C. and only the data for two solutions saturated with both salts are given in Table VI. These solutions

TABLE VI
SOLUBILITY DATA IN THE SYSTEM:
 $\text{Na}_2\text{SO}_3-(\text{NH}_4)_2\text{SO}_3-\text{H}_2\text{O}$ AT 60°C.

Composition of solution, weight %					Solid phases
Na_2SO_3	$(\text{NH}_4)_2\text{SO}_3$	Na_2SO_4	NH_4HSO_3	NH_3	
(8.35	45.08)*	—	—	—	$(\text{NH}_4)_2\text{SO}_3 \cdot \text{H}_2\text{O}$, Na_2SO_3
7.76	44.7	0.74	0	0.08	Not determined
7.69	45.0	0.71	0.08	0	Not determined

*Zil'berman and Ivanov (15).

were obtained by starting with solutions saturated with sodium sulphite and with ammonium sulphite respectively, and adding portions of the other salt until the compositions became constant. It is seen from Table VI that these compositions are practically identical, but these data do not show whether there is formation of a double salt or a solid solution at 60°C. or if dehydration of ammonium sulphite monohydrate occurs. The data obtained, however, are

in fair agreement with those of Zil'berman and Ivanov (15) for a solution saturated with respect to $(\text{NH}_4)_2\text{OS}_3 \cdot \text{H}_2\text{O}$ and Na_2SO_3 .

(4) $\text{NaCl}-\text{Na}_2\text{SO}_3-\text{H}_2\text{O}$ System

(a) 20°C. Data

The data obtained are given in Table VII and are shown plotted in Fig. 5. Between P and C , the solid phase is NaCl , and between Q and L it is $\text{Na}_2\text{SO}_3 \cdot 7\text{H}_2\text{O}$. The space between L and C indicates the existence of an undetermined solid phase.

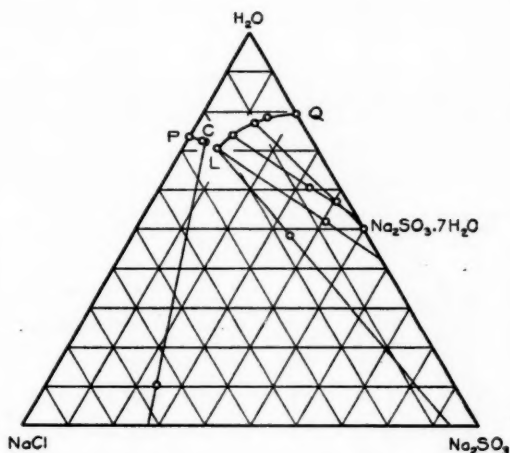


FIG. 5. Sodium chloride - sodium sulphite - water system at 20°C.

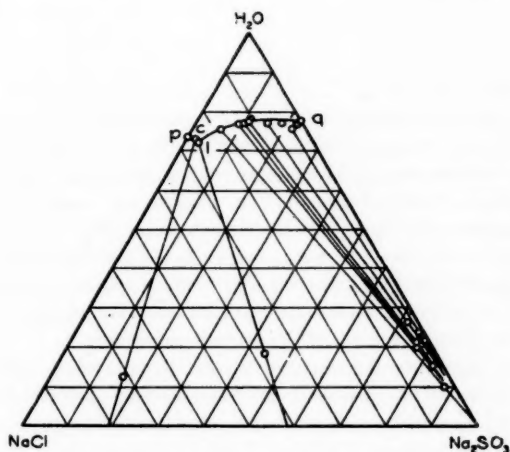


FIG. 6. Sodium chloride - sodium sulphite - water system at 60°C.

TABLE VII
SOLUBILITY DATA IN THE SYSTEM:
NaCl-Na₂SO₃-H₂O AT 20°C. AND AT 60°C.

Point in figure	Composition of solution, weight %			Composition of rest, weight %			Solid phases
	NaCl	Na ₂ SO ₃	Na ₂ SO ₄	NaCl	Na ₂ SO ₃	Na ₂ SO ₄	
At 20°C.							
Fig. 5							
<i>P</i>	26.36	0	—	—	—	—	NaCl
	24.22	3.26	0.22	—	—	—	NaCl
<i>C</i>	23.68	4.35	0.21	65.25	24.28	1.75	Undetermined
<i>L</i>	21.10	7.41	1.24	16.86	34.65	1.18	Undetermined
	21.19	7.61	1.23	7.34	40.60	1.60	Undetermined
	16.73	9.13	1.14	2.95	42.13	2.59	Na ₂ SO ₃ ·7H ₂ O
	16.89	9.20	0.71	6.59	32.78	1.48	Na ₂ SO ₃ ·7H ₂ O
	10.27	12.46	1.04	2.39	40.65	1.24	Na ₂ SO ₃ ·7H ₂ O
	6.76	14.87	0.86	—	—	—	Na ₂ SO ₃ ·7H ₂ O
<i>Q</i>	0	20.58	0.77	—	—	—	Na ₂ SO ₃ ·7H ₂ O
At 60°C.							
Fig. 6							
<i>p</i>	27.03	—	—				NaCl
<i>c</i>	25.77	1.89	0.30	71.8	16.02	0.68	Apparently NaCl+Na ₂ SO ₃
	(24.23	2.36)*					NaCl+Na ₂ SO ₃
<i>l</i>	25.14	3.04	0.16	37.58	44.60	1.12	Apparently NaCl+Na ₂ SO ₃
	18.85	5.98	0.93	2.16	88.3	3.10	Na ₂ SO ₃
	14.03	9.57	0.70	3.34	77.2	2.22	Na ₂ SO ₃
	12.75	10.64	1.05	2.16	83.01	2.66	Na ₂ SO ₃
	11.69	11.46	2.40	2.86	76.50	1.47	Na ₂ SO ₃
	10.88	11.27	1.06	—	—	—	Na ₂ SO ₃
	7.55	15.80	2.04	2.11	72.00	5.40	Na ₂ SO ₃
	4.45	18.90	1.32	0.99	75.75	3.40	Na ₂ SO ₃
	2.98	21.90	1.02	0.76	78.00	6.21	Na ₂ SO ₃
	1.29	22.50	0.65	0.41	76.30	4.43	Na ₂ SO ₃
<i>q</i>	0	22.86	0.67	—	—	—	Na ₂ SO ₃

*Zil'berman and Ivanov (15).

(b) 60°C. Data

Sodium chloride was added to a solution saturated with sodium sulphite (*q*) until a constant composition was reached at *l* (Table VII and Fig. 6). Similarly, when sodium sulphite was added to a solution saturated with sodium chloride the point *c* was obtained. The experiment was repeated several times with the same result being obtained each time. That is, the compositions of the two solutions stopped at *l* and *c* respectively, solid sodium chloride at *l*, and solid sodium sulphite at *c* having little effect on the compositions even after several days' stirring. Thus, there appeared to be an undetermined solid phase present in this system at 60°C. as well as at 20°C.

The following attempts were made to obtain solutions between *c* and *l*, since analysis of the rests from such solutions should give the identity of the solid phase in the region between *c* and *l*. Portions of a filtered solution at *l* were added to three bottles of 150 ml. capacity. To each bottle were added 0.1 gm. of sodium sulphite and 1.0 gm. of sodium chloride. Similarly, a solution

at c was filtered and portions of it were placed in three bottles. To these were added 0.1 gm. of sodium chloride and 1, 2, and 3 gm. of sodium sulphite respectively. These bottles were closed with glass stoppers (greased) and rotated, so that the solids fell from top to bottom of each bottle and vice versa, during a revolution, for seven weeks in a constant temperature bath. At the end of that time the bottles were removed, and analyses were made on the solutions and rests.

The data obtained are given in Table VIII. It will be noted that the sulphate content in solutions c_3 is very low and is evidently in error. The sodium sulphite content in solutions c , c_1 , c_2 , and c_3 shows comparatively little change except

TABLE VIII
NaCl-Na₂SO₃-H₂O SYSTEM AT 60°C.
EXPERIMENTS IN ROTATING BOTTLES

Solution No.	Solution, weight %			Rest, weight %			Remarks
	NaCl	Na ₂ SO ₃	Na ₂ SO ₄	NaCl	Na ₂ SO ₃	Na ₂ SO ₄	
c	25.77	1.89	0.30	71.8	16.02	0.68	
c_1	25.20	1.97	0.62	1.70	87.3	4.70	Soln. c + 0.1 gm. NaCl and 1.0 gm. Na ₂ SO ₃
c_2	25.25	2.08	0.70	1.66	88.6	3.99	Soln. c + 0.1 gm. NaCl and 2.0 gm. Na ₂ SO ₃
c_3	25.55*	2.54	0.04	11.77	79.9	3.25	Soln. c + 0.1 gm. NaCl and 3.0 gm. Na ₂ SO ₃
l	25.14	3.04	0.16	37.58	44.60	1.12	
l_1	25.03	2.93	0.30	66.00	18.37	5.96	Soln. l + 0.1 gm. Na ₂ SO ₃ and 1.0 gm. NaCl
l_2	23.36	2.68	0.56	—	—	—	Soln. l + 0.1 gm. Na ₂ SO ₃ and 1.0 gm. NaCl
l_3	24.72	3.00	0.56	31.99	39.79	4.46	Soln. l + 0.1 gm. Na ₂ SO ₃ and 1.0 gm. NaCl

*Calc. by diff.

in the case of solution c_3 but even in this case it is still considerably below the value for the solution at l . Two grams of sodium sulphite would have been sufficient, had it all dissolved, to move the composition of the solution from c to l . In the case of the experiments in which sodium chloride and a small proportion of sodium sulphite were added to solutions at l (Table VIII), there was no significant decrease in the sulphite content nor increase in the chloride content during seven weeks, for the first and third solutions (l_1 and l_3). In the case of solution l_2 , the decrease in the contents of both sodium chloride and sodium sulphite and the fact that there was insufficient rest for and analysis indicate that water leaked into this bottle.

Because a series of solutions with compositions lying between l and c was not obtained, the results of these experiments do not indicate the nature of the unknown solid phase. A possible explanation of the results may be the formation of solid solutions of sodium sulphate in sodium sulphite, as several such solid solutions are known. It might be, for example, that sodium chloride is in equilibrium with one solid solution of sodium sulphate in sodium sulphite

at c (60°C. diagram) and with a different solid solution at l . In a second paper dealing with the quaternary system the nature of the solid phase between L and C (20°C. data) and between l and c (60°C. data) will be discussed further.

REFERENCES

1. FEDOTIEV, P. P. *Z. physik. Chem.* 49: 162. 1904.
2. GERASSIMOV, I. *Z. anorg. u. allgem. Chem.* 187: 321. 1930.
3. ISHIKAWA, F. and MUROOKA, H. *Cited by J. W. Mellor. A comprehensive treatise on inorganic and theoretical chemistry. Vol. X. Longmans, Green and Co., London, New York, Toronto. 1930. p. 258.*
4. KARSTEN. *Cited by A. Seidell. Solubilities of inorganic and metal organic compounds. Vol. I. 3rd ed. D. Van Nostrand Company, Inc., New York. 1940. p. 1223.*
5. LAUFFENBURGER, R. and BRODSKY, M. *Compt. rend.* 206: 1383. 1938.
6. MONDAIN-MONVAL, P. *Compt. rend.* 174: 1014. 1922; 175: 162. 1922.
7. RENGADE, E. *Chimie & industrie*, 7: 1090. 1922.
8. RESTAINO, S. *Atti 10th Congr. intern. chim. Rome*, 2: 761. 1938.
9. RIVETT, A. C. D. *J. Chem. Soc.* 121: 379. 1922.
10. SBORGI, U. and FRANCO, C. *Gazz. chim. ital.* 51 (II): 1. 1921.
11. SUTTON, F. *Volumetric analysis. 12th ed. P. Blakiston's Son & Co., Inc., Philadelphia. 1935. p. 75.*
12. TOPORESCU, E. *Compt. rend.* 174: 870. 1922; 175: 268. 1922.
13. WURMSER, MLE. *Compt. rend.* 174: 1466. 1922.
14. YARLIKOV, M. M. *Zhur. Priklad. Khim.* 7: 902. 1934.
15. ZIL'BERMAN, YA. I. and IVANOV, P. T. *Zhur. Priklad. Khim.* 14: 939. 1941.

**THE RECIPROCAL SALT-PAIR SYSTEM:
SODIUM CHLORIDE - AMMONIUM SULPHITE - SODIUM
SULPHITE - AMMONIUM CHLORIDE - WATER AT 20°C. AND 60°C.**

PART II: THE QUATERNARY SYSTEM¹

By J. A. LABASH² AND G. R. LUSBY

ABSTRACT

In the above quaternary system at 60°C., besides those representing the four salts at the corners of the Janecke diagram two other saturation areas were found. At 20°C. there are three, and possibly more than three additional areas. In the course of the present work it was not possible to establish the nature of the solid phases in these additional areas of the quaternary system. However, the data of Lewis and Rivett suggest that at least some of these unknown areas may indicate the presence of different solid solutions of sodium sulphate in sodium sulphite. This quaternary system appears to be a rather complex one and much further work remains to be done in order to complete the knowledge of it at 60°C. and 20°C., particularly at the latter temperature.

INTRODUCTION

Zil'berman and Ivanov (6) made a study of the reciprocal salt-pair system: $\text{NaCl}-(\text{NH}_4)_2\text{SO}_3-\text{Na}_2\text{SO}_3-\text{NH}_4\text{Cl}-\text{H}_2\text{O}$ at 60°C. and 85°C., and of the system: $\text{NaCl}-\text{NH}_4\text{HSO}_3-\text{NaHSO}_3-\text{NH}_4\text{Cl}-\text{H}_2\text{O}$ at 25°C. and 60°C. The ultimate purpose of their work was the same as that of the present work, namely, the industrial preparation of sodium sulphite and ammonium chloride from sodium chloride, sulphur dioxide, and ammonia.

The process as developed in this laboratory and used in the plant at Hamilton, Ont. (1), consists essentially in adding sulphur dioxide and ammonia gases to a mother liquor containing sodium chloride in suspension, and centrifuging off the precipitated sodium sulphite at 60°C. The mother liquor is cooled to 20°C., the ammonium chloride which crystallizes out is centrifuged off, and the mother liquor is used for the next cycle.

Such a cyclic process as outlined above is the subject of several German patents dating from 1887. Zil'berman and Ivanov point out that these patents are very vague in regard to the details of the process and that they found it necessary to carry out solubility studies in order to define more precisely the operating conditions. It was for the same reason that the present work was undertaken.

In the previous paper (2) data were given on the four ternary systems associated with the reciprocal salt-pair system: $\text{NaCl}-(\text{NH}_4)_2\text{SO}_3-\text{Na}_2\text{SO}_3-\text{NH}_4\text{Cl}-\text{H}_2\text{O}$ at 20°C. and 60°C. The present paper contains data on the quaternary system.

The experimental methods were essentially the same as those used for the ternary systems.

¹Manuscript received January 17, 1955.

Contribution from Central Research Laboratory, Canadian Industries (1954) Limited, McMasterville, Quebec.

²Present address: Canadian Industries (1954) Limited, Hamilton, Ontario.

EXPERIMENTAL

The presence of sulphate ion as an impurity presents a difficulty in the accurate plotting of the data according to the method of Janecke for reciprocal salt-pairs. Because it was usually not known how the sulphate was distributed between the ammonium and sodium ions, the ionic ratios of these two ions were based on the total sodium and ammonium values.

(1) 60°C. Data

In Fig. 1 it will be noted that there are two saturation areas where the solid phase has not been identified, namely, (a) the area between the lines *cb* and *le*, and (b) the area between the lines *ej* and *do*.

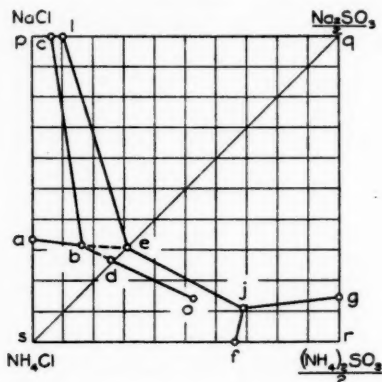


FIG. 1. Sodium chloride - ammonium sulphite - sodium sulphite - ammonium chloride - water system at 60°C.

(a) Area between *cb* and *le* at 60°C.

The points *c* and *l* at the top of this area have already been discussed under the NaCl-Na₂SO₃-H₂O system (2). Ammonium chloride was added in portions to a solution at *c*, in the presence of excess sodium chloride and sodium sulphite, and the solution was analyzed after each addition. In this way several points were obtained along the line *cb*. At *b* the solids were filtered off and each of the three salts sodium chloride, ammonium chloride, and sodium sulphite was added singly, to the filtered solution, which was stirred for several hours in each case. No change in composition occurred and it thus seemed that the solution at *b* was saturated with these three salts. Points along *cb* were also obtained by adding sodium sulphite to solutions plotting to the left of *cb*.

To a solution at *a*, in the presence of excess sodium and ammonium chlorides, sodium sulphite was added and points were obtained along *ab*. The composition became constant at *b*, and was practically the same as that obtained by starting from *c* (Table I).

The point *e* was obtained by adding ammonium chloride to a saturated solution of sodium sulphite and then, after the composition had become

constant, adding sodium chloride. No change in composition occurred when the latter salt was added so the solution at *e* was also apparently saturated with the three salts, sodium chloride, ammonium chloride, and sodium sulphite. Points along the line *le* were obtained by adding sodium chloride to solutions which plotted to the right of this line. In some cases the composition did not stop at this line, but moved into the *cbel* area. The addition of ammonium chloride to a solution on the lower part of the line *le* always caused the composition to move towards the corner *s* of the diagram until the line *be* was reached.

Points on *be* were also obtained by adding sodium chloride to solutions plotting below *be*. Once the composition reached a point on *be*, however, the presence of an excess of solid sodium chloride did not cause the composition to move towards *b*. Also, no noticeable change in composition occurred in a few hours on adding the three salts sodium chloride, ammonium chloride, and sodium sulphite separately to solutions represented by points on the line *be*. There was no difficulty, however, in moving the composition from *b* to *e* by adding ammonium sulphite to a filtered solution at *b*.

(b) Area between *ej* and *do* at 60°C.

When ammonium chloride was added to a saturated sodium sulphite solution, the composition moved along the diagonal from *q* to *e*, where the composition became constant. Similarly, when sodium sulphite was added to a saturated ammonium chloride solution, the composition moved from *s* to *d*. The existence of the two points *d* and *e* indicates the presence of another solid phase, which could be a double salt or a solid solution. Points *d* and *e* were also obtained when these experiments were repeated using solutions which were slightly ammoniacal. This was done because the only known double salt containing sodium and ammonium sulphites has the formula $2\text{Na}_2\text{SO}_3 \cdot (\text{NH}_4)_2\text{S}_2\text{O}_5 \cdot 10\text{H}_2\text{O}$ (4). This double salt was encountered in the present work in certain solutions containing bisulphite ion, but it dissolved readily when the solution was neutralized with ammonia. The possibility of its formation was therefore assumed to have been eliminated by avoiding acidic conditions in the above experiments at the points *d* and *e*, and the existence of the area between *d* and *e* is presumably not due to formation of this double salt.

Chemical analysis and microscopic examination of the rests indicated the presence of sodium chloride, ammonium chloride, and sodium sulphite at *e* and ammonium chloride and sodium sulphite at *d*. The microscopic technique, however, would not have revealed the presence of solid solutions if these had differed only slightly in optical properties from the pure salts. It was decided to investigate the nature of the unknown solid phase by attempting to obtain points between *d* and *e* in the pseudoternary system: $\text{NH}_4\text{Cl}-\text{Na}_2\text{SO}_3-\text{H}_2\text{O}$ in the following manner.

All solids were filtered from a solution at *e*, which was then divided into five portions. To each portion (about 150 gm.) was added 0.1 gm. of sodium sulphite and 1.0 to 2.5 gm. of ammonium chloride, the latter quantity being more than sufficient to move the composition to *d* if it dissolved. Similarly, to each of five portions of filtered liquor at *d* were added 0.2 gm. of ammonium

TABLE I
 RECIPROCAL SALT-PAIR SYSTEM: $\text{NaCl}-(\text{NH}_4)_2\text{SO}_4-\text{Na}_2\text{SO}_4-\text{NH}_4\text{Cl}-\text{H}_2\text{O}$ AT 60°C. AND 20°C.

Line	Composition of solution, weight %						Solid phases
	NaCl	NH ₄ Cl	(NH ₄) ₂ SO ₄	Na ₂ SO ₄	NH ₄ HSO ₄	NH ₃	
At 60°C.							
Point in Fig. 1							
a	13.60	24.70	0	0	0	0	NaCl, NH ₄ Cl
b	5.96	27.17	0	7.24	1.73	0.01 } 0	NH ₄ Cl, Na ₂ SO ₄ , NaCl*
	6.00	27.43	0	7.64	0.80 (NaHSO ₄)		
c	25.77	0	0	1.89	0.30	0	NaCl, Na ₂ SO ₄ *
d	0	30.48	0	12.42	0.76	—	NH ₄ Cl, Na ₂ SO ₄ * NH ₄ Cl, Na ₂ SO ₄ , NaCl
	(0	30.84	0.52	12.84)†	—	—	
e	0	29.20	0.41	14.77	0.62	0.07	NH ₄ Cl, Na ₂ SO ₄ , NaCl*
f	0	17.84	37.72	0	0.91 ((NH ₄) ₂ SO ₄)	—	NH ₄ Cl, (NH ₄) ₂ SO ₄ , H ₂ O
g	0	0	45.0	7.69	0.71	0.08	Na ₂ SO ₄ , (NH ₄) ₂ SO ₄ , H ₂ O
h	0	16.87	34.5	5.23	1.26	0 } 0	NH ₄ Cl, Na ₂ SO ₄ , (NH ₄) ₂ SO ₄ , H ₂ O*
	0	16.87	34.4	5.55	0.64		
i	0	15.89	34.3	6.24	2.29	—	NH ₄ Cl, Na ₂ SO ₄ , (NH ₄) ₂ SO ₄ , H ₂ O
	(0	15.79	35.11	4.25)†	—		
l	25.14	0	0	3.04	0.16	0	NaCl, Na ₂ SO ₄ *
o	0	22.18	20.22	6.68	1.48	—	NH ₄ Cl, Na ₂ SO ₄ *
p	27.03	0	0	0	0	0	NaCl
q	0	0	0	22.86	0.67	0	Na ₂ SO ₄
r	0	0	50.48	0	—	0.13	(NH ₄) ₂ SO ₄ , H ₂ O
s	0	35.37	0	0	0	0	NH ₄ Cl

At 20°C.

Point in Fig. 2

A	—	17.63	14.87	0	0	0	0	0	0	NaCl, NH_4Cl
B	AB	10.24	16.54	0	8.20	0.65	—	—	—	NH_4Cl , Na_2SO_4 , NaCl^*
CB	—	10.47	16.50	0	8.51	0.46	—	—	—	
C	—	23.68	0	0	4.35	0.21	—	—	—	Undetermined
D	—	0.35	21.52	0	16.61	0.44	—	—	—	NH_4Cl , Na_2SO_4^*
E	—	3.86	18.55	0	16.36	0.59	—	—	—	NH_4Cl , Na_2SO_4 , NaCl^*
F	—	0	16.59	23.61	0	1.17 ($(\text{NH}_4)_2\text{SO}_4$)	—	—	—	NH_4Cl , $(\text{NH}_4)_2\text{SO}_4 \cdot \text{H}_2\text{O}$
G	—	0	0	27.43	14.98	0.96 ($(\text{NH}_4)_2\text{SO}_4$)	—	—	—	Undetermined
H	—	0	0	25.75	17.26	1.30 ($(\text{NH}_4)_2\text{SO}_4$)	—	—	—	Undetermined
I	FI DI	0 0	14.58 13.88	17.23 17.88	11.60 10.71	1.51 2.91	0	—	0	NH_4Cl , Na_2SO_4 , $(\text{NH}_4)_2\text{SO}_4 \cdot \text{H}_2\text{O}^*$
J	—	0	13.80	15.78	15.18	0.89	—	—	—	
K	—	0	17.33	1.68	22.25	0.71	—	—	—	NaCl , $\text{Na}_2\text{SO}_4 \cdot 7\text{H}_2\text{O}$, Na_2SO_4
L	—	21.43	0	0	7.44	0.86	—	—	—	Undetermined
N	—	0	19.95	0	18.92	1.45	—	—	—	NH_4Cl , Na_2SO_4^*
P	—	26.36	0	0	0	0	0	0	0	NaCl
Q	—	0	0	0	20.58	0.77	—	—	—	$\text{Na}_2\text{SO}_4 \cdot 7\text{H}_2\text{O}$
R	—	0	0	37.34	0	0.49 ($(\text{NH}_4)_2\text{SO}_4$)	—	—	—	$(\text{NH}_4)_2\text{SO}_4 \cdot \text{H}_2\text{O}$
S	—	0	27.26	0	0	0	0	0	0	NH_4Cl

* Apparent solid phases.
† Zilberman and Iverson (8).

TABLE II
 $\text{NH}_4\text{Cl-Na}_2\text{SO}_4\text{-H}_2\text{O}$ SYSTEM AT 60°C . EXPERIMENTS IN ROTATING BOTTLES

Test sol'n (Fig. 1)	Solution, weight %				Rest, weight %			Remarks		
	NaCl	NH ₄ Cl	(NH ₄) ₂ SO ₄	Na ₂ SO ₄	Na ₂ SO ₄	NH ₄ Cl	Na ₂ SO ₄			
e	0	29.18	0.41	14.90	0.80	0.02	69.4	18.7	1.26	Clear solution divided into five 150 gm. portions and treated as indicated below, for 7 weeks e+0.1 gm. Na ₂ SO ₄ +1.0 gm. NH ₄ Cl
e ₁	0	29.04	0.52	14.66	0.75	—	2.16	89.4	4.54	
e ₂	0	29.15	0.29	14.31	0.80	0.04	Not enough for analysis			e+0.1 gm. Na ₂ SO ₄ +2.0 gm. NH ₄ Cl
e ₃	0	28.80	0.87	14.32	0.84	—	2.30	88.7	—	e+0.1 gm. Na ₂ SO ₄ +2.0 gm. NH ₄ Cl
e ₄	0	29.08	0.29	14.75	0.59	—	4.50	74.9	0.86	e+0.1 gm. Na ₂ SO ₄ +2.5 gm. NH ₄ Cl
e ₅	0	28.98	0.41	14.59	0.98	—	8.14	58.4	1.14	e+0.1 gm. Na ₂ SO ₄ +2.5 gm. NH ₄ Cl
d	0	30.40	0	12.57	0.71	—	25.05	69.0	0.43	Clear solution divided into five 150 gm. portions and treated as indicated below, for 7 weeks d+0.3 gm. NH ₄ Cl+2.0 gm. Na ₂ SO ₄
d ₁	0	29.35	0	12.31	0.86	—	92.0	1.71	4.29	
d ₂	0	30.20	0	12.88	0.56	—	87.8	3.56	1.75	d+0.2 gm. NH ₄ Cl+4.0 gm. Na ₂ SO ₄
d ₃	0.23	29.98	0	12.59	0.84	0.04	65.7	19.51	1.88	d+0.2 gm. NH ₄ Cl+4.0 gm. Na ₂ SO ₄
d ₄	0	29.40	0	12.84	0.49	—	93.1	2.17	2.12	d+0.2 gm. NH ₄ Cl+6.0 gm. Na ₂ SO ₄
d ₅	0	29.82	0.17	12.36	1.35	—	67.9	23.58	1.57	d+0.2 gm. NH ₄ Cl+6.0 gm. Na ₂ SO

chloride and 2 to 6 gm. of sodium sulphite. These solutions and their respective solids were placed in bottles and rotated in the constant temperature bath at 60°C. for six to seven weeks. At the end of that time the solutions and rests were analyzed. In all cases except two (d_1 and d_4), the solution compositions were found not to have changed appreciably and the rests, as indicated by analysis, were mostly ammonium chloride at e and mostly sodium sulphite at d (Table II). Because points were not obtained between d and e , these experiments did not result in the identification of the solid phase between the lines ej and do .

The areas between b and d , and between o and j were not explored; d and o do not represent univariant points but simply the last points determined along the line do . The line do was explored by adding ammonium sulphite to a liquor at d . It was noticed that the composition had a tendency to move across the area between ej and do , so that when one analysis showed the composition to be on do , the analysis after another addition of ammonium sulphite frequently showed the composition to be on ej . To avoid this difficulty, solutions were made up whose compositions were represented by points below do . On addition of anhydrous sodium sulphite in excess, the compositions moved to points on do .

It is interesting to note that the composition found by Zil'berman and Ivanov (6) for the solution saturated with sodium chloride, ammonium chloride, and sodium sulphite corresponds with the composition of the solution at d , which in the present work was found to be not saturated with sodium chloride (Table I and Fig. 1). This difference may be due to a difference in the sulphate content of the two solutions.

When sodium sulphite was added to a solution at f , points were obtained along ff , and the composition became constant at j . Ammonium chloride was added to a solution at g and the composition was followed along gj until j was again reached, as indicated in Table I. Analysis of the rest indicated the presence of anhydrous sodium sulphite, ammonium chloride, and ammonium sulphite, but it was not determined whether the latter was in the form of the hydrate or not.

When ammonium sulphite hydrate was added to a solution at e , along with excesses of sodium sulphite and ammonium chloride, points were obtained along ej until the solution reached a constant composition. It will be seen that the final composition j in this case is somewhat different from the other two compositions, particularly in respect to the ammonium chloride value (Table I). This difference may be due to the higher content of sodium sulphate in this particular solution. The difference between the composition of the solution at j , obtained by Zil'berman and Ivanov, and the present values may also be due to differences in the sulphate contents.

(2) 20°C. Data

The 20°C. data are given in Table I and Fig. 2.

The points C and L have already been mentioned in connection with the ternary system $\text{NaCl}-\text{Na}_2\text{SO}_3-\text{H}_2\text{O}$ at 20°C. (2). To a solution at C in the

between *K* and *H* but this area was not studied sufficiently to establish the boundary line between the hydrated and anhydrous forms of sodium sulphite. The procedure followed in these experiments was to add ammonium chloride to solutions in contact with excess sodium sulphite heptahydrate. The results were inconsistent, possibly because of metastable states of equilibria. No data are given therefore.

The point *I* was obtained by adding anhydrous sodium sulphite to a liquor at *F* in equilibrium with solid ammonium chloride and ammonium sulphite hydrate. The composition became constant at *I* where the solid phases were apparently ammonium chloride, anhydrous sodium sulphite, and ammonium sulphite monohydrate. Points on the line *IG* were obtained by adding anhydrous sodium sulphite to solutions whose compositions plotted below *IG*.

The point *I* was apparently reached also by adding ammonium sulphite monohydrate to a solution at *D* and following the line *DI*. The difference in composition between the two solutions at *I* (Table I) is possibly due to the difference in sulphate content. Several points along *BI* were obtained by adding anhydrous sodium sulphite to solutions below this line. Solutions plotting between *B* and *D* usually moved slowly towards *BE* in the presence of an excess of anhydrous sodium sulphite. In some cases the compositions changed quite quickly on the addition of sodium sulphite, to points between *D* and *E*. On the other hand solutions along *DI* showed little tendency to change even after a week's stirring.

The addition of sodium chloride to solutions along the line *BD* caused the compositions to move immediately to points on *BE*. For example, on taking a solution at *D* in contact with excess ammonium chloride and anhydrous sodium sulphite and adding sodium chloride to it, the new composition corresponded to *E*. The solids were filtered off and the clear solution was stirred separately with each of the three salts. No significant change in composition was observed, which indicated that the solution at *E* was apparently saturated with ammonium chloride, sodium chloride, and anhydrous sodium sulphite.

Solutions along *BE* behaved similarly to those along *be* in the 60°C. diagram. That is, the addition of sodium chloride to a solution on *BE* in the presence of excess ammonium chloride and anhydrous sodium sulphite did not have any noticeable effect on its composition. On the other hand, ammonium sulphite added to solutions along *BE* caused their compositions to move along *BE* to *E*.

By adding ammonium sulphite (in the form of ammonia and sulphur dioxide gases) to a solution on *NJ*, a constant liquor composition was reached at *J*. The filtered solution was tested singly with the three salts—anhydrous sodium sulphite, ammonium chloride, and ammonium sulphite (added in the form of the two gases), but no appreciable change in the liquor composition was noted in any case.

The present data at 20°C. as plotted in Fig. 2 indicate that there are at least three unknown saturation areas one of which, within the region of the points *K*, *H*, *G*, *I*, and *J* may represent solutions in equilibrium with anhydrous

sodium sulphite. A possible explanation of the presence of these unknown saturation areas is discussed below.

GENERAL DISCUSSION

In the 60°C. diagram (Fig. 1), the existence of unknown saturation areas could indicate the presence of double salts or solid solutions of either sodium chloride and sodium sulphite or ammonium chloride and sodium sulphite. It would seem more reasonable, however, to base an explanation of the results on the formation of solid solutions of sodium sulphite and sodium sulphate. (Sulphate was an impurity in the present work.) Such solid solutions are well known as a result of the work of Lewis and Rivett (3, 5). Thus, the line *cb* may represent solutions in equilibrium with sodium chloride and one solid solution of sodium sulphate in sodium sulphite, while in the case of the line *le* the solids may be sodium chloride and a different solid solution. The area between the lines *cb* and *le* (and similarly the area between *bdo* and *ej*) would then be due to the overlapping of two areas which represent solutions saturated with respect to two different solid solutions of sodium sulphate in sodium sulphite. In a similar manner may be explained the existence of unknown saturation areas in the 20°C. diagram. The tendency of sodium sulphate and sodium sulphite to form metastable solid solutions may explain some apparently metastable states of equilibrium encountered in the present study.

The quaternary system is obviously more complicated at 60°C. than the results of Zil'berman and Ivanov indicate, and it is still more complex at 20°C. It is not the intention of the present authors to continue the study of this system of salts but it is hoped that the information presented in these two papers will be of assistance to others in future studies. Much work remains to be done on the quaternary system at 20°C. and 60°C. particularly on the identification of the solid phases, and X-ray diffraction techniques should be very useful in such studies. Literature data on the three ternary systems containing sulphites are also rather scanty, so that salt systems containing sulphites present a large field for phase rule investigations.

REFERENCES

1. COOK, E. J. R. *Can. Chem. Process Ind.* 29: 221. 1945.
2. LABASH, J. A. and LUSBY, G. R. *Can. J. Chem.* 33: 774. 1955.
3. LEWIS, N. B. and RIVETT, A. C. D. *J. Chem. Soc.* 125: 1156, 1162. 1924.
4. MELLOR, J. W. *A comprehensive treatise on inorganic and theoretical chemistry*. Vol. X. Longmans, Green and Co., London, New York, Toronto. 1930. p. 270.
5. RIVETT, A. C. D. and LEWIS, N. B. *Rec. trav. chim.* 42: 954. 1923.
6. ZIL'BERMAN, YA. I. and IVANOV, P. T. *Zhur. Priklad. Khim.* 14: 939. 1941.

ON THE INTERMOLECULAR FORCE FIELD OF NITRILES¹

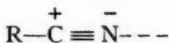
By F. E. MURRAY² AND W. G. SCHNEIDER

ABSTRACT

The nature of the intermolecular force field of the nitriles is considered on the basis of the electron orbital structure and charge distribution of the nitrile group. The directional nature of the force field is due to a well-directed lone pair orbital on the N atom, which may be expected to exhibit strong donor properties, and two π -orbitals which may exhibit weak donor properties. Accordingly with good acceptor molecules such as chloroform and hydrogen chloride, simple 1:1 molecular addition compounds should occur. The existence of molecular complexes of this type was confirmed with the aid of binary freezing-point diagrams which were determined for aceto-, propio-, butyro-, and benzo-nitrile with chloroform and hydrogen chloride. The 1:1 association complex was absent, however, in the system acetonitrile-chloroform. This is accounted for by the stronger association occurring in acetonitrile itself, the nature of which is discussed. The structure of the 1:1 molecular complexes is considered. Additional molecular complexes with lower nitrile mole ratios are indicated in the freezing-point diagrams. Of particular interest are the well-defined compounds appearing in the nitrile-hydrogen chloride systems with the composition $\text{RCN} \cdot 5\text{HCl}$. The possibility that the π -orbitals of the nitrile group may function as donors in these compounds is discussed, and a tentative structure is suggested.

INTRODUCTION

Because of its highly directional character, the intermolecular force field of the nitrile group is of particular interest. Although the nitriles, as for example the alkyl nitriles, RCN , have high dipole moments, the strong molecular association of such molecules cannot in general be attributed primarily to dipole interaction. The charge distribution which gives rise to the strongly polar force field is made up of two π -orbitals which are directed at right angles to each other and centered mainly in the region between the C and N atoms, and of a lone pair orbital centered on the N atom. The latter can be represented approximately by a digonally hybridized sp orbital directed along the CN axis, and it is accordingly an excellent "donor" (7). Thus boron trifluoride, a typical vacant orbital acceptor, forms stable addition compounds with nitriles (4) and hydrogen cyanide associates into linear chains by hydrogen bonding (1). Because the lone pair orbital on the N atom is directed along the molecular axis, it is largely responsible for the high dipole moment of the nitrile group. Moreover, because of the greater electronegativity of the N atom relative to C, the π -orbitals will be displaced somewhat toward the N atom. Accordingly the over-all charge distribution will be such as to make the N atom considerably more negative than the C atom, which may be roughly represented as follows:



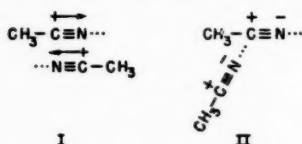
the dotted line indicating the direction of the lone pair orbital.

¹Manuscript received January 21, 1955.

Contribution from the Division of Pure Chemistry, National Research Council, Ottawa, Canada, and the Department of Chemistry, University of Manitoba, Winnipeg, Manitoba. Issued as N.R.C. No. 3562.

²Summer Research Associate, Division of Pure Chemistry, National Research Council, 1954. Present address: Department of Chemistry, University of Manitoba, Winnipeg, Manitoba.

Molecular association in acetonitrile vapor has been studied by Lambert *et al.* (3). From measurements of the second virial coefficient as a function of temperature, it was concluded that dimerization occurs, with a heat of dimerization of approximately 5200 cal./mole. Dimerization was considered to be due to dipole interaction resulting from a parallel orientation of dipoles as shown in (I). This configuration would, however, appear to be extremely



unlikely, since the mutual repulsions of the high charge densities in the region of the CN triple bond would make it unfavorable. The configuration shown in II in which the N lone pair orbital is directed at the C atom of the second molecule would appear to be a more probable one. This structure is closely related to the configuration observed in the crystal of the linear molecule dicyanoacetylene (2); instead of a parallel arrangement of the rod-shaped molecules, the structure is an open one in which the closest approach between neighboring molecules is between the N atom of one molecule and one of the innermost C atoms of the second molecule.

Apart from molecular interactions involving a "donor" action of the N lone pair orbital, there is also the possibility of a similar role by the two π -orbitals of the CN group. Such interaction to form the so-called π -complexes has been observed for the ethylenic and aromatic π -electrons. It is very probable, however, that the "donor" action of the π -electrons in the nitrile group is much weaker than that of the N lone pair orbital and may become significant only in the presence of very strong electron acceptors (acids).

The present work was undertaken in order to obtain a better understanding of the nature of the force field of the nitriles and their molecular associations. It was desired to investigate particularly those molecular associations of the nitriles which will lead to definite compound formation in the solid, the configuration of which can later be established by X-ray methods. Accordingly, the freezing-point diagrams of aceto-, propio-, butyro-, and benzo-nitrile with chloroform and with hydrochloric acid have been determined. Both chloroform and hydrochloric acid may be expected to function primarily only as acceptors, and hence if only the N lone pair orbital of the nitrile group interacts strongly with these reagents, simple 1:1 addition compounds may be expected to appear in the freezing-point diagram.

EXPERIMENTAL

A modified Beckmann freezing-point apparatus was used to obtain cooling curves. The inner glass cell, which contained the mixture being studied, was joined to a vacuum system. A glass stirrer into which was sealed a small iron slug was moved up and down by mechanically driven magnets. Cooling was effected by conduction to liquid nitrogen and the rate could be altered by

changing the pressure in the space between the inner cell and the outer glass tube.

A glass thermocouple well was sealed into the inner cell and temperatures were measured using two copper-constantan junctions. The thermocouple voltage (reference junctions in ice) was recorded continuously during cooling with a recording potentiometer. A platinum resistance thermometer was used to obtain a calibration of the thermocouple-recorder arrangement.

Compositions of the binary liquid mixture were changed by addition of one of the components, either from a pipette or by condensation from a weighing bulb attached to the vacuum system. Hydrogen chloride was added to the nitrile by condensing it into the cell with liquid nitrogen. The amount of gas condensed was obtained by measuring the pressure change in a calibrated volume. Reagent grade chemicals were used throughout without further purification. Interpretation of cooling curves was based on the analysis by Mair *et al.* (5). Temperature measurements were accurate within $\pm 0.5^\circ \text{C}$.

RESULTS

The freezing-point diagrams for chloroform with each of the four nitriles studied are plotted in Fig. 1. In Fig. 2 the corresponding binary diagrams for hydrogen chloride with each of the three alkyl nitriles are shown. The melting points of the addition compounds appearing in these diagrams are collected in Table I.

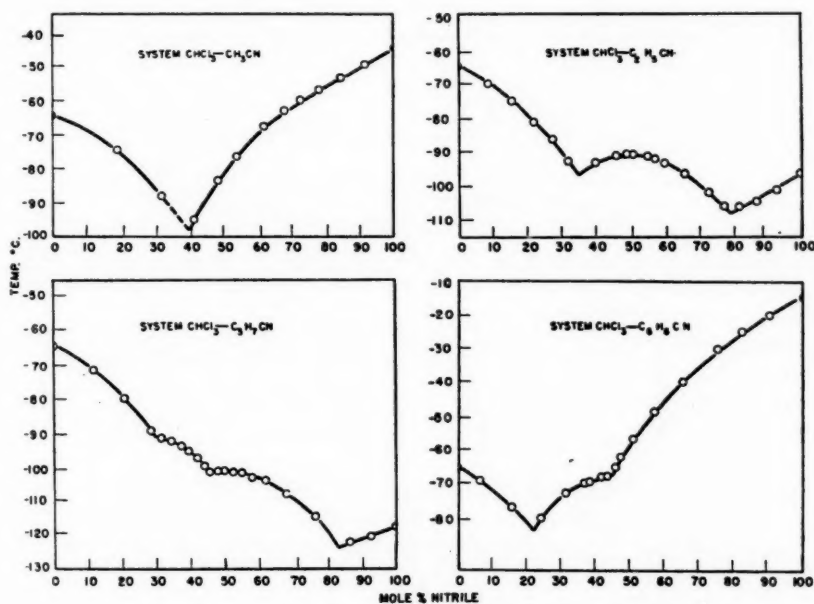


FIG. 1. Freezing-point diagrams for some nitrile-chloroform systems.

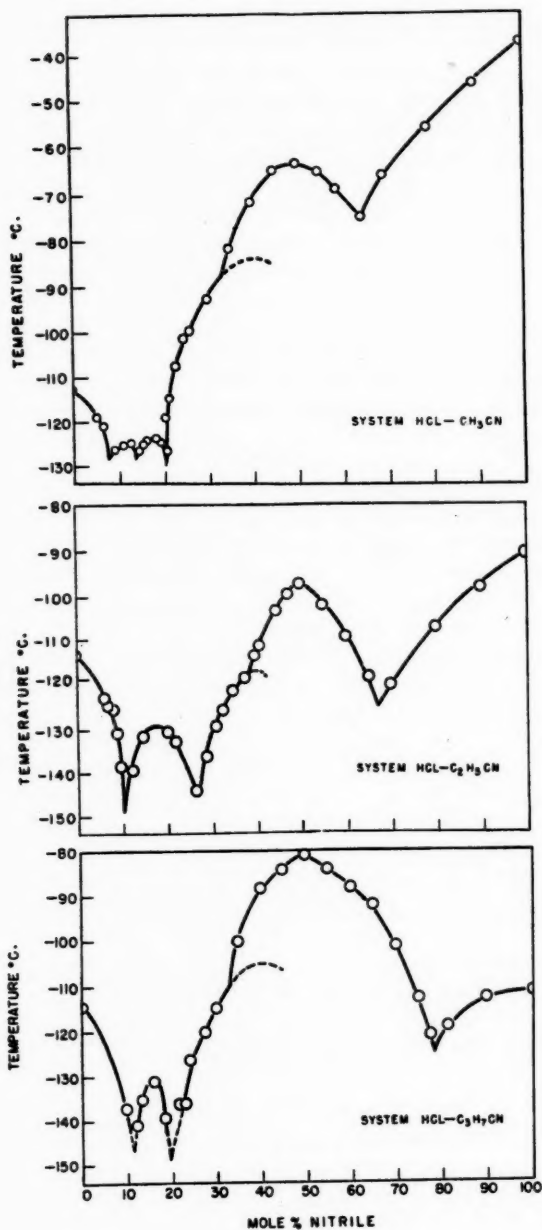


FIG. 2. Freezing-point diagrams for some nitrile - hydrogen chloride systems.

TABLE I
 MELTING POINTS OF MOLECULAR ADDITION COMPOUNDS

Compound	M.p. (° C.)	Compound	M.p. (° C.)
C ₂ H ₅ CN·CHCl ₃	- 90.5	CH ₃ CN·7HCl	-125.0
C ₃ H ₇ CN·CHCl ₃	-101.5	C ₂ H ₅ CN·HCl	- 97.2
C ₃ H ₇ CN·3CHCl ₃	(- 91.5)*	2C ₂ H ₅ CN·3HCl	(-117)*
C ₆ H ₅ CN·CHCl ₃	(- 67.5)*	C ₂ H ₅ CN·5HCl	-129
CH ₃ CN·HCl	- 63.2	C ₂ H ₅ CN·HCl	- 80.6
2CH ₃ CN·3HCl	(- 88)*	2C ₂ H ₅ CN·3HCl	(-109)*
CH ₃ CN·5HCl	-123.6	C ₂ H ₅ CN·5HCl	-130

*Melts incongruently.

DISCUSSION OF RESULTS

The occurrence of intermolecular complexes of both chloroform and hydrogen chloride with the nitriles in a 1:1 mole ratio had been anticipated. The considerations underlying this expectation have been outlined above and the results amply confirm the basic concepts of the nature of the molecular interaction put forward. However, the absence of the 1:1 complex in the chloroform-acetonitrile system was unexpected. The most probable explanation of this anomaly is that acetonitrile is capable of associating with itself more strongly than with chloroform. The nature of the mutual association of acetonitrile molecules has already been referred to; it does not appear likely that this is due to dipole association but results from the positive character of the C atom of the nitrile group. The latter accordingly acts as an acceptor to the donor lone pair orbital on the N atom of a neighboring molecule. In the higher nitriles the positive character of the nitrile C atom is less pronounced owing to the greater inductive effect of the larger alkyl groups. In these nitriles the C atom is now a weaker acceptor than the H atom of the chloroform molecule, with which they accordingly form the 1:1 compound.

If the above explanation for the absence of the 1:1 compound in the acetonitrile-chloroform system is correct, we may expect that with a much stronger acceptor (acid) than chloroform, such as HCl, the mutual association in acetonitrile would be disrupted in favor of the more stable addition compound CH₃CN·HCl. This is confirmed by the freezing-point diagram shown in Fig. 2.

Since the donor lone pair orbital on the N atom of the nitrile group is directed out along the C-N axis the 1:1 addition compounds of the nitriles with chloroform and hydrogen chloride can be assigned the following structures:



where the dotted line indicates the direction of the lone pair orbital. The latter forms a hydrogen bond with the H atom of chloroform and with that of hydrogen chloride. These structures presumably involve a completely linear configuration of nuclei* as follows: C-C≡N- - -H-C in the first com-

*This statement assumes a collinear configuration of the lone pair orbital direction and the H-X acceptor in the hydrogen bond (see Ref. (7)).

pound, and $C-C\equiv N-H-Cl$ in the second, where in each case the first C atom is part of the alkyl group. A determination of the crystal structure of these compounds, which may be expected to have a somewhat open structure, would therefore be of interest.

The 1:1 addition compounds of the nitriles with hydrogen chloride cannot be regarded as salts. The low melting point of these compounds is not compatible with such a structure. On the other hand there is some evidence that in the presence of moisture the addition compound may slowly change to the corresponding salt. Thus if acetonitrile is saturated with hydrogen chloride and allowed to stand at room temperature in the presence of water vapor, white crystals, presumably the salt, are observed to separate from the solution after several days. The transition from a molecular addition compound, in which the binding forces are primarily the electrostatic forces of a hydrogen bond, to that of the corresponding salt may be expected to be favored by the presence of a high dielectric medium such as water. Hydrolysis of the nitrile under these conditions (room temperature) to the corresponding carboxylic acid may however occur to some extent.

The fact that the nitriles do not readily form salts with hydrogen chloride, whereas the corresponding amines do, is of some interest in connection with the relative donor properties exhibited by the nitrogen lone pair orbital in these two classes of compounds. From considerations of the degree of *sp* hybridization occurring in the N lone pair orbital in amines (or ammonia) and in the nitriles, it was previously concluded (7) that the latter should exhibit stronger donor properties. This conclusion is, however, not confirmed by the present results. An alternative relative measure of donor strength of lone pair orbitals is the ionization potential since, for molecules of the type under consideration here, ionization involves removal of an electron from the lone pair orbital. Hence the lower the ionization potential the stronger should be the donor property of the lone pair electrons. The ionization potentials for acetonitrile and methylamine are 12.4 ev. and 9.4 ev. respectively (6), which thus appear to represent more nearly the relative donor strengths indicated by the present experiments.

Additional molecular compounds other than the 1:1 compounds also occur in some of the freezing-point diagrams at lower nitrile concentrations. A number of these have incongruent melting points. Thus butyronitrile forms an incongruent melting compound with chloroform having the probable composition $C_4H_7CN \cdot 3CHCl_3$. The three alkyl nitriles studied all form incongruent melting compounds with hydrogen chloride with the probable composition $2RCN : 3HCl$.

Of particular interest are the well-defined compounds occurring in the alkyl nitrile-HCl systems with the composition $RCN : 5HCl$ (a further compound with even lower nitrile concentration appears in the acetonitrile-HCl system). From the general shape of the freezing-point diagrams, these compounds are evidently much less stable than the corresponding 1:1 compounds. Since they appear in all three nitrile systems, the alkyl group, R, is not a determining factor, and hence the additional donor "centers" which

are evidently brought into play must be attributed to the nitrile group. Apart from the lone pair orbital on the N atom, the only other possible donor "centers" available are the two π -orbitals of the C-N triple bond. Since these orbitals are orthogonal to each other and are directed at right angles to the C-N axis, the configuration shown in Fig. 3 would appear to be the most

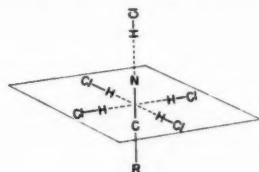


Fig. 3.

probable structure for the 1:5 compounds. One HCl molecule is bonded to the N lone pair, while four HCl molecules are accommodated in a plane at right angles to the molecular axis. It is assumed that each π -orbital can act as donor to two HCl molecules which are directed in the plane at an orientation of 180° . Little is known about the donor properties of π -orbitals, and particularly about those of the "triple" bond. However, if such donor action, even though it is weak, is possible at all, one might expect it to be manifest under the conditions of the present experiments, that is to say at low temperatures and in the presence of a strong small-molecule acceptor such as HCl. Moreover, if the above-postulated structure is correct one might expect analogous structures to occur with hydrogen chloride and acetylene or its derivatives. This possibility is now being investigated.

ACKNOWLEDGMENT

We wish to thank Mr. Yves Lupien for assistance in some of the experimental measurements.

REFERENCES

1. DULMADGE, W. J. and LIPSCOMB, W. N. *Acta Cryst.* 4: 330. 1951.
2. HANNAN, R. B. and COLLIN, R. L. *Acta Cryst.* 6: 350. 1953.
3. LAMBERT, J. D., ROBERTS, G. A. H., ROWLINSON, J. S., and WILKINSON, V. J. *Proc. Roy. Soc. (London)*, A, 196: 113. 1949.
4. LAUBENGAYER, A. W. and SEARS, D. S. *J. Am. Chem. Soc.* 67: 164. 1945.
5. MAIR, B. J., GLASGOW, A. R., and ROSSINI, F. D. *J. Research Natl. Bur. Standards*, 26: 591. 1941.
6. MORRISON, J. D. and NICHOLSON, A. J. C. *J. Chem. Phys.* 20: 1021. 1952.
7. SCHNEIDER, W. G. *J. Chem. Phys.* 23: 26. 1955.

HYDROGEN PEROXIDE AND ITS ANALOGUES

VII. CALORIMETRIC PROPERTIES OF THE SYSTEMS $\text{H}_2\text{O} - \text{H}_2\text{O}_2$ AND $\text{D}_2\text{O} - \text{D}_2\text{O}_2$ ¹

BY PAUL A. GIGUÈRE, B. G. MORISSETTE²,
A. W. OLMOS³, AND O. KNOP⁴

ABSTRACT

The heat of mixing of hydrogen peroxide and water and the heat of vaporization of the mixtures were measured over a wide concentration range at 0° C. with a Bunsen ice calorimeter and at 26.9° with a diphenyl ether calorimeter. The heat capacities of the solutions were determined between these two temperatures. Similar measurements were carried out on the corresponding deuterium compounds. The heat of decomposition of hydrogen peroxide catalyzed by colloidal platinum was also measured at 26.9° as a function of concentration. Correlation of all the results leads to the following recommended values for the thermochemical properties of the pure peroxides in the liquid state at 25° C.

	H_2O_2	D_2O_2
Heat of decomposition (kcal./mole)	23.44 ± 0.02	23.41 ± 0.02
Heat of vaporization (kcal./mole)	12.34 ± 0.03	12.51 ± 0.05
Heat of mixing (cal./mole)	819 ± 2	807 ± 2
Heat capacity (cal./deg. mole)	21.35 ± 0.05	22.9 ± 0.1

A number of related functions are given for convenience in recalculating these quantities to other temperatures. Apart from their practical value the new data are of interest in connection with molecular association and hydrogen bonds.

INTRODUCTION

A previous paper in this series (5) reported measurements of some thermal properties of hydrogen peroxide made at 0° C. in an ice calorimeter. Among these were preliminary results on the heat of decomposition of the liquid at various concentrations, which showed serious discrepancies with other published values. In view of the importance of such data in thermochemical equations involving hydrogen peroxide it was felt desirable to repeat the measurements using a more reliable technique. In order to minimize the importance of corrections to 25° C., the standard temperature, an isothermal calorimeter working with diphenyl ether (m.p. 26.9°) was used as described elsewhere (7). This calorimeter also has the advantages of greater sensitivity and easier operation than the ice calorimeter.

Calculation of the heat of formation of gaseous hydrogen peroxide from the heat of decomposition of the liquid requires knowledge of the heat of vaporization. Therefore, this quantity was also measured at the same temperature as a function of concentration. Comparison of the results with those previously found at 0° C. revealed a strong temperature dependence of the heat of mixing of hydrogen peroxide and water. As only scanty data on this property were available in the literature, the present measurements were extended to include

¹Manuscript received January 14, 1955.

²Contribution from the Department of Chemistry, Laval University, Quebec, Que., with financial assistance from the National Research Council of Canada.

³Holder of a National Research Council Bursary, 1951-52.

⁴Holder of a Scholarship under the Bureau of Scientific Research of the Province of Quebec, 1952-54.

⁵On leave of absence from the Nova Scotia Technical College, Halifax, N.S.

direct determinations of the heat of mixing at both 0° and 26.9° C. from 99% down to fairly low concentrations of peroxide.

The importance of these measurements is twofold. First, they make possible a more exact correlation between the various sets of thermochemical data and a more accurate extrapolation to arrive at the properties of pure hydrogen peroxide. Secondly, they provide much-needed experimental material for testing the validity of proposed theories of solutions of non-electrolytes. Indeed, the system hydrogen peroxide - water is of special interest in that connection as it is probably the simplest binary system with extensive hydrogen bonding. The only systematic investigation of sufficient accuracy to warrant calculation of the relevant thermodynamic functions dealt with vapor pressure of the mixtures (14). However, the results had to be extrapolated considerably beyond the temperature range of the measurements. Even if the present results are only of a modest degree of precision they are valuable in that they provide a direct source of information on the associative properties of the system hydrogen peroxide - water. In the meantime, the availability of mixtures of deuterium peroxide and heavy water was an incentive to extend the investigation to the isotopic system of compounds.

THE SYSTEM $\text{H}_2\text{O} - \text{H}_2\text{O}_2$

So far the heat of decomposition, the latent heat of vaporization, and the heat of mixing of mixtures of hydrogen peroxide and water have been investigated and reported in the literature (cf. (15) for a review). Of these quantities the last one is by far the smallest. It may be obtained indirectly from the other two but the calculations involve differences between two large quantities. To arrive at reasonably precise values the heats of decomposition or vaporization would have to be measured with much greater accuracy than has been done until now. Therefore, it seemed more logical to determine experimentally the heat of mixing of hydrogen peroxide and water and then to use the results to obtain accurate values of the heats of decomposition and vaporization from pertinent data for the pure components.

The temperature dependence of these quantities could be ascertained either directly, by measurements at two or more different temperatures, or indirectly through Kirchhoff's equation. For the latter method the heat capacities of the solutions are needed, and since no reliable data could be found in the literature for this quantity, it was determined at a number of concentrations.

Heat Capacity

The method and experimental details were essentially the same as used previously for measuring the heat capacity of pure liquid hydrogen peroxide (5), except that the initial temperature of the sample was 26.9° C. instead of 25°. The results listed in Table I give an idea of the precision of the measurements. In particular, the average of three determinations with pure water agrees to better than 0.1% with the accepted values of the mean specific heat c_p over the same temperature interval. Extrapolation leads to 0.628 cal./deg. gm. or 21.35 cal./deg. mole for pure H_2O_2 , a value considered fairly accurate on account of the short extrapolation and the practically straight-line

TABLE I
ENTHALPY CHANGES BETWEEN 0° AND 26.9° OF H₂O-H₂O₂ MIXTURES

Concentration, 100 w_p	Weight of solution, gm.	Heat effect measured, cal./gm. solution	c_p , cal./deg. gm.
0	4.1654	26.92	1.002
0	4.2987	27.02	
0	4.0239	26.95	
21.2	4.7556	24.13	0.893
21.2	4.7556	23.97	
21.2	4.7077	23.97	
41.0	4.8261	22.00	0.817
41.0	4.8261	21.98	
60.1	5.2702	20.37	0.757
60.1	5.2702	20.36	
79.1	5.7391	18.73	0.696
79.1	5.7391	18.73	
98.6	5.9067	17.07	0.632
98.6	5.9067	17.03	
98.6	6.6162	16.93	
98.6	5.9879	17.01	
98.6	5.9879	17.00	

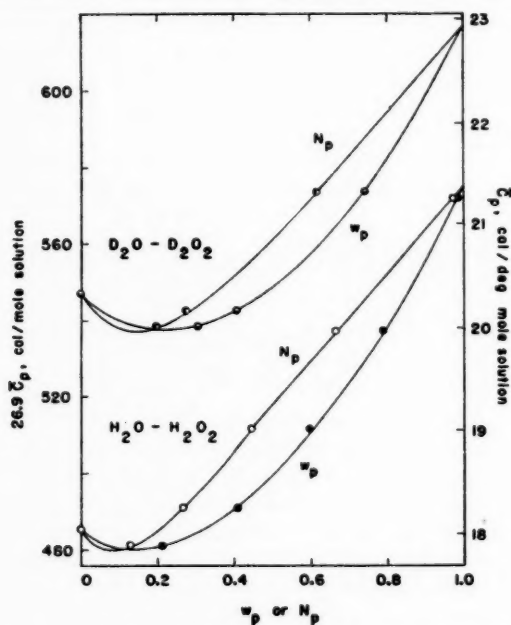


FIG. 1. Molar enthalpy changes and average heat capacities between 0° and 26.9° for H₂O-H₂O₂ and D₂O-D₂O₂ mixtures.

relationship in that range. A slightly higher value, 0.632 cal./deg. gm., has been reported by Foley and Giguère; the discrepancy was traced to a small error in the calibration of the mercury thermometer used by these authors. For the present work a platinum resistance thermometer (Leeds and Northrup, certified at the National Bureau of Standards) was employed.

A plot of the molar enthalpy change of the solutions from 0° to 26.9° C. is shown in Fig. 1 as a function both of the weight fraction w_p and mole fraction N_p of hydrogen peroxide. From a large-scale graph smoothed values were obtained and from these various related properties were derived for convenience in calculating other thermochemical quantities of the peroxide-water mixtures as illustrated below. These derived functions are defined in Table II and their numerical values are given in concentration steps of $10w_p$. For these calculations the following constants were used: oxygen, $C_p = 6.97$; water vapor, $C_p = 7.98$; hydrogen peroxide vapor, $C_p = 10$ cal./deg. mole (11).

TABLE II
SMOOTHED VALUES OF THE AVERAGE HEAT CAPACITIES AND RELATED PROPERTIES
OF H_2O - H_2O_2 MIXTURES BETWEEN 0° AND 26.9°

Concentration		C_p	$\Delta_m C_p^a$	ΔC_p^b	$D_m C_p^c$	$\theta_m C_p^d$	θC_p^e
$100 w_p$	$100 N_p$	cal./deg. mole solution		cal./deg. mole H_2O_2	cal./deg. mole solution		cal./deg. mole H_2O_2
0	0	18.06	0	-8.90	-10.0 ₈	0	9.1
10	5.6	17.87	-0.38	-6.72	-9.7 ₈	0.39	6.92
20	11.7	17.88	-0.57	-4.84	-9.6 ₈	0.59	5.04
30	18.5	18.04	-0.63	-3.41	-9.6 ₈	0.66	3.57
40	26.1	18.27	-0.65	-2.50	-9.7 ₇	0.70	2.68
50	34.6	18.61	-0.59	-1.71	-9.9 ₄	0.66	1.91
60	44.3	19.00	-0.52	-1.18	-10.1 ₄	0.60	1.35
70	55.3	19.48	-0.40	-0.73	-10.3 ₈	0.51	0.92
80	67.9	19.99	-0.31	-0.46	-10.6 ₈	0.44	0.65
90	82.7	20.62	-0.16	-0.19	-10.9 ₈	0.32	0.38
100	100	21.35	0	0	-11.3 ₈	0.19	0.19

$$^a \Delta_m C_p = C_p(\text{solution}) - N_w C_p(H_2O, l) - N_p C_p(H_2O_2, l) = N_p \Delta C_p.$$

$$^b \Delta C_p = (1+n)C_p(\text{solution}) - nC_p(H_2O, l) - C_p(H_2O_2, l).$$

$$^c D_m C_p = N_w C_p(H_2O, g) + N_p C_p(H_2O_2, g) - C_p(\text{solution}).$$

$$^d \theta_m C_p = C_p(H_2O, l) + \frac{1}{2} N_p C_p(O_2, g) - C_p(\text{solution}) = N_p \theta C_p.$$

$$^e \theta C_p = (1+n)C_p(\text{solution}) - (1+n)C_p(H_2O, l) - \frac{1}{2} C_p(O_2, g).$$

Heat of Mixing

Previous measurements of this quantity reported in the open literature are, in chronological order, those of de Forcrand (3), of Roth, Grau, and Meichsner (13), of Evans and Uri (4), and of Kubaschewski and Weber (10). However they covered only a narrow concentration range and the experimental conditions were not always fully stated. For the present work two different experimental techniques were tried in succession. In the first one (experimenter M.) two small test tubes, one fitting inside the other, were used. The inner tube containing the peroxide solution had a very thin bottom so that it could easily be broken with a glass rod that also served as a stirrer. It was

noticed that the thermal leak was always slightly greater after the mixing owing to a slight decomposition of the peroxide by the glass fragments. However, the difference was small (of the order of 0.5 cal./hr.) and the correction was applied from the instant of mixing.

In the second method (experimenter K.), which was applied only to measurements in the diphenyl ether calorimeter, the water was added to the peroxide solution in a small test tube from a long pipette fitted with a rubber bulb. Care was taken that the tip of the pipette did not touch the inside walls of the test tube nor the peroxide solution. The tip of the pipette was formed into a thick-walled capillary and it was coated with a thin film of Halocarbon grease to reduce the size of the drops and prevent them from creeping up the outer wall of the pipette. The amount of water added was determined by difference weighing. To prevent drops of water from falling prematurely into the peroxide solution the pipette was warmed a little before it was filled with water and weighed. Stirring was achieved by means of a small glass-enclosed magnet (Alnico alloy) resting in the peroxide solution. A similar magnet was placed in the bottom of the calorimeter well and so oriented that it repelled the magnet in the test tube. Raising and lowering the latter provided sufficient

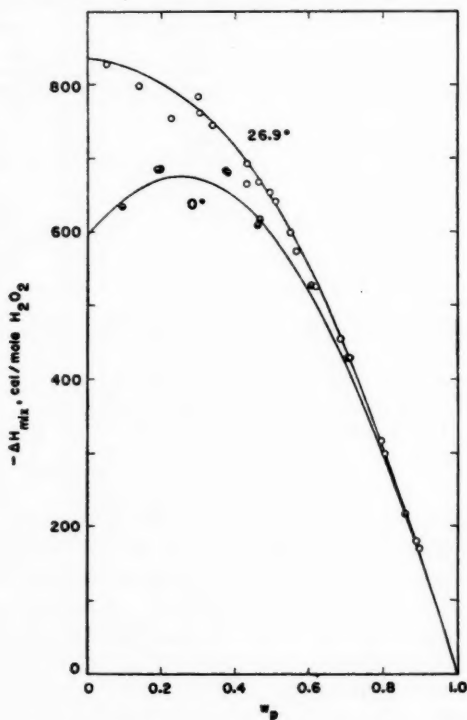


FIG. 2. Heat of mixing of hydrogen peroxide and water at 0° and 26.9° C.

stirring. The progress of the mixing operation could be followed visually to some extent by observing the "schlieren" in the solution but the only safe indication that the mixing was complete was the thermal leak of the calorimeter as shown by the movement of the mercury in the capillary (7).

A run lasted about two hours including the determination of the heat leak of the calorimeter after the reaction. The final concentration of the solution was checked by means of the refractive index; the agreement with the calculated composition was always good. The maximum amount of liquid that could be accommodated in the test tube was only 3 ml. For that reason most of the determinations were carried out with concentrated solutions of peroxide in order to have a good precision on the calorimetric measurements. This had the advantage of minimizing the importance of extrapolation to 100% hydrogen peroxide. On the other hand, it increased the uncertainty at low concentrations because the curve flattens out then (Fig. 2) and the differential heat effect becomes progressively smaller. On recalculating to one mole of peroxide the

TABLE III
EXPERIMENTAL DATA ON THE HEAT OF MIXING OF HYDROGEN PEROXIDE AND WATER

Concentration, 100 w_p		Weight of initial solution, gm.	Heat effect measured cal./mole	Correction applied H_2O_2	$-\Delta H_{mix}$, cal./mole H_2O_2	$-\Delta_m H_{mix}$, cal./mole solution
Initial	Final					
<i>At 0°</i>						
98.7	86.0	2.3589	195	21	216	165
99.4	70.2	1.4583	417	11	428	238
99.4	60.5	0.9868	515	11	526	236
98.7	46.3	2.0358	594	21	615	193
99.4	45.9	0.7660	597	11	608	188
99.4	38.1	0.4854	669	11	680	167
99.4	37.2	0.8316	670	11	681	163
99.4	19.7	0.9546	672	11	683	79
99.4	19.1	0.6033	672	11	683	76
24.5	9.3	1.5709	-42	675	633	33
<i>At 26.9°</i>						
98.7*	89.7	4.9856	148	21	169	139
98.7*	88.9	5.2199	158	21	179	145
97.6†	80.3	1.5465	257	42	299	205
98.7*	79.4	3.0715	297	21	318	213
98.7*	71.0	2.7033	408	21	429	242
88.3†	68.2	1.5431	263	190	453	241
98.7*	62.0	1.8583	504	21	525	244
68.2†	56.5	1.9985	107	465	572	233
98.7*	54.9	1.8496	578	21	599	235
98.7*	50.3	1.8718	622	21	643	224
98.7*	49.6*	2.1562	631	21	652	224
99.4†	46.2	0.8782	657	12	669	209
99.4†	42.9	0.7754	653	12	665	189
98.7*	42.8	1.5030	672	21	693	197
99.3†	33.9	0.8103	734	12	746	160
98.7*	30.1	1.1420	740	21	761	142
99.3†	30.0	0.5437	775	12	787	146
99.3†	22.6	0.4621	739	12	751	101
98.7*	14.0	0.6854	777	21	798	63
98.7*	5.3	0.2939	807	21	828	24

*Observer M.

†Observer K.

experimental error is magnified gradually, so that it is quite large at zero concentration of peroxide.

The experimental results given in Table III refer to both one mole of peroxide, ΔH_{mix} , and one mole of solution, $\Delta_m H_{\text{mix}} = N_p \cdot \Delta H_{\text{mix}}$, as is customary. Graphical extrapolation led to 834 cal./mole for the heat of mixing of the pure peroxide to infinite dilution at 26.9° C. and from this, the correction to be applied to each determination was computed. The results at 26.9° were taken as the basis of the correlation for the following reasons. They are twice as numerous as those at 0° and they were obtained by two different experimenters using two different techniques in one of which, at least, errors due to decomposition of the peroxide were successfully eliminated. Then the measurements were made at a later stage when more experience had been gained. Finally the diphenyl ether calorimeter is more than three times as sensitive as the ice calorimeter and its performance has also been found to be somewhat more regular and reliable.

A set of smoothed values of the heat of mixing at 26.9° were obtained by interpolation and extrapolation from the composite aggregate. As may be seen in Fig. 2 the majority of experimental points fit very closely to the smoothed curve. By means of the equations

$$[1] \quad \Delta H_{\text{mix}}(T^\circ \text{ C.}) = \Delta H_{\text{mix}}(26.9^\circ \text{ C.}) - \Delta C_p \cdot \Delta T$$

and

$$[2] \quad \Delta_m H_{\text{mix}}(T^\circ \text{ C.}) = \Delta_m H_{\text{mix}}(26.9^\circ \text{ C.}) - \Delta_m C_p \cdot \Delta T,$$

where ΔT is the temperature interval from 26.9° and the terms ΔC_p and $\Delta_m C_p$ are taken from Table II, the smoothed values of the heat of mixing given in Table IV were obtained. It may be pointed out here that recalculation of the

TABLE IV
SMOOTHED VALUES OF THE HEAT OF MIXING OF H_2O AND H_2O_2 AT 0° AND 25°

Concentration, 100 w_p	ΔH_{mix} , cal./mole H_2O_2		$\Delta_m H_{\text{mix}}$, cal./mole solution	
	0°	25°	0°	25°
0	597	819	0	0
10	644	812	36	45
20	671	792	79	93
30	671	757	124	140
40	645	707	168	185
50	598	641	207	222
60	518	548	230	243
70	419	438	232	242
80	297	308	202	209
90	158	163	130	135
100	0	0	0	0

data to 0° C. involves no great uncertainty since it does not require knowledge of the instantaneous values of the heat capacity of the solutions, the enthalpy changes having been measured directly between the two very same temperatures. The fit of experimental points to the calculated curve at 0° is not especially good (Fig. 2). In particular it is strange that the two points showing the

greatest discrepancy were duplicated closely. A similar situation occurred in previous measurements of the heat of decomposition (5) and must have originated in the performance of the ice calorimeter.

A plot of the heat of mixing per mole of solution shows that the curve for 26.9° is nearly symmetrical with respect to the axis $N = 0.5$ (Fig. 4). In fact a general second-degree equation derived from all the experimental results in Table III exhibited no significant departure from a symmetrical form. Considering the exceptional nature of the hydrogen peroxide - water mixtures this property is interesting. The dotted line in Figs. 3 and 4 refers to the equation derived by Scatchard, Kavanagh, and Ticknor (14) from their vapor pressure measurements. Their expression

$$[3] \quad \Delta_m H_{mix} = N_p N_w [-1017 + 85(N_p - N_w) + 13(N_p - N_w)^2]$$

leads to much too high values, especially for dilute peroxide solutions, but this is not surprising as the numerical coefficients were chosen in such a way as to give an equation independent of temperature. These authors felt that the accuracy of their measurements did not warrant calculation of the variation of the heat of mixing with temperature. They pointed out that their equation

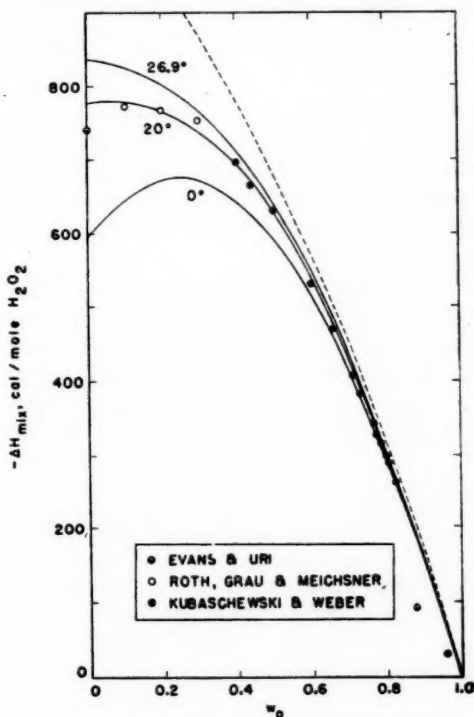


FIG. 3. Comparison of various published data for the heat of mixing of hydrogen peroxide and water with the present ones recalculated to 20° (solid curve).

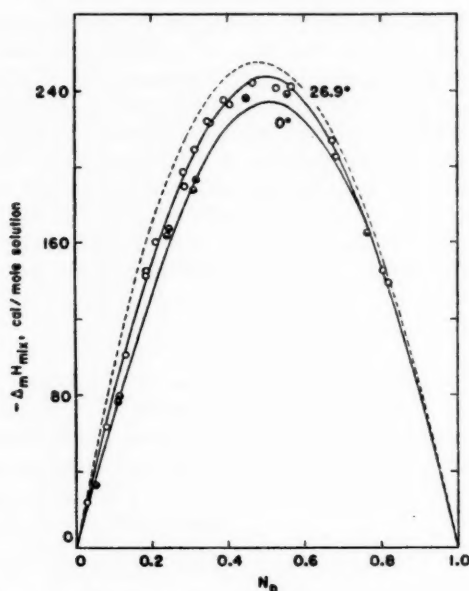


FIG. 4. Heat of mixing, per mole of solution, of hydrogen peroxide and water at 0° and 26.9° C.

should yield more correct values of the heat of mixing in the temperature range of their vapor pressure measurements, namely 60° to 90° C., and this is borne out by the trend of the curves in Fig. 3.

Heat of Vaporization

Measurements of the heat of vaporization at 26.9° were carried out as described before (5) and mostly with concentrated solutions in order to secure a reliable value for the pure peroxide. The quantity obtained by extrapolation, 12,315 cal./mole, was combined with the heat of mixing to obtain the heat of vaporization at various concentrations. Agreement with the experimental results (in Table V) is very good in all cases, the maximum deviation (at

TABLE V
HEAT OF VAPORIZATION OF $H_2O-H_2O_2$ MIXTURES MEASURED AT 26.9°

Concentration, 100 w_p	$\Delta_m H_{vap}$ (expt.), cal./gm. solution	$\Delta_m H_{vap}$ (expt.) kcal./mole solution	$\Delta_m H_{vap}$ (calc.)
99.3	363.7*	12.30	12.30
98.4	366.5†	12.29	12.28
87.4	394.9	12.08	12.08
74.2	428.4	11.86	11.82
48.1	485.3	11.20	11.30

*Average of three determinations.

†Average of four determinations.

74.2% H_2O_2) being less than 0.3%. From these data smoothed values were obtained for 0° and 25° by means of the equation

$$[4] \quad \Delta_m H_{\text{vap}}(T^\circ \text{C.}) = \Delta_m H_{\text{vap}}(26.9^\circ \text{C.}) - D_m C_p \cdot \Delta T.$$

Here again (Table VI) excellent agreement is found with the quantity previously reported for pure hydrogen peroxide at 0°, 12.59 kcal./mole (5).

TABLE VI
CALCULATED VALUES OF THE HEAT OF VAPORIZATION
OF H_2O - H_2O_2 MIXTURES

Concentration, 100 w_p	$\Delta_m H_{\text{vap}}$, kcal./mole solution	
	0°	25°
0	10.76	10.51
10	10.90	10.66
20	11.06	10.81
30	11.23	10.99
40	11.41	11.17
50	11.61	11.36
60	11.81	11.56
70	12.02	11.76
80	12.23	11.96
90	12.43	12.15
100	12.62	12.34

Heat of Decomposition

In view of the difficulties encountered previously with a solid catalyst a colloidal solution of platinum was used this time. It allows a better control of the reaction rate, especially at the beginning, and complete decomposition is more easily achieved. Any dilution effect of the platinum sol must be entirely negligible in the present conditions. The colloidal suspension was prepared after the classical method of Bredig (1) in which an electric arc is struck between platinum wires immersed in distilled water. The circuit comprised a 150-volt battery in series with a 90-ohm shunt and a 22-henry inductance. Because the latter was too low for stable performance the arc lasted only 15–20 sec. at a time. The brownish suspension of platinum was filtered to remove all coarse particles and diluted to a suitable concentration. Then it was placed in a small pipette closed by a stopcock and protected by a tiny glass tube over the tip to prevent drops of the catalyst from falling prematurely in the peroxide solution. The latter was contained in a small test tube in the central well of the calorimeter. Once thermal equilibrium was reached the pipette was taken out of the protective tube and the colloidal solution was added dropwise, very slowly at first, to secure a reasonable reaction rate. Analysis of the residue confirmed that in all cases decomposition was complete. In between runs it was necessary to clean the test tube with aqua regia as otherwise the sample of peroxide decomposed spontaneously owing to traces of platinum adsorbed on the glass.

The results of seven determinations (by experimenter M.) are compared in Table VII with values calculated from the heat of mixing and the heat of

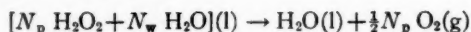
TABLE VII
 HEAT OF DECOMPOSITION OF $\text{H}_2\text{O}-\text{H}_2\text{O}_2$ MIXTURES MEASURED AT 26.9°

Concentration, 100 w_p	$-\Delta H_{\text{dec}}(\text{expt.})$	$-\Delta H_{\text{dec}}(\text{calc.})^*$ kcal./mole peroxide	$-\Delta H_{\text{dec}}(\text{calc.})^\dagger$	$-\Delta_m H_{\text{dec.}}$ kcal./mole solution
24.64	22.66	22.65	23.45	3.35
24.72	22.64	22.65	23.43	3.37
25.10	22.66	22.65	23.45	3.42
49.6	22.79	22.79	23.44	7.83
74.2	23.01	23.05	23.39	13.94
98.5	23.44	23.42	23.46	22.77
98.6	23.42	23.42	23.43	22.82
100	—	Average	23.44 ± 0.02	—

*Of solution at initial concentration w_p .

†Of pure hydrogen peroxide.

decomposition of the pure peroxide averaged from extrapolations of each experimental result (in the fourth column). The latter quantities agree among themselves to within ± 20 cal. except for that at 74.2% H_2O_2 for which the rate of reaction was too fast. When the present results are compared with those of previous authors (5, 12, 13) the only serious discrepancies arise from some of the preliminary measurements of Foley and Giguère considered doubtful at the time. As was done for the other calorimetric properties smoothed values of the heat of the chemical reaction



were calculated for 0° and 25° C. by means of the equations

$$[5] \quad \Delta H_{\text{dec}}(T^\circ \text{C.}) = \Delta H_{\text{dec}}(26.9^\circ \text{C.}) - \theta C_p \cdot \Delta T$$

and

$$[6] \quad \Delta_m H_{\text{dec}}(T^\circ \text{C.}) = \Delta_m H_{\text{dec}}(26.9^\circ \text{C.}) - \theta_m C_p \cdot \Delta T;$$

these values are shown in Table VIII. The quantities thus found for 0° were deemed more reliable than any obtainable from direct determinations with the

 TABLE VIII
 HEAT OF DECOMPOSITION OF $\text{H}_2\text{O}-\text{H}_2\text{O}_2$ MIXTURES AT 0° AND 25°
 CALCULATED FROM EXPERIMENTAL DATA AT 26.9°

Concentration, 100 w_p	$-\Delta H_{\text{dec.}}$ kcal./mole H_2O_2		$-\Delta_m H_{\text{dec.}}$ kcal./mole solution	
	0°	25°	0°	25°
0	22.84	22.62	0.0	0.0
10	22.80	22.62	1.28	1.27
20	22.77	22.64	2.66	2.65
30	22.77	22.68	4.21	4.20
40	22.80	22.73	5.95	5.93
50	22.84	22.80	7.90	7.89
60	22.92	22.89	10.15	10.14
70	23.02	23.00	12.73	12.72
80	23.14	23.13	15.71	15.70
90	23.28	23.27	19.26	19.25
100	23.44	23.44	23.44	23.44

ice calorimeter. As has been remarked before (6) the heat of decomposition of pure hydrogen peroxide in the liquid state is practically temperature-independent.

THE SYSTEM $D_2O-D_2O_2$

The same general pattern was followed in measuring the thermochemical properties of the deuterium compounds except that no determinations of the heat of decomposition were carried out because the amount of isotopic material needed would have been prohibitive. Instead, this quantity was calculated from the corresponding one for hydrogen peroxide and the zero-point energy difference of the two molecules (11). This method (details to be published later) leads, no doubt, to more reliable results than could be achieved experimentally at present. On the whole the calorimetric measurements for the deuterium system of compounds were fewer and less accurate than for the hydrogen compounds because of the difficulty and cost of preparation of deuterium peroxide. In fact this compound has been available in convenient quantities only since the application of the electrodeless discharge method (8).

TABLE IX
ENTHALPY CHANGES, BETWEEN 0° AND 26.9° , OF $D_2O-D_2O_2$ MIXTURES

Concentration, 100 w_p	Weight of solution, gm.	Heat effect measured, cal./gm. solution	c_p , cal/deg. gm. solution
0	5.0822	27.33	1.016
0	5.0822	27.30	
30.46	3.6664	23.25	0.864
40.7	4.5892	22.17	0.825
40.7	4.5892	22.18	
74.2	4.5865	19.21	0.714
74.2	4.5865	19.20	

TABLE X
SMOOTHED VALUES OF THE AVERAGE HEAT CAPACITIES OF $D_2O-D_2O_2$ MIXTURES
BETWEEN 0° AND 26.9°

Concentration, D_2O_2		C_p cal./deg. mole solution	$\Delta_m C_p^a$ cal./deg. mole solution	ΔC_p^b cal./deg. mole D_2O_2	$D_m C_p^c$ cal./deg. mole solution
100 w_p	100 N_p				
0	0	20.3 ₃	0	-9.00	-12.2 ₂
10	5.81	20.1 ₀	-0.40	-6.88	-11.8 ₁
20	12.19	19.9 ₉	-0.67	-5.50	-11.5 ₂
30	19.23	20.0 ₂	-0.83	-4.32	-11.3 ₇
40	27.02	20.1 ₄	-0.88	-3.26	-11.3 ₀
50	35.71	20.3 ₉	-0.87	-2.44	-11.2 ₉
60	45.45	20.7 ₀	-0.82	-1.80	-11.3 ₂
70	56.45	21.1 ₁	-0.69	-1.22	-11.4 ₄
80	68.96	21.6 ₂	-0.51	-0.74	-11.6 ₁
90	83.33	22.2 ₅	-0.24	-0.29	-11.8 ₅
100	100	22.9 ₂	-0	0	-12.0 ₇

^{a, b, c} See Table II for definitions.

Heat Capacity

Three solutions only were measured (Table IX) as the highest concentration of deuterium peroxide available at the time was about 75%. Two determinations with liquid heavy water (99.6% D_2O) gave a value within 1% of that extrapolated from the most recent data (2). As could be expected the experimental points fall on a curve nearly parallel to that for the hydrogen compounds (Fig. 1). This property was relied upon to extrapolate the curve to 100% D_2O_2 . A set of smoothed values of C_p (Table X) were obtained from a large-scale plot. The mean heat capacity of heavy water vapor was taken as 8.13 (9), and that of deuterium peroxide vapor, as 11 cal./deg. mole (11).

Heat of Mixing

The second of the above-described methods was followed for measuring the heat of mixing of deuterium peroxide and heavy water at 26.9° C. As shown in Table XI and Fig. 5 the data are quite extensive, covering the composition range from 98.3% D_2O_2 (the highest concentration ever obtained) for the initial solution, to 7.1% for the most dilute solution. Smoothed values of the heat of

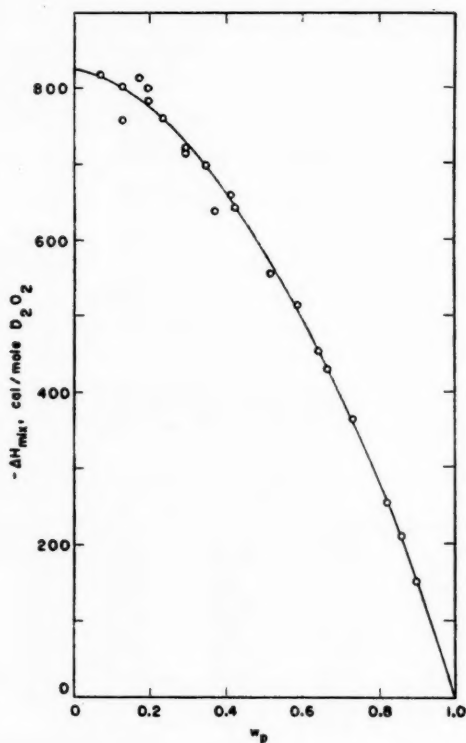


FIG. 5. Heat of mixing at 26.9° C. for the system D_2O - D_2O_2 .

TABLE XI

HEAT OF MIXING OF DEUTERIUM PEROXIDE AND HEAVY WATER AT 26.9°

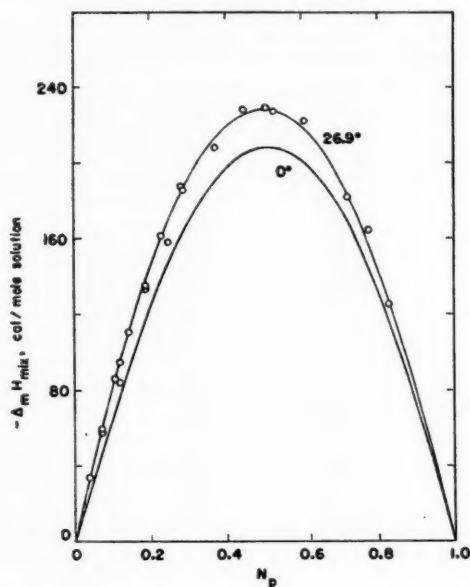
Concentration, 100 w_p		Weight of initial solution, gm.	Heat effect measured	Correction applied cal./mole H_2O_2	$-\Delta H_{mix}$	$-\Delta_m H_{mix}$, cal./mole solution
Initial	Final					
98.3	89.8	2.5190	116	35	151	125
96.6	86.2	2.5689	151	60	211	164
97.0	82.3	2.3050	206	47	253	182
96.6	73.7	1.3482	305	60	365	222
91.0	66.8	1.5401	290	140	430	227
97.0	64.7	1.5836	407	47	454	229
91.0	59.1	1.2938	372	140	512	228
91.0	52.0	1.4379	414	140	555	208
91.0	42.3	1.0702	502	140	642	186
91.0	41.7	0.9641	526	140	660	188
91.0	37.3	0.7956	498	140	638	158
92.6	35.0	0.9318	571	130	701	161
91.0	29.5	0.7595	575	140	715	135
92.0	29.5	0.7509	587	135	722	136
91.2	23.5	0.6828	622	138	760	111
92.0	19.8	0.4617	647	135	782	84
92.0	19.5	0.5502	665	135	800	95
91.2	17.6	0.4828	674	138	812	86
91.2	13.1	0.3359	620	138	758	58
91.2	12.6	0.3286	665	138	803	59
91.2	7.1	0.1749	681	138	819	34

TABLE XII

SMOOTHED VALUES OF THE HEAT OF MIXING OF D_2O AND D_2O_2 AT 0° AND 25°

Concentration, 100 w_p	ΔH_{mix} , cal./mole D_2O_2		$\Delta_m H_{mix}$, cal./mole solution	
	0°	25°	0°	25°
0	582	807	0	0
10	625	797	36	46
20	630	767	77	94
30	612	720	118	138
40	573	655	155	177
50	519	580	186	207
60	447	493	203	223
70	363	394	205	223
80	262	281	180	193
90	142	150	118	125
100	0	0	0	0

mixing were calculated as in the case of the hydrogen peroxide - water system; obviously, the uncertainty of these quantities (Table XII) is greater than for the hydrogen compounds. It is interesting to note that the heat of mixing of the D_2O - D_2O_2 system is smaller than that of the H_2O - H_2O_2 system contrary to the other calorimetric properties. The difference is particularly marked for the $\Delta_m H_{mix}$ function (Fig. 6). The significance of this situation will be considered later in the light of other associative properties of the two binary systems.

FIG. 6. Heat of mixing, per mole of solution, for D_2O - D_2O_2 mixtures.*Heat of Vaporization*

This quantity was the only one measured both at 0° and 26.9° C. for the deuterium compounds. The latter set of data (Table XIII) were used for

TABLE XIII
HEAT OF VAPORIZATION OF D_2O - D_2O_2 MIXTURES MEASURED AT 0° AND 26.9°

Concentration, 100 w_D	$\Delta_m H_{vap}(\text{expt.}),$ cal./gm. solution	$\Delta_m H_{vap}(\text{expt.})$ kcal./mole solution	$\Delta_m H_{vap}(\text{calc.})$
<i>At 0°</i>			
93.0	371.4	12.69	12.70
93.0	368.1	12.56	12.70
49.2	461.4	11.84	11.93
22.2	514.4	11.43	11.48
8.1	541.0	11.24	11.26
<i>At 26.9°</i>			
96.5	354.4	12.43	12.43
94.4	359.4	12.40	12.40
81.0	388.4	12.15	12.18
55.0	442.0	11.71	11.71
53.9	442.2	11.65	11.69
47.0	454.0	11.51	11.57
22.2	498.4	11.09	11.15
8.1	526.4	10.94	10.94

TABLE XIV
SMOOTHED VALUES OF THE HEAT OF VAPORIZATION OF
D₂O-D₂O₂ MIXTURES

Concentration, 100 w _p	$\Delta_m H_{vap}$, kcal./mole solution	
	0°	25°
0	11.15	10.84
10	11.28	10.98
20	11.43	11.14
30	11.58	11.30
40	11.75	11.47
50	11.93	11.64
60	12.10	11.82
70	12.29	12.00
80	12.47	12.18
90	12.65	12.35
100	12.81	12.51

calculating the smoothed values at 0° and 25° (Table XIV) from the heat of mixing and the heat of vaporization of pure deuterium peroxide found by extrapolation. As in the case of water, isotopic substitution by deuterium raises the heat of vaporization of hydrogen peroxide, the effect (170 cal./mole) being about half of that for water (330 cal./mole).

CONCLUSIONS

The present thermochemical data for hydrogen peroxide and its mixtures with water are recommended as superseding previous values because they are based on extensive series of calorimetric measurements closely intercorrelated. The heat of decomposition and heat of vaporization were determined directly on very concentrated solutions in order to arrive at accurate values of these quantities for the pure peroxide. Numerous determinations of the heat of mixing enabled interpolation over the whole concentration range. Finally, from the heat capacities of the mixtures it is possible to recalculate the various properties with fair accuracy over a moderate temperature interval. Although, in general, the calorimetric measurements were executed in such a way as to yield the maximum of internal consistency, it must be remembered, in using the new data, that they are not all known to the same degree of accuracy.

As for the system D₂O-D₂O₂, the above measurements provide us not only with the thermodynamic properties of the pure peroxide, but also with comprehensive data on an isotopic system of compounds, the only one, no doubt, thus investigated so far. In a following paper of this series we intend to present a discussion of these two binary systems from the point of view of the existing theories of solutions of non-electrolytes, together with recalculated values of the excess functions and other associative properties.

ACKNOWLEDGMENT

The authors are grateful to the National Research Council for financial assistance and to Mr. R. L. Wentworth of the Massachusetts Institute of Technology for helpful suggestions.

RÉSUMÉ

On a mesuré à 0° C. dans un calorimètre à glace, et à 26.9° dans un calorimètre à oxyde de phényle les propriétés thermochimiques suivantes de mélanges de peroxyde d'hydrogène et d'eau à différentes concentrations: chaleur spécifique, chaleur de vaporisation, et chaleur de mélange. Des mesures semblables ont ensuite été effectuées sur les composés isotopiques, peroxyde de deutérium et eau lourde. La chaleur de décomposition du peroxyde d'hydrogène catalysée par le platine colloïdal a été déterminée de nouveau avec précision. Par corrélation interne de ces données on est arrivé à un système de fonctions et d'équations permettant de calculer les quantités thermochimiques à toute concentration et sur un intervalle de température modéré.

Outre leur intérêt pratique les nouveaux résultats sont importants du point de vue de la théorie des solutions de liquides associés.

REFERENCES

1. BREDIG, G. Z. Elektrochem. 4: 514. 1898.
2. COCKETT, A. H. and FERGUSON, A. Phil. Mag. 29: 185. 1940.
3. DE FORCRAND, R. Ann. chim. et phys. 15(8): 433. 1908.
4. EVANS, M. G. and URI, N. Trans. Faraday Soc. 45: 224. 1949.
5. FOLEY, W. T. and GIGUÈRE, P. A. Can. J. Chem. 29: 895. 1951.
6. GIGUÈRE, P. A. Can. J. Research, B, 28: 485. 1950.
7. GIGUÈRE, P. A., MORISSETTE, B. G., and OLMOS, A. W. Can. J. Chem. 33: 657. 1955.
8. GIGUÈRE, P. A., SECCO, E. A., and EATON, R. S. Discussions Faraday Soc. No. 14: 104. 1953.
9. KIRSCHENBAUM, I. Physical properties and analysis of heavy water. McGraw-Hill Book Company, Inc., New York. 1951.
10. KUBASCHEWSKI, O. and WEBER, W. Z. Elektrochem. 54: 200. 1950.
11. LIU, I. D. Ph.D. Thesis, Laval University, Quebec, Que. 1954.
12. MATHESON, G. L. and MAASS, O. J. Am. Chem. Soc. 51: 674. 1929.
13. ROTH, W. A., GRAU, R., and MEICHNER, R. Z. anorg. u. allgem. Chem. 193: 161. 1930.
14. SCATCHARD, G., KAVANAGH, G. M., and TICKNOR, L. B. J. Am. Chem. Soc. 74: 3715. 1952.
15. SCHUMB, W. C., SATTERFIELD, C. N., and WENTWORTH, R. L. Hydrogen peroxide. Mass. Inst. Technol. Rept. No. 43. 1953.

COMBINATION AND DISPROPORTIONATION OF ETHYL RADICALS: INFLUENCE OF THE REACTION $H + C_2H_5 = C_2H_6$ ¹

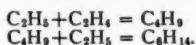
BY MOYRA J. SMITH,² PATRICIA M. BEATTY,³ J. A. PINDER, AND D. J. LE ROY

ABSTRACT

The mercury (¹⁹⁹P₁) photosensitized hydrogenation of ethylene has been studied at room temperature as a function of ethylene concentration, mercury concentration, and light intensity. In addition to combination and disproportionation, ethyl radicals have been shown to take part in the reaction



The conditions favoring this reaction have been established and anomalous values previously found for the ratio of ethane to butane have been explained. The value obtained for the ratio of the rate constants for the disproportionation and combination of ethyl radicals, 0.15 ± 0.01 , is in excellent agreement with the values obtained by other methods. Hexane formation is of some importance at low light intensities and high ethylene concentrations, and is adequately accounted for by the reactions



INTRODUCTION

It is now generally agreed that in systems containing ethyl radicals both combination and disproportionation will take place. From the variety of data discussed by Steacie (13) it is clear that in some instances it is not justifiable to equate the ratio of the rate constants for disproportionation and combination, k_4/k_3 , to $(C_2H_6)/(C_4H_{10})$, $(C_2H_4)/(C_4H_{10})$, or to $\frac{1}{2}((C_2H_6) + (C_2H_4))/(C_4H_{10})$ because of the occurrence of secondary reactions which consume ethylene or because the products may be formed in some other way. When these factors are taken into account both reactions appear to have small or negligible activation energies and steric factors not greatly different from unity (6). Nevertheless, in the case of the mercury photosensitized hydrogenation of ethylene there are differences in the apparent value of k_4/k_3 at room temperature which are greater than the experimental errors.

There is little doubt that the basic mechanism of the reaction at room temperature is the following:



However, from the amounts of ethane and butane formed Moore and Taylor (11) found k_4/k_3 to be 0.17, while Le Roy and Kahn (9) found values ranging from 0.22 to 0.61. In their recent study of the mercury photosensitized hydrogenation of acetylene Cashion and Le Roy (4) found evidence for reactions [3] and [4], although the ratio $(C_2H_6)/(C_4H_{10})$ varied from 0.77 to 1.25.

¹Manuscript received January 27, 1965.

Contribution from the Department of Chemistry, University of Toronto, Toronto, Ontario.

²Present address: Somerville College, Oxford.

³Present address: Division of Applied Chemistry, National Research Council, Ottawa, Ontario.

The latter authors suggested that in systems containing atomic hydrogen, as well as ethyl radicals, "high" values of the ratio might be obtained because of the following reactions:



This set of reactions was first postulated by Darwent and Steacie (5) in order to explain their results on the mercury photosensitized decomposition of ethane. The over-all reaction



would be more likely to occur at high pressures, while the over-all reaction



would be more likely to occur at low pressures. Nevertheless, even at the low pressures (*ca.* 0.5 mm.) used in the Wood-Bonhoeffer discharge method there is some evidence that D atoms will add to ethyl radicals by the analogue of reaction [8] (14, 15). Berlie and Le Roy (2) studied the reaction of H atoms with ethane in a manner which made it possible to detect the occurrence of reaction [8], and their results indicate that it takes place to some extent at pressures as low as 5 mm.

In the present investigation we have been able to show that reaction [8] is of considerable importance in the mercury photosensitized hydrogenation of ethylene at room temperature and that when it is taken into account a value of k_4/k_3 may be obtained which is in good agreement with the most reliable values obtained by other methods.

The following *local* rate equations are obtained for the mechanism consisting of reactions [1], [2], [3], and [4]:

$$d(\text{C}_2\text{H}_6)/dt = k_4 I_a / (k_3 + k_4) \quad [\text{i}]$$

$$d(\text{C}_4\text{H}_{10})/dt = k_3 I_a / (k_3 + k_4). \quad [\text{ii}]$$

It follows that the ratio of the final concentrations, $(\text{C}_2\text{H}_6)_f/(\text{C}_4\text{H}_{10})_f$, should be independent of light intensity and the concentrations and equal to k_4/k_3 .

If reactions [5], [6], and [7] are included in the mechanism the *local* rate equations cannot be solved explicitly unless certain approximations are made. Most of the present experiments were carried out with total pressures of the order of 220 mm., and the carbon balances indicated that reaction [6] was of no importance. The net effect of reactions [5] and [7] will be the consumption of H atoms and ethyl radicals by reaction [8]. Two limiting conditions then arise: (A) the rate of reaction [8] is sufficiently small that the relative concentrations of H atoms and ethyl radicals are not appreciably affected by its occurrence, and (B) the rate of [8] is sufficiently large that it controls the ethyl radical concentration.

For the limiting condition (A) it can be shown that

$$\frac{d(\text{C}_2\text{H}_6)/dt}{d(\text{C}_4\text{H}_{10})/dt} = \frac{k_4}{k_3} + \frac{2k_3(k_3 + k_4)^{1/2} I_a^{1/2}}{k_2 k_3 (\text{C}_2\text{H}_4)}. \quad [\text{iii}]$$

This equation applies to *local* rates and cannot be integrated rigorously without a knowledge of the spatial distribution of I_a and of the radical concentrations. It is possible to calculate I_a as a function of the distance from the front window of the cell from a knowledge of the mercury concentration and the extinction coefficients for the absorption of 2537 Å radiation (which vary across the width of the absorption line), but the calculation can only be carried out for an assumed form for the emission line from the lamp. The rates of diffusion of the various species would also have to be taken into account. The spatial integration of [iii] is therefore fraught with a considerable amount of difficulty. Nevertheless, if a number of experiments are carried out with the same lamp, and using the same mercury concentration, the spatial distribution of I_a will remain constant, and under these conditions it will probably be justifiable to integrate [iii] with respect to time, viz.,

$$\frac{(C_2H_6)_f}{(C_4H_{10})_f} = \frac{k_4}{k_3} + \frac{4.606 k_8 (k_3 + k_4)^{\frac{1}{2}} I_a^{\frac{1}{2}}}{-\Delta(C_2H_4) k_2 k_3} \log \frac{(C_2H_4)_0}{(C_2H_4)_f} \quad [\text{iv}]$$

The quantity I_a in this expression will be the effective average value of I_a .

The expression analogous to [iv] for the limiting condition (B) is

$$\frac{(C_2H_6)_f}{(C_4H_{10})_f} = \frac{3 k_8^2 I_a}{k_2^2 k_3} \cdot \frac{-\Delta(C_2H_4)}{(C_2H_4)_0^3 - (C_2H_4)_f^3} \quad [\text{v}]$$

If we set $(C_2H_4)_0/(-\Delta(C_2H_4)) = \sigma$, equation [v] may be written in the more convenient form,

$$\frac{(C_2H_6)_f}{(C_4H_{10})_f} = \frac{k_8^2 I_a}{k_2^2 k_3} \cdot \frac{1}{-\Delta(C_2H_4) \cdot (C_2H_4)_0(\sigma - 1 + 1/3\sigma)} \quad [\text{vi}]$$

For example, if a constant conversion of 50% is used in each experiment $(\sigma - 1 + 1/3\sigma)$ will be equal to 7/6.

EXPERIMENTAL

A number of exploratory experiments showed that $(C_2H_6)_f/(C_4H_{10})_f$ decreased when either the incident light intensity or the concentration of mercury in the cell was reduced. In both cases this would amount to a reduction of I_a which, in its rigorous definition, is the number of quanta absorbed per unit volume per unit time at a point in the reaction vessel. It was also found that the ratio of ethane to butane increased when the ethylene concentration was decreased at constant hydrogen pressure. Previous work had shown that below 200°C. the ratio was not sensitive to hydrogen pressure over the range from approximately 100 to 300 mm. (9).

Since the preliminary experiments appeared to bear out the predictions of the theory outlined above, a number of experiments were carried out to study in detail the effect of incident light intensity, mercury concentration, and ethylene pressure. In addition, some experiments were performed using a cell with an optical path length of approximately two millimeters. With such a cell the amount of surface exposed to H atoms and ethyl radicals would be

approximately doubled and surface reactions, if they occurred, would be enhanced.

All of the experiments were carried out at room temperature and all pressures were corrected to 25°C. Products were fractionated by low temperature distillation (8) and the C_2 fraction was analyzed for ethylene and ethane by the method of Pyke, Kahn, and Le Roy (12). For the experiments reported here the lamps were of the low pressure type with rare gas carrier; for such lamps the half-width of the emission line is somewhat greater than for a true resonance lamp (10) and the effective reaction zone will penetrate farther into the cell.

EFFECT OF INCIDENT LIGHT INTENSITY

These experiments were carried out in a static system using a 1 liter spherical cell with a plane Vicor window. Initial hydrogen pressures were approximately 180 mm., initial ethylene pressures were approximately 20.5 mm., and the average pressure drop was 10.7 mm. The incident light intensity was varied simply by changing the distance between the lamp and the cell; in this way the rate of pressure drop was varied from 1.42×10^{-3} to 163×10^{-3} mm. min⁻¹.

The values of I_e were unknown and hence the results could only be expressed in relative terms. The inverse square law would not be valid for a finite source and thus the distances from lamp to cell could not be used to obtain relative values of I_e . However, since all of the products are saturated $-\Delta(C_2H_4)$ will be equal to $-\Delta P$, and the rate of pressure drop will be equal to the rate of consumption of ethylene. The latter is equal to $(1 + k_3/(k_3 + k_4))I_e$ for the limiting condition (A), and to I_e for the limiting condition (B).

In Fig. 1 a plot of $(C_2H_6)_f/(C_4H_{10})_f$ against $[(-\Delta P)^{1/2}t]^{-1} \log[(C_2H_4)_0/(C_2H_4)_f]$ is shown; this corresponds to the use of equation [iv], i.e. to the limiting condition (A). It is seen that as I_e approaches zero $(C_2H_6)_f/(C_4H_{10})_f$ becomes linear in $I_e^{1/2}$. The intercept at $I_e = 0$ is 0.146, in good agreement with the values

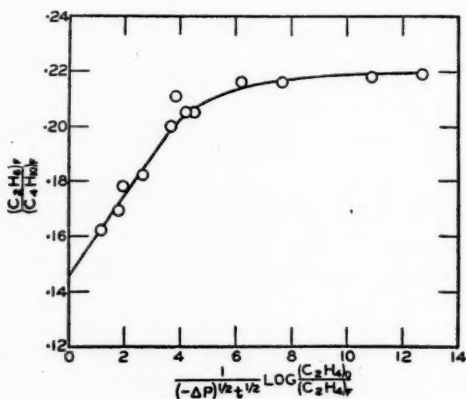


FIG. 1. Test of equation [iv] for variations in incident light intensity.

of k_4/k_3 obtained at room temperature by other methods (*vide* Table I). The decrease in slope which sets in at high light intensities (large values of the abscissa) is not predicted by the present mechanism; the curvature in Fig. 1 is opposite to that predicted on the assumption that the limiting condition (B) obtains at high light intensities. Because of the assumptions involved in the spatial integration of I_a this is not surprising. However, regardless of detailed mechanisms, it is obvious that reaction [8] should become negligible at low light intensities and that under these conditions $(C_2H_6)_f/(C_4H_{10})_f$ should approach k_4/k_3 .

EFFECT OF MERCURY CONCENTRATION

Even though we do not know the spatial distribution of I_a it is clear that a reduction in the mercury concentration in the cell will cause a decrease in the number of quanta absorbed in unit time in any unit volume. According to the present mechanism this should cause a decrease in $(C_2H_6)_f/(C_4H_{10})_f$. A number of experiments were performed with a circulating system in which the gases were passed through a trap containing mercury at temperatures ranging from 27°C. to -12°C. before entering the cell. In each case hydrogen pressures of approximately 220 mm. and ethylene pressures of approximately 17.5 mm. were used. The pressure decreases were not kept as close to 50% of the initial ethylene pressure as in the other experiments and ranged from 5.7 to 14 mm. The incident light intensity was kept constant by fixing the position of the lamp with respect to the cell window. As shown in Fig. 2, the ratio

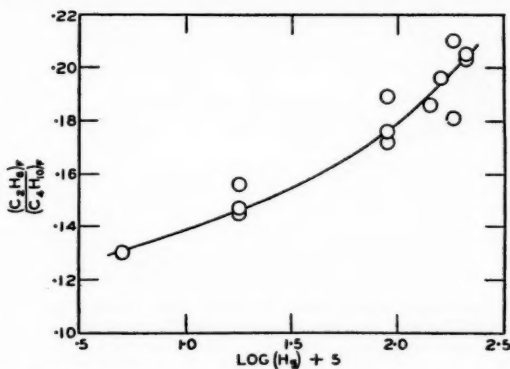


FIG. 2. Influence of the mercury concentration in the cell on the ethane/butane ratio.

$(C_2H_6)_f/(C_4H_{10})_f$ decreases as the mercury concentration is lowered, in agreement with the predictions of the present mechanism. It would be expected, of course, to approach a constant value, k_4/k_3 , as I_a tends toward zero.

EFFECT OF OPTICAL PATH LENGTH

Since, in a mercury photosensitization experiment, most of the light is absorbed very close to the entrance window, an increase in the ratio of the surface to the effective volume of the reaction zone can best be accomplished

by using a cell with a short optical path. The cell was constructed by blowing a bulb in the middle of a piece of quartz tubing and then heating and sucking in one side to form a concave cell with more or less parallel sides approximately two millimeters apart. The side arms of the cell were painted black.

A series of three experiments using this cell and four with a cell having an optical path length of about 10 cm. were made using a circulating system. The same distance between lamp and cell was used in each case. Initial hydrogen pressures were approximately 205 mm.; initial ethylene pressures were approximately 17.5 mm. With the small cell $(C_2H_6)_f/(C_4H_{10})_f$ was $0.22_9 \pm .00_6$; with the large cell it was $0.22_7 \pm .00_7$. It would therefore appear that surface reactions, if they do occur, have no influence on this ratio.

EFFECT OF ETHYLENE CONCENTRATION

A series of experiments was performed in which the initial ethylene pressure was varied from 0.75 mm. to 17.9 mm. using a constant hydrogen pressure of approximately 218 mm. To provide sufficient products for analysis at the lower ethylene pressures a circulating system containing a buffer volume was used. The average fraction of ethylene consumed in any experiment was $0.52 \pm .05$. The results are plotted in Fig. 3 according to equation [iv]. The

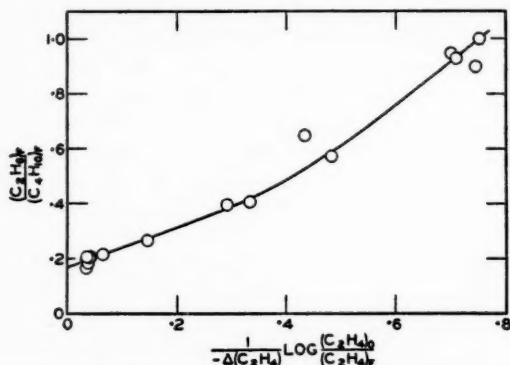


FIG. 3. Influence of ethylene concentration on the ethane/butane ratio. Since approximately 50% of the initial ethylene was used in each experiment, the abscissae are, roughly, $0.6/(C_2H_4)_0$.

value of I_0 should be constant for the series, at least to a first approximation, since both the position of the lamp and the mercury concentration in the cell were fixed. The range of values of $(C_2H_6)_f/(C_4H_{10})_f$ shown in this figure is greater than any obtained previously by the method of mercury photosensitization and illustrates the important effect of ethylene concentration.

The value of k_4/k_2 obtained from the intercept of Fig. 3 is approximately 0.16. Accepting this value, it follows that for initial ethylene pressures of the order of 1 mm., and with the light intensities used in these experiments, approximately four times as much ethane is produced by reaction [8] as by reaction [4].

Fig. 3 shows an appreciable curvature upwards at low ethylene pressures (large values of the abscissa). Such a curvature would be expected if the limiting condition (B) were to come into play. However, it is believed that at least part of this curvature is due to the fact that the rate of circulation of the gases becomes important at low ethylene concentrations.

The circulating pump used had a displacement of $30 \text{ cm}^3 \text{ min}^{-1}$. At high ethylene pressures this would be sufficient to ensure that the partial pressure of ethylene in the gas leaving the cell would not be much less than in the gas entering the cell. But at low ethylene pressures most of the ethylene entering the cell would be consumed. Because these experiments were of short duration much of the gas never left the buffer volume and as a result, although only approximately 50% of the total ethylene was consumed a considerably larger figure would apply to the gas which actually passed through the cell. If this effect could be allowed for the points for low ethylene pressures in Fig. 3 would be moved to the right, thus prolonging the range of linearity of the curve.

HEXANE FORMATION

At low light intensities, particularly at the higher ethylene concentrations, low temperature distillation indicated a product having a vapor pressure in the hexane range. Under the most favorable conditions for its formation it amounted to only 2.1% of the saturated products. Its vapor pressure was determined in the range -52° to -72° using the low temperature still (8) and the values agreed within a range of approximately 5°C . with those calculated for *n*-hexane from the data of International Critical Tables; the thermocouple used had not been calibrated. The vapor pressure at 27°C ., determined as the condensation pressure in a McLeod gauge, was 155 mm., compared to 163 mm. calculated for *n*-hexane.

The most probable method of formation of *n*-hexane is by the sequence



The conditions which were found to be the most favorable for the formation of hexane are the least favorable for the occurrence of reaction [8] and hence it is unlikely that any hexane would be formed by the addition of H atoms to hexyl radicals.

For the limiting condition (A),

$$\frac{d(\text{C}_6\text{H}_{14})/dt}{d(\text{C}_4\text{H}_{10})/dt} = \frac{k_{10}(k_3 + k_4)^{1/2}(\text{C}_2\text{H}_4)}{k_3 I_a^{1/2}} \quad [\text{vii}]$$

It was pointed out previously that the rate of pressure drop should be proportional to the effective average value of I_a , and hence, to a first approximation, $(\text{C}_6\text{H}_{14})_f/(\text{C}_4\text{H}_{10})_f$ should be directly proportional to $(\text{C}_2\text{H}_4)_0/(-\Delta P/\Delta t)^{1/2}$. The data plotted in Fig. 4 show that this is approximately true. Because of the small amounts involved, hexane could not be measured with very great accuracy.

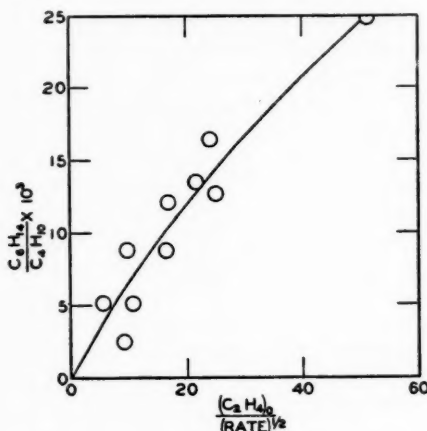


FIG. 4. Correlation of hexane formation with equation [vii]. The effective average value of I_a is assumed to be proportional to the rate of pressure drop.

DISCUSSION

From the present data the most probable value of k_4/k_3 is $0.15 \pm .01$. This is in good agreement with most of the recent work based on other methods, as shown in Table I.

TABLE I
VALUES OF k_4/k_3 OBTAINED BY DIFFERENT METHODS
(Room temperature)

Method	k_4/k_3	Ref.
Photolysis of diethyl mercury	0.35	(6)
Photolysis of propionaldehyde	0.1	(3)
Photolysis of diethyl ketone	$0.12 \pm .02$	(7)
Photolysis of 2,2',4,4' tetradeuterodiethyl ketone	0.1	(16)
Photolysis of azoethane	$0.13 \pm .02$	(1)
This research	$0.15 \pm .01$	

The discrepancies among the values of the ratio $(C_2H_6)/(C_4H_{10})$, obtained by the method of mercury photosensitization can now be understood. Moore and Taylor (11) used an initial ethylene pressure of 40 mm. and their value of 0.17 would therefore be expected to be only slightly larger than k_4/k_3 . Le Roy and Kahn (9), using the full intensity of the lamp and an initial ethylene pressure of 13.3 mm., obtained 0.61 and 0.44 for the ratio; from the pressure drops they observed the final pressures of ethylene would be approximately 1.0 and 1.3 mm., respectively. Using a lower light intensity, initial ethylene pressures of 15.7 mm., and final ethylene pressures of 5.3 and 5.9 mm., they obtained 0.22 and 0.28 for the ratio. Their results are therefore not out of line with those obtained in the present investigation.

Cashion and Le Roy (4) found ethane and butane to be important products in the mercury photosensitized hydrogenation of acetylene and attributed their origin to ethyl radicals produced in the reactions



However, since they found the ethane/butane ratio to be in the range 0.77 to 1.25 they concluded that ethane must be formed in some reaction in addition to [4], namely [8]. An examination of their results shows that for conditions in which [12] would be negligible compared to [2] (i.e. $(\text{H}_2) \rightarrow 0$, their Fig. 2) the ethane/butane ratio would be approximately 1.4. The ethylene concentration in this case would have been zero at the beginning of the experiment and about 0.2 mm. at the end. The large values of the ratio obtained by them can be adequately explained in terms of the present mechanism. They were reluctant to attribute ethane/butane ratios of almost ten times the accepted value of k_4/k_3 solely to the influence of reaction [8] and suggested the additional reaction



It is clear, however, that the last postulate is unnecessary.

ACKNOWLEDGMENT

The authors are grateful to the National Research Council for financial assistance.

REFERENCES

1. AUSLOOS, P. and STEACIE, E. W. R. *Bull. soc. chim. Belges*, 63: 87. 1954.
2. BERLIE, M. R. and LE ROY, D. J. *Discussions Faraday Soc.* No. 14: 50. 1953.
3. BLACET, F. E. and PITTS, J. N. *J. Am. Chem. Soc.* 74: 3382. 1952.
4. CASHION, J. K. and LE ROY, D. J. *Can. J. Chem.* 32: 906. 1954.
5. DARWENT, B. DE B. and STEACIE, E. W. R. *J. Chem. Phys.* 16: 381. 1948.
6. IVIN, K. J. and STEACIE, E. W. R. *Proc. Roy. Soc. (London)*, A, 208: 25. 1951.
7. KUTSCHKE, K. O., WIJNEN, M. H. J., and STEACIE, E. W. R. *J. Am. Chem. Soc.* 74: 714. 1952.
8. LE ROY, D. J. *Can. J. Research*, B, 28: 492. 1950.
9. LE ROY, D. J. and KAHN, A. *J. Chem. Phys.* 15: 816. 1947.
10. MITCHELL, A. G. and LE ROY, D. J. *J. Chem. Phys.* 21: 2075. 1953.
11. MOORE, W. J. and TAYLOR, H. S. *J. Chem. Phys.* 8: 396. 1940.
12. PYKE, R., KAHN, A., and LE ROY, D. J. *Ind. Eng. Chem. Anal. Ed.* 19: 65. 1947.
13. STEACIE, E. W. R. *Atomic and free radical reactions*. Reinhold Publishing Corporation, New York. 1954.
14. TRENNER, N. R., MORIKAWA, K., and TAYLOR, H. S. *J. Chem. Phys.* 5: 203. 1937.
15. TROST, W. R. and STEACIE, E. W. R. *J. Chem. Phys.* 16: 361. 1948.
16. WIJNEN, M. H. J. and STEACIE, E. W. R. *Can. J. Chem.* 29: 1092. 1951.

THE RELATIVE ABUNDANCES OF NEODYMIUM AND SAMARIUM ISOTOPES IN THE THERMAL NEUTRON FISSION OF U^{235} AND U^{238} ¹

By E. A. MELAIKA, M. J. PARKER, J. A. PETRUSKA,² AND R. H. TOMLINSON

ABSTRACT

The relative fission yields of neodymium and samarium isotopes have been measured with a mass spectrometer for samples of natural uranium and U^{235} that had been irradiated with moderated neutrons. The cross sections for neutron capture by Sm^{149} and Sm^{151} have been determined to be $66,200 \pm 2500$ barns and 12,000 barns respectively, relative to the cross section of a B^{10} monitor. The half-lives of Pm^{147} and Sm^{151} have been evaluated to be 2.52 ± 0.08 yr. and ~ 93 yr., respectively, from samarium fission yield data for samples differing in age by seven years.

INTRODUCTION

Inghram, Hayden, and Hess (5) have reported a mass spectrometric determination of the relative abundances of rare earth isotopes separated from fission products in uranium fuel rods. The values obtained were considered to represent relative fission yields of U^{235} , although the previously accepted mass-yield curve (9) for the thermal neutron fission of U^{235} was considerably different in this mass region. Inghram *et al.* pointed out, however, that the mass spectrometric values represent yields for the neutron energy distribution found in thick uranium slugs and do not necessarily correspond to those for the thermal neutron fission of U^{235} . Likewise, the various pile neutron capture cross sections reported by Inghram *et al.* need not be applicable for a thermal neutron energy distribution.

This paper reports the mass spectrometric determination of the relative yields of neodymium and samarium isotopes for the thermal neutron fission of U^{235} and U^{238} . The amount of neutron capture by Sm^{149} and Sm^{151} was large in a sample of uranium for which the integrated neutron flux was monitored with BF_3 . From the observed ratios of the samarium isotopes in this sample, the measured fission yields of samarium isotopes, and the change in the B^{10}/B^{11} ratio for the BF_3 , the neutron capture cross sections of Sm^{149} and Sm^{151} relative to that of B^{10} were obtained. Since the relative abundances of the samarium isotopes were measured at different times after irradiation for the various samples, it was possible to evaluate the half-lives of Sm^{151} and Pm^{147} .

EXPERIMENTAL

For the study of the fission yields for U^{235} , four samples of normal uranium metal were irradiated in the NRX reactor at Chalk River and one at Oak Ridge. A 50 mgm. sample of UO_3 , in which the uranium content was 14.4 atom % U^{233} , 0.6 atom % U^{235} , and 85.0 atom % U^{238} , was irradiated in the

¹Manuscript received January 17, 1955.

Contribution from the Department of Chemistry, Hamilton College, McMaster University, Hamilton, Ontario.

²Holder of a Research Council of Ontario scholarship, 1953-54.

TABLE I
IRRADIATION DATA

Sample	Form	Reactor	Neutron flux, $n/cm.^2/sec.$	t_1 ,* days	t_2 ,† days
A	Uranium metal 20 gm.	NRX, Chalk River thermal column	5.0×10^{10}	81	618
B	Uranium metal 1.6 gm.	NRX, Chalk River	7.0×10^{12}	31	590
C	Uranium metal 30 gm.	Oak Ridge	6.0×10^{11}	18	2950
D	Uranium metal 3.0 gm.	NRX, Chalk River	2.30×10^{12}	36	910
E	50 mgm. UO_3 14.4% U^{235}	NRX, Chalk River	1.23×10^{13}	31	517

*Time of irradiation.

†Time from beginning of irradiation until time of chemical separation and analysis by mass spectrometer.

NRX reactor for the study of U^{235} fission. The irradiation data are summarized in Table I. In no case was the integrated flux greater than 2×10^{19} neutrons/cm.², and hence Pu^{239} did not contribute more than 0.1% to the fission products of either U^{235} or U^{238} . In sample *D*, the contribution from fast neutron fission of U^{238} was estimated from pile data to be 2.5%; it was probably comparable in samples *B* and *C*. Sample *A*, which was irradiated in a thermal column, had essentially no U^{238} fission. Unfortunately, in the case of sample *A*, the time of irradiation was divided into three periods so that the time between periods could not be neglected. Since several determinations of fission yields were made for sample *A* at widely different times, and since there are three corresponding values of t_2 for each of these determinations, the value of t_2 tabulated for sample *A* is only an approximate average.

The uranium, after dissolution in nitric acid, was separated from the fission products either by ion exchange or by precipitation from solution at pH 7 with hydrogen peroxide. The ion exchange method permitted a separation of the neodymium from the samarium and other fission products, whereas the peroxide precipitation method did not. It was found, however, that separation of the rare earths prior to mass spectrometric analysis was not necessary. The peroxide precipitation method was preferred since a much higher chemical yield of neodymium and samarium could be obtained.

The mass spectrometer that was used was a 90° sector instrument with magnetic scanning and a hot filament ion source (2). When a platinum-plated tungsten filament was used, neodymium and samarium samples of 0.01 μ gm. were adequate. The neodymium yields were measured from the NdO^+ ion spectrum at a relatively low filament temperature; the samarium was measured from the Sm^+ ion spectrum which occurred only at a higher filament temperature. The SmO^+ ions also appeared at this higher temperature and were used for the determination of the Sm^{152}/Sm^{154} ratio since a LaO^+ peak at mass 155 tended to interfere with the Sm^{154} metal ion peak when the fission products were not separated from each other. Since, in each case, only mass spectra of

the expected fission isotopes were observed, and since no changes in the ratios were observed with time, it was assumed that no other elements contributed to the mass spectrum of either the samarium or the neodymium.

RESULTS

The relative abundances of the samarium isotopes obtained from the thermal neutron fission in four samples of normal uranium and one sample of uranium containing 14.4% U^{233} are given in Table II. The fission samarium

TABLE II
THE RELATIVE ABUNDANCES OF NEODYMIUM AND SAMARIUM ISOTOPES IN THE THERMAL NEUTRON FISSION OF U^{235} AND U^{233}

Sample		Relative abundances of isotopes					
<i>Neodymium isotopes for U^{235} fission</i>							
		Nd ¹⁴³	Nd ¹⁴⁴	Nd ¹⁴⁵	Nd ¹⁴⁶	Nd ¹⁴⁸	Nd ¹⁵⁰
A	Observed	1.000	(0.713)	0.663	0.502	0.280	0.109
	Relative yield	1.000	(0.912)	0.663	0.502	0.280	0.109
B	Observed	1.000	0.723	0.665	0.506	0.282	0.112
	Relative yield	1.000	0.943	0.665	0.506	0.282	0.112
C	Observed	1.000	0.923	0.666	0.507	0.282	0.110
	Relative yield	1.000	0.923	0.666	0.507	0.282	0.110
D	Observed	1.000	0.820	0.665	0.504	0.280	0.110
	Relative yield	1.000	0.923	0.665	0.504	0.280	0.110
Average		1.000	0.930	0.665	0.505	0.281	0.110
S.D.			±0.012	±0.001	±0.002	±0.001	±0.002
Inghram <i>et al.</i>		1.000	0.860	0.670	0.520	0.304	0.122
<i>Samarium isotopes for U^{235} fission</i>							
		Sm ¹⁴⁷	Sm ¹⁴⁹	Sm ¹⁵⁰	Sm ¹⁵¹	Sm ¹⁵²	Sm ¹⁵⁴
A	Observed	0.724	0.987	0.013	0.393	0.250	0.068
	Relative yield	(2.05)	1.000	0.000	0.398	0.250	0.068
C	Observed	1.864	0.979	0.021	0.374	0.251	0.068
	Relative yield	2.10	1.000	0.000	0.398	0.251	0.068
D	Observed	1.025	0.797	0.203	0.373	0.267	0.068
	Relative yield	2.10	1.000	0.000	0.398	0.251	0.068
Average		2.10	1.000	0.000	0.398	0.251	0.068
S.D.		±0.04				±0.001	±0.000
Inghram <i>et al.</i>		1.96	1.000	0.000	0.405	0.254	0.083
<i>Neodymium isotopes for U^{233} fission</i>							
		Nd ¹⁴³	Nd ¹⁴⁴	Nd ¹⁴⁵	Nd ¹⁴⁶	Nd ¹⁴⁸	Nd ¹⁵⁰
E	Observed	1.000	0.543	0.587	0.441	0.224	0.089
	Relative yield	1.000	0.779	0.587	0.441	0.224	0.089
<i>Samarium isotopes for U^{233} fission</i>							
		Sm ¹⁴⁷	Sm ¹⁴⁹	Sm ¹⁵⁰	Sm ¹⁵¹	Sm ¹⁵²	Sm ¹⁵⁴
E	Observed	0.846	0.405	0.595	0.327	0.373	0.061
	Relative yield	2.81	1.000	0.000	0.422	0.278	0.061

abundances reported as the observed values have been corrected for contamination by natural samarium. The contamination corrections, which were about two to three per cent of the total samarium present, were based on the natural abundances of the samarium isotopes and the measurement of the Sm^{148} which is not formed in fission. In order to obtain the relative cumulative fission yields shown in Table II, it was necessary to take into account several known nuclear processes which occur in the various fission chains which form samarium isotopes. The equations relating the observed ratios to the cumulative fission yields of the samarium isotopes have been given by Inghram *et al.* (5).

Since beta decay in the mass 150 chain from fission terminates at Nd^{150} , the observed Sm^{150} is the result of neutron capture by Sm^{149} . The total relative yield for the mass 149 chain was obtained by direct addition of the Sm^{149} and Sm^{150} abundances. The ratio of the observed Sm^{149} to Sm^{150} is given by equation [1].

$$[1] \quad \frac{N_{149}}{N_{150}} = \frac{1 - \exp(-{}_{62}\sigma^{149}\phi t_1)}{{}_{62}\sigma^{149}\phi t_1 - 1 + \exp(-{}_{62}\sigma^{149}\phi t_1)}$$

where N_{149}/N_{150} = the observed ratio of Sm^{149} to Sm^{150} ,
 ${}_{62}\sigma^{149}$ = the neutron capture cross section for Sm^{149} ,
 ϕ = the neutron flux,
 t_1 = the time of irradiation.

For samples *A* and *C*, the amount of Sm^{149} capture was small and the flux could be estimated only from pile operation data. For sample *D*, however, there was a large amount of Sm^{150} formed, and the flux was accurately determined from the change in the $\text{B}^{10}/\text{B}^{11}$ ratio in a sample of BF_3 that was irradiated simultaneously. The ratio of the $\text{B}^{10}/\text{B}^{11}$ ratio before irradiation to the $\text{B}^{10}/\text{B}^{11}$ ratio after irradiation was found to be 1.029 ± 0.001 . The value of ${}_{50}\sigma^{10}\phi t_1$, where ${}_{50}\sigma^{10}$ is the neutron absorption cross section for B^{10} , was calculated to be 0.0286 ± 0.0010 assuming that all of the change in the ratio of the boron isotopes was due to the $\text{B}^{10}(n, \alpha)\text{Li}^7$ reaction. From the observed ratio N_{149}/N_{150} for sample *D*, a value of 0.472 ± 0.007 was calculated with equation [1] for ${}_{62}\sigma^{149}\phi t_1$. Thus, the ratio ${}_{62}\sigma^{149}/{}_{50}\sigma^{10}$ is 16.5 ± 0.6 at an estimated neutron temperature of 57°C . This ratio corresponds to a neutron capture cross section of $66,200 \pm 2500$ barns if a value of 755 barns (1) is used for the neutron capture cross section of natural boron and 18.83% (4) is used for the natural abundance of B^{10} .

The fission yield of Sm^{151} relative to that of Sm^{149} is given by equation [2] as a function of the observed samarium ratios and the time.

$$[2] \quad \frac{N_{151}}{(N_{149} + N_{150})} = \frac{f_{151}[1 - \exp(-{}_{62}\lambda^{151}t_1 - {}_{62}\sigma^{151}\phi t_1)][\exp(-{}_{62}\lambda^{151}t_2 + {}_{62}\lambda^{151}t_1)]}{f_{149}({}_{62}\lambda^{151} + {}_{62}\sigma^{151}\phi)t_1}$$

where $N_{151}/(N_{149} + N_{150})$ = the ratio of Sm^{151} to Sm^{149} plus Sm^{150} observed at time t_2 ,
 f_{151}/f_{149} = the ratio of the cumulative yields of mass chains 151 and 149,

${}_{62}\lambda^{151}$ = the decay constant of Sm^{151} ,

${}_{62}\sigma^{151}$ = the neutron capture cross section for Sm^{151} ,

ϕ = the neutron flux,

t_1 = the time of irradiation,

t_2 = the time from the beginning of irradiation until the time of chemical separation and isotopic analysis.

If the time of irradiation is short compared to the time of the analysis, and if t_1 is small compared to the half-life of Sm^{151} , equation [2] reduces to equation [3].

$$[3] \quad \frac{N_{151}}{(N_{149} + N_{150})} = \frac{f_{151} \exp(-{}_{62}\lambda^{151} t_2) [1 - \exp(-{}_{62}\sigma^{151} \phi t_1)]}{f_{149} {}_{62}\sigma^{151} \phi t_1}.$$

In the case of samples *A* and *C*, the contribution to mass 150 resulting from neutron capture by Sm^{149} is only 1 to 2%, and, therefore, neutron capture by Sm^{151} will be negligible provided its cross section is less than that of Sm^{149} . Thus, for samples *A* and *C*, equation [3] reduces to equation [4].

$$[4] \quad \frac{N_{151}}{(N_{149} + N_{150})} = \frac{f_{151} \exp(-{}_{62}\lambda^{151} t_2)}{f_{149}}.$$

The observed relative yield at mass 152 is given by equation [5], and its simplified forms, comparable to equations [3] and [4], are given by equations [6] and [7].

$$[5] \quad \frac{N_{152}}{(N_{149} + N_{150})} = \frac{f_{152}}{f_{149}} + \frac{f_{151} {}_{62}\sigma^{151} \phi t_1}{f_{149} ({}_{62}\lambda^{151} + {}_{62}\sigma^{151} \phi)^2 t_1^2} \times [({}_{62}\lambda^{151} + {}_{62}\sigma^{151} \phi) t_2 - 1 + \exp(-{}_{62}\lambda^{151} t_1 - {}_{62}\sigma^{151} \phi t_1)]$$

$$[6] \quad \frac{N_{152}}{(N_{149} + N_{150})} = \frac{f_{152}}{f_{149}} + \frac{f_{151}}{f_{149} {}_{62}\sigma^{151} \phi t_1} [{}_{62}\sigma^{151} \phi t_1 - 1 + \exp(-{}_{62}\sigma^{151} \phi t_1)]$$

$$[7] \quad \frac{N_{152}}{(N_{149} + N_{150})} = \frac{f_{152}}{f_{149}}.$$

Thus, for samples *A* and *C*, the observed Sm^{152} ratios are the actual relative fission yields as shown by equation [7]. The yield of Sm^{151} for these samples, however, is dependent on the half-life of Sm^{151} as shown by equation [4]. From the observed ratios for these two samples, it was possible to solve this equation for both f_{151}/f_{149} and ${}_{62}\lambda^{151}$. For sample *A*, the uncertainty of the value of t_2 in this calculation is not significant. The value obtained for f_{151}/f_{149} is 0.398 and for ${}_{62}\lambda^{151}$ is 0.00747 yr^{-1} which corresponds to a half-life of 93 yr.

The yields of Sm^{151} and Sm^{152} for sample *D* have been set equal to the values obtained from samples *A* and *C*. For sample *D*, ${}_{62}\sigma^{151} \phi t_1$ may then be calculated from either the observed ratio $\text{Sm}^{151}/(\text{Sm}^{149} + \text{Sm}^{150})$ and equation [3], or the observed ratio $\text{Sm}^{152}/(\text{Sm}^{149} + \text{Sm}^{150})$ and equation [6]. These equations give values of 0.090 and 0.080, respectively, for ${}_{62}\sigma^{151} \phi t_1$. From the value of ${}_{62}\sigma^{151} \phi t_1$, the cross section of natural boron, and the natural abundance of B^{10} given

above, values of 12,500 and 11,200 barns are obtained for the neutron capture cross section of Sm^{151} .

The amount of Sm^{147} relative to the amount of Sm^{149} plus Sm^{150} is given by equation [8].

$$[8] \quad \frac{N_{147}}{(N_{149} + N_{150})} = \frac{f_{147}[{}_{61}\lambda^{147}t_1 - \exp(-{}_{61}\lambda^{147}t_2 + {}_{61}\lambda^{147}t_1) + \exp(-{}_{61}\lambda^{147}t_2)]}{f_{149} {}_{61}\lambda^{147}t_1}$$

where ${}_{62}\lambda^{147}$ = the decay constant of Pm^{147} .

In equation [8], there are two unknowns, ${}_{61}\lambda^{147}$ and f_{147}/f_{149} , and these can be evaluated using the observed data from samples *C* and *D* if it is assumed that f_{147}/f_{149} is the same for both samples. A value of $0.275 \pm 0.007 \text{ yr.}^{-1}$ was obtained for ${}_{61}\lambda^{147}$ which corresponds to a half-life of $2.52 \pm 0.08 \text{ yr.}$ The ratio, f_{147}/f_{149} , was found to be 2.10 ± 0.04 . The limits of error assigned to the above values are obtained only from the standard deviations of the mass spectrometric results for samples *C* and *D*. Data for sample *A* were not used for this calculation because of the uncertainty introduced by the three-period irradiation.

Since the samarium yields were determined for only one set of irradiation conditions with U^{235} , the relative fission yields could not be obtained in the same manner as above for U^{235} . In this case, it was necessary to assume a smooth fission mass-yield curve, which gave 0.422 for the ratio f_{151}/f_{149} and 0.278 for the ratio f_{152}/f_{149} .

For this U^{235} sample, neutron capture by Sm^{149} was considerable, and equation [1] was used to solve for ${}_{62}\sigma^{149}\phi t_1$. A value of 2.19 ± 0.09 was obtained. Also, equation [3] may be used to solve for ${}_{62}\sigma^{151}\phi t_1$ if the value of 0.422, interpolated from a smooth yield-mass curve, is taken for the relative yield of mass chain 151 to 149. A value of 0.229 is obtained for ${}_{62}\sigma^{151}/{}_{62}\sigma^{149}$. If a value of 66,200 barns is taken for the value of ${}_{62}\sigma^{149}$, then a value of 15,200 barns is obtained for ${}_{62}\sigma^{151}$.

The results for the relative abundances of the neodymium isotopes in the fission of U^{235} and U^{238} have been given in Table II. The abundances reported as the observed values have already been corrected for contamination by a small amount of natural neodymium. The contamination corrections, which were about 0.5% of the total neodymium present, were based on the natural abundances of the neodymium isotopes and the measurement of Nd^{142} , which is not formed in fission. The relative fission yields take into account the amount of 282-day Ce^{144} which had not decayed to Nd^{144} at the time of analysis. The Ce^{144} correction for sample *C* was negligible.

DISCUSSION

Table II shows that the relative fission yields of the neodymium and samarium isotopes resulting from the thermal neutron fission of U^{235} decrease more rapidly with increasing mass than the yields obtained by Inghram *et al.* (5). The difference (e.g. 11% at mass 150) appears to be real since the precision of either set of data is better than one per cent. This may be the result of different neutron energy distributions, since the fission products analyzed by Inghram *et al.* were obtained from a fuel rod where a large fraction of the

neutrons would have energies of several Mev., whereas in the present work neutron energies were essentially thermal. When fission is induced by particles of very high energy, it is well known that the fission yield curve tends to become more symmetrical. Some evidence of this change has been shown to occur even with fast (fission) neutrons. For example, in the case of Pu^{239} , the relative yield of masses 153/140 was found to be 0.074 for thermal neutrons, whereas the same relative yield was 0.096 for fast (fission) neutrons (12). Whereas the neutron energy may account for the greater part of the difference between the relative yields reported by Inghram *et al.* and those obtained in this work, it is also necessary to consider that fission products contributed by the fast neutron fission of U^{238} and to a smaller extent from the thermal neutron fission of Pu^{239} may have influenced the values obtained by Inghram *et al.*

Apart from the general increase in the slope of the mass-yield curve, the present results indicate that the yield of mass 144 is about 7% greater than the value obtained by Inghram *et al.* and hence could not fall on a smooth curve such as Inghram *et al.* have drawn. The apparently high yield at mass 144 may be taken as evidence for the fine structure predicted for this mass by Pappas (8).

Table II also shows the relative fission yields of the neodymium and samarium isotopes resulting from the thermal neutron fission of U^{235} . These relative yields are probably accurate to within one per cent except at mass 154 where a combination of a low yield and a comparable contamination correction make this particular yield uncertain.

A further correction must be made for the contribution to the fission products from the 0.6 atom % U^{238} present in the sample. The largest correction would occur at Nd^{160} where the relative yield would be reduced by about one per cent if it is assumed that the cross section for the formation of the neodymium isotopes is approximately the same for U^{235} and U^{238} fission. Comparison of the relative yields of neodymium and samarium for U^{235} with those for U^{238} show that the former decrease more rapidly with increase in mass of the fission product. By radiochemical methods, Steinberg *et al.* (13) have obtained yields at masses 144 (3.4%) and 153 (0.078%) while Grummitt and Wilkinson (3) have obtained yields at masses 144 (2.2%) and 147 (0.6%) for thermal neutron fission in U^{235} . Although the agreement between these groups at mass 144 is poor, the relative values obtained by each group confirm the steeper slope of the U^{235} mass-yield curve when compared to the U^{238} mass-yield curve given by Coryell and Sugarman (10).

The value of the half-life of Pm^{147} found in this work is 2.52 ± 0.08 yr. which is longer than the value of 2.26 yr. obtained by Inghram *et al.* (5). The 2.52 yr. value, however, is based on relative abundances measured at different times rather than an assumed yield as was used by Inghram *et al.* The value of 2.52 ± 0.08 yr. compares favorably with the value of 2.6 ± 0.2 yr. obtained by a counting-rate decay method (11).

The half-life of Sm^{151} based on changes in the relative abundances of Sm^{151} in fission products differing in age by about seven years is found to be 93 yr.

Whereas no limit has been set on the accuracy of this value it is considered in reasonable agreement with a value of 73^{+25}_{-14} yr. found by Karraker *et al.* (6) from the change in Sm^{151} abundances over a 3.8 yr. period.

The $66,200 \pm 2500$ barn value obtained for the neutron capture cross section of Sm^{149} is based on a 755 barn cross section for natural boron. Nuclear Data (7) have reported a value of 65,000 barns for the cross section of Sm^{149} averaged for a maxwellian distribution of neutron energies at a temperature of 20.4°C . A value of 47,000 barns for pile neutrons has been reported by Inghram *et al.* (5). This value, however, is not strictly comparable to the other values without more specific information about the neutron energies. A cross section of 12,000 barns has been found for Sm^{151} relative to a 755 barn cross section for natural boron. It is difficult to set a limit of accuracy on this value since the observed changes in the isotopic abundances from which this value was calculated were small. The value of 15,200 barns obtained from the U^{235} data is based on assumed fission yields and hence has unknown reliability. Inghram *et al.* (5) have obtained a cross section of 7200 barns for the pile neutron cross section of Sm^{151} based on assumed fission yields for U^{235} .

Absolute fission yields may be obtained from the relative thermal neutron fission yields of the U^{235} and U^{238} when suitable normalization values are obtained either by radiochemical or isotope dilution methods.

ACKNOWLEDGMENTS

We wish to thank Atomic Energy of Canada Limited for supplying the U^{238} and uranium metal and arranging for the irradiation of samples. The financial support of the National Research Council of Canada and Atomic Energy of Canada Limited is gratefully acknowledged. The authors are indebted to Dr. H. G. Thode and Dr. W. H. Fleming for helpful discussions and the isotopic analysis of the BF_3 .

REFERENCES

1. Atomic Energy Commission. Neutron Cross Section Advisory Group AECU-2040. May 15, 1952.
2. GRAHAM, R. L., HARKNESS, A. L., and THODE, H. G. J. Sci. Instr. 24: 119. 1947.
3. GRUMMITT, W. E. and WILKINSON, G. Nature, 158: 163. 1946.
4. INGHAM, M. G. Phys. Rev. 70: 653. 1946.
5. INGHAM, M. G., HAYDEN, R. J., and HESS, D. C. Phys. Rev. 79: 271. 1950.
6. KARRAKER, D. G., HAYDEN, R. J., and INGHAM, M. G. Phys. Rev. 87: 901. 1952.
7. National Bureau of Standards. Nuclear Data. N. B. S. Circular 499. United States Department of Commerce. 1950.
8. PAPPAS, A. C. Lab. for Nuclear Science Tech. Rept. No. 63. Mass. Inst. Technol. September 15, 1953.
9. Plutonium Project "Nuclei Formed in Fission". Revs. Mod. Phys. 18: 513. 1946.
10. Radiochemical Studies: The Fission Products. Book 3, Appendix B. Edited by Coryell, C. D. and Sugarman, N. McGraw-Hill Book Company, Inc., New York and London. 1951.
11. SCHUMAN, R. P. and CAMILLI, A. Phys. Rev. 84: 158. 1951.
12. STEINBERG, E. P. and FREEDMAN, M. S. Radiochemical Studies: The Fission Products. Book 3, Paper 219. Edited by Coryell, L. D. and Sugarman, N. McGraw-Hill Book Company, Inc., New York and London. 1951.
13. STEINBERG, E. P., SEILER, J. A., GOLDSTEIN, A., and DUDLEY, A. MDCC-1632. United States Atomic Energy Commission. 1947.

CATALYSIS ON FILMS OF ARSENIC, ANTIMONY, AND GERMANIUM¹

BY SIR HUGH TAYLOR

ABSTRACT

Arsenic, antimony, and germanium films laid down on glass surfaces by decomposition of the hydrides have been studied from the standpoint of reaction kinetics in three sets of reactions: the decomposition of hydrides and deuterides, the interaction of hydrides and molecular deuterium, and the exchange reaction of hydrogen and deuterium. Only in the first of these have the surfaces marked catalytic activity. The orders of reaction and the activation energies have been determined. The accelerated catalytic influence of foreign elements, notably antimony in arsine decomposition, has been established. The results obtained contrast strikingly with the properties of clean filaments and evaporated films among the transition elements. The results emphasize the basic importance of chemical factors and de-emphasize the importance of surface cleanliness as a controlling factor in problems of chemisorption and surface catalysis.

It is a pleasant opportunity to outline, in tribute to a lifetime devoted to academic teaching and research by Professor Otto Maass in physical chemistry, some results in an area of physical chemical investigation which, while remote from the area which Professor Maass has so diligently and successfully cultivated, nevertheless has been contemporaneous with that work and has brought to the writer a large measure of the same satisfactions which research and the educational effort bring.

It is proposed to present a summary of some results recently obtained in the Princeton laboratories by a group of postdoctoral students and concerned with the catalytic properties of arsenic, antimony, and germanium films laid down on glass surfaces by the decomposition of the corresponding hydrides at appropriate temperatures. The deposited films act catalytically in the decomposition of the hydrides. Comparative experiments can also be performed on the decomposition of the deuterides. It has also been possible to study the interactions of the hydrides and deuterides among themselves and with molecular hydrogen and deuterium. The exchange reaction between hydrogen and deuterium on the several surfaces has also been examined. The results have a definite bearing on the properties of evaporated metal films which have been intensively studied in recent years in elucidation of the catalytic properties of technical metal catalysts.

Researches by Roberts (3) on the chemisorption of gases on clean flashed tungsten filaments and by Beeck (1) on the adsorption of gases on clean evaporated films of a variety of metals including nickel, iron, tungsten, rhodium, and platinum had emphasized that the activation energy of chemisorption of hydrogen on such clean surfaces was negligible, since it was demonstrably occurring at temperatures in the neighborhood of liquid hydrogen. Such observations gave rise to a very prevalent generalization that if

¹Manuscript received January 26, 1955.

Contribution from the Frick Chemical Laboratory, Princeton University, Princeton, New Jersey, U.S.A.

the metal surfaces were clean the chemisorption of gases might occur without any activation energy. The determination of activation energies of chemisorption of hydrogen on a variety of technical catalysts led to the view that the cause of the activation energy might lie in the impurities present on the surfaces of all technical catalysts.

Such a point of view tended to obscure an obvious fact in the science of catalysis, namely, the very specific activity of particular elements in bringing about catalytic change. The examples of such specificity which could be quoted are legion. It may suffice, however, to recall that whereas iron and osmium surfaces are excellent catalysts in the synthesis of ammonia, nickel, and platinum are obviously inferior. Since all of these metals readily chemisorb hydrogen even down to quite low temperatures, the differences between them in respect to ammonia synthesis would seem to lie in the capacity of these surfaces to chemisorb nitrogen.

Quite recently Trapnell (5) published some comparative data on the interaction of nitrogen, hydrogen, carbon monoxide, ethylene, acetylene, and oxygen with clean evaporated films of some twenty metals between 0 and -183°C . Oxygen chemisorption is universal among the metals studied save in the case of gold. Chemisorption of both nitrogen and hydrogen is limited to transition metals, W, Ta, Mo, Ti, Zr, Fe, and alkaline earth metals such as Ca and Ba. The metals Ni, Pd, Rh, Pt, Cu, Al, K, Zn, Cd, In, Sn, Pb, Ag, and Au do not chemisorb nitrogen in this temperature range but Ni, Pd, Rh, and Pt chemisorb hydrogen. Chemisorption of carbon monoxide, ethylene, and acetylene occurs on the metals which chemisorb both nitrogen and hydrogen and in addition to these Al, Cu, and Au. The metals Zn, Cd, In, Sn, Pb, and Ag do not chemisorb carbon monoxide, ethylene, and acetylene. It is the particular virtue of this study with clean evaporated films that it emphasizes the necessity for activation energy of chemisorption even on clean surfaces.

Dr. M. Boudart in Princeton pointed out that it was possible to expand the area of our knowledge of the chemisorption of hydrogen by a study of the production of films of arsenic, antimony, and germanium by decomposition of the respective hydrides and that the nature of the isotopic hydrogen produced by decomposition of mixtures of hydrides and deuterides of these elements would give clues with respect to the interaction between hydrogen and such surfaces. Further, the constant deposition of fresh elemental product of the reaction, As, Sb, or Ge, on the surface ensured a continuous cleanliness of the surface provided the purity of the original hydrides was secured. A series of researches dealing with these topics is now in process of publication. The present occasion permits a summary survey of the results obtained.

Antimony Surfaces

Dr. K. Tamaru has studied the decomposition of stibine by a static method in the temperature range of 10 to 45°C . The rate is dependent only on the stibine pressure and independent of the hydrogen pressure. The order of reaction in stibine is unity at 45°C . and decreases with decreasing temperature

reaching 0.75 at 10°C. At 40 cm.-Hg stibine pressure the activation energy of the reaction is 8.8 kcal./mole, with lower values at lower pressures. The rate of decomposition of deuterostibine is slightly lower than that for stibine under similar conditions.

A feature common to all three surfaces can now be indicated. Stibine decomposition in presence of deuterium at 25°C. did not produce any hydrogen deuteride which shows that no exchange reaction between hydrogen and deuterium occurs at that temperature on the antimony surface. Decomposition of a mixture of stibine and deuterostibine produced a large proportion of hydrogen deuteride.

Stibine decomposes very slowly on the glass surface of a clean vessel but as antimony is deposited on the glass the rate accelerates until after 200 cm.-Hg of stibine have been decomposed the rate becomes reproducible. When a small amount of oxygen is introduced into the stibine there is a small acceleration in reaction rate but very considerably less than that to be noted subsequently in the decomposition of germane.

The evidence indicates that at the higher temperature limit of 45°C. in the measurements the chemisorption of stibine on the surface determines the rate of reaction. As the temperature is lowered the desorption of hydrogen, resulting from the decomposition of the stibine, from the antimony surface becomes slow enough to be comparable with the chemisorption process. The order of the reaction decreases and at sufficiently low temperatures where desorption of hydrogen became determinant the order would be zero. The data indicate a transition over the temperature range employed between the two kinds of rate process.

Arsenic Surfaces

The decomposition of arsine can be studied only in a much higher temperature range, between 218 and 278°C. Dr. Tamaru overcame a difficulty which had prevented good kinetic measurements by van't Hoff and Kooj (2) and by Stock and co-workers (4). This difficulty lay in the inability to form a coherent arsenic film on the surface of glass. Tamaru solved this problem by first laying down on the glass surface a coherent film of antimony on which by subsequent decomposition of arsine a coherent film of arsenic was formed. These experiments demonstrated that arsine decomposes slowly on glass even at 350°C. but decomposes more rapidly on antimony surfaces than it does on arsenic surfaces. On the antimony surface the original rate of arsine decomposition is relatively rapid, the rate decreasing as the antimony becomes covered with arsenic, constant rates of decomposition being secured after some ten experiments, this rate being assumed to be characteristic of a coherent arsenic film. In such a manner the kinetics and the activation energy of arsine decomposition on such arsenic films have been successfully obtained. We hope to be able to characterize the surfaces by electron diffraction studies.

The reaction is first order with respect to arsine and independent of hydrogen concentration. The apparent activation energy on arsenic surfaces is 23.2 kcal./mole. In the decomposition of a mixture of arsine and deutoarsine at

255°C. intermolecular exchange occurs as revealed by infrared spectroscopy. The decomposition product contains a high percentage of hydrogen deuteride. When arsine is decomposed with molecular deuterium at this temperature no hydrogen deuteride is found, indicating no exchange between hydrogen and deuterium on the arsenic surface. Analysis of the experimental data indicates that the chemisorption of arsine is the rate determining step on arsenic surfaces.

Germanium Surfaces

Dr. P. J. Fensham who initiated this whole experimental program found that the decomposition of germane and deuterogermane on germanium films did not differ significantly in velocity. He demonstrated that the product from the decomposition of mixtures of germane and deuterogermane contained considerable amounts of hydrogen deuteride in the product hydrogen. On the other hand, germane-deuterium mixtures and molecular hydrogen-deuterium mixtures contained minimal amounts of hydrogen deuteride after reaction.

Dr. Tamaru examined the kinetics of the decomposition in greater detail and succeeded in showing that a zero order surface-catalyzed decomposition of germane occurs simultaneously with a first-order homogeneous decomposition in the gas phase in the temperature range 230 to 330°C. The kinetic expression in cylindrical vessels with surface to volume ratios from 1 to 7.5 cm.⁻¹ was expressible by an equation

$$v = k_0 + k_1 p$$

where v is the observed velocity, k_0 and k_1 the zero and first order constants respectively. For the two reactions the activation energies were 41.2 and 51.4 kcal./mole respectively. By filling the reaction vessel with glass wool and thus enhancing the zero order reaction some 30-fold the surface zero order reaction became dominant and the first order reaction negligible. Even in the unpacked cylindrical vessels the ratios of k_0 to $k_1 p$ were such that below 10 cm. working pressure of germane the reaction was kinetically closely zero order.

The surface reaction evidently occurs on a surface practically covered with chemisorbed GeH_2 radicals and adsorbed hydrogen atoms, the evaporation of which in the steady state determines the rate of the surface reaction. That Fensham did not observe marked hydrogen deuteride formation in his experiments with germane-deuterium mixtures means either that his surface reaction was dominant in his experimental conditions over the homogeneous reaction or that this latter, if it were occurring, proceeds via $\text{GeH}_2 + \text{H}_2$ rather than via $\text{GeH}_3 + \text{H}$. The presence of H atoms in the latter type of decomposition would ensure considerable formation of hydrogen deuteride via the homogeneous chain-reaction exchange process $\text{H} + \text{D}_2 = \text{HD} + \text{D}$, followed by $\text{D} + \text{H}_2 = \text{HD} + \text{H}$.

Some interesting added facts emerged from the kinetic measurements. Arsine decomposes very slowly on germanium surfaces at 302°C., much more slowly than on antimony and arsenic surfaces. Nevertheless, in presence of minor amounts of arsine the rate of decomposition of germane is measurably

accelerated. Apparently, the deposition of As atoms in the germanium surface enhances the catalytic activity for germane decomposition.

Much more striking effects resulted from the introduction of small amounts of oxygen into the germane. Rapid reaction between the two gases occurs. The decomposition of residual germane on the oxygen-contaminated germane surface was markedly greater than on a pure germanium surface. Further, the accelerating influence persists through successive runs with pure germane. This indicates that the oxygen impurity retains its position and effect in the germanium surface in spite of further deposition of germanium in the decomposition process. The accelerating action of oxygen contamination in the germanium surface contrasts strikingly with the pronounced inhibitory effects of oxygen contamination on iron-synthetic ammonia catalysts.

DISCUSSION

The obvious conclusion from these researches is that while clean arsenic, antimony, and germanium surfaces activate the X—H bond in the several hydrides they none have any marked activation efficiency with respect to the H—H bonds in the temperature range 10 to 330°C. It follows that chemistry is involved in the process of chemisorption and that cleanliness of the elemental surface cannot substitute for the chemical factors involved. The influence of arsenic and oxygen impurities in the hydride decomposition processes on these surfaces is additional evidence in the same direction. It is expected that further studies, now in progress, will correlate these catalytic data with the growing body of data on the solid state physics of germanium.

The experience gained in the present studies makes it possible to approach the general problem of chemisorption of gases on these surfaces. Such work is in progress and will permit a correlation with the data that are being accumulated on the adsorption of gases on single crystals, notably of germanium, of such importance in the modern use of transistors.

ACKNOWLEDGMENTS

My thanks are due to Drs. Boudart, Fensham, and Tamaru for permission to make use of the data that are in process of detailed publication elsewhere. These postdoctoral workers have been assisted either by the fellowship provided to Princeton University by the Shell Fellowship Committee of the Shell Companies Foundation, Inc., of New York City, or by a research project sponsored by the Office of Naval Research, N6onr-27018 on Solid State Properties and Catalytic Activity. To both these sources of support I wish to express the indebtedness of Princeton University for their generous assistance.

REFERENCES

1. BEECK, O. *Advances in catalysis*. Academic Press, Inc., New York. 1950. p. 151.
2. *Etudes de dynamique chimique*. Muller and Co., Amsterdam. 1884. p. 83.
3. ROBERTS, J. K. *Proc. Roy. Soc. (London)*, A, 152: 477. 1935.
4. STOCK, A., GOMOLKA, F., and HEYNEMANN, H. *Ber.* 40: 532. 1907.
STOCK, A., ECHENDIA, E., and VOIGT, P. R. *Ber.* 41: 1319. 1908.
5. TRAPNELL, B. M. W. *Proc. Roy. Soc. (London)*, A, 218: 566. 1953.

PRELIMINARY STUDY OF PHOTOCHEMICAL BEHAVIOR IN THE SYSTEM NITROGEN DIOXIDE - ETHANE¹

BY T. M. ROHR² AND W. ALBERT NOYES, JR.

ABSTRACT

The addition of ethane to nitrogen dioxide either during exposure to radiation transmitted by pyrex, or afterwards, reduces the amount of oxygen formed. At room temperature this is apparently due to the effectiveness of ethane in promoting the reverse reaction of nitric oxide and oxygen to form nitrogen dioxide. At temperatures over 100° there is a reaction which uses oxygen atoms produced in the primary process. Nitroethane (or nitrosoethane) is formed along with carbon monoxide, carbon dioxide, and some methane. The results suggest that acetaldehyde is an intermediate, but acetaldehyde could not be detected because it would react thermally with nitrogen dioxide. It is not possible to give a complete explanation of the results, but suggestions can be made which might form the basis for later work.

The photochemical reaction between nitrogen dioxide and methane has been studied, but no evidence for reaction found (4). The oxygen atoms almost certainly produced in the primary process might react either with nitrogen dioxide or with methane, and the rate of the former reaction seemed to be sufficiently great to obscure the latter. Hardeck and Kopsch (5) showed that oxygen atoms produced in a discharge tube react with ethane with an estimated activation energy of 7 kcal.

It was hoped in starting this investigation to obtain information both about the reactions of oxygen atoms with ethane and possibly also about the reactions of hydroxyl radicals. As so often happens, the course of the reaction is complex, and only suggestions can be made about some of the steps. A few semiquantitative estimates of relative rates can be made.

EXPERIMENTAL

Nitrogen dioxide was prepared by heating lead nitrate in a stream of oxygen, condensation by dry ice - acetone, and fractional distillation. The middle third was retained and stored at the temperature of liquid nitrogen. Stopcocks were lubricated with Myvacene-S (Dow-Corning) which proved not to be attacked by nitrogen dioxide as far as could be ascertained.

Ethane (Phillips Petroleum Company, Research Grade) appeared upon hydrogenation to contain traces of ethylene. It was mixed with nitrogen dioxide at 160° to remove ethylene and the ethane was distilled from a trap at -150°.

Mercury vapor was mostly kept out of the reaction cell by a trap immersed in dry ice - acetone. Final traces were eliminated by admission of nitrogen dioxide and evacuation just before a run. Initial pressures of reactants were measured by a Bourdon gauge.

¹Manuscript received January 7, 1955.

Contribution from the Department of Chemistry, University of Rochester, Rochester, N. Y.

²Postdoctoral Fellow 1952-54 under a grant made to the Department of Chemistry, of the University of Rochester, by the Doctors Camille and Henry Dreyfus Foundation.

A Hanovia Alpine burner Type S-100 was used, and the radiation (except in the first series of runs) passed through Corning Filter No. 7740 to remove radiation below 3000 Å. The beam was collimated by a quartz lens and completely filled the cell which was 2.5 cm. in diameter and 20 cm. in length. A magnetically driven glass stirrer largely prevented the development of local concentration gradients.

Owing to the nature of the products the complete analysis proved to be difficult, and not all products have been completely identified.

The gases were condensed immediately after reaction to eliminate the reverse reaction



The products not condensed by supercooled liquid nitrogen at -210° were removed by a Toepler pump. These would consist of oxygen, nitrogen (if any), carbon monoxide, methane, and possibly traces of nitric oxide. The latter would, however, mainly be held back by formation of nitrogen trioxide with nitrogen dioxide. In a few runs when the nitrogen dioxide was nearly used up, nitric oxide might appear in this fraction.

Oxygen, carbon monoxide, and methane were determined by methods previously described (8).

The separation of condensable products proved to be difficult. Carbon dioxide could not be separated from the large amount of ethane present. After removal of the ethane at -155° , the residue was condensed in a cold finger subsequently filled with mercury. After a few hours' standing nitrogen dioxide was reduced to nitric oxide which could be pumped off at -150° . The remaining products were volatilized and burned to carbon dioxide over a copper oxide furnace at 650° and the pressure of carbon dioxide measured. Blank runs showed that nitroethane could be quantitatively determined in this way.

RESULTS

Blank runs showed no thermal reaction between nitrogen dioxide and ethane to occur at temperatures up to 160° , the highest temperature used in these experiments.

The results may be summarized briefly as follows:

(a) The addition of carbon dioxide (120 mm.) to nitrogen dioxide (5 mm.) did not affect the rate of production of gas uncondensed at -210° . Ratio of amounts with carbon dioxide to blanks at 108° : 1.03, 1.00.

(b) The addition of ethane (100 mm.) to nitrogen dioxide (5 mm.) reduces the amount of gas uncondensed at -210° (mainly oxygen) by the following ratios: 25° (1.09); 108° (0.54, 0.59); 160° (0.57).

In a series of experiments at 25° the oxygen yield was about the same whether or not ethane was added, and it was not influenced by variation in ethane pressure. The formation of condensable products in these experiments is probably due to impurities in the ethane, because with each successive run the amount diminished and it became zero after the sixth run.

In experiments at 108° and at 160° the decrease of the oxygen yield in the presence of ethane, compared to that either without ethane or merely with addition of carbon dioxide, cannot be explained by postulating that the missing oxygen is used for the oxidation of ethane even if one assumes the formation of products which escape detection by analysis. The presence of ethane favors the reaction of oxygen with nitric oxide as the following experiments showed.

If after radiation of 5 mm. of nitrogen dioxide at 160° for four hours the products were condensed immediately after turning off the light, one obtained 4.88×10^{-6} moles of oxygen. If the gases were condensed 30 min. after turning off the light, one obtained only 4.39×10^{-6} moles of oxygen. One tenth of the oxygen therefore was used by reacting with nitric oxide during this period of time. Addition of 50 mm. of ethane, immediately after radiation, greatly accelerated this reverse reaction since only 2.46×10^{-6} moles of oxygen were left after 30 min. Thus 50% was used in the same period.

(c) Nitroethane shows continuous absorption below about 3000 Å (2, 13), but no observable products were formed when the gas was irradiated under the conditions of the present experiments. Moreover there was no observable thermal reaction between nitroethane and nitrogen dioxide at temperatures up to 160°.

(d) When mixtures of nitrogen dioxide (5 mm.) and nitroethane (0.04 mm.) were irradiated, the rate of production of gas not condensed at -210° was unaffected by the presence of the nitroethane. When nitroethane was present at pressures of 27-35 mm., the yield of non-condensables was reduced to about half that in the blank runs. The non-condensables were oxygen and carbon monoxide. Products not volatile at -150° would not have been detected.

(e) When mixtures of ethane (usually 100 mm.) and of nitrogen dioxide (5 mm.) were irradiated at 160°, the gas uncondensed at -150° (measured as carbon dioxide, see above) was formed at a constant rate. In four runs of 4,

TABLE I
RESULTS WITH NITROGEN DIOXIDE - ETHANE MIXTURES
($P_{\text{NO}_2} = 5$ mm., $P_{\text{C}_2\text{H}_6} = 100$ mm., $T = 160^\circ$, Alpine burner, pyrex filter)

Time, hours	Products not condensable at -210° moles $\times 10^6$			Products condensable at -150° (measured as CO ₂)
	O ₂	CO	CH ₄ (or N ₂)	
4	2.49	0.49	—	1.24
4	2.15	0.40	—	0.78
12	1.96	0.23	0	2.4
18	0.35	0.19	0.004	3.3
25.5	0.35 (total)			Not measured
42	0	0.45	0.013	Not measured
52.7	0	0.48	0.017	Not measured
52.7*	0	0.65	0.013	Not measured

*0.085 mm. oxygen added. This shows oxygen to disappear.

12, 18, and 52.7 hr., the moles $\times 10^6$ formed per hour were 0.19, 0.20, 0.19, and 0.17, respectively. On the other hand, oxygen was formed in short runs but could not be detected at the end of long runs. Carbon monoxide was formed to an increasing extent along with small amounts of methane (or nitrogen). Table I shows the results.

(f) Some experiments were made with mixtures of nitrogen dioxide and of acetaldehyde as shown in Table II.

TABLE II

RESULTS WITH NITROGEN DIOXIDE - ACETALDEHYDE MIXTURES

(T = 160°, P_{NO_2} = 5 mm., $P_{\text{CH}_3\text{CHO}}$ = 1.5 mm., Time: 4 hr., Alpine burner, pyrex filter)

Moles of products $\times 10^6$				
O ₂	CO	CH ₄ (or N ₂)	NO	CO ₂
0 ^a	0	0	0	0
			4.59	> 9.0 ^b
0 ^d	0.22	0	> 7.2	3.1
0	0.47	0	4.1	> 9.0
0 ^e	0.89	0	0	> 9.0
0 ^c	0.20	0		

^aBlank with no nitrogen dioxide.^bThermal reaction.^c100 mm. ethane also present.^d P_{NO_2} = 2.5 mm.^e P_{NO_2} = 10 mm.

It is evident that there is a thermal reaction between nitrogen dioxide and acetaldehyde even at room temperature but that this reaction does not lead to methane formation.

DISCUSSION

The absorption characteristics of the system nitrogen dioxide - nitrogen peroxide have been carefully studied by Hall and Blacet (3). Since this mixture had a total pressure of 5 mm. in the present work, it can be shown from the data of Giauque and Kemp (1) that the pressure of nitrogen peroxide at 25° would be 0.17 mm. At wave lengths of 3130 and 3650 Å the absorption will be almost exclusively by nitrogen dioxide and not by nitrogen peroxide even at room temperature, and absorption by the latter will be entirely negligible at the higher temperatures used (1, 3).

The photochemistry of nitrogen dioxide has been carefully studied (7, 10). The primary process is undoubtedly



and this is followed by



The yield of the primary process must be high, and in the absence of foreign gases Equation [3] must occur nearly quantitatively. When foreign gases are added, Equation [3] will compete with other reactions of oxygen atoms. The latter, under conditions of the present experiments, are almost certainly

formed in the normal (³P) state. Kinetic energies of the oxygen atoms after primary dissociation might be equivalent to 4 kcal. at 3650 Å and 8 kcal. at 3130 Å provided dissociation proceeds immediately before vibrational energy can be lost by collision. Unless steric factors are high for hot oxygen atom reactions, one would not expect to find noticeable "hot atom" effects.

If ethane is added to nitrogen dioxide, the first reaction of oxygen atoms should be



The data show this reaction to be negligible at 25° compared to Equation [3] since (a) the amount of oxygen formed is almost the same in the presence and in the absence of ethane; (b) products condensed at -150° but not at -210° are negligible if the ethane has been previously exposed to radiation in the presence of nitrogen dioxide. Apparent reaction is due therefore to impurities in the ethane at this temperature.

The rate of the reaction



is not known with precision but may have a low activation energy (12). The first reaction of ethyl radicals formed from either Equation [4] or Equation [5] should be



where $\text{C}_2\text{H}_5\text{NO}_2$ is probably nitroethane but might be ethyl nitrite. Mass spectrographic analysis tends to favor the latter.

It is not possible to obtain a precise estimate of the activation energy of Equation [4]. From the results at 160° $E_a - E_0 \sim 3$ kcal. if Equation [3] and Equation [4] have the same steric factors. This result is probably low since with such a low activation energy and similar steric factors reaction [4] should compete more successfully than it does with reaction [3] at 25°. On the other hand if one takes 'condensables at -150°' divided by 'non-condensables at -210°' as a measure of the ratio of rate of Equation [4] to rate of Equation [3], one obtains from the results at 108° and at 160° a value of 8 kcal. This is based on results with considerable scatter and is not a reliable figure. One may merely say that probably the activation energy of Equation [4] is less than 10 kcal. in agreement with the work of Harteck and Kopsch (5). An activation energy of 5 kcal. or more is compatible with the results at 25°.

Oxygen atoms evidently do react with nitroethane but at a somewhat slower rate than with ethane. Hirschlaff and Norrish (6) suggest a reaction of oxygen atoms with nitroethane to give ethylene and the latter in the present system would give dinitroethane and would escape analysis by the procedure used. The probable formation of small amounts of methane and of larger amounts of carbon monoxide suggests that acetaldehyde is an intermediate. This could be formed easily from ethyl nitrite (11). This would disappear rapidly either by thermal reaction with nitrogen dioxide or by a reaction with radicals or excited molecules.

One of the striking points is the formation of oxygen during the early stages of the reaction and its subsequent disappearance. This would indicate that as

reaction proceeds, some radical or atom is produced which reacts much more rapidly with oxygen than with nitrogen dioxide and other molecules present. Not over 20% of the nitrogen dioxide would have disappeared during even the longest run. Thus this radical or atom must have a rate of reaction with oxygen of the order of magnitude of 10 to 100 times as fast as with nitrogen dioxide. Alkyl radicals may fulfill this requirement and so might possibly oxygen atoms.

The amount of carbon monoxide produced was not affected markedly by varying (a) the ethane pressure; (b) the nitrogen dioxide pressure; (c) the time. Blank runs showed that this lack of variation with conditions is not due to impurities.

Oxygen atoms react much less readily with carbon monoxide than with oxygen (9), but carbon monoxide may react with ozone or with peroxy radicals in the system. A detailed study of the reason why carbon monoxide apparently reaches a steady state might prove of interest.

ACKNOWLEDGMENT

This work was supported in part by contract with the Office of Naval Research, United States Navy. We wish to thank Mr. R. C. Wilkerson, Celanese Corporation of America, Clarkwood, Texas, for mass spectrographic analyses.

REFERENCES

1. GIAUQUE, W. F. and KEMP, J. D. *J. Chem. Phys.* 6: 40. 1938.
2. GOODEVE, J. W. *Trans. Faraday Soc.* 30: 504. 1934.
3. HALL, T. C., JR. and BLACET, F. E. *J. Chem. Phys.* 20: 1745. 1952. This article gives references to earlier work.
4. HARRIS, L. and SIEGEL, B. M. *J. Am. Chem. Soc.* 63: 2520. 1941.
5. HARTECK, P. and KOPSCH, U. *Z. physik. Chem. B*, 12: 327. 1931.
6. HIRSCHLAFF, E. and NORRISH, R. G. W. *J. Chem. Soc.* 1580. 1936.
7. HOLMES, H. H. and DANIELS, F. *J. Am. Chem. Soc.* 56: 630. 1934.
8. MARCOTTE, F. B. and NOYES, W. A., JR. *Discussions Faraday Soc.* No. 10. 236. 1951.
9. NOYES, W. A., JR. and LEIGHTON, P. A. *The photochemistry of gases*. Reinhold Publishing Corporation, New York. 1941. p. 253 gives a review of this subject.
10. NOYES, W. A., JR. and LEIGHTON, P. A. *The photochemistry of gases*. Reinhold Publishing Corporation, New York. 1941. p. 400 gives a review of this subject.
11. STEACIE, E. W. R. *Atomic and free radical reactions*. Vol. 1. Reinhold Publishing Corporation, New York. 1954. p. 239.
12. STEACIE, E. W. R. *Atomic and free radical reactions*. Vol. 2. Reinhold Publishing Corporation, New York. 1954. p. 607.
13. THOMPSON, H. W. and PURKINS, T. F. *Trans. Faraday Soc.* 32: 674. 1936.

FURTHER DEGRADATION REACTIONS OF ANNOTININE¹

BY F. A. L. ANET² AND LÉO MARION

ABSTRACT

Both the hydroxylactone obtained by the action of chromous chloride on annotinine chlorohydrin, and the unsaturated lactone B prepared by the action of the same reagent on the hydroxylactone, contain a secondary nitrogen and a vinyl group. The unsaturated lactone A which accompanies the hydroxylactone is a cyclic allylamine which on oxidation with potassium permanganate yields an amino acid $C_{14}H_{19}O_4N$. These facts make it possible to explain the reaction of chromous chloride with annotinine chlorohydrin. The amino acid can be dehydrogenated to an acid containing a free carboxyl and a lactamic grouping ($C_{14}H_{15}O_5N$) but no longer containing a lactone ring. The lactamic acid which seems to contain a benzene ring is readily decarboxylated to a neutral substance $C_{13}H_{15}ON$, showing color reactions and ultraviolet absorption similar to those of strychnine.

Annotinine, $C_{16}H_{21}O_3N$, was found (9) to react with hydrochloric acid to form annotinine chlorohydrin, $C_{16}H_{22}O_3NCl$, which was reduced (10) with chromous chloride to a mixture of "unsaturated lactone A", $C_{16}H_{21}O_2N$, and "hydroxylactone", $C_{16}H_{23}O_3N$. The latter compound on more vigorous treatment (10) with chromous chloride in strongly acidic solution gave "unsaturated lactone B", $C_{16}H_{21(23)}O_2N$. The two unsaturated lactones each contained a readily reducible double bond and gave two different dihydro-derivatives (10). The relationship of these compounds has now been clarified and affords supporting evidence for MacLean and Prime's suggestion (8) of the presence of the system $\begin{array}{c} \diagup N-CH_2-CH-C \diagdown \\ \quad \quad \quad O \end{array}$ in annotinine and also for the modifica-

tion of this scheme to $\begin{array}{c} \diagup N-CH_2-CH-CH \diagdown \\ \quad \quad \quad O \end{array}$ suggested by Wiesner *et al.* (6).

Following MacLean and Prime we can write $\begin{array}{c} \diagup N-CH_2-CH-CH \diagdown \\ \quad \quad \quad Cl \quad OH \end{array}$ as a grouping in annotine chlorohydrin instead of $\begin{array}{c} \diagup N-CH_2-CH-CH \diagdown \\ \quad \quad \quad OH \quad Cl \end{array}$, although

the evidence adduced by these authors for the former arrangement is meager. It does allow, however, of a simple interpretation for the chromous chloride reduction products, which is not possible with the alternate cleavage of the oxide ring of annotine (see below).

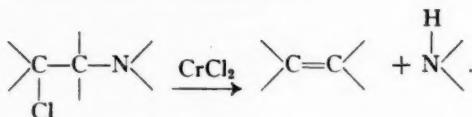
Chromous chloride is known to reduce various chlorinated derivatives of the senecio alkaloids, e.g., chloroisoheliotridene (1) by replacement of the halogen by hydrogen. Julian *et al.* (7) found that chromous chloride reduced

¹Manuscript received January 25, 1955.

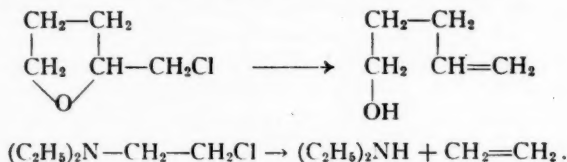
Contribution from the Division of Pure Chemistry, National Research Council, Ottawa, Canada. Issued as N.R.C. No. 3570.

²National Research Council of Canada Postdoctorate Fellow. Present address: Department of Chemistry, University of Ottawa, Ottawa.

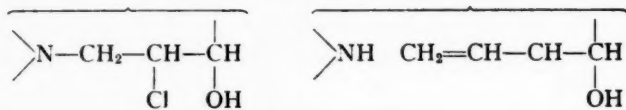
steroid *vic*-dihalides to the corresponding unsaturated compounds. In both of these reductions, chromous chloride behaves in much the same way as does zinc in neutral or acidic conditions. Fieser and Ettore (5) found that zinc and acetic acid converted certain steroid *vic*-chlorohydrins to the olefins and therefore it would be anticipated that chromous chloride could effect the same reaction. Furthermore, it is only a simple extension to consider β -chloroamines which could react as below (see also Fig. 1)



That this extension is not unjustified is shown by the work of Paul (11) who showed that the reduction by metallic sodium of cyclic ethers of *vic*-chlorohydrin and of β -chloro*tert.*amine proceeds analogously, e.g., in the case of tetrahydrofurfuryl chloride and β -chloroethyldiethylamine,



It was found in the present work that the hydroxylactone was unsaturated and yielded a dihydro-derivative on hydrogenation and formaldehyde on ozonolysis. Although the action of acetyl chloride failed to give the expected product (10), treatment of the hydroxylactone with acetic anhydride produced a neutral O,N-diacetyl derivative (infrared bands 1740 and 1678 cm^{-1} in Nujol). The hydroxylactone was obviously not formed by simple replacement of the chlorine of annotinine chlorohydrin by hydrogen, but its formation could be readily explained by analogy to the reactions outlined above.



The unsaturated lactone A would be expected to be the olefin VIII (Fig. 1) corresponding to annotinine chlorohydrin, and this was substantiated by the reactions of the unsaturated lactone A which behaved as a cyclic allylamine. Its pK_a was 7.06 whereas that of its dihydro-derivative was 8.48 (cf. Ref. 14), and it gave a methosulphate which was smoothly hydrogenolized in the presence of Adams' catalyst with the uptake of two moles of hydrogen and the formation of a tertiary base X ($\text{C}_{17}\text{H}_{27}\text{O}_2\text{N}$). Oxidation of the unsaturated lactone A with potassium permanganate yielded an amino acid XV isolated as the sulphate, $\text{C}_{14}\text{H}_{19}\text{O}_4\text{N} \cdot \frac{1}{2}\text{H}_2\text{SO}_4$, which was identical with the oxidation

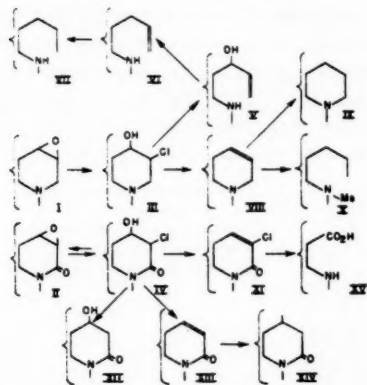


FIG. 1. Partial formulae of degradation products.

product obtained as described by Wiesner *et al.* (6) from the anhydro derivative of annotinine lactam chlorohydrin XI (8).

The relation of the unsaturated lactone B to the other products was obscured by the fact that its infrared spectrum showed no NH band although that of its dihydro-derivative did contain such a band. Yet it formed a neutral N-acetyl derivative (infrared band at 1762 cm^{-1}) which yielded formaldehyde on ozonolysis. The easy reduction of the unsaturated lactone B to its dihydro-derivative, and the low intensity of its ultraviolet absorption at short wave lengths also indicated the presence of a terminal methylene group. The dihydrolactone B also gave a N-acetyl derivative (infrared band at 1755 cm^{-1}).

The infrared spectra in carbon disulphide of the unsaturated lactone B and its dihydro-derivative were very similar and were consistent with the presence of a vinyl group in the former. We therefore assign the partial formulae VI and VII to these compounds respectively. This is also consistent with a re-investigation of the empirical formulae of this series which showed that the unsaturated lactone B was definitely $\text{C}_{16}\text{H}_{23}\text{O}_2\text{N}$ and not $\text{C}_{16}\text{H}_{21}\text{O}_2\text{N}$.

Annotinine lactam chlorohydrin (IV) which can be prepared either by oxidation (10) of annotinine chlorohydrin, or by treatment (8, 10) of annotinine lactam with hydrochloric acid gave two main products on chromous chloride reduction. These were identical with the compounds $\text{C}_{16}\text{H}_{21}\text{O}_4\text{N}$ and $\text{C}_{16}\text{H}_{19}\text{O}_4\text{N}$ prepared previously (8) by MacLean and Prime. Since the compound $\text{C}_{16}\text{H}_{19}\text{O}_4\text{N}$ was dehydrated (8) with phosphorus oxychloride to the second compound $\text{C}_{16}\text{H}_{17}\text{O}_4\text{N}$, the two products may be allotted the partial structures XII and XIII respectively. It may be noted that XIII is produced in the chromous chloride reduction under conditions that are not sufficient to dehydrate XII, which agrees with the mechanism proposed above. MacLean and Prime (8) found that catalytic or Clemmensen reduction of annotinine lactam chlorohydrin gave XII and XIV (Fig. 1). It is most probable that XII and XIII are the primary reduction products and that XIII is further reduced

to XIV. Indeed, as expected, XII could not be hydrogenated (8). The action of phosphorus oxychloride, or prolonged treatment with boiling hydrochloric acid convert (8) annotinine lactam chlorohydrin to a compound $C_{16}H_{19}O_3NCl$ which may be represented by XI (Fig. 1). Confirmation of the structures of XI and XIII is given by their ultraviolet spectra shown in Fig. 2 with those of

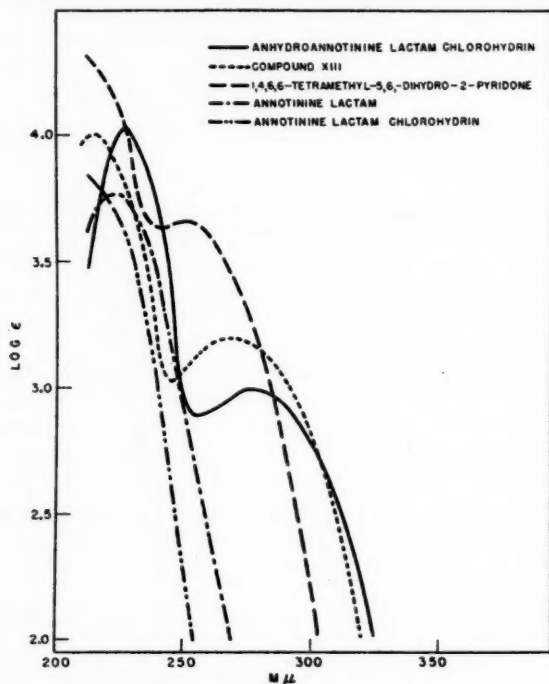


FIG. 2. Ultraviolet spectra in alcohol.

1,4,6,6-tetramethyl-5,6-dihydro-2-pyridone (12), annotinine lactam, and annotinine lactam chlorohydrin. The absorption bands of XI and XIII are at a longer wave length than would be expected when compared with the model compound, but there seems to be no doubt that a conjugated system is present. An $\alpha\beta$ -unsaturated lactam system is also indicated by the infrared absorption spectra of XI and XII which contain two bands in the carbonyl region whereas the spectra of the saturated lactams contain only one band (cf. Edwards and Singh (4)). The spectra of all the compounds in Fig. 1 had a band at about 1780 cm^{-1} indicative of a γ -lactone group.

The amino acid XV, $C_{14}H_{19}O_4N$, was dehydrogenated in the presence of palladium on barium sulphate at $200\text{--}250^\circ$ to an acid XVI, $C_{14}H_{15}O_3N$. The new acid no longer showed the γ -lactone band in its infrared spectrum but showed bands at 1715 , 1620 , and 1575 cm^{-1} in Nujol (curve 1, Fig. 4) and at

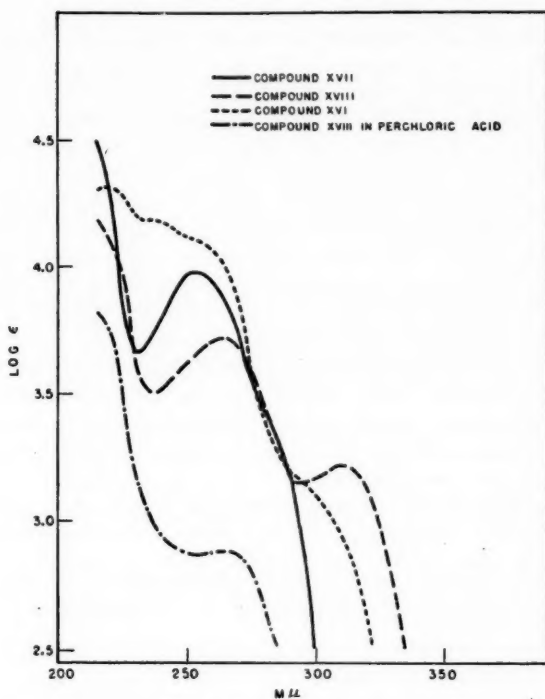


FIG. 3. Ultraviolet spectra.

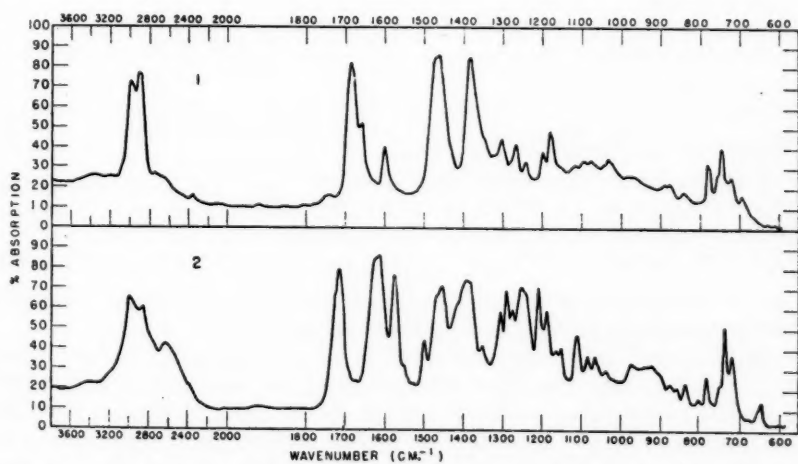
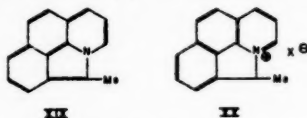


FIG. 4. Infrared absorption spectra: curve 1, compound XVI; curve 2, compound XVII.

1692, 1665, 1610, and 1575 cm^{-1} in chloroform solution which are consistent with the presence of a carboxyl, an amide group, and a benzene ring. The ultraviolet spectrum is shown in Fig. 3. The dehydrogenated acid was decarboxylated by heating with copper powder to a neutral compound XVII, $\text{C}_{11}\text{H}_{11}\text{ON}$ (m.p. 70°). The ultraviolet spectrum of XVII is shown in Fig. 3 and the difference from that of the acid indicates that the carboxyl group is directly attached to the chromophoric system in the acid. The infrared spectrum in Nujol contained no bands in the NH region, but bands at 1685 and 1660 cm^{-1} (weak) assigned to an amide group and at 1600 cm^{-1} (benzene ring) (curve 2, Fig. 4). The bands were shifted in chloroform solution to 1655 and 1600 cm^{-1} . Although the compound appears not to contain an NH band it is probable that an NH group is present, for if a benzene ring is present, as is almost certain (see also below) the dehydrogenated acid must contain one less ring than the acid XV. A carbon-nitrogen fission seems more likely than a carbon-carbon fission, and would result in the formation of a NH group. The ultraviolet spectrum of XVII is very similar to that of strychnine (13) and like this alkaloid, XVII gave an intense violet color with 80% sulphuric acid and a trace of chromic acid (Otto reaction).

Unfortunately, we have not been able to secure more than very small amounts of XVII. Reduction of XVII with lithium aluminum hydride in ether solution gave a weak base, which formed a crystalline picrate, m.p. 172° (decomp.). The base XVIII gave an intense red color with nitric acid or with ferric chloride and its ultraviolet spectrum, shown in Fig. 3, is roughly similar to that of strychnidine (13). In strong acid the spectrum changed to that of an isolated benzene ring.

More drastic dehydrogenation of annotinine itself at 300° over palladium gave a small amount of 7-methylquinoline, isolated as the picrate. Wiesner *et al.* (3) have recently studied the selenium dehydrogenation of annotinine and have isolated 8-*n*-propylquinoline as well as another base and a neutral nitrogen-containing substance. The formation of both 7-methyl- and 8-*n*-propylquinoline in the dehydrogenation of annotinine under different conditions is puzzling. With reference to the neutral nitrogen containing substance obtained in the selenium dehydrogenation, it may be stated that the structure XIX suggested by Wiesner *et al.* (3) for this substance seems highly unlikely

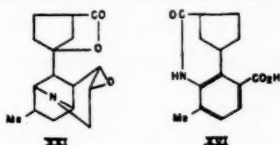


as it is the anhydro base of XX and, therefore, would be expected to revert to the quaternary salt XX in the presence of acid.

On the other hand, the structure XXI that we suggested for annotinine in our preliminary note (2) does not explain the formation of 8-*n*-propylquinoline by dehydrogenation. According to the views of Wiesner *et al.* (6) on the relactonization of various annotinine derivatives to compounds containing a new γ -lactone, the acid XV should contain the grouping

$$\begin{array}{c} | & | & | \\ \text{O}-\text{C}-\text{C}-\text{C}-\text{CO}_2\text{H} \\ | & | & | \end{array}$$
 Hence, the dehydrogenation of XV should give an *o*-phthalic acid derivative, because one of the carboxyl groups has been shown to be attached to a benzene ring. This is not so, however, for the other carboxyl group becomes involved in amide formation with the nitrogen atom that is attached to the benzene ring. Thus, the relactonization theory, although attractive, presents difficulties which can only be surmounted by assuming either a change in the carbon skeleton in the formation of XVI, or that the lactone ring in some of the derivatives of annotinine is larger than five-membered in spite of the infrared evidence.

It appears plausible that one of the rings in annotinine may be larger than six-membered and that the formation of quinoline derivatives in the dehydrogenations involves a rearrangement. However, formula XXI which we have tentatively suggested earlier (2) to represent annotinine possesses the merit



that it permits the representation of the dehydrogenated acid XVI by a structure which is consistent with its ultraviolet absorption and its color reactions.

EXPERIMENTAL

Optical rotations were determined in a 1 dcm. tube. Ultraviolet absorption spectra were determined on a Beckmann spectrophotometer, Model D.U. Infrared absorption spectra were measured on a Perkin-Elmer double beam instrument, Model 21. Values of pK_a were determined in 50% methanol-water with a Beckmann pH meter (Model G) fitted with a glass and a calomel electrode; 0.1 *N* hydrochloric acid used for the titration was delivered from a microburette.

Unsaturated Lactone B

The compound prepared as described earlier (10) was twice crystallized from *n*-hexane from which it was obtained as colorless glistening prisms, m.p. 135–136°. Calc. for $C_{11}H_{12}O_2N$: C, 73.53; H, 8.87; 1 act. H, 0.386%. Found: C, 73.82; H, 8.86; (on sample sublimed at 10^{-4} mm.) C, 73.70, 73.79; H, 8.93, 8.82; act. H (at room temp.) 0.00%, (at 100°), 0.448%. $pK_a = 8.44$.

Dihydro Lactone B

The compound prepared as described before (10) was recrystallized from *n*-hexane and dried *in vacuo* at room temperature. Calc. for $C_{11}H_{14}O_2N$: C, 72.96; H, 9.57. Found: C, 73.12; H, 9.34%. $pK_a = 8.44$.

Acetyl Unsaturated Lactone B

Unsaturated lactone B (25 mgm.) in acetic anhydride (5 ml.) was heated on a steam bath for half an hour. The mixture was poured into water and after

hydrolysis of the excess acetic anhydride, made alkaline with sodium hydroxide and extracted with ether. The ether extract was washed with acid and then with water, dried, and evaporated. The residue, after recrystallization from *n*-hexane, had m.p. 137–138°, depressed to 125° by the starting product. Calc. for $C_{11}H_{14}O_4N$: C, 71.25; H, 8.31. Found: C, 70.96; H, 8.17.

Acetyl Dihydro Lactone B

This compound was prepared as described above for the unsaturated analogue and after recrystallization from *n*-hexane it formed fine needles, m.p. 141–142°. Calc. for $C_{11}H_{17}O_3N$: C, 70.79; H, 8.91. Found: C, 71.11, 71.44; H, 8.92, 8.86.

Unsaturated Lactone A

The compound (10) after sublimation *in vacuo* had m.p. 130–132°; pK_a , 7.06; $[\alpha]_D^{24} = -70^\circ$ (*c*, 2.6 in ethanol).

Dihydro Lactone A

The compound (10) after sublimation *in vacuo* had m.p. 110°; pK_a , 8.48; $[\alpha]_D^{24} = -35^\circ$ (*c*, 1.4 in ethanol).

Hydroxylactone

A sample of hydroxylactone (10) was sublimed *in vacuo* after which it had m.p. 174°; pK_a , 8.21; $[\alpha]_D^{22} = -30^\circ$ (*c*, 1.42 in ethanol).

Dihydro Hydroxylactone

Hydroxylactone (0.25 gm.) in methanol (15 ml.) was hydrogenated in the presence of Adams' catalyst (20 mgm.). Absorption of 23.4 ml. of hydrogen (*ca.* 1 mole) was complete after 2.5 minutes. The platinum was filtered off and the filtrate evaporated to dryness. Recrystallization of the residue from *n*-hexane gave long brittle needles, m.p. 141–142°. For analysis the compound was sublimed *in vacuo*. Calc. for $C_{11}H_{16}O_3N$: C, 68.78; H, 9.02. Found: C, 68.97; H, 9.26%. pK_a , 8.00; $[\alpha]_D^{22} = -65^\circ$ (*c*, 1.47 in ethanol). The dihydroxylactone was unaffected by prolonged boiling with chromous chloride in concentrated hydrochloric acid.

Ozonolysis of Hydroxylactone

Hydroxylactone (80 mgm.) in pure carbon tetrachloride (15 ml.) was ozonized at -10° for about two minutes. Water (10 ml.) and hydrochloric acid (1 ml.) were added, followed by a hot saturated solution of 2,4-dinitrophenylhydrazine in 15% hydrochloric acid (5 ml.). The mixture was refluxed for 15 min., cooled, and extracted with benzene (twice). The dried extract was evaporated to 20 ml. and the yellow solution passed through a short column of neutral alumina (activity II–III), which was then washed with a little benzene. The eluate was evaporated to dryness *in vacuo* and the residue crystallized from hexane. Yellow needles (14.6 mgm. 24%), m.p. 162–163°, were obtained. There was no depression of melting point with authentic formaldehyde 2,4-dinitrophenylhydrazone of m.p. 163–164°, and the infrared absorption spectra of the two compounds were identical.

Ozonolysis of Acetyl Unsaturated Lactone B

The lactone (63 mgm.) was ozonized in carbon tetrachloride solution (10 ml.) at 0° until ozone appeared from the guard tube containing water (10 ml.). The combined water and carbon tetrachloride solution was boiled for half an hour and then mixed with a solution of 2,4-dinitrophenylhydrazine in hydrochloric acid. The cooled mixture was extracted three times with benzene, and the combined dried extract passed through a column of alumina which was then washed with benzene. The benzene eluate gave on evaporation formaldehyde 2,4-dinitrophenylhydrazone (3.5 mgm.), m.p. 160–161°, undepressed by the authentic compound. Elution of the column with benzene containing methanol (3%) gave a fraction which, after two crystallizations from methanol, was obtained as yellow needles, m.p. 218–219°, and was not further investigated.

Unsaturated Lactone A Methosulphate

Unsaturated lactone A (200 mgm.) was dissolved in benzene (5 ml.) and allowed to stand 40 hr. with freshly distilled dimethyl sulphate (0.2 gm.). The faintly yellow prisms which separated were collected and recrystallized from methanol-ether. The methosulphate formed colorless prisms, m.p. 234–235°. Calc. for $C_{11}H_{11}O_2N \cdot (CH_3)_2SO_4$: C, 56.09; H, 7.06. Found: C, 56.28; H, 7.23.

Reduction of Unsaturated Lactone A Methosulphate

Unsaturated lactone A methosulphate (72 mgm.) was hydrogenated in water (10 ml.) in the presence of Adams' catalyst (7 mgm.). Absorption of 2 moles of hydrogen took 15 min. The filtered solution was made alkaline with ammonia and the glistening needles which separated were collected. The base was recrystallized from *n*-pentane and for analysis was sublimed *in vacuo*, m.p. 90–91°. Calc. for $C_{17}H_{17}O_2N$: C, 73.60; H, 9.81. Found: C, 73.67; H, 9.89%.

O,N-diacetyl Hydroxy Lactone

Hydroxylactone (60 mgm.) was heated at 100° with acetic anhydride (4 ml.) for three hours and the mixture then diluted with water (10 ml.) and kept for two hours. The mixture was extracted three times with ether and the combined extracts were washed with aqueous sodium carbonate and then with water. The residue obtained after evaporation of the ether from the dried extract crystallized from hexane in prisms, m.p. 124–126°. After several crystallizations the melting point was raised to 132–133°. Calc. for $C_{16}H_{17}O_4N$: C, 66.46; H, 7.53. Found: C, 66.62; H, 7.85%.

Chromous Chloride Reduction of Annotinine Lactam Chlorohydrin

Annotinine lactam (1.69 gm.) was boiled with concentrated hydrochloric acid (40 ml.) for 40 min. To the mixture was added, in an atmosphere of nitrogen, a filtered solution of chromous chloride, prepared from chromic chloride (30 gm.), concentrated hydrochloric acid (40 ml.), water (60 ml.), and amalgamated zinc (25 gm.). The mixture was refluxed under nitrogen for

2.5 hr., diluted with water (500 ml.), and the cold solution extracted with chloroform four times (total volume: 200 ml.). The dried extract was evaporated to dryness *in vacuo*. The residue (0.84 gm.) was triturated with benzene, filtered, and crystallized from aqueous ethanol from which it separated as prisms, m.p. 300° (decomp.), undepressed by the compound $C_{11}H_{11}O_4N$ prepared as described by MacLean and Prime (8). The benzene solution was chromatographed on alumina (activity II-III). Elution with benzene gave a small amount of low melting product, followed by a main fraction (0.4 gm.), m.p. 174-175° after crystallization from acetone-pentane. It was identical (mixed m.p.) with the compound $C_{11}H_{11}O_4N$ prepared as described by MacLean and Prime (8). Hydrogenation of this compound (0.1 gm.) with Adams' catalyst (20 mgm.) in ethanol (20 ml.) resulted in the uptake of 1 mole of hydrogen and the substance isolated had m.p. 176-177° identical with the compound $C_{11}H_{11}O_4N$ of MacLean and Prime.

Oxidation of Unsaturated Lactone A

The unsaturated lactone A (1 gm.) was dissolved in acetone (100 ml.) and treated with powdered potassium permanganate until the pink color was unchanged for five minutes. The filtered manganese dioxide was suspended in water and brought into solution by passing sulphur dioxide through the solution. Continuous ether extraction of the mixture gave after evaporation of the ether a viscous liquid containing some crystals. The product was crystallized from methanol-ether to yield colorless prisms (0.25 gm.), m.p. 232° (decomp.); $[\alpha]_D^{25} -31^\circ$ (*c*, 1.7 in water) of the sulphate of XV. Calc. for $C_{11}H_{11}O_4N \cdot \frac{1}{2}H_2SO_4$: C, 53.48; H, 6.41. Found: C, 53.67; H, 6.64%. The compound was identical as shown by infrared spectra and mixed melting point with the amino acid sulphate prepared as described by Wiesner *et al.* (6) (see below). The compound showed only end absorption in the ultraviolet (log ϵ , 2.58 at 210 $m\mu$).

Oxidation of Anhydro Annotinine Lactam Chlorohydrin (XI)

Annotinine lactam chlorohydrin (10) (1.83 gm.) was dissolved in dry pyridine (80 ml.) and mixed with phosphorus oxychloride (3 ml.). The mixture became warm and was kept for five hours at room temperature. It was poured into water, the pyridine neutralized with hydrochloric acid, and the mixture extracted with chloroform (four times). The combined extract was dried and evaporated to dryness. The residue was crystallized from methanol giving a total of 1.53 gm. of product, m.p. 186-187°. This modification gave a much better yield of XI than MacLean and Prime's method (8). Anhydro annotinine lactam chlorohydrin (0.95 gm.) in acetone (200 ml.) was oxidized with potassium permanganate (1.35 gm.). The mixture was worked up as described above and gave 0.3 gm. of the sulphate of XV, m.p. 232° (decomp.).

Dehydrogenation of $C_{11}H_{11}O_4N$ (XV)

The above amino-acid sulphate (0.13 gm.), barium carbonate (0.04 gm.), and 5% palladium - barium sulphate (0.5 gm.) were mixed and stirred with water (0.5 ml.). The dried mixture was heated in an atmosphere of nitrogen at 200° for one hour and the temperature was gradually raised to 250° during the

course of three hours. The product was extracted with ether several times, and the ether extract washed with acid. The ether was then extracted with 5% sodium carbonate solution. The ether solution generally contained a small amount of XVII formed by decarboxylation of XVI. The aqueous extract was acidified with hydrochloric acid and extracted with ether. Evaporation of the dried extract left a residue, crystallizing from benzene-pentane in colorless needles (0.018 gm.), m.p. 250° (decomp.); $[\alpha]_D^{25} + 47^\circ$ (c, 0.9 in ethanol). Calc. for $C_{14}H_{18}O_3N$: C, 68.55; H, 6.16; N, 5.71; equiv. wt. 245.3. Found: C, 68.90, 68.71; H, 6.35, 6.19; N, 5.87; equiv. wt. 250.

Decarboxylation of the Acid $C_{14}H_{18}O_3N$ (XVI)

The acid $C_{14}H_{18}O_3N$ (10 mgm.) was mixed with copper powder (20 mgm.) in a tube. The mixture was heated with a free flame, when a colorless oil distilled on the cooled parts of the tube. The oil crystallized on cooling and was purified by repeated sublimation *in vacuo*. The colorless prisms then had m.p. 70° and gave an intense violet color when a trace of the compound in 80% sulphuric acid was treated with a few drops of dilute chromic acid. Calc. for $C_{13}H_{17}ON$: C, 77.58; H, 7.51. Found: C, 77.40; H, 7.45%.

Lithium Aluminum Hydride Reduction of $C_{13}H_{17}ON$ (XVII)

The neutral compound $C_{13}H_{17}ON$ (10 mgm.) in dry ether was refluxed with a large excess of lithium aluminum hydride in ether for three hours. The mixture was decomposed with water and sodium hydroxide, and the ether layer separated and mixed with ethereal picric acid. The precipitate was recrystallized from methanol-ether when it was obtained as yellow prisms, m.p. 172° (decomp.). The regenerated base was obtained as an oil which gave an intense red color with ferric chloride solution and with concentrated nitric acid. There was insufficient pure material for elementary analysis.

Dehydrogenation of Annotinine

Annotinine (1.2 gm.) was mixed with 5% palladium-barium sulphate (1 gm.) and heated to 310° during the course of two hours. The cooled mixture and distillate was extracted twice with ether (10 ml. in all). The ether solution was extracted three times with dilute hydrochloric acid and the combined extract made strongly alkaline with sodium hydroxide. The mixture was distilled until 10 ml. of distillate had collected. The distillate was extracted with ether, and the ether evaporated. The residue was mixed with picric acid in methanol (3 ml.), and the crystals, which formed gradually, were collected by centrifugation. Three more crystallizations from methanol gave long yellow needles, m.p. 238–240°, and in admixture with 7-methylquinoline picrate of m.p. 240–241°, 239–241°. The infrared spectra of the two samples were virtually identical. The original ether extract containing the neutral products from the dehydrogenation gave a strong Ehrlich reaction in the cold and possibly contained indole derivatives, but no crystalline picrate was obtained.

ACKNOWLEDGMENT

The authors wish to express their gratitude to Dr. R. Norman Jones and Mr. R. Lauzon of these laboratories for taking the infrared absorption spectra.

REFERENCES

1. ADAMS, R. and MAHAN, J. G. *J. Am. Chem. Soc.* 65: 2009. 1943.
2. ANET, F. A. L. and MARION, L. *Chemistry & Industry*, 1232. 1954.
3. BANKIEWICZ, C., HENDERSON, D. R., STONNER, F. W., VALENTA, Z., and WIESNER, K. *Chemistry & Industry*, 1068. 1954.
4. EDWARDS, O. E. and SINGH, T. *Can. J. Chem.* 32: 683. 1954.
5. FIESER, L. F. and ETTORE, R. *J. Am. Chem. Soc.* 75: 1700. 1953.
6. HENDERSON, D. R., STONNER, F. W., VALENTA, Z., and WIESNER, K. *Chemistry & Industry*, 544. 1954; 852. 1954.
7. JULIAN, P. L., COLE, W., MAGNANI, A., and MEYER, E. W. *J. Am. Chem. Soc.* 67: 1728. 1945.
8. MACLEAN, D. B. and PRIME, H. C. *Can. J. Chem.* 31: 543. 1953.
9. MANSKE, R. H. F. and MARION, L. *J. Am. Chem. Soc.* 69: 2126. 1947.
10. MEIER, H. L., MEISTER, P. D., and MARION, L. *Can. J. Chem.* 32: 268. 1954. MEIER, H. L. and MARION, L. *Can. J. Chem.* 32: 280. 1954.
11. PAUL, R. and TCHELITCHEFF, S. *Compt. rend.* 238: 2089. 1954; PAUL, R. and RIOBE, O. *Compt. rend.* 224: 475. 1947.
12. PICCINI, G. *Atti accad. sci. Torino*, 43: 554. 1907.
13. PRELOG, V. and SZPILFOGEL, S. *Helv. Chim. Acta*, 28: 1169. 1945.
14. VEXLEARSCHI, G. and RUMPF, P. *Compt. rend.* 236: 939. 1953.

FREE RADICALS BY MASS SPECTROMETRY

VII. THE IONIZATION POTENTIALS OF ETHYL, ISOPROPYL, AND PROPARGYL RADICALS AND THE APPEARANCE POTENTIALS OF THE RADICAL IONS IN SOME DERIVATIVES¹

By J. B. FARMER² AND F. P. LOSSING

ABSTRACT

The ionization potentials of ethyl, isopropyl, and propargyl radicals have been measured by electron impact on radicals produced by thermal decomposition of appropriate compounds. The values are: ethyl 8.78 ± 0.05 ev., isopropyl 7.90 ± 0.05 ev., and propargyl 8.25 ± 0.08 ev. From the appearance potentials of these ions in various compounds, the following values of bond dissociation energies were obtained:

$D(\text{C}_2\text{H}_5-\text{H}) = 98.5 \pm 2.3,$	$D(s\text{-C}_3\text{H}_7-\text{H}) = 86.7 \pm 2.3,$
$D(s\text{-C}_3\text{H}_7-\text{I}) = 42.4 \pm 2.3,$	$D(s\text{-C}_3\text{H}_7-\text{Br}) = 58.8 \pm 2.3,$
$D(s\text{-C}_3\text{H}_7-\text{Cl}) = 73.3 \pm 2.3,$	$D(\text{CH} \equiv \text{C} \cdot \text{CH}_2-\text{I}) = 45.7 \pm 3.2,$
$D(\text{CH} \equiv \text{C} \cdot \text{CH}_2-\text{Br}) = 57.9 \pm 3.2$ kcal./mole, assuming no kinetic energy of the products.	

INTRODUCTION

The ionization potential of the ethyl radical was measured by Fraser and Jewitt (5) by directing a beam of ethyl radicals and other products from the decomposition of lead tetraethyl into an ionization gauge detector. They found $I(\text{C}_2\text{H}_5) = 10.6 \pm 0.8$ ev., a value which was undoubtedly too high because of the presence of reaction products such as ethylene. Hipple and Stevenson (7) measured the ionization potential of the ethyl radical by electron impact on radicals produced by the thermal decomposition of lead tetraethyl in a quartz capillary furnace opening into the ionization chamber of a mass spectrometer. By this means they found $I(\text{C}_2\text{H}_5) = 8.67 \pm 0.1$ ev., a value which, taken in conjunction with the appearance potential of C_2H_5^+ in the mass spectrum of ethane, 12.92 ± 0.1 ev. (23), led to a dissociation energy of the $\text{C}_2\text{H}_5-\text{H}$ bond of 4.25 ± 0.2 ev. or 98.0 ± 4.6 kcal./mole. This is in good agreement with the average electron impact value of 4.20 ± 0.04 ev. (96.9 ± 1 kcal./mole) recently quoted by Stevenson (21) and the value of 98 ± 2 kcal./mole obtained by photobromination (1).

The ionization potential of the isopropyl radical has not previously been measured directly, but a value of 7.45 ± 0.1 ev. has been derived from the appearance potentials of C_3H_7^+ in the mass spectra of isobutane, isopentane, and 2,3-dimethyl butane, the heats of formation of these compounds, and the bond dissociation energies of CH_3-H and $\text{C}_2\text{H}_5-\text{H}$ (20). This value, together with the appearance potential of the C_3H_7^+ ion in the mass spectrum of propane, 11.67 ± 0.1 ev. (24), leads to a dissociation energy for the $s\text{-C}_3\text{H}_7-\text{H}$ bond of 4.22 ± 0.2 ev. (97.3 ± 4.6 kcal./mole). This appears to be high by comparison with Stevenson's electron impact average of 4.09 ± 0.09 ev.

¹Manuscript received January 14, 1955.

Contribution from the Division of Pure Chemistry, National Research Council, Ottawa, Canada. Issued as N.R.C. No. 3571.

²N.R.C. Postdoctorate Fellow 1953-1955.

(94.3 ± 2 kcal./mole) and with the Butler and Polanyi pyrolysis value of ~ 89 kcal./mole (19).

As far as the authors are aware, no published measurements or predictions of the ionization potential of the propargyl radical ($\text{CH}_2\text{C}\cdot\text{CH}_3$) have been made. The radical does not appear to have been identified previously, although it has been suggested that its thermal stability might be high (27).

EXPERIMENTAL

Production of the Radicals

The fact that ethyl and isopropyl radicals are much less stable thermally than methyl, allyl, or benzyl radicals, whose ionization potentials were reported in an earlier paper (13), required a modification of the reactor used previously. In a reactor of the type described in earlier papers (14, 15) the residence time was sufficiently long to allow the disappearance of an appreciable fraction of the radicals at the temperature ($\sim 660^\circ\text{C}$.) at which mercury diethyl or azo-isopropane decomposed. Although these radicals were found in considerable abundance under these conditions (12), the presence of appreciable amounts of the decomposition, disproportionation, and combination products caused serious interference at the parent peak of the radical. In order to reduce this interference a furnace was constructed in which the residence time would be shorter. This furnace was similar in design to that used by Hipple and Stevenson (7) and consisted of a quartz tube of 1.5 mm. internal diameter surrounded at the end by a heater, 2 cm. in length, cut from tantalum sheet in the shape previously described (15). The heater was enclosed in a quartz sheath sealed to the end of the quartz tube. A cylindrical radiation shield of Nichrome V surrounded the sheath. The furnace was mounted coaxially with the hole in the top plate of the ionization chamber, at a distance of about 1 mm. The compound was admitted to the reactor through a molecular-flow leak without the use of helium as a carrier. With this arrangement the pressure in the reactor was very low ($\sim 10^{-3}$ mm.) and second-order products were considerably reduced. The dissociation products of the radicals were still present but in reduced amounts.

(a) Ethyl Radicals

The decomposition of mercury diethyl at about 800°C . gave rise to ethyl radicals, butane, ethane, ethylene, and hydrogen. A small amount of undecomposed mercury diethyl was also present. Out of a combined peak height of 497 cm. at mass 29 using 50 ev. electrons, a net peak height of 249 cm. for the ethyl radical was obtained after subtraction of the contributions from ethane, butane, $\text{C}^{13}\text{C}^{13}\text{H}_4$, and mercury diethyl. The ratio of ethane to butane at 800°C . was 0.36:1. This ratio of disproportionation (k_1) to combination (k_2) (0.36) is not greatly different from that found ($k_1/k_2 = 0.1$ to 0.3) at lower temperatures (2, 10). If significant, this result would suggest that

$$E_{\text{combination}} \approx E_{\text{disproportionation}}$$

However, at the very low pressures involved ($\sim 10^{-3}$ mm.) it is questionable whether the ethane and butane arise from homogeneous disproportionation

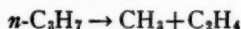
and combination reactions rather than from surface reactions. Some butane may also be formed directly from mercury diethyl under these conditions.

(b) *Isopropyl Radicals*

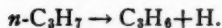
As in the case of ethyl, the production of a high concentration of isopropyl radicals presented experimental difficulties owing to the thermal instability of the radicals. In the high pressure reactor, the decomposition of azoisopropane in a stream of helium at 6.5 mm. was almost complete at 665°C. The increase in the mass 43 peak at low electron energies showed the isopropyl radical to be present. At this temperature some isopropyl radicals were decomposing, the products being propylene and hydrogen almost exclusively (12). By the use of a retractable furnace (9) in the high pressure reactor, the product of dimerization of the radicals was found to be mainly 2,3-dimethyl butane with a small amount of another hexane, possibly 2-methyl pentane, showing that the radicals were indeed isopropyl radicals. In the low pressure reactor, azoisopropane was 90% decomposed at 655°C. At this temperature the mass 43 peak height was 1030 cm. After subtracting the contributions from 2,3-dimethyl butane, propane, and undecomposed azoisopropane, a peak height of 329 cm. for the isopropyl radical remained.

(c) *n-Propyl Radicals*

Attempts to produce the *n*-propyl radical in quantities sufficient for ionization potential measurements were unsuccessful. The decomposition of azo-*n*-propane at 665°C. in the high pressure reactor resulted in the formation of methyl radicals and ethylene in approximately equal amounts, together with nitrogen, *n*-hexane, propane, propylene, and some ethane formed from the combination of the methyl radicals (12). The mode of decomposition of *n*-propyl appears to be almost entirely by



and not by



This is in agreement with conclusions drawn from kinetic studies (19).

(d) *Propargyl Radicals*

The decomposition of propargyl iodide at 1000–1100°C. in either the high-pressure or the low-pressure reactor resulted in a good yield of propargyl radicals. The dimer, 1,5-hexadiyne, was also formed.

Measurement of the Ionization Potentials

The method of calibrating the voltage scale using a number of standards was the same as that used previously (13). In this case the calibration line was found to have a slope of unity within the precision of measurement. Krypton was added to the gas stream as a reference standard, and the difference between the appearance potential of the radical peak and the appearance potential of the krypton mass 84 peak was determined by the method of extrapolated voltage differences (28). The net peak height for the radical ion at 50 ev. was determined by subtracting the contributions from dimers and other prod-

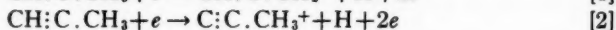
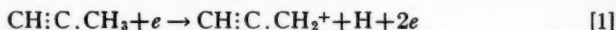
ucts as described above. Ionization efficiency curves for the radical ions from these products were measured to ensure that no contributions to the peaks could occur at the low electron energies at which the voltage difference measurements were made. The only correction of this kind found to be necessary was a small correction to the krypton mass 84 peak as a result of the 2,3-dimethyl butane formed from isopropyl radicals. This correction was evaluated from measurements of the mass 84 peak in the absence of krypton, other conditions being the same.

Measurement of the Appearance Potentials

As found by Stevenson and Hipple (23) a significant correction to the mass 29 peak was required in the measurement of $A(C_2H_5^+)$ from ethane. The appearance potential of $C_2H_4^+$ from ethane is appreciably lower than that of $C_2H_6^+$ (23). Consequently the mass 28 peak is many times as high as the mass 29 peak at electron energies a few volts above $A(C_2H_5^+)$. The isotopic $C^{12}C^{13}H_4^+$ peak from $C_2H_4^+$ was found to account for almost one-third of the mass 29 peak under these conditions. The correction to mass 29 was calculated from the natural abundance of C^{13} assuming that no difference in the ionization efficiency curves of $C^{12}C^{12}H_4^+$ and $C^{12}C^{13}H_4^+$ or in the ratio of formation of the ions would occur as a result of isotopic factors. This correction raised the observed value of $A(C_2H_5^+)$ by about 0.2 ev. as was found by Stevenson and Hipple (23).

The ionization efficiency curves for $A(C_2H_5^+)$ from the halides showed curved δV vs. I plots and the extrapolated values being apparently low by 0.4 to 0.6 ev. are not reported here. The cause of this discrepancy is not obvious. I^- ions from the iodide were found, but only to the extent of about one part in 6000 of the $C_2H_5^+$ ion. This amount should not appreciably lower the appearance potential, and in any case the ion may arise by a secondary process. The formation of ethyl radicals by pyrolysis on the filament followed by diffusion back into the ionization chamber would lower the observed appearance potential. However, it is difficult to see, in view of the thermal instability of ethyl, why this effect should be larger than for the more stable methyl or allyl radicals.

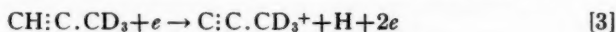
The appearance potential of the mass 39 ion from propyne was not measured since this ion may arise by two different processes



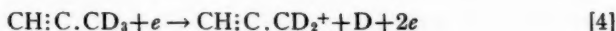
depending on which hydrogen atom is lost. In order to find out the extent to which process [2] occurs, the mass spectrum of a sample of $CH:C.CD_3$, kindly prepared by Dr. L. C. Leitch, was examined. The isotopic purity of the sample was determined from the mass spectrum obtained with electrons of energy sufficient to form the molecular ion but insufficient to form dissociation products (25). As shown in Table I, the sample was about 80% $CH:C.CD_3$.* In the 50-volt spectrum, after the parent ions have been subtracted in the

*The improbable rearrangement product $CD:C.CD_3H$ was assumed to be absent.

ratio of their abundance, the fragment ion at mass 42 can arise only by



and that at mass 41 mainly by



with a small contribution from the impurity

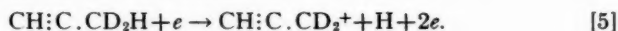
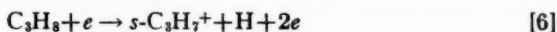


TABLE I
MASS SPECTRA OF TRIDEUTEROPROPYNE

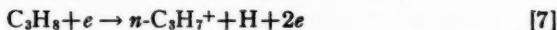
Mass No.	Peak height at low energy	Mole %	Peak height at 50 ev.	Parent ions	Fragment ions
44	0.2	1.1	—	—	—
43	15.0	79.4	2015	2015	—
42	2.8	14.8	798	376	422
41	0.5	2.7	1482	69	1413
40	0.35	2.0	—	—	—

If the contribution from process [5] is ignored, the ratio H loss/D loss from CH:C.CD_3 is then $422/1413 = 0.30$. It is possible, however, to correct for process [5] on the assumption that its probability is one half the sum of the probabilities of process [1] and process [2]. The contribution of process [5] to the mass 41 peak is then $376 \times \frac{1}{2} \times \text{ratio mass 39/mass 40 in propyn}$ (0.859). The fragment peak at mass 41 resulting from process [4] is then $1413 - (376 \times \frac{1}{2} \times 0.859) = 1252$, and the corrected ratio of H loss/D loss is $422/1252$ or 0.337. This is almost exactly $\frac{1}{3}$, suggesting that after a propyne molecule has been struck by a 50-volt electron, the four hydrogens in the excited ion are equivalent and the loss of a hydrogen atom from either end occurs on a statistical basis. Unfortunately the isotopic purity of the sample was not sufficiently high to give appearance potentials for processes [3] and [4] free from interference.

The same inherent ambiguity exists in the mass 43 peak from propane. It has, however, been reported that this ion is mainly $s\text{-C}_3\text{H}_7^+$ (18, 26). In addition, it is possible to say that the process



will have a lower appearance potential than the process



since $I(n\text{-C}_3\text{H}_7) > I(s\text{-C}_3\text{H}_7)$ and $D(n\text{-C}_3\text{H}_7\text{—H}) > D(s\text{-C}_3\text{H}_7\text{—H})$. In view of these considerations it is very probable that $A(\text{C}_3\text{H}_7^+)$ corresponds to process [6] and that the derived dissociation energy can be assigned to the $s\text{-C}_3\text{H}_7\text{—H}$ bond.

RESULTS AND DISCUSSION

The individual and average values obtained for the ionization potentials of the three radicals are given in Table II, together with some measured and calculated values from the literature. The appearance potentials of the radical ions from the derivatives are given in Table III. The dissociation energies for the radical-atom bonds, derived on the assumption that no kinetic energy term is involved, are also given in Table III for comparison with values from the literature. The limits of error shown should be regarded as limits of precision and not of absolute error.

TABLE II
IONIZATION POTENTIALS OF THE FREE RADICALS ETHYL, ISOPROPYL, AND PROPARGYL

Radical	Source	Ionization potential (ev.)			
		Individual values	Average	Literature value	Method
Ethyl	Mercury diethyl	8.80	8.78 \pm 0.05	8.67 \pm 0.1	Direct electron impact (7)
		8.79			
		8.76			
		8.78			
Isopropyl	Azoisopropane	7.01	7.90 \pm 0.05	7.43 \pm 0.1	A(<i>s</i> -C ₃ H ₇ ⁺) from isoalkanes (20)
		7.93		7.73	Calculated (4)
		7.88		7.81	Calculated (22)
		7.90			
Propargyl	Propargyl iodide	8.23	8.25 \pm 0.08		
		8.23			
		8.28			

Ethyl

The average value for the ionization potential of the ethyl radical, 8.78 \pm 0.05 ev., agrees with that of 8.67 \pm 0.1 ev., measured by Hipple and Stevenson, within the combined limits of error. The appearance potential of C₂H₅⁺ from ethane, 13.05 \pm 0.05 ev., lies within the estimated limits of error of the three previous measurements. Using the present data for *I*(C₂H₅[•]) and *A*(C₂H₅⁺), *D*(C₂H₅-H) = 4.27 \pm 0.10 ev. (98.5 \pm 2.3 kcal./mole). This result is perhaps just significantly higher than the average value from electron impact data (21), and within the limits set by the photobromination data (1).

As described above, the appearance potentials of the ethyl ion from the halides were anomalously low, and no reliable values for the dissociation energies of the ethyl-halide bonds could be obtained. It would be interesting to study the ionization efficiency curves for the ethyl ion from these compounds using some means of detecting fine structure (3, 17).

Isopropyl

The measured ionization potential of the isopropyl radical, 7.90 \pm 0.05 ev., is considerably higher than the 7.43 \pm 0.1 ev. derived from the appearance potentials of *s*-C₃H₇⁺ in the mass spectra of isoalkanes and from the relevant heats of formation (20). It is, in fact, very close to the 7.94 \pm 0.1 ev. derived in the same way for the *n*-propyl radical (21). As discussed in a previous section, there appeared to be no doubt of the identity of the isopropyl radical on the basis of the dimer formed. Even if some *n*-propyl radicals were initially

TABLE III
APPEARANCE POTENTIALS AND BOND DISSOCIATION ENERGIES

Substance	Ion	Appearance potential (ev.)			Bond dissociation energy (kcal./mole)		
		This work	Literature	Reference	This work	Literature	Reference
Ethane	Ethyl	13.05±0.05	12.92±0.1	(23)	98.5±2.3	98±2	(1)
			12.81±0.2	(11)		96.9±1	(21)
			12.71±0.4	(16)			
Propane	Isopropyl	11.66±0.05	11.67±0.1	(24)	86.7±2.3	~89	(19)
			11.5±0.3	(11)		94.3±2	(21)
			11.76±0.1	(16)			
Isopropyl iodide	Isopropyl	9.74±0.05	—	—	42.4±2.3	46	(19)
Isopropyl bromide	Isopropyl	10.45±0.05	—	—	58.8±2.3	—	—
Isopropyl chloride	Isopropyl	11.08±0.05	—	—	73.3±2.3	—	—
Propargyl iodide	Propargyl	10.23±0.06	—	—	45.7±3.2	—	—
Propargyl bromide	Propargyl	10.76±0.06	—	—	57.9±3.2	—	—

formed, they would decompose very rapidly at the temperature of the reactor as was found in the attempt to produce the *n*-propyl radical. With the present method of plotting the ionization efficiency curves, the measured ionization potential would be high if some contribution to the 50 ev. peak at mass 43 had been neglected in calculating the net radical peak height at 50 ev. A decrease of 10% in the net 50 ev. peak height would lower the ionization potential by only 0.05 ev. The four individual values for $I(s\text{-C}_3\text{H}_7)$ given in Table III were obtained in two separate experiments separated by an interval of a few days.

The appearance potential of mass 43 from propane (11.66 ± 0.05 ev.) is in good agreement with previously measured values (11, 16, 24). However the value of $D(s\text{-C}_3\text{H}_7\text{—H})$ from the present data

$$A(s\text{-C}_3\text{H}_7^+) - I(s\text{-C}_3\text{H}_7) = 11.66 - 7.90 = 3.76 \pm 0.10 \text{ ev.,}$$

or 86.7 ± 2.3 kcal./mole, would appear to be considerably too low by comparison with the electron impact average of 94.3 ± 2 kcal. The derived dissociation energies for the isopropyl-halide bonds also appear to be low, although the absence of reliable kinetic data for these bonds makes comparison difficult. The appearance potential data for the isopropyl ion would suggest that the measured ionization potential is too high by about 0.3 ev. It is interesting to note that two values of the ionization potential calculated by Franklin and Field (4) (7.73 ev.) and by Stevenson (22) (7.81 ev.) on the basis of a simplified molecular orbital method, both lie between the presently measured value and the average electron impact value. The calculated value of Franklin and Field, 7.73 ev., was based on $I(\text{CH}_3) = 10.07$ ev. and $I(\text{C}_2\text{H}_5) = 8.67$ ev., that of Stevenson on the later value for methyl $I(\text{CH}_3) = 9.96$ ev. and $I(\text{C}_2\text{H}_5) = 8.67$ ev. Using $I(\text{CH}_3) = 9.96$ and $I(\text{C}_2\text{H}_5) = 8.78$ as measured in this work, the same calculation of the ionization potential of the isopropyl radical gives 7.97 ev. In view of the assumptions and simplifications necessary in such a calculation, it is doubtful whether this result can be considered as support for the high value for $I(s\text{-C}_3\text{H}_7)$ found here. It would appear that further work is necessary to resolve the discrepancy.

Propargyl

The ionization potential of the propargyl radical, 8.25 ± 0.08 ev., is only slightly higher than the 8.16 ± 0.03 ev. found for the allyl radical (13). This difference is considerably smaller than that between the ionization potentials of propyne (10.43 ± 0.1 ev.) (6) and propylene (9.84 ev.) (8).

The dissociation energies of the propargyl-halide bonds are not known from other sources for comparison purposes, but the derived values seem rather low in view of the high temperature required to dissociate propargyl iodide.

REFERENCES

1. ANDERSON, H. C. and VAN ARTSDALEN, E. R. J. Chem. Phys. 12: 479. 1944.
2. AUSLOOS, P. and STEACIE, E. W. R. Bull. Soc. chim. Belges, 63: 87. 1954.
3. FOX, R. E., HICKAM, W. M., and KJELDAAS, T. Phys. Rev. 89: 555. 1953; 90: 386. 1953.
4. FRANKLIN, J. L. Private communication.
5. FRASER, R. G. J. and JEWITT, T. N. Proc. Roy. Soc. (London), A, 160: 563. 1937. Phys. Rev. 50: 1091. 1936.

6. GAUTHIER, F. and PILON, J. R. Unpublished work.
7. HIPPLE, J. A. and STEVENSON, D. P. *Phys. Rev.* 63: 121. 1943.
8. HONIG, R. E. *J. Chem. Phys.* 16: 105. 1948.
9. INGOLD, K. U. and LOSSING, F. P. *J. Chem. Phys.* 21: 1135. 1953.
10. IVIN, K. J., WIJNEN, M. H. J., and STEACIE, E. W. R. *J. Phys. Chem.* 56: 967. 1952.
11. KOFFEL, M. B. and LAD, R. A. *J. Chem. Phys.* 16: 420. 1948.
12. LOSSING, F. P., INGOLD, K. U., and HENDERSON, I. H. S. *Applied Mass Spectrometry*, Institute of Petroleum, London 1954.
13. LOSSING, F. P., INGOLD, K. U., and HENDERSON, I. H. S. *J. Chem. Phys.* 22: 621. 1954.
14. LOSSING, F. P., INGOLD, K. U., and TICKNER, A. W. *Discussions Faraday Soc.* No. 14: 34. 1953.
15. LOSSING, F. P. and TICKNER, A. W. *J. Chem. Phys.* 20: 907. 1952.
16. MITCHELL, J. J. and COLEMAN, F. F. *J. Chem. Phys.* 17: 44. 1949.
17. MORRISON, J. D. *J. Chem. Phys.* 19: 1305. 1951.
18. SCHISLER, D. O., THOMPSON, S. O., and TURKEVICH, J. *Discussions Faraday Soc.* No. 10: 46. 1951.
19. STEACIE, E. W. R. *Atomic and free radical reactions*. Reinhold Publishing Corporation, New York. 1954.
20. STEVENSON, D. P. *Discussions Faraday Soc.* No. 10: 35. 1951.
21. STEVENSON, D. P. *Trans. Faraday Soc.* 49: 867. 1953.
22. STEVENSON, D. P. Abstracts A.C.S. Meeting. Kansas City. April 1954.
23. STEVENSON, D. P. and HIPPLE, J. A. *J. Am. Chem. Soc.* 64: 1588. 1942. (Corrected to $I(\text{argon}) = 15.77 \text{ ev.}$)
24. STEVENSON, D. P. and HIPPLE, J. A. *J. Am. Chem. Soc.* 64: 2769. 1942.
25. STEVENSON, D. P. and WAGNER, C. D. *J. Am. Chem. Soc.* 72: 5612. 1950.
26. STEVENSON, D. P. and WAGNER, C. D. *J. Chem. Phys.* 19: 11. 1951.
27. SZWARC, M. *Discussions Faraday Soc.* No. 10: 143. 1951.
28. WARREN, J. W. *Nature*, 165: 810. 1950.

THE HYDRATION OF PLASTER OF PARIS¹

BY FRASER W. BIRSS² AND T. THORVALDSON

ABSTRACT

The hemihydrate of calcium sulphate labelled with calcium-45 or sulphur-35 was hydrated in a supersaturated solution of calcium sulphate at 21°C. The distribution of the radioactive isotope between the solution and the solid phases and the concentration of the solution throughout the period of hydration were measured. The exchange of calcium ions between crystalline gypsum and its solution was also studied. The experimental results are discussed from the viewpoint of the mechanism involved. They are found to be in agreement with a mechanism which postulates a single passage of the structural units of the solid hemihydrate through the solution and not consistent with one of direct hydration without temporary independent existence of the products in the liquid phase.

INTRODUCTION

The availability of radioactive isotopes provides a new method for the study of reactions between slightly soluble substances and aqueous solutions. A paper by Graham, Spinks, and Thorvaldson (1) on the hydrolysis and hydration of tricalcium silicate and β -dicalcium silicate illustrates some of the possibilities of the method. The experimental results obtained by these workers are readily interpreted on the basis of the theory of Le Chatelier, that the anhydrous silicates pass into solution and react to form less soluble hydrated silicates, which then separate out of the supersaturated solution. They are not so readily interpreted on the basis of the direct hydration of the silicate in the solid state, with only calcium hydroxide splitting off to enter the hydrating liquid.

As the study of the hydration of these silicates is complicated by the variable lime-silica ratio and the gel-like nature of the hydrated silicates, it was considered desirable to apply the method to a simpler system. The hydration of plaster of Paris was selected because of its historical and scientific interest in relation to the chemistry of cements.

There are several points of difference between the hydration of tricalcium silicate and of plaster of Paris. In the case of the silicate labelled with calcium-45 two methods are available for following the progress of the reaction, i.e. the determination of (i) the alkalinity and (ii) the activity³ of the liquid phase, while in the case of plaster of Paris labelled with calcium-45 or sulphur-35 only the second method is available. The solubility of the hydrated silicate in solutions of calcium hydroxide is extremely small while the solubility of gypsum in water is much higher and supersaturation of the order of fourfold with respect to the hydration product may be obtained during hydration of the hemi-

¹ Manuscript received January 25, 1955.

Contribution from the Department of Chemistry, University of Saskatchewan, Saskatoon, Sask., with financial support from the National Research Council of Canada. This paper represents a part of a thesis submitted by one of us (F. W. B.) as partial requirement for the degree of Master of Arts.

²Holder of a bursary from the National Research Council of Canada.

³The terms "active", "inactive", and "activity" will be used to refer to radioactivity and not to the chemical activity of the materials under discussion.

hydrate. The ratio of lime to silica in the silicate changes during the hydration and this ratio in the product varies with the concentration of lime in the solution, while the corresponding stoichiometric ratio of the calcium sulphate remains unchanged. Furthermore, the hydrolysis of the silicate is a comparatively long process, starting off fairly rapidly with the rate tapering off with time, while the hydration of the hemihydrate of calcium sulphate begins very slowly and continues at a steadily accelerating rate.

Assuming a "through-solution" mechanism for the conversion of the hemihydrate to the dihydrate, a mathematical expression for the progressive change in the activity of the liquid phase may readily be developed in a similar manner to that used in the case of the hydration of tricalcium silicate (1). Two complicating factors may enter: (i) substantial changes in the concentration of the hydrating liquid due to the formation of supersaturated solutions with subsequent precipitation of gypsum, and (ii) exchange of Ca^{45} or S^{35}O_4 ions between the solution and the hydration product after precipitation. These must be considered in applying the theoretical equation to the experimental data.

EXPERIMENTAL

Materials

Calcium sulphate dihydrate was prepared from reprecipitated "alkali-free" calcium carbonate. The latter was dissolved in hot dilute hydrochloric acid, calcium sulphate precipitated slowly with ammonium sulphate, washed, and dried over plaster of Paris. The radioactive samples were prepared by addition of a suitable amount of $\text{Ca}^{45}\text{Cl}_2$ or $\text{H}_2\text{S}^{35}\text{O}_4$, obtained from Atomic Energy of Canada, to the solution before the precipitation. The sample of gypsum labelled with calcium-45 was completely crystalline, composed mainly of thin prisms varying in thickness from 0.002 to 0.01 mm. with an occasional crystal as much as 0.025 mm. thick. The loss on dehydration agreed well with the theoretical value for the dihydrate.

The gypsum was dehydrated in an oven at 85–87°C. in a slow current of air. The time required to reduce the moisture content to that of the hemihydrate was about eight hours when further dehydration almost stopped. The Ca^{45} -labelled sample used for the hydration appeared to be mainly in the form of elongated fibrous plates, composed of aggregates of small crystals. The sample labelled with S^{35}O_4 ions was composed of smaller particles. The water content of the samples was close to the theoretical value for the hemihydrate.

Determination of the Activity of the Solutions

The activity of the solutions was determined on 0.500-ml. portions, at least in triplicate, after precipitation of the calcium as oxalate and evaporation to dryness, using an end window Geiger-Mueller tube (window thickness 1.7 mgm. per sq. cm.; scale of 64 scaler) and an electric timer. The geometry was kept constant and enough counts were made to reduce the probable error to less than 2%. Corrections were made for background, for self-absorption when necessary, and for the resolving time error of the tube-scaler assembly above counting rates of 25 registers per min.

Exchange of Calcium Between Gypsum Crystals and Solution

Freshly precipitated gypsum crystals were digested for a long period of time, first at 38°C. and then at 21°C., and after filtration were dried over plaster of Paris. The sample was composed of long prisms of fairly uniform thickness of from 0.004 to 0.007 mm. with an occasional crystal measuring 0.003 mm. In the exchange experiments 0.05-gm. samples were shaken in pyrex centrifuge tubes with 9 ml. water at 21°C. for four weeks, 1 ml. of a saturated solution of calcium sulphate labelled with calcium-45 was then added, the shaking was continued, and individual tubes were removed from time to time for counting the solution. The ratio of solid to dissolved calcium sulphate in the system was about 1:1. The room was thermostatted at 21°C.

The calculated activity at time of mixing, assuming no exchange, was 15.16 registers per min. for 0.5 ml. of solution. Counts were made on separate tubes at 30 sec.; 20, 40, and 60 min.; two, four, and six hours after adding the calcium-45 activity. The values obtained were (reg./min./0.5 ml.) 15.08, 15.12, 15.22, 15.21, 15.13, 15.07, and 15.03, respectively. For the conditions and duration of these experiments it appears that exchange of calcium ions between the solid and solution does not significantly affect the activity within the accuracy of counting.

In our hydration experiments with plaster of Paris one might expect greater exchange owing to smaller crystals and higher specific surface. A second series of experiments was therefore made to attempt to determine exchange rates with very small crystals. These were prepared by shaking together in pyrex centrifuge tubes weighed quantities of precipitated calcium carbonate and equivalent amounts of 0.1 molar sulphuric acid. Within two minutes the calcium carbonate had completely dissolved, followed by the formation of a voluminous precipitate of hydrated calcium sulphate. After rapid centrifuging, samples of the clear supersaturated liquid were removed for analysis to determine the concentration of the solution and the weight of solid (by difference). A standard solution of calcium sulphate labelled with calcium-45 was immediately added to each tube and the tubes shaken to allow exchange to take place. The total time required for these manipulations up to the beginning of the exchange shaking was approximately six minutes. From time to time tubes were centrifuged and the solution counted. The concentration of the solution was determined in each case and corrections applied to the count for self-absorption on the basis of previously determined values for the concentrations found.

The crystals formed by the action of the acid on the carbonate, separated from the mother liquor by rapid filtration two minutes after mixing, were fine prisms mostly less than 0.0015 mm. in diameter. At this stage the mother liquor was highly supersaturated with respect to gypsum, containing as much as five times the saturation value. The concentration after dilution with the active solution was still three to four times the saturation value. After an additional period of shaking with the mother liquor for 12 min. (i.e. the period required for complete hydration in the experiments described below) the crystals had grown considerably; many of them were more than 0.002 mm. in diameter and the solution was approaching saturation.

The experimental conditions were in some ways similar to those of the hydrations described below. The total weight of calcium sulphate in the system and the volume used were the same. The concentrations of the solutions at the beginning of the exchange shaking were of the same order as those at the beginning of the hydration runs. On the other hand in the exchange experiments the activity of the solution and the specific activity of the solute were at the maximum at the beginning when the size of the crystals was at a minimum while in the hydration runs the total and specific activities of the solute were at a minimum at the beginning when the crystals of gypsum were of minimum size. Thus the conditions were more favorable to high exchange in the present experiments than in the hydration runs.

The per cent exchange of calcium was calculated, correction being made for the activity removed from the solution by precipitation. This correction, which was based on the mean specific activity of the solute during the exchange period, is probably too small, since most of the precipitation occurred during the first half of the time interval when the specific activity is near the maximum, thus making the value attributed to exchange too large. The average value obtained for exchange was 2.2% in 10 min. and 4.8% in 20 min. This amounts to about 3% for a 12-min. period, the time required for the hydration runs. The great increase in the size of the crystals during this period suggests that the exchange is mainly due to recrystallization of the original inactive finely divided precipitate. As long as there are a large number of small crystals present subject to recrystallization, the rate of this process probably increases as the concentration of the solution falls giving proportionally greater exchange during the longer periods. While we were mainly interested in what happened during the first 12 min., the experiments were continued up to 24 hr. The approximate values obtained for the per cent exchange for the longer periods indicated that the rate of exchange increased up to a maximum in about one hour, then fell slowly, and that 100% exchange was approached in 24 hr. The question of exchange in the hydration experiments will be discussed later.

The Hydration of Plaster of Paris Labelled With Calcium-45

If one brings the active solid hemihydrate into contact with a saturated solution of gypsum it dissolves, producing, before any precipitation occurs, an active solution which is highly supersaturated with respect to the dihydrate. To reduce such dissolution of the active sulphate it is necessary to prepare an inactive supersaturated solution and to use this as the hydrating liquid.

The hydrating solution was prepared by adding successive portions of the inactive hemihydrate to freshly boiled and cooled redistilled water until apparently no further solution occurred on vigorous shaking. Five-milliliter portions of the centrifuged solution were placed in a number of 15-ml. centrifuge tubes each containing 44.0 mgm. of the radioactive plaster of Paris. These were immediately stoppered with serum bottle caps and shaken vigorously for a definite period of time. After centrifuging, three 0.500-ml. samples of the solution were withdrawn for determination of concentration (evaporation and weighing on a microbalance) and three samples for counting. Three

series of runs were made. The experimental values for the initial concentration of the hydrating liquid of the three series of runs were 4.42, 4.40, and 4.41 mgm. (expressed as the hemihydrate) per 0.5 ml. The average value 4.41 mgm./0.5 ml. was used in all the calculations. The maximum activity in the solution was, in each case, recorded at 11.7 min. The data for one of the series of runs are recorded in Table I. All the determinations of the activity for the three runs and the corresponding values for the concentration of the hydrating liquid are plotted in Fig. 1.

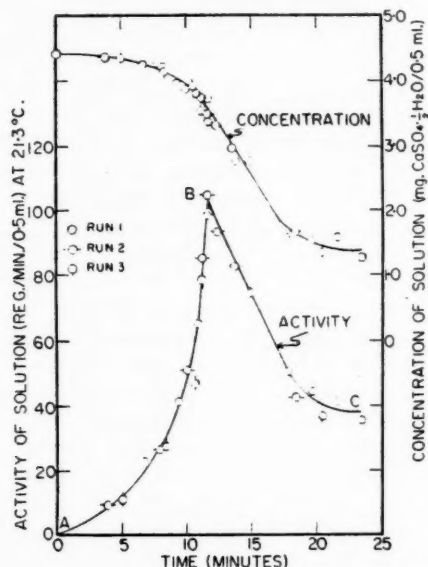


FIG. 1. The liberation of activity to the solution and the changes in concentration when 44 mgm. of the hemihydrate of calcium sulphate, labelled with calcium-45 (specific activity 43.1 reg./min./mgm.), were hydrated in 5 ml. of inactive calcium sulphate solution.

TABLE I
HYDRATION OF 44.0 MGm. Ca^{45} -LABELLED PLASTER OF PARIS* IN 5 ML. SUPERSATURATED SOLUTION OF INACTIVE CALCIUM SULPHATE AT 21.3°C.

Shaking period, min.	Centrifuging period, min.	Concentration of solution†	Count,‡ reg./min./0.5 ml.
0	0	4.40	0
3.8	3.0	4.37	9.7
7.8	3.1	4.28	26.5
10.0	2.8	3.88	50.7
11.2	2.9	3.74	85.0
11.7	3.1	3.50	105.0
12.35	2.7	3.32	93.6
13.6	2.9	2.98	82.5
18.4	3.2	1.68	42.4

*Specific activity of the plaster of Paris = 43.1 reg./min./mgm.

†Expressed as milligrams of plaster of Paris per 0.5 ml. of solution.

‡Corrected for background, self-absorption, and resolving time but not for changes in concentration of the solution.

The Hydration of Plaster of Paris Labelled with Sulphur-35

Three similar runs were made with the sample of plaster of Paris labelled with sulphur-35. The same types of curves were obtained both for the development of activity in the hydrating liquid and for changes in concentration. The maximum activity in the liquid was attained in a shorter time (approximately nine minutes) possibly owing to the smaller particles of the sample or to presence of more gypsum nuclei. There was somewhat greater variability in the experimental results. Otherwise there was no essential difference between the curves obtained for the hydration of the two samples of hemihydrate labelled with calcium-45 and sulphur-35.

DISCUSSION

Derivation of the Theoretical Expression for the Activity of the Solution

An expression for the relation between the extent of hydration and the activity of the hydrating solution may be derived on the basis of a through-solution mechanism. The derivation given below assumes:

(i) Constant concentration of the solution, i.e. that the rate of precipitation of gypsum is at all times equivalent to the rate of solution of the hemihydrate.

(ii) No exchange of the active ion between the solution and the hydrate after precipitation.

(iii) Rapid enough shaking so that the dissolved radioactive isotope is at all times essentially uniformly distributed throughout the solution.

Let a = moles of inactive CaSO_4 in the original solution,

m = moles of labelled solid hemihydrate placed in the system,

b = the specific activity per mole of the hemihydrate,

x = moles of labelled hemihydrate which have passed into the solution,

$f(x)$ = the specific activity of the calcium sulphate in the liquid phase.

Consider the hydration of dx moles of active plaster of Paris, releasing an activity $b dx$ to give a solution of specific activity $f(x)$. The sulphate precipitates as gypsum carrying down an activity $f(x) dx$ from the solution. The net activity liberated to the solution during the process is $b dx - f(x) dx$. When x moles of the plaster of Paris have thus passed through the solution the activity in the solution becomes

$$\int_0^x (b dx - f(x) dx) = bx - \int_0^x f(x) dx.$$

One can evaluate $f(x)$ in terms of a , b , and x and integrate this expression by a method similar to that used by Graham, Spinks, and Thorvaldson (1), thus obtaining the expression for the activity in solution = $ab(1 - e^{-x/a})$. Dividing by mb the total activity in the system and multiplying by 100 one obtains the percentage of total activity in the solution = $(100a/m)(1 - e^{-x/a})$.

In place of "moles CaSO_4 " one may use the weight of CaSO_4 , $\text{CaSO}_4 \cdot \frac{1}{2}\text{H}_2\text{O}$, or $\text{CaSO}_4 \cdot 2\text{H}_2\text{O}$ in the system, or weight of any of these per unit volume of solution provided the basis of reference is the same for all quantities. In the discussion of the hydration experiments in this paper the concentration of

calcium sulphate in solution is always expressed in terms of milligrams of the hemihydrate per 0.5 ml. of solution.

The End Point of the Hydration

In each series of the hydration runs with the Ca^{45} -labelled sample, the maximum activity of the hydrating liquid was attained in 11.7 min. The question presents itself: was the hydration complete at this point or was an increase in activity due to subsequent hydration masked by a lowering due to precipitation? This question is answered by consideration of the specific activity of the calcium sulphate in the solution after the 11.7-min. point (Fig. 1, curve BC). If the specific activity of the solute remains constant, then precipitation is the only process taking place.⁴ Calculation of the specific activity at points between 11.7 and 20.0 min. gave a constant value, i.e.,

$$[\text{activity (reg./min./0.5 ml.)}]/[\text{concentration (mgm./0.5 ml.)}] = 29.$$

This indicates that after the 11.7-min. point the only factor affecting the activity of the solution was precipitation and that the hydration was therefore essentially complete at this point.

The Correction for Changes in Concentration of the Hydrating Liquid

Before comparing the experimental values for the activity of the hydrating liquid during the period of hydration (Fig. 1, curve AB) with those calculated by use of the theoretical equation, correction must be made for changes in concentration. The gradual decrease in the concentration of the solution indicated in Fig. 1 corresponds to the removal of continually increasing amounts of activity. For the ascending portion (AB) of the hydration curve the change in concentration is comparatively small while after the end point of the hydration it is much more rapid until the solution approaches saturation with respect to gypsum.

An approximate value for the lowering of the activity of the solution due to the decrease in concentration during any small time-interval is given by the expression

$$(w_i - w_f) \left[\frac{1}{2} (a_i/w_i + a_f/w_f) \right]$$

where w_i and w_f are the concentrations at the beginning and end, respectively, of the interval, and a_i and a_f are the corresponding activities of the solution. The expressions a_i/w_i and a_f/w_f represent the specific activities of the calcium sulphate in the hydrating liquid at the beginning and end, respectively, of the time interval.

The calculated corrections for the period of hydration, using nine time-intervals, are given in Table II. Doubling the number of intervals does not change the corrected final a_f value materially.

The corrected experimental value for the activity of the solution at the end of the hydration period (i.e. at 11.7 min.) is 116 reg./min./0.5 ml. or 61% of the total activity of the system. The corresponding value for complete hydration calculated from the theoretical equation is 63% of the total activity.⁵

⁴An exception to this statement would be the unlikely case where two or more compensating processes in addition to precipitation occur in the system.

⁵For total exchange the calculated value for the activity of the solution at the end point of the hydration, for our experimental conditions, is 76 reg./min./0.5 ml., or 40% of the total activity of the system.

TABLE II
HYDRATION OF PLASTER OF PARIS
Correction of experimental activities for changes in concentration

Time interval (min.)	0-5	5-7	7-8	8-9	9-10	10-10.5	10.5-11	11-11.5	11.5-11.7
Activity* at beginning of interval (a_i)	0	11.8	20.5	28.5	38.2	50.5	57.5	73	95
Activity at end of interval (a_f)	11.8	20.5	28.5	38.2	50.5	57.5	73.0	95	105
Conc.† of soln. at beginning of interval (w_i)	4.41	4.36	4.25	4.20	4.10	3.95	3.87	3.76	3.62
Conc. of soln. at end of interval (w_f)	4.36	4.25	4.20	4.10	3.95	3.87	3.76	3.62	3.57
Decrease in conc.	0.05	0.11	0.05	0.10	0.15	0.08	0.11	0.14	0.05
Calc. activity removed by change in conc.	0.1	0.4	0.3	0.8	1.7	1.1	1.9	3.2	1.4
a_f correction for change in conc. of soln.	11.9	21.0	29.3	39.8	53.8	61.9	79.3	105	116
Per cent of total activity in soln.	6.3	11.1	15.5	21.0	28.3	32.6	41.8	55	61

*All activities are expressed as registers per minute per 0.5 ml.

†All concentrations are expressed as milligrams plaster of Paris per 0.5 ml.

These values may be considered to be in good agreement as any lack of thorough mixing of the solution during the hydration would tend to cause precipitation of gypsum in regions of high activity and thus lower unduly the activity of the solution. There is likely to be some lowering of activity due to this cause near the end of the hydration when the rate of reaction is very high and the diffusion of the calcium ions through a film adhering to the solid may become the limiting factor. Furthermore, the experimental values obtained at the 11.7-min. point are likely to be below the true maximum, as a slight displacement along the time axis, either way, from the true end point (which is not necessarily exactly 11.7 min.) would give lower values for the activity. For these reasons the maximum experimental value at 11.7 min. was used in the calculation of the final corrected maximum instead of the average for the three series of runs. The close reproducibility of the three series of experimental runs is an indication of the clock-like regularity of the hydration process under given conditions.

The Question of Exchange

The theoretical equation gives a measure of the exchange of the radioactive isotope between the solid and the solution, resulting from the dissolution of the active hemihydrate and the essentially simultaneous precipitation of an equivalent amount of an active dihydrate. Exchange of calcium occurring during the hydration period but after separation of the solid hydration product would reduce the experimental value for the activity of the solution below those values calculated by the equation. Recrystallization during the period of hydration through the solution of very small crystals with redeposition on larger ones, which means a second passage of the calcium sulphate through the solution, would also lower unduly the activity of the solution.

There is considerable evidence indicating that the effect of these processes on the experimental values for the activity of the hydrating liquid is small. The experiments described above indicate that the rate of exchange of the calcium ion between gypsum and its saturated solution, after the system has attained equilibrium, is negligible for the time of exposure involved in our experiments. During the hydration the surfaces of the growing crystals are continually in radioactive exchange equilibrium with the calcium sulphate in the solution. For further exchange the radioactive ion must pass from the surface to the zone of lower radioactivity inside the crystal. The very low rate of diffusion of the calcium ion in the crystalline solid therefore determines the rate of exchange.

The gypsum prisms formed in the hydration runs were of fairly uniform size, mainly 0.003 to 0.004 mm. in diameter, with very few less than 0.002 mm. This suggests a regular growth of the crystals during the hydration period and indicates that near the end of the hydration there were very few crystals small enough to take part in a recrystallization process. Such recrystallization would also be inhibited by the very high supersaturation of the solution right up to the end of the hydration period.

During the early part of the hydration period when both exchange through diffusion, due to the high specific surface, and exchange through recrystalliza-

tion, due to the small size of the crystals of gypsum, would be at a maximum, both the rate of hydration and the activity of the solution are very low. Less than 5% of the plaster of Paris is hydrated during the first third and less than 10% during the first half of the hydration period (see Fig. 3) thus favoring the growth of the gypsum nuclei present in the solution to a size where the tendency for recrystallization is reduced or eliminated. Even if there were considerable exchange during this early period the over-all effect for the hydration of the whole sample would be small.

The constancy of the specific activity of the dissolved solid in the post-hydration period is perhaps the strongest evidence for the absence of appreciable exchange effects through diffusion or recrystallization during the period of hydration, for such processes, if operating, would be expected to carry beyond the end point.

The experimental findings are therefore in agreement with the assumption that the structural units of crystalline plaster of Paris pass through the solution during the hydration and that the theoretical equation is applicable to the process.

The Rate of Hydration

From the corrected experimental values for the per cent of total activity found in the solution (Table II) one may calculate, by means of the theoretical equation, the percentage of the plaster of Paris hydrated (i.e. $100x/m$) corresponding to any given activity or the end of any time interval. Fig. 2 gives the calculated per cent hydration vs. the corrected activity of the solution and Fig. 3 the rate curve for the hydration at 21.3°C. under the conditions of our experiments.

Another approximation of the extent of hydration may be derived directly from the experimental data if the through-solution mechanism is assumed. In any interval, x_i moles of labelled hemihydrate pass into solution releasing an activity bx_i to the solution. If no concurrent precipitation took place the activity of the solution would become $a_i + bx_i$ and the concentration $w_i + x_i$. Upon precipitation the solution assumes an activity a_f which is directly proportional to the final concentration attained, w_f .

$$\begin{aligned} a_f &= [w_f / (w_i + x_i)] (a_i + bx_i) \\ \text{and} \quad x_i &= (a_i w_f - a_f w_i) / (w_f b - a_f) \end{aligned}$$

Calculations based on this approximation yield results in good agreement with those given in Figs. 2 and 3 if the intervals are sufficiently small.

It is of interest to note that the shape of our rate curve, which was obtained with a very low ratio of the hemihydrate to solution, is in general agreement with the thermal curve obtained by Weiser and Moreland (2) with a very high ratio of plaster to water (50 gm. to 30 ml.). The period of slow hydration at the beginning ("inhibition period") is attributed by these authors to dearth of crystal nuclei of the hydration product and was found to be shortened or eliminated by the addition of small amounts of finely crystalline gypsum to the plaster.

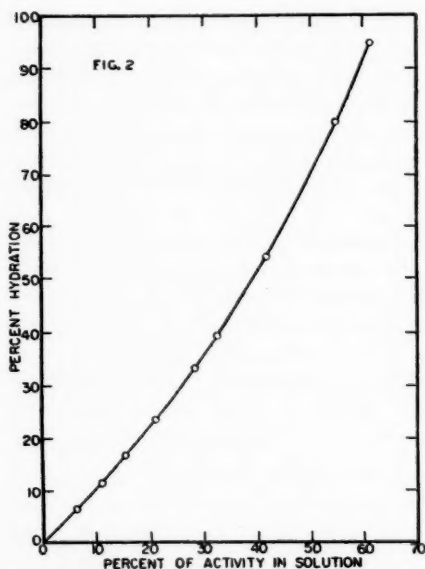


FIG. 2. The relation between the per cent of active plaster of Paris hydrated and the per cent of the total activity found in the hydrating liquid.

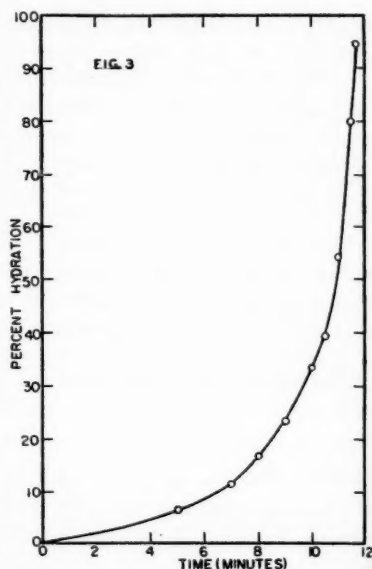


FIG. 3. The rate curve for the hydration of plaster of Paris at 21.3°C.

The Hydration of Plaster of Paris Labelled with Sulphur-35

The above discussion also applies to the data obtained with the sample of plaster of Paris labelled with S^{35} . The final value for the activity corrected for the effect of precipitation was 62% of the total activity in the system as compared to 64%, the value required by the theory for hydration by a through-solution mechanism under our experimental conditions.

GENERAL CONCLUSION

The experimental results for the hydration of plaster of Paris are in agreement with those calculated for a through-solution mechanism, while they are not consistent with the assumption of any mechanism of direct hydration without the solid passing into solution. Direct hydration alone would not give rise to activity in the solution. If one assumes that the first step of the process is a surface reaction between the crystals of the hemihydrate and water one would have to postulate that the dihydrate formed passes into solution and maintains the high supersaturation of the solution with respect to gypsum crystals during the period of hydration.

REFERENCES

1. GRAHAM, W. A. G., SPINKS, J. W. T., and THORVALDSON, T. *Can. J. Chem.* 32: 129. 1954.
2. WEISER, H. B. and MORELAND, F. *J. Phys. Chem.* 36: 1. 1932.

THE MECHANISM OF THE HYDRATION OF CALCIUM OXIDE¹

BY FRASER W. BIRSS² AND T. THORVALDSON

ABSTRACT

Three samples of calcium oxide, designated as A, B, and C, were prepared from calcium carbonate labelled with calcium-45. A was heated to constant weight at 700°C.; B was heated an additional three hours at 1400 to 1550°C.; and C was heated six hours at the same temperature. The samples were hydrated in a supersaturated lime solution at 21°C., the development of activity and the changes in concentration of the solution being determined. The activity entering the solution accounted, according to theory, for the following percentages of the samples passing through the solution during the hydration: A, 27%; B, 57%; C, 94%. These results indicate that sample C ("dead-burnt" lime) hydrated by a "through-solution" mechanism, but that A and B either hydrated partly according to some other mechanism, such as a vapor phase process in the pores of the particles of lime, or the calcium ions failed to reach the bulk of the hydrating liquid before precipitation as calcium hydroxide.

INTRODUCTION

Three cases of hydration, namely of tricalcium silicate, β -dicalcium silicate, and the hemihydrate of calcium sulphate, have been studied by the newly developed method of using radioactive elements as tracers (1, 2). The experimental evidence available on the mechanism of the hydration of the two silicates has in the past been rather inconclusive. However, it is generally considered that when plaster of Paris is brought into contact with a large excess of water, the solid passes into solution and then crystallizes out as gypsum. The results of the experiments with the hemihydrate of calcium sulphate labelled with calcium-45 or sulphur-35 (1) were found to be compatible with such a "through-solution" mechanism, thus giving, when combined with the previous findings (2), indirect support to the theory of a similar mechanism for hydration of the silicates.

Calcium oxide was selected for similar experiments because of the violence of its reaction with water. It was thought that the tracer method applied to this reaction might give support to the alternative theory that some solids react directly with water, hydrating without passing through the solution in the process. It is well known that when calcium oxide is brought into contact with water, solutions highly supersaturated with respect to crystalline calcium hydroxide are formed, and that these solutions shed the excess hydroxide rather slowly. Thus it is evident that, at least in part, the solid passes through the solution. However, if the predominant reaction is a direct one between water and solid lime without the latter passing into solution, then the tracer method should disclose this and might show that the hydration goes completely by this path if a highly supersaturated solution of lime is used as the hydrating liquid.

¹Manuscript received January 25, 1955.

Contribution from the Department of Chemistry, University of Saskatchewan, Saskatoon, Sask., with financial support from the National Research Council of Canada. This paper represents a part of a thesis submitted by one of us (F. W. B.) as partial requirement for the degree of Master of Arts.

²Holder of a bursary from the National Research Council of Canada.

EXPERIMENTAL

The experimental procedures were very similar to those described in the preceding paper (1) by Birss and Thorvaldson on the hydration of plaster of Paris. The methods and the precautions used to ensure accuracy of the measurements of radioactivity were the same. The work was done in a room thermostatted at $21 \pm 0.1^\circ\text{C}$.

Three samples of calcium oxide, A, B, and C, were prepared from calcium carbonate of high purity, labelled with calcium-45, by the various heat treatments indicated in Table I.

Supersaturated solutions containing from 1.26 to 1.35 gm. of inactive³ calcium oxide per liter were used as the hydrating liquids so as to reduce, as far as possible, further increase in concentration through solution of active lime during the hydration. Fifty-milliliter aliquots of the supersaturated calcium hydroxide solution were shaken with freshly ignited 0.05-gm. samples ($\pm 1\%$) of active calcium oxide in sealed 100-ml. gold or silver lined steel tubes. At intervals tubes were centrifuged, 25 ml. of the clear liquid titrated with 0.06 *N* hydrochloric acid, and five 0.500-ml. samples counted. Duplicate series of hydrations were run with each sample of calcium oxide.

RESULTS

The three samples of lime showed considerable differences in their behavior on hydration. In each case the concentration of the supersaturated hydrating liquid increased; with samples B and C to a much greater extent than with sample A. Sample C, which gave the highest supersaturation, required the longest time for complete hydration. Some observations on the hydrations follow.

Sample A.—The concentration of the hydrating liquid rose rapidly from an initial 1.26 to 1.33 gm. CaO/liter (10 min.), then more slowly to 1.35 gm./liter (30 min.). The same value was obtained at 60 min., with a slight decrease during the next 60 min. The activity of the solution reached a maximum in 30 to 50 min. The duplicate series were not in close agreement.

Sample B.—The concentration rose from 1.29 to 1.44 gm. CaO/liter in five minutes, reached 1.46 to 1.47 gm./liter at 20 min., then remained almost constant until the two-hour test. The activity of the solution reached a maximum in 60 min., and showed very slight decrease at the two-hour test.

Sample C.—The concentration rose from the initial of 1.34 gm. CaO/liter to as high as 1.52 gm./liter in 5 to 10 min., then fell rapidly, reaching 1.30 gm./liter at four hours and 1.28 gm./liter at eight hours. The activity of the solution increased rapidly during the first 10 min., then slowly up to the four-hour test, and then fell slightly during the next four hours. The duplicate determinations of the two series with this sample were in fairly good agreement.

The apparent times required for complete hydration were:

Sample A, 30–50 min.; Sample B, one hour; Sample C, four hours.

³The terms "inactive", "active", and "activity" will be used to refer to radioactivity and not to the chemical activity of the materials under discussion. The Ca^{45} was supplied by Atomic Energy of Canada.

"Through-solution" Hydration of Lime

A theoretical expression for the liberation of radioactivity by a labelled sample of the hemihydrate of calcium sulphate when hydrated in a solution of inactive calcium sulphate has been developed in the preceding paper (1). The expression holds also for the case of the through-solution hydration of lime labelled with Ca^{45} in a solution of inactive calcium hydroxide, namely:

$$\text{Per cent of total activity in the solution} = (100a/m)(1 - e^{-x/a})$$

where a = moles of inactive lime in the original solution,

m = moles of labelled calcium oxide placed in the system,

x = moles of labelled calcium oxide which have passed into solution during the hydration.

The limitations in the application of the expression to the experimental data have been discussed in the preceding paper (1).

The experimental results obtained with sample C will be considered first. Fig. 1 gives the plot for the changes in the activity of the hydrating liquid with time, and the corresponding changes in the concentration of the solution. It also gives the plot of the experimental values of the activity in the solution corrected for the changes in the concentration, by the method described in the preceding paper (1). The corrected experimental activity at the maximum is 67.4% of the total activity of the system as compared with 70.5%, the theoretical value for complete hydration by a through-solution mechanism. This may be considered to be reasonable agreement because of probable errors which would tend to lower the experimental activity. Assuming complete radioactive exchange equilibrium between the lime in the solid and solution at the end of the hydration would give only 55% of the activity in the solution.

Discussion of Errors

The errors affecting the experimental results have been discussed at length in the preceding paper, and will therefore be considered only briefly here. The rapid reaction at the beginning of the hydration may result in incomplete mixing and consequent precipitation of the hydrated lime in regions of high

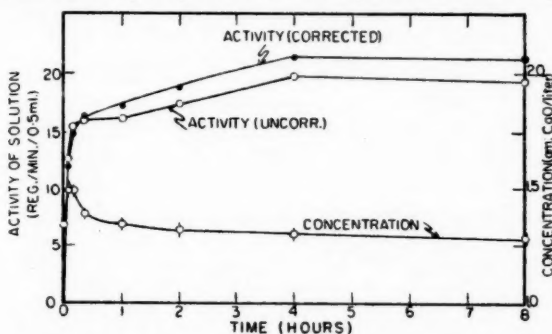


FIG. 1. The liberation of activity to the solution and the changes in concentration when 0.05-gm. samples of calcium oxide (heated six hours at 1400–1550°C.) labelled with calcium-45 (specific activity 63.2 reg./min./mgm.) were hydrated in 50 ml. of inactive lime solution 1.34 gm. CaO/liter).

activity. This would lower the observed activity in the liquid. In the hydration of plaster of Paris a similar danger was present near the end of the hydration period. The experimental measurement of activity at the four-hour point (Sample C, Fig. 1), which was taken as the maximum value, is not necessarily the true peak, thus possibly giving too low a maximum. However, as the slope of the curve at this point is small, the error is probably not large.

Exchange of calcium ions between the liquid and solid after the precipitation of the calcium hydroxide would lower the activity but the error is probably not large since the drop in activity, after correction for precipitation, from the four-hour to the eight-hour value is within the probable experimental error of counting. Direct determination of exchange by shaking inactive calcium hydroxide crystals with a solution of labelled calcium hydroxide (ratio of solid to dissolved calcium hydroxide six to one) gave a marked drop in the activity of the solution on mixing, probably owing to exchange of calcium ions between the liquid and the large area of surface of the thin calcium hydroxide plates. This was followed by a slow decrease in the activity of the solution. Surface exchange does not affect the results in the hydration experiments as the surface of the crystals is at all times in exchange equilibrium with the solution. When the initial drop in activity observed in the exchange experiments is eliminated and correction is made for the ratio of calcium hydroxide in the solid and liquid phase (0.8 to 1 in the hydration runs), the direct experiments give an estimated drop in activity of about 0.1% per hour for the conditions of the hydration experiments. This is of the order of the drop observed between four and eight hours in the hydration of sample C.

During the very rapid hydration of sample C in the first 10 min. when, by calculation, about 60% of the sample was hydrated, very small crystals of calcium hydroxide were probably formed. These would be subject to recrystallization, thus depressing the activity of the solution. During the 10–60 min. period (Fig. 1) the activity (lower curve) is depressed by the drop in the concentration of the solution. This correction has been made in the upper curve. However, the apparently low values for the one and two hour points on the "corrected" curve are probably due to recrystallization and the low experimental value for activity of 67.4 instead of the theoretical 70.5% may be mainly due to this factor.

Thus one must conclude that in the case of sample C there is no evidence of direct hydration of the solid calcium oxide without passage of the solid into solution during the over-all hydration process.

Comparison of the Hydration of Samples A, B, and C

The activity values obtained for the hydration liquids were corrected for changes in concentration (1). From the figures obtained the proportion of the calcium oxide apparently hydrated by a through-solution mechanism was calculated by means of the theoretical equation. The results are given in Fig. 2 and in Table I.

The marked difference in the behavior of the three samples is apparently due to the heat treatments. The sample of calcium carbonate was composed

TABLE I
 COMPARISON OF DATA FOR CaO SAMPLES A, B, AND C

Sample	A	B	C
Heat treatment	20 hr. at 700°C.	3 hr.* at 1400-1550°C.	6 hr.* at 1400-1550°C.
Maximum activity of liquid (corr.) (as % of total activity)	{ 31.0 26.1 Mean 28.6	45.4 46.1 45.8	67.3 67.4 67.4
Calc. % CaO hydrated "through-solution" (mean)	32	57	94

*After 20 hr. at 700°C. The samples were ground lightly to break up aggregates and ignited two hours at 950°C. before use.

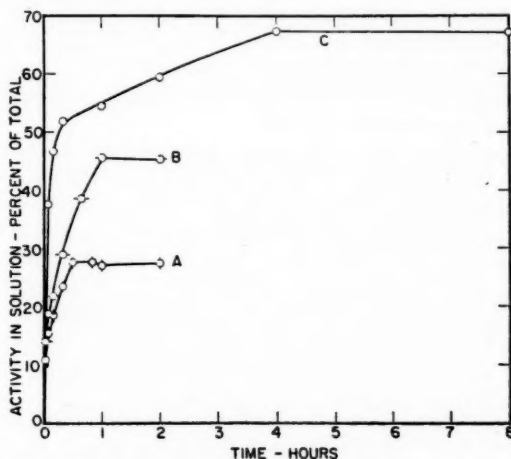


FIG. 2. Comparison of the activity liberated to the solution on hydration of three samples of calcium oxide labelled with calcium-⁴⁵ (see Table I).

of crystals mainly 0.022 to 0.04 mm. in diameter. Sample A retained the shape of the original crystals and microscopic measurements indicated only slight shrinkage. The particles of samples B and C had to a great extent lost their original shape, were smaller, and some sintering had occurred.

Hedin and Thorén (3) have made a very thorough study of volume changes during the ignition of calcium carbonate at various temperatures. They have concluded that ignition at low temperatures produces particles of oxide of extremely loose structure composed of very small crystals of calcium oxide and having a large amount of internal pore space, but that progressive heating at higher temperatures gives closer packing and finally a compact crystalline material. They consider that the high rate of slaking of soft burnt lime is due to a large area of internal surface at which slaking can take place, while dead-burnt lime slakes only at the external surface of the particles. Hedin and

Thorén have further concluded from their studies on the hydration of calcium oxide that the first step of slaking is merely the dissolution of the oxide and that this solution presumably occurs by direct formation of ions. However, they do not exclude the possible formation of hydroxide in the solid but consider that the supersaturation is due to the direct dissolution of calcium oxide.

The results obtained with sample A could be explained on the assumption that the particles possess a large amount of internal surface and that a large proportion of the hydration of the oxide and precipitation of the hydroxide occurs in the capillaries and pores of the particles. This would, in part, prevent the radioactive ions of calcium from entering the bulk of the hydrating liquid. The average activity developed in the solution by this sample corresponded to a 32% hydration, through-solution. One would then assume that internal hydration occurs to a much lesser extent in sample B, which gave a calculated 57% through-solution hydration, while it is absent in sample C, where the normal through-solution mechanism becomes evident with sufficient time lag between solution and precipitation for approaching complete uniformity of concentration in the hydrating liquid.

On the basis of the above one might perhaps assume that essentially the mechanism of the hydration of the three samples is the same. There is, however, the question of the mechanism of the "internal" hydration. Does water, as liquid, enter the pore space, in which case the hydration might occur in liquid films, or does only water vapor pass into the capillaries giving a vapor phase reaction with the solid? Our experiments do not answer these questions but they indicate that sample C, which probably corresponds to "dead-burnt" lime, hydrates by a "through-solution" mechanism. While the "ionic" solution of the calcium oxide seems probable, the possibility that calcium hydroxide is first formed and then dissolves is not excluded.

REFERENCES

1. BIRSS, F. W. and THORVALDSON, T. *Can. J. Chem.* 33: 870. 1955.
2. GRAHAM, W. A. G., SPINKS, J. W. T., and THORVALDSON, T. *Can. J. Chem.* 32: 129. 1954.
3. HEDIN, R. and THORÉN, Å. *Swed. Cement Concrete Inst. Stockholm, Bull. No. 16.* 1949.

THE ELECTRICAL CONDUCTANCE OF STRONG ELECTROLYTES: A TEST OF STOKES' EQUATION¹

BY A. N. CAMPBELL AND E. M. KARTZMARK

ABSTRACT

The equation recently put forward by Wishaw and Stokes, purporting to reproduce the equivalent conductance of concentrated solutions of strong electrolytes, has been tested by applying it to the experimental data of Campbell, Kartzmark *et alii*. The agreement between the calculated and observed values of Λ is astonishingly good, in the case of lithium nitrate up to a concentration of 7 molar. The deviations found for silver nitrate and ammonium nitrate are attributed to ion-pair formation and a dissociation "constant" deduced (for silver nitrate) which does show approximate constancy; a similar calculation by Stokes for ammonium nitrate shows even better constancy. Since the Stokes' equation is fully theoretical and contains only quantities to which physical meaning can be attached, it is to be preferred to any empirical, or semiempirical, equation. The Stokes' equation, being merely an extension of the Debye-Hückel-Onsager concept, cannot be expected to apply to concentrations greater than, say, 5 *N*. Attention is again drawn to the empirical observation that in the region of very high concentration the plot of Λ versus $\log C$ is a true straight line.

For a number of years, the present authors in collaboration with others (1) have been determining the equivalent conductances of concentrated solutions of strong electrolytes, at various temperatures and at concentrations up to that of the molten salt (at sufficiently high temperature). This they have done in a purely experimental manner, since they lacked any theoretical equation which could be tested by their results, and there was no picture of the mechanism of conduction in strong solutions. The Debye-Hückel-Onsager equation, which requires a straight line relation between Λ and \sqrt{C} , is only valid in the extremely dilute region, say up to 0.01 *N*; at high concentrations it even gives negative values for Λ . It is unnecessary here to go into detail, since the situation is summarized by Harned and Owen in their well-known book (4, pp. 144-158). Suffice it to say that attempts have been made to extend the Debye-Hückel-Onsager equation by the addition of further terms to the \sqrt{C} term. The best known of these are the equations of Onsager and Fuoss (7) and of Shedlovsky (8); the latter, however, is purely empirical. At best, these equations represent the variation of equivalent conductance with concentration only up to, say, 1.0 *N*.

Quite recently, Wishaw and Stokes (9) have produced an equation which is an extension of Onsager's equation, taking into account the effect of finite ionic size² (and Falkenhagen's evaluation of the relaxation effect (3)). The Wishaw-Stokes equation is

$$\Lambda = \left(\Lambda^\circ - \frac{B_2 \sqrt{C}}{1 + B_2 \sqrt{C}} \right) \left(1 - \frac{B_1 \sqrt{C.F}}{1 + B_1 \sqrt{C}} \right) \frac{\eta^\circ}{\eta}$$

¹ Manuscript received January 17, 1955.

Contribution from the Department of Chemistry, University of Manitoba, Winnipeg, Manitoba.

² "The term \bar{a} [distance of closest approach of the ions] is not the sum of the crystallographic radii of the appropriate ions (probably owing to the increase in effective radius of the ions due to their solvation sheaths), and must therefore be determined empirically." Kortüm-Bockris (5).

The symbols have the following meaning:

Λ = equivalent conductance at concentration C ,

Λ° = limiting equivalent conductance,

$B_1 = 8.20 \times 10^5 / (\epsilon T)^{3/2}$, where ϵ = dielectric constant of solvent,

$B_2 = 82.5 / \eta^\circ (\epsilon T)^{1/2}$, where η° = viscosity of solvent,

$B = 50.29 / (\epsilon T)^{1/2}$,

η = viscosity of solution,

\bar{a} = mean distance of closest approach of ions, (\AA),

$F = \frac{(e^{0.2929Ka} - 1)}{0.2929Ka}$ where K = quantity in Debye-Hückel theory given by

$K^2 = \left[\frac{4\pi N e^2}{1000 \epsilon k T} \right] C(\nu_1 z_1^2 + \nu_2 z_2^2)$ and a = mean distance of closest approach (cm.).

Other symbols have their usual meanings.

Wishaw and Stokes have tested their equation using their own data for ammonium chloride and for ammonium nitrate (the latter data are identical with our own). For ammonium chloride they find good agreement up to 5 N (± 1 mho), while the discrepancies observed with the ammonium nitrate results are attributed to ion-pair formation, and a dissociation constant is evaluated which is reasonably constant up to 6 N .

As our results are more extensive than those of Wishaw and Stokes and apply at different temperatures, it seems appropriate to test their very interesting equation using our results. Before doing so, however, some comment is necessary. In a letter from Dr. Stokes he makes use of the following words: "I am rather sorry that your extensive conductivity measurements refer to nitrates; the behaviour of these is less simple and respectful towards the theory than that of chlorides, etc. . . . I believe the ion-pair formation in nitrates is genuine—it ties up with the thermodynamic data and the diffusion fairly convincingly. . . . For silver nitrate I should suggest an \bar{a} something between 3.5 and 4 \AA ; not the crystallographic value. According to Bjerrum, one should really take $\bar{a} = 3.57$ for the ionized part of a one: one electrolyte which forms ion-pairs, but this parameter is fairly elastic. The greatest difficulty in applying the theory to ammonium nitrate or silver nitrate at temperatures other than 25° is that we have no activity coefficient data to use in calculating the ion-pair dissociation-constant K . However, the theory may still be used to estimate α , the degree of dissociation of the ion-pairs, and to compare it at different temperatures. It is quite possible that α will be nearer to unity at your higher temperatures; the behaviour of the function $e^2/\epsilon k T$ ought to correlate with the amount of ion-pair formation at a given concentration at various temperatures. This function has the values 7.135 at 25°; 7.225 at 35°; 7.935 at 95°; all $\times 10^4$."

We have applied the Stokes equation to our data for silver nitrate and ammonium nitrate, at 25°, 35°, and 95°, and to potassium chloride (6) at 25°, and to lithium nitrate at 25° (unpublished data by Dr. G. Debus, working in this laboratory).

In using Stokes' equation, the quantities which may require arbitrary selection are \tilde{a} and Δ° ; F is not such a quantity. Δ° is well known or can be found from the ionic conductances, for all common electrolytes at 25°, but at other temperatures it becomes a matter of guesswork (in the absence of further experimental work). \tilde{a} is occasionally known (at 25°) but usually again only a probable value can be assigned. According to Bjerrum, \tilde{a} should have a fixed value of 3.57 for the ionized part of a 1:1 electrolyte which forms ion-pairs. This value, however, can be altered within reasonable limits and still retain its physical meaning but it must not vary with temperature. In other words, such a value of \tilde{a} is chosen (varying, say, between 3 and 4 Å) as fits the data for 25° (Δ° is known without ambiguity for this temperature) and this value of \tilde{a} is used for calculations at other temperatures.

There remains what Stokes calls "the vexed question" of a viscosity correction. While admitting that a viscosity correction is necessary, and that this correction is not given by the ordinary bulk viscosity, he is nevertheless forced to use this bulk viscosity. Stokes thinks there is "some justification" for this. The particular substances investigated by him, ammonium chloride and ammonium nitrate, exhibit anomalous viscosity, that is, up to quite high concentrations, the viscosity is somewhat less than that of water and never, even at the highest concentrations, much greater. Silver nitrate and lithium nitrate, which are used in our calculations, form very viscous solutions at high concentrations. It is fair to point out that some of the deviation observed may be due to the use of a viscosity correction which may be only approximate.

CALCULATIONS

Our calculations are contained in Tables I to IV. It should be emphasized once again that the choice of \tilde{a} and Δ° (except at 25°) is only guesswork but this does not detract from the value of Stokes' equation; it merely requires further experimental work. Ion-pair formation has been assumed with silver nitrate and a dissociation constant calculated using the activity coefficients given in Harned and Owen (4). The calculation was not carried beyond the point at which $\alpha (= \Lambda_{\text{exp}}/\Lambda_{\text{calc}})$ appeared to increase with further concentration. A similar calculation has already been made for ammonium nitrate by Wishaw and Stokes (10). The results for Λ_{exp} and Λ_{calc} are graphed in Figs. 1 to 5.

DISCUSSION

Obviously, the values of Δ obtained are dependent on the values of \tilde{a} chosen (and of Δ° if this is not known) but the general behavior is the same, whatever value of \tilde{a} is chosen. For example, a value of \tilde{a} may be chosen (e.g. 2.30 for silver nitrate) which may reproduce rather well the observed results over the initial range (up to 3 *N* for silver nitrate) and then give systematically decreasing values of Δ up to the limit of saturation. If it is objected that the value of 2.30 is too low to have physical significance and the more reasonable value of 4.35 assumed, then the initial calculated values are somewhat too high and later values finally become too low. In other words, the behavior is qualitatively the same. We have used a number of alternative \tilde{a} values in the case

TABLE I

C	Λ_{exp}	Λ_{calc}		α (for $\lambda = 4.35$)	K
		$\lambda = 2.3$	$\lambda = 4.35$		
I. Silver nitrate at 25°, $\Lambda^\circ = 133.36$					
0.0005	131.36	131.36	131.39	0.999	—
0.001	130.51	130.57	130.62	0.999	—
0.005	127.20	127.31	127.56	0.997	—
0.01	124.76	125.00	125.32	0.996	2.41
0.02	121.41	121.93	122.52	0.991	2.07
0.05	115.24	116.36	117.55	0.980	2.08
0.1	109.14	109.84	112.81	0.967	2.98
1.004	77.82	78.69	89.20	0.872	2.52
1.998	64.20	63.90	76.29	0.842	2.74
3.028	54.97	53.21	65.63	0.838	3.10
4.000	48.50	44.69	56.46	0.859	3.96
5.029	43.14	37.77	48.64	0.887	
6.006	38.55	31.87	41.58	0.927	
7.012	34.70	26.79	35.36	0.981	
8.011	31.20	22.46	30.09		
9.010	27.99	18.21	24.44		
9.709	26.1	16.09	21.67		
II. Silver nitrate at 35°, $\Lambda^\circ = 158.43^*$					
0.986	132.5	129.7	133.2	0.995	
1.4023	85.37	83.0	97.1	0.879	
1.7757	79.55	76.8	91.6	0.868	
3.0322	65.41	60.5	75.6	0.865	
3.8230	58.91		66.8	0.882	
4.2306	56.06		62.9	0.892	
III. Silver nitrate at 95°, $\Lambda^\circ = 340.6^*$					
0.0534	298.3		295.2		
0.1	278.0		281.4	0.988	
1.220	172.7		199.9	0.864	
2.189	147.8		165.8	0.891	
2.967	130.8		141.2	0.926	
4.829	103.1		104.1	0.990	
6.591	84.88		77.57		
8.830	48.12		54.27		
9.906	61.28		45.60		
11.876	50.35		39.0		

* Calculated using the temperature coefficients of conductance from (1).

The constants B , B_1 , B_2 at 95° were calculated using the dielectric constant data of Wyman and Ingalls (10), and viscosity data from I.C.T.

TABLE II

<i>C</i>	Λ_{exp}	Λ_{calc}	α		<i>C</i>	Λ_{exp}	Λ_{calc}	α
<i>I. Ammonium nitrate at 25°, $\Lambda^\circ = 144.84$; $\lambda = 4.85$</i>								
0.001	142.0	142.01	—		1.004	101.32	110.35	0.918
0.002	141.4	140.93	—		1.993	91.95	104.62	0.879
0.005	138.7	138.87	—		2.982	84.28	97.79	0.862
0.01	136.2	136.84	—		4.020	76.78	91.58	0.838
0.02	133.3	134.20	—		5.014	70.00	84.68	0.827
0.05	128.0	129.80	0.986		6.036	63.12	76.49	0.825
0.07	125.5	127.98	0.981		7.015	56.73	69.31	0.819
0.10	122.7	125.82	0.975		8.011	50.36	61.26	0.822
0.20	116.9	121.02	0.966		9.043	43.93	53.37	0.823
0.50	108.0	113.64	0.950		10.004	38.19	45.05	0.848
					11.282	31.3	35.90	0.872
<i>II. Ammonium nitrate at 35°, $\Lambda^\circ = 171.78$; $\lambda = 4.85$</i>								
0.0538	153.1	152.03	—		2.450	103.2	114.2	0.904
1.023	119.4	125.8	0.949		7.671	59.84	68.65	0.872
1.694	111.0	120.3	0.923		9.409	47.46	52.52	0.904
1.9104	108.2	118.7	0.912					
<i>III. Ammonium nitrate at 95°, $\Lambda^\circ = 365$; $\lambda = 4.85$</i>								
0.0878	306.2	307.0	0.997		6.632	116.0	125.2	0.927
0.194	275.3	285.4	0.965		7.95	97.81	105.3	0.929
0.9963	234.8	237.6	0.988		8.74	88.04	95.4	0.923
1.525	213.6	222.4	0.960		10.12	72.44	74.0	0.979
2.576	185.6	203.8	0.912		11.13	61.99	63.4	0.978
3.600	166.9	182.7	0.914		13.31	42.07	41.4	—
4.221	154.7	162.2	0.954		14.81	28.71	35.92	0.799

NOTE. *K* values (for 25°) have been calculated by Wishaw and Stokes (9), whose experimental results are in close agreement with ours.

TABLE III
POTASSIUM CHLORIDE AT 25°, $\Lambda^\circ = 149.86$; $\lambda = 4.6$

<i>C</i>	Λ_{exp}	Λ_{calc}	$\frac{\Lambda_{\text{exp}}}{\Lambda_{\text{calc}}}$
0.0005	147.81	147.78	
0.001	146.95	146.91	
0.005	143.55	143.71	0.999
0.01	141.27	141.68	0.997
0.02	138.34	138.91	0.996
0.05	133.37	134.19	0.994
0.10	128.96	129.88	0.993
0.20	123.9	125.0	0.991
0.50	117.2	117.29	0.999
1.00	111.9	111.96	0.999

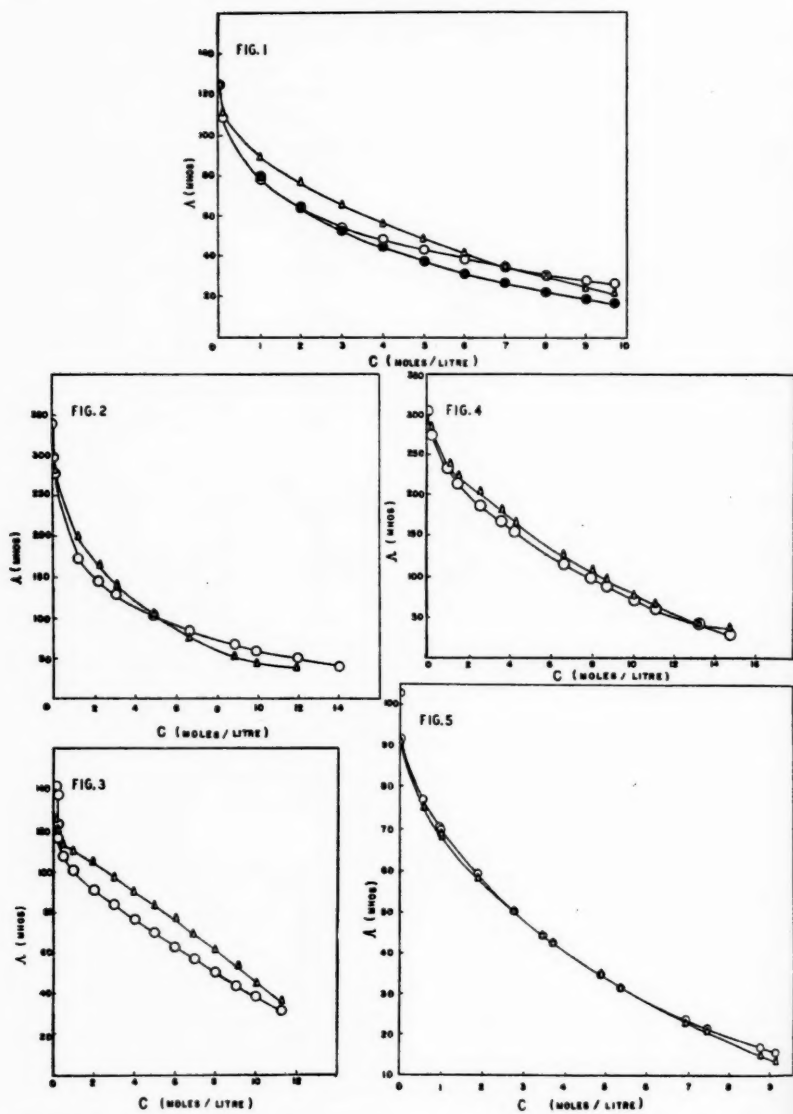


FIG. 1. AgNO_3 at 25°C . \circ experimental; \triangle calculated, $\bar{\lambda} = 4.35$; \bullet calculated, $\bar{\lambda} = 2.30$, $\Delta^\circ = 133.36$.
 FIG. 2. AgNO_3 at 95°C . \circ experimental; \triangle calculated, $\bar{\lambda} = 4.35$, $\Delta^\circ = 340.6$.
 FIG. 3. NH_4NO_3 at 25°C . \circ experimental; \triangle calculated, $\bar{\lambda} = 4.35$, $\Delta^\circ = 144.84$.
 FIG. 4. NH_4NO_3 at 95°C . \circ experimental; \triangle calculated, $\bar{\lambda} = 4.35$, $\Delta^\circ = 365$.
 FIG. 5. LiNO_3 at 25°C . \circ experimental; \triangle calculated, $\bar{\lambda} = 4.5$, $\Delta^\circ = 110.13$.

TABLE IV
 LITHIUM NITRATE AT 25°; $\Lambda^\circ = 110.13$

C	η/η_0	Λ_{exp}	Λ_{calc}				
			$\bar{a} = 3.5$	$\bar{a} = 4.0$	$\bar{a} = 4.5$	$\bar{a} = 5.0$	$\bar{a} = 6.0$
0.00997	1.005	102.79	101.94	102.04	102.3	102.5	102.47
0.09902	1.013	91.74	90.42	91.05	90.88	91.46	92.45
0.5526	1.063	76.86	75.52	—	75.18	76.82	79.04
0.9579	1.109	70.26	70.01	—	68.75	70.15	
0.9951	1.111	69.78			68.33	69.86	
1.8855	1.221	58.95			58.22	59.44	
2.7401	1.351	50.60	56.66		50.41	52.02	
3.4560	1.490	44.72			44.44	45.96	
3.6980	1.534	42.81			42.78	44.26	
4.857	1.826	34.69			34.89	35.86	
5.337	1.984	31.66			31.43	32.58	
6.916	2.637	23.52			22.69	23.50	
7.427	2.914	21.24			20.31	20.99	
8.725	3.849	16.51			14.86	15.40	
9.130	4.218	15.20			13.34	13.93	

of lithium nitrate, to demonstrate this. In view of Dr. Stokes' remark that nitrates are liable to ion-pair formation, in general we have preferred those values of \bar{a} which give a calculated Λ greater than that we have observed, and from the α -value thus obtained we have calculated a dissociation constant; for silver nitrate it is reasonably constant. The agreement between Λ_{exp} and Λ_{calc} for lithium nitrate, using an \bar{a} value of 4.5 Å, is so close, i.e. $\alpha \sim 1$, that we prefer these results and therefore we have not attempted to calculate a dissociation constant. This means that we believe there is no ion-pair formation in lithium nitrate solutions up to at least 7 N. Such deviations as do occur may be due to the viscosity correction being uncertain (*vide supra*, p. 889). This leaves the problem of explaining why lithium nitrate should not form ion-pairs, while other nitrates do, but a ready explanation offers itself in the well-known fact, or supposition, that the lithium ion is highly hydrated, in comparison with other univalent ions.

The equation of Stokes seems to us to constitute a major advance, in that it carries the Debye-Hückel-Onsager concepts up to a concentration of from 3 to 5 N. It is of course true that the figures obtained are far from exhibiting that close correspondence with the experimental results which an empirical equation might give but this is not the point. A similar objection might be made to van der Waals' equation of state, as contrasted with other empirical and semiempirical equations, but van der Waals' equation is still the best for teaching and theoretical purposes, because of the clear and relatively simple picture it gives of the structure of a compressed gas. The same may be said of Stokes' equation; it supplies a mechanism of conductance up to a region of truly high concentration.

The essential virtue of Stokes' equation is that it is entirely free from empiricism, every quantity contained in it having a clear physical meaning. It may be objected that \bar{a} , the distance of closest approach of the ions, is really only an empirical constant, but against this there are the strong objections that

it is always of the order of magnitude that would be expected and, above all, is independent of temperature. We note that, in agreement with Stokes' suggestion, the α -values are larger at the higher temperatures (using of course the same λ values), that is, ion-pair formation is less. As would be expected, the calculated results, measured in terms of so-called α -values, become meaningless above a concentration of about 5 *N*.

For solutions of the highest concentration and for anhydrous melts it may be that an entirely new theory is called for. In this connection, we cannot help referring again to an observation made by Mr. John Herron (2), when working with us, viz. that from the region of, say, 5 *N* (where the Stokes' equation begins to break down) the plot of Λ against $\log C$ is a rigorously straight line. This has recently been confirmed by Debus' observations on lithium nitrate (up to 9*N*). To say that any quantity plotted against $\log C$ would be a straight line or that the curve is merely approaching a straight line is incorrect; the curve is absolutely straight by any test with which we are acquainted. The observation is quite empirical but, if it is accepted, any proposed theory will have to account for this.

REFERENCES

1. CAMPBELL, A. N. and KARTZMARK, E. M. *Can. J. Research, B*, 28: 43, 161. 1950; *Can. J. Chem.* 30: 128. 1952. CAMPBELL, A. N., KARTZMARK, E. M., BISSETT, D., and BEDNAS, M. E. *Can. J. Chem.* 31: 303. 1953. CAMPBELL, A. N., GRAY, A. R., and KARTZMARK, E. M. *Can. J. Chem.* 31: 617. 1953. CAMPBELL, A. N., KARTZMARK, E. M., BEDNAS, M. E., and HERRON, J. T. *Can. J. Chem.* 32: 1051. 1954.
2. CAMPBELL, A. N., KARTZMARK, E. M., BEDNAS, M. E., and HERRON, J. T. *Can. J. Chem.* 32: 1051. 1954.
3. FALKENHAGEN, H., LEIST, M., and KELBG, G. *Ann. Physik*, 6(II): 51. 1952.
4. HARNED, H. S. and OWEN, B. B. *The physical chemistry of electrolytic solutions*. Reinhold Publishing Corp., New York. 1943.
5. KORTUM-BOCKRIS. *Textbook of electrochemistry*, Vol. 1. Elsevier Publishing Company, Maastricht. 1951. p. 191.
6. MACINNES, D. A. *Principles of electrochemistry*. Reinhold Publishing Corp., New York. 1939. p. 339.
7. ONSAGER, L. and FUOSS, R. M. *J. Phys. Chem.* 36: 2689. 1932.
8. SHEDLOVSKY, T. *J. Am. Chem. Soc.* 54: 1405. 1932.
9. WISHAW, B. F. and STOKES, R. H. *J. Am. Chem. Soc.* 76: 2065. 1954.
10. WYMAN, J., Jr. and INGALLS, E. N. *J. Am. Chem. Soc.* 60: 1182. 1938.

STUDIES ON CARRAGEENIN: THE EFFECT OF SHEAR RATE ON VISCOSITY¹

BY C. R. MASSON AND D. A. I. GORING

ABSTRACT

The viscosity of aqueous solutions of carrageenin of high molecular weight was markedly dependent on the rate of shear. The shear-dependence increased with decrease in the concentration of added electrolyte. Because of curvature, extrapolation of $[\eta]$ to zero rate of shear was not possible. The Huggins interaction coefficient, k' , increased with decrease in rate of shear; k' also increased with increase in concentration of added electrolyte. In water, maxima of η_{sp}/c were observed at concentrations of carrageenin equivalent to the ionic impurities in the distilled water used. At higher concentrations the data fitted the Fuoss equation at rates of shear of 200 and 100 sec^{-1} but not below 100 sec^{-1} . The constants A and D both increased with decrease in rate of shear.

INTRODUCTION

The polysaccharide carrageenin, a water-soluble extract of the red alga *Chondrus crispus*, is of interest as a naturally occurring polyelectrolyte of high molecular weight. Solutions of carrageenin show a wide range in viscosity (2, 6, 8, 9) depending on the method of preparation and treatment of the extract. The intrinsic viscosity, $[\eta]$, is important as a means of characterizing any given sample.

It has been shown previously (8) that the viscosity of solutions of carrageenin of relatively low molecular weight is similar to that of other polyelectrolytes, while for extracts of higher molecular weight the viscosity becomes shear-dependent. The present work is part of an attempt to establish some general measurement of viscosity independent of rate of shear or intermolecular interaction. This paper describes the effect of shear rate on the viscosity of aqueous solutions of carrageenin, both in the presence and absence of added salts.

EXPERIMENTAL

Preparation of Extract

Carrageenin was extracted with water at 80°C. from the residue of a preliminary extraction at 30°C.–40°C. In order to obtain a product of high molecular weight care was taken to avoid undue degradation or bacterial contamination.

The extract was filtered through a No. 10 "Selas" porcelain filter and precipitated in four volumes of 95% ethanol. The white fibrous material was washed in absolute ethanol and ether, dried *in vacuo*, ground to pass a 20-mesh screen, and stored at -13°C. This extract is referred to in this and subsequent work as "Extract G". A preliminary osmometric determination of its molecular weight gave a value of 2,500,000.

Recent work (6, 12, 13) has shown that carrageenin contains at least two components, distinguishable mainly by their gelling tendencies. Although no

¹Manuscript received January 17, 1955.

Contribution from the Maritime Regional Laboratory, National Research Council, Halifax, Nova Scotia. Issued as N.R.C. No. 3569.

attempt was made in the present investigation to separate these components, recent results (6) indicated that a hot extract prepared in the above manner consists largely of the gelling fraction.

Preparation of Solutions

Solutions were made up as required by tumbling at room temperature. The sodium salt of the polyelectrolyte was used in all experiments. This was prepared by passing a solution of concentration 0.1 to 0.2 gm. dl.⁻¹ down a column of Amberlite IR 100 ion exchange resin. Final clarification was achieved with a No. 02 Sela filter element.

Buffering salts were added by mixing known volumes of the carrageenin with a stronger salt solution. The three ionic conditions studied were (1) distilled water, (2) *M*/30 sodium phosphate at pH 7.0 (referred to as *M*/30 phosphate), (3) *M*/30 sodium phosphate plus *M*/20 sodium chloride at pH 7.0 (referred to as *M*/12 phosphate/NaCl).

Viscosity Measurements

Capillary viscometers, each equipped with a series of bulbs to provide different hydrostatic heads, were employed. Various designs were tried in order to cover as wide a range of shear gradients as possible.

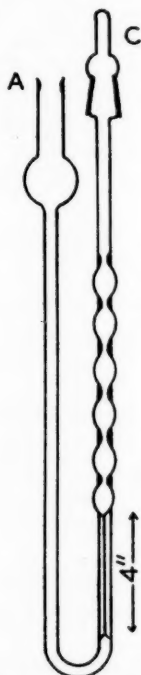


FIG. 1. Viscometer for checking on the possibility of drainage errors.

Three of the viscometers were similar to the one described by Schurz and Immergut (11). By using various lengths of capillary tubing a range of shear gradients for water between 221 and 2135 sec^{-1} was obtained. Where measurements were taken with different viscometers over the same range of shear gradients, the difference between the results was less than two per cent.

The design of a fourth viscometer, shown in Fig. 1, was such as to allow the liquid to flow into the dry bulbs, thus providing a check on the possibility of drainage errors. The viscometer was filled through *A* with cap *C* closed. Sufficient time was allowed for temperature equilibrium to be established, cap *C* was then removed, and the time required to fill each bulb in turn was noted. The range of shear gradients covered was 607 to 2061 sec^{-1} . Results obtained with this instrument for a highly viscous aqueous solution agreed within experimental error with data from one of the other viscometers. Thus drainage errors were inappreciable.

Measurements were made at 25°C. in thermostats controlled to $\pm 0.05^\circ\text{C}$. or better. Kinetic energy corrections were applied to all the results. Viscometers were calibrated by measuring the flow times of glycerol-water mixtures of known density and viscosity. Kinetic energy corrections were calculated for each bulb by the usual method. In one viscometer the correction for water in the bulb with the highest shear was 6% of the flow time and the correction decreased with increasing time of flow. All other corrections were lower than this and in several viscometers were negligible. The intrinsic viscosity, $[\eta]$, was obtained from the specific viscosity, η_{sp} , by the usual relationship

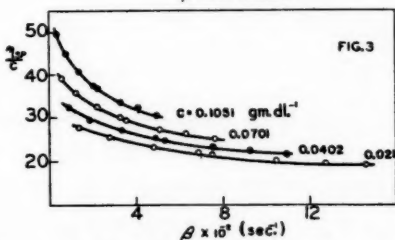
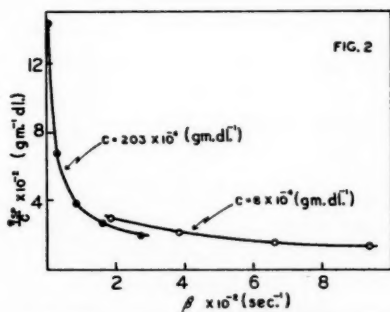


FIG. 2. η_{sp}/c vs. β for Extract G in water.

FIG. 3. η_{sp}/c vs. β for Extract G in *M*/12 phosphate/NaCl.

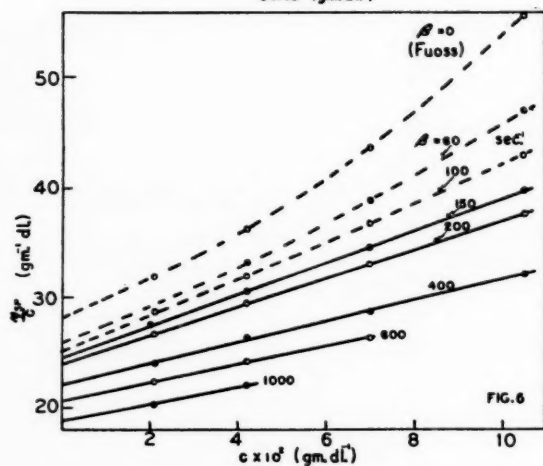
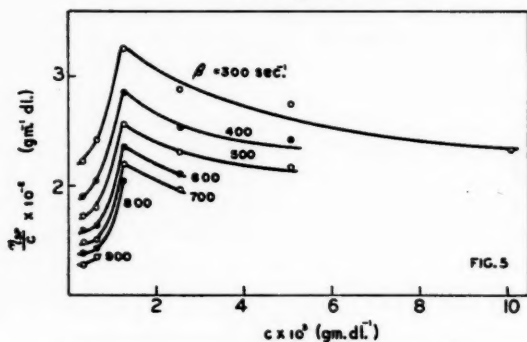
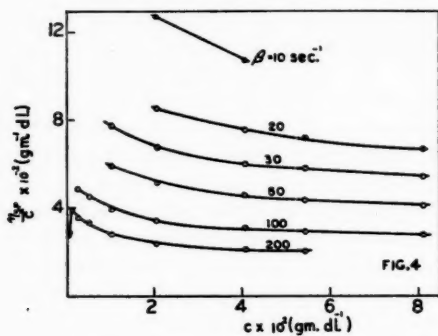


FIG. 4. Isoshear graphs of η_{sp}/c vs. c for Extract G in water. Values of β are from 10-200 sec^{-1} .

FIG. 5. Isoshear graphs of η_{sp}/c vs. c for Extract G in water. Values of β are from 300-900 sec^{-1} .

FIG. 6. Isoshear graphs of η_{sp}/c vs. c for Extract G in $M/12$ phosphate/NaCl.

$$[1] \quad [\eta] = (\eta_{sp}/c)_{c \rightarrow 0}$$

The average shear gradient, β , was calculated from

$$[2] \quad \beta = 8V/3\pi r^3 t$$

where V is the volume of bulb, r is the radius of capillary, and t is the time of flow.

RESULTS

Experimental curves of η_{sp}/c vs. β for various concentrations of Extract G in water and $M/12$ phosphate/NaCl are given in Figs. 2 and 3. From such curves, values of η_{sp}/c at constant shear were derived and isoshear graphs of η_{sp}/c vs. c (Figs. 4, 5, and 6) were drawn. In $M/12$ phosphate/NaCl, as shown in Fig. 6, η_{sp}/c varied linearly with c except for the slight curvature at $\beta = 60 \text{ sec}^{-1}$. Extrapolation to $c = 0$ gave values of $[\eta]$ corresponding to definite shear rates. Similar results were obtained with $M/30$ phosphate; $[\eta]$ is plotted against β in Fig. 7 for both sets of measurements.

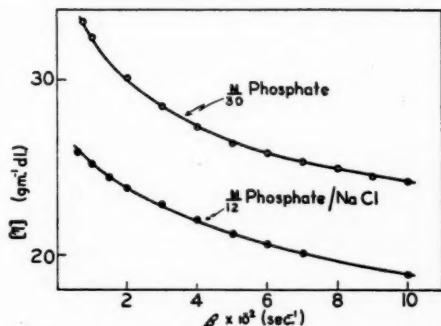


FIG. 7. Intrinsic viscosity vs. shear rate for Extract G in $M/30$ phosphate and $M/12$ phosphate/NaCl.

The isoshear graphs for Extract G in water did not permit extrapolation to zero concentration. At low shear rates (Fig. 4) the plots were curved upwards; at higher shear rates, where measurements could be carried to very low concentrations, distinct maxima in the plots were observed (Fig. 5).

DISCUSSION

The results fit the general pattern of polyelectrolyte behavior. Solutions containing added electrolyte behave like those of uncharged polymers, with the exception that curvature is noted in the plots of η_{sp}/c against c at low rates of shear (Fig. 6). This makes it difficult to obtain accurate values of $[\eta]$ at low shear rates. In addition, since the plot of $[\eta]$ vs. β (Fig. 7) is also curved, the value of $[\eta]$ at zero rate of shear can not be determined by extrapolation with any degree of accuracy.

An interesting feature of these measurements concerns the magnitude of the Huggins (7) interaction coefficient, k' . As shown in Table I, k' increases with

TABLE I
VALUES OF k' AT VARIOUS SHEAR GRADIENTS FOR EXTRACT G IN $M/30$ PHOSPHATE
AND $M/12$ PHOSPHATE/NaCl

β sec. ⁻¹	$k' \times 10^3$	
	$M/30$ phosphate	$M/12$ phosphate/NaCl
1000	117	
700	140	193
600	147	193
500	153	196
400	156	198
300	161	208
200	169	232
150		248
100		281

decreasing shear rate. Solutions of high molecular weight carrageenin have been shown to have a yield point which increases at higher concentration (8). Thus an increase in the concentration dependence of η_{sp}/c at low rates of shear might be expected. A similar dependence of k' on shear gradient has recently been noted (10) for solutions of cellulose and cellulose nitrate.

It is also of interest that the values of k' are higher with $M/12$ phosphate/NaCl than with $M/30$ phosphate, when comparison is made at the same rate of shear or the same intrinsic viscosity. This is the opposite behavior to that anticipated if the effect of adding salt is to cause a further coiling of the molecule in solution. A possible explanation is that neutralization of the charges on the polymer chain by the addition of electrolyte results in a decrease in electrostatic repulsion between neighboring chains thereby allowing an increase in some structure-forming tendency. In the case of carrageenin, the latter effect may predominate under the conditions studied. This interpretation is consistent with the gelling tendency of solutions of certain fractions of carrageenin (6) on the addition of electrolytes. A detailed interpretation of this anomaly must await the development of an adequate theory of polyelectrolyte solutions.

Regarding the measurements in the absence of added salts (Figs. 4 and 5), the occurrence of maxima similar to those observed here has been noted by Conway and Butler (1) for dilute solutions of thymus nucleic acid. Fuoss and Cathers (4) have shown that for solutions containing traces of added salt, such maxima are to be expected when the concentration of ions from the polyelectrolyte and salt are roughly equivalent. The specific conductance of the distilled water was approximately 2×10^{-6} mho cm.⁻¹ This could be attributed to sodium chloride in a concentration of 2×10^{-5} M . The maxima in the curves occur at a carrageenin concentration of 0.0012 gm. dl.⁻¹ The sulphate content (as OSO_3^-) of carrageenin is approximately 25% giving a value of 384 for the equivalent weight. The "molar" concentration of carrageenin was therefore 3×10^{-5} M . The occurrence of maxima in the viscosity curves in this region is thus probably due to the suppression of ionization by foreign cations in roughly equivalent concentration. Such effects have been

predicted by Flory and Osterheld (3) but can only be observed with polyelectrolytes of high molecular weight where viscosity measurements are still practicable at very low concentrations.

The curves shown in Fig. 4 have been plotted according to the equation of Fuoss and Cathers (4)

$$[3] \quad z = \eta_{sp}/c = \frac{A}{1+Bc^{\frac{1}{2}}} + D.$$

Previous work (8) has shown that this equation adequately fits the viscosity-concentration relationship for carrageenin of low molecular weight. In the present work, the occurrence of maxima at $c = 0.0012$ gm. dl.⁻¹ makes the shape of the curves of η_{sp}/c vs. c uncertain at low concentrations. It was assumed, however, that this would not influence η_{sp}/c at concentrations above 0.01 gm. dl.⁻¹

From the linear plots of η_{sp}/c vs. $c^{-\frac{1}{2}}$, values of D were obtained at various shear rates. As shown in Fig. 8, D is markedly shear-dependent, increasing rapidly at low values of β . Since D represents the reduced specific viscosity at $c = \infty$, this means that even in concentrated solutions the molecule is rod-shaped. Values of D are higher than the corresponding intrinsic viscosities in salt solutions indicating that the coiling effect of a high concentration of polyelectrolyte is not as great as that of small quantities of added salt.

In Fig. 9, plots of $1/(z-D)$ vs. $c^{\frac{1}{2}}$ at various shear rates are shown. The plots are linear for shear rates of 200 and 100 sec.⁻¹ but become curved at lower shear. For $\beta = 200$ and 100 sec.⁻¹, A was respectively 800 and 1240 gm.⁻¹ dl. also

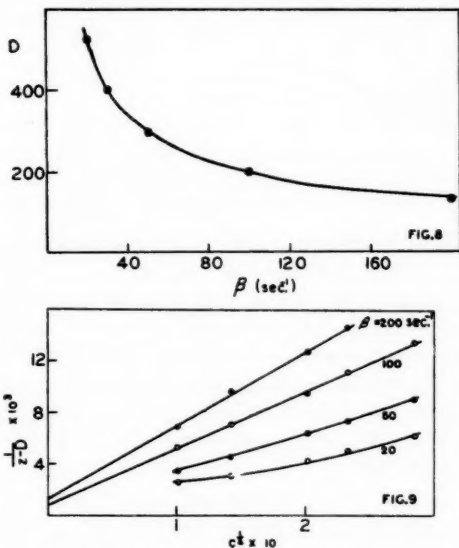


FIG. 8. Variation of D with rate of shear for Extract G in water.

FIG. 9. Graph of $1/(z-D)$ vs. $c^{\frac{1}{2}}$ for Extract G in water.

showing marked shear-dependence. Values of $46 (\pm 5)$ and $55 (\pm 8)$ were obtained for the constant B at 200 and 100 sec^{-1} respectively. These values are similar to those obtained previously with a low molecular weight sample (8).

The data have also been analyzed by the method of Goldberg and Fuoss (5), in which $1/\eta$ is plotted against $\eta\dot{\gamma}$. For Extract G in water (Fig. 10) the results are similar to those obtained by these authors for aqueous solutions of poly-*n*-N-butyl-4-vinylpyridine. At high concentrations the relationship is linear, but extrapolation yields apparently negative values of $1/\eta$, indicating curvature near the origin. At lower concentrations the relationship is non-linear and extrapolation is uncertain.

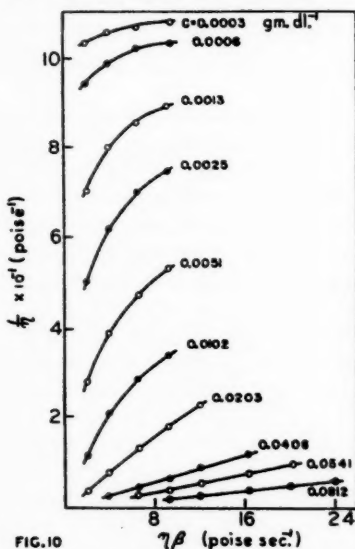


FIG. 10

FIG. 10. Graph of $1/\eta$ vs. $\eta\dot{\gamma}$ for Extract G in water.

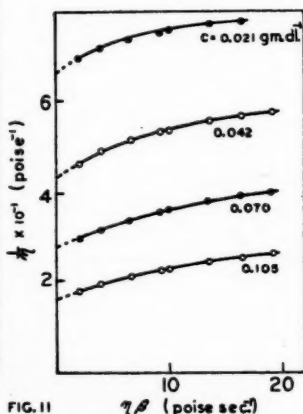


FIG. 11

FIG. 11. Graph of $1/\eta$ vs. $\eta\dot{\gamma}$ for Extract G in $M/12$ phosphate/ NaCl .

For the results in $M/12$ phosphate/ NaCl , the curvature in these plots was not so pronounced (Fig. 11), and the method was applied to obtain a rough estimate of the value of $[\eta]$ at zero rate of shear. The curve of η_{sp}/c vs. c at zero rate of shear which is obtained in this way is included in Fig. 6.

Other empirical methods which have been described in the literature have been applied to the above results in attempts to extrapolate to zero rate of shear. All methods tried were unsuccessful; for characterization of the polyelectrolyte it appears best at present to use the value of $[\eta]$ at some arbitrary shear rate above 100 sec^{-1} .

ACKNOWLEDGMENTS

The authors are indebted to Dr. E. Gordon Young for help and advice in preparing the manuscript, and also to Messrs. G. W. Caines and J. MacAulay for technical assistance.

REFERENCES

1. CONWAY, B. E. and BUTLER, J. A. V. *J. Polymer Sci.* 11: 277. 1953.
2. COOK, W. H., ROSE, R. C., and COLVIN, J. R. *Biochim. et Biophys. Acta*, 8: 595. 1952.
3. FLORY, P. J. and OSTERHELD, J. E. *J. Phys. Chem.* 58: 653. 1954.
4. FUOSS, R. M. and CATHERS, G. I. *J. Polymer Sci.* 4: 97. 1949.
5. GOLDBERG, P. and FUOSS, R. M. *J. Phys. Chem.* 58: 648. 1954.
6. GORING, D. A. I. and YOUNG, E. G. *Can. J. Chem.* 33: 480. 1955.
7. HUGGINS, M. L. *J. Am. Chem. Soc.* 64: 2716. 1942.
8. MASSON, C. R. and CAINES, G. W. *Can. J. Chem.* 32: 51. 1954.
9. ROSE, R. C. *Can. J. Research, F*, 28: 202. 1950.
10. SCHURZ, J. *J. Polymer Sci.* 10: 123. 1953.
11. SCHURZ, J. and IMMERGUT, E. H. *J. Polymer Sci.* 9: 279. 1952.
12. SMITH, D. B. and COOK, W. H. *Arch. Biochem. and Biophys.* 45: 232. 1953.
13. SMITH, D. B., COOK, W. H., and NEAL, J. L. *Arch. Biochem. and Biophys.* 53: 192. 1954.

THE HEAT OF WETTING OF SILK FIBROIN BY WATER¹

BY H. BRIAN DUNFORD² AND JOHN L. MORRISON³

ABSTRACT

The heats of wetting by water of silk fibroin initially containing various amounts of adsorbed and desorbed water have been measured. These measurements along with the water vapor adsorption isotherm of Hutton and Gartside have been used to calculate the integral and differential heats, free energies, and entropies of adsorption. In contrast with cellulose, silk containing desorbed water evolves less heat than that containing adsorbed water. This fact suggests that any contribution by a heat of swelling term is very small for silk fibroin, so that the calculated thermodynamic properties probably can be assigned almost entirely to the adsorption process. The changes in the heats and entropies of adsorption appear to parallel the sequence of changes in film formation as revealed by surface area calculations.

Bull (2) determined the water vapor adsorption isotherms of a large number of proteins including silk fibroin at 25° and 40°C. Dole and McLaren (4) and Davis and McLaren (3) corrected and extended Bull's thermodynamic calculations of the water-protein systems. In these calculations, isosteric heats of adsorption were obtained by applying the Clausius-Clapeyron equation to the adsorption isotherms at the two different temperatures. Much uncertainty in this method of determining heats of adsorption occurs in the low and high water vapor pressure regions, yet it is these regions that are very important in understanding the nature of the adsorption process.

Direct measurement of the heats of wetting of water by silk fibroin over the whole range of vapor pressures are reported here. With these data and the adsorption isotherm of Hutton and Gartside (11), the thermodynamic functions have been calculated. The only reported similar measurements that have come to our attention were made at four initial water contents by Hedges (8).

EXPERIMENTAL

Rotating Adiabatic Calorimeter

A rotating adiabatic calorimeter as originally designed by Lipsett, Johnson, and Maass (13, 14) was used with some small modifications (1, 5).

The heat capacity of the calorimeter was obtained by the method used for the original apparatus (13). This consisted of measuring the heat of solution of sodium chloride in water, using sets of two determinations with the same salt-water ratios but differing absolute amounts of reactants. The average heat capacity for seven sets of determinations was within 0.08 calories of the calculated value of 13.09 calories. Although this is an error of 0.6% for the metal container, it is only 0.1% for the total heat capacity when the 50 ml. of accurately weighed water used for all heat of wetting measurements is included.

¹Manuscript received January 18, 1955.

Contribution from the Department of Chemistry, University of Alberta, Edmonton, Alberta. Based on a thesis submitted to the School of Graduate Studies, University of Alberta, in partial fulfillment of the requirements for the M.Sc. degree. Presented in part to the Annual Conference of the Chemical Institute of Canada, Windsor, Ontario, June 4-6, 1953.

²Present address: Department of Chemistry, McMaster University, Hamilton, Ontario.

³Associate Professor, Department of Chemistry, University of Alberta, Edmonton, Alberta.

Evacuated Glass Calorimeter

The heat of wetting measurements were carried out in air. To determine the magnitude of the heat effect arising from the desorption of the air by water, some heat of wetting measurements were made in a simple vacuum calorimeter.

The glass reaction cell of the calorimeter was similar to that of Howard and Culbertson (10) and consisted of two compartments, one of about 20 ml. volume to hold the evacuated silk sample, and the other of about 50 ml. to hold the water. Upon breaking the hook-shaped thin glass partition between the two compartments, the water came in contact with the silk. The whole assembly, including glass cell, Beckmann thermometer, 50 ohm resistance wire, and glass stirring rod, was immersed in xylene (low heat capacity liquid) contained in a Dewar flask (inside dimensions: 6.7 cm. diameter by 28 cm. height). The top was sealed as completely as possible by a waxed cork. The glass cell was discarded after an experiment.

The temperature rise of the wetting process was simulated electrically so that it was unnecessary to determine the heat capacity of the calorimeter.

Silk Fibroin

Japanese raw silk was kindly supplied by Belding-Corticelli Ltd., Montreal. It was degummed by the method of Sookne and Harris (19).

Drying and Moistening Procedures

Most samples were dried by a procedure similar to that of Hedges (8). A stream of compressed air was passed successively through absorbent cotton, sulphuric acid scrubbers, sodium hydroxide pellets, and magnesium perchlorate towers. The dry air entered a copper coil and desiccator inside an oven at $105 \pm 1^\circ\text{C}$. After it was dried for two hours in the oven desiccator, the sample was placed in a specially designed desiccator (16) over phosphorus pentoxide for 30 min. to cool.

If the sample was being used to determine the heat of wetting at the above dryness, the container for drying the sample was the inner box of the calorimeter. If, however, the sample was being prepared for heats of wetting measurements at finite initial moisture contents, the drying container was a weighing bottle. After the dry weight of the silk was obtained, the weighing bottle was placed over an aqueous sulphuric acid solution of concentration necessary to give the required initial moisture content. Then, after at least three days, the sample was transferred as rapidly as possible to the inner box of the calorimeter, covered by the weighed greased lid, and reweighed to determine the moisture content.

Some heat of wetting measurements were made on samples from which water had been partially desorbed. First, the samples were placed over distilled water, and then over various aqueous sulphuric acid solutions.

Bull's data as well as the present measurements are on a vacuum-dry basis. Three samples which had been previously dried by the above method were dried for two hours in an Aberhalden vacuum drying apparatus which uses boiling water as a heat source. These determinations showed that the oven-

dried samples contained 0.20% moisture on the vacuum-dry basis. The heat of wetting of one of these samples was determined.

Finally, for the heat of wetting measurements of evacuated samples, the silk was dried *in vacuo* at 105°C. by an electric furnace.

RESULTS AND CALCULATIONS

Net Heat of Adsorption

The heats of wetting of silk fibroin at 25°C. and equilibrated with various amounts of water, both adsorbed and desorbed, are given in Table I and Fig. 1. For comparison, Hedges' four determinations (8) are included in Fig. 1. A comparison of the degree of precision of our calorimetry with that of Hedges may be shown by the fact that, in our case, the mean deviation of three determinations at 0.20% moisture content is ± 0.03 cal. gm.⁻¹, while the mean deviation of Hedges' four values for the heat of wetting of dry wool is ± 0.4 cal. gm.⁻¹.

The measurements of the heat of wetting of seven evacuated samples in the Dewar calorimeter gave an average of 15.94 ± 0.11 cal. gm.⁻¹. Since these values agree with the result obtained in the presence of air, the air has no measurable effect. Also, the value of the initial, vacuum-dried sample (15.93) was confirmed by a different type of calorimeter.

The integral net heats of adsorption, ΔH , in calories per 100 gm. silk fibroin (above the heat of condensation of water vapor to liquid) have been calculated from the heats of wetting by the method of Dole and McLaren (4) (See also Wahba (21)).

In our case, the *heat of wetting*, q_0 , of 100 gm. dry protein is evolved by Process 1.

(1) Protein (dry at $p = 0$) + excess liq. H₂O (at p_0) \rightarrow Protein (with excess liq. H₂O at p_0), in which p_0 is the vapor pressure of pure water at 25°C.

TABLE I
HEATS OF WETTING OF SILK FIBROIN CONTAINING ADSORBED AND DESORBED WATER VAPOR

Adsorption		Adsorption		Desorption	
Water content, %	Heat of wetting, cal.	Water content, %	Heat of wetting, cal.	Water content, %	Heat of wetting, cal.
0.00	15.93	8.38	4.03	1.24	12.47
0.20	15.71	8.45	3.70	1.45	11.72
0.54	14.64	9.73	2.98	3.82	8.83
0.71	14.40	10.39	2.51	5.64	6.31
0.86	14.09	11.87	1.83	7.59	4.36
1.11	13.24	12.11	1.68	9.98	2.48
2.52	10.92	14.19	1.13		
2.56	10.78	14.20	1.03		
4.14	8.51	16.4	0.69		
4.23	8.37	23.9	0.34		
5.80	6.42	25.2	0.19		
5.90	6.39				

Note: Water content is in per cent of the dry weight of fibroin. The heats of wetting are given in calories per gram of dry fibroin.

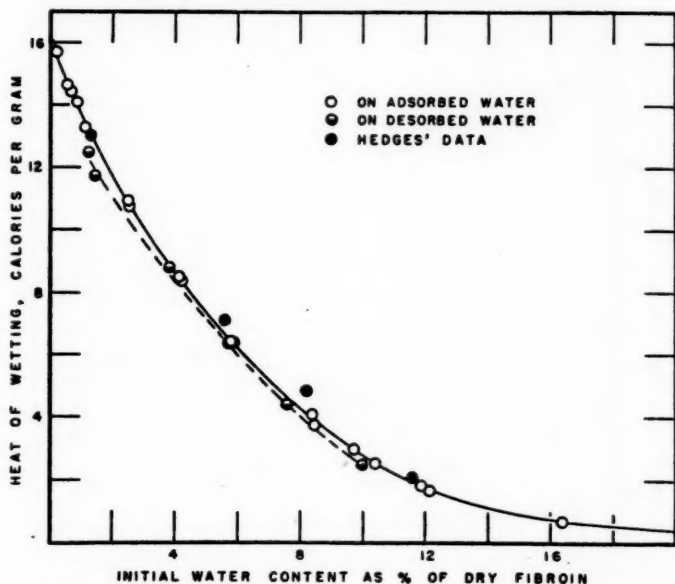


FIG. 1. The heats of wetting by water of silk fibroin containing various amounts of adsorbed and desorbed water.

When 100 gm. protein has been equilibrated in water vapor at pressure p and has taken up n moles of water, the *heat of wetting*, q , is evolved by Process 2.

(2) Protein (with n H₂O at p) + excess liq. H₂O (at p_0) → Protein (with excess liq. H₂O at p_0).

TABLE II

CALCULATED THERMODYNAMIC PROPERTIES OF THE SILK-WATER SYSTEM AT 25°C.

n	P/P_0	$-\Delta H$	$-\Delta F$	$-\Delta S$	$-\overline{\Delta H}$	$-\overline{\Delta F}$	$-\overline{\Delta S}$
0	0	0	0	0	4665	—	—
0.05	.015	215	151	0.22	3880	~2400	~4.97
0.10	.040	390	265	0.42	3170	1820	4.53
0.20	.150	660	414	0.83	2460	1125	4.48
0.30	.300	900	503	1.33	2230	705	5.12
0.35	.377	1010	535	1.59	2160	575	5.32
0.40	.452	1105	561	1.88	1750	475	4.28
0.50	.588	1255	600	2.20	1210	320	2.99
0.60	.703	1360	625	2.47	870	210	2.21
0.70	.777	1435	642	2.66	600	150	1.51
0.80	.830	1490	655	2.80	440	110	1.11
0.90	.868	1520	665	2.87	270	85	0.62
1.00	.898	1545	672	2.93	155	65	0.30
1.20	.938	1560	683	2.94	50	35	0.05
1.40	.965	1570	688	2.96	—	—	—

Note on units: n , moles per 100 gm. fibroin; ΔH and ΔF , calories per 100 gm. fibroin; $\overline{\Delta H}$ and $\overline{\Delta F}$, calories per mole of water; ΔS , entropy units per 100 gm. fibroin; $\overline{\Delta S}$, entropy units per mole of water.

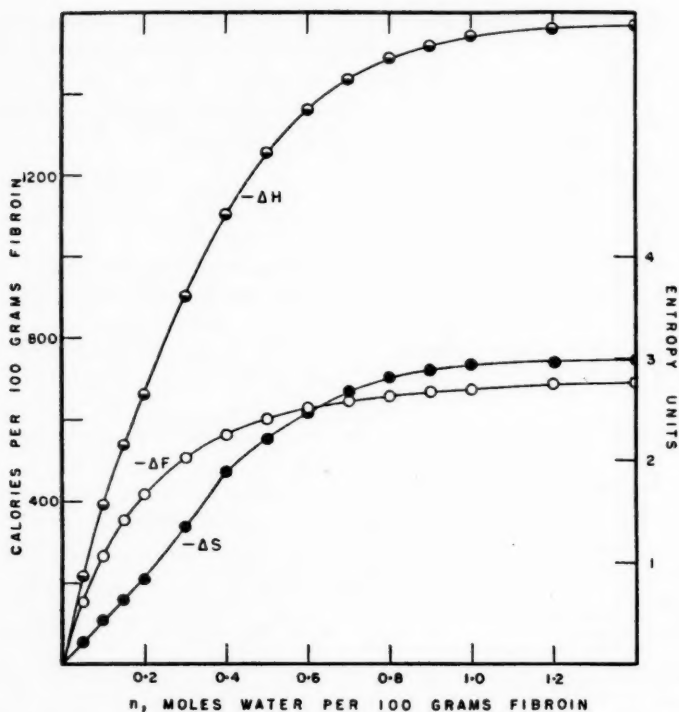


FIG. 2. The integral heat, free energy, and entropy of adsorption of water by silk fibroin.

Subtraction of Process 2 from Process 1 gives Process 3:

(3) Protein (dry at $p = 0$) + n H₂O (at p_0) → Protein (with n H₂O at p), with the evolution of $(q_0 - q)$ calories/100 gm. dry protein, or ΔH , the integral net heat of adsorption.

Our Process 3 is the same as Dole and McLaren's Process (4). Values of ΔH are given in Table II and Fig. 2.

The differential net heats of adsorption, $\overline{\Delta H}$, given in Table II and Fig. 3, were obtained by careful graphical differentiation of the plot of ΔH vs. n , the number of moles of water adsorbed per 100 gm. fibroin.

Free Energy of Adsorption

The integral and differential free energies of adsorption of water on a protein are obtained from the vapor adsorption isotherm. Following Dole and McLaren (4), the differential free energy, $\overline{\Delta F}$, is given by

$$\overline{\Delta F} = RT \ln (P/P_0)$$

and the integral free energy, ΔF , of our Process 3 is given by

$$\Delta F = -RT \int_0^n \ln (P/P_0) + nRT \ln (P/P_0).$$

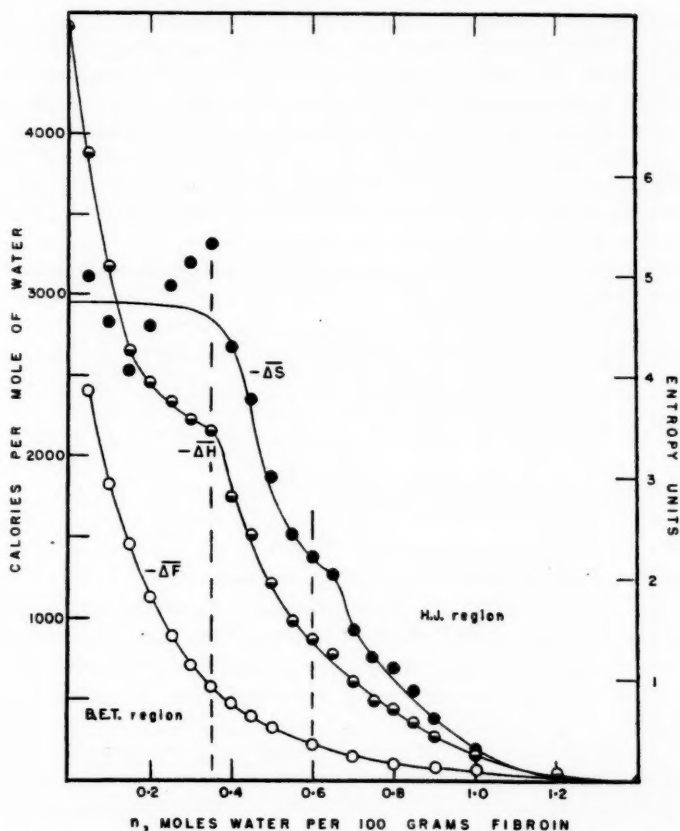


FIG. 3. The differential heat, free energy, and entropy of adsorption of water by silk fibroin.

A number of attempts were made to obtain a reproducible adsorption isotherm with a vacuum apparatus like that used by Wiig and Juhola (22) for charcoal. Although the middle and upper pressure parts of the adsorption branch matched the corresponding parts of the isotherm of Hutton and Gartside (11), the amount adsorbed in the low pressure region was lower than that obtained by them and others (2, 18). It was realized that the determination of the correct isotherm is a major project in itself.

Fortunately, Hutton and Gartside (11) have carried out an exhaustive study of the water isotherm on silk at 25°C. They found that degummed silks of Japanese, Chinese, and Italian origins gave practically the same isotherm, and by both the vacuum and the desiccator methods.

Dunford and Morrison (6) have shown that the Brunauer, Emmett, and Teller equation and the Harkins-Jura equation, although applying to the opposite extremes of Bull's water-protein systems, gave the same monolayer

adsorption for each protein. Liang's method (12) was used to correlate the two equations. These equations were applied to the isotherm of Hutton and Gartside. The B.E.T. plot gave a straight line over the relative pressure range 0.07 to 0.35, with a monolayer content, X_m , of 4.49 gm. water per 100 gm. silk fibroin. The H.J. plot gave a straight line over the relative pressure range 0.60 to 0.97 (and probably to 1.00), with $X_m = 4.46$ gm. It is considered that this coincidence of X_m values further validates the isotherm. The same test applied to our isotherm failed to produce a straight line for the B.E.T. plot, while it gave a value of $X_m = 4.48$ gm. for the H.J. plot.

Thus, the water vapor adsorption isotherm of Hutton and Gartside was used to calculate ΔF and $\overline{\Delta F}$, the results of which are given in Table II and Figs. 2 and 3.

Entropy of Adsorption

The integral and differential net entropies of adsorption, calculated by the well known equations

$$\Delta S = (\Delta H - \Delta F)/T$$
$$\text{and } \overline{\Delta S} = (\overline{\Delta H} - \overline{\Delta F})/T,$$

are given in Table II and Figs. 2 and 3.

DISCUSSION

Comparison with Calculations of Davis and McLaren

The results shown in Figs. 2 and 3 may be compared with the corresponding calculations of Davis and McLaren (3), based on Bull's data (2). In contrast with their results, the present integral heats and entropies in Fig. 2 reach higher values and approach maximum values as saturation vapor pressure is reached.

The differential heats and entropies in Fig. 3 show similar general features to those of Davis and McLaren except at the extremes of the vapor pressure range. In the low pressure range, a mean value of about -4.7 e.u. is suggested for $\overline{\Delta S}$, the differential entropy change. Entropy values of this order of magnitude are maintained until appreciably above a B.E.T. monolayer film content. The value of -4.7 e.u., which is much less than the value of nearly -8 obtained by Davis and McLaren, is still sufficient to suggest chemisorption of water as proposed by Pauling (17). The fact that the entropy does not fall off until a film content 40% above the monolayer is reached suggests that some water in the second layer is very tightly held.

In the region of high vapor pressure, the upswing in the negative differential heats and entropies calculated by Davis and McLaren are not found in the present calculations; instead, $-\Delta \overline{H}$ and $-\Delta \overline{S}$ decrease regularly to those of liquid water. However, Davis and McLaren doubt the reality of their upswings.

Heat of Wetting Hysteresis

In interpreting thermodynamic calculations of adsorption systems, the question of how much of the changes arise from the adsorbate and the adsorbent respectively must be determined. This is particularly true of protein-water systems, in which swelling phenomena and even solution may occur.

The silk fibroin - water system appears to be a relatively simple one, so that the thermodynamic changes can be fairly definitely identified with purely adsorption phenomena. The fact that fibroin is very accessible to water, independently of its structure, so that its water vapor adsorption isotherm is unaffected by solution and reprecipitation (15) does not in itself eliminate the possibility of swelling phenomena. Wool, which shows swelling properties, behaves similarly to silk in that its adsorption isotherm is largely unaffected by the destruction of its structure. However, while the *amounts* adsorbed may be unaffected, the energy relations may be profoundly affected.

No comparison of silk with wool is possible because Hedges (8) who measured the heats of wetting of wool by water did not make measurements on "desorbed" samples. However, Argue and Maass (1) made measurements for cellulose and found that the heats of wetting on the 'desorbed' samples were significantly *higher* than for the corresponding 'adsorbed' samples. This is generally explained by including a heat of swelling term in the net heat of wetting on an 'adsorbed' sample, part of which would not be included in the heat of wetting of a 'desorbed' sample. In our case, if there is any heat of swelling, it is probably very small because the desorption heats of wetting are *below* the adsorption heats.

It must be remembered that both silk fibroin and cellulose give the same type of sorption isotherm hysteresis. At equal moisture contents, water is more tightly held on the desorption branch. Therefore we would expect the heat of wetting to be *less* for the desorption side if there are no phenomena occurring other than pure adsorption.

Adsorption Areas

Adsorption area measurements assist in the interpretation of the thermodynamic properties of adsorption systems. In the case of the silk fibroin - water system, it was shown (6) in common with all Bull's data that the B.E.T. and H.J. area equations when applied to the two parts of the adsorption isotherm gave coincident monolayer values ($X_m = 4.48$ gm. H_2O per 100 gm. fibroin). This confirms the observation of Mellon, Korn, and Hoover (15) that swelling phenomena do not appear to affect the accessibility of water molecules to the molecular chains of fibrous proteins. The coincidence of monolayer areas has been interpreted by Dunford and Morrison (6) to indicate that the upper part of the isotherm involves the formation of a condensed film above the monolayer laid down in the first part of the isotherm. This interpretation confirms the observations of Hoover and Mellon (9) who, by applying a polarization theory to protein-water sorption isotherms, showed "that sorption on active sites occurs at low vapor pressures and that sorption at higher vapor pressure is due to this prior sorption".

Finally, let us consider what happens when vapor saturated silk fibroin is immersed in liquid water. An attempt was made to measure the area of the protein by the absolute method of Harkins and Jura (7). A sample was kept above pure water for three days attaining 25.2% moisture content before being immersed in the calorimeter. The heat of wetting was 0.19 cal. gm.⁻¹. However,

the saturation moisture content of silk fibroin is 36% (11) and extrapolation to this water content gave a value of less than 0.10 cal. (Wahba (20) found 0.30 cal. gm.⁻¹ for cellulose under the same conditions). Assuming that the heat of immersion of the vapor saturated fibroin does not include swelling energy, the Harkins and Jura 'absolute' area is less than 3.5 sq. meters gm.⁻¹, compared with the isotherm area of 158 sq. meters gm.⁻¹. This suggests that near the relative vapor pressure of unity, the spaces between the molecular protein chains are completely filled with water and that the area 3.5 sq. meters gm. may correspond to the external area of the fibrils.

Conclusion

The area and thermal measurements and calculations of the silk fibroin-water system are consistent; in Fig. 3, the differential heat and entropy curves indicate a transition from monolayer and multilayer formation to a condensed film, which in turn becomes indistinguishable from liquid water. If swelling occurs, its effect is not reflected in either the amounts or energies of adsorption.

ACKNOWLEDGMENTS

We wish to thank Dr. H. W. Habgood of the Alberta Research Council, Edmonton, for helpful discussions. Acknowledgments are also made to the National Research Council and the General Research Committee of the University of Alberta for grants in aid of this work.

REFERENCES

1. ARGUE, G. H. and MAASS, O. *Can. J. Research*, 12: 564. 1935.
2. BULL, H. B. *J. Am. Chem. Soc.* 66: 1499. 1944.
3. DAVIS, S. and McLAREN, A. D. *J. Polymer Sci.* 3: 16. 1948.
4. DOLE, M. and McLAREN, A. D. *J. Am. Chem. Soc.* 69: 651. 1947.
5. DUNFORD, H. B. Thesis, University of Alberta, Edmonton, Alta. 1952.
6. DUNFORD, H. B. and MORRISON, J. L. *Can. J. Chem.* 32: 558. 1954.
7. HARKINS, W. D. and JURA, G. *J. Am. Chem. Soc.* 66: 1362. 1944.
8. HEDGES, J. J. *Trans. Faraday Soc.* 22: 178. 1926.
9. HOOVER, S. R. and MELLON, E. F. *J. Am. Chem. Soc.* 72: 2562. 1950.
10. HOWARD, F. L. and CULBERTSON, J. L. *J. Am. Chem. Soc.* 72: 1185. 1950.
11. HUTTON, E. A. and GARTSIDE, J. *J. Textile Inst. Trans.* 40: T161. 1949.
12. LIANG, S. C. *J. Phys. & Colloid Chem.* 55: 1410. 1951.
13. LIPSETT, S. G., JOHNSON, F. M. G., and MAASS, O. *J. Am. Chem. Soc.* 49: 925. 1927.
14. LIPSETT, S. G., JOHNSON, F. M. G., and MAASS, O. *J. Am. Chem. Soc.* 49: 1940. 1927.
15. MELLON, E. F., KORN, A. H., and HOOVER, S. R. *J. Am. Chem. Soc.* 71: 2761. 1949.
16. MORRISON, J. L., CAMPBELL, W. B., and MAASS, O. *Can. J. Research*, B, 15: 447. 1937.
17. PAULING, L. *J. Am. Chem. Soc.* 67: 555. 1945.
18. ROWEN, J. W. and BLAINE, R. L. *Ind. Eng. Chem.* 39: 1659. 1947.
19. SOOKNE, A. M. and HARRIS, M. *J. Research Natl. Bur. Standards*, 23: 299. 1939.
20. WAHBA, M. *J. Phys. & Colloid Chem.* 52: 1197. 1948.
21. WAHBA, M. *J. Phys. & Colloid Chem.* 54: 1148. 1950.
22. WHIG, E. O. and JUHOLA, A. J. *J. Am. Chem. Soc.* 71: 561. 1949.

THE ADSORPTION OF NITROGEN, OXYGEN, AND ARGON BY GRAPHITE¹

BY H. L. McDERMOT AND J. C. ARNELL

ABSTRACT

The adsorption of nitrogen, oxygen, and argon by three Acheson graphites has been measured at liquid nitrogen and liquid oxygen temperatures. The isotherms were Type II in the B.E.T. classification and displayed two kinds of hysteresis. The first kind was attributed to the presence of pores in the graphite and the second kind to intercrystalline swelling.

INTRODUCTION

This paper describes an investigation of three artificial graphites manufactured by the Acheson Colloids Corporation. Very little detailed adsorption work has been done with graphites of this type with a view to elucidating their structure. Barrer (2) has measured the adsorption of nitrogen, argon, and hydrogen by an Acheson graphite over a considerable temperature range and has calculated isosteric heats from the isotherms. He found that the graphite was energetically heterogeneous to all three gases and that the heats in the case of nitrogen were unaffected by the addition of chemisorbed oxygen to the surface of the graphite. He concluded therefore that the heterogeneity was a property of the carbon structure. In the opinion of the authors, the weakness of this work lies in the fact that very few adsorption points were measured at each temperature and no desorption points at all were determined. Bartell and Dodd (4) measured the adsorption of nitrogen at liquid nitrogen temperatures by a number of carbons which included two Acheson graphites. The purpose of the work was to measure the surface area of the carbons so that only a small number of points were determined and only in the case of the diamond powder were desorption points taken. It is stated that no desorption points were measured for the graphite because reversibility for nitrogen adsorption had been established at liquid oxygen temperatures. Bartell and Dodd do not indicate to what pressures these measurements were carried, but it will be shown in the present paper that reversibility of the nitrogen isotherm at 90°K. is by no means a criterion for reversibility unless pressure measurements are extended to well over an atmosphere. Because of the lack of data on these graphites, it was decided to undertake a detailed study of three typical artificial graphites. The first step was to measure isotherms at low temperatures using as adsorbates nitrogen, oxygen, and argon. Unusual hysteresis effects were encountered and therefore a detailed study was made on one graphite using nitrogen as the adsorbate. For comparative purposes the nitrogen isotherm of a nonporous carbon black was also determined.

¹Manuscript received January 17, 1955.

Contribution from the Defence Research Chemical Laboratories, Ottawa, Canada. Issued as DRCL Report No. 184.

EXPERIMENTAL AND RESULTS

Samples of three graphites of surface areas up to $100 \text{ m}^2/\text{gm.}$ were supplied by the Acheson Colloid Corporation. They were designated as Lot 6226, Lot 6131, and No. 39. For the purpose of this paper they have been designated as G-1, G-2, and G-3, respectively.

Nitrogen was supplied by the Canadian Liquid Air Co. It was stated to be 99.5% nitrogen and was used without further purification.

Oxygen was also supplied by the Canadian Liquid Air Co. and specified as 99.9% oxygen.

The argon used was Matheson Research Grade and was rated as 99.9% pure.

The adsorption isotherms were measured by means of a standard volumetric adsorption apparatus. For the isotherms at 77.5°K. and 90.0°K. , open baths of liquid nitrogen and liquid oxygen were used. The maximum variation in the temperature of these baths was $\pm 0.2^\circ$. For the isotherm at 70.6°K. , a cryostat was used the temperature of which was controlled and measured by a nitrogen thermometer. The temperature of the cryostat was regulated to better than $\pm 0.02^\circ$. Before commencing adsorption measurements the samples of graphite were outgassed by evacuation at 120°C. for at least 12 hr.

The isotherm for the adsorption of nitrogen by G-1 is shown in Fig. 1. The isotherm is Type II in the B.E.T. classification and displays a normal hysteresis loop from saturation down to a relative pressure of 0.45. Several scanning curves are also shown illustrating the effect of desorption from pressures below saturation. Below a relative pressure of 0.45, an unusual desorption curve

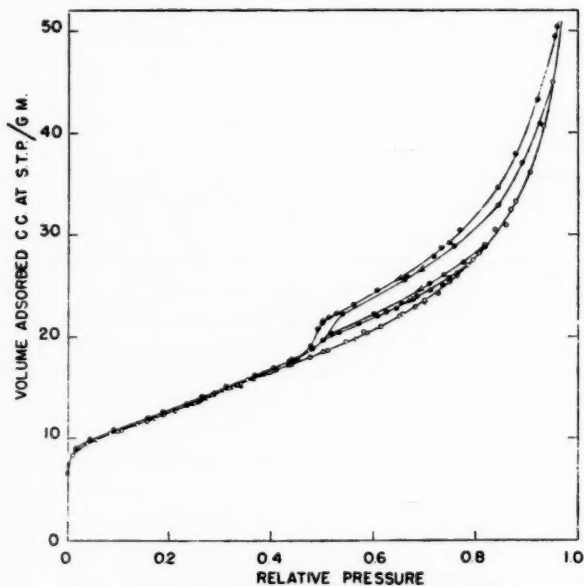


FIG. 1. Isotherm of nitrogen sorbed by G-1 at 77.5°K.

approximately parallel to the adsorption curve and slightly above it was found. The separation of the curves at this part of the isotherm is small, but is nevertheless believed to be real. Over ten separate adsorption-desorption cycles were carried out with this system and in every case the desorption points were observed to lie slightly above the adsorption points despite the fact that desorption was begun from a variety of relative pressures (all above the inception of the hysteresis loop). If for example a cumulative error existed, a different separation would be anticipated for each relative pressure chosen for the commencement of desorption. This was not found to be the case. However when desorption was carried out at pressures below the inception of the hysteresis loop then no hysteresis at all was observed. This point is illustrated by Fig. 2, which shows the isotherm of nitrogen adsorbed by G-1 at

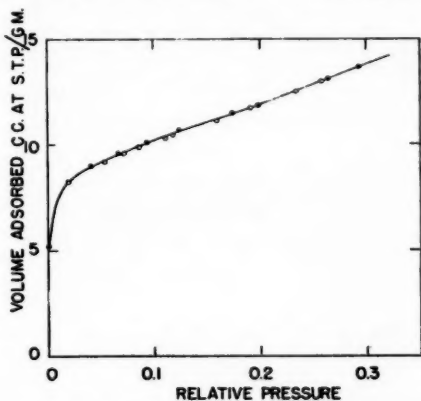


FIG. 2. Isotherm of nitrogen sorbed by G-1 at 90.0°K.

90.0°K. The characteristics outlined for the adsorption isotherm of nitrogen on G-1 were found to be typical of the nitrogen isotherms of all these graphites.

As the initial measurements with G-1 revealed the unusual hysteresis effects referred to above, experiments were conducted to discover if these effects stemmed from the packing of the powder in the adsorption cell. In the first of these experiments, the nitrogen isotherm was remeasured using 1 gm. of graphite instead of 10 gm. The results are plotted in Fig. 3 along with the original isotherm. There is no discernible difference between the two sets of data. In a second experiment, a 1 gm. sample was spread out (approximately 1 mm. in depth) on circular trays arranged on a vertical rod and separated from each other by washers. Before filling with graphite, the trays were washed with organic solvents to remove machining compounds and were thoroughly dried. The adsorption of nitrogen was then measured. The isotherm is shown in Fig. 4 along with that determined for a 1 gm. sample in bulk. Although the adsorption is somewhat greater for the sample on trays at high relative pressures, the hysteresis effects remained substantially unchanged. It was concluded therefore that the unusual hysteresis effects were real. No explana-

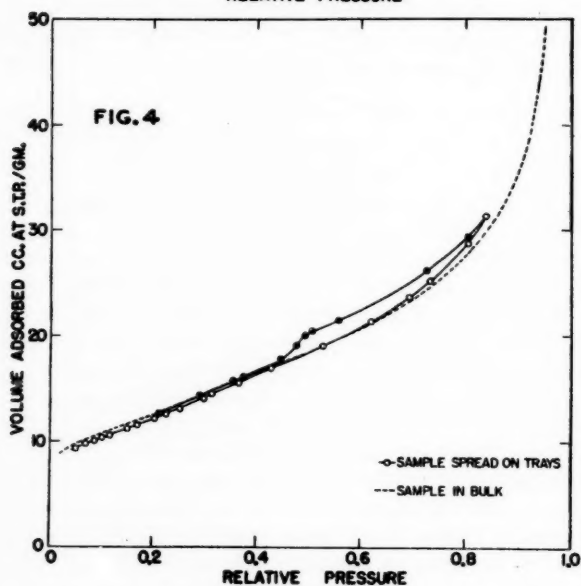
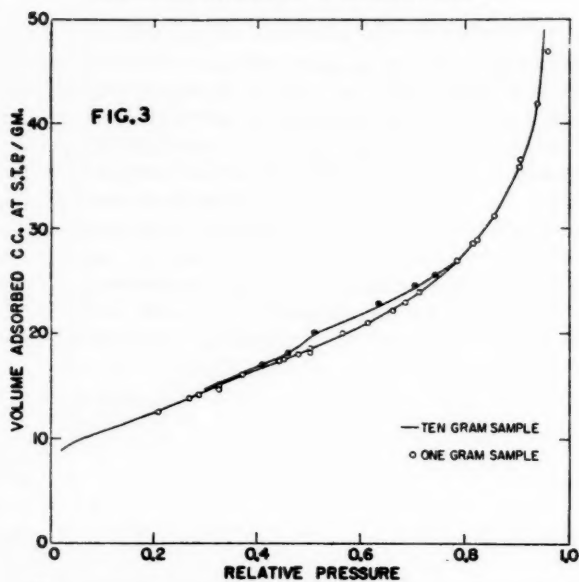


FIG. 3. Sorption isotherms of nitrogen by G-1 at 77.5°K. showing the effect of variations in sample size.

FIG. 4. Sorption isotherms of nitrogen by G-1 at 77.5°K. showing the effect of sample dispersion.

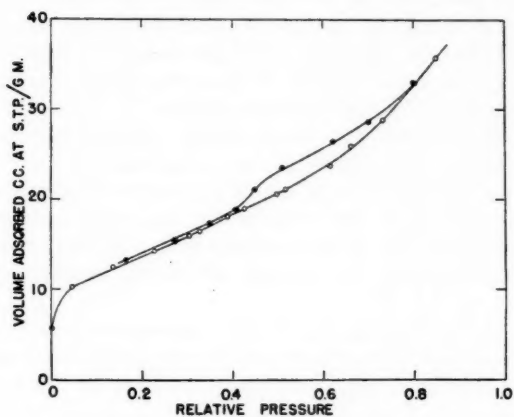


FIG. 5. Isotherm of oxygen sorbed by G-1 at 90.0°K.

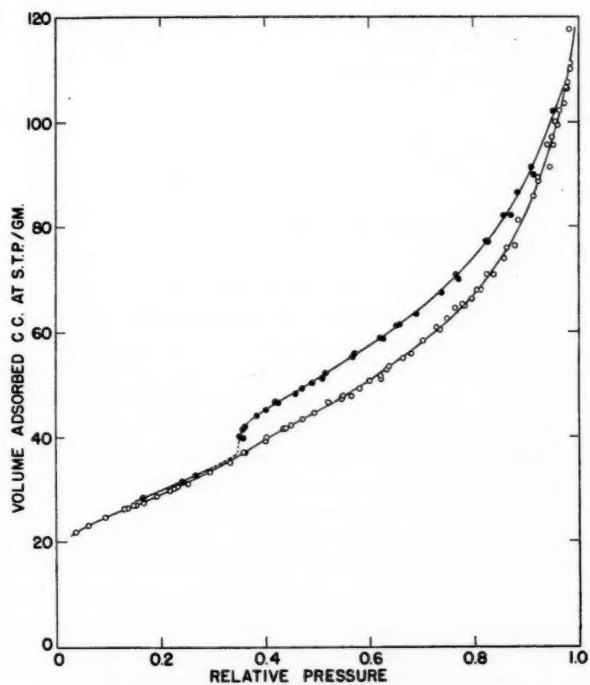


FIG. 6. Isotherm of argon sorbed by G-2 at 77.5°K.

tion has been found for the difference between the isotherms of the "bulk" sample and the "dispersed" sample. The reproducibility of the measurements indicates that the effect is real and not due to experimental error. An obvious speculation is that some packing is occurring in the "bulk" sample which hinders adsorption at higher relative pressures.

It was then suspected that the hysteresis phenomena observed in the adsorption isotherms of nitrogen by these graphites were due to the graphite structure. To confirm this suspicion, measurements were made with two other gases, oxygen and argon. Fig. 5 shows the adsorption isotherm of oxygen on G-1 at 90.0°K. and Fig. 6 the isotherm of argon on G-2 at 77.5°K. These isotherms clearly display the features previously described for the nitrogen isotherms.

Finally, a closer investigation of these phenomena was made utilizing the G-3 nitrogen system. This system was chosen because the separation of the lower part of the desorption curve from the adsorption curve was found to be greater for G-3 than for the other graphites. The isotherms for the adsorption

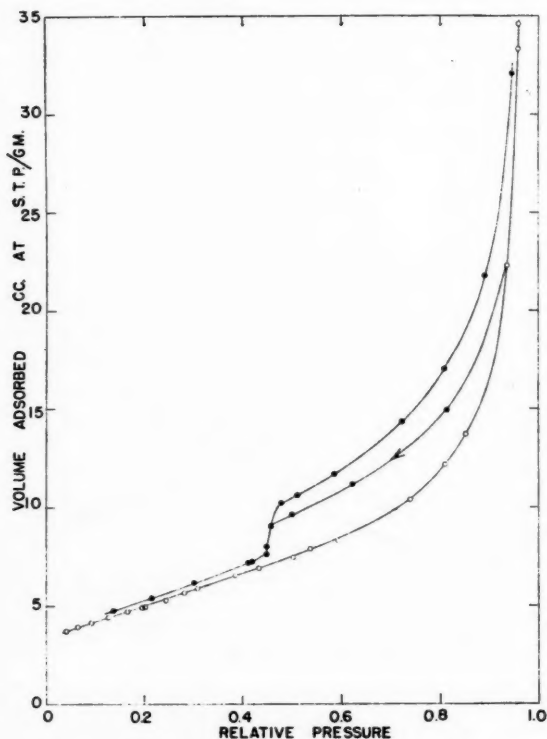


FIG. 7. Isotherm of nitrogen sorbed by G-3 at 77.5°K.

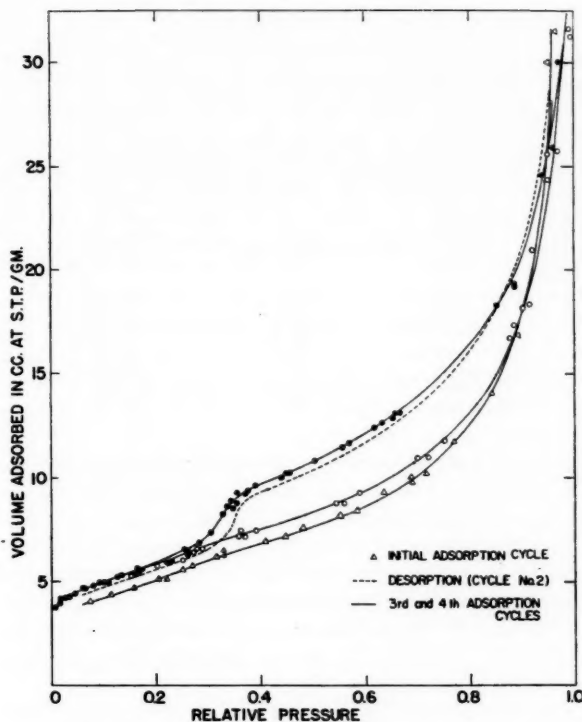


FIG. 8. Isotherm of nitrogen sorbed by G-3 at 70.6°K.

of nitrogen by G-3 at 77.5°K. and at 70.6°K. are shown in Figs. 7 and 8 respectively. It will be observed that the form of the isotherm at 77.5°K. is qualitatively similar to that for G-1 which is depicted in Fig. 1.

The data plotted in Fig. 8 are taken from these series of runs, with up to four successive adsorption cycles for a series. Except for the first cycle of a series, a typical adsorption cycle was begun by readsorption from the lowest desorption point of the previous cycle, without altering the bath temperature. Between each series the graphite was given the standard outgassing treatment. The initial adsorption curve is seen to be considerably below the subsequent ones. After the second adsorption cycle, the hysteresis loop closes completely and a reversible section of the isotherm is observed below the beginning of the loop. The dotted line and the points just below the upper of the two adsorption curves represent data from the second adsorption cycle, which appears to be a transition cycle between the first and final adsorption cycles. It can be seen from Figs. 7 and 8 that the separation of the adsorption curves is greater at 70.6°K. than it is at 77.5°K. This is partly the effect of the extra cycling at 70.6°K. and partly the effect of the lower temperature.

DISCUSSION

The foregoing results have shown that the low temperature isotherms of the three graphites considered are Type II with hysteresis.

The adsorption curves obey the B.E.T. equation from $p/p_0 = 0.08$ to $p/p_0 = 0.30$. The values of V_m derived from the B.E.T. plots and the surface areas calculated from them are given in the following table. In every case the data used were taken from the initial adsorption isotherm.

Graphite	Adsorbate	Temperature, °K.	V_m , cc. at S.T.P.	Area, m. ² /gm.
G-1	Nitrogen	77.5	10.35	45.3
G-1	Nitrogen	90.0	9.86	41.6
G-1	Oxygen	90.0	11.49	43.4
G-2	Nitrogen	77.5	21.97	96.2
G-2	Argon	77.5	23.92	82.0
G-3	Nitrogen	77.5	4.21	18.4
G-3	Nitrogen	70.6	4.44	17.3

Closer examination has revealed two distinct types of hysteresis. The first type is represented by a wide loop extending from saturation down to a relative pressure of approximately 0.45. It is illustrated by a closed loop in Fig. 8. The second hysteresis effect is a much smaller one which takes the form of a slight elevation of the desorption curve above the adsorption curve at relative pressures below the beginning of the main hysteresis loop. This effect is most clearly shown in Fig. 8, which also shows that readsorption without evacuation follows the desorption branch until the main hysteresis loop is reached after which a new path is taken.

The first type of hysteresis is believed to be evidence that these graphites are porous. Moreover in agreement with the ideas of Wheeler (7) and of Barrett, Joyner, and Halenda (3) on the mechanism of the sorption of vapors in pores, it is believed that the loops are a result of the presence of pores greater than four to six molecular diameters. These arguments have been previously advanced by McDermot and Arnell (6) to explain the presence of hysteresis loops in the isotherms of wide-pored charcoals and their absence in narrow-pored charcoals. Thus the hysteresis loops are thought to be similar for the charcoals and for the graphites though the similarity may be masked by the widely different surface areas and porosities. The postulated mechanism of adsorption and desorption is briefly as follows: layer adsorption occurs on the walls of the pores until the layers build up to a point where they coalesce to form a meniscus after which capillary condensation may occur in that pore. Thus capillary condensation is occurring in the small pores while layer adsorption is taking place in larger pores which have not yet formed a meniscus. Hysteresis arises because adsorption takes place by a mixture of layer adsorption and capillary condensation, whereas desorption occurs by evaporation from pores that are initially full of liquid. An adsorbed layer is left on the walls as capillary evaporation proceeds, but the process is not the reverse of the adsorption process owing to delay in meniscus formation on the adsorption branch. This mechanism does not of course exclude any contributions to hys-

teresis that may be made by pore constrictions, but these are only important when an attempt is made to evaluate pore distributions. Further support for these ideas is offered by Carman (5), who has measured the isotherm of CF_2Cl_2 on Linde silica powder and on the same powder compressed into a plug of known porosity. A hysteresis loop was obtained for sorption by the plug and a reversible isotherm for the powder. More vapor was sorbed on the adsorption branch of the isotherm by the plug than by the powder until the plug was filled with liquid at which point sorption ceased. This behavior is in accord with the postulated hypothesis, because at a given relative pressure layer adsorption would be greater on a curved surface than on a plane one. In order to demonstrate that the hysteresis loops discussed here are characteristic of sorption by a porous material, an experiment similar to Carman's was performed using as a porous carbon a sample of G-2 and as a nonporous carbon a sample of Spheron 9 supplied by the Godfrey L. Cabot Co. Arnell and Henneberry (1) calculated the surface area of this carbon black from adsorption, permeability, and electron microscope data and found approximate agreement by all three methods. This is taken to be good evidence that Spheron 9 is nonporous. The adsorption of nitrogen at 77.5°K. by G-2 and by Spheron 9 is compared in Fig. 9. As Spheron 9 has a slightly larger surface area than G-2 the data are plotted as V/V_m versus p/p_0 rather than directly on the basis of volumes adsorbed. It will be observed that although the curves coincide initially the adsorption curve for the graphite rises above that of the carbon black. These results are qualitatively similar to those of Carman (5), and are considered sufficient proof that G-2 is porous.

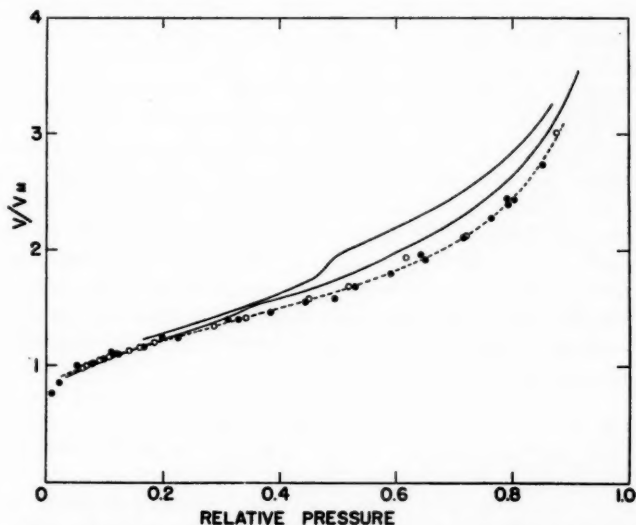


FIG. 9. Comparison between the sorption of nitrogen by G-2 and Spheron 9 at 77.5°K. Solid line represents the isotherm of G-2 and the dashed line that of Spheron 9.

The second hysteresis effect is most clearly observed in the adsorption isotherm of nitrogen on G-3 at 70.6°K. which is plotted in Fig. 8. It has been found that if one proceeds along the lower adsorption curve to a pressure at which the two curves are still well separated and then desorbs a reversible isotherm is obtained. If however adsorption is taken to a point where the two adsorption curves merge, then on desorption the upper curve is attained on completion of the main hysteresis loop. Moreover readsorption then takes place along the upper curve. Once the upper curve has been reached, it is only possible to regain the lower curve by warming the sample to the point where virtually all the nitrogen is desorbed. To sum up, the transition to the upper curve is only possible after the sorption of a considerable quantity of nitrogen, but once it has occurred it cannot be reversed. This type of behavior is characteristic of a sorption system which swells, and indeed the upper and lower adsorption branches in Fig. 8 are very similar in form to the isotherm of water sorbed by cellulose. It will be instructive to review the cellulose-water system and show that the resemblance noted above is not merely superficial. In the cellulose-water system swelling takes place along the adsorption branch and is only complete at saturation when the water has completely penetrated the structure. On desorption the path followed lies above the adsorption path because water which was able to enter the structure when it was swollen is trapped and can only be removed by completely drying the cellulose. Thus the initial adsorption curve can only be retraversed by completely drying the cellulose or in part by adding enough water to reswell the cellulose. By analogy it is believed that when sufficient gas is adsorbed by the graphite, the crystallites swell because of intercrystalline penetration. Once this penetration has occurred, some molecules are trapped and can only be removed by warming the graphite and desorbing all the gas. The analogy is not perfect because it is possible to scan the loop of the cellulose-water isotherm, but not the two adsorption curves of Fig. 8. The explanation is believed to be the following: on the sorption of water, cellulose swells gradually and continuously over the whole course of the adsorption loop and similarly on desorption water is lost gradually from the interior of the fiber. Hence the fiber can be reswollen from the partially dried state or dried from the partially swollen state, the amount of trapped water depending on the degree of swelling. In contradistinction, the graphite swells only when a critical quantity of nitrogen is sorbed and the process is sudden and irreversible. Once swelling has occurred, the quantity of trapped nitrogen is fixed and the lower curve cannot be attained without complete desorption.

REFERENCES

1. ARNELL, J. C. and HENNEBERRY, G. O. *Can. J. Research*, A, 26: 29. 1948.
2. BARRER, R. M. *Proc. Roy. Soc. (London)*, A, 161: 476. 1937.
3. BARRETT, E. P., JOYNER, L. G., and HALENDA, P. P. *J. Am. Chem. Soc.* 73: 373. 1951.
4. BARTELL, F. E. and DODD, C. G. *J. Phys. & Colloid Chem.* 54: 114. 1950.
5. CARMAN, P. C. and RAAL, F. A. *Proc. Roy. Soc. (London)*, A, 209: 59. 1951.
6. McDERMOT, H. L. and ARNELL, J. C. *Can. J. Chem.* 30: 177. 1952.
7. WHEELER, A. Presentations at Catalysis Symposia, Gibson Island A.A.A.S. Conferences. June 1945 and June 1946.

THE MANNICH CONDENSATION OF COMPOUNDS CONTAINING ACIDIC IMINO GROUPS¹

BY CAURINO CESAR BOMBARDIERI² AND ALFRED TAURINS

ABSTRACT

The synthesis of several new Mannich bases was accomplished by the condensation of secondary amines and formaldehyde with the following compounds: (1) 2-pyrrolidone, (2) 2,4-thiazolidinedione, (3) hydantoin, (4) 5,5-dimethylhydantoin, (5) uracil, (6) ethylnitramine, and (7) *n*-butylnitramine.

INTRODUCTION

While much work has been done on the Mannich condensation of compounds containing acidic hydrogen on carbon, considerably fewer data are available on the Mannich reaction of substances possessing active hydrogens on nitrogen, as it can be seen from this historical introduction.

Feldman and Wagner (6) prepared piperidinomethyl derivatives of succinimide, phthalimide, and carbazole. In their study of morpholinomethyl derivatives of urea and substituted ureas, Weaver, Simons, and Baldwin (13) condensed morpholinomethanol with phthalimide and succinimide. *N*-(Morpholinomethyl)- and *N*-(piperidinomethyl)-phthalimide were also synthesized by Moore and Rapala (12). The condensation of benzothiazole-2-thione and related compounds with formaldehyde and secondary amines was described in the German patent 575,114 in 1933. The purpose of the latter work was to prepare methylenediamine derivatives for use in the rubber industry.

Bachman and Heisey (1) condensed benzimidazole and benzotriazole with formaldehyde and secondary amines. Baker, Querry, Kadish, and Williams (2) prepared two Mannich bases of 4-quinazolone in reactions with formaldehyde, piperidine, and morpholine respectively. The Mannich condensation of pyrazole was studied by Huttel and Jochum (9). Butenandt and Hellmann (3) studied the reaction of hydantoin with formaldehyde and piperidine. However, they did not investigate the reaction product further. The most recent work on the synthesis of *N*-Mannich bases has been published by Hellmann and Löschmann (8). They describe the condensation of isatin, phthalimide, succinimide, and carbazole and give a few references on the previous publications of other authors.

That the alkylnitramines undergo a condensation with piperidinomethanol was observed by Franchimont (7) as early as 1910. However, he did not give any data on analysis and properties of the reaction product.

The objective of this work was to investigate the Mannich condensation of the cyclic imino compounds containing one or two imino groups in addition to the carbonyl groups as the hydrogen activators. We also studied the condensation of alkylnitramines in which the nitro group activates the hydrogen atom of the imino group.

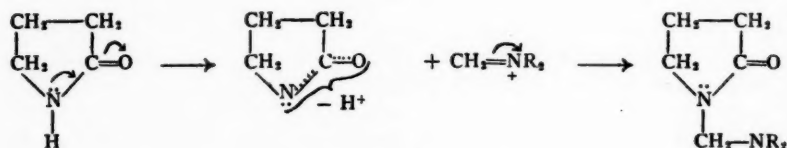
¹Manuscript received January 18, 1955.

Contribution from the Organic Chemistry Laboratory, McGill University, Montreal, Quebec, with the financial assistance of the National Research Council of Canada, Ottawa.

²Holder of a National Research Council Studentship 1953-1954.

DISCUSSION

We consider the replaceability of a hydrogen of the imino group by halogens or by metals, or by both, as the guiding principle enabling us to indicate the compounds possessing the ability to react in the Mannich condensation. On the bases of a similar behavior of ketones and imides in the reactions of halogenation and salt formation via enolization, we can assume that the Mannich condensation in both groups of compounds must follow the same course. Lieberman and Wagner (11) postulated the formation of a carbanion from a C—H acid compound as a necessary step in this reaction. It is reasonable to assume that the N—H acidic substance undergoes an analogous change to give a mesomeric anion in which the negative charge is located in the group N=C=O. The formation of the Mannich base may be visualized as the addition of the intermediate methylene-ammonium cation or the protonated dialkylaminomethanol at the mesomeric anion, as in the example of the reaction of 2-pyrrolidone.



Most of the condensations of imino carbonyl compounds were carried out using free secondary bases, but not their salts because of the sensitivity of the N—CH₂—N bond towards acids. However, in a few cases the condensation was successful using even secondary amino hydrochlorides. Thus 2-pyrrolidone [2-pyrrolidinone] was successfully condensed with morpholine and piperidine bases, and dimethylamine hydrochloride as well.

2,4-Thiazolidinedione (4, 14) possesses acidic properties and forms alkali and silver salts. It reacted very easily at 0° with morpholine, piperidine, and dimethylamine. Even methylamine reacted with two molecules of the 2,4-thiazolidinedione to give (VII). Both hydantoin [2,4-imidazolidinedione] and 5,5-dimethylhydantoin [5,5-dimethyl-2,4-imidazolidinedione] demonstrated their ability to react in the Mannich condensation with two molecules of formaldehyde and two molecules of morpholine. No reaction products were obtained in the attempted condensations of both hydantoins with piperidine and dialkylamines respectively.

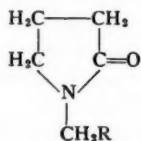
We found that uracil [2,4-(1H, 3H)-pyrimidinedione] reacted with morpholine and formaldehyde to give 1-(morpholinomethyl)uracil. Despite the close resemblance to uracil, dihydrouracil did not react in the Mannich reaction.

In this work, alkylnitramines were prepared by the procedure of Curry and Mason (5). The attempted condensations of alkylnitramines with formaldehyde and secondary amines under reflux gave no desired products. However, the condensation succeeded when the reaction mixture was kept at 0° for 12 hr. It was found that dimethylamine and diethylamine did not undergo the Mannich condensation with *n*-butyl- and ethyl-nitramine. All attempts to form Mannich bases using methylnitramine were unsuccessful.

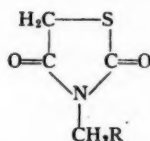
For the purpose of identification, the ultraviolet spectra of alkylnitramines and their derivatives were determined in absolute alcohol (DU Beckman spectrophotometer).

Compound	λ_{\max} , m μ	ϵ_{\max}
Methylnitramine	230	14010
Ethylnitramine	227-232	28230
<i>n</i> -Butylnitramine	231-233	9727
N-(Morpholinomethyl)-ethylnitramine	232	6603
N-(Morpholinomethyl)- <i>n</i> -butylnitramine	234	2931

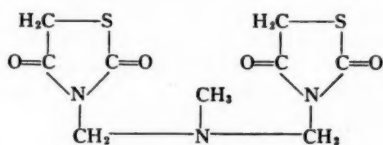
Although the observed values of λ_{\max} are in agreement with the reported absorption spectra (10), the values of the molecular extinction coefficients are considerably higher than those given for methyl- and *n*-butyl-nitramine.



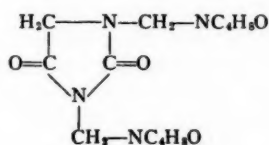
I: R = NC₄H₉O
 II: R = NC₃H₇O
 III: R = N(CH₃)₂



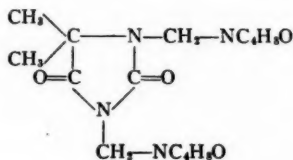
IV: R = NC₃H₇O
 V: R = NC₄H₉O
 VI: R = N(CH₃)₂



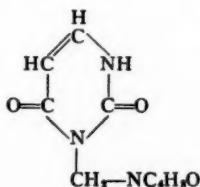
VII



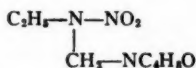
VIII



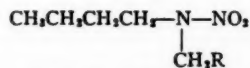
IX



X



XI



XII: R = NC₃H₇O
 XIII: R = NC₄H₉O

EXPERIMENTAL

1-(Morpholinomethyl)-2-pyrrolidone (I)

In a 50 ml. three-necked flask, a solution containing 2.55 gm. (0.03*M*) of 2-pyrrolidone in 20 ml. of water and 2.8 gm. (0.03*M*) of morpholine was placed. The mixture was stirred and 2.7 ml. (0.03*M*) of 35% formaldehyde was added slowly. The reaction mixture was refluxed at 100° for one hour. Upon cooling, the solution was extracted with chloroform and the extract was concentrated by distillation on a water bath. To this residue, 25 ml. of ethanol was added and the solution was concentrated by further distillation. After 12 hr., solid white crystals of I appeared which, after several crystallizations, melted at 68.5–69.5°. The total yield was 1.5 gm. (27.2%). The yield of I was increased to 2.1 gm. (37.8%) when the reaction time was extended to two hours.

Anal. Calc. for $C_6H_{10}N_2O_2$: N, 15.26%. Found: N, 15.12%.

1-(Piperidinomethyl)-2-pyrrolidone (II)

The compound II was prepared by refluxing the mixture of 2.55 gm. of 2-pyrrolidone, 2.7 ml. of 35% formaldehyde, 2.7 ml. of piperidine, and 20 ml. of water at 100° for one-half hour in the same manner as described for the above experiment. A precipitate was crystallized from ethanol and yielded 1.5 gm. (27.4%) of white crystals which melted at 47.5–49°.

Anal. Calc. for $C_{10}H_{16}N_2O$: N, 15.37%. Found: N, 15.25%.

1-(Dimethylaminomethyl)-2-pyrrolidone (III)

The reaction mixture of equimolar amounts (0.03*M*) of 2-pyrrolidone, 35% formaldehyde, dimethylamine hydrochloride, and 20 ml. of water was heated at 68° for one-half hour with constant stirring. The solution was cooled, made alkaline with 20% solution of potassium carbonate, and extracted with chloroform. The extract was evaporated and fractionally distilled to yield 1.5 gm. (37.4%) of a liquid product (III), b.p. 64–67° at 1 mm. pressure.

Anal. Calc. for $C_7H_{14}N_2O$: N, 19.7%. Found: N, 19.72%.

3-(Piperidinomethyl)-2,4-thiazolidinedione (IV)

To the solution of 3.5 gm. of 2,4-thiazolidinedione in 15 ml. of ethanol, an equimolar amount of formaldehyde and piperidine was added at 0°. In short time, crystals of IV appeared. After crystallization from absolute ethanol 6.17 gm. (95.9%) of white crystals, m.p. 76–77°, was obtained.

Anal. Calc. for $C_9H_{14}N_2O_2S$: C, 50.44; H, 6.58; N, 13.02%.

Found: C, 50.69; H, 6.55; N, 13.04%.

3-(Morpholinomethyl)-2,4-thiazolidinedione (V)

This substance was formed with great ease by the interaction of 2,4-thiazolidinedione, formaldehyde, and morpholine and was obtained as white crystals, m.p. 147°, in 99.9% yield.

Anal. Calc. for $C_8H_{12}N_2O_3S$: N, 12.95%. Found: 13.05%.

3-(Dimethylaminomethyl)-2,4-thiazolidinedione (VI)

The condensation product VI was obtained by a similar procedure in a yield

of 71.5%. It gave white crystals which after crystallization from absolute alcohol melted at 82°.

Anal. Calc. for $C_8H_{10}N_2O_2S$: C, 41.36; H, 5.79; N, 16.08%.

Found: C, 41.60; H, 5.92; N, 16.05%.

N-Methyl-N,N-bis(2,4-thiazolidinedionomethyl)amine (VII)

A mixture of 3.5 gm. of 2,4-thiazolidinedione dissolved in 15 ml. of ethanol and 2.7 ml. of 35% formaldehyde was cooled to 0° and 4.85 ml. of 25% methylamine solution was added dropwise. The reaction product was crystallized from absolute ethanol to yield 4.34 gm. (50%) of soft white crystals, m.p. 144–145°.

Anal. Calc. for $C_9H_{11}N_3O_4S_2$: N, 14.52%. Found: N, 14.59%.

The above experiment was repeated using a 2:2:1 mole ratio of 2,4-thiazolidinedione, formaldehyde, and methylamine respectively. The yield was increased to 7.1 gm. (83%).

1,3-Di(morpholinomethyl)hydantoin (VIII)

To the heated solution of 3 gm. (0.03M) of hydantoin in 20 ml. of water, 5.6 ml. of morpholine was added and 5.4 ml. of 35% formaldehyde was introduced dropwise. The mixture was stirred and heated at 85° for 15 min. The reaction product was extracted from the cold solution with chloroform. After recrystallization from ethanol VIII yielded 2 gm. (22%) of white crystals, m.p. 144–145.5°.

Anal. Calc. for $C_{13}H_{22}N_4O_4$: N, 18.84%. Found: 18.76%.

Acid Hydrolysis of VIII

Dry hydrogen chloride gas was bubbled through the solution of 0.3 gm. of VIII in 25 ml. of absolute ethanol. A white precipitate of hydantoin, m.p. 218°, separated (lit. m.p. 220°).

1,3-Di(morpholinomethyl)-5,5-dimethylhydantoin (IX)

The condensation of 5,5-dimethylhydantoin with morpholine and formaldehyde in molar ratio 1:2:2 respectively, was carried out at 90° for 30 min. The product was recrystallized from ethanol to yield 3.9 gm. (39.8%) of white crystals, m.p. 134–134.5°.

Anal. Calc. for $C_{18}H_{26}N_4O_4$: N, 17.1%. Found: N, 17.02%.

1-(Morpholinomethyl)uracil (X)

Uracil (3.4 gm.) dissolved in 40 ml. of water and morpholine (2.8 ml.) were cooled to 0° and 2.7 ml. of 35% formaldehyde was slowly added. A precipitate was formed which after crystallization from alcohol yielded 2.16 gm. (56%) of white crystals, m.p. 208–209°.

Anal. Calc. for $C_9H_{13}N_3O_2$: N, 19.89. Found: N, 19.92%.

N-(Morpholinomethyl)ethylnitramine (XI)

The reaction mixture of ethylnitramine, morpholine, and formaldehyde in molar ratio 1:1:1 respectively, was allowed to stand for 12 hr. at 4°. The product XI was crystallized from petroleum ether (b.p. 65–110°). The yield

of white plates, m.p. 86–87°, of XI was 92%.

Anal. Calc. for $C_7H_{16}N_3O_3$: C, 44.43; H, 7.99; N, 22.2%.

Found: C, 44.61; H, 8.0; N, 21.97%.

N-(Piperidinomethyl)-*n*-butylnitramine (XII)

A solution of 7.1 gm. of *n*-butylnitramine in 20 ml. of alcohol was cooled to 0° and 5.4 ml. of 35% formaldehyde was added dropwise. To this mixture, 5.4 ml. of piperidine was slowly introduced and the flask was kept at 0° for 12 hr. The alcohol was evaporated and the residue fractionally distilled. The total yield of XII was 4.6 gm. (35.7%; b.p. 97–100°) at 1 mm.

Anal. Calc. for $C_{10}H_{21}N_3O_2$: C, 55.78; H, 9.83; N, 19.52%. Found: C, 55.34; H, 10.08; N, 18.79%.

N-(Morpholinomethyl)-*n*-butylnitramine (XIII)

The substance XIII was prepared by the method described as above, with the exception that the reaction product was crystalline and it separated from the solution. It was crystallized from petroleum ether (b.p. 30–60°) and obtained as white crystals, m.p. 53–53.5°, in 97.6% yield.

Anal. Calc. for $C_9H_{19}N_3O_3$: N, 19.34%. Found: N, 19.62%.

REFERENCES

1. BACHMAN, G. B. and HEISEY, L. V. J. Am. Chem. Soc. 68: 2496. 1946.
2. BAKER, B. R., QUERRY, M. V., KADISH, A. F., and WILLIAMS, J. H. J. Org. Chem. 17: 35. 1952.
3. BUTENANDT, A. and HELLMANN, H. Z. physiol. Chem. 284: 168. 1949.
4. CLAEISSON, P. Ber. 10: 1346. 1877.
5. CURRY, H. M. and MASON, J. P. J. Am. Chem. Soc. 73: 5041, 5043. 1951.
6. FELDMAN, J. R. and WAGNER, E. C. J. Org. Chem. 7: 31. 1942.
7. FRANCHIMONT, M. A. P. N. Rec. trav. chim. 29: 296. 1910.
8. HELLMANN, H. and LÖSCHMANN, I. Chem. Ber. 87: 1684, 1690. 1954.
9. HUTTEL, R. and JOCHUM, P. Ber. 85: 820. 1952.
10. JONES, R. N. and THORN, G. D. Can. J. Research, B, 27: 828. 1949.
11. LIEBERMAN, S. V. and WAGNER, E. C. J. Org. Chem. 14: 1001. 1949.
12. MOORE, M. B. and RAPALA, R. T. J. Am. Chem. Soc. 68: 1657. 1946.
13. WEAVER, W. I., SIMONS, J. K., and BALDWIN, W. E. J. Am. Chem. Soc. 66: 222. 1944.
14. WHEELER, H. L. and BARNES, B. Am. Chem. J. 24: 60. 1900.

DISINTEGRATION-RATE DETERMINATION BY 4π -COUNTING

PART II. SOURCE-MOUNT ABSORPTION CORRECTION¹

BY B. D. PATE² AND L. YAFFE

ABSTRACT

The various methods in use for determining the correction for absorption due to the source mount used in a 4π -counter are discussed, and experiments conducted to test the validity of the correction, arising from these methods, for β emitters of varying end-point energies. The methods all give erroneous corrections for low energy β emitters and possible reasons for the errors introduced by the 'sandwich method' are discussed. An 'absorption curve' type method is proposed which is shown to give more accurate correction factors.

A. INTRODUCTION

In a previous publication (8), we have discussed the principles of 4π -counting and described the design of counting chamber used in this laboratory. We also discussed the errors to which the final disintegration-rate value is subject and the conditions under which the first of these—departure from unit counter response probability—is minimized. In the present paper, we shall discuss corrections for the second of the sources of error, namely absorption of radiation in the mounting film on which the source is deposited.

For determinations involving nuclides emitting monoenergetic radiation, such as α radiation and conversion electrons, of such an energy that the range of the particle in the source-mount material is greater than its path length in the film used, no source-mount absorption correction is necessary. As long as a sufficient number of ion pairs are produced by the ionizing particle to trigger the counting circuit, each disintegration will be recorded. The majority of determinations for which a 4π proportional counter will be employed, however, involve β radiation with a continuous distribution of particle energies; in this case a fraction of the emitted particles will always be absorbed by the film, the fraction being larger the smaller the end point of the beta spectrum.

We have already (7) described techniques developed in this laboratory for the production of films, for use in 4π -counters, of a superficial density of 5–10 $\mu\text{gm./cm}^2$. For disintegration-rate determinations of moderate precision with β radiation of moderate or high energy, the use of films of this thickness allows absorption of radiation in the source mount to be neglected. For work of the greatest precision, however, and particularly that with the weaker β emitters, the absorption loss must be accurately evaluated and a correction made. The use of very thin films is nevertheless still of considerable advantage, since the magnitude of the correction is reduced, and the final disintegration-rate value less sensitive to errors in the correction.

¹Manuscript received January 17, 1965.

Contribution from the Radiochemistry Laboratory, Department of Chemistry, McGill University, Montreal, Quebec, with financial assistance from the National Research Council of Canada and Atomic Energy of Canada Ltd.

²Holder of a National Research Council Studentship.

Three methods of determining the absorption correction have been described in the literature: the so-called "sandwich" procedure, calculation from 2π and 4π counting rates, and the use of absorption curves.

(i) The "sandwich" procedure has been described by Hawkins *et al.* (3). The counting rate given by a source mounted on a known thickness of mounting film is determined, and then a second determination made with an identical film superimposed over the first so as to sandwich the source. The observed reduction of counting rate was applied as a correction to the single film value to arrive at the source disintegration rate, and the validity of this procedure was taken to be apparent "from a consideration of the contribution to the counting rate from each hemisphere". However, Smith (11) found that applying the sandwich procedure to similar sources of, for instance, S^{35} using sets of films of differing superficial density lead to results for the disintegration rate differing by as much as seven per cent. The results should of course be independent of the thickness of films used.

(ii) Seliger and co-workers (5, 9) have attempted to develop mathematical relationships which would allow calculation of the source disintegration rate from measured 2π - and 4π -, single and sandwiched film counting rates. The resulting formulae as quoted in the second and more rigorous of the two papers (5) were:

$$(a) \quad (N_t - N_b)/(N_T - N_b) = 2\beta_f + \tau \approx \tau$$

where N_t and N_b are the counting rates observed in the top and bottom half-counters respectively, N_T is the counting rate observed from both halves combined, β_f is the fractional back-scattering factor, and τ the fractional absorption factor for the film used as source mount.

$$(b) \quad (N_T - N_s)/(2N_T - N_s) = \tau/2$$

where N_s is the counting rate obtained with the source sandwiched between two similar films. The value of τ obtained from these equations was then to be substituted into

$$N_0 = N_T/(1 - \tau/2)$$

to obtain N_0 , the true disintegration rate of a source where no self-absorption corrections have to be made.

As is common with calculations of this sort (11), the combination of a continuous distribution of beta energies with energy-dependent scattering and absorption coefficients and a complex geometrical arrangement make the problem analytically very difficult without the adoption of several simplifications. For example: Among those employed by Seliger *et al.* were the supposition that the absorption and scattering characteristics of β radiation were unaffected by the scattering process (e.g. degradation of the energy spectrum was neglected) and, in several places in the derivation, the assumption that β_f and τ were small compared to unity.

The latter may be true in the region of beta energies and film thicknesses where the absorption correction is in any case insignificant, but with lower beta energies where an accurate correction is required, both coefficients are

by no means negligible, and vary rapidly with changing beta energy. In particular, the back-scattering effect observed in a 4π geometry is found to be considerably larger than in conventional counter systems. The 4π -counter will respond to particles having undergone scattering at low angles to the source mount, and low angle scattering is evidently important even with thin films made from a material of low average atomic number. Using a 4π -counter, Meyer-Schützmeister and Vincent (6) have reported an 8% back-scattering for S^{35} β particles from 30–40 $\mu\text{gm./cm.}^2$ cellulose films, Houtermans *et al.* (4) reported similar results for P^{32} , and Borkowski (1) found 5% back-scattering of Na^{24} β radiation from 50 $\mu\text{gm./cm.}^2$ of Formvar.

Thus the over-all 2% accuracy claimed by Mann and Seliger (5) for their absorption correction is probably over-rated when one is using β emitters of low energy (e.g. Ni^{63} , C^{14} , S^{35} , etc.).

(iii) The 'absorption curve method' used to correct the results obtained from end-window counters for the absorption of radiation suggests itself as a corrective technique applicable to this case. A procedure of this sort was used by the workers at Göttingen (4, 6). They made a series of counting-rate measurements with a source mounted on a film, and with increasing thicknesses of aluminum foil placed *over* the source, and used the curves obtained to correct the original counting rate. However, such a procedure would appear to be open to the same objections as the ordinary sandwich procedure.

A study of the variation of counting rate as a function of the actual mount thickness was first carried out by Smith (11). He commenced with a source mounted on aluminum of 260 $\mu\text{gm./cm.}^2$ and took measurements of the counting rates obtained with the source backed by increasing thicknesses of this material. The curve obtained on plotting the results was observed to be approximately linear, and Smith assumed that the value obtained by extrapolating back to zero mount thickness represented the source disintegration rate. However, this value was found to be low compared with the counting rate observed with a similar source mounted on 30 $\mu\text{gm./cm.}^2$ of cellulose acetate, by 3% in the case of S^{35} , and 1.5% in the case of Co^{60} . The discrepancy probably arose from a change of slope in the absorption curve below 260 $\mu\text{gm./cm.}^2$ superficial density, such as was observed by Suzor and Charpak in another connection (12). Provided sufficiently thin films and a suitable technique were used, this type of procedure would be expected to produce the most accurate means of correcting for mount absorption, the results being independent of any assumptions regarding counter mechanisms and so on. The anomalous back-scattering effects observed by Yaffe and Justus (13) and Glendenin and co-workers (2) would not be expected to cause any disturbing effects.

B. EXPERIMENTAL PROCEDURE AND RESULTS

For the following experiments, we have used the chamber and ancillary equipment described in the previous publication (8), operating under the conditions found to give unit response probability. We have performed two sets of experiments:

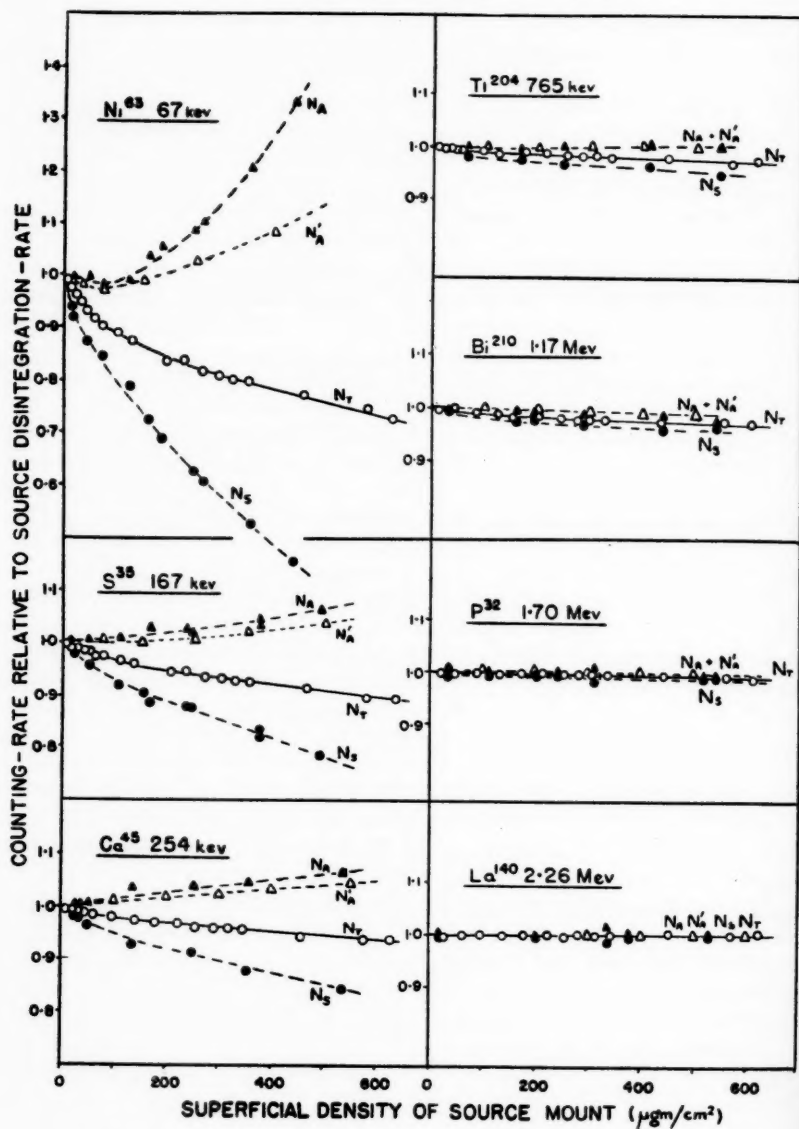


FIG. 1. Source-mount absorption characteristics for a series of beta emitters.

(i) *Single Film Source-mount Absorption Characteristics*

A series of counting-rate measurements was taken for each nuclide of the series of seven β emitters of increasing end-point energy, and four emitters of differing forms of radiation, whose nuclear characteristics were described earlier (8). For each of a series of increasing source-mount superficial densities, we have measured the total counter counting rate (N_T) with the anodes connected in parallel to the amplifying system. The source mounts used were of gold-coated VYNS film (7) mounted on a 1 mm. aluminum diaphragm of aperture 2.5 cm. in diameter. The thinnest films employed were of 5 to 10 $\mu\text{gm./cm.}^2$ superficial density, and increasing thickness was obtained:

(a) up to about 70 $\mu\text{gm./cm.}^2$ by allowing a series of films of known superficial density to adhere to the back of the initial mount;

(b) above 70 $\mu\text{gm./cm.}^2$ by temporarily placing in contact with the back surface of the mount, in position in the chamber, each of a series of standardized films of increasing superficial density.

The results of these experiments are shown plotted in Figs. 1 and 2. Data as shown are for "weight-less" sources. Experiments with Ni^{63} have shown that identical results are obtained even for source thicknesses where self-absorption of the order of 80 to 90% occurs.

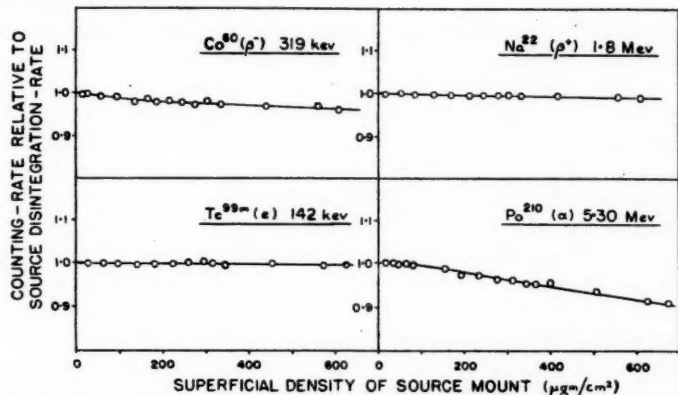


FIG. 2. Source-mount absorption characteristics for emitters of other forms of radiation.

(ii) *Sandwich Characteristics*

A second series of measurements was taken using the series of seven β emitters described above as shown in Fig. 1. In this case sources of each nuclide were prepared on a series of films of increasing superficial density and the following quantities measured: the total counting rate with the anodes in parallel with a single mount (N_T), and the total counting rate with a second identical sandwiching film added (N_S). From these values the expected disintegration rate of the sources used has been calculated by the procedure of Hawkins *et al.* (N_A) and by the more rigorous of the procedures of Seliger and co-workers (N_A'). The results are shown plotted as a function of source-mount

superficial density in Fig. 1, with the true source disintegration rates normalized to a common value for each nuclide using the curves for N_T obtained in the first series of experiments.

C. DISCUSSION

(a) The Sandwich Procedure

The results shown in Fig. 1 give a fairly complete picture of the accuracy of the sandwich procedure as a function of mount thickness and β end-point energy, whether applied by the method of Hawkins *et al.* (3) or by the NBS method (5, 9, 10), and are in accord with those found by Smith (11). Though the procedure may be said to work fairly well at higher particle energies, where the mount absorption is small in any case, at lower energies, where accurate information is desirable, it becomes progressively less and less useful. The fact that the calculation of the disintegration rate leads to results that vary considerably (for example in the case of Ni^{63}) with source mount thickness would indicate that the mathematical treatment was oversimplified.

(b) The Absorption Curve Procedure

The anomalous results obtained by this method by Smith (11) using mounts with a superficial density in excess of $260 \mu\text{gm./cm.}^2$ are readily understood on

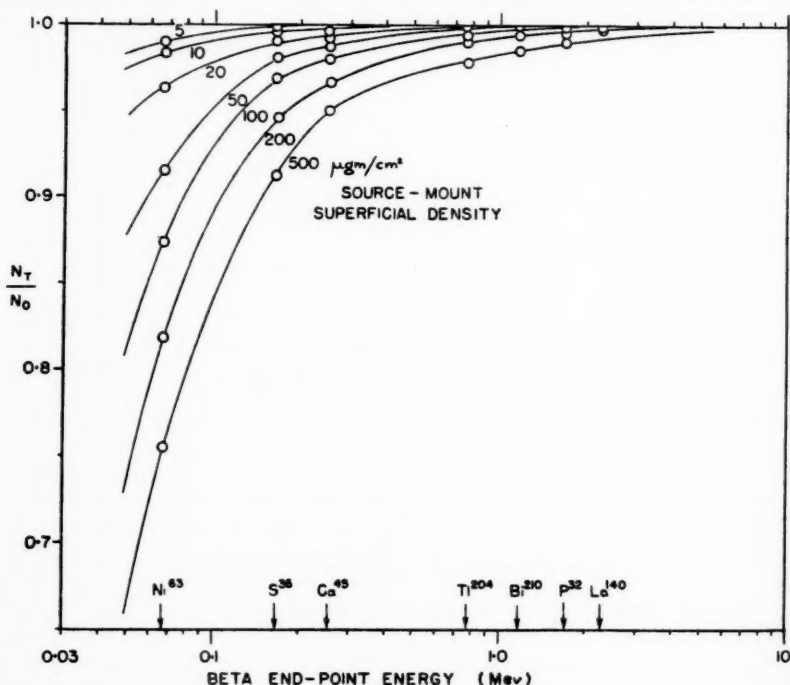


FIG. 3. Absorption parameter (N_T/N_0) as a function of beta end-point energy, for a series of film thicknesses.

a basis of the curves for N_T shown in Fig. 1. Extrapolation of the approximately linear portion of the curves obtained at higher mount thicknesses would take no account of the initial fall in counting rate, particularly pronounced at low β end-point energies, due to progressive absorption by the source mount of the softest radiation in the beta energy spectrum.

For work of moderate precision the data in Fig. 1 may be used directly to correct observed single-film results for source-mount absorption. In order to allow interpolation to intermediate β energies, the data are replotted in Fig. 3 with the absorption parameter (N_T/N_0) as a function of beta end-point energy for a series of film thicknesses. Clearly several approximations are introduced by use of the data in this way, including a neglect of variation in the form of the beta energy spectrum with nature of the beta transition (degree of forbiddenness etc.) and of the additional complication of nuclear gamma emission when this is present. Also, obviously the transition must be recognized as a beta transition and the end-point energy known.

For work of maximum precision, the procedure adopted to obtain our experimental results is recommended. In this case, the source material is mounted on the thinnest film available, and the counting rate N_T measured as a function of increasing mount thickness as outlined above. The disintegration rate is obtained by extrapolating to zero mount thickness.

The accuracy of the disintegration-rate value, arrived at in this way, can also be judged from Fig. 1. It is limited by the statistical deviation of the counting rates measured, and by the accuracy with which the superficial density values are known (7). No error of significance should be introduced by the technique of allowing additional films to adhere to the original mount, and we estimate that the error in the final disintegration-rate value can be reduced to about $\pm 0.2\%$ in the case of the weakest beta radiation studied, and probably to less than this at higher particle energies. We find this method satisfactory in routine use, the necessary measurements and manipulations taking very little more time than those required for the conventional sandwich procedure.

In the case of a beta emitter of unknown energy, once the disintegration rate is known from the absorption curve procedure, Fig. 3 may be used to derive from the observed value of N_T/N_0 a crude but nevertheless useful estimate of the end-point energy of the spectrum. This technique replaces those commonly used with end-window counters, which are inapplicable in a 4π steradian-geometry.

It is of interest to consider why the value of source disintegration rate predicted by the sandwich procedure should vary with increasing source-mount thickness, and in general differ (widely at low beta energies) from the figure unequivocally indicated by the absorption curve method. The reasons for variations in the separate counting rates of the hemispheres above and below the source mount, and in the rate of coincidences between the two half-counters, are various and will be discussed in the fourth paper of this series. However, the change in total counting rate (N_T) can only be due to increased absorption of radiation in the mounting film or reduction of particle energy to below that

required to trigger the counter. It has been shown in paper one of this series (8) that, under the adopted operating conditions, substantially all particles entering the counter gas produce the necessary minimum ionization and trigger the counter.

It is proposed to leave the quantitative analysis of the relative contribution of the various scattering and absorption processes to paper four of this series, in which a more complete set of data for the half-counter counting rates and coincidence rates observed with different forms and energy of radiation under different conditions will be presented.

One should, however, perhaps consider the data for N_T for Po^{210} shown in Fig. 2. Po^{210} is an α emitter of 5.30 Mev. energy which has a range of ~ 5.1 mgm./cm.² in air, and therefore using known atomic stopping powers one can compute the range in the film to be 4.9 mgm./cm.² Hence, with film superficial densities of up to at least 600 $\mu\text{gm.}/\text{cm.}^2$ no fall in N_T with increasing d might be expected, whereas an approximately linear decrease is observed. One observes in this case (α emission) that the rate of coincidences between the two half-counters is very small ($< 0.1\%$ of N_0) and that N_T is substantially the sum of the counting rates of the upper hemisphere (which is constant with increasing d) and of the lower hemisphere (which decreases linearly with increasing d). Thus, the observed effect is due solely to absorption of α particles in the film, which at the film thicknesses used should be small in view of the mono-energetic nature of the emission.

However, if the film thickness is again d and the range of the radiation in film material is R , as in Fig. 4, then of those α particles emitted in the 2π steradian angle towards the film, only those inside the cone of half-angle

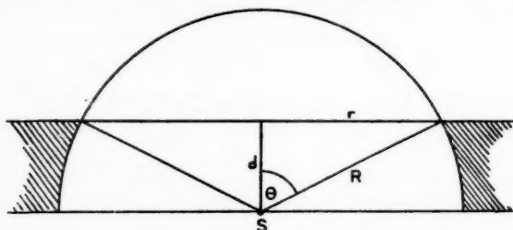


FIG. 4. Film absorption of α radiation (schematic).

subtended by the radius r will emerge into the gas volume and register. The proportion of the total radiation emitted outside this cone and totally absorbed in the film can be shown to be $(2\pi rd)/4\pi R^2$ for large values of θ

$$\begin{aligned} &= rd/2R^2 \\ &\approx d/2R \end{aligned}$$

in agreement with the observed linearity with d . In a film thickness corresponding to 600 $\mu\text{gm.}/\text{cm.}^2$, the loss by absorption is found to be 6.5% compared to an observed value of 7.5%. The agreement is fair considering the assumptions made regarding the range of Po^{210} α particles in the film material.

The absence of apparent decrease of N_T with d in the case of the (mono-energetic) conversion electrons from Tc^{99m} (Fig. 2) is presumably due to their longer range (26 mgm./cm.²) and the influence of back-scattering.

ACKNOWLEDGMENTS

The authors wish to thank the National Research Council of Canada and Atomic Energy of Canada Ltd. for grants-in-aid. We would also like to express our appreciation to Dr. R. E. Bell for valuable discussions. One of us (B. D. P.) wishes to thank N.R.C. for assistance in the form of a Studentship.

REFERENCES

1. BORKOWSKI, C. J. Conference on Absolute β Counting. Prelim. Rept. Nuclear Sci. Ser. N.R.C., Washington, D.C. No. 8: 55. 1950.
2. GLENDENIN, L. E. Conference on Absolute β Counting. Prelim. Rept. Nuclear Sci. Ser. N.R.C., Washington, D.C. No. 8: 20. 1950.
3. HAWKINGS, R. C., MERRITT, W. F., and CRAVEN, J. H. Proceedings of Symposium: Maintenance of Standards. Natl. Phys. Lab. May, 1951. H.M. Stationery Office, London. 1952.
4. HOUTERMANS, F. G., MEYER-SCHÜTZMEISTER, L., and VINCENT, D. H. Z. Physik, 134: 1. 1952.
5. MANN, W. B. and SELIGER, H. H. J. Research Natl. Bur. Standards, 50: 197. 1953.
6. MEYER-SCHÜTZMEISTER, L. and VINCENT, D. H. Z. Physik, 134: 9. 1952.
7. PATE, B. D. and YAFFE, L. Can. J. Chem. 33: 15. 1955.
8. PATE, B. D. and YAFFE, L. Can. J. Chem. 33: 610. 1955.
9. SELIGER, H. H. and CAVALLO, L. J. Research Natl. Bur. Standards, 47: 41. 1951.
10. SELIGER, H. H. and SCHWEBEL, A. Nucleonics, 12 (No. 7): 54. 1954.
11. SMITH, D. B. Brit. Atomic Energy Rept. A.E.R.E. I/R 1210. 1953.
12. SUZOR, F. and CHARPAK, G. Compt. rend. 234: 720. 1952.
13. YAFFE, L. and JUSTUS, K. M. J. Chem. Soc. Suppl. S. 341. 1949.

SIMULTANEOUS SURFACE EXCHANGE STUDIES USING BOTH CATION AND ANION¹

BY R. M. STOW² AND J. W. T. SPINKS

ABSTRACT

Labelled Sr^{++} and SO_4^{--} have been used simultaneously to measure the apparent surface area of a SrSO_4 precipitate by the direct radioactive method. The values found differ by about 90%. By contrast, when labelled Pb^{++} and SO_4^{--} are used to measure the apparent surface area of PbSO_4 , the values found are in close agreement. The results are discussed with reference to the kinetics of surface exchange reactions.

INTRODUCTION

The heterogeneous exchange between the ions on the surface of a solid and the ions in a solution has been widely used as the basis for the radioactive method for determining the "active" surface area of a solid. The method was introduced by Paneth and Vorwerk (4), and has been the subject of numerous investigations (for recent summaries, see (3, 8)). There appears to be a very rapid primary exchange, involving only the surface layer of the solid, followed by a much slower secondary exchange which may involve penetration of ions into the crystal. In the primary exchange, equilibrium is reached in a few minutes. According to Paneth, at equilibrium $N_s^1/N_s = N_L^1/N_L$ where N_s^1 = number of tracer atoms (or ions) on the surface, N_s = total number of this species of atoms (or ions) on the surface, N_L^1 = number of tracer atoms (or ions) in the bulk of the solution, and N_L = total number of this species of atoms (or ions) in the bulk of the solution. N_s is readily calculated knowing N_s^1 , N_L^1 , and N_L , and from this the surface area, $S = N_s l^2$, can be calculated. l^2 is the effective area of the tagged atom (or ion) on the surface and is given by $l^2 = (\text{M.W.}/aNd)^{2/3}$ where M.W. = the formula weight of the solid, a = number of gram atoms (or gram ions) of the tagged species of atoms per formula weight of solid, N = Avogadro's number, and d = density.

Using Paneth's method, tracers isotopic with either cation or anion of the precipitate should, on the basis of simple theory, yield the same surface area. However, Imre (1, 2) has suggested that surface exchange may not be quite so simple as Paneth suggests. He suggests rather that for the surface exchange equilibrium $(N_s^1/N_s)(N_L/N_L^1) = K$, where $K = K_0 e^{-E/RT}$ and is not necessarily unity. K_0 is a symmetry factor which is equal to unity for self-adsorption systems (e.g. Pb^{++} on PbSO_4). For self-adsorption, $K = e^{-E/RT}$, K being called the 'activation' factor and E the 'activation energy'. This terminology is perhaps unfortunate since it seems to imply that we are dealing with kinetics of exchange reactions whereas in fact we are dealing with measurements of exchange equilibrium. Imre states that different K values result for the exchange of Pb^{++} and CrO_4^{--} on PbCrO_4 but suggests that the K values will

¹Manuscript received January 10, 1955.

Contribution from the Department of Chemistry, University of Saskatchewan, Saskatoon, Saskatchewan, with financial assistance from the National Research Council of Canada.

²Died while a student in Cambridge, England, 1951.

be the same for the exchange of Pb^{++} and SO_4^{--} on PbSO_4 . The availability of S^{35} , Sr^{90} , and Pb^{212} has made it possible to test this hypothesis with precipitates of SrSO_4 (7) and PbSO_4 . In some experiments surface exchange was carried out with either cation or anion labelled; in other experiments, both cation and anion were labelled in the same experiment.

EXPERIMENTAL

Radioactive Materials

S^{35} was obtained from Chalk River in the form of an aqueous solution of sulphuric acid. Tests showed that all the S^{35} was in the form of SO_4^{--} and that the half life and absorption half thickness were in agreement with published values (6). Sr^{90} , obtained from Chalk River as SrCO_3 , was converted to the acetate to form a stock solution (5). Immediately prior to a surface exchange experiment, the Y^{90} daughter was separated from the Sr^{90} by adding yttrium holdback carrier and precipitating Sr as the sulphate. The precipitated SrSO_4 was washed with a small amount of saturated SrSO_4 solution.

Pb^{212} was obtained from the emanation from thorium hydroxide (5). No attempt was made to remove the 60.5-min. half life daughter, Bi^{212} .

Strontium Sulphate

The strontium sulphate used was that prepared in 1946 by Singleton (5) and kept in contact with strontium sulphate solution since that time.

Lead Sulphate, Suspension S (Precipitate Prepared Using Excess Sulphate)

The first precipitate was prepared using 5% excess sulphate. A solution of 250 gm. reagent grade lead nitrate in 650 ml. distilled water was added with stirring to 300 ml. of a sulphuric acid solution. The addition took place over a period of one hour. When the addition was complete, a test of the filtrate showed it to contain excess sulphate ion. The precipitate was washed, with accompanying stirring, with 15 1-liter portions of distilled water over a period of one month.

Lead Sulphate, Suspension L (Precipitate Prepared Using Excess Lead)

This precipitate was prepared in a manner similar to that described for Suspension S except that the chemicals were added in the reverse order, and a 5% excess of lead, instead of sulphate, was used. A test of the filtrate, after the mixing of the chemicals, showed an excess of lead ion.

The washing scheme for this precipitate was identical to that for Suspension S.

Saturated Solutions of the Precipitates in Water

The individual washings of a precipitate were accomplished by agitating the precipitate for 24 hr., with 1-liter portions of distilled water, by means of an electrically driven stirrer. When the last agitation of a precipitate in any particular set of washings had been completed, the suspension was allowed to settle and some of the solution decanted, filtered, and saved. The solution

³The more convenient Sr^{89} was not readily available at that time (1949-50).

obtained was thus a saturated solution of the precipitate compound in water at room temperature, as given by the precipitate at that stage of washing.

Solutions Containing Sr^{90}

A small amount of highly active strontium sulphate precipitate, freed from yttrium, was stirred with a quantity of saturated inactive strontium sulphate solution. As exchange between the precipitate and solution occurred, activity entered the solution. After approximately one hour, when the solution had attained a sufficient degree of activity,⁴ the mixture was allowed to settle and the solution decanted and filtered. Solutions containing Sr^{90} were thus obtained without introducing additional strontium or foreign ions.

Solutions Containing $\text{S}^{35}\text{O}_4^-$

One-tenth of a milliliter of the stock solution of $\text{S}^{35}\text{O}_4^-$ obtained from Chalk River was diluted to 1 ml. with distilled water. To approximately 400 ml. of saturated inactive strontium or lead sulphate solution a sufficient quantity (0.15 ml.) of the diluted stock solution was added to give an activity of 80 counts per sec. per 5 ml.

Solutions Containing ThB

After the platinum foil in the emanation apparatus had been collecting activity for two days, the foil was removed and rinsed in a quantity of saturated inactive lead sulphate solution. After 15 min. the platinum foil was removed and the solution was ready for use.

Measurement of Radioactivity

Counting equipment consisted of an Atomic Instrument Company Scale of 64 scaler and an end-window Geiger tube. The usual corrections for resolving time and background were made. Backscattering corrections were avoided by always using identical 1 ml. Pt dishes, diameter 2.2 cm., for counting. Statistical counting errors were reduced to about 1% by recording 10,000 counts. Self-absorption corrections were eliminated by preparing all samples containing a given radionuclide in such a way that they contained the same weight of absorbing agent. Thus, samples from experiments with the strontium sulphate precipitate were all counted with the residue left upon evaporation of 5 ml. of saturated strontium sulphate solution. This residue weighs approximately 0.62 mgm., equivalent to 0.2 mgm. per sq. cm. when evaporated on dishes of 2.2 cm. diameter. Similarly, samples from experiments with the lead sulphate precipitates have been counted with the residue, weighing approximately 0.20 mgm., from 5 ml. of saturated lead sulphate solution.

Miscellaneous Equipment

A mechanical shaker was used to keep samples agitated during the absorption experiments.

Thirty-milliliter glass stoppered flint glass bottles were used as shaking bottles, the same as in previous experiments (5).

Suspensions were stirred with an electrically driven stirrer.

⁴Radioactivity.

Experimental Procedure

The procedure was essentially the same as that used in the previous work on strontium sulphate (5, 6). After the precipitate suspension had been agitated by a mechanical stirrer for at least five minutes, an aliquot of the suspension, usually 5 ml., was withdrawn by pipette and placed in a shaking bottle. An aliquot, usually 15 ml., of the appropriate active solution was then pipetted into the bottle and shaking on the mechanical stirrer was begun immediately. The temperature was room temperature, approximately 20°C. Shaking time was measured from the time the solution had completely drained into the shaking bottle. When shaking was complete the bottle was removed and centrifuged for approximately one minute. Five milliliters of the supernatant liquid was then withdrawn by pipette and evaporated in successive portions in a 1-ml. platinum dish on a semimicro water bath.

The radioactivity of the sample in the Pt dish was then measured under an end-window Geiger tube.

It is necessary to know the starting activity of the active solution before admixture with the precipitate, as well as the activity after mixing, if the amount adsorbed by the precipitate in an exchange experiment is to be obtained by difference. The procedure used in measuring the starting activity of an aliquot of active solution was such that the starting activity samples went through all experimental operations except the actual addition of the precipitate. The effects of adsorption, if any, of tracer ions on equipment were thus made to cancel out. The starting activity samples were made by transferring an aliquot of inactive solution to a shaking bottle and adding the same volume of active solution as used in the exchange experiment. The solution was shaken for a time, then a portion was withdrawn and evaporated on a sample dish. The aliquot of inactive solution to which active solution was added was equal in volume to the volume occupied by liquid in an aliquot of the precipitate suspension. For example, the volume occupied by liquid in a 5 ml. aliquot of strontium sulphate suspension was $(5 - 0.24) = 4.76$ ml., the volume of the solid precipitate being 0.24 ml.

The amount of precipitate suspension and the amount of active solution used in each experiment were so chosen that roughly 50% adsorption or exchange of activity would occur. At 50% adsorption the accuracy of the experiment is at a maximum.

The weight of precipitate in an aliquot of suspension was determined by transferring a number of aliquots to a Gooch filter crucible, filtering, drying in an oven (105°C.) overnight, and weighing.

Corrections for the Growth of Y^{90} from Sr^{90}

The sample was measured first without an absorbing screen and then with an absorbing screen of thickness 231 mgm./sq. cm. between it and the Geiger tube. This reduced the Sr^{90} count to less than 0.2% but transmitted 39% of the Y^{90} count. Multiplying the second count by 100/39 and subtracting this from the first count gave the count due to Sr^{90} .

Counting of S^{35} in the Presence of Sr^{90} Plus Y^{90}

By counting the sample through a screen of 17.4 mgm./sq. cm. thickness all the S^{35} radiations were cut out. Combining this count with a knowledge of the fraction of the Sr-Y radiations transmitted by this screen and a measurement of the amount transmitted by a 231 mgm./sq. cm. screen allowed the calculation of both S^{35} and Sr^{90} activities in a given sample.

Counting of S^{35} in the Presence of ThB

The ThB was measured by counting the sample behind a 17.4 mgm./sq. cm. screen which absorbed the S^{35} radiations. The S^{35} was measured six days later when all the ThB had decayed.

Method of Calculation

The starting activity and the activity of the exchange samples belonging to a particular set of experiments were first corrected for background. They were then brought to the same basis by taking into account any dilution that had occurred as a result of the experimental procedure.

When dealing with Sr^{90} the next step in the calculations was the correction for growth of daughter activity.

After applying these corrections the quantity of activity adsorbed by the precipitate was obtained by difference. Substitution was then made in the ratio on the left side of the fundamental equation:

$$\frac{\text{No. tracer anions or cations in soln.}}{\text{No. tracer anions or cations in surf.}} = \frac{\text{No. of anions or cations in soln.}}{\text{No. of anions or cations in surf.}}$$

The quantity "number of anions or cations in solution" is calculated from the solubility of the precipitate in water. For strontium sulphate, formula weight 183.7 and solubility in water 0.1233 gm. per liter (7), the number of strontium or sulphate ions per milliliter of saturated solution is

$$0.1233 \times 6.02 \times 10^{23} / 1000 \times 183.7 = 4.04 \times 10^{17} \text{ ions per ml.}$$

For lead sulphate, formula weight 303.3 and solubility in water 2.56×10^{-4} moles per liter at 20°C., the corresponding figure is 1.54×10^{17} ions per ml. Using the formula given in the Introduction, the area per molecule is, for strontium sulphate (density 3.96 gm. per ml.), $(183.7 / 3.96 \times 6.02 \times 10^{23})^{2/3} = 1.81 \times 10^{-16}$ sq. cm. The corresponding area for lead sulphate (density 6.2 gm. per ml.) is 1.88×10^{-16} sq. cm.

*Typical Calculations**(a) Exchange of Sr^{90} at the Surface of a Strontium Sulphate Precipitate*

Five milliliters of a suspension of strontium sulphate was added to 15 ml. of saturated strontium sulphate solution containing Sr^{90} . The mixture was shaken for 10 min. and then centrifuged. Five milliliters of the centrifugate was evaporated and counted. After correcting for yttrium, the activity was 23.65 registers/min. (1 reg. = 64 counts). Five milliliters of the original solution gave 52.9 reg./min. Thus, the percentage activity adsorbed or exchanged = $(1 - 23.65/52.9) \times 100 = 55.3\%$. The weight of $SrSO_4$ in the suspension was

1.1315 gm. and the total volume of solution was 19.76 ml. Thus, the number of ions in the surface per gram of precipitate equals

$$\frac{55.3}{44.7} \times \frac{19.76 \times 4.04 \times 10^{17}}{1.1315} = 8.55 \times 10^{18}.$$

The surface area per gram, corresponding to 8.55×10^{18} ions in the surface, is equal to $8.55 \times 10^{18} \times 1.81 \times 10^{-15} = 15,500$ sq. cm.

(b) *Combined Sr^{90} and $\text{S}^{35}\text{O}_4^-$ Experiment*

An experiment was conducted in which 5 ml. of a suspension of strontium sulphate were shaken with 15 ml. saturated strontium sulphate solution containing approximately equal activities of Sr^{90} and $\text{S}^{35}\text{O}_4^-$. Shaking time was 10 min. The results are recorded in Table I.

TABLE I
EXCHANGE EXPERIMENT USING BOTH S^{35} AND Sr^{90}

	Activity, registers/min., corrected for background	
	Starting activity sample	Exchange sample
1. No screen	61.7	33.4
2. 17.4 mgm./sq. cm. screen	20.1	9.56
3. 231 mgm./sq. cm. screen	0.53	0.50
4. Calculated Sr^{90} activity passing 231 mgm./sq. cm. screen	0.04	0.02
5. Y through 231 mgm./sq. cm. screen ((3) - (4))	0.49	0.48
6. Y, no screen ((5) . 100/39)	1.25	1.23
7. Y through 17.4 mgm./sq. cm. screen (0.95(6))	1.19	1.17
8. Sr^{90} through 17.4 mgm./sq. cm. screen ((2) - (7))	18.91	8.39
9. Sr^{90} , no screen ((6)/(0.56))	33.8	14.95
10. S^{35} , no screen ((1) - (9) - (6))	26.7	17.2

$$\% \text{ Sr adsorbed} = [(33.8 - 14.95)/33.8]100 = 55.8;$$

$$\% \text{ S}^{35} \text{ adsorbed} = [(26.7 - 17.2)/26.7]100 = 35.5.$$

These figures correspond to areas of 16,200 and 7050 sq. cm. per gram of precipitate, respectively.

RESULTS

SrSO_4

The effect of time of shaking on percentage adsorption of $\text{S}^{35}\text{O}_4^-$ on SrSO_4 is shown in Fig. 1, together with the corresponding figures for the exchange of Sr^{++} by the same precipitate (see Ref. (5)) in experiments done two years earlier. As before, there is a very rapid primary exchange followed by a much slower secondary exchange. The primary exchange is essentially complete in about ten minutes, and as a consequence this time of shaking has been rather arbitrarily chosen as the point at which to calculate surface area in most experiments.

Shaking time, 10 min.

(a) Using Sr^{90} only, average area per gm. = 15,000 sq. cm. (cf. Singleton, 12,800 sq. cm., in 1947).

(b) Using Sr^{90} and S^{35} simultaneously; based on Sr^{90} , area per gm. = 16,200 sq. cm.; based on $\text{S}^{35}\text{O}_4^-$, area per gm. = 7050 sq. cm.

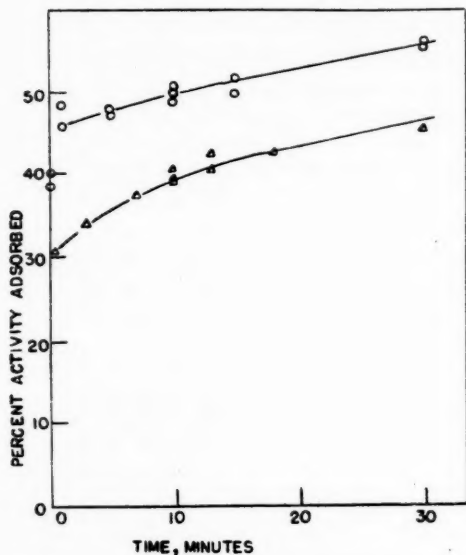


FIG. 1. Variation of percentage adsorption of ions on a strontium sulphate precipitate, with time of shaking; O, Sr^{90} (Singleton 1947), Δ , $\text{S}^{35}\text{O}_4^-$ (Stow 1949).

The precipitate was then washed with six 1-liter portions of distilled water and the exchange experiments repeated with the following results:

Based on $\text{S}^{35}\text{O}_4^-$, average area per gm. = 7830 sq. cm.

Based on Sr^{90} , average area per gm. = 14,400 sq. cm.

Washing the precipitate thus had very little effect on the apparent surface area.

Celestine

A single, well-formed crystal of celestine⁵ was reduced to a fine powder using an agate mortar and pestle. The powder was washed by stirring with 10 successive 300-ml. portions of water over a period of 40 hr. and then used in exchange experiments with labelled Sr^{++} and SO_4^- . Shaking 8.5 gm. powdered celestine with 8.5 ml. saturated SrSO_4 solution for 20 min. resulted in 65.5% adsorption of SO_4^- and 75% adsorption of Sr^{++} . The relative surface areas as measured by Sr^{++} and SO_4^- were thus in the ratio $(75/25)(34.5/65.5) = 1.58$ (cf. 1.9 for SrSO_4 prepared in the laboratory). The surface area per gram as measured by Sr^{++} was 2140 sq. cm.

PbSO₄; Suspensions S and L

Results for time of shaking experiments with PbSO_4 suspensions are recorded in Figs. 2 and 3.

In four of the experiments both SO_4^- and Pb^{++} were labelled; in the remainder, one ion only was labelled. For Suspension S the percentage adsorptions of SO_4^- and Pb^{++} were not significantly different and the difference was only

⁵Obtained from Ward's Natural Science Establishment.

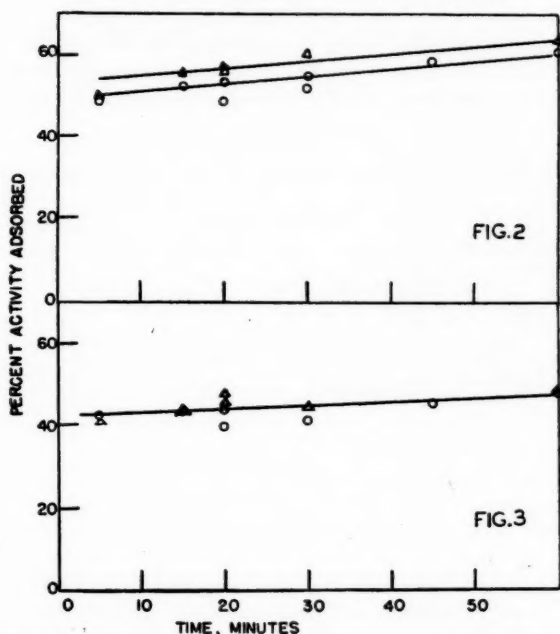


FIG. 2. Variation of percentage adsorption of ions on a lead sulphate precipitate, Suspension L, with time of shaking; O, ThB; Δ , $S^{35}O_4^-$.

FIG. 3. Variation of percentage adsorption of ions on a lead sulphate precipitate, Suspension S, with time of shaking; O, ThB; Δ , $S^{35}O_4^-$.

slight for Suspension L. The mean surfaces per gram of precipitate (20 min. shaking) are 2160 and 3650 sq. cm. for S and L, respectively.

The precipitate was then washed with six 1-liter portions of distilled water and the exchange experiment repeated. Again the percentage adsorptions for a given suspension were not significantly changed by the washing for either ThB or $S^{35}O_4^-$. Thus washing the precipitate had little effect on the surface area.

DISCUSSION

The foregoing experiments, in which two labelled ions have been used simultaneously to measure the degree of exchange at a surface consisting of the two ions, indicate that the degree of exchange is not necessarily the same for the two ions. The statistical mechanical approach of Imre has indicated that factors other than those considered by Paneth may sometimes be involved. It is of particular interest that his prediction that the degrees of exchange for Pb^{++} and SO_4^{--} on $PbSO_4$ would be the same is borne out by the present experiments. It is also of some interest that the degrees of exchange for Sr^{++} and SO_4^{--} on $SrSO_4$ differ markedly from one another, both for artificially prepared $SrSO_4$ and for the naturally occurring celestine. While altogether too few experiments have been done to warrant any speculation concerning the origin of the differ-

ence, it might possibly be due to differing hydration energies of the Sr^{++} and SO_4^{--} ions. However the present experiments do indicate that this method, and possible extensions of it, does provide a powerful tool for investigating the behavior of ions at surfaces. Further experiments have been planned.

ACKNOWLEDGMENT

We are grateful to the National Research Council of Canada for financial aid.

REFERENCES

1. IMRE, L. *Kolloid-Z.* 99: 147. 1942.
2. IMRE, L. *Kolloid-Z.* 106: 39. 1944.
3. PANETH, F. A. *J. chim. phys.* 45: 205. 1948.
4. PANETH, F. A. and VORWERK, W. *Z. physik. Chem.* 101: 445. 1922.
5. SINGLETON, R. H. and SPINKS, J. W. T. *Can. J. Research, B*, 27: 238. 1949.
6. STOW, R. M. Thesis, University of Saskatchewan, Saskatoon, Sask. 1950.
7. STOW, R. M. and SPINKS, J. W. T. *J. Chem. Phys.* 17: 744. 1949.
8. WAHL, A. C. and BONNER, N. A. *Radioactivity applied to chemistry*. John Wiley & Sons, Inc., New York. 1951.

INTERFACIAL POTENTIALS¹

By J. T. DAVIES AND SIR ERIC RIDEAL

ABSTRACT

A new relation between interfacial distribution potentials and interfacial surface (contact) potentials is presented. By a suitable choice of experimental system either distribution potentials or surface potentials may be measured separately; results are in good agreement with theory. Surface potentials are shown to be made up of several independent components. The rates of decay of surface potentials are also discussed.

The origin of interfacial potentials between oil and water, important as biological analogies, has long been a matter of some controversy. Many of the early experiments were conducted with salicylaldehyde or *o*-toluidine as the oil phase, and the potential differences measured when different organic salts were added changed slowly with time during the experiments. Beutner (4, 5) believed that the potential differences arise from the free charge at the interface due to an unequal distribution of the various cations and anions across the interface. The distribution potential difference caused by this process may be termed after Lange the ψ or outer potential. Baur (3) on the other hand believed the changes were due to selective ionic adsorption at the oil-water interface. Such surface or interfacial potentials may be represented by ΔV or by $\delta\chi$ in Lange's nomenclature.

After much controversy Baur accepted Beutner's explanation as to their origin. Some years later Dean, Gatty, and Rideal (15) showed theoretically that if one or more types of ions can dissolve in both oil and water no *stable* interfacial potential ΔV can be measured.

Whether the older potential differences were distribution or surface potentials has been summed up by Adam (1):

"It seems quite likely, however, that both (Beutner and Baur) were right, according to circumstances; although the final potential when thermodynamic equilibrium is attained is not an adsorption potential, the establishment of this equilibrium probably takes a very long time".

Indeed, since the paper of Dean, Gatty, and Rideal (15), it has become clear that the time for decay of the surface potential ΔV determines whether we measure $\Delta\psi$ or ΔV when different organic salts are added. In this paper we shall estimate such times, and confirm that with polar oils at equilibrium only $\Delta\psi$ is measured. Although ψ may take a considerable time to reach equilibrium, owing to the slow diffusion of the salts, and although a diffusion potential (6) may also be measured while this occurs, the surface potential ΔV must decay to zero extremely rapidly in the systems of Beutner and Baur.

Further, by a suitable choice of oils, it has now become possible to measure potential changes ascribable wholly to ψ or to V .

¹Manuscript received February 7, 1955.

Contribution from Department of Physical Chemistry, University of London, King's College, London, England.

(a) DISTRIBUTION POTENTIALS

According to Nernst's theory of distribution potentials, these are measured when the salt has an appreciable solubility in the oil and they arise from the different solubilities of the positive and negative ions in the two phases. We can express this in the following manner:

$$B_+ = \exp[(\mu_+^0 - \mu_+^o)/RT] \text{ or } RT \ln B_+ = \mu_+^0 - \mu_+^o,$$

$$B_- = \exp[(\mu_-^0 - \mu_-^o)/RT] \text{ or } RT \ln B_- = \mu_-^0 - \mu_-^o,$$

where B_{\pm} refers to the ionic distribution coefficients, and μ^0 the standard chemical potential. Subscripts o and w refer to the oil and water phases respectively.

These different solubilities of the two ions cause a potential between the two phases, as shown in Fig. 1.

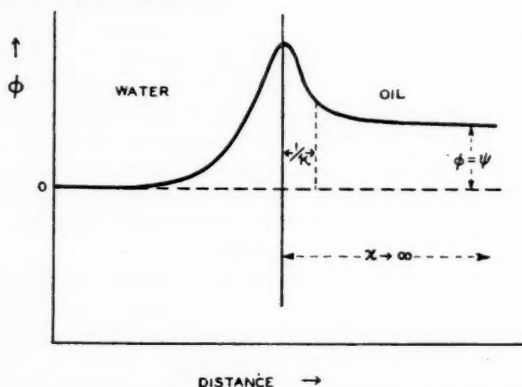


FIG. 1. Variation of ϕ (relative to the interior of the water phase) near an oil-water interface. The oil is assumed polar. The distance from the interface is represented by x , and measurements are made where $x \rightarrow \infty$ compared with the ionic double layer thickness $1/\kappa$.

The water phase is generally assigned zero potential, while the oil phase has a potential in Lange's notation ϕ (sometimes termed the inner or Galvani potential). If positive ions (e.g. tetramethylammonium) dissolve preferentially in the oil phase, while (say) chloride ions tend to remain in the water, ϕ is positive. The potential ϕ includes both ψ and V thus: $\phi = \psi + V$, or in Lange's notation, $\phi = \psi + \chi$.

We now relate ϕ to B_+ and B_- by means of their electrochemical potentials, $\bar{\mu}$. The Faraday unit is written F .

$$[1] \quad \bar{\mu}_+ = \mu_+^0 + RT \ln {}_w c_+$$

$$[2] \quad \bar{\mu}_+ = \mu_+^0 + RT \ln {}_o c_+ + \phi F$$

$$[3] \quad \bar{\mu}_- = \mu_-^0 + RT \ln {}_w c_-$$

$$[4] \quad \bar{\mu}_- = \mu_-^0 + RT \ln {}_o c_- - \phi F$$

At equilibrium:

$$[5] \quad {}_w\bar{\mu}_+ = {}_o\bar{\mu}_+$$

and

$$[6] \quad {}_w\bar{\mu}_- = {}_o\bar{\mu}_-$$

Further, each phase must be electrically neutral, therefore

$$[7] \quad {}_w c_+ = {}_w c_-$$

and

$$[8] \quad {}_o c_+ = {}_o c_-$$

By substitution of equations [1] to [4] into equations [5] and [6], we find:

$${}_w\mu_+^0 + RT \ln {}_w c_+ = {}_o\mu_+^0 + RT \ln {}_o c_+ + \phi F$$

and

$${}_w\mu_-^0 + RT \ln {}_w c_- = {}_o\mu_-^0 + RT \ln {}_o c_- - \phi F$$

If we subtract, remembering equations [7] and [8], we obtain:

$$({}_w\mu_+^0 - {}_o\mu_+^0) - ({}_w\mu_-^0 - {}_o\mu_-^0) = +2\phi F$$

or

$$RT \ln B_+ - RT \ln B_- = 2\phi F$$

or

$$[9] \quad \phi = \phi_{x=\infty} = (RT/2F) \ln(B_+/B_-)$$

Here $\phi_{x=\infty}$ is defined as in Fig. 1, ϕ being measured far from the interface when x is great compared with the Debye-Hückel term $1/\kappa$. Equation [9] is the required relation between ϕ , B_+ , and B_- . If B_+ is large compared with B_- , ϕ is positive.

It can easily be shown that if S is the ratio (conc. salt in oil)/(conc. salt in water),

$$[10] \quad S = (B_+ \cdot B_-)^{1/2}$$

Hence, from equations [9] and [10],

$$\phi = (RT/2F) \ln(S^2/B_-^2)$$

Although the absolute potentials ϕ are not measurable, we can determine differences in ϕ for (say) NaI and KI. Then B_- is constant, and

$$\Delta\phi = (RT/F) \ln(S_{\text{NaI}}/S_{\text{KI}})$$

Since ΔV should theoretically not contribute to $\Delta\phi$ in such systems (15), and since $\Delta\phi = \Delta\psi + \Delta V$, if x tends to infinity,

$$[11] \quad \Delta\phi = \Delta\psi = (RT/F) \ln(S_{\text{NaI}}/S_{\text{KI}})$$

Further, as we may see from inspection of equation [9], $\Delta\phi$ is independent of the common ion. Thus $\Delta\phi$ or $\Delta\psi$ is the same if chlorides are considered instead of iodides in equation [11], since

$$[12] \quad \Delta\phi = (RT/2F) \ln(B_{\text{Na}^+}/B_{\text{K}^+})$$

Karpfen and Randles (18) have recently set up the cell shown in Fig. 2. They found good agreement between theory, as given by equation [11], and experiment.

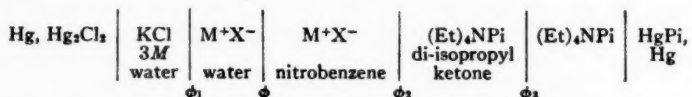


FIG. 2. Cell for measuring $\Delta\phi$ at interface of water and a polar oil such as nitrobenzene (18). Salt bridges are chosen so that when the salt MX is changed, the measured potential change is $\Delta\phi$, i.e. ϕ_1 , ϕ_2 , and ϕ_3 remain constant. In such an experiment $\Delta\phi$ is measured across thicknesses of solvent great compared with the thickness of the interfacial electrical double layers. Pi is picrate.

Results are shown in Table I, the distribution coefficients for simple salts in nitrobenzene having been found by Davies (7). The agreement is strong support for the validity of equation [11] if the oil is polar. Similar evidence in favor of equation [11] has recently been forthcoming from Göttingen, where Dr. Strehlow and his colleagues have been working along similar lines.

TABLE I

System (see Fig. 2)	$\Delta\phi$ calculated from distribution experiments (7), using equations [11] and [12]. Quoted from (18)	$\Delta\phi$ (observed) (18)
K ⁺ replaced by (Et) ₄ N ⁺	-124 mv.	-126 mv.
K ⁺ replaced by Na ⁺	-50 mv.	-53 mv.
Cl ⁻ replaced by I ⁻	+95 mv.	+102 mv.

(b) SURFACE POTENTIALS IN RELATION TO DISTRIBUTION POTENTIALS

If now an oil is chosen in which practically no salt can dissolve (e.g. a paraffinic oil such as decane), an ionic double layer cannot build up completely in the thickness of oil (e.g. 1 mm.) available. Hence equation [8] does not apply to measurements with this oil, although, since the system is by definition at equilibrium in that the free energy is minimal for this thickness of oil, equations [1] to [7] still hold.

Dividing the potential at the oil side of the interface into V (due either to a dipole array formed by spreading or by adsorption or to a charged film) and $\psi_{x=\infty}$ (see Fig. 3) we shall show that if the oil solubilities of the interfacial film and of the salt present are very small, only ΔV contributes to the measured change in ϕ when a film is spread.

From the above equations, if equation [8] is no longer true, equation [9] is extended to:

$$[13] \quad \phi = \frac{RT}{2F} \ln \left(\frac{B_+}{B_-} \right) - \frac{RT}{2F} \ln \left(\frac{c_+}{c_-} \right)$$

in which c_+ and c_- refer to ionic concentrations in the oil at the point where

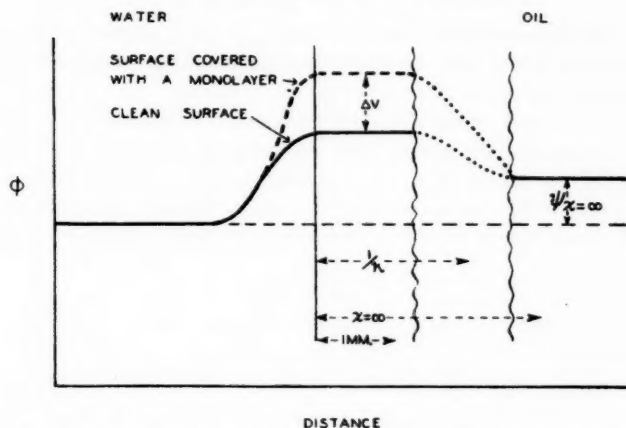


FIG. 3. Variation of ϕ (relative to the interior of the water phase) at the interface with a paraffinic oil. Measurements are made with x (~ 1 mm.) less than $1/\lambda$.

ϕ is measured. To express these concentrations in terms of measurable quantities, we apply the equations of Boltzmann in the form:

$$[14] \quad c_{+} = (c_{+})_{x=\infty} \times \exp[-e(V - \psi_{x=\infty})/kT]$$

and

$$[15] \quad c_{-} = (c_{-})_{x=\infty} \times \exp[+e(V - \psi_{x=\infty})/kT]$$

and, in the hypothetical region of oil at $x = \infty$, where the electrical double layer is complete,

$$[16] \quad (c_{+})_{x=\infty} = (c_{-})_{x=\infty}.$$

Hence equation [13] becomes:

$$\phi = \frac{RT}{2F} \ln \left(\frac{B_{+}}{B_{-}} \right) - \frac{RT}{2F} \ln \exp[-2e(V - \psi_{x=\infty})/kT].$$

The double layer is complete at $x = \infty$, so $\phi_{x=\infty} = \psi_{x=\infty}$ and hence, according to equation [9],

$$\psi_{x=\infty} = \frac{RT}{2F} \ln \left(\frac{B_{+}}{B_{-}} \right).$$

Therefore

$$\phi = \psi_{x=\infty} + \frac{2RTe}{2kTF} (V - \psi_{x=\infty})$$

$$\text{or} \quad \phi = \psi_{x=\infty} + (V - \psi_{x=\infty})$$

$$\text{or} \quad \phi = V.$$

Here ϕ is independent of B_{+} and B_{-} , and

$$[17] \quad \Delta\phi = \Delta V (= \delta\chi, \text{ Lange nomenclature}).$$

From the above considerations we note that with a polar oil in a cell of the type shown in Fig. 2, we can make measurements with direct current (18) to test equation [11]:

$$[11] \quad \Delta\phi = \Delta\psi = (RT/F)\ln(S_{NaI}/S_{KI}) .$$

With a non-conducting oil, the vibrating plate method (8, 9) must be employed. This is a capacity method, and depends upon alternating current, since no measurable direct current can pass through a non-conducting oil, in which salts are effectively insoluble. To such potentials, equation [17] applies:

$$[17] \quad \Delta\phi = \Delta V .$$

To test the theories we thus require different oils: if the oil is polar, $\Delta\phi$ should depend only on the distribution coefficients, and not on ΔV ; but if the oil is paraffinic, $\Delta\phi$ should depend on ΔV and not on S , the distribution coefficient.

If the non-aqueous phase is so non-polar that ions cannot appreciably dissolve in it, the interfacial potential will alter only if an interfacial film is formed—the partition coefficients being assumed to be unaltered by the interfacial monolayer. Ions are unstable in air near a water surface, and no double layer can therefore form above a water surface; thus the measurement (23) of film potentials at the air–water surface is rendered possible and equation [17] can be tested, where ΔV is the difference of potential between the clean water surface and one on which a film has been spread, as shown in Fig. 3. Such potential changes are perfectly stable with time, no decrease ever having been observed with insoluble films. Exactly similar results are obtained, though the experimental technique is different (8, 9, 12), with paraffinic oils, as shown in Fig. 4. The petrol-ether used in this experiment is made up of decane and near homologues.

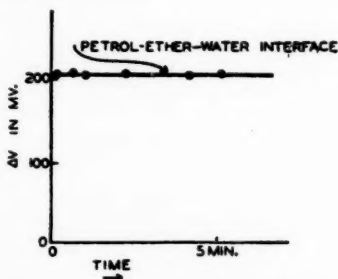


FIG. 4. Surface potential for monolayer of $C_{18}H_{37}N(CH_3)_3^+$ spread to 92 \AA^2 per chain between petrol-ether and water. The latter contained $1.0 \text{ } N$ NaCl. The potential does not change with time (12).

Again, if the paraffinic oil be replaced by a fairly polar oil there should, by equation [11] which is now applicable, be no change in potential between the system with a clean interface and one with a monolayer at the interface. Only if the distribution coefficient is changed will the potential alter. This is in full accord with experiment.

If, however, we study a very slightly polar oil, spreading a film and measuring the potential difference $\Delta\phi$ (equation [17]), this should now slowly decrease to zero, since, if the oil is slightly polar, ions from the water will redistribute themselves and set up a new double-layer in the oil. During this process of ionic redistribution (Fig. 5) we pass from the region of applicability

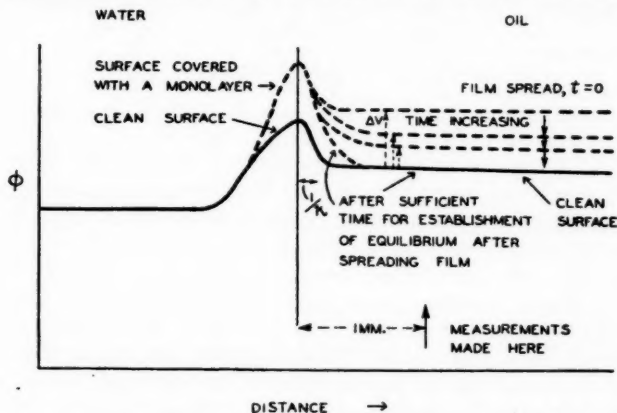


FIG. 5. Potential redistribution on oil side of interface after spreading a film if the oil is slightly polar. The (negatively charged) ionic atmosphere slowly builds up in the oil till ΔV has decreased to zero, provided that the thickness of oil used is sufficient to dissolve the necessary ions.

of equation [17] to that of equation [11]. The latter predicts $\Delta\phi$ should be zero, since a monolayer will not appreciably affect the distribution coefficients. Thus the potential difference $\Delta\phi$ due to the spread film should decrease with time and, if a complete double layer can form in the oil, will eventually become zero. This is borne out by experiment (Fig. 6).

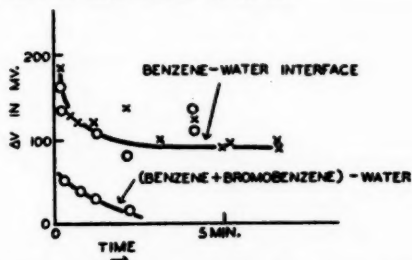


FIG. 6. Interfacial potentials of film of $C_{12}H_{27}N(CH_3)_3^+$ spread to 92 \AA^2 per chain between water and slightly polar oils. The decrease in ΔV with time reflects the change from the region of applicability of equation [17] to that of equation [11]. Crosses denote potentials measured with the vibrating plate apparatus (8, 9) and circles those found with the radioactive source method (2).

We can now proceed further and observe that if the times for the potential to decay to one half its initial value are found, a rough correlation with the

TABLE II

Non-aqueous phase	Calculated concentration of Cl^- in non-aqueous phase	Depth of ionic atmosphere, i.e. $1/\kappa$	Time calculated for Cl^- to reach equilibrium positions after film was spread	Observed time of decay of ΔV to $1/e$ of original value
Air	$10^{-16}N$	10^{14} cm.	10^{14} sec.	∞
Petrol-ether (decane)	$10^{-13}N$	10^8 cm.	10^{11} sec.	∞
Benzene	$10^{-11}N$	5×10^{-3} cm.	~ 1 sec.	60 sec.
Benzene + bromobenzene	$10^{-9}N$	5×10^{-4} cm.	~ 0.01 sec.	~ 1 sec.

rates of diffusion of the counter-ions from the water into the oil (to build up the new double layer) might be expected. In Table II this is shown, the calculated times (12) being functions of the polarity of the oil, i.e. of the equilibrium concentration of chloride ions immediately on the oil side of the interface. From here the ions must diffuse through the oil to a mean distance of $1/\kappa$ (the Debye-Hückel function) away from the interface. Although benzene is only slightly more polar than paraffins, it dissolves more water, so that ions in benzene can be at least partly hydrated and in consequence more ions can dissolve in benzene than in petrol-ether. Thus interfacial potentials at the benzene-water interface decrease with time, although those at the paraffin-water interface are stable.

(c) COMPONENTS OF ΔV , THE SURFACE POTENTIAL

Throughout this paper the orientation of the dipoles at the water surfaces has been neglected, and by definition $\phi_{\text{H}_2\text{O}} = 0$. If ψ , the free charge, is zero in the water, the absolute potential $\phi_{\text{H}_2\text{O}}$ is V or χ , the potential of the water dipoles. Although questions of absolute potentials have been avoided in the present work, it is interesting to note that V has been estimated for the air-water surface. The figures range, however, from -0.5 volts to $+0.4$ volts (21).

If, however, a monolayer is spread on a clean water surface, the water dipoles will be reoriented about the film-forming molecules, because of the new dipoles introduced into the surface. This change, for each molecule spread

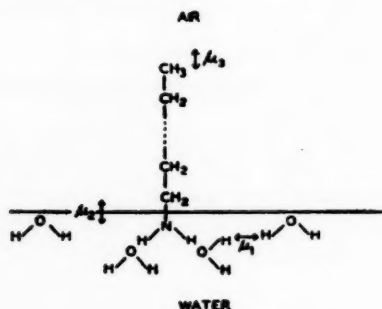


FIG. 7. Components μ_1 , μ_2 , and μ_3 of the surface potential ΔV for an electrically neutral monolayer.

in the monolayer, will be denoted μ_1 . The dipoles of the film-forming molecules (e.g. C—NH₂ in a long-chain amine) will also contribute to ΔV by an amount depending on the dipole moment μ_2 . A third component of ΔV for electrically neutral films spread at the air-water surface is μ_3 , the moment of the bond (e.g. C—H) at the upper limit of the monolayer (Fig. 7). If we apply the Helmholtz formula for an array of n dipoles per cm.², and if they are all vectorially additive in the vertical direction (Eucken), we obtain:

$$[18] \quad \Delta V = 4\pi n\mu = 4\pi n\mu_1 + 4\pi n\mu_2 + 4\pi n\mu_3$$

where μ is an over-all dipole moment including all components.

Unfortunately μ_1 cannot be measured, so it is usual to combine this term with μ_2 , especially since the reorientation of the water dipoles, given by μ_1 , probably depends on μ_2 , as in Fig. 7.

The term μ_3 is normally constant since paraffinic chains are usual in surface active molecules, so that then equation [18] becomes for an electrically neutral film:

$$[19] \quad \Delta V = 4\pi n\mu = 4\pi n\mu_D$$

where $\mu_D = \mu_1 + \mu_2 + \mu_3$, characteristic of the dipole of the head-group (e.g. C=O, C—NH₂) of the molecules in the monolayer.

In recent years there has been added interest in substituted hydrocarbon chains, and to investigate these we use [18] in the form:

$$[20] \quad \Delta(\Delta V) = 4\pi n(\Delta\mu_3).$$

Thus by comparing films with the same numbers of molecules per cm.², spread at the same interface, and having the same polar head groups, we measure the difference in potential due to substitution of the —CH₃ group at the upper

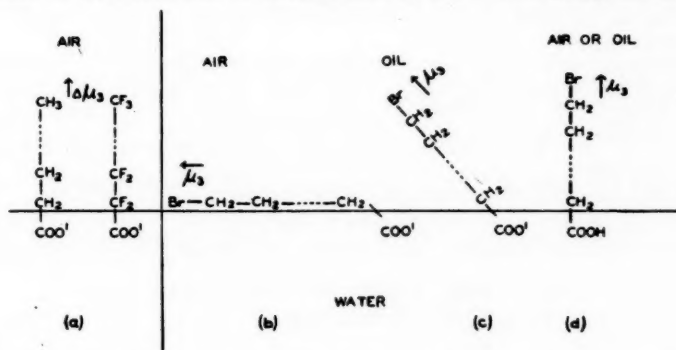


FIG. 8. (a) Anions of an aliphatic acid and of a perfluoro acid spread at the air-water interface. The difference in ΔV is due to the change in μ_3 , the vertical dipole moment of the uppermost bond (19).

(b) Anion of ω -bromohexadecanoic acid at air-water interface. The vertical component of μ_3 is zero (13).

(c) Anions of ω -bromohexadecanoic acid at decane-water interface. Vertical component of μ_3 now appreciable, as the ω -bromo group is easily lifted into the oil (13).

(d) Molecule of ω -bromohexadecanoic acid in close-packed film at pH 4 at air-water surface. The dipole μ_3 is now relatively large (17).

limit of the film by (say) $-\text{CH}_2\text{Br}$ or $-\text{CF}_3$, as shown in Fig. 8. Some results are shown in Table III. That $\Delta\mu_3$ is less than the dipole of the carbon-halogen link suggests that there is mutual polarization of the dipoles in condensed films (first and last examples in Table III). Further, the dipoles of such ω -halogen links are unlikely to be oriented vertically, but rather at half the tetrahedral angle (17).

TABLE III
VARIATIONS IN μ_3 FOR DIFFERENT FILMS AT THE AIR-WATER AND OIL-WATER INTERFACES

Film	ΔV	$\Delta(\Delta V)$	$\Delta\mu_3$ (vertical component of dipole differences in ω -bonds)	Difference in μ for ω -bond and C—H bond from bulk measurements
Myristic acid with carboxyl group ionized (25 Å, air-water)	-50 mv.	-900 mv. (19)	-600 mD. (see Fig. 8a)	-1800 mD.
Perfluorodecanoic acid with carboxyl group ionized (25 Å, air-water)	-950 mv.			
Hexadecanoic acid on 1 N NaOH at 66 Å, air-water	-28 mv.	0 (13)	0 (see Fig. 8b)	-1900 mD.
ω -Bromohexadecanoic acid on 1 N NaOH at 66 Å, air-water	-28 mv.			
ω -Bromohexadecanoic acid on 1 N NaOH at 66 Å, oil-water	-160 mv.	-132 mv. (13)	-230 mD. (see Fig. 8c)	-1900 mD.
Hexadecanoic acid pH4 air-water (20 Å)	+390 mv.			
ω -Bromohexadecanoic acid, pH4, air-water (20 Å)	-870 mv.	-1260 mv. (17)	-660 mD. (see Fig. 8d)	-1900 mD.

If now we consider a charged film of $\text{C}_{18}\text{H}_{37}\text{N}(\text{CH}_3)_3^+$ ions, an additional term ψ_0 for the electrostatic potential of the interface relative to the subjacent layers of liquid is necessary. Thus equations [18] and [19] become:

$$[21] \quad \Delta V = 4\pi n\mu = 4\pi n\mu_1 + 4\pi n\mu_2 + 4\pi n\mu_3 + \psi_0,$$

$$[22] \quad \Delta V = 4\pi n\mu = 4\pi n\mu_D + \psi_0,$$

or

$$[23] \quad \mu = \mu_D + \mu_0$$

where μ_0 is the dipole contribution of the electrical double layer.

At low surface coverages, ψ_0 may be expected to contribute to μ a dipole moment (Fig. 9) given by the product of the mean thickness of the ionic double layer (the Debye-Hückel term $1/\kappa$) and the charge thus separated per molecule, i.e. one electron. Both these quantities are large (e.g. $1/\kappa$ may be

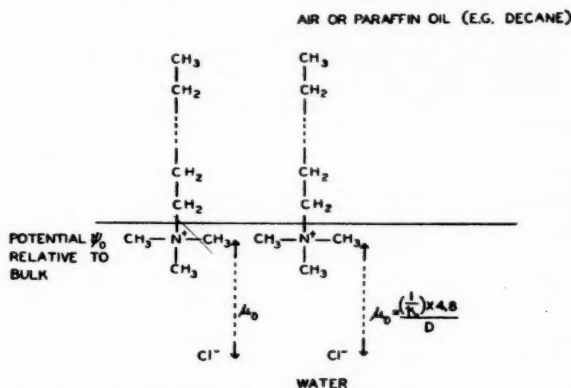


FIG. 9. A monolayer of $C_{13}H_{27}N(CH_3)_3^+$ at air-water or decane-water interface. The mean depth of the Cl^- counter-ions is $1/\kappa$, and this makes possible very large dipole contributions if the ionic strength is low (Table IV). The electrostatic potential at the interface is ψ_0 relative to the bulk of the aqueous phase.

several hundred Angstrom units), so very large dipole moments may be expected. To treat the double layer as an array of dipoles in this manner we have assumed that the dielectric constant D of the water is always 80 in the electrical double layer, and that the charges are far enough apart in the surface for their mutual interactions to be neglected. Thus:

$$[24] \quad \mu_{n \rightarrow 0} = \frac{(1/\kappa) \times 4.8}{D}$$

and hence, by [23],

$$[25] \quad \mu = \mu_D + \frac{(1/\kappa) \times 4.8}{D}$$

Comparison of μ thus calculated with the experimental results at different ionic strengths (8) is made in Table IV. The value of μ_D is 400 mD. throughout (11). Although the dipole moments, especially on $10^{-4} N$ solution ($1/\kappa = 300 \text{ \AA}$), are very high, the potentials at 1000 \AA (Table IV) are not very great. However, since n is then only 10^{13} , μ is large by equation [22]. At greater surface concentrations (n increasing), ΔV increases only slightly, and μ falls steeply owing to mutual interaction of the electrical charges (8).

Equation [22] can also be tested (10) using the Gouy equations for ψ_0 :

$$[26] \quad \psi_0 = \frac{2kT}{e} \sinh^{-1} \left(\frac{134 \times 10^{-18} \times n}{\sqrt{c}} \right).$$

Comparison with experiment is made in Table V, combining equations [22] and [26]:

$$[27] \quad \Delta V = 4\pi n \mu_D + \frac{2kT}{e} \sinh^{-1} \left(\frac{134 \times 10^{-18} \times n}{\sqrt{c}} \right).$$

These considerations all apply to the air-water or decane-water interface. If, however, a polar oil is used, ΔV for charged films is found (see above) to

TABLE IV

CALCULATED AND MEASURED DIPOLE MOMENTS μ FOR COMPLETELY IONIZED FILMS OF $C_{18}H_{37}N(CH_3)_3^+$ AT THE AIR-WATER OR DECAH-WATER INTERFACES. THE DISTANCE $1/\kappa$ IS GIVEN BY $3/\sqrt{c}$ Å, WHERE c IS THE SALT CONCENTRATION

NaCl concentration, c	μ (calculated)*	μ (measured (8))	Potential ΔV at $n = 10^{13}$ (1000 Å ² per chain)
$2 N$ ($1/\kappa = 2.1$ Å)	528 mD.	500 mD. as $n \rightarrow 0$	22.5 mv.
$10^{-1} N$ ($1/\kappa = 9.5$ Å)	970 mD.	1026 mD. as $n \rightarrow 0$	43 mv.
$10^{-2} N$ ($1/\kappa = 30$ Å)	2200 mD.	2700 mD. as $n \rightarrow 0$	86 mv.
$10^{-3} N$ ($1/\kappa = 95$ Å)	6100 mD.	6170 mD. as $n \rightarrow 0$	124 mv.
$10^{-4} N$ ($1/\kappa = 300$ Å)	18,400 mD.	19,300 mD. as $n \rightarrow 0$	220 mv.

* $\mu = 400 + \frac{(1/\kappa) \times 4.8}{D}$; the figure of 400 mD. for μ_D is from Ref. 11.

TABLE V

TEST OF EQUATION [27]. DATA FOR $C_{18}H_{37}N(CH_3)_3^+$ (11, 10). AS BEFORE, $\mu_D = 400$ mD.

Function of ΔV	Calculated	Experimental
$\left(\frac{\partial(\Delta V)}{\partial \log c}\right)_n$	- 59 mv. = $\frac{2.303kT}{e}$ if c not too high	-57 mv. to -62 mv.
$\left(\frac{\partial(\Delta V - 4\pi n \times 400)}{\partial \log n}\right)_c$	+118 mv. = $\frac{2 \times 2.303kT}{e}$ if n not too low	+110 mv.
$\Delta V - 4\pi n \times 400 = \psi_0$ ($n = 3.33 \times 10^{13}$)	+108 mv.	+112 mv.
$\Delta V - 4\pi n \times 400 = \psi_0$ ($n = 6.67 \times 10^{13}$)	+142 mv.	+145 mv.

be zero at equilibrium, in agreement with the theory of Dean, Gatty, and Rideal (15). They pointed out that a compensative electrical double layer must also be set up in a polar oil (whether or not ψ_0 is zero), and this, represented here as ψ_{oil} , must at equilibrium be given by:

$$[28] \quad \Delta V = 4\pi n \mu_D + \psi_0 + \psi_{\text{oil}} = 0.$$

GENERAL DISCUSSION

That the Gouy equations, based on the assumption of a uniformly charged and impenetrable film in contact with counter-ions which are point charges, predict so accurately ψ_0 up to high ionic strengths had been interpreted (14) in terms of compensation of the effects of the finite sizes of the counter-ions with the penetration of some of the counter-ions between the charged groups

constituting the film. This conclusion has been supported by studying the surface viscosity and interfacial reaction kinetics as ψ_0 changes.

In the last few years various authors have measured interfacial potentials with cells of the type shown in Fig. 2. Thus McMullen (20) found that the introduction of cetyltrimethylammonium bromide into an octyl alcohol-water system caused a potential $\Delta\phi$ of about 130 mv. although this decayed rapidly. Similar results were found with amyl-acetate. On the other hand Dupeyrat and Guastalla (16), using nitrobenzene as oil, found $\Delta\phi$ to be constant at 400 mv. when a myristyl-trimethylammonium salt was added. We consider that distribution potentials ($\Delta\psi$ of equation [11]) and diffusion potentials are responsible for all these results, the very thin layers of oil used by McMullen eventually making possible distribution potentials at *both* oil-water interfaces ($\Delta\phi_2 \sim \Delta\phi$ in Fig. 2, owing to diffusion). The potential of Dupeyrat and Guastalla is certainly a stable $\Delta\psi$, though rather higher than found by Powell and Alexander (22), whose measurements are more difficult to interpret. They used the contact potential method, ionizing the air gap above the oil layer (and possibly the oil itself) with a mesothorium source. Interfacial potentials due to cetyltrimethylammonium bromide added to the water were usually constant after the first few minutes, and then it was found that $\Delta\phi$ varied in the order:

$$\Delta\phi(\text{air}) \gg \Delta\phi(\text{amyl acetate}) > \Delta\phi(\text{octyl alcohol}) .$$

This sequence is in the reverse order of the dielectric constants. Powell and Alexander interpret these $\Delta\phi$ measurements as ΔV potentials, though by comparison with the results of Fig. 6 and Table II this seems unlikely, especially as they claim that the equilibrium postulated by Dean, Gatty, and Rideal (15) must be very slow in attainment since their potentials are stable with time after a few minutes. We consider that Powell and Alexander's oil-water results are probably distribution potentials or may sometimes be due to diffusion to and adsorption at the upper (oil-air) interface. Distribution potentials would be expected to decrease with increasing dielectric constant of the oil, since B_+ depends on $\epsilon\mu_+$.

Our considerations concerning the adsorption and ion partition potential differences which may develop at liquid-liquid interfaces and the effects of an added electrolyte on their magnitude can evidently be extended to the case in which, for example, a lipoid-like membrane is inserted between two aqueous phases. The best known method of estimating the various components of a membrane potential into phase boundary and diffusion potentials has been laid on a sure foundation by the investigations of Kurt Meyer and T. Teorell.

CONCLUSION

In general $\Delta\phi = \Delta\psi + \Delta V$, but by choosing polar and paraffinic oils, we can separate $\Delta\psi$ and ΔV thus:

$$\begin{aligned} \Delta\phi &\cong \Delta\psi = f(B_+, B_-) && \text{polar oil,} \\ \Delta\phi &\cong \Delta V = f(n, \mu) && \text{paraffinic oil.} \end{aligned}$$

From our results we conclude that Beutner was indeed correct—Baur's adsorption potentials (surface potentials) either cannot be detected or are very transient for polar oils. Only with recent techniques for investigating interfacial potentials between water and pure paraffinic oils can stable oil-water interfacial potentials (ΔV or $\delta\chi$) be measured (8, 9). This lends strong support to the theory of Dean, Gatty, and Rideal (15).

Surface potentials have been analyzed into components from the dipoles of the polar "head groups" of film-forming molecules, from the dipoles at the upper end of the carbon chain, and from ionic redistributions if the film is electrically charged.

REFERENCES

1. ADAM, N. K. The physics and chemistry of surfaces. Oxford University Press, Oxford. 1944. p. 361.
2. ALEXANDER, A. E. Trans. Faraday Soc. 37: 117. 1941.
3. BAUR, E. *et al.* Z. Elektrochem. 19: 590. 1913; 32: 547. 1926.
4. BEUTNER, R. *et al.* Z. Elektrochem. 19: 319, 467. 1913.
5. BEUTNER, R. *et al.* Science, 104: 569. 1946.
6. BONHOEFFER, K. F., KAHLWEIT, M., and STREHLOW, H. Z. physik. Chem. 1: 21. 1954.
7. DAVIES, J. T. J. Phys. & Colloid Chem. 54: 185. 1950.
8. DAVIES, J. T. Nature, 167: 193. 1951.
9. DAVIES, J. T. Z. Elektrochem. 55: 559. 1951.
10. DAVIES, J. T. Proc. Roy. Soc. (London), A, 208: 224. 1951.
11. DAVIES, J. T. Trans. Faraday Soc. 48: 1052. 1952.
12. DAVIES, J. T. Trans. Faraday Soc. 49: 683. 1953.
13. DAVIES, J. T. Trans. Faraday Soc. 49: 949. 1953.
14. DAVIES, J. T. and RIDEAL, SIR ERIC. J. Colloid. Sci. Suppl. 1: 1. 1954.
15. DEAN, R. B., GATTY, O., and RIDEAL, E. K. Trans. Faraday Soc. 36: 161. 1940.
16. DUPEYRAT, M. and GUASTALLA, J. Colloque sur les composés superficiellement actifs. Paris. 1955.
17. GEROVICH, M. and FRUMKIN, A. J. Chem. Phys. 4: 624. 1936.
18. KARFFEN, F. M. and RANDLES, J. E. B. Trans. Faraday Soc. 49: 823. 1953.
19. KLEVENS, H. and DAVIES, J. T. J. Am. Chem. Soc. In press.
20. McMULLEN, A. I. Ph.D. Thesis, Cambridge. 1948.
21. PARSONS, R. In Modern aspects of electrochemistry. Edited by J. O'M. Bockris and B. E. Conway. London. 1954. p. 124.
22. POWELL, B. D. and ALEXANDER, A. E. J. Colloid. Sci. 7: 482, 493. 1952.
23. SCHULMAN, J. H. and RIDEAL, E. K. Proc. Roy. Soc. (London), A, 130: 259. 1931.

CYSTINE AS AN ADDITION AGENT IN THE ELECTRODEPOSITION OF COPPER¹

By A. J. SUKAVA² AND C. A. WINKLER

ABSTRACT

The steady state polarization of 100 mv. in acid copper sulphate electrolyte, at 2 amp./dm.², appears to consist of 45 to 50 mv. activation overpotential to deposit aquo-copper complexes, 20 to 25 mv. concentration polarization, and about 30 mv. polarization due to hydrogen ion interference. The presence of cystine in the electrolyte gave rise to polarization-time curves similar to those observed previously with gelatine. The increase of polarization caused by cystine appears to be due to an obstructive effect of adsorbed cystine (or its copper complex), together with an increase of concentration polarization. Cystine alone probably does not affect the activation overpotential. Addition of sufficient chloride virtually eliminated the polarization due to obstruction by cystine, possibly by acting as an electron bridge or by forming more readily dischargeable chloro-cystine-copper complexes. Chloride also eliminated the increment in concentration polarization caused by cystine. Attainment of a minimum total steady state polarization of about 40 mv. in the presence of cystine and chloride appeared to reflect an increase of surface, hence a decrease of true current density with time of deposition. The addition agent behavior of methionine was, in most respects, similar to that of cystine. The behavior of thiourea at low concentrations appeared to be complicated, but the effects of chloride were similar to those observed with gelatine.

INTRODUCTION

Since gelatine is probably the most commonly used addition agent in the electrodeposition of copper, much work has been done in this laboratory and elsewhere to study its behavior in this capacity. An understanding of its action is clouded, however, by the complex structure of the gelatine molecule, and it has seemed desirable to find, if possible, a simple amino acid with which the addition agent effect of gelatine might be closely simulated. A previous study with glutamic acid (1) indicated that this substance was not a satisfactory substitute for gelatine. The present paper recounts similar studies with some simple thioamino acids.

EXPERIMENTAL

Polarization measurements were made with the equipment and procedure outlined in earlier papers (1, 10). All chemicals were reagent grade, and water was twice distilled from alkali. The standard electrolyte contained 125 gm./liter $\text{CuSO}_4 \cdot 5\text{H}_2\text{O}$ and 100 gm./liter H_2SO_4 . The composition of other electrolytes used in the study will be specified as required. The Haring cell contained 150 ml. of electrolyte in all experiments, and measurements were made at 24.5° C. throughout the study.

Each cathode surface was brought to a standard condition by electro-deposition from standard electrolyte at 24.5° C. at 3 amp./dm.² for 30 min.,

¹ Manuscript received January 14, 1955.

² Contribution from the physical chemistry laboratory, McGill University, Montreal, with financial assistance from the National Research Council, Ottawa, and the Consolidated Mining and Smelting Co., Trail, B.C.

³ Holder of a Cominco Research Fellowship. Present address: Department of Chemistry, University of Western Ontario, London, Ontario.

followed by deposition at 2 amp./dm.² until steady state polarization (100 ± 5 mv.) was attained (4).

RESULTS

Initial Cathode Polarization in Absence of Addition Agent

In an earlier study (10) it was observed that, at 2 amp./dm.², the polarization rose almost instantaneously to about 100 mv. in the standard electrolyte, and then increased slowly to a slightly higher steady state value. A more detailed study of the behavior with the cathode ray oscilloscope or the Brush recorder has shown that a zero time* polarization of 85 to 90 mv. was followed by an increase to about 115 mv. after one to two minutes, and a subsequent decrease during about 30 min. to the steady state value. Typical results are shown in Fig. 1. Transition from the behavior represented in Fig. 1B to that of Fig. 1C was essentially complete after interruption of the current for one to two minutes. This indicates that the time for dissipation of the cathode film is about the same as that for attainment of the initial maximum polarization and for formation of the cathode film (2).

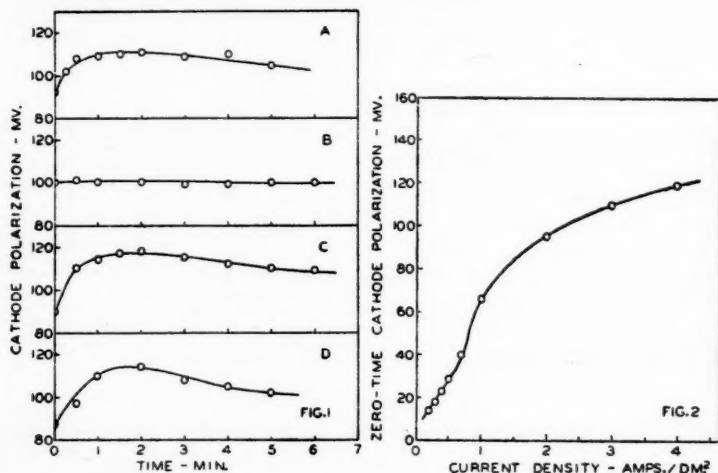


FIG. 1. Initial cathode polarization-time relation for standard electrolyte and standard cathode surface.

- A. Cathode film absent at zero time (new standard electrolyte).
 B. Cathode film present at zero time (current switched off and immediately re-established).
 C. Cathode film absent at zero time (current switched off and cell left undisturbed for four hours).
 D. Cathode film absent at zero time (current switched off and solution stirred for one minute).
 FIG. 2. Zero-time cathode polarization - current density relation with standard electrolyte and standard cathode surface.

The concentration polarization at the steady state was found to range from 20 to 25 mv. Hence the true zero time polarization presumably should have been 75-80 mv. It is probable that the higher value recorded includes

*Zero time is taken as the time at which a first polarization value could be identified.

some initial build-up of concentration polarization before the first reading was obtained on the C.R.O. or Brush recorder.

The effect of current density on the zero time polarization (Brush recorder) in the absence of cathode film is shown in Fig. 2. The linear relation at low current densities is similar to that observed for other polarization values under different conditions (3, 11, 12); at current densities above 0.6 amp./dm.² the polarization was, within experimental error, linear with the logarithm of the current density.

Cathode Polarization in the Presence of Cystine

The initial polarization pattern observed when cystine was added to the standard electrolyte resembled that previously observed with gelatine (10). The presence of cystine caused the polarization to pass through an early maximum, P_{\max} (after a fraction of a second), then through a minimum, P_{\min} (after about two seconds), followed by a gradual rise to the steady state value, P_s . As with gelatine, the values of P_{\max} and P_{\min} increased with immersion time, i.e. the time the electrode was in contact with the electrolyte before electrolysis was begun. The following data were obtained with 50 mgm./liter cystine and 2 amp./dm.²:

Immersion time (min.)	Initial polarization (mv.)	
	(maximum at 0-0.05 sec.)	(minimum at 1-2 sec.)
1	150	120
5	177	122
10	205	125
15	235	145
30	270	155
50	275	155
85	292	157

The time to attain P_{\max} showed no definite dependence on immersion time. A constant immersion time of five minutes was adopted for routine purposes, and is applicable to the remainder of the discussion.

The value of P_{\max} , and to a lesser extent that of P_{\min} , was found to increase steadily with increased cystine concentration (Fig. 3A). The times to P_{\max} and to P_{\min} decreased with increased concentration of cystine. Both P_{\max} and P_{\min} always exceeded the lowest zero-time polarization (80 mv.) measured in the absence of addition agent.

The steady state polarization was found to be related to cystine concentration as shown in Fig. 3B. The values for concentrations of cystine below about 10 mgm./liter are approximate only, since there was a continued slight decrease of polarization even after five to seven hours electrolysis. The concentration polarization at the steady state, obtained with the C.R.O. (13), also showed a definite, though somewhat erratic, increase with increased cystine concentration (Fig. 3C).

Effect of Chloride on the Polarization in the Presence of Cystine

Addition of various amounts of chloride ion to standard electrolyte containing 20 mgm./liter cystine showed that the depolarizing effect of chloride

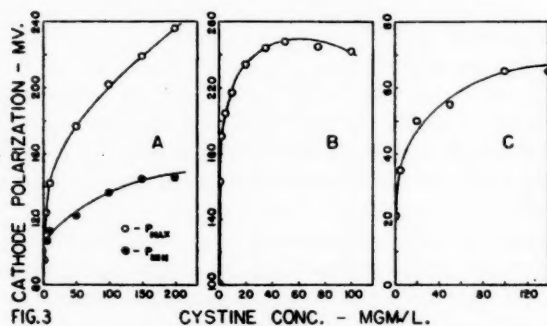


FIG. 3

CYSTINE CONC. - MGM/L.

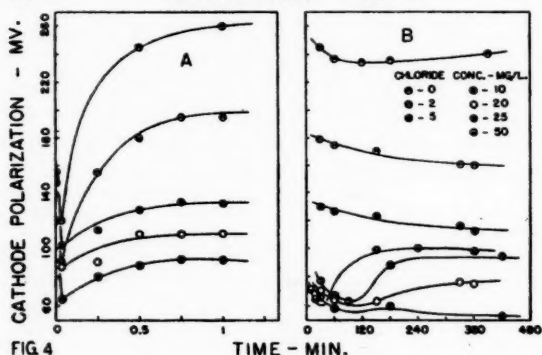


FIG. 4

TIME - MIN.

FIG. 3. Cathode polarization - cystine concentration relations.

A. Initial maximum and minimum polarizations.

B. Steady state polarization.

C. Concentration polarization at steady state.

FIG. 4. Cathode polarization-time relations in the presence of 20 mgm./liter cystine and different amounts of chloride.

A. Initial polarization-time pattern.

B. Polarization-time pattern after prolonged electrolysis.

was immediate (Fig. 4A). Concentrations of chloride higher than about 15 mgm./liter eliminated the influence of cystine to give a behavior, during the first minute, almost identical with that observed in the absence of addition agent. Much higher chloride concentrations (50 to 100 mgm./liter) reduced the initial polarization further by 15 to 20 mv. Following upon the immediate depolarization due to chloride were the slower changes shown in Fig. 4B. These were not due to chemical changes other than electrode processes, since aging the solutions prior to electrolysis had no effect.

The steady state polarization as a function of chloride concentration is shown in Fig. 5A. The minimum polarization (about 50 mv. at 12 mgm./liter chloride) was always accompanied by a coarse, irregular deposit.

The effect of cystine concentration on the position of the minimum in the steady state polarization - chloride concentration curve is shown in Fig. 5B.

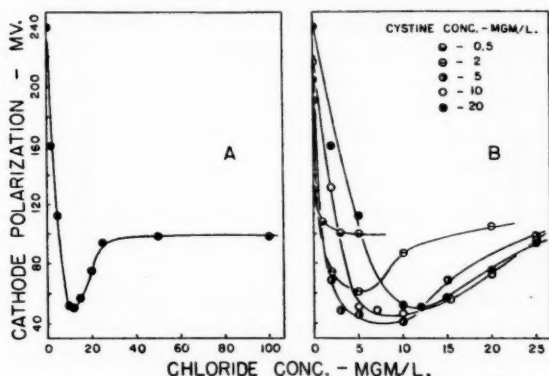


FIG. 5. Steady state cathode polarization-chloride concentration relations for different concentrations of cystine.

A. Effect of wide range of chloride concentrations with 20 mgm./liter cystine.

B. Effects of low chloride concentrations with different amounts of cystine.

It would seem that approximately 40 mv. represents the lower limit to which the polarization may be reduced by chloride in the presence of cystine for the conditions of electrolysis used.

The initial polarization in the presence of cystine and chloride is determined largely by the surface condition of the electrode. This was shown by the following experiment: A solution containing 5 mgm./liter cystine and 10 mgm./liter chloride was electrolyzed (starting with a standard surface electrode), at 2 amp./dm.², to the steady state polarization of 40 mv. The solution was removed from the cell and the cell thoroughly rinsed with water and standard electrolyte to remove as much adsorbed cystine and chloride as possible. Electrolysis was then resumed with fresh electrolyte of the same composition as in the first electrolysis. During the first electrolysis with a standard surface cathode a sharp decrease in polarization from 92 mv. to a minimum at 65 mv. occurred after two seconds. This was followed by an increase during the next half minute to 110 mv. and a subsequent decrease to the steady state value after about three hours. The second electrolysis showed a small decrease in polarization (55 mv. to 50 mv.) during the first two seconds, which was succeeded by an increase to 70 mv. after 1.5 min., and thereafter by a decrease to the steady state value in about the same time as the first electrolysis. Repetition of the experiment with a steady state surface obtained at a polarization of 105 mv. in electrolyte containing 2 mgm./liter cystine and 20 mgm./liter chloride gave initial polarization values in the second electrolysis that were within 5 mv. of those in the first electrolysis. Evidently, the steady state and standard electrode surfaces were essentially identical in this last experiment.

Concentration polarization at 2 amp./dm.² in the presence of different concentrations of cystine and chloride had the following values:

Cystine conc. (mgm./liter)	Chloride conc. (mgm./liter)	Concentration polarization (mv.)
0.5	1	20
2	20	20
5	5	20
5	10	20
10	50	20
20	0	50
20	1	35
20	10	25
20	12	25
20	20	20
20	50	20
20	100	20

It would appear that the presence of amounts of chloride above the concentrations corresponding to the minima in the steady state polarization - chloride concentration curves reduced the concentration polarization effectively to the value observed in the absence of addition agent.

The effect of acid concentration of the electrolyte on the initial polarization maximum was determined in the absence and presence of cystine, at 2 amp./dm.², with a standard cathode surface. Not only was the initial maximum polarization a linear function of acid concentration in both systems, but the increase of polarization in the presence of cystine over that in its absence was virtually constant at the different acid concentrations, thus:

Cystine conc. (mgm./liter)	Acid conc. (gm./liter)	Polarization (mv.)		
		Initial max.	Steady state	Concentration
0	25	60	—	
0	50	70	64	25
0	75	77	87	25
0	100	85	99	25
0	150		107	25
20	50	128	203	50
20	75	137	233	50
20	100	146	234	50
20	150	—	235	50

While the steady state polarizations indicate roughly parallel behavior with acid concentration in the presence and absence of addition agent, changes in surface characteristics at the cathode undoubtedly influence these values somewhat. For example, the surface corresponding to the steady state polarization with 50 gm./liter acid, in the absence of cystine, showed microscopically a rough, irregular structure, in contrast to the smoother texture of the initial standard surface.

If the relation between initial maximum polarization and acid concentration is assumed to be linear down to zero acid concentration, the contribution made by acid of a given concentration to the total polarization may be estimated by extrapolating to zero acid concentration and noting the difference between the polarization for zero acid and that at the given acid concentration. This treatment of the data yields a value of about 30 mv. for the contribution by acid to the polarization at a standard cathode surface in electrolyte containing 100 gm./liter acid.

Cathode Polarization in the Presence of Methionine

With methionine alone as addition agent, the initial polarization-time relations, the variation of initial polarization maximum with methionine concentration, and the relations of steady state total and concentration polarization values with methionine concentration, were all quite similar to the corresponding relations when cystine was the addition agent.

When chloride was added in conjunction with methionine, the depolarizing action was immediate, as it was with cystine. However, prolonged electrolysis revealed some differences in the behavior of the two addition agents. In particular, with higher chloride concentrations (5 to 25 mgm./liter) there were no minima in the polarization-time curves with methionine, while at all chloride concentrations the change of polarization to the steady state was slower. The steady state polarization showed the same type of relation with chloride ion concentration as that observed with cystine. The only difference appeared to be that the minimum polarization (again, about 40 mv.) was obtained with 5 mgm./liter, instead of 12 mgm./liter, chloride ion concentration, when the concentrations of the addition agents were 20 mgm./liter.

Cathode Polarization in the Presence of Thiourea

The cathode polarizations obtained with concentrations of thiourea of 3 mgm./liter and lower, though not those with higher concentrations, were found to be very irreproducible. Moreover, they were found to vary considerably with age of the stock solution of electrolyte containing the addition agent, possibly as a result of oxidation by cupric ion. After about 10 days, the solution contained a yellowish precipitate, apparently free sulphur.

Regardless of the age of the electrolyte and with concentrations of thiourea up to 3 mgm./liter, the polarization-time curves consisted of an early low polarization stage (70-90 mv.) followed by an increase, perhaps due to an anodic oxidation product, to a higher value (200-220 mv.) after about one hour electrolysis. The polarization during the initial stage increased at first with age of solution, then decreased to a limiting low value of about 70 mv. after eight days. The higher second stage value was practically eliminated by such aging when the thiourea concentration was 2 mgm./liter or less. When the electrolyte containing 3 mgm./liter thiourea was treated with hydrogen peroxide at room temp, then warmed to decompose excess peroxide, the resulting solution decreased the polarization to a steady state value of 70 mv., unaltered by further electrolysis.

Addition of chloride to freshly prepared electrolyte containing 10 mgm./liter thiourea gave steady state polarization values with a minimum at about 160 mv., corresponding to a chloride concentration of about 2 mgm./liter. (The polarization with 10 mgm./liter thiourea alone was about 240 mv.) With higher chloride concentrations, the deposits had a very rough and nodular structure. The behavior, including the high value of the minimum polarization, is reminiscent of the previous observations with gelatine as the addition agent.

DISCUSSION

The increase in initial polarization maximum, P_{\max} , with increased immersion time in the presence of cystine is strong evidence for the prior adsorption of cystine on the copper cathode. The time required to attain a steady state in respect of adsorption is probably increased by simultaneous corrosion at the copper surface. Adsorption prior to electrolysis should, of itself, result in an increase of zero time polarization values with increase of cystine concentration in accordance with an adsorption isotherm type of relation. On the other hand, P_{\max} might be expected to include additional polarization due to cataphoretic migration to the cathode of positively charged cystine (or cysteine) when electrolysis is begun. (It may be assumed that cysteine is formed by cathodic reduction.) This, too, should increase with increase of cystine concentration. Hence, the sustained increase of P_{\max} in Fig. 3A appears to be reasonable. On the other hand, a maximum in P_{\max} with immersion time might be expected, since in these experiments a constant addition agent concentration was used, and the contribution due to cataphoresis should be substantially constant.

The presence of subsequent minimum and steady state polarizations as electrolysis is continued may be explained in the manner suggested previously for the similar behavior with gelatine (10).

The rapid increase of steady state polarization as the cystine concentration is increased might be attributed to adsorption of cystine, with consequent decrease of active area and increase of true current density. Alternatively, it might be due to adsorption of copper-cystine complexes from which copper is discharged with difficulty or not at all. For standard electrolyte and a standard surface, the activation overpotential of 45 to 50 mv.* presumably corresponds to discharge of the aquo-complex. Only by consideration of the effect of chloride does it seem possible to suggest a reason for the increase of polarization in the presence of cystine over that observed in its absence.

From the data presented, it is evident that all but 40 to 50 mv. of the total steady state polarization in the presence of cystine can be overcome by addition of an appropriate amount of chloride. It seems reasonable to assume that this residual polarization is due mainly to concentration polarization plus an overpotential caused by hydrogen ions, acting perhaps as a barrier to approach of the copper ions to the cathode.† Values of these polarizations somewhat less than the 20 mv. and 30 mv. respectively estimated for the standard surface might be expected if the rougher surfaces laid down in the presence of cystine are of larger active area and the true current density therefore less. In this event, there would remain some (probably small) activation polarization at the steady state.

The amount of chloride necessary to give the 40–50 mv. minimum steady state polarization in the presence of cystine reduced the *initial* (one to two

*Determined as the difference between the total polarization (100 mv.) and the sum of the concentration polarization (20 to 25 mv.) and that due to hydrogen ion (30 mv.).

†Since the increase of polarization due to increased acid concentration was essentially the same in the absence and presence of cystine, it seems doubtful that adsorption of hydrogen ions on the copper surface is responsible for the contribution to polarization made by hydrogen ions.

minutes) polarization to approximately the level (100 mv.) obtained in the absence of addition agent. Since the concentration and hydrogen ion contributions to the 100 mv. polarization are essentially the same (20 mv. and 30 mv. respectively) in the standard electrolyte and in the presence of cystine, the remaining 50 mv. in both cases probably also represents the same activation overpotential for discharge of aquo-complexes. It seems significant that the levels of the initial polarizations, with amounts of chloride capable of yielding minimum steady state polarizations, were but little influenced by the amount of cystine present. This would indicate that the activation overpotential involved is independent of cystine, and this would be true if it involved the aquo-complex.

With a chloride concentration much larger than that necessary to give a minimum steady state polarization (50 mgm./liter chloride with 20 mgm./liter cystine) the *initial* polarization (i.e. after one to two minutes) was some 15 mv. lower than the value for standard electrolyte. This lowering presumably represents a decrease in activation overpotential to about 30-35 mv. This cannot correspond to facilitated deposition from a chloro-aquo-complex since chloride ion (5 to 10 mgm./liter) in the absence of other addition agents increases the steady state polarization by about 15 mv. for the conditions of the present experiments (9). It might, however, represent discharge of a chloro-cystine-copper complex.

On the basis of the data and analysis presented above, the steady state polarization *in excess of about 100 mv.*, due to cystine alone, might reasonably be attributed to an increment (about 30 mv.) in concentration polarization, plus a component of the polarization arising from the obstructive influence of adsorbed cystine or cystine-copper complexes. Virtual elimination of this component of the polarization by chloride might be explained by facilitated electron transfer through an electron bridge, in the manner suggested by Heyrovsky (5), or by the formation of more readily dischargeable chloro-cystine-copper complexes, in accordance with Lyons' views (6, 7). The tendency for the initial activation overpotential in the cystine-chloride system to attain, with excess chloride, a lower value than that corresponding to discharge of the aquo-complex, as discussed previously, gives some support, perhaps, to the second suggestion.

The increment in concentration polarization caused by cystine may be explained if the cystine-copper complex is less readily discharged than the aquo-complex. A reaction of the type



would then proceed to the right under kinetic conditions of current flow and be restored to equilibrium when the current is stopped only by further hydrolysis of the cystine complex, corresponding to the observed increment in concentration polarization. Rapid formation of directly dischargeable chloro-cystine complexes on addition of chloride would render formation of aquo-complexes by the above reaction less significant as a factor in maintaining current flow, hence in determining the magnitude of the concentration polar-

ization. With sufficient chloride, the limiting concentration polarization of 20 mv. probably reflects diffusion and convection effects only.

The increase in polarization caused by increasing the chloride concentration above the point of minimum polarization with cystine and methionine may be attributed to accumulation and adsorption of colloidal cuprous chloride on the cathode, as discussed previously for gelatine (8). The delay of about one hour, after electrolysis is begun, before the rise in polarization is noted suggests that the cuprous chloride originates at the anode (1). The magnitude of the overpotential caused by adsorption of cuprous chloride may be estimated by taking advantage of the observation that the surface laid down at 100 mv. *steady state* overpotential in the presence of cystine plus excess chloride was microscopically similar to that obtained at 100 mv. steady state overvoltage in standard electrolyte. If this be taken to indicate that the true current densities were approximately equal in the two systems, a hydrogen ion contribution of about 30 mv. may be ascribed to both polarizations. Also, the activation overpotential for discharge of chloro-cystine complexes at the 100 mv. steady state polarization should have about the same value as that estimated previously (30–35 mv.) for these complexes at a standard surface in the absence of adsorbed cuprous chloride, i.e. from the initial polarization values. These polarization values, together with 20 mv. concentration polarization give, by subtraction from the 100 mv. total steady state polarization, a value of 15–20 mv. for the overpotential due to adsorption of cuprous chloride at the steady state. A similar value is obtained from McConnell's value of 115 mv. for the effect of chloride alone (9), by introducing the hydrogen ion and concentration polarization values given above, together with the previously estimated activation overpotential of 45–50 mv. for discharge of aquo-complexes.

REFERENCES

1. ADAMEK, S. and WINKLER, C. A. *Can. J. Chem.* 32: 931. 1954.
2. BRENNER, A. *Proc. Am. Electroplaters' Soc.* 28. 1941.
3. GARDAM, G. E. *Discussions Faraday Soc.* No. 1: 182. 1947.
4. GAUVIN, W. and WINKLER, C. A. *Can. J. Research, A*, 21: 37. 1943.
5. HEYROVSKY, J. *Discussions Faraday Soc.* No. 1: 212. 1947.
6. LYONS, E. H. *J. Electrochem. Soc.* 101: 363. 1954.
7. LYONS, E. H. *J. Electrochem. Soc.* 101: 376. 1954.
8. MANDELCORN, L., MCCONNELL, W. B., GAUVIN, W., and WINKLER, C. A. *J. Electrochem. Soc.* 99: 84. 1952.
9. MCCONNELL, W. B. Ph.D. Thesis, McGill University, Montreal, Que. 1949.
10. PARSONS, B. I. and WINKLER, C. A. *Can. J. Chem.* 32: 581. 1954.
11. SHREIER, L. L. and SMITH, J. W. *Trans. Faraday Soc.* 50: 393. 1954.
12. TAFT, R. and MESSMORE, H. E. *J. Phys. Chem.* 35: 2585. 1931.
13. TURNER, R. C. and WINKLER, C. A. *J. Electrochem. Soc.* 99: 78. 1952.

MICROCALORIMETRIC DETERMINATION OF THE CRITICAL CONCENTRATION AND THE MOLECULAR DIMENSIONS OF POLYVINYL ACETATE IN SOLUTION¹

BY MICHEL PARENT² AND MARCEL RINFRET

ABSTRACT

Heats of mixing of polyvinyl acetate fractions with *s*-tetrachloroethane and methanol have been determined for the low concentration region. At the lowest concentrations the graphs of ΔH vs. volume fraction are linear as predicted by the van Laar, Scatchard, and Hildebrand theory. As the concentration increases, an inflection point appears, the enthalpy increment being smaller for a short concentration interval and then resuming its former value up to the limit of the range studied. The position of the critical interval depends on the solvent employed and on the molecular weight of the fraction. An equation, based on Flory's theory, has been developed for predicting the critical concentration from intrinsic viscosity. Assuming that, at the critical concentration, the molecules are just coming into contact, it is possible to calculate the diameter of the sphere equivalent to a molecule. Comparison of the dimensions obtained from the critical concentration and the root-mean-square end-to-end distance of the molecule calculated by the Flory equation leads to agreement within 10%.

INTRODUCTION

The existence in high polymer solutions of a critical concentration, above which the macromolecules are entangled, was first postulated by Staudinger (9). More recently, Boyer and Spencer (1) have made a survey of the literature on the subject and Streeter and Boyer (10) have demonstrated its existence by viscosity measurements on highly dilute solutions of polystyrene. Further microcalorimetric studies of heats of mixing by Daoust and Rinfret (2) and determinations of partial molal volumes by Horth and Rinfret (5) give results in accord with the findings of Boyer and co-workers. The purpose of this paper is to show the dependence of the critical concentration on the nature of the solvent and the molecular weight of the solute. Moreover it will be shown that it is possible to deduce the dimensions of the macromolecule in solution from the critical concentration.

Most high polymers are amorphous and are often considered as very viscous liquids. The enthalpy change in mixing with a solvent is therefore given by the van Laar, Scatchard, and Hildebrand theory (4),

$$[1] \quad \Delta H_M \approx \Delta E_M = V_M B \Phi (1 - \Phi),$$

V_M being the total volume of mixture, and Φ the volume fraction of the solute. B is a parameter characterizing the net heat of interaction between solute and solvent. According to Scatchard (8),

$$[2] \quad B = C_{11} + C_{22} - 2C_{12}$$

where C_{11} , C_{22} , and C_{12} are the interaction energies per milliliter (also called

¹Manuscript received January 28, 1955.

Contribution from the Department of Chemistry, University of Montreal, Montreal, Quebec. This paper is taken in part from the Ph.D. thesis of Michel Parent.

²Holder of the C.I.L. Fellowship 1952-54. Present address: Centre de Recherches sur les Macromolécules, Strasbourg, France.

cohesive energy densities) between similar and dissimilar molecules. It can be shown that for similar molecules, the cohesive energy density per milliliter is given by:

$$[3] \quad C_{11} = (\Delta E_v/V)_1 \quad \text{and} \quad C_{22} = (\Delta E_v/V)_2$$

where ΔE_v is the energy of vaporization per mole and V , the molar volume of species 1 and 2 respectively. It has not been possible to calculate C_{12} for dissimilar molecules, and it has been postulated by Scatchard that:

$$[4] \quad C_{12} = (C_{11} \cdot C_{22})^{1/2}$$

Using [2], [3], and [4] equation [1] can be rewritten:

$$[5] \quad \Delta H_M = V_M \left[\left(\frac{\Delta E}{V} \right)_1^2 - \left(\frac{\Delta E}{V} \right)_2^2 \right] \Phi(1-\Phi).$$

Equation [5] indicates that all heats of mixing are positive. That many mixtures are accompanied by a negative heat evolution shows that the Scatchard postulate [4] is only valid for limiting cases. Where C_{12} is much different from the value given in [4] because of specific interaction between solute and solvent, B can take negative as well as positive values but is still a measure of the net heat of solute-solvent interaction.

Since polymer-solvent interactions take place between a molecule of solvent and an adjacent short segment of polymeric chain, the net energy of interaction should be independent of chain length. This will be shown to be true by the constancy of parameter B over a large range of molecular weights for a given polymer-solvent pair.

EXPERIMENTAL

A polyvinyl acetate fraction of molecular weight 29,000 was available from a previous investigation (2). A sample of Gelva-15, from Canadian Resins and Chemicals Co., of average molecular weight 60,000 was dissolved in 2% acetone solution and precipitated by water into seven main fractions using a method derived from Flory (3). Fractions were kept under vacuum over phosphoric anhydride.

The *s*-tetrachloroethane was of Eastman grade, stored over "Drierite", and distilled before use. Methanol was an acetone-free sample from Brickman Co. and was distilled, at high reflux ratio, in a 35 theoretical plates fractionating column. The microcalorimetric technique was essentially the same as already described (2). An improvement over the results obtained previously was effected by an even greater elimination of evaporation losses and the metallization of the Pyrex calorimeter cells to promote better heat conduction to the thermocouples. These cells were first chemically silvered and then a thin coat of copper was deposited by electrolysis. Intrinsic viscosities were determined with modified Ubbelohde viscometers as described elsewhere (2).

RESULTS

Table I together with Figs. 1-3 shows the heats of mixing of polyvinyl acetate fractions of various molecular weights in methanol and *s*-tetrachloro-

TABLE I

HEATS OF MIXING OF POLYVINYL ACETATE IN METHANOL AND *s*-TETRACHLOROETHANE AT 25° C.

Fraction mol. wt.	$\Phi(1-\Phi)$ $\times 10^3$	ΔH_M , cal.	V_M , ml.	$\Delta H_M/V_M$	B , cal. per ml.
<i>Methanol</i>					
536,000	4.38	.217	7.141	.030 ₄	6.9
	5.01	.221	6.584	.033 ₅	6.7
	6.44	.299	6.406	.046 ₇	7.3
	7.56	.317	6.305	.050 ₂	6.6
	8.82	.354	6.289	.056 ₁	—
	11.98	.458	6.184	.074 ₁	6.9
	15.93	.637	6.086	.105	7.1
	19.32	.747	5.983	.125	6.9
	23.5	.996	6.400	.156	7.0
255,000	4.02	.203	7.001	.029 ₀	7.2
	7.06	.361	7.309	.049 ₄	7.0
	7.99	.399	7.354	.054 ₄	6.8
	9.92	.447	6.319	.070 ₇	7.1
	11.03	.594	7.758	.078 ₁	6.9
	11.98	.544	7.005	.077 ₇	—
	12.91	.627	7.375	.085 ₀	—
	14.20	.564	6.199	.090 ₀	6.9
	15.70	.774	7.680	.101	6.9
	19.58	.849	6.546	.130	7.0
29,000	7.93	.403	7.128	.056 ₁	7.1
	11.98	.575	6.709	.085 ₇	7.1
	15.67	.690	6.082	.113	7.2
	16.95	.626	5.081	.123	7.3
	18.09	.875	6.654	.132	7.3
	19.28	.662	5.133	.129	—
	19.82	.525	3.825	.137	7.2
<i>s-Tetrachloroethane</i>					
536,000	1.04	— .148	6.526	— .022 ₇	— 21.9
	1.53	— .196	6.511	— .030 ₁	— 19.7
	1.75	— .237	6.441	— .036 ₁	— 21.0
	2.03	— .332	8.014	— .041 ₁	—
	2.13	— .326	7.598	— .043 ₁	—
	2.52	— .222	4.834	— .045 ₁	— 21.0
	3.52	— .532	8.028	— .066 ₁	— 20.9
	4.69	— .799	8.764	— .091 ₁	— 20.9
	5.70	— .821	7.394	— .111	— 20.7
	6.49	— .978	7.625	— .128	— 20.8
	6.84	— .893	6.484	— .138	— 21.2
255,000	1.26	— .215	8.072	— .026 ₁	— 21.1
	2.01	— .347	8.269	— .041 ₁	— 20.9
	2.44	— .366	7.493	— .048 ₁	— 21.5
	2.99	— .321	5.319	— .060 ₁	— 21.4
	3.63	— .630	8.715	— .072 ₁	— 20.9
	3.95	— .593	7.454	— .079 ₁	— 21.1
	4.95	— .752	7.320	— .103	— 21.5
	5.04	— .783	7.650	— .102	— 21.0
	6.43	— 1.03 ₁	7.881	— .131	— 21.0
191,000	1.02	— .147	6.932	— .021 ₁	— 20.8
	2.02	— .317	7.856	— .040 ₁	— 19.9
	2.52	— .372	7.149	— .052 ₁	— 20.6
	3.00	— .416	6.624	— .062 ₁	— 21.0
	3.49	— .524	7.319	— .071 ₁	— 20.5
	3.79	— .554	7.278	— .076 ₁	— 21.1
	4.01	— .595	7.396	— .080 ₁	— 20.9
	5.07	— .794	7.725	— .103	— 20.9
	6.01	— .966	7.898	— .122	— 20.9
29,000	2.49	— .436	8.278	— .052 ₁	— 21.2
	3.50	— .551	7.364	— .074 ₁	— 21.4
	4.53	— .728	7.363	— .098 ₁	— 21.8
	5.04	— .784	7.246	— .108	— 21.5
	5.98	— 1.03	7.857	— .131	— 21.9
	6.96	— 1.09	7.243	— .150	— 21.5
	9.96	— 1.26	5.854	— .214	— 21.5
	10.87	— 1.50	6.547	— .230	— 21.5
	12.14	— 1.62	6.268	— .259	— 21.7

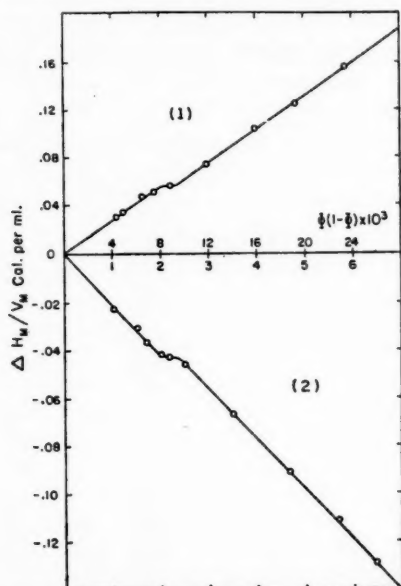


FIG. 1. Heats of mixing at 25° C. of polyvinyl acetate (mol. wt. 536,000) in: (1) methanol, (2) *s*-tetrachloroethane.

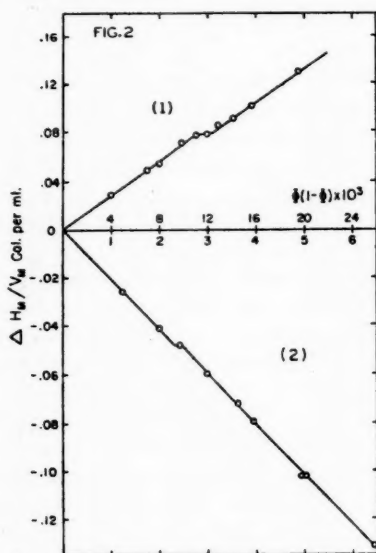


FIG. 2. Heats of mixing at 25° C. of polyvinyl acetate (mol. wt. 255,000) in: (1) methanol, (2) *s*-tetrachloroethane.

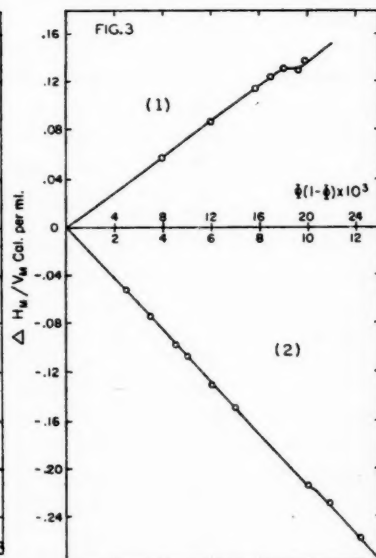


FIG. 3. Heats of mixing at 25° C. of polyvinyl acetate (mol. wt. 29,000) in: (1) methanol, (2) *s*-tetrachloroethane.

ethane. The values of B given in the table are derived from equation [1] below the critical concentration and from the following equation above the inflection point:

$$[6] \quad \Delta H_M/V_M = B\Phi(1 - \Phi) + C$$

where C is the parallel displacement of the curve before and after the inflection point, along the $\Delta H_M/V_M$ axis.

The molecular weights of the fractions M_v were calculated from an equation given by Wagner (11) for polyvinyl acetate in solution in acetone at 25° C.:

$$[7] \quad \log M_v = 1.47 \log[\eta] + 5.519.$$

Table II gives the intrinsic viscosities, at 25° C., of the various fractions of polymer in the two solvents used in this study.

TABLE II
INTRINSIC VISCOSITIES OF POLYVINYL ACETATE FRACTIONS
IN METHANOL AND *s*-TETRACHLOROETHANE AT 25° C.

M_v	$[\eta]$ in methanol	$[\eta]$ in <i>s</i> -tetrachloroethane
536,000	0.79	2.10
255,000	0.62	1.54
191,000	—	1.00
29,000	0.25	0.42

DISCUSSION

When the results given here are compared with those of Daoust and Rinfret (2) a great improvement is noticed. This must be ascribed to a more elaborate experimental technique, as described above, and to a greater care in reducing impurities in polymer and solvent such as elimination of all trace of moisture. A relatively slight increase in accuracy has shown that the curves of $\Delta H_M/V_M$ vs. Φ such as that of Fig. 4 (of Reference 2, above) were actually straight lines. With this knowledge it was possible to make a better choice of concentrations to be investigated and to reject spurious results due to losses by evaporation and other causes.

Figs. 4 and 5 show the displacement of the inflection point with molecular weight for a poor solvent, methanol, and a very good solvent, *s*-tetrachloroethane. The values of the parameters B and C together with the critical concentration are given in Table III. The accuracy of positioning of the inflection point for the low molecular weight fraction (Fig. 3) is lower than that of the other fractions, but the experimental results (Table I) show that the inflection points are real even if their final position is subject to slight revision. A remarkable feature is that after the inflection point the slope of the curves, B , resumes its former value. Parameter B is also quite constant over the range of molecular weight; any slight change with molecular weight might be ascribed to previous history of the polymer fraction. Similar remarks can be made about C , although here there may be a real effect in the higher value found in both solvents with the 536,000 molecular weight fraction.

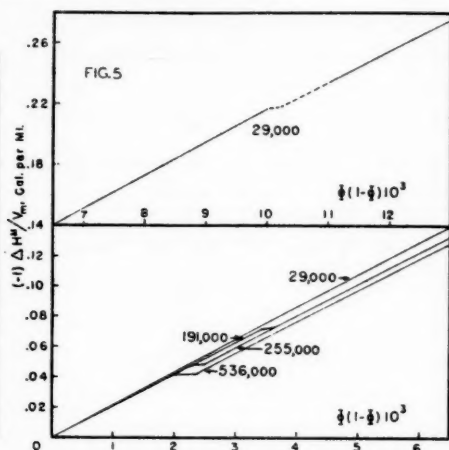
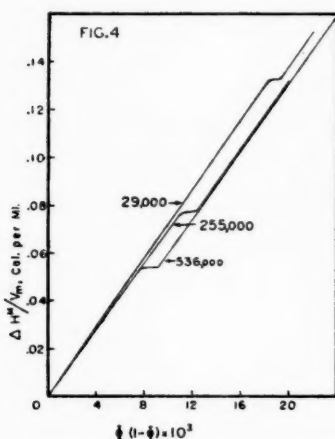


FIG. 4. Heats of mixing at 25° C. of various polyvinyl acetate fractions in methanol.
 FIG. 5. Heats of mixing at 25° C. of various polyvinyl acetate fractions in *s*-tetrachloroethane.

TABLE III
 PARAMETERS *B* AND *C* AND THE CRITICAL CONCENTRATION FOR VARIOUS
 FRACTIONS IN METHANOL AND *s*-TETRACHLOROETHANE

Solvent	Fraction mol. wt.	Critical volume fraction $\times 10^3$	<i>B</i> , cal. per ml.	<i>C</i> , cal. per ml. $\times 10^3$
Methanol	536,000	0.86	+ 6.9	-0.9
	255,000	1.2 ₁	+ 7.0	-0.7 ₁
	29,000	1.9 ₂	+ 7.2	-0.6
<i>s</i> -Tetrachloroethane	536,000	0.22	-20.9	+0.7
	255,000	0.24	-21.1	+0.4
	191,000	0.35	-20.7	+0.3 ₁
	29,000	1.05	-21.6	+0.4 ₁

As stated in the introduction, parameter *B* measures the net heat of interaction per contact of polymer segment - solvent molecule times the number of such contacts per segment. Although the total number of contacts between polymer and solvent increases with concentration, *B* will be essentially constant at low concentrations. At the moment of critical concentration Weissberg, Simha, and Rothman (12) have shown that the random polymer coils would be compressed because of the tendency of a polymer molecule to exclude all others from the space it occupies. Since this phenomenon occurs at only one concentration, it appears as a parallel displacement of the curves and parameter *C* is not affected by concentration. This effectively amounts to a new spatial distribution of polymer and solvent in the solution. An interesting property of the critical concentration lies in its use in the calculation of the dimension of the polymer molecule in solution. By making the assumption

that at this point each molecule occupies a sphere that has a diameter equal to the end-to-end distance of the chain, this dimension can be calculated. Given A the side of a cube occupied by N_s spheres of diameter D one finds for closed-packed spheres:

$$[8] \quad N_s = 1.41 A^3/D^3.$$

If $A = 10$ cm. the number of spheres becomes the number per liter. This number N_s is also given by:

$$[9] \quad N_s = (m_c \times N)/M$$

where N is Avogadro's number, m_c , the critical concentration in grams per liter, and M , the molecular weight of the polymer. From [8] and [9], it is found that:

$$[10] \quad D = 13.3(M/m_c)^{1/3} \text{ \AA}.$$

The dimensions obtained from equation [10] are given in Table IV where they are compared with the value of $(\bar{r}^2)^{1/2}$, the root-mean-square separation of

TABLE IV
MOLECULAR DIMENSIONS OF POLYVINYL ACETATE IN SOLUTION AT 25° C.

Solvent	Fraction mol. wt.	D in \AA equation [10]	$(\bar{r}^2)^{1/2}$ in \AA equation [11]
Methanol	536,000	500	580
	255,000	350	420
	29,000	140	150
s-Tetrachloroethane	536,000	790	810
	255,000	600	570
	191,000	480	450
	29,000	180	180

polymer chain ends from Flory's equation:

$$[11] \quad (\bar{r}^2)^{1/2} = (M[\eta]/\phi)^{1/2} \text{ cm.}$$

where ϕ is a universal constant derived by Kirkwood and Riseman (6), who found the value 3.6×10^{21} , and recently determined experimentally by Newman, Krigbaum, Laugier, and Flory (7). Their best value is given as 2.5×10^{21} .

Concordance of the two methods in Table IV for calculating molecular dimensions is good enough to suggest equating D and $(\bar{r}^2)^{1/2}$ to give:

$$[12] \quad 13.3(M/m_c)^{1/3} = (M[\eta]/\phi)^{1/2} \times 10^8$$

and therefore:

$$[13] \quad m_c = 5.9/[\eta] \quad \text{and}$$

$$[14] \quad \Phi_c = 5.9 \times 10^{-3}/(d_p \times [\eta])$$

where Φ_c is the critical volume fraction and d_p the density of the polymer.

Because of the differences between D and $(\bar{r}^2)^{\frac{1}{2}}$ in Table IV, this equation should be taken as a semiquantitative guide to the value of the critical concentration, until further investigation.

ACKNOWLEDGMENTS

We wish to express our thanks to Canadian Industries Limited for providing a Fellowship to one of us (M.P.). We are also grateful to the National Research Council for grants in aid of research and summer assistance.

REFERENCES

1. BOYER, R. F. and SPENCER, R. S. *J. Polymer Sci.* 5: 375. 1950.
2. DAOUST, H. and RINFRET, M. *Can. J. Chem.* 32: 492. 1954.
3. FLORY, P. J. *J. Am. Chem. Soc.* 65: 372. 1943.
4. HILDEBRAND, J. H. and SCOTT, R. L. *The solubility of nonelectrolytes*. 3rd ed. Reinhold Publishing Corporation, New York. 1950.
5. HORTH, A. and RINFRET, M. *J. Am. Chem. Soc.* 77: 503. 1955.
6. KIRKWOOD, J. G. and RISEMAN, J. *J. Chem. Phys.* 16: 565. 1948.
7. NEWMAN, S., KRIGBAUM, W. R., LAUGIER, C., and FLORY, P. J. *J. Polymer Sci.* 14: 451. 1954.
8. SCATCHARD, G. *Chem. Revs.* 8: 321. 1931.
9. STAUDINGER, H. *Die hochmolekularen Verbindungen*. Verlag von Julius Springer, Berlin. 1932. p. 128.
10. STREETER, D. J. and BOYER, R. F. *J. Polymer Sci.* 14: 5. 1954.
11. WAGNER, R. H. *J. Polymer Sci.* 2: 21. 1947.
12. WEISSBERG, S. G., SIMHA, R. S., and ROTHMAN, S. *J. Research Natl. Bur. Standards*, 47: 298. 1951.

SOME THERMODYNAMIC CONSIDERATIONS OF SURFACE REGIONS

SURFACE TENSION, ADSORPTION, AND ADSORPTION HYSTERESIS¹

By E. A. FLOOD

ABSTRACT

Thermodynamic conditions for equilibrium between bodies which exert forces upon one another are discussed. The two bodies are treated as assemblies of infinitesimal volumes of pure components and the influence of the mutual potential fields examined. The results provide a thermodynamic description of surface tension and certain types of adsorption phenomena, as well as throwing considerable light on adsorption hysteresis.

INTRODUCTION²

In general where any two bodies are in contact with one another, they exert forces upon each other, usually only the very short range forces being of importance thermodynamically. As a consequence of these short range forces, when considering equilibria within the interfacial region, we cannot "regard as immaterial the position . . . of the various homogeneous parts of which . . ." each body is composed, as done by Gibbs (7) in deducing the phase rule. In general, these short range forces give rise to potentials of position.

The influence of these potentials on the thermodynamic conditions for equilibrium may be treated formally, in much the same way as the influence of the gravitational potential is treated. However, in the case of the gravitational potential, the force function of the field is treated as though it is independent of the state of the substance, while in the case of the interaction between two bodies, the "potential" is almost certainly influenced by the state

¹Manuscript received January 21, 1955.

Contribution from the Division of Pure Chemistry, National Research Council, Ottawa, Canada. Issued as N.R.C. No. 3581. An Abstract of this paper was presented at the Symposium on Problems Relating to Adsorption of Gases by Solids at Kingston, Ontario, September 10-11, 1954. The text of the paper presented at the Symposium appears in the special issue of the Canadian Journal of Chemistry covering the Symposium (5).

²A primary object of this enquiry is to obtain some insight into the physical factors which control rates of flow of fluids through porous adsorbents. The author is greatly indebted to Dr. Otto Maass of McGill University for encouragement and assistance in the pursuit of this problem.

In the case of adsorption of condensable gases, liquid-vapor interfaces as well as solid-vapor interfaces are to be expected. Accordingly, it is necessary to know something of the natures of these surface regions in order to discuss "surface" flow mechanisms.

Evidence has been presented previously that where adsorbates are contained within pores which are fairly large compared with molecular dimension (10^{-7} to 10^{-8} cm.) adsorbates may be regarded as Polanyi compressed films, and that flow mechanisms of such films are essentially those of classical laminar flow, but flow rates are controlled by density and pressure gradients (both normal and parallel to the direction of flow) that are functions of the surface forces. These adsorbate gradients are very different from the directly observable or applied "gradients" of the gas outside the range of the surface forces. Generally adsorbate gradients are not directly observable and must be measured indirectly or inferred from measurements of adsorbate densities, surface tensions, surface energies, or other measurable average properties. Where we can determine adsorbate density gradients and can assume that the adsorbate behaves as a single substance, we can calculate corresponding pressure gradients, and make considerable progress in relating net flow rates to the physical structure of these fine grained porous adsorbents; while where the adsorbate cannot be regarded as a single component fluid the problem of correlating the permeability with the structure of an adsorbent, if at all possible in any literal sense, is much more complex.

of the bodies in contact (i.e., the potential of position may be a function of the density, pressure, and temperature as well as of the mass).

When two bodies of different kinds of matter are in contact with one another, the different kinds of material will eventually diffuse into one another to a greater or lesser degree, and the whole system everywhere must be regarded ultimately as a two component system. However, there are many cases where these diffusive processes are so slow, or where the equilibrium states are such, that the two bodies, including the interfacial regions, may be regarded as two distinct volumes each consisting of a single component. Evidently we must assume in such cases that the surface "potential" is such that, as the "boundary" of one of these volumes of pure component is approached, very strong repulsive forces are called into play ultimately limiting the density of this component to vanishing values (i.e. preventing interpenetration). When the two bodies in contact are more or less rigid solids, the short range surface forces acting between the bodies will give rise to states of stress in the interfacial regions which differ from those prevailing throughout the bulk phases. These states of stress will be accompanied by deformations, or states of strain, in the interfacial region which will result in small over-all deformations of the two bodies as they are brought into contact. If, however, one of the bodies is a highly compressible fluid, the density of the fluid in the interfacial region will be very materially influenced by the surface forces, resulting in comparatively large changes in volume of the compressible fluid as a result of its being brought into contact with the solid, i.e., adsorption will occur.

Thus we may consider the whole of the volume of the compressible fluid (or gas) as constituting a single component system bounded by regions of complex potential fields which are functions of the pressure, temperature, and natures of the gas and solid.

We confine our interest to cases where all the material of the compressible component in the interfacial region is fluid, and we shall inquire into the thermodynamic conditions for equilibrium which must prevail in such complex single component fluid systems. While the thermodynamic conditions for equilibrium in constant potential fields are discussed in standard texts, the thermodynamics of the more general case where the force function of the field may depend on the density, pressure, and temperature of the fluid has been largely ignored.

In Part I of what follows, we present some general thermodynamic considerations of the equilibrium conditions which must prevail in complex single component fluid systems; in Part II, these ideas are applied to surface tension problems; and in Part III, they are applied to gas adsorption problems.³

It is shown that these ideas lead to a plausible detailed thermodynamic description of surface tension phenomena, and that in the case of adsorption phenomena, they predict results capable of experimental verification.

³When applied to adsorption theory, the thermodynamic considerations lead to what is essentially a Polanyi (14) adsorption potential theory, but where the "potential" of the surface is variable, i.e., is a function of the equilibrium pressure of the gas, the density of the adsorbate, etc., thus providing for so-called "co-operative effects".

I. SINGLE COMPONENT COMPLEX FLUIDS

Thermodynamics is, strictly, a science of observable quantities and hence is a science dealing with the properties of matter in bulk. Accordingly, the validity of the assigning of thermodynamic properties to elementary volumes of material is open to question.

Tolman (19) in his theory of surface tension treats elementary laminar volumes as thermodynamic systems and discusses the validity of such treatments. When we consider the pressure gradients, energy gradients, etc. of a gas in a gravitation field, we assume that such gradients are continuous. Thus we tacitly assume that laminae of infinitesimal dimensions have thermodynamic properties. It is evident that when we deal with helium we may take as the thickness of a lamina a dimension considerably less than that of the diameter of the spherical molecule, only those molecules whose centers of mass lie within the lamina being considered as "contained" within the elementary laminar volume. In this way it is quite possible to construct statistical model fluids that are very accurate descriptions of real gases, and which are equally applicable to infinitesimal volumes and to large finite volumes, equally applicable to volumes small or large compared with molecular dimensions. If the fluid molecules are dipoles and may be subject to orientation in a field, the situation is somewhat more complex and it might seem that we must consider adjacent laminae as consisting of different "kinds of material" as would be the case in an ionic crystal. In the latter case the long range order is a permanent condition, a state of the system, and even after very long periods of time, neighboring elementary laminar volumes cannot be regarded as consisting of the same substance, i.e., they are not reversibly convertible into one another by any ordinary sort of thermodynamic process (e.g., layers containing almost wholly chloride ions and layers containing sodium ions are not thermodynamically interconvertible). If, however, any orientation forces can be resolved into forces and couples acting on and about molecular mass centers, a statistical model fluid can be constructed such that elementary volumes regardless of size can be regarded as elementary thermodynamic systems containing the same component as the whole assembly of elementary volumes. Without looking more closely into statistical details of such problems, we shall define a single component fluid complex as follows: an assembly of elementary fluid volumes, where every elementary volume is thermodynamically identical with an equal elementary volume of a single fluid in some bulk state, the bulk state being in reversible equilibrium with externally applied forces no matter how bizarre these forces may be. Thus the state of each elementary volume corresponds exactly to a bulk state of a single substance under specific external forces. All the elementary volumes are thus inherently capable of reversible thermodynamic conversion into another. Since we will be mainly concerned with fluids, we shall assume that pressures of elementary volumes are equal in all directions and that all pressure, energy, density gradients, etc. are continuous. The forces transmitted across boundaries of adjacent elementary volumes are necessarily equal.

Thermodynamic Equilibria in Single Component Complexes

When two bodies exert forces upon one another, the energy associated with separating them is not strictly a property of either body alone. However, we may arbitrarily fix the energy of one of these bodies and consider it as being in a reference state and accordingly assign the energy of separation to the second body. This is the normal procedure when considering equilibrium in a force field. Since in the usual derivations of the conditions for equilibrium in force fields the force field is assumed independent of the state of the body, it is necessary to re-examine the equilibrium when the potential of position of unit mass may be a function of the volume of the mass.

The condition that changes in thermodynamic states of a system under the action of external forces shall be reversible is that the heat received by the system during such changes shall be equal to the change in the energy of the system plus the maximum work which the system can do against the external forces if such a maximum exists. When no potential of position is involved and the only work is associated with a change in volume, this condition for reversibility is expressed by the well-known equation

$$dE_0 = TdS - pdv + \mu_0 dm$$

where E_0 is the intrinsic energy, T the temperature, S the entropy, p the pressure, v the volume, μ the intrinsic thermodynamic potential, and m the mass.

When a "potential" of position is involved we can write where

$$\begin{aligned} [1] \quad dE &= dE_0 + d\omega = TdS - pdv + \mu_0 dm + d\omega \\ &= TdS - pdv + \mu_0 dm + \Omega dm \\ &= TdS - pdv + \mu_0 dm + \frac{\partial}{\partial m} \int_{x_0}^x f(x) dx \cdot dm \\ &= TdS - pdv + \mu dm \end{aligned}$$

where

$$d\omega = \Omega dm = \frac{\partial}{\partial m} \int_{x_0}^x f(x) dx \cdot dm,$$

and $(\partial/\partial m) \int_{x_0}^x f(x) dx$ represents the maximum or reversible work associated with moving unit mass at constant S and v from the initial position x_0 to the final position x . This work is assumed dependent only on the initial and final positions in the potential field. Such fields are sometimes referred to as scalar fields. It is implied that in the reference state corresponding to x_0 , $f(x)$ is zero. Other relations expressed by the equations are self-explanatory.

By definition of the single component complex, Equation [1] is applicable to every element of volume of the assembly, and accordingly an equation of similar form is applicable to assemblies of these volumes. The conditions for equilibrium between these volumes will depend upon the physical conditions assumed applicable within the complex, or between elements of the complex and a reference volume. Since the complex is essentially a fluid mass, heat and

matter may be assumed to be in a state of flux between the various parts. Accordingly we assume the following physical conditions: (a) increments of heat-energy and mass, independently, may flow in to or out of any of the volumes concerned, (b) no work is involved in the transport of entropy through finite distances, (c) the transport of mass through finite distances involves performance of work against the force function of the field. With these conditions, following exactly the method of Gibbs, it can readily be shown that the necessary and sufficient conditions for equilibrium throughout the complex are: (a) uniformity of temperature, (b) uniformity of total potential per unit mass, μ or $\mu_0 + \Omega$. Evidently the existence of potentials of position that may be functions of the volume as well as of the mass of the substance concerned does not change the basic equilibrium conditions applicable to systems in constant potential fields.

Equation [1] may be written in the form

$$\begin{aligned} dF &= -SdT + vdp + \mu_0 dm + \frac{\partial}{\partial m} \int_{x_i}^x f(x) dx \cdot dm \\ &= -SdT + vdp + \mu dm \end{aligned}$$

where $F = E - TS + pv$ and $\mu = \partial F / \partial m = \partial E / \partial m$, etc.

Assuming that $F(T, p = 0, x, m = 0) = 0$ and that $\int_{x_i}^x f(x) dx = 0$ when $m = 0$, we can write for the potential F of any mass m of fluid at any position x under any pressure p ,

$$F = \int_{p=0, m=0}^{p, m} (vdp + \mu dm),$$

the path of integration corresponding to increasing the mass of material at some position x while v , p , and μ take particular values for various values of m .

We suppose that the complex is in equilibrium with a bulk reference fluid of uniform properties, and that the complex remains in reversible equilibrium with the bulk reference fluid throughout a path where the density and pressure of the reference fluid vary from zero to specified values.

Assigning the value x_0 to the bulk reference state and the value x_{a_i} to the i th element of the complex, we can write for equal masses of material at x_0 and x_{a_i}

$$F_0(p_1, m_i, x_0) = \int_{p=0, m=0}^{p=p_1, m=m_i} (vdp + \mu_0 dm),$$

$$F_{a_i}(p_{a_i}, m_i, x_{a_i}) = \int_{p=0, m=0}^{p=p_{a_i}, m=m_i} (vdp + \mu_{a_i} dm),$$

and $F_0 = F_{a_i}$ and $\mu_0 = \mu_{a_i}$ throughout the path of integration. Also we may write

$$F_{a_i} = \int_{p=0, m=0}^{p=p_1, m=m_i} (vdp + \mu_0 dm) + \int_{p_1, x_0}^{p_{a_i}, x_{a_i}} vdp + \int_{x_0, p_{a_i}}^{x_{a_i}, p_{a_i}} f(x) dx$$

where

$$\int_{p_1, x_0}^{p_{a1}, x_0} v dp + \int_{x_0, p_{a1}}^{x_{a1}, p_{a1}} f(x) dx = \int_{p_1, x_{a1}}^{p_{a1}, x_{a1}} v dp + \int_{x_0, p_1}^{x_{a1}, p_1} f(x) dx.$$

It will be noted that $\int_{p_1, x_0}^{p_{a1}, x_0} v dp$ is not necessarily equal to $\int_{p_1, x_{a1}}^{p_{a1}, x_{a1}} v dp$. When they are equal, the equation of state (v of p , T constant) is independent of the field. When the integrals are not equal, the force function of the field is a function of v .

We may suppose the uniform reference fluid broken up into elementary volumes δv_i of mass δm_i equal to the mass of each elementary volume of the complex δv_{a1} at x_{a1} . For the equilibrium between these elementary volumes, the x coordinates remaining constant while δm_i and the pressures vary, we have

$$\delta v_{1i} \cdot \delta p_1 + \mu_0 \delta m_i = \delta v_{a1} \cdot \delta p_{a1} + \mu_{a1} \delta m_i,$$

and since $\mu_0 = \mu_{a1}$,

$$\sum_i \delta v_{a1} \cdot \delta p_{a1} = \delta p_1 \cdot \sum_i \delta v_{1i} = \frac{\delta p_1}{\rho_1} \sum_i \delta v_{a1} \cdot \rho_{a1}.$$

Therefore

$$v_a \delta \bar{p}_a^* = v_a \bar{p}_a \cdot \frac{\delta p_1}{\rho_1}$$

where the density of the uniform reference fluid is ρ_1 , and $\rho_1 = \delta m_i / \delta v_{1i}$. Hence

$$[2] \quad \bar{p}_a^* = \int_{p=0, m=0}^{p=p_1, m=m} \bar{p}_a / \bar{p}_1 \cdot dp_1.$$

Thus the volumetric mean pressure \bar{p}_a^* can be determined if the volumetric mean density \bar{p}_a is known as a function of p_1 , i.e., if m and v_i are known functions of the pressure, p_1 , of the reference gas along a path of thermodynamic reversibility where the equilibrium pressures vary from zero to p_1 while m varies from 0 to m .

It will be noted that since \bar{p}_a and ρ_1 are positive, \bar{p}_a^* is necessarily positive for any path of thermodynamic reversibility where the equilibrium pressure increases from zero to p_1 . If, however, other paths of thermodynamic reversibility intersect this path at points below p_1 , say at p_1' , so that if the pressure of reference fluid is raised from zero to p_1 and then reduced to p_1'' below p_1' , the system may follow the second path from p_1' to p_1'' and

$$\begin{aligned} \bar{p}_a^* &= \int_0^{p_1} \frac{\bar{p}_a}{\rho_1} \cdot dp_1 + \int_{p_1}^{p_1'} \frac{\bar{p}_a}{\rho_1} dp_1 + \int_{p_1'}^{p_1''} \frac{\bar{p}_a'}{\rho_1} dp_1 \\ &= \int_0^{p_1'} \frac{\bar{p}_a}{\rho_1} \cdot dp_1 - \int_{p_1'}^{p_1''} \frac{\bar{p}_a'}{\rho_1} \cdot dp_1. \end{aligned}$$

If the second integral is larger than the first, \bar{p}_a^* may be negative.

When $\bar{p}_a > \rho_1$, $\bar{p}_a^* > p_1$ and the potential of position of the reference fluid is greater than the average potential per unit mass of the complex.

The mean "potential" difference between the complex and the reference fluid may be expressed by

$$\sum_i \frac{\bar{p}_{a,i} - p_1}{\bar{\rho}_{a,i} |_{p_1 - p_{a,i}}} \cdot \rho_{a,i} \cdot \delta v_{a,i} = -\omega$$

where $\bar{\rho}_{a,i} |_{p_1 - p_{a,i}}$ is the mean density of the reference fluid over the pressure interval p_1 to $p_{a,i}$. Thus

$$\omega = c v_a (p_1 - \bar{p}_a^*)$$

where c is a dimensionless positive quantity. If $\bar{p}_a^* > p_1$, $c \geq 1$. If the material is incompressible in all of the ranges p_1 to $p_{a,i}$, $c = 1$. In general ω will be dependent on the distribution function, $v(\omega)$, of the complex and upon the equation of state of the reference fluid. It will be noted that $\Omega(x_{a,i} - x_0, p_1)$ is not necessarily the same as $\Omega(x_{a,i} - x_0, p_{a,i})$. Thus in general we cannot determine ω when \bar{p}_a^* can be determined unless the fluid is incompressible in the various pressure intervals p_1 to $p_{a,i}$. If the reference fluid is a condensable gas and p_1 is above the saturation pressure, that is p_1 is the pressure of the reference liquid, then if the liquid is practically incompressible, we can obtain a measure of ω , i.e., $\omega = v_a (p_1 - \bar{p}_a^*)$.

Phase Rule Considerations

We have assumed that each elementary volume or lamina is thermodynamically identical with equal elementary volumes of the fluid in some bulk state. Accordingly elementary volumes having the same p , T , and μ but different densities are to be regarded as different phases in the sense of the phase rule. However, the fundamental thermodynamic equation has in addition to S , v , and m one more variable, namely, that measuring the force function of the field, $f(x)$. When v of p (T and m constant) is not influenced by $f(x)$, if the potential of position $\Omega(x - x_0, p_1)$ vanishes at three values of x in the surface region, and the corresponding laminae have three different densities for given values of T , p , and μ , the system will be invariant in the sense of the phase rule. But if the relation between v and p is influenced by $f(x)$, then where $f(x)$ is not zero, the density of a fluid lamina for given values of p may differ from the density where $f(x)$ is zero. Since $\Omega(x - x_0, p_1)$ may vanish for some value of x for which $f(x)$ does not vanish, we may have $\Omega(x - x_0, p_1)$ zero for three values of x , while $f(x)$ is zero for only two of these values. Under these circumstances, we may have two density states corresponding, say, to normal liquid and vapor, and a third density state where $f(x)$ is large, while the system is still monovariant in the phase rule sense.

We cannot, in general, suppose a fluid divided into laminae and treat the "spreading pressure" of each layer as an independent variable in order to calculate the phase "variance". However, when a force field is involved $p_{a,i}$ will in general differ from p_1 and may be regarded as constituting a measure of the potential of the field and of $f(x)$ (cf. Rowley and Innes (16)).

In Part II of this paper the interface between a liquid and vapor of a single substance will be treated as a single component complex and in Part III the boundary of a fluid or gas in contact with a solid of a different kind of substance will be similarly treated. While both cases are essentially similar, in the former

case both bulk phases consist of a single component while in the latter case the two bulk phases are different components. In both cases surface forces are assumed to be classical.⁴

II. SURFACE TENSION

The Liquid-Vapor Interface, A Single Component Complex Fluid

Consider a liquid separated from its vapor by a flat interface. Far from the interface the net hydrostatic pressures of the liquid and of the vapor are the same and are, of course, positive. The interfacial region, however, exhibits a tension, and accordingly negative pressures or negative stress intensities are to be expected in this region. If following Tolman (19) we think of the interface as made up of very thin laminae parallel with the surface and if we suppose the material constituting these laminae to be fluid so that stress intensities acting on elementary volumes (i.e., laminae) are equal in all directions, we must suppose a sharp pressure gradient to exist along the normal to the surface, the gradient vanishing within the body of the liquid and within the vapor.

Let $p(x)$ be the pressure of the fluid as a function of x , where x is the distance along a normal to the surface, measured from liquid to gas. If h is the thickness of the interface, the thickness of the region wherein $p(x)$ varies with x , then

$\int_x^{x+h} p(x) dx \equiv \bar{p}(x) \cdot h$ is the net parallel surface force exerted by unit area of the surface region, and $\bar{p}(x)$ is the mean value of the stress intensities exerted by the various laminae parallel with the surface. If $\bar{p}(x)$ is negative, $-\bar{p}(x) \cdot h$ is literally a positive "surface tension". The work done by the surface system when the surface of area σ is increased by $d\sigma$, the thickness remaining constant, is, of course, $\bar{p}(x) \cdot h \cdot d\sigma$. Hence the corresponding Helmholtz free energy change is given by $(\partial A / \partial \sigma)_{T,h} = -\bar{p}(x) \cdot h = \gamma$. Thus, this "surface tension", γ , is unambiguously the Helmholtz free energy per unit surface.

It may be remarked that considerable confusion (18) exists in the literature dealing with the relations between "surface tension" and "surface free energy". This confusion arises partly from following Lewis and Randal (11) and equating the change in Gibbs free energy, F (where $F = E - TS + pV$), of the surface to the work of stretching the film, i.e., in writing $dF_T = \gamma d\sigma$ instead of

"If the energy states of molecules of the fluid with respect to the surface force field are continuous and the distribution of these states largely classical in character, the detailed structure of all of the energy states at a given temperature will be largely characteristic of the fluid in some bulk state. Accordingly, fluid laminae under the influence of such fields will behave as a single substance in the sense that laminae of the bulk states of fluid can exist in equilibrium with external forces in states that are thermodynamically practically identical with corresponding laminae in the force field. However, when the energy states of the molecules in the surface layers are quantized and the surface forces large, the detailed structure of the energy states at any given temperature may be quite different from those of any bulk state of the pure fluid. Accordingly, laminae under the influence of such potential fields will not behave as the same substance, thermodynamically, as the bulk fluid, and the assembly of surface laminae cannot be treated as an assembly of volumes of a single component."

A pure component of a chemical compound or of a solution is, in general, capable of reversible transformation with the same substance in the compound or solution. For such a process $\Delta F = 0$, but ΔA , ΔE , $\Delta S \neq 0$. For the special case of an ideal gas solution where each gas behaves as a vacuum to each other gas ΔF , ΔA , ΔE , $\Delta S = 0$ but $\Delta v \neq 0$, $\Delta \bar{p} \neq 0$. When ΔF , ΔA , ΔE , ΔS , Δv , $\Delta \bar{p}$, etc. = 0 the forces of interaction between the bodies in the combined system take the place of the external forces of the pure components. The latter case may be called "mechanical" or "physical" interaction, as distinct from the first case of "chemical" interaction and from the second case of pure "solution".

equating the Helmholtz free energy to this work, i.e., instead of writing $dA_T = \gamma d\sigma$.⁵ However, these difficulties are due mainly to the fact that some authors treat the surface as an isolated thermodynamic system distinct from the material lying on either side of it, while others define surface tension by $(\partial A / \partial \sigma)_{T, \dots} = \gamma$ where the operation $(\partial A / \partial \sigma)_{T, \dots}$ is applied to systems containing surfaces and bulk material. Thus in the latter case, a distortion of a solid at constant volume would yield a "surface free energy" or "surface tension" quite different from the "surface tension" that would be obtained if the process $(\partial A / \partial \sigma)_{T, \dots}$ corresponded to increasing the number of crystals while decreasing their size, their shapes remaining constant. In the case of liquids with flat surfaces, if $(\partial A / \partial \sigma)_{T, \dots}$ corresponds to the process of changing the shape of the container of a liquid-gas system so that the surface area of the interface is increased while the volume remains constant,

$$(\partial A / \partial \sigma)_{T, \dots} = [\bar{p}(x) - p_0] h$$

where p_0 is the vapor pressure of the liquid. Evidently the operation $(\partial A / \partial \sigma)_{T, \dots}$ applied to a system containing surfaces and bulk material does not in general constitute a measure of a definite quantity, the operation being capable of yielding a variety of "surface tensions" depending upon further particulars not specified by the operation.

In the case of a liquid the actual net force of the surface tension is one of its most striking characteristics and is directly measurable. In most cases the methods of measurement of the surface tension of a liquid correspond closely to the operation $(\partial A / \partial \sigma)_T$ applied to the surface layer only. Accordingly, in what follows we shall consider that surface tension is the net parallel mechanical force actually exerted by the surface. Thus we put $-\bar{p}(x) \cdot h = \gamma$.⁶

In general, if a surface has an energy per unit surface area, under equilibrium conditions the surface energy will be a minimum consistent with its entropy. Thus the flat surface will not be quite smooth, but will have a somewhat greater area than the flat surface, the excess area corresponding to the thermal energy of motion of the surface as a whole. In the absence of gravitational and other external fields, changes in position of the interface will have no effect on the equilibrium within the systems. If we suppose the surface region divided into geometrically flat elementary laminae parallel with the mean position of the surface region and of area equal to the apparent area of the "flat" interface separating a liquid from its vapor, the assembly of laminar

⁵Replacing p by $\bar{p}(x) \cdot h \cdot \sigma$ then for the surface system only, $dw = \bar{p}(x) \cdot h \cdot d\sigma$, $dA_T = -\bar{p}(x) \cdot h \cdot d\sigma$, $dF_T = h \cdot \sigma \cdot d\bar{p}(x)$, and if $\bar{p}(x)$ is constant, $dF_T = 0$. Thus increasing the area of a flat surface is, formally, exactly equivalent to increasing the volume of a phase in equilibrium with other phases. If a system consists of bulk phases and surface phases so that the potential per unit mass is given by $\mu = E - TS + p\sigma - \gamma\sigma$, etc., we should write $dF = -SdT + vdp - \sigma d\gamma$, and when T , p , and γ are constant, $dF = 0$ irrespective of any work done when stretching the surface or when increasing the volume.

⁶Some writers regard the "surface tension" as a fiction but regard the surface free energy as real. This is much like regarding the pressure of a gas as a fiction but its thermodynamic potential as real (1). In the case of ionic substances "surface free energy" phenomena might be exhibited by very marked gradients in electrical charge density and corresponding gradients in mass density. In this case mechanical stress gradients in the surface regions might be quite negligible and the actual "surface tension" practically zero.

volumes will constitute, thermodynamically, a single component complex as defined in Section I above. Evidently all of the thermodynamic relations applicable to the single component fluid complex are applicable to liquid-vapor systems including the interfacial regions when these interfacial regions are fluid throughout.

It will be noted that, in general, the mean pressure of laminae within the interfacial region will be negative if the surface tension is positive. If we regard the vapor as the reference fluid and the interfacial region as the complex, the interfacial region cannot be formed reversibly along a constant temperature path of increasing pressure of the reference gas. Thus if we fill a fixed volume with vapor of a condensable substance and increase the pressure until a liquid-vapor interface is formed, if the interface is of finite dimensions and has a positive surface tension, some irreversibility is involved in the process (cf. p. 984). However, we may suppose the volume filled with vapor above the critical temperature and then cooled reversibly so that the meniscus can form reversibly. Along this path \bar{p}_a^* and $\bar{p}(x)$ can become negative reversibly. To form a strictly flat interface by such a process in the absence of other sources of potential, it would appear necessary that the fixed volume be of infinite size. Accordingly, in the absence of condensing surfaces the formation of the flat meniscus by a strictly reversible process would appear to be experimentally unattainable. However, a spherical drop could be formed by such a process at constant volume. Of course, as pointed out by Gibbs (7) curved surfaces of tension cannot be in, strictly, stable reversible equilibrium with any source of constant pressure, in the absence of condensing surfaces or other sources of potential.

Thermodynamic Description of a Fluid Liquid-Vapor Interface

Writing $\Omega(x)$ as the potential of position as a function of the distance x along the normal to the surface, we may take $\Omega(x)$ as zero within the body of the liquid far from the interface. Evidently $\Omega(x)$ must become positive in regions of negative pressure and finally vanish in the interior of the vapor. Accordingly, $\Omega(x)$ must have at least one maximum. Since

$$\begin{aligned}\frac{dF}{dx} &= v \frac{dp}{dx} + \frac{d\Omega}{dx} = 0, \\ v \frac{dp}{dx} &= -\frac{d\Omega}{dx} = f(x)\end{aligned}$$

everywhere along the normal to the surface. When $\Omega(x)$ is a maximum or a minimum $f(x)$ and dp/dx are necessarily zero. Further, as before, taking h as the thickness of the surface region, i.e., the region where $\Omega(x)$ may differ from zero,

$$\int_0^h \frac{dp}{dx} dx = \overline{\frac{dp}{dx}} \cdot h = 0$$

for flat surfaces, and also

$$\int_0^h f(x) dx = \int_0^h v \frac{dp}{dx} dx = v \cdot \overline{\frac{dp}{dx}} \cdot h = 0.$$

The latter two necessary conditions impose a considerable constraint on possible forms of $\Omega(x)$, $p(x)$, and $v(x)$. Thus, if $\Omega(x)$ has only one extreme value and that a maximum at x_m , $0 < x_m < h$. Then since the specific volume $v(x)$ increases by large factors as the vapor is approached from the liquid and the mean value of $v(x)$ on the liquid side of x_m (i.e., in the range 0 to x_m) is less than that on the vapor side of x_m , it follows that the specific volume on the liquid side of x_m must rise to greater values than on the vapor side. Hence, the rapid increase in volume must occur mainly on the liquid side of x_m . The point x_m is the point at which $\Omega(x)$ is a maximum and $p(x)$ a minimum; accordingly in this case the minimum pressure must occur in the region where $v(x)$ is large, i.e., in regions where densities are comparable with vapor densities. The relations are illustrated in Fig. 1. From physical considerations dilute gases cannot exert negative pressures. Accordingly, the relations illustrated in Fig. 1 could only apply to systems where gas densities were relatively high and/or surface tensions small or negative. (If $\bar{p}(x)$ is less than p_0 , the system will exhibit "surface tension" behavior, but if $\bar{p}(x)$ is positive the surface tension is negative.) Evidently, in cases where surface tensions are high and vapor densities much less than liquid densities $\Omega(x)$ cannot have the simple form indicated in Fig. 1. In the case of the flat interface where the bulk liquid and vapor have equal pressures, if $\Omega(x)$ has more than one extreme value in the interval $0 < x < h$, there must be at least three equal values of $p(x)$ in this interval. Thus, there must be at least three laminae having different densities but equal values of T , p , and μ . Accordingly, $(\partial F/\partial p)_x$ must be a function of x ; i.e. the "equation state" must be influenced by the force field. Otherwise the system would be invariant in the sense of the phase rule (cf. I, p. 985). In Fig. 2A the relations between the various functions are shown, assuming $\Omega(x)$ to have the simplest form consistent with a positive surface tension, and $v(x)$ to have a plausible maximum and minimum.

It will be noted that whatever the shape of the curve $\Omega(x)$, if $f(x)$ is positive for any value of x in the interfacial region it must also have negative values. Thus, if material is attracted toward the liquid on the liquid side of the x_m , it must be repelled from the liquid somewhere in the region $x_m < x < h$. Some authors treat the surface forces as though a net thermodynamic potential difference existed between the liquid and its vapor.

The relations indicated in Fig. 2A correspond physically with a case where the "interface" adsorbs its own vapor, i.e., both the density and pressure rise as the interface is entered from the vapor. These relations are consistent with some statistical mechanical descriptions of an interface (20). It is not, of course, necessary from thermodynamic considerations alone that $v(x)$ have a maximum and a minimum.

The $v(x)$ curve as drawn is intended to suggest that in order for molecules to enter the more or less close packed liquid structure some selection is involved resulting in a reduction in density of the "transition" laminae. In the case of very dense liquids this "surface" might behave very much like a solid surface and allow only limited penetration, i.e., a comparatively large percentage of the molecules "striking the surface" would be reflected.

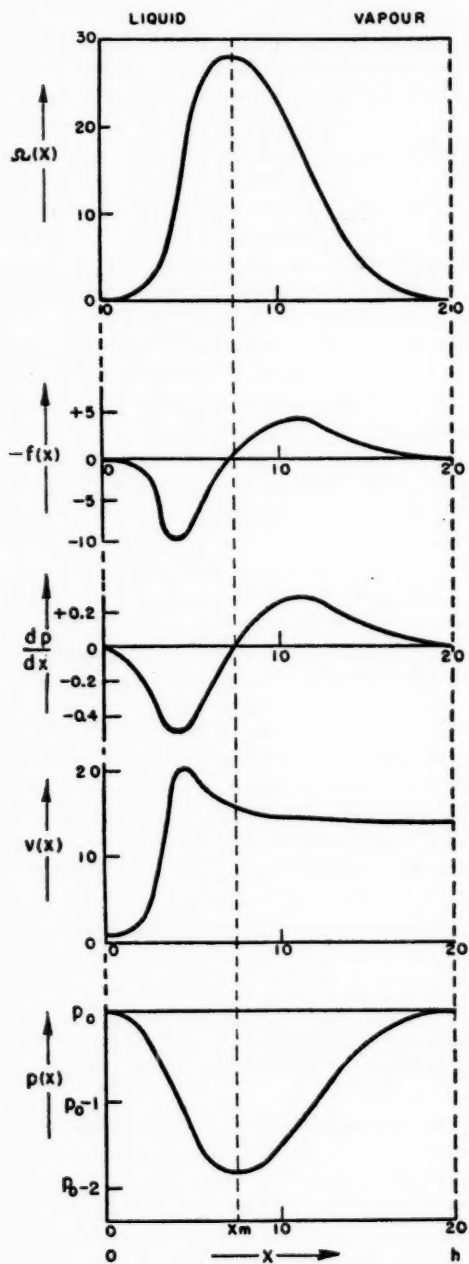


FIG. 1.

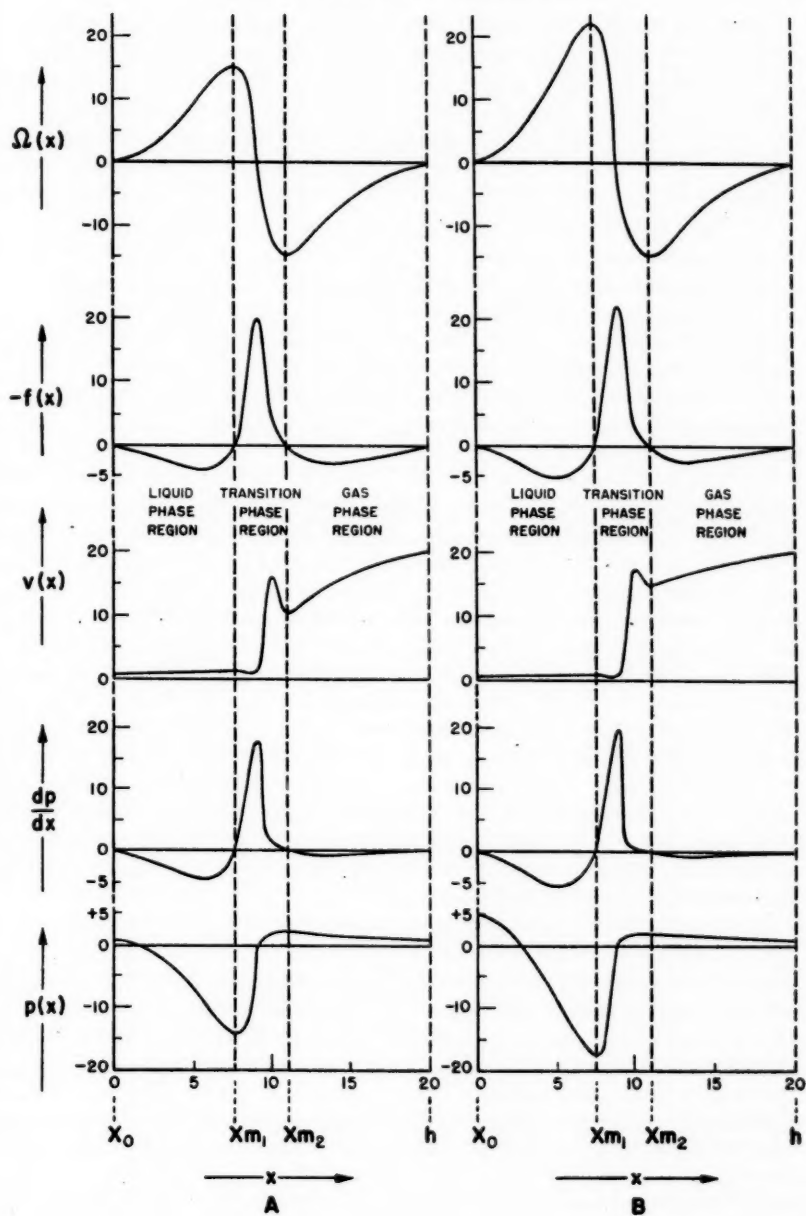


FIG. 2.

Referring to Fig. 2A, at the maximum of $\Omega(x)$, $f(x) = 0$ and $v(x)$ must be that corresponding to normal bulk liquid under the corresponding negative stress. Thus in the region $0 \leq x \leq x_m$, we regard the fluid as being essentially normal liquid under negative hydrostatic stress; in the region $x_m \leq x \leq h$ the fluid is normal gas; while in the intermediate region the equation of state v of p is materially influenced by the force field. Thus in the region where $\Omega(x) \rightarrow 0$ but $f(x)$ approaches a maximum, the fluid is neither normal liquid nor normal gas but is in a transition state.

Capillary Rise and Depression

As a variation of the "flat" interface illustrated by Fig. 2A we may suppose the whole system raised or lowered in a potential field independent of surface potential fields. If we impose the condition $dF = 0$ for this variation the conditions are analogous to capillary rise or depression.

In order that $dF = 0$, the relative changes in liquid and gas pressures will be more or less proportional to densities. Accordingly, the $p(x)$ curve must be distorted so that $\int_0^h (dp/dx) dx \neq 0$. However, for small rises or depressions $\bar{p}(x)$ and $\bar{\Omega}(x)$ will not be changed appreciably, since the magnitudes of $\bar{p}(x)$, $p(x_m)$, etc. are large compared with the pressure changes introduced by the rise or depression. For large depressions, analogous to the effect of curvature on very small droplets, the pressure changes may be comparable with $\bar{p}(x)$. In such cases to retain constancy of surface tension either $\Omega(x)$ must change or the surface thickness, h , or both must change. A natural assumption is that the tendency of the surface to adsorb its own vapor becomes less on surfaces concave toward the dense phase and hence that $\Omega(x)$ is changed. Fig. 2B illustrates a "capillary depression" of the hypothetical system illustrated by Fig. 2A, the values of $\bar{p}(x)$ and h being unchanged, but $v(x)$, $p(x)$, and $\bar{\Omega}(x)$ distorted so that there is a net pressure difference between liquid and vapor. The surface tensions and the surface thicknesses are the same for the two cases, but $\Omega(x)$ is greater for the depressed curved surface. Rice (17) has pointed out that γ might be expected to increase with increasing pressure, in view of the Lewis (11) relation,

$$(\partial\gamma/\partial p)_{v,T} = (\partial v/\partial \sigma)_{p,T}.$$

Since γ is essentially a mean volumetric stress intensity, the interpretation of this equation, if valid at all, is obscure. In general one would expect $\Omega(x)$ to be due largely to the density gradient in the surface region and consequently that changes in the vapor-liquid equilibrium conditions which tended to make the density and compressibility differences vanish would also tend to make $\Omega(x)$ vanish. Both large increases or decreases in vapor pressures would tend toward reducing density and compressibility differences between liquid and vapor. Accordingly, we should expect $\Omega(x)$ to be a maximum for nearly flat surfaces. Thus for exceedingly minute gas bubbles or drops γ should be materially less than that corresponding to the flat surface and the pressure differences across small spheres reach a maximum and finally practically vanish as the radius diminishes.

Thickness of the Interface

For convenience of illustration the difference between the specific volumes of liquid and vapor has been taken much less than is the case with liquid-vapor systems such as water. The magnitudes of the negative pressures are also much smaller with respect to vapor pressures than is the case in ordinary systems of appreciable surface tension.

In the case of the water interface $-\bar{p}(x) \cdot h \approx 70$ dynes cm^{-1} at room temperature. If the thickness of the interface, h , lies between 10 and 1 Å, the mean negative pressure or mean stress intensity must lie between 7 and 70 hundred atmospheres. Evidently such large tensile stresses cannot be sustained in the more dilute regions of the fluid interface and hence practically the whole contribution to $\bar{p}(x)$ must come from the region where the fluid has high tensile strengths, high densities, and low compressibilities, i.e., from the liquid region of the interface. The maximum tensile stress in this region will exceed the mean tensile stress by factors depending on the relative thicknesses of these regions, the factors being the greater, the smaller the ratio of the thickness of the dense region to the thickness of the whole interface. In the case illustrated in Fig. 2A this factor is about five and correspondingly, the maximum tensile stress is between 35 and 3.5 thousand atmospheres for total film thicknesses between 1 and 10 Å. The film thickness as measured by the Rayleigh method will be the region of rapid change of refractive index and thus will be the region of rapid increase in specific volume. The thickness of the water interface as measured by Raman and Ramdas (15) using the Rayleigh method is about 1 Å. If the relative thicknesses of the various regions are as illustrated, the total film thickness is somewhat less than 10 Å and the maximum tensile stress of the order of 4×10^3 atmospheres. It seems very improbable that this figure can be much too low since it is comparable with the measured tensile strength of some metals.

The Laplace (10) method of calculating the tensile strength of liquids, neglecting the quite appreciable heat of "evaporation" of monomolecular layers, leads to values of the order of 25×10^3 atmospheres which are almost certainly too high. Further, owing to relaxation effects, it seems unlikely that the maximum negative stress sustained in the surface layers of a free surface will be as large as the tensile strength of the bulk liquid.

Thus it would appear that the maximum tensile stress in the surface region of liquid water is of the order of 10^3 atmospheres or less and hence that the thickness is of the order of 10 Å or more.

Surface Potential

Finally a word may be said concerning the factors giving rise to the surface potential $\Omega(x)$. The energy of a vapor is, of course, in general much greater than the energy of the corresponding liquid. The heat energy or TS energy change from liquid to vapor is somewhat greater than the internal energy change (i.e., by $p_0 \Delta v$). In order that a positive potential of position exist $\Delta(E + p_0 v)/\Delta x$, p_0 constant, must exceed $T\Delta S/\Delta x$. We may ascribe the positive potential of position as being, in the main, due to an increase in energy without

a compensating increase in entropy. In the dense part of the interface where the fluid compressibility is small, any increase in volume, i.e., a small increase in mean distance of nearest neighbors, will give a large energy increase with little change in entropy. Proceeding further toward the gas the region is reached where fluid extensibility is large and the rapid increase in volume is accompanied by a large increase in entropy. In the case indicated in Fig. 2A the negative potential of position corresponds to a condition where the entropy of the nearly gaseous layers is larger with respect to their energy than prevails in the body of the gas. Ultimately these laminae correspond to states of "supersaturation" of the vapor. While laminae near the liquid or vapor side may be expected to have the normal equation of state of bulk liquid or gas, in the intermediate regions the relations between p , T , and μ or E , S , and v (per unit mass) will depend upon $f(x)$.

We may express the total potential of the surface, ω , as follows (cf. p. 985):

$$\omega = - \sum_{\delta v_{at}} \frac{p_{at} - p_0}{\rho_{at}|_{p_0 - p_{at}}} \cdot \rho_{at} \cdot \delta v_{at},$$

and since in this case $\delta v_{at} = \sigma \delta x_i$ and $p_{at} = p(x)$, we may write

$$\begin{aligned} \omega &= \sigma \int_0^h \frac{[p_0 - p(x)]}{\rho(x)|_{p_0 - p(x)}} \cdot \rho(x) \delta x \\ &= c\sigma[p_0 - \bar{p}(x)] \cdot h = c\sigma[p_0 h + \gamma] \end{aligned}$$

where $c > 1$. Since in cases where the surface tension is large, by far the greater mass of material lies in the regions where fluid compressibilities are small (i.e., where $c = 1$) and the pressures are of large negative magnitudes, ω is very nearly equal to $\gamma\sigma$. Thus γ is practically energy per unit surface. Where compressibilities are high throughout the surface region (near the critical temperature) ω will be greater than $\gamma\sigma$. Further, we should expect ω to consist partially in a decrease in entropy as well as an increase in energy. Thus near the critical region γ will not constitute a measure of surface energy.

III. ADSORPTION AND ADSORPTION HYSTERESIS

If in adsorption processes adsorbates and adsorbents retain their own individual properties, adsorbates at suitable temperatures and equilibrium pressures may be regarded as single component complex fluids as defined in Part I of this paper. In such cases all of the thermodynamic relations applicable to the single component complex are applicable to the adsorbates. Thus we have at once a method of calculating the mean volumetric pressures of the adsorbates from isotherm data, provided that the relevant isotherms represent paths of thermodynamic reversibility.

From Part I, the mean volumetric adsorbate pressure will be given by

$$\bar{p}_a = \int_0^1 \frac{\bar{p}_a}{\rho_1} d\rho_1 = \alpha p_1$$

and α can be calculated from isotherm data (6). The corresponding change in

reversible (elastic) volumetric mean state of stress of the solid can be shown to be related to the adsorbate stress by the following equation,

$$[3] \quad v_a \cdot \bar{p}_a^* + v_c \bar{p}_c^* = (v_a + v_c) p_1$$

where v_a and v_c are the volumes of adsorbate and solid; $v_a + v_c$ is the total volume of the porous body; \bar{p}_a^* and \bar{p}_c^* are the changes in volumetric mean states of stress of the void volume v_a and solid volume v_c , respectively, while p_1 is the change in hydrostatic state of stress of the whole porous body.

From Equation [3] we get at once

$$\bar{p}_c^* = (1 + \phi - \phi\alpha) p_1$$

where $\phi = v_a/v_c$, $\bar{p}_a^* = \alpha p_1$, and \bar{p}_c^* refers to the actual change in elastic state of stress of the adsorbent as a result of the adsorption reaction.⁷

If we are interested in comparing changes in linear dimensions of an adsorbent due to adsorption of gas, we can expect a correlation between these dimensional changes and its change in state of stress. The change in linear dimension per unit length will be a function of the change in linear average state of stress. If \bar{p}_c^* , the mean volumetric change of stress, were a measure of a change of hydrostatic stress (as would be the case if \bar{p}_a^* were a uniform hydrostatic pressure equal to p_1), \bar{p}_c^* would be the same as the change in linear average stress, \bar{p}_c^1 . If in a given direction the solid were perfectly uniform in cross section and its surface field uniform in this direction, then \bar{p}_c^* and \bar{p}_c^1 would be the same. However, in general, these quantities are not equal. Let us write

$$\begin{aligned} \bar{p}_c^* &= p_1 + (\bar{p}_c^*)', \\ \bar{p}_c^1 &= p_1 + (\bar{p}_c^1)', \end{aligned}$$

where \bar{p}_c^* is considered as consisting of the hydrostatic stress p_1 due to the gas pressure and the additional stress $(\bar{p}_c^*)'$ due to interaction with the gas, i.e., due to its surface field. Similarly, $(\bar{p}_c^1)'$ is the additional linear stress due to interaction. While in the general case $(\bar{p}_c^1)'$ may be greater or less than $(\bar{p}_c^*)'$, if the surface forces are more or less uniform but the cross section variable, the ratio $(\bar{p}_c^1)' / (\bar{p}_c^*)'$ will be greater than unity and the ratio will be a constant descriptive of the structure of the adsorbent. Putting $(\bar{p}_c^1)' = K(\bar{p}_c^*)'$ we get $\bar{p}_c^1 = (1 + K\phi - K\phi\alpha) p_1$. Hence for isotropic solids which obey Hooke's law we can write

⁷Following Gibbs (7) we can write for a solid or for an assembly of solid systems

$$[A] \quad dE = TdS = \sum [X_s' \delta(dx/dx')] dx dy dz = TdS - \bar{p}_c^* dv$$

where $\sum [X_s' \delta(dx/dx')]$ and $-\bar{p}_c^*$ represent the generalized state of stress of the element of volume $dx dy dz$. Thus $-\bar{p}_c^*$ represents the volumetric mean adiabatic strain energy per unit volumetric strain. The variation in Gibbs free energy corresponding to a variation in reversible state of strain, all other independent variables remaining constant, may be written $dF = v_c d\bar{p}_c^*$ where v_c is the total volume of the assembly of solid volumes. It is important to note that these relations imply that release of the stress (i.e. putting $\bar{p}_c^* = 0$) will be accompanied by the spontaneous release of the strain, the elements $dx dy dz$ becoming identical with the reference elements $dx' dy' dz'$. Thus Equation [A] cannot be used to describe strains beyond the elastic limit or irreversible strains. In the case of a so-called self-strained body, the state of strain of the body as a whole is to be taken as zero when the matter comprising the body is everywhere statistically at rest and no external forces are operative.

$$[4] \quad \delta l/l = -\frac{1}{3}\beta(1+K\phi-K\phi\alpha)p_1,$$

where l is the length of the sample and β its compressibility. Where the dilation (or contraction) is isotropic we do not need to introduce the Poisson ratio. If the adsorbent is not isotropic both " β " and K will differ in different directions. In very extreme cases where K is very different in different directions, corrections of the Poisson contraction type will be necessary, and must be known or inferred for accurate correlation of experimental results.

It has been shown (6) that Equation [4] can be used to describe experimental data fairly well.⁹ Accordingly the view that the adsorbate may be regarded as a single component complex appears to have considerable validity. The factor K in so far as it is determined by the solid structure will be a constant and thus have the same value for different gases at various temperatures. However, if the mechanism of adsorption changes, the value of K will change. Thus as we have shown (6) K will have different values for a given solid structure when the void volume is filled with liquid under a uniform pressure (e.g. extreme cases of capillary condensation) as compared with the case where the adsorbate is condensed in layers upon the surface.

Adsorption and Adsorption Hysteresis

In general when considerable adsorption occurs, the apparent potential of the surface is modified by molecular interactions of the adsorbate, i.e., the "potential" is a function of the equation of state of the gas. If the gas is condensable, liquid-gas interfaces will form and these interfaces introduce additional "potentials" of position which must be combined with the surface potentials. However, as long as the isotherm represents a path of thermodynamic reversibility, the mean volumetric pressure of the adsorbate will be given by Equation [2] of Part I.

The formation of adsorbate liquid-gas interfaces may lead to irreversible adsorption. The adsorption mechanism commonly referred to as "capillary condensation" is inherently a thermodynamically irreversible process. While the thermodynamics of hysteresis and reversible and irreversible adsorption have been treated by Hill (8) and others using statistical mechanical models, there are a number of inferences that can be drawn from purely thermodynamic considerations which are important and quite independent of any models.

The usual method of measuring adsorption isotherms is to expose the initially evacuated adsorbent to sources of constant gas pressure. When equilibrium is attained at each pressure, the thermodynamic potentials of the gas and adsorbate are the same, thus $\partial F/\partial m_1$, the partial molar free energy or thermodynamic potential of the adsorbate, equals dF/dm_1 , the thermodynamic potential of the gas, and in each case,

$$\Delta F = \int_{m_1=0, m_2}^{m_1, m_2} \frac{\partial F}{\partial m_1} dm_1 = \int_{m_1=0}^{m_1} \frac{dF}{dm_1} \cdot dm_1$$

⁹This assumes that the compressibility of the solid is uniform and not changed by the adsorption. Even where the fundamental equations are strictly applicable, i.e., where the adsorbent changes only in state of stress, if the accompanying change in volume is large, β will be neither uniform nor constant.

⁹The validity of Equation [4] may be considered as a criterion for judging the validity of the potential theory of adsorption. If Equation [4] is valid the surface forces behave as a "potential".

and in the case of the gas,

$$\Delta F = \int_0^{p_1} v_1 dp_1.$$

If the adsorbate behaves as a single component complex so that the volume of the adsorbate has a physical meaning,

$$\Delta F = \int_{\bar{p}_a=0}^{\bar{p}_a^*} v_a d\bar{p}_a^*.$$

However, all of these relations assume that v_1 or m_1 (the mass adsorbed) and hence that F and μ are known as functions of p_1 or that p_1 is known as a function of m_1 . If the equilibrium gas pressure is anywhere a decreasing function of m_1 , say at m_1' , the system would be mechanically unstable when containing the mass m_1' and would spontaneously fill irreversibly to some value m_1'' . The equilibrium pressures and hence the potentials corresponding with the filling would not be observable in this case under ordinary experimental conditions. Such mechanisms as the "Cohan" (3) or any other "capillary condensation" mechanism would lead to such results.

Suppose, for example, that the equilibrium gas pressure as a function of the mass adsorbed has the form shown in Fig. 3.¹⁰ The line CF is the only line¹¹

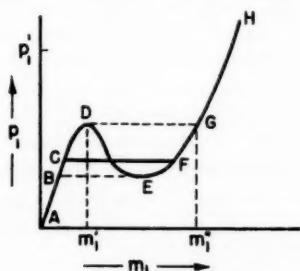


FIG. 3.

along which the mass may increase at constant pressure and give the correct value of ΔF . If the filling is premature, i.e., occurs at lower pressures along the line BE , the apparent observed value of ΔF from $p_1 = 0$ to some point $p_1 = p_1'$ will be too large, while if the filling occurs at higher pressures, e.g. along DG , the apparent value of ΔF will be too small.

If $p_1(m_1)$ has the form shown above, and the adsorbate behaves as a single component complex regardless of mechanism of adsorption, \bar{p}_a^* , the adsorbate pressure, will be a function of p_1 having the form shown in Fig. 4.¹² The point C of Fig. 4 corresponds with the line CF of Fig. 3. If the adsorption actually

¹⁰ $p_1(m_1)$ is assumed as measured in a small constant volume apparatus. $p_1(m_1)$ cannot, of course, have any such form when exposed to sources of m_1 at constant pressure.

¹¹ The position of CF is obtained from a plot of v_1 against p_1 using Maxwell's rule of equal areas (cf. Hill (8)).

¹² Assuming suitable relative magnitudes of corresponding gas and adsorbate densities.

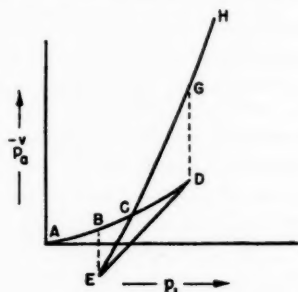


FIG. 4.

followed the curve of Fig. 3 the corresponding adsorbate pressures would follow the curves AD , DE , EH in Fig. 4. If the adsorption follows the path $ABEH$ of Fig. 3 the corresponding path in Fig. 4 will be $ABEH$. If the adsorption follows $ADGH$ of Fig. 3 the adsorbate pressure will follow $ADGH$ of Fig. 4. In the former of the irreversible cases the adsorbate pressures will become negative, while in the latter case they will be positive throughout.

It is to be emphasized that \bar{p}_a^* , the adsorbate pressure, can only become negative on *adsorption* if the filling occurs at equilibrium pressures below the line CF . If the filling occurs along CF or at pressures above CF , \bar{p}_a^* will be positive. In order that the adsorbent, if reasonably isotropic, contract on adsorption, i.e., on increasing the equilibrium pressures, the net adsorbate pressure must become negative and this can only occur if the filling occurs irreversibly along a path lying below CF . The fact that in some cases quite appreciable contractions are observed in the lower pressure regions of increasing pressure indicates that $p_1(m_1)$ is a decreasing function of m_1 in these lower pressure regions. This may be construed as evidence of the existence of "capillary condensation" or of some equivalent mechanism such as the "two-dimensional condensation" of Pierce (13).

When the filling of the adsorbate volume is irreversible whether above or below the line CF the observed " ΔF " (i.e. $\int_0^{p_1} v_1 dp_1$) is not an accurate measure

of the actual ΔF of the adsorbate and the application of thermodynamic relations based on such values of ΔF will be in error. Such errors are to be expected when liquid-vapor surface tensions are high.

While as pointed out by Hill (8) we would normally expect that irreversible transitions would be delayed (i.e. occur above CF of Fig. 3) the fact that contractions are observed on increasing pressure paths indicates that these transitions are premature (i.e., occur below CF). The absence of appreciable hysteresis in these regions together with the fact that contractions on desorption and adsorption are of much the same magnitude indicates that on *desorption* the transition is *delayed*. This apparently anomalous behavior may be due to the difference in sign of the temperature effect of adsorption and

desorption. Thus if the hypothetical constant pressure (p_s') line at the higher temperature lies below that at the lower temperature (e.g. if $\partial p_s'/\partial t$ is negative in these regions (cf. Coolidge (4)) the transition may occur, as expected, above the line corresponding to the actual temperature of the adsorbent, the adsorbate pressures being positive at the adsorbent temperature but becoming negative on cooling to the isothermal bath temperature. The reverse temperature effect would be expected on desorption and thus tend to equalize the adsorption and desorption states actually obtained.

In general, if the actual quantity of material per "site" "area" or "pore" for which $p_1(m_1)$ has the form of Fig. 3 is very small, filling of these sites irreversibly may be controlled by minor differences in experimental procedures. In addition there may be little apparent difference between adsorption and desorption isotherms, depending on the distribution of pressures corresponding to CF lines for the various sites. If, however, the quantity of material is large so that there are large differences in mass m_1 per site as CF is traversed, filling of these sites will in general occur at pressures above CF and the emptying (desorption) occur below CF . This will, in general, lead to marked hysteresis. In the extreme case of the filling of large void volumes, such volumes will fill with liquid only at pressures above saturation but the liquid will persist considerably below saturation if separated from the equilibrium gas by small pores. If appreciable areas of liquid-vapor surfaces having appreciable positive tensions are formed along paths of increasing pressures some irreversibility must be involved. Where a considerable mass of adsorbate is under a net negative pressure due, say, to capillary condensation and where this condition is reached along a path of increasing gas equilibrium pressures, the irreversibility will be large and ΔF quite different from the observed value of $\int_0^{p_1} v_1 dp_1$. Under these circumstances \bar{p}_0^* as measured by the observed value of αp_1 will be seriously in error and is apt to be of the wrong sign. The mean adsorbate pressure, in some cases, may be estimated by adding "Kelvin" adsorption and "reversible" adsorption, but in general these pressures are not additive quantities.

It is quite possible for the adsorption isotherm to represent a path of almost perfect thermodynamic reversibility from zero gas pressures up to saturation, and that a considerable part of the desorption branch also represents such a path even when the hysteresis is large, so that the two thermodynamically reversible branches are widely different. In this case ΔF and \bar{p}_0^* can be correctly calculated from the observed data along the two reversible branches. Of course, the desorption curve must eventually meet the adsorption curve at lower relative pressures and hence involve considerable irreversibility in these regions of the desorption branch.

In general where the theoretically reversible continuous curve $p_1(m_1)$ has negative values of $\partial p_1/\partial m_1$, observed reversible isotherms will be stepwise.

Finally if $p_1(m_1)$ is nowhere for any site (area or pore) a decreasing function of m_1 , ΔF will be given accurately by $\int_0^{p_1} v_1 dp_1$ applied to the equilibrium gas

and \bar{p}_a^* by $\int_0^{p_1} \bar{p}_a/p_1 \cdot dp_1$, or αp_1 , quite regardless of whether liquid-vapor interfaces of any form are present or not. In such cases the "tension" of any liquid-vapor interfaces must be negative, i.e., pressures in these surfaces must be positive.

Adsorption Isotherm

The validity of the Polanyi (14) potential theory of adsorption is commonly based on the ability to calculate adsorption isotherms of a variety of gases at various temperatures from the characteristic curve for one representative gas. This, of course, involves the assumptions that the "potential" of the surface is the same for each gas and is independent of the temperature. It assumes that the equations of state of the gases concerned are known reasonably well. Although there are many exceptions, it is indeed surprising to what an extent these rather violent assumptions have been confirmed. Without any reservations concerning the nature of the potential field, if Equation [4] above is valid it constitutes strong evidence of the essential validity of the Polanyi theory. Thus our previously reported experimental results may be taken as confirmation of Polanyi's compressed film hypothesis. McBain's (12) "disproof" of the potential theory was based on considerations of adsorbate pressures. Some of the fallacies in McBain's "disproof" have been pointed out by Brunauer (2). Our results indicate that such considerations instead of contributing to a "disproof" of the compressed film hypothesis" lend very considerable support to it. Adsorption equilibrium is, of course, thermodynamic equilibrium. Accordingly, in its broadest sense, the "potential" theory is necessarily correct. We usually limit the "potential" theory of adsorption to processes where the adsorbate may be regarded as a single substance and thus distinguish "physical adsorption" from chemical reaction, and from solution. In its most restricted sense the "potential theory" is limited further to those cases where the "surface potential" is constant. The principal weakness of the potential theory of adsorption lies in its generality, since even in its most restricted form almost any type of adsorption isotherm can be consistent with it, as has been shown by many authors. Even if we assume that a condensable gas obeys the ideal gas law exactly, below the saturation pressure, and that above saturation it is an incompressible liquid of density unity, ignoring liquid-vapor interfaces a great variety of isotherm shapes can be generated depending on the form of the volumetric distribution of the "potential" of the surface region as well as upon the magnitude of the mean potential with respect to RT .¹³

¹³Let $V(\Omega) d\Omega$ be the volume of the surface region having a potential lying between Ω and $d\Omega$, and let

$$V(\Omega) = v_a/h) \Omega e^{-\Omega/a}, \quad 0 \leq \Omega \leq \infty.$$

Taking v_a as $\frac{1}{2}$ cc. per gram of adsorbent and neglecting the concentration of vapor, one gets

$$x/m = \frac{1}{2} (p/p_a)^a [1 - \log(p/p_a)^a]$$

where $a = 2RT/\mu\bar{\Omega}$. Fig. 5 shows a plot of this equation for various values of a . Evidently to determine whether or not experimental points fall on such curves or on, say, a Freundlich curve, we must be very sure of the experimental data and resort to rather elaborate mathematical analysis of these data (cf. Honig (9)).

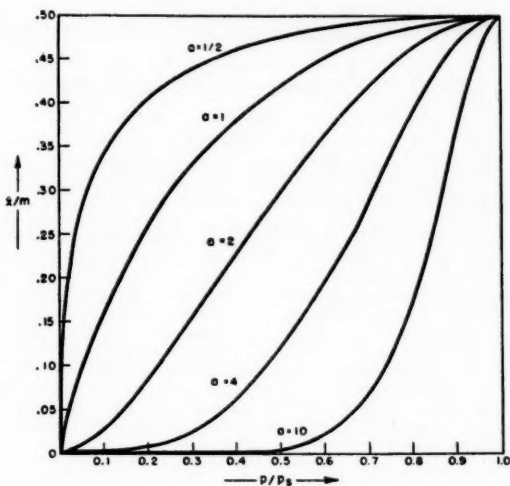


FIG. 5.

Since we cannot deduce an equation of state of a single homogeneous substance from purely thermodynamic considerations, it is evident that we cannot deduce an adsorption isotherm from such considerations. All so-called "thermodynamic" derivations of adsorption isotherms are based either directly or indirectly on assumed equations of state of both the equilibrium gas and the corresponding adsorbed material.

REFERENCES

1. BROWN, R. C. *Proc. Phys. Soc. (London)*, 59: 429. 1947.
2. BRUNAUER, S. *The adsorption of gases and vapors*. Princeton University Press, Princeton, N.J. 1943.
3. COHAN, L. H. *J. Am. Chem. Soc.* 60: 433. 1938.
4. COOLIDGE, A. S. *J. Am. Chem. Soc.* 49: 708. 1927. (cf. S. Brunauer Ref. (2)).
5. FLOOD, E. A. and HUBER, M. *Can. J. Chem.* 33: 203. 1955.
6. FLOOD, E. A. and HEYDING, R. D. *Can. J. Chem.* 32: 660. 1954.
7. GIBBS, J. W. *Collected works*. Yale University Press, New Haven, Conn. 1948.
8. HILL, T. L. *J. Chem. Phys.* 15: 767. 1947.
9. HONIG, J. M. and ROSENBLUM, P. C. *Can. J. Chem.* 33: 193. 1955.
10. LAPLACE. In J. R. Partington's *An advanced treatise on physical chemistry*. Vol. II. Longmans, Green and Co., London. 1951.
11. LEWIS, G. N. and RANDAL, M. *Thermodynamics*, McGraw-Hill Book Company, Inc., New York. 1923.
12. MCBAIN, J. W. and BRITTON, G. T. *J. Am. Chem. Soc.* 52: 2198. 1930.
13. PIERCE, C. and SMITH, R. *J. Phys. & Colloid Chem.* 54: 784. 1950.
14. POLANYI, M. *Verhandl. deut. physik. Ges.* 15: 55. 1916.
15. RAMAN, C. V. and RAMDAS, L. A. *Phil. Mag.* 3: 220. 1927.
16. ROWLEY, H. H. and INNES, W. B. *J. Phys. Chem.* 46: 537. 1942.
17. RICE, O. K. *J. Chem. Phys.* 15: 333. 1947.
18. SHUTTLEWORTH, R. *Proc. Phys. Soc. (London)*, A, 62: 167. 1949.
19. TOLMAN, R. C. *J. Chem. Phys.* 16: 758. 1948.
20. WYLLIE, G. *Proc. Roy. Soc. (London)*, A, 197: 383. 1948.

OXIDATION OF ALKENES BY MERCURIC SALTS¹

BY D. A. SHEARER AND GEORGE F WRIGHT

ABSTRACT

The α -oxymercurials of cyclohexene, 2-methyl-1-phenylpropene-1, and the geoisomers of stilbene have been shown to be the intermediates in the oxidation of these alkenes by mercuric nitrate and other salts, usually in methanol. These intermediates are stable in the oxidation environment and their alkoxy groups appear intact in the oxidation product; indeed organomercurials without vicinal alkoxy groups are likewise oxidized. The reaction products from alkenes in methanol are 1,2-dimethoxyethanes, 1,1-dimethoxyethanes, and (with mercuric nitrate) 1-methoxy-2-nitroxyethanes, formation of the latter being most rapid. The oxidation is stereospecific, each geoisomer yielding its characteristic diastereomeric products. It is catalyzed by acids such as nitric acid but not by nitrate ion, though neither affect the ratio of products. This over-all second-order reaction, first-order in organomercurial and first-order in mercuric salt, becomes over-all first-order with mercuric acetate when it is catalyzed by boron fluoride. Combination of the catalyst with the organomercurial must be rate-controlling. The similarity of the oxidation and the acid decomposition reactions of organomercurials is discussed.

The oxidation of alkenes by mercuric salts is not a new reaction (3, 2, 25) but interest has recently been revived because of its application to sterol dehydrogenation (4, 5, 38, 39). A mechanism for the sterol dehydrogenation has been proposed involving a "mercurinium ion" (33) but it seems to be inconsistent with the observed formation of mercurous salts rather than metallic mercury. On the other hand, another mechanism has been suggested (11) for the oxidation of cycloalkene by mercuric salts (20, 36, 37) which does not take into account the equilibration: $2\text{HgOAc} \rightleftharpoons \text{Hg} + \text{Hg}(\text{OAc})_2$. Neither mechanism is consistent with the earlier observations that two equivalents of mercuric salt are involved in the oxidation of an alkene to an alkadiene or an alkenyl ester as well as to a glycol derivative (7) or rearrangement product (10, 30).

The consumption of two equivalents of mercuric salt per equivalent of alkene was confirmed by Brook and Wright (10) who also proposed a mechanism for the conversion of cyclohexene to formylcyclopentane not involving the intermediacy of an oxymercurial. These workers thought that an oxymercurial could not be involved because "hydroxymercuration with mercuric nitrate is not a significant reaction in water". We have now found this statement to be incorrect.

The error of Brook and Wright lay in dilution of their reaction aliquots with excess aqueous sodium chloride. The hydrochloric acid generated in this way decomposed the mercurial. Alternatively if cyclohexene is mixed with an equivalent each of mercuric nitrate and nitric acid (1 molar) and diluted after 10 min. into *one equivalent* of cold aqueous sodium chloride a maximal 80% yield of 2-hydroxy-1-chloromercuricyclohexane may be isolated. The equilibrium is shifted to afford a 63% yield when the system is 2 molar in nitric acid.

¹Manuscript received January 21, 1955.

Contribution from the Chemical Laboratory, University of Toronto, Toronto, Ontario.

Kinetic studies* show that the oxidation of cyclohexene by two equivalents of aqueous mercuric nitrate proceeds through the intermediate mercurial, and that the over-all second-order kinetics are first-order in respect of mercurial and of mercuric nitrate, *i.e.* the oxymercuration of the alkene is so fast that the subsequent oxidation is rate-controlling. Table I shows, by comparison of Expt. 1 with Expts. 2, 3, and 4, that the rate is enhanced by addition of nitric acid, but the effectiveness does not increase in direct proportion to the concentration. Expt. 5 has been carried out with an excess of mercuric nitrate and the rate has been calculated by the expression

$$kt = [2.303/(a-b)] \log [b(a-x)/\{a(b-x)\}], \quad [i]$$

where a is the concentration of mercuric salt *after mercuration is assumed to have occurred*, and b is the concentration of mercurial assumed to form instantly at zero time while $a-x$ and $b-x$ are corresponding values after certain time

TABLE I
REACTION OF CYCLOHEXENE WITH AQUEOUS MERCURIC NITRATE AT $25.0 \pm 0.1^\circ\text{C}$.

Expt. No.	Initial molarities			Molarities after mercuration			Second-order rate constant k (l. moles ⁻¹ min. ⁻¹)	% Investigated
	Hg(NO ₃) ₂	C ₆ H ₁₀	HNO ₃	Hg(NO ₃) ₂	Mercurial	HNO ₃		
1	.50	.25	—	.25	.25	0.25	.0259 ± .0008	71.8
2	.50	.25	1.0	.25	.25	1.25	.0473 ± .0041	60.6
							.0476 ± .0017	57.7
3	.50	.25	1.5	.25	.25	1.75	.0489 ± .0036	60.1
4	.50	.25	2.0	.25	.25	2.25	.0505 ± .0014	62.0
							.0520 ± .0043	69.8
5	.50	.125	1.0	.375	.125	1.125	.0447 ± .0043	75.0

intervals. Agreement of this rate constant with that obtained from systems containing a comparable amount of nitric acid (Expt. 2) shows that the rates are independent of cyclohexene concentration because the alkene is very rapidly converted to the mercurial. These results are valid for about 60% of the reaction, after which the rate falls off markedly. The deviation from simple second-order kinetics is not unexpected since the isolable yield of product, formylcyclopentane, has never exceeded 45% of theoretical.

This oxidation of cyclohexene is not limited to use of aqueous mercuric nitrate alone. The reaction proceeds in methanolic mercuric nitrate solution (two equivalents with one equivalent of both cyclohexene and nitric acid, each 0.25 molar) but 41 hr. are required for 65% of oxidation, in contrast to two hours for 60% of oxidation in the aqueous system. It may be significant that the intermediate methoxymmercurial is a more stable compound than the hydroxymmercurial which is intermediate in the aqueous system. The product from the methanolic system seems to be the dimethylacetal of formylcyclo-

* A referee has adversely but correctly questioned the value of kinetic data based on this complex reaction which is not in stoichiometric balance, and in which the limited analytical precision precludes wide variation in reagent concentration. Indeed the kinetic studies only have value in so far as the same conclusions can be drawn from experiments using four different alkenes.

pentane according to the sluggish reaction with 2,4-dinitrophenylhydrazine. The same product is obtained when 2-methoxycyclohexylmercuric nitrate is treated with mercuric nitrate in methanol.

The conversion of cyclohexene to formylcyclopentane is not limited to use of the nitrate salt. A 45% combined yield of the aldehyde and cyclopentanecarboxylic acid is obtained with mercuric sulphate and molar sulphuric acid; the reaction is comparable in rate with that of the nitrate salt, but is difficult to follow kinetically because mercurous sulphate precipitates during the reaction. The reaction is much slower in aqueous mercuric benzenesulphonate containing benzenesulphonic acid, but the same products are obtained. Thus the anion can be varied within limitations (chloride is ineffective and acetate is unduly slow). But the mercury is necessary. Nitrate salts of barium, cadmium, copper II, iron III, lead, zinc, and bismuth are ineffective in the oxidation either of cyclohexene or of its oxymercurials.

The oxidation study has been extended to 2-methyl-1-phenylpropene-1 (I). This compound has previously been methoxymercurated. The 2-methoxy-2-methyl-1-phenylethylmercuric salt thus obtained has been converted by means of iodine or bromine to substances which essentially are oxidation products of the alkene (6). The action of methanolic mercuric nitrate on 2-methyl-1-phenylpropene-1 or 2-methoxy-2-methyl-1-phenylethylmercuric nitrate (VI) does not produce two of these products (3-phenylbutanone-2 and 2-methyl-2-phenylpropanal) but the third, 1,2-dimethoxy-1-methyl-2-phenylpropane (II), is obtained in fair yield. Additionally the mercuric nitrate oxidation yields a higher boiling compound, seemingly 2-methoxy-2-methyl-1-phenylpropyl nitrate (III), since it gives a positive diphenylamine test for nitrate and is reduced by zinc and acetic acid to a 71% yield of 2-methoxy-2-methyl-1-phenylpropanol-1 (IV, characterized as its *p*-nitrobenzoate). Although previously reported (35) this alcohol actually was unknown (6). However it has

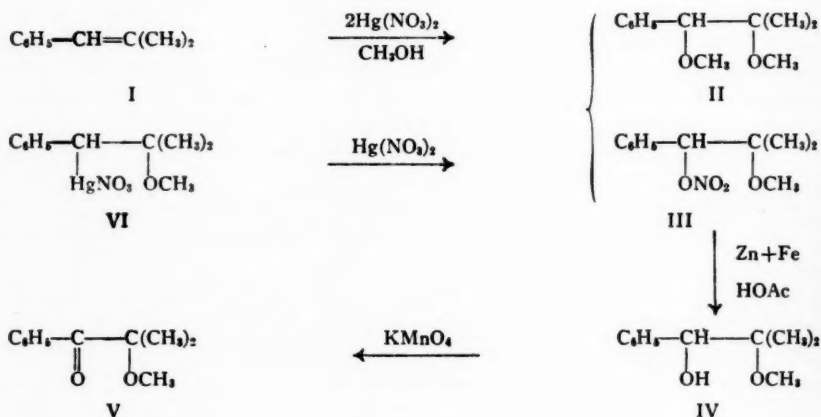


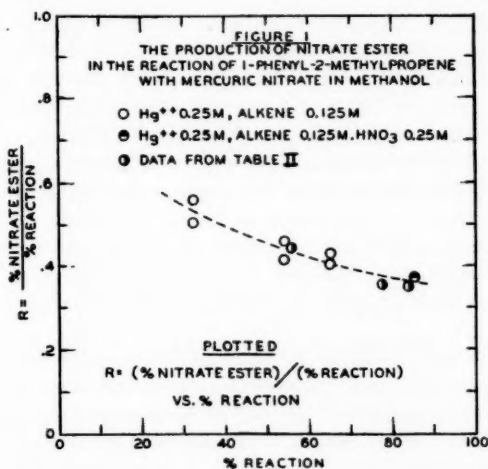
TABLE II

REACTION OF 1-PHENYL-2-METHYLPROPENE AND OF 1-PHENYL-2-METHOXY-2-METHYL-PROPYLMERCURIC NITRATE WITH MERCURIC NITRATE IN METHANOL

Expt. No.	Initial molarities				Time (hr.)	Yields, %			Ratio, nitrate ester: total yield
	Alkene	Mercurial	Hg(NO ₃) ₂	70% HNO ₃		Dimethyl ether	Nitrate ester	Total	
1	.25	—	.52	.5	0.5	31	25	56	.45
2	.25	—	.52	—	20	50	28	78	.36
3	—	.25	.26	—	48	54	30	84	.36

now been identified by oxidation to the known 2-methoxy-2-methyl-1-phenylpropanone (V).

The relative yields of II and III from either the alkene I or its mercurial VI are shown in Table II. The apparent augmentation of III is due to incompleteness of Expt. 1 and not to presence of nitric acid. It is shown clearly in Fig. 1 that the ratio of II to II+III is related to duration of reaction; i.e. nitroxylation is faster than methoxylation. Although nitric acid is ineffective in changing



the ratio of nitrate ester to ether, it does increase the rate of reaction. This effect is shown by the first four experiments in Table III in which the rates have been calculated on the assumption that formation of the oxymercurial VI is virtually complete at the onset of oxidation. Then if b is the initial concentration of this mercurial VI and a is the initial concentration of mercuric

nitrate after mercuration, the rate may be calculated according to equation [i] where x is extent of oxidation at time t . The comparable rates of Expts. 3 and 4 indicate that this assumption is approximately true; further the data show that the oxidation is first-order in mercurial and first-order in mercuric nitrate. The effectiveness of nitric acid may be due to its acidity since the over-all second-order rate is enhanced markedly by addition of water to the system

TABLE III
REACTION OF 1-PHENYL-2-METHYLPROPENE WITH MERCURIC NITRATE IN METHANOL
AT 25°C.

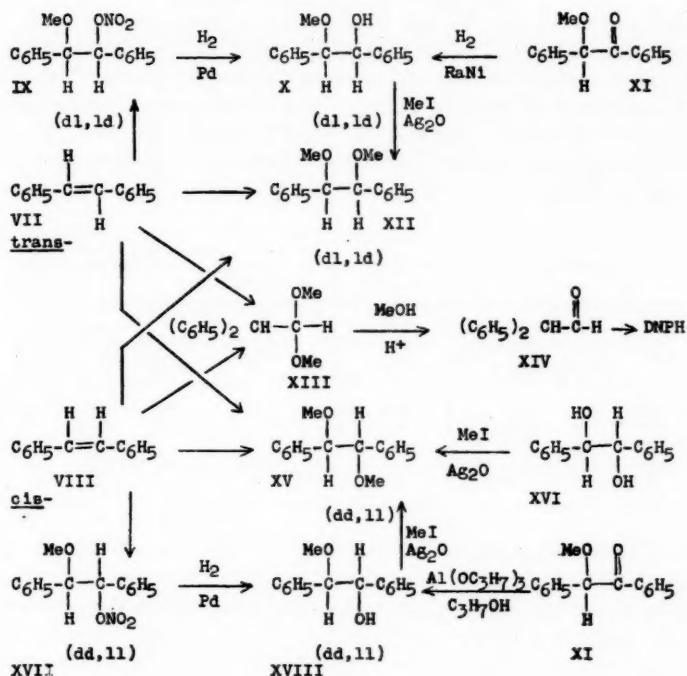
Expt. No.	Initial molarities			Molarities after mercuration			Molarity of other reagents	Second-order specific rate k (l. moles ⁻¹ min. ⁻¹)	% Investi- gated
	Hg(NO ₃) ₂	Alkene	HNO ₃	Hg(NO ₃) ₂	Mercurial	HNO ₃			
1	.125	.0625	—	.0625	.0625	.0625	—	.103 ± .008	66.0
2	.25	.125	—	.125	.125	.125	—	.114 ± .010	68.6
3	.25	.125	.125	.125	.125	.250	—	.130 ± .010	62.5
4	.25	.083	.125	.167	.083	.208	—	.123 ± .016	86.6
5	.25	.125	—	.125	.125	.125	H ₂ O 5.6	.420 ± .020	83.6
6	.25	.125	—	.125	.125	.125	NO 0.01	.092 ± .013	51.5

(Expt. 5). It may be noted (Expt. 6) that nitric oxide is ineffective in alteration of the rate.

The complexity of the reaction is indicated by oxidation of 2-methyl-1-phenylpropene-1 with two equivalents of other mercuric salts. Aqueous mercuric sulphate in two days gives a 70% yield of 2-methyl-1-phenylpropanediol-1,2 and no sulphate ester although aqueous mercuric nitrate seems to yield a compound not the diol (to be reported in detail in the future). Methanolic mercuric trifluoroacetate in two days gives 50% of 1,2-dimethoxy-1-phenyl-2-methylpropane contaminated with a trace of 3-phenylbutanone-2. Methanolic mercuric acetate does not react appreciably with 2-methyl-1-phenylpropene-1 until 0.5 equivalent of boron trifluoride etherate is added. After the rapid oxymercuration is complete the subsequent formation of 1,2-dimethoxy-1-phenyl-2-methylpropane is first-order over-all ($k = 1.16 \times 10^{-3}$ min.⁻¹), as if co-ordination with the boron fluoride were the rate-determining step.

Some years ago the oxidation of the 2-methoxy-1,2-diphenylethylmercuric chlorides was reported (7) and these studies have now been elaborated by use of pure *cis*- and *trans*-stilbenes* as well as their oxymercurials. Each of the geoisomeric alkenes yields, besides the original alkene, three characteristic crystalline products as well as a common oil, 1,1-dimethoxy-2,2-diphenylethane (XIII), when each is treated with two equivalents of methanolic mercuric nitrate.

*The question of *cis*-stilbene purity has always been vexing. Although this geoisomer has usually been thought to melt below 0°, Brackman and Plesch recently (8) reported the melting point to be 5–6°, decreasing to 0.62° with age. Many years ago material of high melting point was available in our laboratory but subsequently could not be obtained. Now we have found that pure (40) *cis*-stilbene (which is best obtained without distillation of the mercurial decomposition product) is dimorphic. The form most readily obtained melts at –24 to –23° (uncorr.) but when this melt is seeded with *cis*-stilbene, m.p. 1.5–3.0° (uncorr.), it resolidifies and then melts entirely at the higher temperature.



These products are listed below in the order that they are separated by elution from an alumina column by frontal displacement:

From *cis*-stilbene

- | | |
|---------------------|---|
| (VIII) <i>cis</i> | (1) stilbene |
| (XVII) <i>dd,ll</i> | (2) 2-methoxy-1,2-diphenylethyl nitrate |
| (XII) <i>dl,ld</i> | (3) 1,2-dimethoxy-1,2-diphenylethane |
| (XIII) | (4) diphenylacetaldehyde dimethylacetal |
| (XV) <i>dd,ll</i> | (5) 1,2-dimethoxy-1,2-diphenylethane |

From *trans*-stilbene

- | |
|--------------------|
| <i>trans</i> (VII) |
| <i>dl,ld</i> (IX) |
| <i>dl,ld</i> (XII) |
| (XIII) |
| <i>dd,ll</i> (XV) |

The *cis*-stilbene is conveniently identified by methoxymercuration with mercuric acetate while *trans*-stilbene is identified by mixture melting point. The two diastereomeric nitrate esters, only one of which is obtained from each geoisomeric stilbene, were hitherto unknown. They have been identified by analysis and by catalytic hydrogenation with palladium-on-charcoal (24) to the diastereomeric 2-methoxy-1,2-diphenylethanol which in turn have been configurationally characterized. The (*dl,ld*)-methoxydiphenylethanol (X) (19), which also is obtained almost quantitatively by Raney nickel reduction of benzoin methyl ether (XI), is converted by Purdie methylation to the configurationally-known (*dl,ld*)-1,2-dimethoxy-1,2-diphenylethane (XII) (19). The (*dd,ll*)-methoxydiphenylethanol (XVIII), which may also be obtained by

fractional crystallization of the diastereomeric mixture from aluminum isopropoxide reduction of benzoin methyl ether (XI), is likewise related by methyl iodide-silver oxide methylation to the known (*dd, ll*)-1,2-dimethoxy-1,2-diphenylethane (XV) (13). Finally the 1,1-dimethoxy-2,2-diphenylethane (XIII), which obviously arises by 1,2-rearrangement in these systems, is identified by analysis and by conversion to the 2,4-dinitrophenylhydrazone of 2,2-diphenylethanal (XIV).

TABLE IV
A COMPARISON OF THE REACTIONS OF *cis*- AND *trans*-STILBENES WITH MERCURIC NITRATE IN METHANOL

Alkene	Time (hr.)	Per cent yields of products					Recovered alkene, %	Fraction of total products			
		<i>dl, ld</i> Ether	<i>dd, ll</i> Ether	Nitrate ester	Acetal	Total		<i>dl, ld</i> Ether	<i>dd, ll</i> Ether	Nitrate ester	Acetal
<i>cis</i> -	48			(<i>dd, ll</i>) 37.8	39.0	96.0	1.2	.025	.17	.39	.41
	11	2.5	16.7	34.2	34.6	88.9	3.7	.011	.21	.38	.39
<i>trans</i> -	40	21.8	2.3	(<i>dl, ld</i>) 33.6	20.6	78.3	10.9	.28	.029	.43	.26
	41	22.4	1.0	35.3	24.4	83.1	14.7	.27	.012	.42	.29

The yields of these oxidation products from *cis*- and *trans*-stilbenes are shown in Table IV. The stereospecificity which completely gives *dd, ll*-2-methoxy-1,2-diphenylethyl nitrate (XVII) from *cis*-stilbene and the *dl, ld* diastereomer (IX) from *trans*-stilbene is also preponderant for the 1,2-dimethoxy-1,2-diphenylethanes although a yield of 2-3% of the *dl, ld* diether (XII) arises from VIII. Also 1-2% of *dd, ll* diether (XV) arises from *trans*-stilbene. Both render stereospecificity incomplete. However in large part these oxidation products are characteristic of over-all apex-base (*trans*) addition to the geoisomers.

Recovery of alkene as shown in Table IV is much greater when *trans*-stilbene is oxidized, by contrast to the *cis* geoisomer. But this might be expected if the methoxymercurials are intermediates in these oxidations since the oxymercuration of *trans*-stilbene has been shown (40) to be less complete than that of *cis*-stilbene. Finally one may note in Table IV that the ratio (0.68) of acetal yields for *trans*- versus *cis*-stilbene is roughly inversely proportional to the ratio (0.72) of the diether yields from *cis*- versus *trans*-stilbene. By contrast the ratio of nitrate ester yields is 0.9. This contrast may be due to the more rapid formation of nitrate ester versus diether if methoxylation must compete with relatively slow 1,2-rearrangement.

Addition of nitric acid to the system comprising methanolic mercuric nitrate and each of the stilbenes accelerates reaction with the *cis* geoisomer and retards it with the *trans* form although, as is shown in Table V, the ratios of product yield are essentially unchanged. It is probable then that nitric acid exerts a dual effect by accelerating the oxidation of the intermediate oxymercurial but also by decreasing the equilibrium concentration of the oxymercurial. The favorable equilibrium of the *cis*-stilbene system favors the first effect, while the adverse equilibrium in the *trans*-stilbene system is accentuated owing to the latter effect.

TABLE V
ADDITION OF NITRIC ACID TO METHANOLIC SYSTEMS 0.26 MOLAR IN
MERCURIC NITRATE AND 0.125 MOLAR IN STILBENES

Geo- isomer	Molarity HNO ₃	Time, hr.	% Yield of products				Recovered stilbene, %	% of total product		
			Ether	Ester	Acetal*	Total		Ether	Ester	Acetal
<i>cis</i>	0	11	19	34	36	89	4	21	39	40
<i>cis</i>	0.25	4	19	34	35	88	6†	22	38	40
<i>trans</i>	0	40	22	34	23	79	11	28	43	29
<i>trans</i>	0.25	88	16	31	18	65	14	24	48	28
<i>trans</i>	0.50	88	14	27	19	60	14	24	45	31

*The small yield of nonpreponderant ether has been included with the acetal.

†Recovered stilbene half *trans*.

TABLE VI
REACTION OF *trans*-STILBENE WITH MERCURIC NITRATE IN METHANOL
EFFECT OF VARYING THE CONCENTRATION OF REAGENTS

Initial molarities		Time, hr.	Per cent yield of products				Recovered alkene, %	% of total product		
Hg(NO ₂) ₂	<i>trans</i> - Stilbene		Ether	Ester	Acetal	Total		Ether	Ester	Acetal
.13	.0625	47	22	32	22	76	14	29	42	29
.26	.125	40	22	34	23	79	11	28	43	29
.52	.25	46	21	32	25	78	5	26	42	32
.39	.125	48	24	33	21	78	2	31	42	27

The data of Table VI show that the ratios of products are practically unaffected by fourfold variation in the concentrations of *trans*-stilbene and mercuric nitrate in methanol. Likewise the augmentation of ionic strength by inclusion of lithium nitrate (Table VII) does not affect the yield of *dl,ld*-2-methoxy-1,2-diphenylethyl nitrate (IX) until the concentration is very large, but it does alter markedly the ratio of diether (XII) to acetal (XIII). This effect is not unexpected when a 1,2-rearrangement is involved, and the relatively slow methoxylation ought to be affected more than the rapid nitroxylation. The effect of added lithium nitrate does seem to show that methoxylation and, especially, nitroxylation are not directly dependent on the ionic species.

TABLE VII
REACTION OF 0.625 MOLAR *trans*-STILBENE AND 0.13 MOLAR MERCURIC
NITRATE IN METHANOL WITH ADDED LITHIUM NITRATE

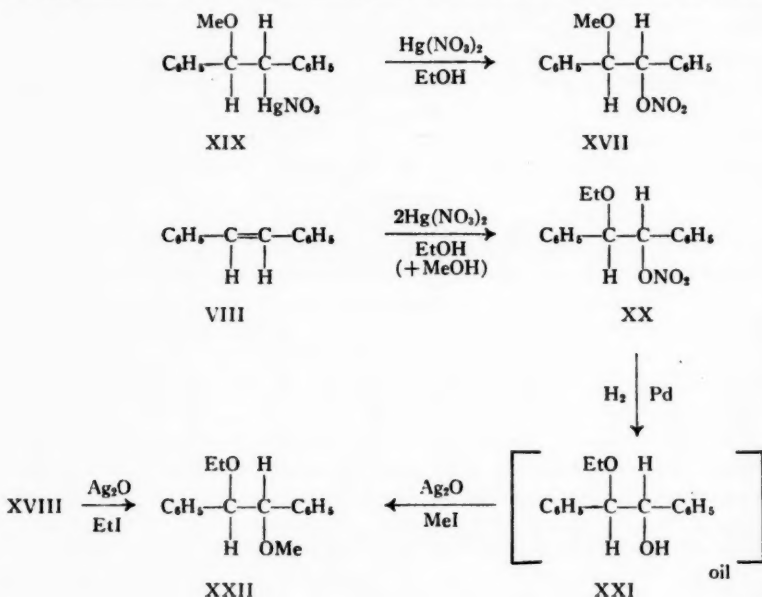
Molarity LiNO ₃	Time, hr.	Per cent yields of products				Recovered alkene, %	% of total product		
		Ether	Ester	Acetal	Total		Ether	Ester	Acetal
0	40	22	34	23	79	11	28	43	29
0.0625	47	20	29	20	69	9	30	41	29
0.25	48	12	29	29	70	7	17	42	41
0.75	48	17	34	30	81	9	21	41	37
1.25	47	10	23	20	53	13	19	43	38
3.50	46	13	28	38	79	8	16	36	48

Before kinetic studies of the stilbene oxidation are considered it seems advisable to establish unequivocally that the oxymercurials are intermediate in the reaction. This has been done in three different ways of which the first is a

demonstration that organomercurials in general are oxidized by mercuric salts of oxy acids. When benzylmercuric nitrate in methanol is shaken with an equivalent of mercuric nitrate for 40 hr. the products are mercurous nitrate, a 46% yield of benzyl methyl ether, and a 15% yield of benzyl nitrate. Toluene in this environment is unaffected, so the reaction does not involve hydrolytic decomposition of the mercurial. Actually hydrolysis may be deleterious to the oxidation since the less stable *sec*-butylmercuric nitrate gives only a 5% yield of *sec*-butyl nitrate and no other product.

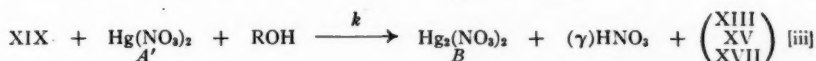
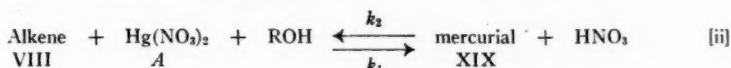
Secondly it can be shown that the oxymercurial is formed rapidly under the conditions of oxidation. When *cis*-stilbene is treated with two equivalents of a 0.125 molar methanolic solution of mercuric nitrate for 10 min. and then drowned in cold dilute aqueous sodium chloride the mercurous salt which is formed indicates that 8-9% of oxidation already has occurred, but the remainder of the precipitate (washed with hexane to remove stilbene) is 2-methoxy-1,2-diphenylethylmercuric chloride in 78% yield. It is believed that this yield represents an equilibrium concentration since it is depressed to 74% and to 73% by inclusion into the reaction system of two or four equivalents of nitric acid; these additions only increase the amount of oxidation to 10%.

Thirdly we have demonstrated that the oxymercurial rather than the alkene is the species which undergoes oxidation. When α -2-methoxy-1,2-diphenylethylmercuric nitrate (XIX) is treated with mercuric nitrate in ethanol a 39% yield of (*dd, ll*)-2-methoxy-1,2-diphenylethyl nitrate (XVII) is obtained, as compared with the 35% yield of this diastereomer obtained by oxidation of *cis*-stilbene from which the α mercurial is derived. If oxidation of the mercurial



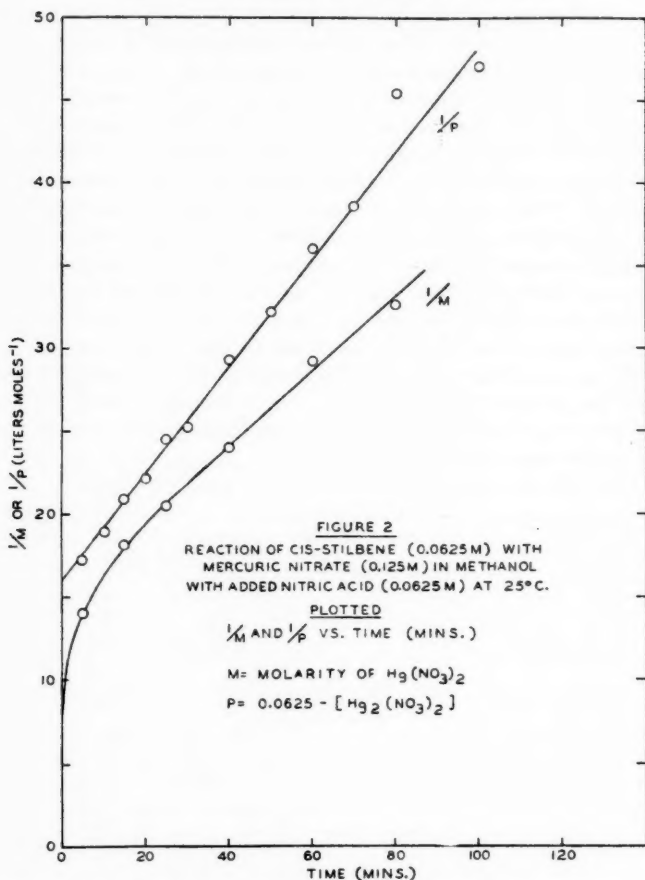
had involved appreciable reversion to the alkene the product would have been the ethoxy nitrate (XX). The proof is valid unless the single equivalent of methanol which would be formed by decomposition of the methoxymercurial to the alkene were to be selected for the oxidation process from a large excess of ethanol. This doubt has been dispelled by treatment of *cis*-stilbene with two equivalents of mercuric nitrate in ethanol containing one equivalent of methanol. The product in 25% yield is evidently (*dd, ll*)-2-ethoxy-1,2-diphenylethyl nitrate (XX) since it is reduced by palladium-on-charcoal to ammonia and an oil. This oil must be (*dd, ll*)-2-ethoxy-1,2-diphenylethanol (XXI) since treatment with methyl iodide and silver oxide produces (*dd, ll*)-1-ethoxy-2-methoxy-1,2-diphenylethane (XXII), identical according to mixture melting point with that prepared by ethylation with silver oxide and ethyl iodide of (*dd, ll*)-2-methoxy-1,2-diphenylethanol (XVIII). Therefore it seems to be definite that the alkene reacts with two equivalents of mercuric nitrate, first to form the oxymercurial, the carbon-metal linkage of which is replaced by nitroxilation (and presumably by alkoxylation) without involvement of the vicinal oxy linkage.

Thus for kinetic study the oxidation of *cis*-stilbene by alcoholic mercuric nitrate may be described by two equations:



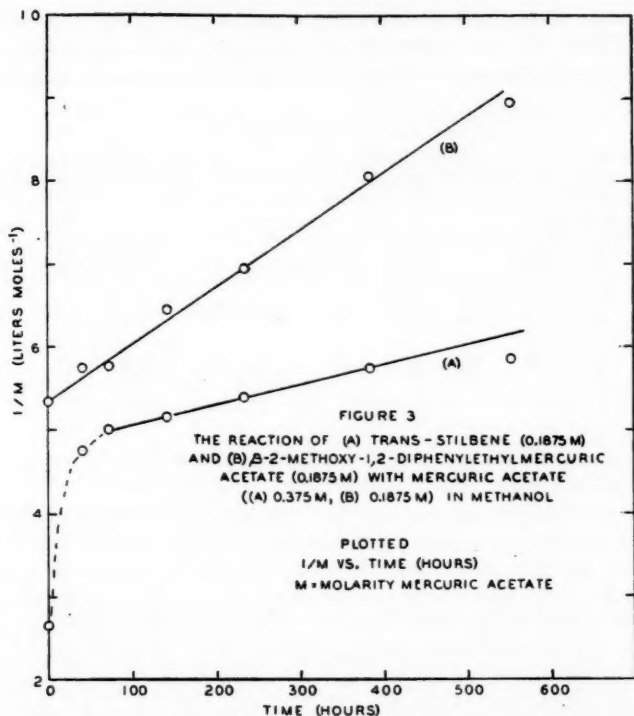
where γ is the fraction of nitrate ester (XVII) to total products. No general integrated equation has been devised (29) to express the kinetic behavior of such a reacting system, especially in consideration of the observed catalytic effect of nitric acid. However the knowledge that $k_1 \gg k_2 \gg k$ in the reaction with *cis*-stilbene makes this system amenable to study if the effect of nitric acid is neglected by examination of the early stages of reaction. This expedient is probably workable because the catalytic effect of nitric acid opposes its equilibrium-depressant effect in the first reaction. Then the kinetics may be described in terms of [iii] and if a is the initial concentration of A' and b is the concentration of XIX (or A) the second-order relationship of equation [i] is applicable.

However since k_1 is not infinitely larger than k_2 it is apparent that analytically it is better to follow the appearance of mercurous salt rather than the disappearance of mercuric salt. This preference is exemplified in Fig. 2 (see also Table XIII) wherein the combined rate of oxymercuration (reaction [ii]) and oxidation (reaction [iii]) is not apparent as a second-order relationship in $1/M$ but may be so interpreted in $1/P$. But this expedient is ineffective in the oxidation of *trans*-stilbene in methanol for several reasons. Firstly the system is not initially homogeneous. Secondly it is probable that k_2 actually is larger than k_1 and both are comparable with k . Nevertheless a roughly determined rate constant ($0.017 \text{ l. moles}^{-1} \text{ min.}^{-1}$) has been calculated showing



at least that the over-all oxidation of the *trans*-isomer is slower than that of the *cis* form. Since mercurials easily decomposed according to reaction [ii] are usually oxidized more easily according to reaction [iii] it would seem that the slow rate of *trans*-stilbene oxidation is due to an especially unfavorable equilibrium in reaction [ii].

Probably because the reaction becomes more quickly homogeneous, and possesses a more favorable equilibrium in the mercuration step (like reaction [ii]), the kinetics of the oxidation of *trans*-stilbene by mercuric acetate in methanol (7) are more amenable for study than oxidation with mercuric nitrate though both mercurous nitrate and acetate are separable from mercuric salt. Titration of unchanged mercuric acetate after chloroform extraction of mercurial (41) provides concentration values of A' (reaction [iii]) from which reciprocals are plotted versus time (Curve A, Fig. 3). Despite the marked initial curvature characterizing the slow attainment of a steady-



state concentration of β -2-methoxy-1,2-diphenylethylmercuric acetate the remainder of the curve is sufficiently linear for calculation of 0.39×10^{-4} l. moles $^{-1}$ min. $^{-1}$ as a second-order specific rate constant. However a better evaluation is possible since it is realized that the mercurial is an intermediate in the oxidation. Direct reaction of β -2-methoxy-1,2-diphenylethylmercuric acetate (from the chloromercurial and silver acetate) with one equivalent of methanolic mercuric acetate occurs according to Curve B, Fig. 3, the slope of which gives a realistic second-order rate constant of 1.2×10^{-4} l. moles $^{-1}$ min. $^{-1}$.

The products of the reactions of *cis*- and *trans*-stilbenes, as well as their characteristic oxymercurials, with methanolic mercuric acetate (containing boron fluoride etherate) are shown in Table VIII. The results, obtained by chromatographic separation, resemble those obtained with mercuric nitrate since *trans*-stilbene (VII) yields chiefly (*dl,ld*)-1,2-dimethoxy-1,2-diphenylethane (XII) together with a small amount of the (*dd,ll*)-diastereomer (XV), while the converse distribution of diastereomeric diethers is obtained from *cis*-stilbene. However it is notable that the ratio (ca. 4 : 1) of (*dd,ll*) to (*dl,ld*) diastereomer obtained from *cis*-stilbene is somewhat smaller than the ratio (*dl,ld*) to (*dd,ll*) (ca. 21 : 1) of these diastereomers obtained from *trans*-stilbene and methanolic mercuric acetate. Similar but lesser differences (diastereo-

meric ratios of *ca.* 7 : 1 for *cis*-stilbene and *ca.* 15 : 1 for *trans*-stilbene) are found (Table IV) for reactions of comparable duration with methanolic mercuric nitrate. Since the reactions with mercuric acetate are slower than those

TABLE VIII

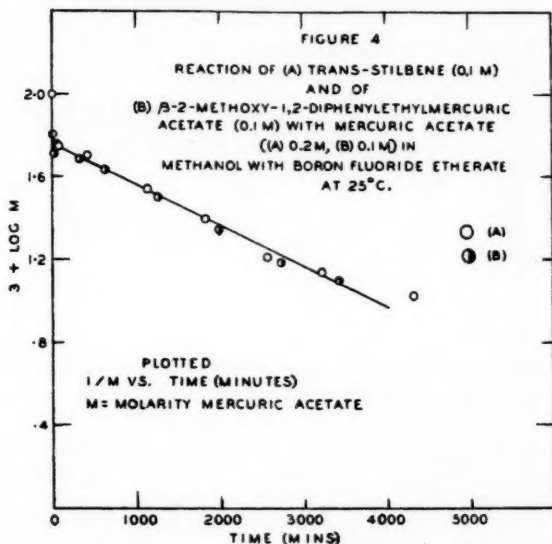
REACTION OF *cis*- AND *trans*-STILBENES AND OF α - AND β -2-METHOXY-1,2-DIPHENYLETHYL-MERCURIC ACETATES IN METHANOL WITH 0.02 *M* BORON FLUORIDE ETHERATE

Hg(OAc) ₂	Initial molarities		Time, hr.	% Yields of products				Recovered alkene, %	% of total products		
	Mercurial	Stilbene		(<i>dl,ld</i>) Diether	(<i>dd,ll</i>) Diether	Acetal	Total		(<i>dl,ld</i>) Diether	(<i>dd,ll</i>) Diether	Acetal
<i>cis</i> -Stilbene	—	.05	58	5.2	22.6	8.0	35.8	6.6	15	63	22
.10	—	—	118	6.2	28.4	13.6	48.2	8.3	13	59	28
<i>trans</i> -Stilbene	—	.05	117.5	44.4	2.1	14.0	60.5	12.2	73	35	24
.10	—	—	146	41.2	1.9	22.7	65.8	6.4	63	3	34

utilizing mercuric nitrate, and (as will be explained below) when the highly acidic methoxytrifluoboric acid is present, the systems described in Table VIII will suffer *cis-trans* isomerism (9). Although the exact position of the *cis-trans* equilibrium between the stilbenes is still in doubt (12) it is at least 95% *trans*. It might then be expected that, despite the faster rate of *cis*-stilbene mercuration, the preponderance of *trans*-stilbene following small extents of geoisomerization would tend to accentuate the diastereomeric ratio of (*dl,ld*) to (*dd,ll*). Evidence for some geoisomerization during the oxidation is provided by the observation that *cis*-stilbene recovered from the oxidations contains some *trans*-isomer. In consequence of these observations it is conceivable that the oxidation reaction is entirely stereospecific, and the nonstereospecific product is a consequence of side-reaction during experiments of long duration. Significant to this argument are the yields of 1,1-dimethoxy-2,2-diphenylethane (Table VIII) which are about the same for *cis*- and *trans*-stilbenes in these slow reactions with mercuric acetate, although they are quite different for the more rapid reactions with mercuric nitrate (Table IV).

It has been noted that the experiments described in Table VIII include boron trifluoride etherate (the methylate behaves identically) which has been shown previously (7) to accelerate oxidation of alkenes and their mercurials by mercuric acetate. The type, if not ratios, of products is the same if the catalyst is not used, but of course the yields are meager and are contaminated with products of side-reactions caused, for example, by the slow oxidation of methanol by mercuric acetate which takes place in absence of alkenes. However we have necessarily assumed, because of experimental difficulties of isolation, that the kinetic results of the uncatalyzed reaction of stilbenes with mercuric acetate give about the same amounts of products as those which have been isolated from reactions which are catalyzed with boron fluoride.

The kinetic behavior of the boron-fluoride-catalyzed reaction is quite different from that of the uncatalyzed reaction. In presence of the catalyst the reaction is first-order over-all up to at least 70% of completion. This behavior



is evident in Fig. 4 where the logarithm of mercuric acetate concentration has been plotted against time of reaction with *trans*-stilbene (Curve A) and its mercurial (Curve B) in presence of boron fluoride. The linearity is that expected of a first-order reaction although the initial stages indicate that oxymercuration, though rapid, does not go to completion; conversely the oxymercurial when used initially seems to decompose reversibly so as to regenerate mercuric acetate. This behavior is shown more clearly in Fig. 5, describing reaction of β -2-methoxy-1,2-diphenylethylmercuric acetate in methanol with boron fluoride alone. Disappearance of mercuric and appearance of mercurous salt have been determined simultaneously. At first there is a rapid appearance of mercuric acetate which then remains relatively constant at a ratio of $2 \text{ Hg}(\text{OAc})_2 : 8 \text{ oxymercurial}$ until, after about five hours, it begins to increase. The increase undoubtedly is due to shifting equilibrium caused by acetic acid generated by the oxidation which, according to the generation of mercurous salt, is proceeding continually.

The significance of the catalyst in respect of the first-order kinetics is shown in Table IX, where the rate is found to be directly proportional to the boron fluoride concentration. Also significant is the fact that the first-order oxidation rate of either *cis*-stilbene or its derivative, α -2-methoxy-1,2-diphenylethylmercuric acetate, is approximately the same as that of *trans*-stilbene or the β -methoxymercurial. This similarity is shown by comparison of Expts. 1 and 2, Table X, with the rate constant (5.56×10^{-4}) for the comparable experiment with β -2-methoxy-1,2-diphenylethylmercuric acetate in Table IX. Expts. 3 and 4, Table X, also are comparable, although the recorded rate constants are different because Expts. 3-7 were analyzed for mercurous salt

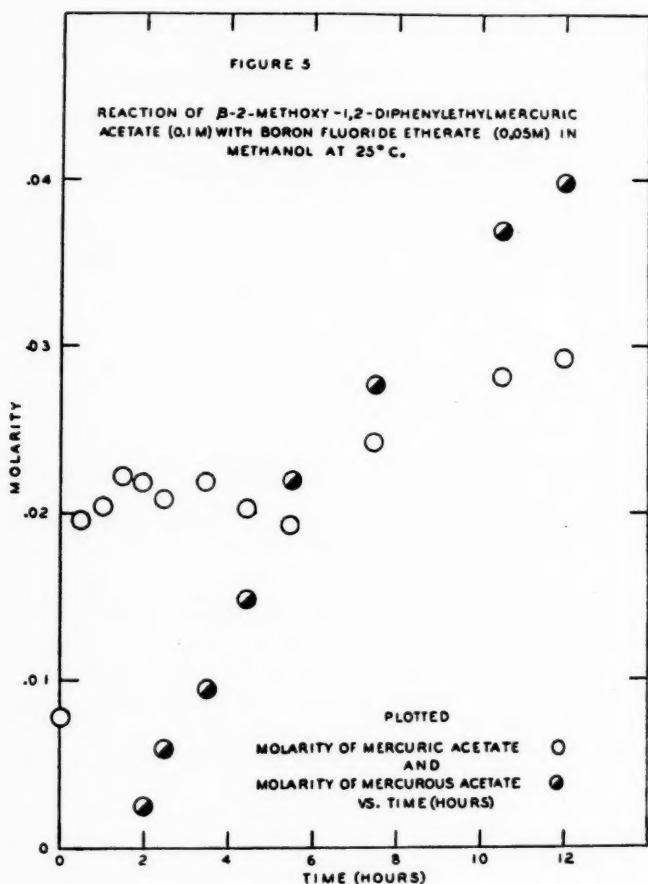


TABLE IX
REACTION OF β -2-METHOXY-1,2-DIPHENYLETHYLMERCURIC ACETATE (0.1 M)
WITH MERCURIC ACETATE (0.1 M) IN METHANOL WITH BORON FLUORIDE
ETHERATE AT 25°C.

Molarity of $\text{BF}_3 \cdot \text{etherate} (M_{\text{BF}_3})$	First-order spec. rate $k \text{ (min.}^{-1}\text{)}$	k/M_{BF_3}
.03	3.22×10^{-4}	.0107
.04	5.56	.0139
.06	7.76	.0129
.08	9.29	.0116

TABLE X
REACTION OF *cis*-STILBENE WITH MERCURIC ACETATE IN METHANOL CATALYZED
BY BORON FLUORIDE AT 25°C.

Expt. No.	Initial molarities			Molarities after mercuration			First-order k (min. ⁻¹)	Per cent investi- gated
	Hg(OAc) ₂	<i>cis</i> - Stilbene	BF ₃ ·Et ₂ O	Hg(OAc) ₂	Mercurial	HOAc		
1	—	—*	.02	.05	.05	—	$5.05 \pm .25 \times 10^{-4}$	79
2	.1	.05	.02	.05	.05	.05	$5.68 \pm .30$	75
3	.2	.1	.02†	.1	.1	.1	$3.95 \pm .05$	66
4	.2	.1	.02	.1	.1	.1	$4.08 \pm .10$	69
5	.1	.05	.02	.05	.05	.05	$4.62 \pm .11$	72
6	.25	.1	.02	.15	.1	.1	$4.70 \pm .17$	70
7	.20	.05	.02	.15	.05	.05	$6.77 \pm .36$	88

* Mercurial used instead of alkene.

† BF₃ gas in methanol.

while mercuric acetate was determined in the first two experiments. The rate constants are more accurate when calculated from mercurous salt analyses.

Inspection of Expt. 7, Table X, shows that first-order kinetics no longer are valid when the molar ratio of mercuric acetate to *cis*-stilbene becomes large. The same type of deviation is observed when the ratio of mercuric acetate to β -2-methoxy-1,2-diphenylethylmercuric acetate is 2:1 rather than 1:1 ($k = 5.35$ versus 4.9×10^{-4} min.⁻¹). Additionally the apparent rate seems to increase as the reactions with excess of mercuric acetate proceed. These behaviors are exemplified by comparison of the detailed kinetic data of Expt. 4 (and Expts. 6 and 7 are similar) with Expt. 7 in Table X. The comparison is delineated in Table XI in terms of calculated first- and second-order rate constants. No satisfactory integral order can be defined for Expt. 7, in contrast to the first-order kinetic agreement for Expt. 4.

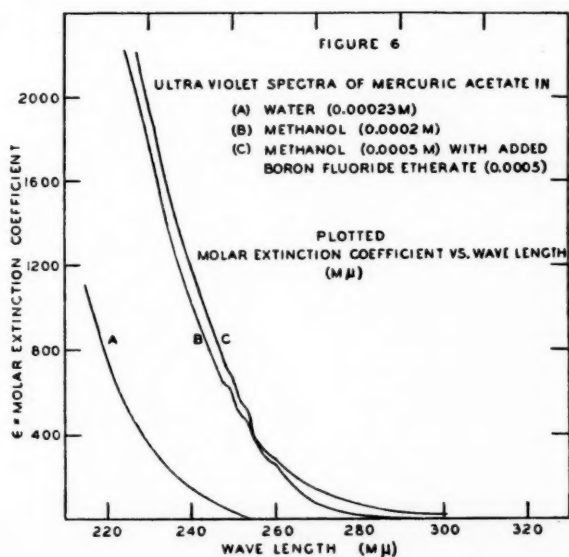
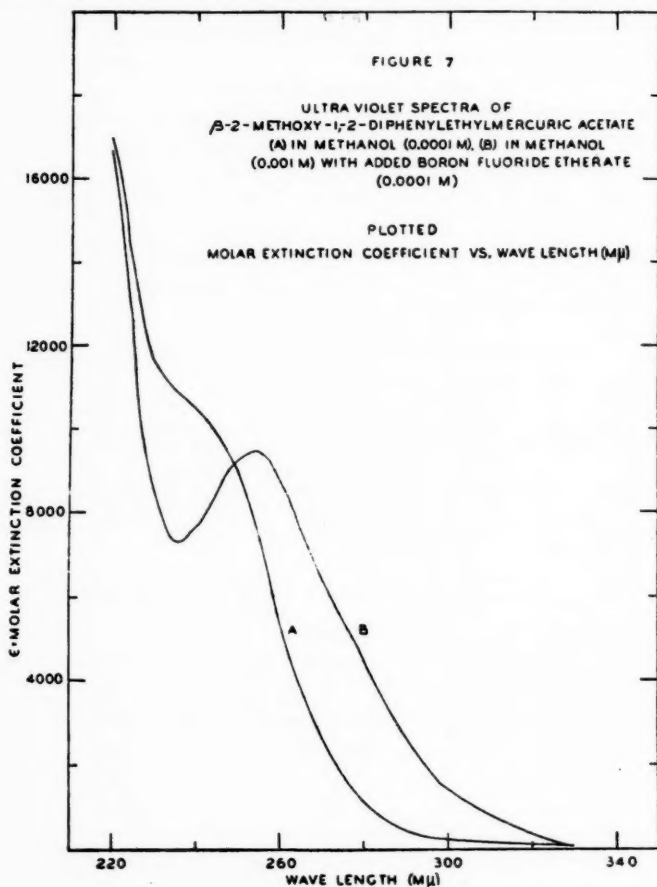
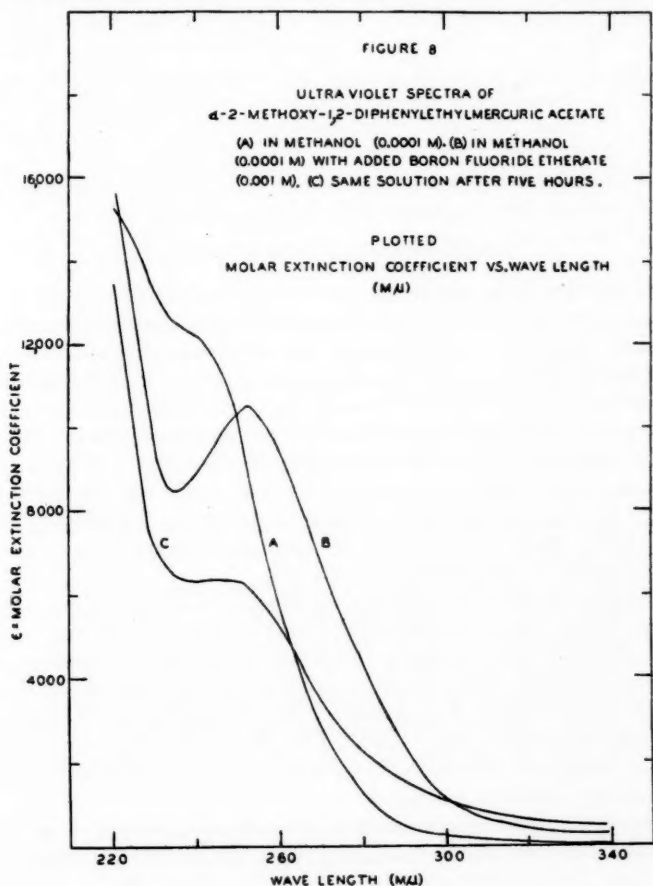


TABLE XI
THE REACTION OF *cis*-STILBENE WITH MERCURIC ACETATE IN METHANOL WITH
ADDED BORON FLUORIDE ETHERATE AT 25°C.

Expt. 4 Mercuric acetate, 0.1 M; mercurial, 0.1 M			Expt. 7 Mercuric acetate, 0.15 M; mercurial, 0.05 M		
Time (min.)	k_1 (min. ⁻¹)	k_2 (l. moles ⁻¹ min. ⁻¹)	Time (min.)	k_1 (min. ⁻¹)	k_2 (l. moles ⁻¹ min. ⁻¹)
130	4.61×10^{-4}	4.82×10^{-3}	120	4.13×10^{-4}	4.06×10^{-3}
250	4.33	4.59	240	6.53	4.41
380	4.24	4.56	370	6.44	4.45
460	4.05	4.45	465	6.50	4.56
590	4.01	4.53	695	6.32	4.51
710	4.01	4.64	870	6.61	4.76
880	3.92	4.69	1420	6.90	5.25
1430	3.94	5.30	1780	7.34	5.75
1790	4.09	6.02	2850	7.50	6.26
2865	4.10	7.83			

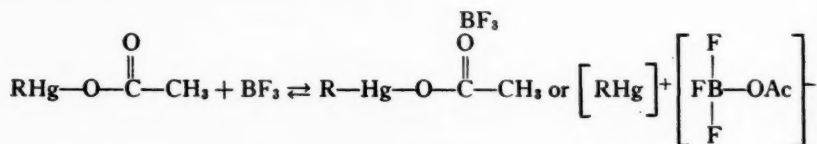


In order to evaluate these results the ultraviolet spectra of some of these systems have been examined. It may be seen in Fig. 6 that aqueous mercuric acetate ($0.00023 M$) is as transparent as water at wavelengths longer than $255 m\mu$ but methanolic mercuric acetate ($0.0005 M$) begins to absorb at $300 m\mu$ and is completely opaque at $220 m\mu$. The addition of boron fluoride etherate ($0.0005 M$) to this latter solution does not change its absorption. On the other hand it is seen in Fig. 7 that methanolic β -2-methoxy-1,2-diphenylethylmercuric acetate ($0.0001 M$) begins to absorb at about $340 m\mu$ and the absorption rises steadily until a single inflection is found ($E_{\text{molar}} = 11,000$) at $240 m\mu$. Addition of boron fluoride etherate ($0.001 M$) to this solution has a profound effect. The absorption rises more steeply from $340 m\mu$ to a peak at $253 m\mu$ ($E_{\text{molar}} = 9500$) and then dips to a trough of transmission ($E_{\text{molar}} = 7000$) at $235 m\mu$. The α -2-methoxy-1,2-diphenylethylmercuric acetate in methanol shows essentially the same behavior (Fig. 8). However its solution containing

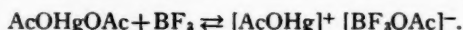


10 equivalents of boron fluoride has been examined further, with respect to time. After five hours it is found that the peak has almost disappeared, as if a complex were decomposing to give substances of greater transparency than those contained in the original system. These substances cannot include appreciable amounts of the stilbenes since the *cis*-isomer absorbs strongly at 270 $m\mu$ while the *trans* form absorbs at 300 $m\mu$.

It would seem from these data that the combination of boron fluoride with acetate involves the rate-controlling step, which should then be first-order. Furthermore, since the ease of oxidation of alkenes (and of course the intermediate oxymercurial) is greater with salts of strong acids rather than weak ones, the boron fluoride must be creating a salt of a strong acid. The creation of an u.v. absorption region when boron fluoride is added to the oxymercurial, and the disappearance of this band at a rate commensurate with that of oxidation, indicates the reaction:



but the deviation from first-order kinetics with consequent acceleration when mercuric acetate is in large excess ought to involve the reaction:



Thus the rate of oxidation by mercuric salts seems to depend on the acid involved with the mercury and, especially, with the intermediate organomercurial. However it is doubtful that the acid is functioning in an ionic form. The effectiveness of acids (HNO_3 , H_2SO_4 > HClO_4 > $\text{C}_6\text{H}_5\text{SO}_3\text{H}$, CF_3COOH) does not correspond with the dissociation of these acids in water. Certainly in media such as ethanol, nitric acid is largely non-dissociated (15, 16, 21, 28). The ion concentration would have to be very low, but in this circumstance the reaction would have to be very sensitive to added ions. It has been shown (Table VII) that the oxidation as such is unaffected by addition of lithium nitrate. From these considerations it would seem that the acid and its salts were not active in the oxidation as free ions.

The effect of acid in the oxidation has an additional significance. It is known, and has further been demonstrated in the present report, that acids cause decomposition of oxymercurials, which then revert to the parent alkene. But those oxymercurials which are most stable toward acid decomposition are also most difficult to oxidize. For example, hydroxyethylmercuric nitrate and 2,2'-dinitratomercuridiethyl ether (which actually can be prepared from ethylene in acid solutions of mercuric salts) are recovered unchanged after treatment with mercuric nitrate in methanol.

Of course the hydrolytic decomposition and the oxidation of oxymercurials have other characteristic resemblances. Both seem to be stereospecific in the

sense that diastereomeric oxymercurials tend to revert by acid decomposition to the geoisomer from which they were originally derived, while oxidation gives derivatives characteristic of this geoisomer. This would seem to preclude the postulation of a carbonium ion intermediate in either reaction. The demonstration in the present report that the vicinal alkoxy group is not involved directly in the oxidation renders improbable the participation of an epoxonium ion. It would seem likely that molecular species are operative in both reactions either by ion-pair exchange (giving HgX^+ and X^- in the acid decomposition versus HgX^- in the oxidation) or by homopolar exchange giving HgX radicals from which mercuric or mercurous salts could be formed.

EXPERIMENTAL*

Acidic Hydroxymercuration of Cyclohexene

A solution 0.5 molar in mercuric nitrate and 1.0 molar in nitric acid was treated with cyclohexene equivalent to the mercuric salt. After 10 min. the system was poured into 0.1 molar aqueous sodium chloride equivalent to the cyclohexene. The yield of α -2-hydroxycyclohexylmercuric chloride, m.p. 145–147°, was 79%. A 20-min. experiment gave the identical yield. When the reaction system was 1.0 molar in mercuric nitrate and 2.0 molar in nitric acid the otherwise identical experiment gave a 63% yield.

Formylcyclopentane and Its Derivatives

(a) From Mercuric Nitrate - Cyclohexene

To a solution of 68.6 gm. (0.2 mole) of mercuric nitrate monohydrate in 400 ml. of water containing 12.6 ml. (0.2 mole) of 70% nitric acid was added with vigorous stirring 10.1 ml. (0.1 mole) of cyclohexene. After 84 hr. the system (which contained 0.8 gm. of free mercury) was extracted with four 50-ml. portions of chloroform. Distillation yielded 2.22 gm. (23%) of formylcyclopentane, b.p. 40–50° (8 mm.), n_D^{20} 1.4460, and 1.54 gm. (14%) of cyclopentanecarboxylic acid, b.p. 94° (8 mm.) n_D^{20} 1.4597. The residue, separated from 0.11 gm. of mercurous salt, was crystallized from 95% ethanol, 1.20 gm. (12%) of 2,4,6-tricyclopentyl-1,3,5-trioxane, m.p. 123–125°, identified by mixture melting point.

(b) From Mercuric Nitrate and 2-Hydroxycyclohexylmercuric Nitrate

When 8.38 gm. (0.025 mole) of 2-hydroxycyclohexylmercuric chloride was shaken with 50 ml. of water containing 4.25 gm. (0.025 mole) of silver nitrate and 5 ml. of methanol for 70 min. the precipitate of silver chloride weighed 3.71 gm. (92%). To the filtrate was added 8.54 gm. (0.026 mole) of mercuric nitrate in 50 ml. of water. The system was azeotropically distilled at 8 mm. and 35° for two hours. No cyclohexene was found in the ice-cooled or dry-ice-cooled receivers but 0.93 gm. (38%) of formylcyclopentane, b.p. 75–85° (94 mm.), was obtained by distillation of the ether extract. No cyclopentanecarboxylic acid was found.

*Melting points have been corrected against reliable standards. X-ray diffraction patterns were determined using Cu K_α (Ni filtered) radiation at relative intensities I/I_1 and d spacings in Angstrom units.

(c) *From Methanolic Mercuric Nitrate - Cyclohexene*

A system containing 6.86 gm. (0.02 mole) of mercuric nitrate, 0.63 ml. (0.01 mole) of 70% nitric acid, and 1.01 ml. (0.01 mole) of cyclohexene in 40 ml. of methanol was studied kinetically by removal of 10-ml. aliquots into 40 ml. of 5% aqueous sodium chloride. After 17.5, 41.5, and 114 hr. the mercurous chloride weighed 0.28, 0.77, and 0.89 gm. respectively, representing oxidation to the extent of 24, 65, and 76%. The filtrate from the third aliquot on treatment with a solution of 2,4-dinitrophenylhydrazine in 2 *N* hydrochloric acid yielded 0.12 gm. of formylcyclopentane dinitrophenylhydrazone (17% based on cyclohexene), m.p. 148–152°, with X-ray diffraction pattern [10] 4.05; [6] 5.12; [5] 7.48; [4] 3.20; [1] 3.40; [0.5] 3.05, 2.44, 2.03, identical with an authentic specimen.

(d) *From Mercuric Nitrate and 2-Methoxycyclohexylmercuric Nitrate*

A quantitative yield of silver chloride was obtained when 3.49 gm. (0.01 mole) of α -2-methoxycyclohexylmercuric chloride was treated with 1.70 gm. (0.01 mole) of silver nitrate. The remainder of the system after three days with 3.25 gm. (0.01 mole) of mercuric nitrate was diluted with 100 ml. of water and extracted with 125 ml. of ether in four portions. This extract, washed with alkali and with water and dried with magnesium sulphate, was distilled to yield only 0.54 gm. (55%) of formylcyclopentane, n_D^{20} 1.4495, identified as the dinitrophenylhydrazone. The extracted aqueous dilution liquor yielded mercurous chloride quantitatively upon treatment with aqueous sodium chloride.

(e) *From Cyclohexene and Mercuric Sulphate*

After 11 hr. a system comprising 43.4 gm. (0.2 mole) of mercuric oxide in 50 ml. of 6 molar sulphuric acid (0.3 mole), 340 ml. of water, and 10.1 ml. (0.1 mole) of cyclohexene gave a negative test for mercuric salt. The suspension was flash-distilled at 10–12 mm. into receivers at -15° and -80° . Extraction of the distillate yielded 3.5 gm. (37%) of formylcyclopentane, b.p. 65–68° (75–76 mm.), identified as the dinitrophenylhydrazone. Extraction of the 96% yield of mercurous sulphate with chloroform gave an oil which, combined with the residue from distillation of the aldehyde, yielded about 0.8 gm. (7%) of cyclopentanecarboxylic acid, b.p. 80–90° (9 mm.).

(f) *From Cyclohexene and Other Mercuric Salts*

After five days a system comprising 9.48 gm. (0.06 mole) of benzenesulphonic acid, 4.34 gm. (0.02 mole) of mercuric oxide, and 1.01 ml. (0.01 mole) of cyclohexene was filtered to remove 0.12 gm. (3%) of free mercury. Treatment of the filtrate with sodium chloride followed by extraction with ether gave successively 3.65 gm. (77%) of mercurous chloride and 0.39 gm. of oil which gave the dinitrophenylhydrazone of formalcyclopentane. By contrast no trace of the aldehyde was obtained from mercuric phosphite.

2-Methyl-1-phenylpropene (I) Purification

The preparation according to Tiffeneau and Orékoﬀ (35) gave a product in 90% yield, b.p. 75–86° (15–17 mm.), redistilled for 75% over-all yield, b.p. 75–79° (12–14 mm.), n_D^{20} 1.5376, d_4^{20} 0.903, m.p. -66 to -63° . After conversion

to 2-methoxy-2-methyl-1-phenylethylmercuric chloride (6), m.p. 78.5–80°, which was crystallized, the alkene was recovered by decomposition of the mercurial with 1 : 1 methanol – concentrated hydrochloric acid, aqueous dilution, and petroleum ether extraction. The distilled product boiled at 65.5–66° (12 mm.) or 75–77° (18 mm.), n_D^{20} 1.5405, and seemed to exist in polymorphic forms. Crystallization by rapid cooling gave a melting point of about –56°; if maintained at this temperature the sample resolidified, then melted at –50° to –48°.

2-Methyl-1-phenylpropene with Mercuric Salts

(a) With Mercuric Nitrate in Methanol

The addition of 17.0 gm. (0.052 mole) of mercuric nitrate to 100 ml. of methanol produced a yellow precipitate, principally mercuric oxide, but it redissolved within two minutes when 3.65 ml. (0.025 mole) of 2-methyl-1-phenylpropene was added. After 20 hr. the system was filtered from 4.74 gm. of mercurous nitrate. The filtrate, diluted with 200 ml. of water and thrice extracted with a total of 200 ml. of ether, was then treated with sodium chloride to precipitate mercurous chloride. Since the remaining liquor with hydrogen sulphide gave 0.6 gm. of mercuric sulphide, the total recovery of mercury is 98%.

The ether solution, washed with water, 5% alkali, and water, then dried with magnesium sulphate, contained 4.66 gm. of oil which was distilled (8 mm.) to yield two lots of impure (40%) 1,2-dimethoxy-2-methyl-1-phenylpropane (II), b.p. 94–100° (n_D^{20} 1.4966), m.p. 0–6°, and b.p. 100–106° (n_D^{20} 1.4980), finally purified by fractional freezing of the 2.11 gm. total, m.p. 8–11.5°, identified by mixture melting point (6). After an intermediate fraction, b.p. 106–122°, 0.57 gm. (n_D^{20} 1.5027), there distilled 1.30 gm. (23%) at 124–126° (n_D^{20} 1.5083) 2-methoxy-2-methyl-1-phenylpropyl nitrate (III). Anal.: Calc. for $C_{11}H_{18}O_4N$: N, 6.22. Found: N, 5.96. The intermediate and final fractions were contaminated with small amounts of benzaldehyde or its acetal, identified by preparation of its dinitrophenylhydrazone, m.p. 237–238°, with unchanged mixture melting point. The amount of benzaldehyde was enhanced by addition of nitric acid to the original system. Essentially the same yields of principal products were obtained (according to refractive indices) when 2-methoxy-2-methyl-1-phenylpropylmercuric nitrate replaced the 2-methyl-1-phenylpropene in the original system, although contamination with benzaldehyde was diminished.

In order to demonstrate that the nitrate ester is formed more rapidly than the 1,2-dimethoxy-2-methyl-1-phenylpropane a system comprising 2.029 gm. (0.00625 mole) of finely ground mercuric nitrate and 0.459 ml. (0.00313 mole) of 2-methyl-1-phenylpropene made up to 25 ml. with methanol was maintained at 25°. One series of 1-ml. aliquots was withdrawn periodically and analyzed according to kinetic methods outlined below. Another set of 5-ml. aliquots was periodically diluted with 10 ml. of 0.1 *N* nitric acid. The ether extract (40 ml.) of this diluate was extracted with two 10-ml. portions of 5% sodium sulphate, then diluted to exactly 50 ml. with ether. Two 10-ml. aliquots

of this solution were evaporated, treated with *m*-xylene and sulphuric acid (42), and examined through a blue filter in the Klett Summerson colorimeter using potassium nitrate as a standard. A second experiment was performed with inclusion of 0.262 ml. (0.00625 mole) and at 29°. A single analysis was performed after 130 min. Results are outlined in Table XII.

TABLE XII
RATE OF NITRATE ESTER FORMATION IN REACTION OF MERCURIC NITRATE
WITH 2-METHYL-1-PHENYLPROPENE

Expt.	Time, min.	% Reaction (Y)	% Nitrate ester (X)	Ratio X/Y
1	30	32	17	0.53
1	70	54	24	0.44
1	120	66	27	0.42
2	130	86	30	0.35

(b) *With Mercuric Trifluoroacetate in Methanol*

Mercuric trifluoroacetate was prepared by solution of 10.83 gm. (0.05 mole) of mercuric oxide in 10 ml. (0.147 mole) of trifluoroacetic acid. After the initial evolution of heat a further 5-ml. portion of trifluoroacetic acid was added, and the whole was heated on the steam bath until solution was almost complete. The hot suspension was filtered through sintered glass and chilled to 0°. The white crystals were filtered off and vacuum dried, 10.9 gm. (53%), m.p. 164–168° with softening at 158°. The X-ray diffraction pattern was: [20] 10.00; [18] 10.64; [16] 15.49, 13.71; [14] 4.90; [12] 7.82, 4.18; [10] 4.07, 3.40, 3.15; [8] 4.48, 3.53; [6] 5.27, 3.91, 2.98, 2.66, 2.28; [4] 6.91, 3.76, 2.93, 2.36, 2.23, 2.03; [2] 6.44, 5.49, 4.76, 3.33, 2.77, 2.00, 1.96, 1.93; [1] 7.49, 5.71, 2.59, 2.48. Anal.: Calc. for $\text{Hg}(\text{CF}_3\text{COO})_2$; Hg, 47.0. Found: Hg, 46.7.

To a solution of 4.27 gm. (0.01 mole) of mercuric trifluoroacetate in 20 ml. of methanol was added 0.73 ml. (0.005 mole) of 2-methyl-1-phenylpropene. Dilution with 25 ml. of water after two days and extraction with 20 ml. of chloroform gave a solution which, washed with water, 2 *N* hydrochloric acid, 5% aqueous alkali and water, then dried, was distilled at 16 mm. giving 0.45 gm., b.p. 106–111°, n_D^{20} 1.4999, and 0.17 gm., b.p. 110–120°, n_D^{20} 1.5080, and 0.21 gm. of residue. The first fraction (m.p. –16 to –6°) was converted in part to 3-phenylbutanone-2 dinitrophenylhydrazone with the methanolic hydrochloride reagent and was identified by mixture melting point. According to the 1.98 gm. of mercurous chloride obtained from the diluted reaction liquor by hydrochloric acid treatment the oxidation reaction was 84% complete.

(c) *With Mercuric Sulphate in Water*

To the bright yellow precipitate obtained when 21.7 gm. (0.1 mole) of mercuric oxide was shaken with 200 ml. (0.2 mole) of molar sulphuric acid was added 7.31 ml. (0.05 mole) of 2-methyl-1-phenylpropene. After shaking for two days 23.5 gm. (95%) of mercurous sulphate was filtered off and washed with methanol and ether. The filtrate was extracted with this ether and with three more 25-ml. portions of ether and three 50-ml. portions of chloroform.

Evaporation of the combined, dried extract left 5.80 gm. (70%) of 2-methyl-1-phenylpropanediol-1,2 which crystallized slowly, m.p. 47–62°. Crystallization from diethyl ether and petroleum ether (b.p. 40–50°) gave 4 gm., m.p. 63–63.5°, identified by mixture melting point with an authentic sample.

2-Methoxy-2-methyl-1-phenylpropanol-1 (IV)

A solution of 0.78 gm. (0.0035 mole) of 2-methoxy-2-methyl-1-phenylpropyl nitrate in 7 ml. of acetic acid was warmed gently while small amounts of zinc dust and iron powder were added until a test sample no longer gave a blue color with diphenylamine and sulphuric acid. The dark-brown mixture was filtered into 30 ml. of water containing 15 gm. of potassium carbonate (pH 8). A triple extraction with 40 ml. total of ether removed an oil, b.p. 118–124° (12 mm.), 0.44 gm. (70%), n_D^{20} 1.5177, m.p. 17–23° (actual yield probably only half this apparent 70%). A repeated partial freezing raised this melting point to 36–39°. This alcohol, still impure, was identified by preparation of derivatives.

After oxidation of 0.08 gm. of the impure alcohol with one equivalent of alkaline permanganate at 0° the mixture was extracted with ether and the extract evaporated. The oil was dissolved in methanol and the dried solution was treated with 2,4-dinitrophenylhydrazine to yield 0.03 gm. of α -methoxy-isobutyrophenone dinitrophenylhydrazone, m.p. 124–127°, which, crystallized from methanol and from 20 : 1 petroleum ether – benzene, melted at 139–140° (0.01 gm.). The X-ray powder diagram was: [10] 10.97, 3.54; [9] 3.09; [7] 9.25, 4.13; [6] 6.21, 3.97; [5] 6.75, 5.53, 3.23; [4] 4.87; [3] 4.31, 2.82; [2] 2.97. Comparison with this powder diagram and by mixture melting point showed that this derivative was identical with that obtainable from the known ketone (1).

trans-Stilbene with Methanolic Mercuric Nitrate

A clear solution was obtained after one hour from 0.90 gm. (0.005 mole) of *trans*-stilbene and 3.41 gm. (0.0105 mole) of mercuric nitrate in 40 ml. of methanol. Dilution with 100 ml. of water after 38 hr. gave a mixture which was thrice extracted with a total of 70 ml. of ether. Treatment of the aqueous layer with 10 ml. of saturated sodium chloride precipitated 2.28 gm. (92%) of mercurous chloride.

The etherous extract, washed with 5% alkali and water, then dried with sodium sulphate, was evaporated leaving 1.19 gm. of semisolid, of which a benzene solution of 339 mgm. was chromatographed on non-activated 80–200 mesh Alcoa alumina in a column 29 × 1.6 cm. Elution with benzene gave 10 fractions: 1, 10 ml. (29 mgm.), m.p. 110–119°; 2, 11 ml. (131 mgm.), m.p. 85–89°; 3, 10 ml. (42 mgm.), m.p. 120–135°; 4, 10 ml. (27 mgm.), m.p. 139.5–140.5°; 5, 10.5 ml. (11 mgm.), oily solid; 6, 10 ml. (32 mgm.), oil; 7, 11 ml. (21 mgm.), oil; 8, 16 ml. (12 mgm.), oil; 9, 15.5 ml. (1 mgm.); 10, 40 ml. (9 mgm.), m.p. 89–91°.

Fraction 1, crystallized from ethanol, was *trans*-stilbene (VII), m.p. 121–123°, identified by mixture melting point. Fraction 2 was crystallized four times from methanol, m.p. 91.4–92.0°, and this (*dl,ld*)-2-methoxy-1,2-diphenylethyl nitrate (IX) gave a positive test with diphenylamine and sulphuric acid.

Anal.: Calc. for $C_{18}H_{18}O_4N$: C, 65.9; H, 5.50; N, 5.13. Found: C, 66.2; H, 5.69; N, 5.09. X-Ray diffraction pattern: [10] 3.79; [7] 9.25, 3.39; [5] 5.65, 5.50, 5.18; [4] 7.62, 6.13, 3.97; [3] 4.29, 4.16; [2] 3.26, 3.02; [1] 4.79, 2.90, 2.79. Fraction 3 is an impure specimen of fraction 4, which is almost-pure (*dl,ld*)-1,2-dimethoxy-1,2-diphenylethane (XII) as was authenticated by mixture melting point and by X-ray diffraction pattern: [10] 5.21; [9] 4.98; [8] 4.76, 3.50; [7] 5.96; [6] 4.01; [4] 9.45, 4.53, 4.44; [3] 6.91, 6.53, 3.37, 3.28; [2] 3.21; [1] 3.13, 3.03, 2.99, 2.81, 2.76. Disregarding fraction 5, the next three, 6, 7, and 8, were combined (n_D^{20} 1.5280) and evidently comprised in large part diphenylacetaldehyde dimethyl acetal (XIII) since it gave no active hydrogen and no carbonyl addition in the Grignard machine, yet slowly yielded the 2,4-dinitrophenylhydrazone of diphenylacetaldehyde (m.p. 143–146°) when it was treated with the methanolic hydrochloride reagent. Two crystallizations from ethanol or chloroform–petroleum ether (b.p. 60–70°) or from methanol–ethyl acetate raised this melting point to 150.2–150.5°. Anal.: Calc. for $C_{20}H_{14}O_4N_4$: C, 63.8; H, 4.29; N, 14.9. Found: C, 63.7; H, 4.24; N, 14.6. The X-ray diffraction pattern was: [10] 15.6; [8] 5.20, 3.65, 3.18; [7] 4.60, 3.94; [6] 6.93; [5] 7.73; [4] 5.64, 5.40. When this derivative was prepared from authentic diphenylacetaldehyde, b.p. 165–166° (12 mm.), n_D^{20} 1.5878, d_4^{20} 1.09, it was found to be identical with the analyzed sample. Fraction 10 was shown by mixture melting point to be (*dd,ll*)-1,2-dimethoxy-1,2-diphenylethane. Its X-ray diffraction pattern was: [10] 6.30, 3.55; [9] 5.01, 4.95; [6] 7.28; [5] 8.58, 4.26, 4.13; [4] 3.32; [3] 5.43, 4.74; [2] 5.88, 3.76; [1] 3.96, 3.06, 2.90.

(dl,ld)-2-Methoxy-1,2-diphenylethanol (X)

(a) From Benzoin Methyl Ether

The procedure of Irvine and Weir (19) was altered by reduction with Raney nickel in ethanol at 27° and 1–2 atmospheres. The product (97%) melted at 100–102°, X-ray diffraction pattern: [10] 5.14; [9] 3.63, 3.42; [7] 8.66, 3.90; [6] 4.66; [4] 12.7, 6.39, 5.64, 4.27, 3.98; [3] 4.88, 3.82, 3.74; [1] 3.34. The configuration was demonstrated by treatment of 1.14 gm. (0.005 mole) with 7.10 gm. (0.05 mole) of methyl iodide and 4.35 gm. (0.016 mole) of fresh gradually-added silver oxide under reflux for five hours. The product (83%) m.p. 140–142° after crystallization was identical (mixture melting point) with that obtained by methylation of hydrobenzoin.

(b) From (dl,ld)-2-Methoxy-1,2-diphenylethyl Nitrate (IX)

A solution of the nitrate ester (27 mgm., 0.0001 mole) in 4 ml. of 1 : 1 dioxane–ethanol was hydrogenated at atmospheric pressure over 0.1 gm. of palladium-on-charcoal (17). The system, containing ammonia, was filtered and evaporated, 19 mgm. (83%), m.p. 97.5–100°. Crystallization from ethanol–water raised the melting point to 100.5–101.8°. The compound was identical with that obtained by procedure (a).

(c) From Stilbene Oxide and Methyl Nitrate – Nitric Acid

When 0.196 gm. (0.001 mole) of stilbene oxide (34) (m.p. 68–69°) in 10 ml. of methanol was treated with 0.154 gm. (0.002 mole) of methyl nitrate (b.p.

65–66°, n_D^{20} 1.3754, d_4^{20} 1.192) at 27° for 29 hr. it was recovered unchanged. However when 0.105 ml. (0.0025 mole) of absolute nitric acid was added the system upon vacuum evaporation after 42 hr. yielded 0.226 gm. of yellow solid, m.p. 40–90°. Chromatography on alumina did not yield any methoxy nitrate ester or dimethoxy compound but 97 mgm., m.p. 91–96°, was obtained, from which (*dl,ld*)-2-methoxy-1,2-diphenylethanol, m.p. 99.5–100.5°, was identified (after crystallization from petroleum ether (b.p. 60–70°) and ethanol–water) by mixture melting point. Both (*dl,ld*)-1,2-dimethoxy-1,2-diphenylethane and (*dl,ld*)-2-methoxy-1,2-diphenylethyl nitrate were found to be stable in the reaction system.

cis-Stilbene with Methanolic Mercuric Nitrate

A shaken suspension of 3.41 gm. (0.0105 mole) of mercuric nitrate and 0.43 gm. (0.0024 mole) of *cis*-stilbene (40) in 40 ml. of methanol was clear after five minutes. After 48 hr. the system was diluted into 80 ml. of water. The diluate, extracted with three 10-ml. portions of chloroform, was then treated with 10 ml. of saturated aqueous sodium chloride to precipitate 1.33 gm. (0.0055 mole) of mercurous chloride. Addition of ammonia to the filtrate then precipitated 1.09 gm. (0.0043 mole) of aminomercuric chloride to give a total of 93% of the original mercury.

The chloroform extract, washed with 5% alkali and with water and dried over sodium sulphate, was evaporated to leave 0.703 gm., semicrystalline, of which 0.242 gm. in benzene was chromatographed as was described for the oxidation of *trans*-stilbene. Fraction 1, 3 mgm., was *cis*-stilbene; 2, 94 mgm., m.p. 87–93°; 3, 6 mgm., m.p. 115–138°; 4, 81 mgm., oil; 5, 31 mgm., m.p. 85–91°. Fraction 2 was twice crystallized from methanol and once from ethanol, m.p. 93.6–93.9°. The X-ray diffraction pattern of this (*dd,ll*)-2-methoxy-1,2-diphenylethyl nitrate (XVII, which gave a blue color with diphenylamine and sulphuric acid) was measured: [10] 10.77, 10.39, 4.08, 4.04; [9] 6.94, 6.73; [8] 7.43, 7.25; [7] 5.18, 5.09, 2.78; [5] 3.64, 3.36; [4] 3.19; [3] 8.07, 7.79, 6.15, 5.30, 4.98. A mixture melting point with the (*dl,ld*)-diastereomer was depressed. Anal.: Calc. for $C_{16}H_{14}NO_4$: C, 65.9; H, 5.50; N, 5.13. Found: C, 65.9; H, 5.80; N, 5.02. Fraction 3, when crystallized from methanol, melted at 138–140°, identified as (*dl,ld*)-1,2-dimethoxy-1,2-diphenylethane by mixture melting point and X-ray diffraction pattern. Fraction 4 was converted to diphenylacetaldehyde 2,4-dinitrophenylhydrazone, m.p. 145–146°, with the methanolic hydrochloride reagent. After crystallization (m.p. 150°) it was authenticated by mixture melting point. Fraction 5 was identified by mixture melting point and X-ray diffraction pattern as (*dd,ll*)-1,2-dimethoxy-1,2-diphenylethane (XV).

(dd,ll)-2-Methoxy-1,2-diphenylethanol (XVIII)

(a) From Benzoin Methyl Ether and Aluminum Isopropoxide

A mixture of 2.12 gm. (0.01 mole) of benzoin methyl ether, 4.0 gm. (0.02 mole) of aluminum isopropoxide, and 35 ml. of isopropyl alcohol in a Hahn apparatus (14) was slowly distilled (28 ml.) until acetone (dinitrophenylhydrazine test) no longer was produced. The cooled residue, diluted with 35 ml.

of 7% hydrochloric acid, was twice extracted with ether. The extract (washed with 5% alkali and water, and sodium-sulphate-dried) was evaporated, 1.88 gm., m.p. 55–59°. By fractional crystallization from petroleum ether (b.p. 60–70°) the more soluble component was separated, m.p. 54.5–55.5°; X-ray diffraction pattern: [10] 5.21; [7] 8.66, 5.71; [6] 4.77; [5] 6.65; [3] 5.01; [2] 4.35, 4.07, 4.00, 3.85, 3.74, 3.49; [1] 13.4, 3.69. Anal.: Calc. for $C_{16}H_{16}O_2$: C, 78.9; H, 7.07. Found: C, 78.4; H, 7.16. The configuration was confirmed by methyl iodide – silver oxide methylation; 0.094 gm. (99%), m.p. 80–88°, was crystallized from 0.5 ml. of methanol, m.p. 92–93°. This (*dd, ll*)-1,2-dimethoxy-1,2-diphenylethane (XV), identical with that obtained by methylation of isohydrobenzoin, was compared by mixture melting point and X-ray diffraction pattern.

(b) *By Reduction of (dd, ll)-2-Methoxy-1,2-diphenylethyl Nitrate (XVII)*

The procedure used for the (*dl, ld*)-diastereomer gave a 75% yield, m.p. 50–52°. After crystallization from petroleum ether (b.p. 60–70°) this (*dd, ll*) isomer, m.p. 54.3–55.5°, was identified by mixture melting point and X-ray diffraction pattern.

α -2-Methoxy-1,2-diphenylethylmercuric Chloride

After about four minutes a strongly shaken mixture of 1.07 gm. (0.0033 mole) of mercuric nitrate and 0.281 gm. (0.0016 mole) of *cis*-stilbene in 25 ml. of methanol at 25° was clear. After 10 min. of reaction time the system was added to 25 ml. of cold 0.4 *N* aqueous sodium chloride. The precipitate, 0.737 gm., was extracted with chloroform, then with methanol to remove mercuric chloride, leaving 0.129 gm. (17%) of mercurous chloride.

The evaporated chloroform solution (0.584 gm.) was washed with 1 ml. of petroleum ether (b.p. 60–70°) to leave 0.548 gm., m.p. 132–139°. After crystallization from ethanol the product (m.p. 141–143°) was identified by mixture melting point.

α -2-Methoxy-1,2-diphenylethylmercuric Nitrate (XIX) with Ethanolic Mercuric Nitrate

After 1.118 gm. (0.0025 mole) of α -2-methoxy-1,2-diphenylethylmercuric chloride and 0.425 gm. (0.0025 mole) of silver nitrate in 10 ml. of anhydrous ethanol was shaken for 35 min. and the silver chloride (0.354 gm. or 0.0025 mole) was filtered and washed with 10 ml. of anhydrous ethanol, the combined filtrate and washings were shaken with 0.845 gm. (0.0026 mole) of mercuric nitrate for 72 hr. Filtration removed 1.047 gm. (0.004 mole) of mercurous nitrate; the filtrate, diluted with an equal volume of water, was thrice extracted with 5-ml. portions of chloroform and was treated then with dilute hydrochloric acid. The precipitated mercurous chloride weighed 0.31 gm. (0.001 mole).

The water-washed chloroform extract was dried and evaporated, leaving 0.633 gm. This product was partially chromatographed, as outlined above, to yield two fractions. The first was crystallized from petroleum ether (b.p. 60–70°), 0.237 gm. (39%), identified as (*dd, ll*)-2-methoxy-1,2-diphenylethyl

nitrate, m.p. 93.5–94°, by mixture melting point. The second fraction, which was oily and weighed 0.290 gm., was treated with hot methanolic 2,4-dinitrophenylhydrazine hydrochloride reagent, yielding the derivative, m.p. 133–138°. After crystallization from ethyl acetate – methanol, m.p. 150–151°, this diphenylacetaldehyde dinitrophenylhydrazone was identified by mixture melting point. If the oil is the diethyl acetal the yield is 43% of theoretical.

(dd,ll)-2-Ethoxy-1,2-diphenylethyl Nitrate

To a mixture of 1.69 gm. (0.0052 mole) of mercuric nitrate in 20 ml. of anhydrous ethanol containing 0.080 gm. (0.0025 mole) of methanol (shaken until the solid had disintegrated) was added 0.4506 gm. (0.0025 mole) of *cis*-stilbene and the mixture was shaken vigorously for 48 hr. After dilution with water the system was thrice extracted with a total of 20 ml. of chloroform. The aqueous layer yielded 0.0049 mole of mercurous chloride when it was treated with aqueous sodium chloride.

The water-washed chloroform extract was dried and evaporated to leave 0.658 gm. of an oil. Chromatography of 258 mgm. of this oil by the method outlined above yielded 29 mgm., m.p. 48–68°, and 80 mgm., m.p. 67–73°, as well as 117 mgm. of an oil. The 80 mgm. portion was crystallized from petroleum ether (b.p. 60–70°), 52 mgm., m.p. 74–75°. Recrystallization raised this melting point to 74.8–75.5°; X-ray diffraction pattern: [10] 3.88; [5] 10.04, 4.82; [4] 4.58, 4.13; [3] 2.94. Anal.: Calc. for $C_{16}H_{17}NO_4$: C, 66.9; H, 5.97; N, 4.88. Found: C, 67.3; H, 6.14; N, 4.68. The residue from the evaporated crystallization liquors melted at 57–69°, 27 mgm.

(dd,ll)-1-Ethoxy-2-methoxy-1,2-diphenylethane (XXII)

(a) From (dd,ll)-2-Methoxy-1,2-diphenylethanol (XVIII)

Gradual addition of 0.46 gm. (0.002 mole) of fresh silver oxide to 83 mgm. (0.0036 mole) of the alcohol in 2.0 ml. (0.0025 mole) of boiling ethyl iodide during four hours gave a mixture which was filtered and evaporated; 89 mgm. slowly crystallized, m.p. 51–54°. A benzene solution, passed through 10 gm. of Alcoa alumina in a column, gave a fraction (79 mgm.), m.p. 54–55°, which was crystallized from 0.3 ml. of petroleum ether (b.p. 40–50°), m.p. 55.2–55.5°, with X-ray diffraction pattern: [10] 6.48; [9] 5.24; [5] 9.16, 7.13, 4.20; [4] 3.81, 3.57, 3.44. Anal.: Calc. for $C_{17}H_{20}O_2$: C, 79.7; H, 7.86. Found: C, 79.7; H, 7.97.

(b) From (dd,ll)-2-Ethoxy-1,2-diphenylethyl Nitrate (XX)

Hydrogenation of 36 mgm. (0.00125 mole) of the nitrate ester with palladium-on-charcoal as outlined earlier yielded 30 mgm. of oil which was methylated with silver oxide and methyl iodide. The crude product in benzene was passed through 2 gm. of Alcoa alumina in a column and the main fraction upon evaporation slowly crystallized, m.p. 53–54.5°. A mixture melting point with product prepared by procedure (a) was not lowered.

β -2-Methoxy-1,2-diphenylethylmercuric Acetate

After shaking 5.0 gm. (0.0112 mole) of β -2-methoxy-1,2-diphenylethylmercuric chloride and 1.87 gm. (0.012 mole) of silver acetate in 40 ml. of

methanol for one hour in the dark the mixture was filtered from silver chloride (100%). Vacuum evaporation of the filtrate left 5.35 gm. (100%), m.p. 100–104°. Solution in 15 ml. of methanol followed by dilution with 8 ml. of water gave 4.22 gm., m.p. 103.5–105°. After crystallization from 95% ethanol the X-ray diffraction pattern of the compound, m.p. 104.5–105.5°, was determined: [10] 11.04; [9] 4.16; [8] 3.43; [6] 4.38; [5] 5.79, 4.58; [3] 3.73; [1] 7.59, 5.27, 4.95. Anal.: Calc. for $C_{17}H_{18}HgO_3$: Hg, 42.6. Found: Hg, 42.4. The product was identified by reconversion to the chloromercurial by treatment of a methanolic solution with aqueous sodium chloride.

cis- or trans-Stilbene or the Corresponding Methoxymercurials with Methanolic Mercuric Acetate and Boron Fluoride Etherate at 25°

The reaction with *trans*-stilbene is typical. A solution of 0.90 gm. (0.005 mole) of *trans*-stilbene, 3.19 gm. (0.01 mole) of mercuric acetate (crystallized from acetic acid), and 0.28 gm. (0.002 mole) of boron fluoride etherate was made up to 100 ml. with dry methanol. The reaction was followed by titration of 2-ml. aliquots with thiocyanate solution after they had been diluted with water and extracted with chloroform. After five days the system was filtered to remove 1.70 gm. (65%) of mercurous acetate. The filtrate, evaporated and diluted with water, was thrice extracted with chloroform. The extract, washed with 5% alkali, water, and then dried and evaporated, yielded 1.055 gm. of semisolid. Chromatography of 277 mgm. as described before yielded 26 mgm. of stilbene, 130 mgm. of impure (*dl,ld*)-1,2-dimethoxy-1,2-diphenylethane, m.p. 137–139° (mixture melting point at 140–141.5° after crystallization from ethanol), 40 mgm. of diphenylacetaldehyde acetal, converted to its 2,4-dinitrophenylhydrazone, m.p. 145–147°, purified 149–150°, m.m.p., and finally 6 mgm. of impure (*dd,ll*)-1,2-dimethoxy-1,2-diphenylethane, crystallized from methanol to melt at 90–91°, m.m.p.

Benzylmercuric Nitrate and Methanolic Mercuric Nitrate

A mixture of 6.54 gm. (0.02 mole) of benzylmercuric chloride (22), m.p. 105–105.5°, and 3.40 gm. (0.02 mole) of finely-ground silver nitrate in 20 ml. of methanol was vigorously shaken for several hours, then filtered to remove 2.75 gm. (0.019 mole) of methanol-washed silver chloride. Then 6.83 gm. (0.021 mole) of mercuric nitrate was added and the system was shaken nine hours and let stand 30 hr. After filtration to remove 0.17 gm., infusible, the system was diluted with an equal volume of water and four times extracted with 50 ml. total of chloroform. The extract, washed with cold 5% aqueous sodium hydroxide and water, then dried over sodium sulphate, was distilled, yielding two discreet fractions. The first one (0.90 gm., 46%) was benzyl methyl ether, b.p. 62–70° (15 mm.), n_D^{20} 1.5042; redistilled at 168–171° (750 mm.), n_D^{20} 1.5040, m.p. –61 to –56°, it was identified by mixture melting point with an authentic sample, b.p. 170.5°, n_D^{20} 1.5034, m.p. –56 to –54° (31).

The second fraction, b.p. 65–75° (1.5 mm.), n_D^{20} 1.5212 (0.47 gm., 15%), was redistilled at 66–72° (1–2 mm.), n_D^{20} 1.5204, m.p. –21 to –19°, and then frozen fractionally, m.p. –19.5 to –15°. Anal.: Calc. for $C_7H_7NO_3$: NO_3 , 40.5. Found: NO_3 , 40.0. This benzyl nitrate was identified by mixture melting point

with an authentic sample (26), b.p. 99–100° (16 mm.), n_D^{20} 1.5211, m.p. –17 to –15° (uncorr.). When toluene was subjected to the same reaction conditions used for the mercuric neither of the products was detected and no mercurous salt was formed.

sec-Butyl Nitrate

A mixture of 5.86 gm. (0.02 mole) of *sec*-butylmercuric chloride (27), m.p. 128.5–129.3°, and 3.40 gm. (0.02 mole) of finely-ground silver nitrate in 25 ml. of methanol was shaken for 30 min. After filtration from 2.93 gm. of silver chloride the filtrate with 20 ml. of methanolic washings was shaken with 6.83 gm. (0.021 mole) of mercuric nitrate for 10 hr., then filtered to remove 3.33 gm. (30%) of mercurous nitrate. The filtrate diluted with water was ether extracted and the extract, water and alkali washed, was dried and distilled to yield a fraction, b.p. 120–123° (750 mm.), 0.12 gm. (5%), n_D^{20} 1.4006. This product was identified as *sec*-butyl nitrate by its physical constants (23), by a positive test with diphenylamine–sulphuric acid, and by uptake of hydrogen over palladium-on-charcoal to the extent of 96% of that expected for *sec*-butyl nitrate with consequent formation of ammonia.

2,2'-Dinitratomercuridiethyl Ether with Methanolic Mercuric Nitrate

Both this compound and hydroxyethylmercuric nitrate were prepared by the method of Hoffmann and Sand (18) and both were stable toward 10% nitric acid although they were decomposed by hydrochloric acid. When a methanolic solution of dinitratomercuridiethyl ether was shaken for five days with mercuric nitrate there was no evidence for mercurous salt formation, even when some water was added to the system.

Methods of Analysis for Kinetic Studies

When analysis for mercuric salts in absence of chlorides was possible the method of thiocyanate titration following chloroform extraction (41) was used. However the interference by mercurous salt frequently made this method unusable and the procedure of Personne (32) was refined for our purpose. By this refinement a 1 or 2 ml. aliquot (which might be about 0.5 molar in total inorganic mercury I and II) was added to 10 ml. of water in a separatory funnel and 1 ml. of 1 *N* nitric acid was added to prevent hydrolysis of the inorganic mercury salts. Three extractions with 5-ml. portions of chloroform were made for removal of organomercurial, then the aqueous layer was rinsed into 10 ml. of 2 *N* hydrochloric acid. The resulting precipitate of mercurous chloride was filtered off after 20 or 30 min. with celite as filter-aid, and washed at least four times. Filtrate and washings were combined and treated with 10 ml. of 0.19 *N* potassium iodide solution. The clear solution was diluted to a volume of about 80 ml. and was titrated with standardized (against red mercuric oxide in nitric acid) 0.1 *N* mercuric nitrate solution to the first appearance of a permanent red color due to mercuric iodide. Best results are obtained using a dark background and side-lighting. The titer value was subtracted from a blank carried out similarly on the potassium iodide solution. It is important that the final volume of each analyzed solution be nearly the same.

$$\text{Molarity of Hg}^{++} = \frac{\text{normality}}{2} \cdot \frac{(\text{vol. of blank titer} - \text{vol. of sample titer})}{\text{volume of aliquot}}$$

Since 2-hydroxycyclohexylmercuric salts cannot be extracted quantitatively by chloroform the kinetic study of cyclohexene oxidation by aqueous mercuric nitrate does not include the extraction step and the aliquot is added directly to dilute hydrochloric acid which decomposes the hydroxymercurial and precipitates the mercurous salt at the same time. In this event the rate must be calculated on the assumption that the oxymercuration has gone rapidly to completion (see equation [i]).

The determination of mercurous salt above, or of both mercurous and mercuric salt, is obviously better suited to a kinetic study of oxidation by mercuric salt than is a determination of the mercuric salt alone, especially since the organomercurial is involved as an intermediate. Two methods have been employed.

In the first method, after extraction of the organomercurial the mercurous salt is precipitated but then filtered and washed by suction on a micro filtering crucible from which it is dissolved and oxidized by warming with 2 ml. of *aqua regia* until solution is complete. This solution is diluted, treated with potassium iodide, and titrated as described before,

$$\text{Hg}_2^{++} = \frac{\text{normality}}{4} \cdot \frac{\text{blank titer} - \text{sample titer}}{\text{volume of aliquot}},$$

while the mercuric salt is determined as before.

The second method is iodometric. After extraction of the organomercurial the aqueous layer is rinsed into a solution of 0.5 gm. of potassium iodide in 10 ml. of 2 *N* hydrochloric acid plus 5 ml. of 0.1 *N* standard iodine solution. Titration is then carried out with 0.1 *N* standard thiosulphate using a starch endpoint because of a tendency for the final solution to be slightly yellow.

Kinetic studies based on this determination of mercurous salt are shown in Table XIII, depicting the reaction of *cis*-stilbene with mercuric nitrate in methanol at 25°. Rates calculated from data corresponding to the 1/*P* curve, Fig. 2, show (Expts. 1 and 2, 3 and 4, 5 and 6) a satisfactory second-order relationship dependent on the concentration of nitric acid, which exerts an accelerating effect.

TABLE XIII

REACTION OF *cis*-STILBENE WITH MERCURIC NITRATE IN METHANOL AT 25° ± 0.1°C.

Expt. No.	Initial molarities			Molarities after mercuration			Second-order specific rate constant, l. moles ⁻¹ min. ⁻¹	% Investigated
	Hg(NO ₃) ₂	<i>cis</i> -Stilbene	HNO ₃	Hg(NO ₃) ₂	Mercurial	HNO ₃		
1	.0937	.0313	.125	.0625	.0313	.156	.293 ± .012	73
2	.125	.0313	.125	.0938	.0313	.156	.294 ± .009	88
3	.125	.0625	.125	.0625	.0625	.189	.338 ± .009	68
4	.156	.0625	.125	.0938	.0625	.188	.335 ± .007	84
5	.125	.0625	.250	.0625	.0625	.312	.402 ± .006	72
6	.125	.0625	.375	.0625	.0625	.437	.413 ± .006	74

REFERENCES

1. ASTON, J. G., CLARKE, J. T., BURGESS, K. A., and GREENBERG, R. B. *J. Am. Chem. Soc.* 64: 300. 1942.
2. BALBIANO, L. *Gazz. chim. ital.* 36, I: 237. 1906. *Ber.* 42: 1503. 1909.
3. BALBIANO, L. and PAOLINI, V. *Ber.* 35: 2994. 1902; 36: 3575. 1903.
4. BARTON, D. R. H. *J. Chem. Soc.* 516. 1946.
5. BARTON, D. R. H. and ROSENFELDER, W. J. *J. Chem. Soc.* 2381. 1951.
6. BERMAN, L., HALL, R. H., PYKE, R. G., and WRIGHT, G. F. *Can. J. Chem.* 30: 541. 1952.
7. BIRKS, A. M. and WRIGHT, G. F. *J. Am. Chem. Soc.* 62: 2412. 1940.
8. BRACKMAN, D. S. and PLESCH, P. H. *J. Chem. Soc.* 2188. 1952.
9. BRACKMAN, D. S. and PLESCH, P. H. *J. Chem. Soc.* 1289. 1953.
10. BROOK, A. G. and WRIGHT, G. F. *Can. J. Chem.* 29: 308. 1951.
11. COPE, A. C., NELSON, N. A., and SMITH, D. S. *J. Am. Chem. Soc.* 76: 1100. 1954.
12. DOWNING, D. C. and WRIGHT, G. F. *J. Am. Chem. Soc.* 68: 141. 1946.
13. FISCHER, H. O. L. and TAUBE, C. *Ber.* 59: 855. 1926.
14. HAHN, A. *Ber.* 43: 420. 1910. *Cf. Org. Syntheses*, 20: 27. 1940.
15. HARTLEY, W. N. *J. Chem. Soc.* 81: 556. 1902.
16. HARTLEY, W. N. *J. Chem. Soc.* 83: 221. 1903.
17. HARTUNG, W. H. *J. Am. Chem. Soc.* 50: 3373. 1928.
18. HOFFMANN, K. A. and SAND, J. *Ber.* 33: 1340. 1900.
19. IRVINE, J. C. and WEIR, J. *J. Chem. Soc.* 91: 1390. 1907.
20. JEFFRIES, P. R., MACBETH, A. K., and MILLIGAN, B. *J. Chem. Soc.* 705. 1954.
21. JONES, R. N. and THORN, G. D. *Can. J. Research, B*, 27: 580. 1949.
22. KHARASCH, M. S., PINES, H., and LEVINE, H. *J. Org. Chem.* 3: 347. 1938.
23. KORNBLUM, N., PATTON, J. T., and NORDMANN, J. B. *J. Am. Chem. Soc.* 70: 746. 1948.
24. KUHN, L. *J. Am. Chem. Soc.* 68: 1761. 1946.
25. LEYS, A. *Bull. soc. chim.* [4] 1: 262, 633. 1907.
26. LUCAS, G. R. and HAMMETT, L. P. *J. Am. Chem. Soc.* 64: 1928. 1942.
27. MARVEL, C. S. and CALVERY, H. O. *J. Am. Chem. Soc.* 45: 820. 1923.
28. MEEN, R. H. and WRIGHT, G. F. *J. Org. Chem.* 19: 391. 1954.
29. MEYER, J. *Z. physik. Chem.* 67: 257. 1909.
30. MORTON, A. A. and PENNER, H. P. *J. Am. Chem. Soc.* 73: 3300. 1951.
31. OLSON, W. T. *et al.* *J. Am. Chem. Soc.* 69: 2451. 1947.
32. PERSONNE, J. *Compt. rend.* 56: 951. 1863.
33. RUYLE, W. V. *et al.* *J. Am. Chem. Soc.* 76: 2604. 1953.
34. TIFFENEAU, M. and LEVY, J. *Bull. soc. chim.* [4] 39: 781. 1926.
35. TIFFENEAU, M. and OREKOFF, A. *Bull. soc. chim.* [4] 29: 816. 1921.
36. TRIEB, W. and BAST, H. *Ann.* 561: 165. 1948.
37. TRIEB, W., LUCIUS, G., KOGLER, H., and BRESLAUER, H. *Ann.* 581: 59. 1953.
38. WINDAUS, A. *Ann.* 552: 135, 142. 1942.
39. WINDAUS, A. and LINSERT, O. *Ann.* 465: 157. 1928.
40. WRIGHT, G. F. *Can. J. Chem.* 30: 268. 1952.
41. WRIGHT, G. F. *J. Am. Chem. Soc.* 57: 1993. 1935.
42. YAGODA, H. *Ind. Eng. Chem. Anal. Ed.* 15: 27. 1943.

THE PHOTOINITIATED ADDITION OF MERCAPTANS TO OLEFINS

II. THE KINETICS OF THE ADDITION OF *n*-BUTYL MERCAPTAN TO 1-PENTENE^{1,2}

BY M. ONYSZCHUK³ AND C. SIVERTZ⁴

ABSTRACT

The detailed kinetics involved in the photoinitiated addition of *n*-butyl mercaptan to 1-pentene is presented. It has been shown that side reactions such as propagation and α -dehydrogenation are relatively negligible and the principal mechanism comprises attack by thiyl radical followed by transfer with mercaptan by the alkyl radical. The velocity constant of the attack step is estimated to be 7×10^6 and that of the transfer step 1.4×10^6 liters/mole-sec. These values together with approximate termination velocity constants are shown to explain the kinetics over a wide range of concentration.

INTRODUCTION

In the first study (2) rates were observed for only *equal* concentrations of mercaptan and olefin. This preliminary work emphasized the need for a more general formulation of the kinetics and the inadmissibility of simplifying assumptions with regard to terminations. The mechanism previously proposed (2) involved an attack step followed by a transfer step but the isolation of each of these was not accomplished. It was therefore the principal object of this work to vary the concentrations of reagents over a wide range and test the proposed reaction scheme in terms of a more general kinetic description, and if possible to measure both the attack and transfer velocity coefficients.

BASIC REACTIONS: UNCONJUGATED VINYL

The basic reactions and consequent steady state equations are presented in considerable detail in this paper to form a foundation of symbolism and theory for subsequent papers. Some estimates of incidental velocity coefficients at 30°C. are included to help in forming a judgment of the reactions which need to be considered.

In this paper we discuss only the photoinitiated addition of *n*-butyl mercaptan to unconjugated vinyls, and proceed to break the over-all process up into the various steps involved. Velocity constants are in liters moles⁻¹ sec⁻¹.

Origin of Radicals

As in previous work (2) the origin of radicals is through the photolysis of 2,2'-azo-bis-isobutyronitrile designated Q₂, using a filter system which forbids activation of reactants:



where $k(I)$ is the rate of origin of kinetic chains (moles/liter-sec.). In the

¹Manuscript received January 13, 1955.

Contribution from the Department of Chemistry, University of Western Ontario, London, Ont. This work was supported by funds provided by the National Research Council of Canada.

²The first paper of this series is Reference (2).

³Graduate student 1962. Present address—University of Cambridge, Cambridge, England.

⁴Associate Professor of Chemistry, University of Western Ontario, London, Ontario.

present treatment we will assume that \dot{Q} radicals have negligible concentration compared to all others and that they disappear by transfer with mercaptan:



Initiation

The thiyl radical attacks monomer to produce an unconjugated radical designated \dot{X} , e.g. $\text{RSCH}_2\dot{\text{C}}\text{HCH}_2\text{CH}_2\text{CH}_3$ results from an attack on 1-pentene. That the addition was counter Markovnikov was proved by product analysis.



Propagation

Nothing much is known of the propagation of \dot{X} radicals into monolefins in the liquid phase. If we extrapolate James and Steacie's (5) values to 30° for the gas phase propagation of C_2H_5 radicals into 1-heptene and also their dehydrogenation constant, it may be shown that the kinetic chain would be of the order of unity, owing to degradative transfer, even in the absence of mercaptan. Consequently we can neglect propagation.



Chain Transfer

In the presence of sufficient mercaptan the principal transfer reaction is



where P is addition product.

At low mercaptan concentrations we have reason to believe that there may be significant α -hydrogen transfer with the production of the strongly stabilized allylic radical designated \dot{A} .



This value for k_{3a} is that for the dehydrogenation of 1-heptene in the gas phase determined by James and Steacie (5).

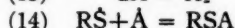
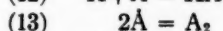
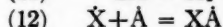
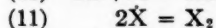
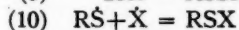


Finally reaction (7) is reversible, hence



Since $k_{3a}'/k_{3A} = K$, the equilibrium constant for (7), we can estimate K through bond energies to be somewhat less than unity. The value of $k_{3A} = 100$ is about the transfer constant of isoprenyl radical previously reported (2).

Termination



In the light of the experimental results to be reported we have found it expedient to deal with the system:

*Recent work in this laboratory indicates that the value 6×10^{11} previously reported is an average for RS and \dot{X} with $k_4' > k_5'$.

(1) assuming the geometric mean for the crossed terminations and including the α -dehydrogenation,

(2) neglecting α -dehydrogenation and making no simplifying assumption with regard to cross terminations.

Total Radical Termination

With the assumption of the geometric mean for crossed termination two added constants suffice to express all termination constants in terms of one. Let $k_4 = u^2 k_6$, $k_8 = \sigma^2 k_6$, then all terminations may be expressed as $k_6(uR\dot{S} + \sigma\dot{A} + \dot{X})^2$.

Here we write $k_4 = 2k_4'$, $k_6 = 2k_6'$, $k_8 = 2k_8'$, and $k_6 = 2\sqrt{k_4'k_8'} = \sqrt{k_4k_8}$. Such a definition of the crossed termination k_6 is suggested by elementary collision theory since the collision number for unlike species is twice that for single. With this convention the expression $k_6[uR\dot{S} + \sigma\dot{A} + \dot{X}]^2$ is equal to the rate of disappearance of *all* radicals. We may note that in terms of the approximate values of k_4 , k_6 , and k_8 given above $u \div 2$, $\sigma \div 0.1$.

STEADY STATE EQUATIONS

The radical whose steady state is described is shown on the left. Since all terminations except those for \dot{Q} radicals are included, the rate detail for terminations is implied by the letters T . For example

$$T_{II} = k_4(R\dot{S})^2 + k_5(R\dot{S})(\dot{X}) + k_9(R\dot{S})(\dot{A}).$$

$$I \quad \dot{Q} \quad k(I) = k_3^0(RSH)(\dot{Q})$$

$$II \quad R\dot{S} \quad k_3^0(RSH)(\dot{Q}) + k_{3A}(RSH)(\dot{A}) + k_{3X}(RSH)(\dot{X}) \\ = k_1(R\dot{S})(M) + k_{3a}'(R\dot{S})(M) + T_{II}$$

$$III \quad \dot{A} \quad k_{3a}'(R\dot{S})(M) + k_{3a}(\dot{X})(M) = k_{3A}(RSH)(\dot{A}) + T_{III}$$

$$IV \quad \dot{X} \quad k_1(R\dot{S})(M) = k_{3X}(RSH)(X) + k_{3a}(M)(\dot{X}) + T_{IV}.$$

Summation to infinity yields

$$[1] \quad k(I) = \Sigma T = k_6[uR\dot{S} + \sigma\dot{A} + \dot{X}]^2.$$

The reaction rate measured dilatometrically is

$$[2] \quad R = k_1(R\dot{S})(M) = k_{3X}(RSH)(\dot{X})$$

providing we neglect T_{IV} and $k_{3a}(M)$ compared to $k_{3X}(RSH)$. The former is not permissible, as $RSH \div 0$. For *long* kinetic chains we can express $(R\dot{S})$ and (\dot{A}) in terms of (\dot{X}) through IV and III. This value of (\dot{X}) substituted in [2] yields

$$[3] \quad R = k_{3X}(RSH)\omega_6 / \left[1 + u \frac{k_{3X}(RSH)}{k_1(M)} + \sigma \frac{k_{3a}(M)}{k_{3A}(RSH)} \right]$$

after elimination of insignificant terms. In [3], $\omega_6 = \sqrt{k(I)/k_6}$. Owing to the last term in the denominator of [3] this equation predicts *lower* rates at *low mercaptan* than would be the case if $k_{3a} = 0$. If α -dehydrogenation is neglected equation [3] can take a linear form, viz.,

$$[4] \quad \frac{1}{R} = \frac{1}{k_{3X}(RSH)\omega_6} + \frac{u}{k_1(M)\omega_6},$$

from which on varying RSH at constant (M_0)

$$[5] \quad u k_{3X}/k_1 = \text{Intercept}(M_0)/\text{slope}.$$

By the same procedure the rate may be expressed in terms of the $R\dot{S}$ radical (equation [2]).

$$[6] \quad R = k_1(M)\omega_6/[u + k_1(M)/k_{3X}(\text{RSH})\{1 + k_{3a}(M)/k_{3A}(\text{RSH})\}].$$

No sigmoidal form of R vs. M such as that implied in [3] for R vs. RSH is now apparent, but the rate should fall at high M values owing to k_{3a} . Again if $k_{3a} = 0$ [6] can be written in a similar form to [4]

$$[7] \quad R = k_1(M)\omega_6/u[1 + k_1(M)uk_{3X}(\text{RSH})]$$

which in linear form yields

$$[8] \quad uk_{3X}/k_1 = \text{slope}/\text{intercept}(\text{RSH}_0).$$

Cross Termination

If the cross termination is not given by the geometric mean we can represent it quite generally thus: $k_6 = \phi\sqrt{k_4k_6}$ in which ϕ may have any value from 0 upwards. When this is included in the solution for the steady states it readily follows that equation [3] neglecting α -hydrogen reactions now becomes:

$$[9] \quad R_1 = k_{3X}(\text{RSH})\omega_6/[1 + 2\phi br + b^2r^2]^{\frac{1}{2}}$$

where $b = uk_{3X}/k_1$ and $r = (\text{RSH})/(M)$. Similarly [7] becomes

$$[10] \quad R_2 = k_1(M)\omega_6 br/u[1 + 2\phi br + b^2r^2]^{\frac{1}{2}}.$$

As rates R_1 are measured, varying RSH at constant M_0 a limiting value of [9] is implied at ($r \rightarrow \infty$) $R_1^\infty = k_1(M_0)\omega_6/u$. Similarly $R_2^\infty = k_{3X}(\text{RSH}_0)\omega_6$ ($r \rightarrow 0$). Consequently we can write [9] and [10] in terms of the two constants b and ϕ , and the limiting rates R_1^∞ and R_2^∞ viz.,

$$[11] \quad R_1 = R_2^\infty r/[1 + 2\phi br + b^2r^2]^{\frac{1}{2}},$$

$$[12] \quad R_2 = R_1^\infty b/[1 + 2\phi br + b^2r^2]^{\frac{1}{2}}.$$

METHODS

In general the methods employed were those described in the first paper (2) except that a new apparatus was constructed employing a series of four quartz lenses to collimate and focus the mercury arc light in a manner similar to that of Bartlett *et al.* (3).

The ultraviolet light source was a Hanovia A H-8, 85-watt lamp. The photosensitizer was again 2,2-azo-isobutyronitrile (AIN) employed in such concentration as to absorb not more than 20% of the light in the cell. Corning filters 9863 and 5840 were used to isolate radiation capable of photolyzing the AIN alone. Dilatometer technique was identical with that previously described (2).

EXPERIMENTAL

1-Pentene—Phillips Petroleum Research Grade was used without further purification.

Normal butyl mercaptan—Eastman Kodak's white label was distilled under an atmosphere of nitrogen through a 40-plate Todd column. The middle cut retained had the following properties: b.p. 98.0°C. at 750 mm., $n_D^{20} = 1.4410$. **Benzene**—Merck's Reagent Grade Thiophene-free was used without further purification.

Azo-isobutyronitrile was prepared by the method of Overberger *et al.* (7); m.p. 102.5–103.5°C.

The following series of experiments were carried out. All concentrations are expressed in moles/liter. *n*-Butyl mercaptan is represented as BuSH. Temperature was constant at 25°C.

TABLE I

	(AIN) 10^3	(1-Pentene)	(<i>n</i> -BuSH)	$10^7k(I)$
Series I	3.15	1.59	1.61	1.1
Series II	3.15	4.8	0.803(const.)	1.1
Series III	3.15	0.797(const.)	4.8	1.1

$k(I)$ values were determined by the method of Reference (1).

RESULTS AND DISCUSSION

Series I was designed to show the reproducibility of rate measurements, which is shown in Fig. 1. The measured rates are 0.159, 0.161, 0.161, and 0.16 mm./sec.

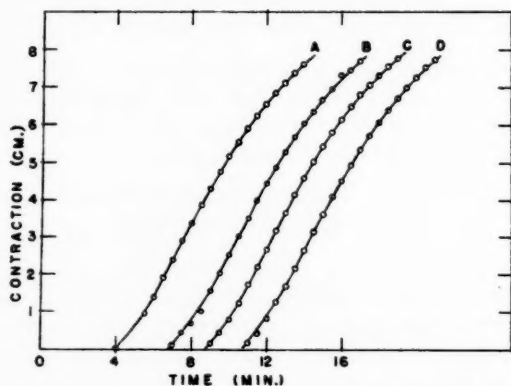


FIG. 1. Dilatometric measurement of the rate of addition of *n*-butyl mercaptan to 1-pentene, showing reproducibility of rate measurements. Series I.

Butyl Mercaptan and 1-Pentene

Series II—Analysis of the data plotted in Fig. 2, in the light of the theory, proceeded by attempting first to fit equation [6]. This suggested that the last term in the denominator was so small that it could not be distinguished from possible effects due to the considerable changes in environment as the composition was altered. In general the shape of the curve in Fig. 2 is that anticipated

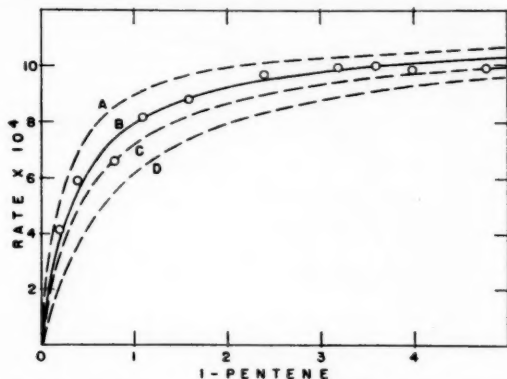


FIG. 2. Rate of addition of mercaptan as a function of 1-pentene at constant mercaptan (0.803 moles/liter). Series II. Curve A: $b = 0.3$, $\phi = 1$; Curve B: $b = 0.5$, $\phi = 1$; Curve C: $b = 0.5$, $\phi = 1.5$; Curve D: $b = 1.0$, $\phi = 1$.

by equation [7] or [12]. We could then proceed to apply equation [7] which assumes the geometric mean or equation [12] which does not. The result of the first alternative in terms of the linear form of equation [7], Fig. 3, yields an intercept $1/k_{3X}(\text{RSH})_0 \omega_8 = 900$ liter sec./mole, and a slope $u/k_1 \omega_8 = 360$ sec., and hence a value of $u k_{3X}/k_1 = b \div 0.5$. The application of equation [12] is discussed below.

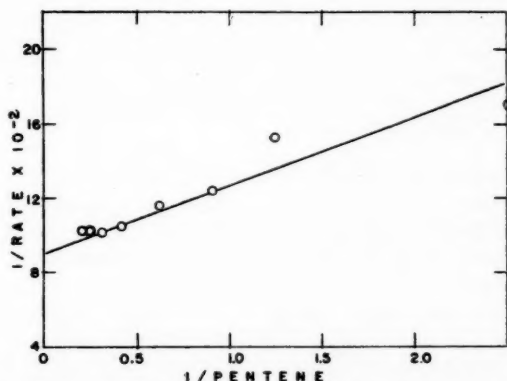


FIG. 3. Plot of data in Fig. 2 according to linear form of equation [7]. Intercept = 900 liter-sec./mole, slope = 360 sec.

Series III—The data are plotted in Fig. 4. From Series II we have values for $k_{3X}\omega_8$ and $u k_{3X}/k_1$, and hence "calculated" rates neglecting α -dehydrogenation can be determined. These are shown in Fig. 2B and 4B. A glance at the latter shows that the rates are lower than calculated in both low and high mercaptan regions. It is hence obvious that the linear form [4] cannot apply to

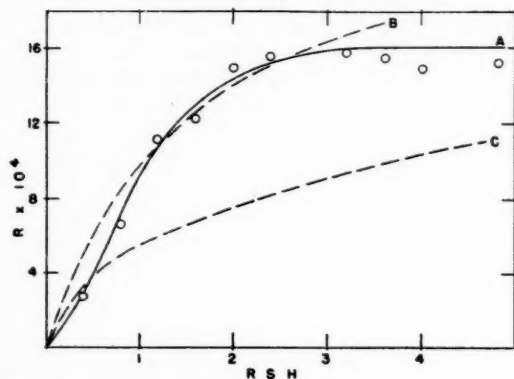


FIG. 4. Rate of addition of mercaptan as a function of mercaptan, 1-pentene constant (0.797 moles/liter). Series III. Curve A: smoothed experimental curve. Curve B: $b = 0.5$, $\phi = 1$; Curve C: $b = 0.5$, $\phi = 6$.

all values of mercaptan. Nevertheless the *general form* is that anticipated by [3] or [11] proceeding from a region where rates are dependent on mercaptan through a *transition region* to one in which rate is independent of mercaptan. Moreover the relative value of constants, viz., $u k_{3x}/k_1 = 0.5$ determined from Series II, does locate the position of the transition region. The deviation at low mercaptan may be partly imputed to some α -dehydrogenation (equation [3]). Another obvious reason for low rates could be the neglect of termination by Q radicals (basic reaction (2)) which cannot be valid at low mercaptan concentrations. There is nothing in the kinetics which anticipates the sharp levelling off of rates at *high* mercaptan and we can only surmise that this is due to the considerable changes in environment. Also shown are curves A and D, Fig. 2, which indicate the sensitivity to $b = u k_{3x}/k_1$ values when $\phi = 1$. Fig. 4 shows in curve C the effect of $\phi = 6$, $b = 0.5$.

Application of Equations [11] and [12]: Non-geometric Termination

Considering that α -dehydrogenation appears to be close to negligible we may with more confidence apply equations [11] and [12]. It should be noted that only unique values of ϕ and b will satisfy both equations. It was found that when $b = 0.5$ and $\phi = 0.5$ a reasonably good fit of the data is again obtained (Fig. 5). However the data can hardly discriminate between this interpretation and that of the geometric mean. Our main conclusions are (a) the cross termination is close to the geometric mean, (b) the value of $u k_{3x}/k_1$ appears to be quite closely given as 0.5 at 25°C., (c) deviations from the anticipated rate curves at high mercaptan values are probably due to environmental effects on the mechanism, but the general form is that predicted by the basic reactions given.

Estimation of Absolute Velocity Constants

While it was not the object of this work to determine the velocity coefficients and no half-life measurements were made, we may estimate these by taking

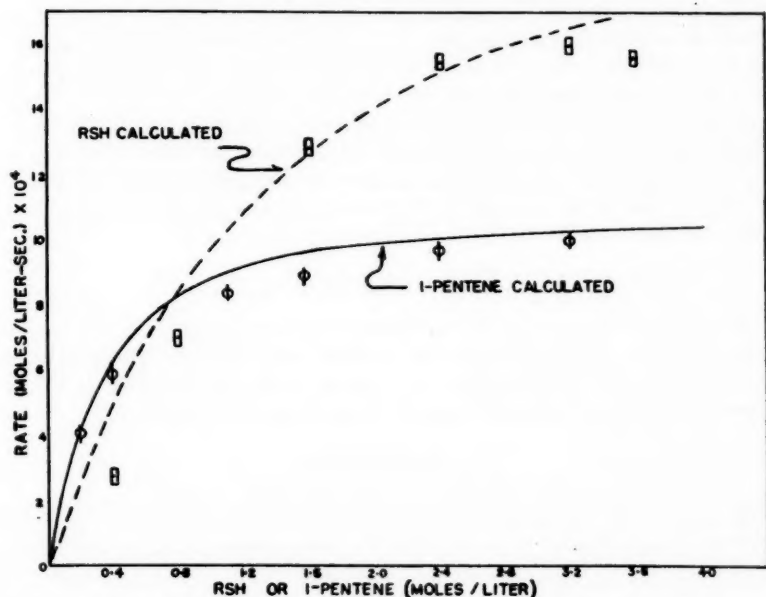


FIG. 5. Plot of equations [11] and [12] with $b = 0.5$, $\phi = 0.5$, showing agreement with measured rates.

$k_6 = 10^{11}$ which corresponds to 5×10^{10} for k_6' , the recombination constant of \dot{X} radicals. This value is somewhat lower than that previously reported (2) and higher than Ivin and Steacie (4) report for C_2H_5 radicals in the gas phase, viz., 1.56×10^{10} . This value for k_6 together with the $k(I)$ (Table I) for the series yields $\omega_6 \div 10^{-9}$. From Fig. 3 we found $1/k_{3X}(RSH_0)\omega_6 = 900$ or alternatively that $R_2^\infty = k_{3X}(RSH_0)\omega_6$ (Fig. 2) $= 1.1 \times 10^{-3}$. Therefore since $(RSH_0) = 0.8$, $k_{3X} = 1.1 \times 10^{-3}/0.8 \times 10^{-9} = 1.4 \times 10^6$ liter/mole-sec. If we take k_4 for the $R\dot{S}$ radical as 6×10^{11} (2), then $u = 2.45$ and hence $k_1 = 7 \times 10^6$. This happens also to yield for $u k_{3X}/k_1$ the value $2.45 \times 1.4 \times 10^6/7 \times 10^6 = 0.52$, which is hence consistent with the direct experimental value.

GENERAL CONCLUSIONS

(1) The "calculated" curves shown in Fig. 5 are seen to be in substantial agreement with the experimental results except for high mercaptan concentrations. In consequence we can presume that the mechanism of the photo-initiated addition of mercaptan to 1-pentene does in fact take place in two independent steps: an attack step ($k_1 = 7 \times 10^6$) and a mercaptan transfer step ($k_{3X} = 1.4 \times 10^6$).

(2) With regard to equation [7] it should be noted that the last term in the denominator $k_1(M)/uk_{3X}(RSH)$ is equal to $(\dot{X})/u(R\dot{S})$ and hence measures the relative abundance of these radicals. On the plateau of Fig. 2 we may

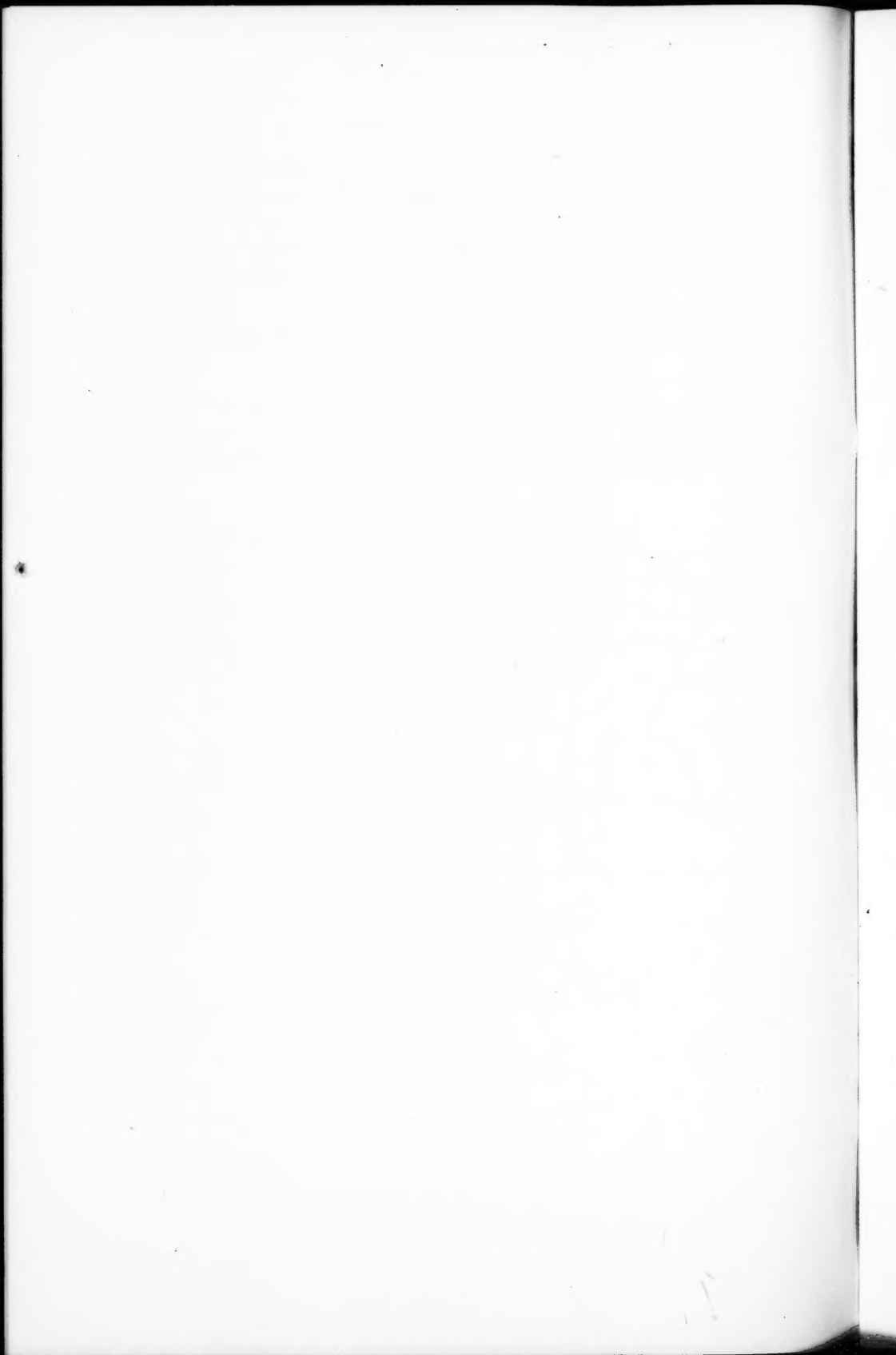
hence presume that $(\dot{X}) > (R\dot{S})$, and a half life in this region may be assigned to the \dot{X} radical. In a similar manner we might isolate the $R\dot{S}$ radical. Melville, Robb, and Tutton (6) were the first to point out that when such measurements of half lives are combined with one made in a region of obvious cross-termination the cross-termination velocity constant k_c could be measured. It is concluded here that such a procedure is valid only (a) if it has been shown that such side reactions as α -dehydrogenation are negligible, (b) if no propagation occurs, (c) provided the regions where radicals may be taken as isolated have been defined experimentally such as shown in this paper.

ACKNOWLEDGMENTS

We are grateful for financial assistance from the National Research Council and one of us, M. Onyszchuk, for a scholarship from the Ontario Research Council and also for permission to publish these results from the Associate Committee of the National Research Council on Synthetic Rubber.

REFERENCES

1. BACK, R. and SIVERTZ, C. Can. J. Chem. 32: 1061. 1954.
2. BACK, R., TRICK, G., McDONALD, C., and SIVERTZ, C. Can. J. Chem. 32: 1078. 1954.
3. BARTLETT, P. D. and KWART, H. J. J. Am. Chem. Soc. 72: 1051. 1950.
4. IVIN, K. J. and STEACIE, E. W. R. Proc. Roy. Soc. (London), A, 208: 25. 1951.
5. JAMES, D. G. L. and STEACIE, E. W. R. Private communication.
6. MELVILLE, H. W., ROBB, J. C., and TUTTON, R. C. Discussions Faraday Soc. 10: 5595. 1951.
7. OVERBERGER, C. G., O'SHAUGHNESSY, M. T., and SHALIT, H. J. J. Am. Chem. Soc. 71: 2161. 1949.



Free Radicals by Mass Spectrometry. VII. The Ionization Potentials of Ethyl, Isopropyl, and Propargyl Radicals and the Appearance Potentials of the Radical Ions in Some Derivatives— <i>J. B. Farmer and F. P. Lossing</i> - - - - -	861
The Hydration of Plaster of Paris— <i>Fraser W. Birss and T. Thorvaldson</i> - - - - -	870
The Mechanism of the Hydration of Calcium Oxide— <i>Fraser W. Birss and T. Thorvaldson</i> - - - - -	881
The Electrical Conductance of Strong Electrolytes: A Test of Stokes' Equation— <i>A. N. Campbell and E. M. Kartzmark</i> - -	887
Studies on Carrageenin: The Effect of Shear Rate on Viscosity— <i>C. R. Masson and D. A. I. Goring</i> - - - - -	895
The Heat of Wetting of Silk Fibroin by Water— <i>H. Brian Dunford and John L. Morrison</i> - - - - -	904
The Adsorption of Nitrogen, Oxygen, and Argon by Graphite— <i>H. L. McDermot and J. C. Arnell</i> - - - - -	913
The Mannich Condensation of Compounds Containing Acidic Imino Groups— <i>Caurino Cesar Bombardieri and Alfred Taurins</i>	923
Disintegration-rate Determination by 4π -Counting. Part II. Source-mount Absorption Correction— <i>B. D. Pate and L. Yaffe</i>	929
Simultaneous Surface Exchange Studies Using Both Cation and Anion— <i>R. M. Stow and J. W. T. Spinks</i> - - - - -	938
Interfacial Potentials— <i>J. T. Davies and Sir Eric Rideal</i> - - - -	947
Cystine as an Addition Agent in the Electrodeposition of Copper— <i>A. J. Sukava and C. A. Winkler</i> - - - - -	961
Microcalorimetric Determination of the Critical Concentration and the Molecular Dimensions of Polyvinyl Acetate in Solution— <i>Michel Parent and Marcel Rinfret</i> - - - - -	971
Some Thermodynamic Considerations of Surface Regions. Surface Tension, Adsorption, and Adsorption Hysteresis— <i>E. A. Flood</i>	979
Oxidation of Alkenes by Mercuric Salts— <i>D. A. Shearer and George F Wright</i> - - - - -	1002
The Photoinitiated Addition of Mercaptans to Olefins. II. The Kinetics of the Addition of <i>n</i> -Butyl Mercaptan to <i>l</i> -Pentene— <i>M. Onyszchuk and C. Sivertz</i> - - - - -	1034

Contents

	Page
Foreword— <i>R. L. McIntosh</i> - - - - -	725
Studies in the Polyoxyphenol Series. IX. The Synthesis of Papaverine and Papaveraldine by the Pomeranz-Fritsch Method— <i>Donald A. Guthrie, Arlen W. Frank, and C. B. Purves</i> - - -	729
The Vapor Phase Photolysis of Hexafluoroacetone in the Presence of Methane and Ethane— <i>P. B. Ayscough, J. C. Poianyi, and E. W. R. Steacie</i> - - - - -	743
Free Radical Recombination in the Photolysis of Acetone— <i>S. N. Naldrett</i> - - - - -	750
The Determination of Molecular Weight— <i>A. F. Sirianni and I. E. Puddington</i> - - - - -	755
Particle Motions in Sheared Suspensions. III. Further Observations on Collisions of Spheres— <i>R. St. J. Manley and S. G. Mason</i>	763
The Reciprocal Salt-pair System: Sodium Chloride - Ammonium Sulphite - Sodium Sulphite - Ammonium Chloride - Water at 20°C. and 60°C. Part I. Ternary Systems— <i>J. A. Labash and G. R. Lusby</i> - - - - -	774
The Reciprocal Salt-pair System: Sodium Chloride - Ammonium Sulphite - Sodium Sulphite - Ammonium Chloride - Water at 20°C. and 60°C. Part II. The Quaternary System— <i>J. A. Labash and G. R. Lusby</i> - - - - -	787
On the Intermolecular Force Field of Nitriles— <i>F. E. Murray and W. G. Schneider</i> - - - - -	797
Hydrogen Peroxide and Its Analogues. VII. Calorimetric Properties of the Systems $H_2O - H_2O_2$ and $D_2O - D_2O_2$ — <i>Paul A. Giguère, B. G. Morissette, A. W. Olmos, and O. Knop</i> - - - - -	804
Combination and Disproportionation of Ethyl Radicals: Influence of the Reaction $H + C_2H_5 = C_2H_6$ — <i>Moyra J. Smith, Patricia M. Beatty, J. A. Pinder, and D. J. Le Roy</i> - - - - -	820
The Relative Abundances of Neodymium and Samarium Isotopes in the Thermal Neutron Fission of U^{235} and U^{238} — <i>E. A. Melaika, M. J. Parker, J. A. Petruska, and R. H. Tomlinson</i> - - - -	830
Catalysis on Films of Arsenic, Antimony, and Germanium— <i>Sir Hugh Taylor</i> - - - - -	838
Preliminary Study of Photochemical Behavior in the System Nitrogen Dioxide - Ethane— <i>T. M. Rohr and W. Albert Noyes, Jr.</i> -	843
Further Degradation Reactions of Annotinine— <i>F. A. L. Anet and Léo Marion</i> - - - - -	849

(Continued on inside)

